UNIVERSITE DE LA MEDITERRANEE (AIX-MARSEILLE II)

Ecole Doctorale des Sciences de la Vie et de la Santé

Année 2011 N° attribué par la bibliothèque

THESE

Pour obtenir le grade de
Docteur en Sciences de l'Université de la Méditerranée

Spécialité
NEUROSCIENCES

Présentée par
CLEMENT MENUET

Vieillissement physiologique et pathologique du contrôle nerveux de la respiration : Etude chez des souris sauvages et transgéniques

Thèse dirigée par : **Dr. GERARD HILAIRE**

Membres du Jury :

M. le Docteur	JEAN-RENE CAZALETS	INCIA - Université Bordeaux 2	(Rapporteur)
M. le Professeur	DAVID KATZ	Case Western Reserve University - Cleveland	(Rapporteur)
M. le Docteur	CHRISTIAN STRAUS	EFR - G.H. Pitié-Salpétrière	(Rapporteur)
M. le Professeur	ANDRE NIEOULLON	IBDML - Université de la Méditerranée	(Examinateur)
M. le Professeur	FRED VAN LEUVEN	LEGTEGG - Katholieke Universiteit Leuven	(Examinateur)
M. le Docteur	CHRISTIAN GESTREAU	CRN2M - Université Paul Cézanne	(Co-Directeur)
M. le Docteur	GERARD HILAIRE	CRN2M - Université Paul Cézanne	(Directeur)

A mes parents,

à mes sœurs,

à Murielle.

« La connaissance s'acquiert par l'expérience, tout le reste n'est que de l'information. »

Albert Einstein

Remerciements

Cette thèse aura été pour moi une expérience très enrichissante, à la fois scientifique et humaine. Je souhaite ici remercier et rendre hommage à toutes les personnes qui m'ont aidé et soutenu dans la réalisation de ce travail, mais aussi dans la vie "hors labo".

En premier lieu, je souhaite remercier Monsieur le Docteur Gérard Hilaire, mon directeur de thèse. Joseph Joubert disait, « Le génie commence les beaux ouvrages, mais le travail seul les achève ». Cette citation trouve tout son sens lorsque l'on connaît Gérard, qui m'aura impressionné tout au long de ma thèse par sa capacité hors du commun à initier des projets de recherches particulièrement pertinents, et à les mener à bout de main de maître, par un travail acharné. Je suis honoré d'avoir été le dernier étudiant dirigé par Gérard, qui m'aura tellement apporté tant sur le plan scientifique que humain, me distillant régulièrement des conseils de "vieux briscard". Gérard, je souhaite vous remercier très chaleureusement pour cette merveilleuse expérience de vie que vous m'avez apportée, et je vous souhaite bon vent pour votre retraite bien méritée.

Je tiens également à remercier fortement Monsieur le Docteur Christian Gestreau, mon co-directeur de thèse. Christian aura été d'une aide inestimable tout au long de ma thèse, et en particulier dans ma découverte et mon apprentissage du domaine de la commande centrale respiratoire. Christian possède notamment une passion pour la science et une connaissance scientifique extraordinaires, et son souci pour l'exactitude, la pertinence de sa pensée dans les débats qui animent notre communauté scientifique, et sa promptitude à me transmettre son savoir, m'auront guidé tout au long de ma thèse. Christian, tu as toujours été là, dans les bons et dans les mauvais moments, comme les galères de manips qui ne marchent pas, et ce malgré ton emploi du temps surchargé. Un grand merci pour tout, et j'espère que nos chemins se recroiseront un jour, pourquoi pas en Australie ?

Je remercie vivement l'ensemble des membres du Jury de ma thèse pour avoir accepté d'évaluer ce travail de recherche.

Je remercie Monsieur le Docteur Jean-René Cazalets, Monsieur le Professeur David Katz, et Monsieur le Docteur Christian Straus, d'avoir accepté de consacrer une partie de leur été à l'examination de ce mémoire de thèse. Je suis très honoré de vous avoir eu comme rapporteurs de thèse, vos carrières scientifiques et publications respectives étant pour moi des références à suivre. J'ai hâte de vous rencontrer lors de la soutenance de ma thèse, afin de pouvoir enfin dialoguer avec vous.

Je remercie Monsieur le Professeur André Nieoullon d'avoir accepté d'être examinateur de ma thèse malgré vos nombreuses responsabilités, votre présence à mon oral est un grand honneur pour moi.

Enfin, un grand merci à Monsieur le Professeur Fred Van Leuven, qui au-delà de son rôle d'examinateur dans cette thèse, m'aura accompagné tout au long de ces trois dernières années *via* une collaboration extrêmement constructive. Je souhaite vous adresser un remerciement tout particulier, tant j'ai apprécié mes séjours dans votre laboratoire à Leuven. Vous m'avez toujours soutenu et m'avez encadré avec des conditions de travail exceptionnelles, sans parler d'un enseignement particulier sur la fermentation du houblon en Belgique avec Travaux Pratiques !

Je remercie très chaleureusement tous les membres de l'équipe MP3-Respiration et du laboratoire CRN2M en général.

Monsieur le Professeur Alain Enjalbert, je vous remercie de m'avoir accueilli au sein de votre laboratoire.

Nicolas, tu as été celui qui m'a mis le pied à l'étrier, et tout au long de ma thèse tu as toujours été là pour m'enseigner des techniques expérimentales, me conseiller et m'orienter. Nous avons partagé beaucoup de temps, au labo et en congrès notamment, je te remercie énormément pour tout. Tu es désormais MCF à Bobigny, je te souhaite le meilleur pour le futur, mais je ne doute pas que ce sera le cas !

Jorge, comment ne pas apprécier quelqu'un d'aussi gentil, enthousiaste et prévenant que toi ? Ton soutien m'aura tellement aidé notamment dans certaines passes difficiles. Egalement, le hasard fait parfois bien les choses, les divers effets de l'EPO m'ont toujours très intéressés, et voilà que le spécialiste de l'impact de l'EPO sur la respiration vient au labo ! Nous avons partagé une année de déboires expérimentaux, mais aussi de belles réussites, notre collaboration s'est vite transformée en amitié sincère et je sais que l'on se reverra, très bientôt certainement ! Un grand merci, et un « huge hug » !

Je remercie fortement Florence et Julie, votre bonne humeur quotidienne aura toujours égayé le labo. J'ai beaucoup apprécié les discussions et moments partagés, et vos nombreux conseils m'ont bien aidé. Bonne chance dans votre nouveau labo, et à bientôt !

Je souhaite également remercier Michèle (Bevengut), qui m'aura apporté de précieux conseils notamment en immunohistologie et en anatomie, et pour son fabuleux sens de la cuisine !

Un grand merci à Valéry, tant pour les manips et en particulier l'imagerie confocale, que pour sa sympathie et sa gentillesse au quotidien.

Un remerciement tout particulier pour Anne-Marie et Michèle (Morel), vos présences au labo étaient un souffle de jeunesse (et oui !), j'appréciais particulièrement votre dynamisme et votre gentillesse. Vous représentez ce qu'il y a de meilleur à Marseille, et m'avez beaucoup aidé au quotidien. Notamment, merci beaucoup à Anne-Marie pour votre aide dans l'analyse de certaines données en pléthysmographie, et pour avoir relu et corrigé les fautes d'orthographe et les coquilles de mon manuscrit de thèse. Je vous souhaite une bonne retraite, très active !

Un grand remerciement à deux proches collaborateurs avec lesquels j'ai eu la chance de travailler, Monsieur le Docteur Mathias Dutschmann, et Monsieur le Docteur Yuri Schvarev. Mathias, tes travaux de recherche ont inspiré certaines de mes manips, et je suis heureux d'avoir pu travailler avec toi, et peut-être de remettre ça dans peu de temps à Melbourne ! Yuri, grâce à toi j'en connais un peu plus sur la Russie et surtout la Sibérie, faire ta connaissance aura été mouvementé mais très agréable ! A bientôt je l'espère.

Je souhaite remercier très amicalement et rendre hommage à mes collègues étudiants et post-doctorants. Par ordre d'apparition :

Keda, il s'en est passé des choses pendant ces trois années où nous avons partagé le même bureau ! Des bonnes et des moins bonnes, mais que de souvenirs, ton "British touch" et ton caractère décapant nous ayant assuré de grands moments. Bonne chance pour la dernière ligne droite, et j'espère que tu t'épanouiras pleinement dans la réalisation de tes projets futurs !

Hanan et Théodora, j'ai beaucoup apprécié les bons moments passés avec vous au labo et en dehors, malgré les misères que vous me faisiez subir ;) (surtout Hanan…). Hanan, j'ai eu la chance de partager un passage crucial de ta vie étudiante, qui t'a conduite à l'obtention brillante d'une bourse de thèse. Désormais, ton avenir dans la recherche nous amènera à se

revoir, et c'est tant mieux, j'ai quelques revanches à tenir ! Théo, j'ai beaucoup apprécié le temps passé avec toi au labo, et je te souhaite le meilleur pour le futur.

Nazim, tu auras été le premier étudiant de M1 que j'ai pu encadrer, et tu resteras certainement l'un des meilleurs qu'il me sera donné de connaître. J'ai beaucoup apprécié ton esprit brillant et ta soif de connaissance, ce qui est d'ailleurs reconnu car tu vas débuter une thèse qui s'annonce extraordinaire. Bonne chance, bon courage, et surtout à très bientôt, peut-être en congrès !

Seb, j'ai vécu cette dernière année de thèse tambours battant, et heureusement que tu étais là pour m'aider à décompresser ! Tu n'es arrivé au labo que récemment, mais on a vite partagé de bonnes parties de rigolade (à en pleurer…). Tu représentes les valeurs qui me sont chères dans la recherche, un esprit brillant et humble, et je suis sûr que tu décrocheras la position que tu mérites tant !

Un grand merci aux nombreux autres étudiants, que j'ai moins eu la chance de connaître et côtoyer, mais avec qui j'ai pu partagé quelques instants, et en particulier Adeline, Marie-Solenne et Fannie, bon courage pour vos thèses respectives.

Egalement, je remercie toutes les personnes avec qui j'ai pu collaborer et qui m'ont toujours apporté leur aide et leur soutien.

En particulier, les collègues du laboratoire de Leuven, Tomasz, Hervé, Peter, Annicke, Hermann, Natalia, Bénédicte, Brechje, Clara, Anna, Lies, Justin, Benoît et les autres. A chacun de mes voyages à Leuven, je savais que j'allais me sentir bien en terre belge notamment grâce à vous.

Je remercie Madame le Docteur Françoise Muscatelli, ainsi que Anne et Fabienne, pour notre collaboration très intéressante sur les souris Necdin. Anne, je te souhaite une bonne soutenance de thèse, et bonne chance pour la suite !

Merci à Monsieur le Docteur Giuseppe Testa et à Thomas, pour avoir initié une collaboration avec nous sur l'histone déméthylase JMJD3, qui s'annonce très prometteuse.

Je tiens à adresser un remerciement spécial à mon ancien directeur de recherche Monsieur le Docteur Laurent Arsac, qui a encadré mes stages de recherche de M1 et de M2 dans le laboratoire RMSB (Résonnance Magnétique des Systèmes Biologiques) à Bordeaux, et qui m'a communiqué sa passion pour la Science. Merci Laurent de m'avoir permis mes premiers pas dans la recherche, ta simplicité mêlée à ton excellence scientifique sont pour moi un exemple à suivre. De plus, je tiens à te remercier de ne pas m'avoir tenu gré, et même de m'avoir encouragé dans ma volonté de faire ma thèse à Marseille sous la direction de Gérard Hilaire, malgré mon obtention d'une bourse de thèse à Bordeaux. Je remercie aussi Monsieur le Professeur Jean-Michel Franconi qui m'avait accueilli au sein de son laboratoire, le RMSB, et qui m'a toujours aidé et soutenu.

La thèse, c'est aussi la vie "hors labo", où les amis et la famille jouent un rôle fondamental. Je tiens à leur présenter un grand merci, car j'ai eu la chance d'être très bien entouré. Egalement, j'ai pu bénéficier de terrains de jeu fantastiques autour de Marseille, avec la mer Méditerranée (où il peut y avoir des vagues surfables, parfois, et où tous les surfeurs ne s'appellent pas Brice…), les calanques et leurs superbes falaises, les Alpes, paradis du ski de rando et de l'alpinisme, et où quelques beaux projets restent en attente…

Les amis :

Mes potes (et amis !) les "bobos", Seb et Aurélien, avec Rémi et Fred, nos traditionnels surftrips annuels sous l'égide de la "over roots hardcore surftrip association"

m’ont tellement fait du bien. Egalement, avec les "nouveaux", les Thou’s bros, on aura vraiment vécu ensemble des moments extraordinaires. Dans la continuité, merci à Meghan, Darina et Majo d’avoir apporté cette magnifique note multiculturelle à notre dernier trip au Mexique, un vrai melting pot de beauté et de joie ! Vivement les prochains, et merci pour ce superbe cadeau de thèse avec un surftrip au Portugal 3 jours après la soutenance ! A bientôt en Australie, pour un petit tour en Océanie… !

Je passe de la mer à la montagne, pour un grand merci à Jeff, avec qui on a partagé tant d’aventures en grimpe, en ski de rando et en alpinisme. Pour moi, tu es une référence en ce qui concerne l’importance du mental et de la volonté dans la réussite. Continue à semer tes mouchoirs de partout, et vivement nos prochaines escapades Alpines !

Marcoman, éminent membre de la team Mezoute, grâce à toi certains projets en ski de rando sont devenus réalisables (en tout cas, c’est mieux que le solo !). Vivement notre premier 5.1 ensemble ! Et vivement ce fameux GR20, prévu comme carotte de fin de thèse, et justement en mode "mezoute"…

Xavier, nous avons vécu des événements très durs et pénibles ensemble pendant cette thèse, qui nous ont rapprochés et dont on est sortis plus forts. J’y ai perdu certaines illusions, mais j’y ai gagné un ami. Tu seras le troisième larron du GR20, pour que l’on vive enfin des moments de bonheur ensemble, où tu pourras mettre en pratique ta théorie de "la douleur n’est qu’une information, libre à nous de l’écouter, ou pas !".

Un grand merci à mes autres amis proches, que je n’ai pas pu voir autant que souhaité, mais qui me soutenaient de loin, Claire, Jimmy, Guillaume, Chips, Cédric, Guilhem, et les autres.

Je remercie aussi Nico et Shanti, on se verra peut-être en Indo, et Ben et Gaëlle, bon courage pour cette nouvelle aventure que d’avoir un enfant ! Je n’oublie pas non plus les potes du rugby à la fac, qui m’auront permis de décompresser entre midi et 2 durant cette dernière année *via* des plaquages bien appuyés et de bonnes tranches de rigolade !

La famille :

Je remercie toute ma famille, mes grands-parents, oncles et tantes, cousins et cousines, qui m’ont soutenu et accompagné tout au long de cette thèse, notamment avec les repas traditionnels et gargantuesques des fêtes de fin d’année toujours aussi joyeuses en votre compagnie. Un remerciement spécial pour Philippe, qui a épluché mon manuscrit de thèse durant l’été à la recherche des fautes d’orthographe et des coquilles, l’ayant lu deux fois ! Quelle belle endurance de marathonien !

Je n’en serais pas là aujourd’hui sans mes parents, qui ont toujours eu confiance en moi, m’ont toujours encouragé, et surtout qui se sont toujours mis en 4 afin de soutenir mes projets, mes études etc. Maman et Papa, je vous dois tout, ce que je suis et ce que j’ai fait, merci infiniment.

Merci à mes sœurs, Meije, Tiphaine et Ondine, qui m’ont toujours accompagné, ont souvent joué le rôle de garde fou dans mes projets, et qui contribuent merveilleusement à maintenir une ambiance familiale chaleureuse. Après nous avoir régulièrement hébergés Murielle et moi à Toulon, à nous de vous héberger en Australie !

Enfin, merci à celle avec qui j’ai le bonheur de partager ma vie depuis plus de 5 ans, Murielle, "Doude", mon amour. Tu as choisi de me suivre à Marseille, et tu m’as tellement aidé et soutenu pendant ces trois dernières années, que je ne sais comme te rendre la pareille. Notre voyage "down under" s’annonce riche en aventures, en tout cas une magnifique occasion de consolider notre vie à 2 !

Pour terminer, merci à vous, qui avez eu le courage de lire ces remerciements jusqu’au bout, rendant hommage à toutes les personnes citées, et donc à ce travail de thèse !!

Publications et Communications

1 - Publications

1.1 - Articles à comité de lecture

Soumis à **J. Neurosci. : Menuet C.,** Borghgraef P., Voituron N., Gielis L., Gestreau C., Dutschmann M., Van Leuven F., Hilaire G.; *Isoflurane anaesthesia precipitates airway dysfunction and tauopathy in pre-symptomatic Tau.P391L mice.*

Soumis à **J. Physiol. (London) : Menuet C.,** Khemiri H., de la Poëze d'Harambure T., Gassmann M., Hilaire G., Gestreau C., Soliz J.; *Excessive erythrocytosis and high levels of erythropoietin in blood and brain blunt the hypercapnic ventilatory response in mice.*

Accepté dans **Plos One : Menuet C.*,** Cazals Y.*, Gestreau C., Borghgraef P., Gielis L., Dutschmann M., Van Leuven F., Hilaire G.; *Tauopathy alters ultrasonic vocalization in Tau.P301L mice: possible implication for declining language disorders* **- *ont contribué de manière égale.**

Menuet C., Borghgraef P., Matarazzo V., Gielis L., Lajard A.M., Voituron N., Gestreau C., Dutschmann M., Van Leuven F., Hilaire G. ; *Raphé tauopathy alters serotonin metabolism and breathing activity in terminal Tau.P301L mice: Possible implications for tauopathies and Alzheimer's disease.* **Resp. Physiol. Neurobiol.** 2011 Sep 15;178(2):290-303.

Menuet C., Kourdougli N., Hilaire G., Voituron N. ; *Differences in serotoninergic metabolism possibly contribute to différences in breathing phenotype of FVB/N and C57Bl/6J mice.* **J. Appl. Physiol.** 2011 Mar 17.

Voituron N., Shvarev Y., **Menuet C.,** Bevengut M., Fasano C., Vigneault E., El Mestikawy S., Hilaire G. ; *Fluoxetine treatment abolishes the in vitro respiratory response to acidosis in neonatal mice.* **Plos One** 2010 Oct 26;5(10):e13644.

Hilaire G., Voituron N., **Menuet C.**, Ichiyama R.M., Subramanian H.H., Dutschmann M. ; *The role of serotonin in respiratory function and dysfunction.* **Resp. Physiol. Neurobiol.** 2010 Nov 30;174(1-2):76-88.

Voituron N., **Menuet C.**, Dutschmann M., Hilaire G. ; *Physiological definition of upper airway obstruction in mouse model for Rett Syndrome.* **Resp. Physiol. Neurobiol.** 2010 Sep 30;173(2):146-56.

Voituron N., Zanella S., **Menuet C.,** Lajard A.M., Dutschmann M., Hilaire G. ; *Early abnormalities of post-sigh breathing pattern in a mouse model of Rett Syndrome*. **Resp. Physiol. Neurobiol.** 2010 Feb 28;170(2):173-82.

Dutschmann M.*, **Menuet C**.*, Stettner G.M.*, Gestreau C., Borghgraef P., Devijver H., Glies L., Hilaire G., Van Leuven F. ; *Upper airway dysfunction of Tau-P301L mice*

correlates with tauopathy in mid-brain and ponto-medullary brainstem nuclei. **J. Neurosci.** 2010 Feb 3;30(05):1810-21 **- *ont contribué de manière égale.**

Voituron N., Zanella S., **Menuet C**., Dutschmann M., Hilaire G. ; *Early breathing defects after moderate hypoxia or hypercapnia in a mouse model of Rett Syndrome*. **Resp. Physiol. Neurobiol.** 2009, Aug 31;168 (1-2):109-18.

Menuet C., Arsac L. ; *Muscle [Phosphocreatine] dynamics during exercise: implication for understanding the regulation of muscle oxidative metabolism*. **J. Physiol. (London)** 2008, Jul 1;586(13):3027-9.

1.2 - Actes de congrès

Voituron N., **Menuet C.**, Lajard A.M., Hilaire G. ; *Mecp2 and Breathing Symptoms in a Mouse Model of Rett Syndrome: On the trail of GABA involvement.* **Dev. Neurosci.** 2010, 8, vol 28, 691-692.

Menuet C., Dutschmann M., Stettner G.M., Gestrau C., Hilaire G., Van Leuven F. ; *Brainstem Tauopathy in Tau-P301L mice induces upper airway dysfunction: possible implication for Alzheimer disease.* **Fund. Clin. Pharmacol.** 2010, 24, 19-19.

2 - Communications orales

2.1 - Congrès Internationaux

Menuet C., Jaworski T., Dewachter I., Lechat B., Gielis L., Borghgraef P., Devijver H., Hilaire G., Van Leuven F. ; *GSK3 controls breathing activity, upper airway function and life span of Tau-P301L mice*. The 10th International Conference on Alzheimer's and Parkinson's Disease, 9 au 13 mars 2011, Barcelone, Espagne.

Menuet C., Voituron N., Kourdougli N., Borghgraef P., Gielis L., Devijver H., Van Leuven F., Hilaire G. ; *Isoflurane anesthesia of young Tau-P301L mice precipitates upper airway dysfunction*. Australian Neuroscience Society 31st annual meeting, 31 janvier au 3 février 2011, Auckland, Nouvelle Zélande.

Menuet C., Khemiri H., Gassmann M., Hilaire G., Gestreau C., Soliz J. ; *Blunted hypercapnic ventilatory response in transgenic mice overexpressing erythropoietin.* The VIII World Congress on High Altitude Medicine and Physiology, 8-12 août 2010, Arequipa, Pérou.

Menuet C., Dutschmann M., Stettner G.M., Gestreau C., Hilaire G., Van Leuven F. ; *Upper airway dysfunction and brainstem tauopathy in ageing Tau-P301L mice: possible implication for Alzheimer disease.* Australian Neuroscience Society 30th Annual Meeting / Australian Physiological Society 50th Anniversary Meeting (ANS/AuPS 2010), 31 janvier au 3 février 2010, Sydney, Australie.

2.2 - Congrès Nationaux

Menuet C., Hilaire G. ; *Upper airway dysfunction and brainstem Tauopathy in ageing Tau-P301L mice : possible implication for Alzheimer disease.* Colloque de l'Ecole Doctorale des Sciences de la Vie et de la Santé, Marseille, France, 31 mai au 1ier juin 2010.

Menuet C., Dutschmann M., Stettner G.M., Gestreau C., Hilaire G., Van Leuven F. ; *Brainstem Tauopathy in Tau-P301L mice induces upper airway dysfunction: possible implication for Alzheimer disease.* 5ème congrès de Physiologie, Pharmacologie et Thérapeutique (P2T), Bordeaux, 23-25 mars 2010.

Voituron N., Zanella S., **Menuet C.**, Lajard A.M., Quintin L., Dutschmann M., Hilaire G. ; *GABA deficits, early breathing abnormalities and late breathing symptoms in mouse model of Rett syndrome.* 5ème congrès de Physiologie, Pharmacologie et Thérapeutique (P2T), Bordeaux, 23-25 mars 2010.

Menuet C., Dutschmann M., Stettner G.M., Gestreau C., Hilaire G., Van Leuven F. ; *Tauopathie et dysfonctionnement des voies aériennes supérieurs chez la souris : implication possible pour la maladie d'Alzheimer.* Huitièmes journées scientifiques de l'IFR Jean Roche, Marseille/la Baume, Novembre 2009.

3 - Communications affichées

3.1 - Congrès Internationaux

Menuet C., Voituron N., Kourdougli N., Borghgraef P., Gielis L., Devijver H., Van Leuven F., Hilaire G. ; *Isoflurane anesthesia induces upper airway dysfunction in young Tau-P301L mice*. The 10th International Conference on Alzheimer's and Parkinson's Disease, 9 au 13 mars 2011, Barcelone, Espagne.

Borghgraef P., **Menuet C.**, Devijver H., Gielis L., Gijsen H., Moechars D., Hilaire G., Van Leuven F. ; *Inhibition of O-GlcNAcase mitigates motor and breathing defects and prolongs survival of Tau-P301L mice*. The 10th International Conference on Alzheimer's and Parkinson's Disease, 9 au 13 mars 2011, Barcelone, Espagne.

Voituron N., **Menuet C.**, Lajard A.M., Hilaire G. ; *Mecp2 and Breathing Symptoms in a Mouse Model of Rett Syndrome: On the trail of GABA involvement*. 18th Biennial Meeting of the International Society for developmental Neuroscience, Estoril, Portugal, 6-9 juin 2010.

Voituron N., Zanella S., **Menuet C**., Dutschmann M. Hilaire G. ; *Early breathing anomalies in a mouse model of Rett syndrome.* The 10th annual Rett syndrome symposium, Chicago, USA, Juin 2009.

Voituron N., Zanella S., **Menuet C.**, Dutschmann M. and Hilaire G. *Early alterations of respiratory regulations in a mouse model of Rett Syndrome.* International symposium on respiratory control, Saint-Maximin, France, Décembre 2008.

3.2 - Congrès Nationaux

Menuet C., Hilaire G. ; *Upper airway dysfunction and brainstem Tauopathy in ageing Tau-P301L mice : possible implication for Alzheimer disease.* Colloque de l'Ecole Doctorale des Sciences de la Vie et de la Santé, Marseille, France, 31 mai au 1ier juin 2010.

Menuet C., Dutschmann M., Stettner G.M., Gestreau C., Hilaire G., Van Leuven F. ; *Brainstem Tauopathy in Tau-P301L mice induces upper airway dysfunction: possible implication for Alzheimer disease.* 5ème congrès de Physiologie, Pharmacologie et Thérapeutique (P2T), Bordeaux, 23-25 mars 2010.

Voituron N., Zanella S., **Menuet C.**, Lajard A.M., Quintin L., Dutschmann M. et Hilaire G. ; *GABA, anomalies respiratoires pré-symptomatiques et symptômes respiratoires chez un modèle murin du Syndrome de Rett*. Huitièmes journées scientifiques de l'IFR Jean Roche, Marseille/la Baume, Novembre 2009.

4 - Prix

Prix étudiant, 10ème Colloque de la Société des Neurosciences, Marseille, 24 au 27 mai 2011.

Prix du meilleur poster, Colloque de l'Ecole Doctorale des Sciences de la Vie et de la Santé, Marseille, France, 31 mai au 1ier juin 2010.

Prix du meilleur poster, 5ème congrès de Physiologie, Pharmacologie et Thérapeutique (P2T), Bordeaux, 23-25 mars 2010.

Prix de communication orale, 8ième journées scientifiques de l'IFR Jean Roche, Marseille/la Baume, Novembre 2009.

Résumé

De nouveaux enjeux émergent dans le domaine de la Santé en raison du vieillissement de la population et du développement inquiétant de la Maladie d'Alzheimer (MA). Chez le sujet sain ou pathologique, peu d'études ont porté sur le vieillissement du contrôle nerveux de la respiration, en dépit de son rôle crucial pour l'oxygénation du cerveau. Cette thèse présente des recherches translationnelles, réalisées chez la souris, pour étudier le vieillissement physiologique et pathologique du contrôle nerveux de la respiration. Chez des souris transgéniques, modèles reconnus de la MA et du syndrome de Rett, nous décrivons le développement de neuropathologies respiratoires graves, conduisant à un décès prématuré. Nous montrons pour la première fois qu'une tauopathie du tronc cérébral altère le fonctionnement des voies aériennes supérieures, la vocalisation et la respiration. De plus, nos travaux suggèrent un rôle délétère de l'anesthésie pour la MA et identifient des pistes thérapeutiques nouvelles. En conclusion, nos travaux chez la souris peuvent avoir des retombées particulièrement intéressantes notamment pour la MA.

Summary

New issues are emerging in the field of Health care due to ageing of the population and the alarming development of Alzheimer's Disease (AD). In healthy or pathological living being, very few studies are dealing with the ageing of the respiratory nervous control, in spite of the crucial role of respiration for brain oxygenation. This thesis presents translational research performed in mice to examine the physiological and pathological ageing of the respiratory nervous control. In mice from two transgenic strains, recognized models for AD and Rett syndrome, we describe the development of drastic respiratory neuropathologies leading to premature death. In the AD mouse model, we show for the first time that brainstem tauopathy triggers dysfunctions of the upper airways, impairs vocalization and alters respiration and respiratory control. In addition, our work suggests a deleterious effect of anaesthesia for AD and identifies new therapeutic strategies. This mouse research could well contribute to significant improvements in AD care.

Sommaire

Présentation Générale de la Thèse ---- 3
Liste des abréviations ---- 7

INTRODUCTION ---- 11
Introduction générale : de l'oxygène à la respiration ---- 13
I - NEUROPHYSIOLOGIE DE L'ACTE MOTEUR RESPIRATOIRE DU MAMMIFERE ---- 17
1 - Modalités de décharges nerveuses respiratoires ---- 18
1.1 - L'inspiration (I) ---- 19
1.2 - La post-inspiration ou expiration précoce (E1) ---- 19
1.3 - L'expiration tardive (E2) ---- 20
2 - Sites de projection axonale et modalités de décharges des neurones respiratoires ---- 22
2.1 - Sites de projection axonale des neurones respiratoires ---- 22
2.2 - Modalités de décharges des neurones respiratoires ---- 23
3 - Anatomie du réseau respiratoire ---- 25
3.1 - Noyaux respiratoires pontiques ---- 26
3.1.1 - Le noyau de Kölliker-Fuse (KF) et le complexe parabrachial (LPB et MPB) ---- 28
3.1.2 - Les noyaux noradrénergiques A5 et A6 ---- 28
3.2 - Noyaux respiratoires bulbaires ---- 29
3.2.1 - Le groupe respiratoire parafacial (pFRG) ---- 30
3.2.2 - Le noyau rétrotrapézoïde (RTN) ---- 30
3.2.3 - Le complexe de Bötzinger ---- 31
3.2.4 - Le complexe de PréBötzinger ---- 31
3.2.5 - Les noyaux ambigu et para-ambigu ---- 32
3.2.6 - Le groupe respiratoire ventral ---- 32
3.2.7 - Le noyau du faisceau solitaire et le groupe respiratoire dorsal ---- 32
II - DEVELOPPEMENT ET MATURATION DE LA COMMANDE RESPIRATOIRE ---- 35
1 - Embryogenèse d'oscillateurs couplés et respiration prénatale ---- 35
1.1 - Naissance du groupe respiratoire parafacial embryonnaire et du noyau de PréBötzinger, ou la recherche du « Nœud Vital » ---- 36
1.2 - Un « nœud vital » isolé suffisant pour générer du "gasp", mais pas de l'eupnée ---- 38
1.3 - Vers une conciliation entre les deux grandes écoles de la rythmogenèse respiratoire ? ---- 40
2 - Maturation postnatale et "apprentissage" respiratoire ---- 42
2.1 - Maturation postnatale du système respiratoire ---- 42
2.2 - La post-inspiration, une phase cruciale du cycle respiratoire sous le contrôle du « centre pneumotaxique » ---- 43
3 - Le Syndrome de Rett, une pathologie neurodéveloppementale qui altère la respiration ---- 46
3.1 - Signes cliniques du syndrome de Rett et mutations du gène *MECP2* ---- 46
3.2 - Syndrome de Rett et troubles respiratoires ---- 48
III - REGULATIONS ET PLASTICITE RESPIRATOIRES ---- 51
1 - Les bioamines, modulateurs privilégiés de la respiration ---- 51
1.1 - Les catécholamines ---- 51
1.2 - La sérotonine ---- 53
1.2.1 - Métabolisme de la 5-HT ---- 53
1.2.2 - Anatomie du réseau sérotoninergique ---- 54
1.2.3 - Influence de la 5-HT sur le CPG respiratoire ---- 56
1.2.4 - Sérotonine et perspectives ---- 58
2 - Chémosensibilité, réponses respiratoires à l'hypoxie et à l'hypercapnie, et réflexe de Hering-Breuer ---- 59
2.1 - Sensibilité périphérique à l'O_2, au CO_2 et au pH ---- 60
2.2 - Sensibilité centrale à l'O_2, au CO_2 et au pH ---- 63
2.2.1 - Sensibilité centrale à l'O_2 ---- 63
2.2.2 - Sensibilité centrale au pH et au CO_2 ---- 65
2.3 - Erythropoïétine et réponse ventilatoire à l'hypoxie ---- 70
2.4 - Récepteurs à l'étirement pulmonaire et réflexe de Hering-Breuer ---- 72
3 - L'eupnée : physiologie d'un patron moteur indispensable à la plasticité fonctionnelle du réseau respiratoire ---- 74
3.1 - Plasticité fonctionnelle du réseau respiratoire ---- 75

3.2 - Un cas particulier, la vocalisation ---- 76
IV - PHYSIO/PATHOLOGIE DU VIEILLISSEMENT ET RESPIRATION ---- 83
1 - Théories du vieillissement ---- *83*
2 - Vieillissement du système respiratoire ---- *84*
2.1 - Vieillissement de la pompe ventilatoire, poumons et cage thoracique ---- 84
2.2 - Vieillissement de la valve respiratoire, les voies aériennes supérieures ---- 86
2.3 - Vieillissement de la chémosensibilité ---- 88
3 - Protéine tau et tauopathies ---- *90*
3.1 - La protéine tau ---- 90
3.1.1 - Biochimie de la protéine tau ---- 90
3.1.2 - Fonctions de la protéine tau ---- 92
3.2 - Les tauopathies ---- 94
3.2.1 - La maladie d'Alzheimer ---- 94
3.2.1.1 - Les plaques ß-amyloïdes ---- 95
3.2.1.2 - La neurodégénérescence induite par tau ---- 97
3.2.2 - La démence frontotemporale et les autres tauopathies ---- 104
3.3 - Structures et fonctions neurovégétatives dans la tauopathie ---- 106

RESULTATS ---- 109
I - SYNDROME DE RETT ET TROUBLES RESPIRATOIRES, ETUDES CHEZ LA SOURIS *MECP2*$^{-/y}$ ---- 111
1 - Défauts respiratoires précoces après une hypoxie ou une hypercapnie modérée chez un modèle murin du Syndrome de Rett ---- *113*
2 - Anormalités précoces de la respiration post-soupir chez un modèle murin du Syndrome de Rett ---- *125*
3 - Définition physiologique de l'obstruction des voies aériennes supérieures chez un modèle murin du Syndrome de Rett ---- *137*
II - ETUDES DES REGULATIONS RESPIRATOIRES INDUITES PAR LE CO_2 ET LA SEROTONINE ---- 151
1 - Les différences de métabolisme sérotoninergique contribuent potentiellement aux différences de phénotype respiratoire des souris FVB/N et C57Bl/6J ---- *153*
2 - Le rôle de la sérotonine dans la fonction et la dysfonction respiratoires ---- *165*
3 - Le traitement à la fluoxétine abolit la réponse respiratoire à l'acidose in vitro chez la souris nouveau-née ---- *179*
4 - L'érythrocytose excessive et des hauts niveaux d'érythropoïétine dans le sang et dans le cerveau diminuent la réponse ventilatoire à l'hypercapnie chez la souris ---- *189*
III - TAUOPATHIE ET TROUBLES RESPIRATOIRES, ETUDES CHEZ LES SOURIS TAU-P301L ---- 233
1 - La dysfonction des voies aériennes supérieures des souris Tau-P301L corrèle avec la tauopathie dans les noyaux mésencéphaliques et ponto-bulbaires du tronc cérébral ---- *235*
2 - La tauopathie dans les raphés altère le métabolisme de la sérotonine et l'activité respiratoire chez les souris Tau-P301L terminales : implications potentielles pour les tauopathies et la maladie d'Alzheimer ---- *249*
3 - Altérations liées à l'âge de la vocalisation ultrasonore des souris Tau-P301L : implication potentielle pour les troubles progressifs du langage ---- *265*
4 - L'anesthésie à l'isoflurane précipite la tauopathie et les dysfonctions des voies aériennes supérieures chez les souris Tau-P301L pré-symptomatiques ---- *297*

DISCUSSION ---- 325
I - SYNTHESE DES RESULTATS PRESENTES DANS CETTE THESE ---- 327
II - INFLUENCE DU GENOTYPE SUR LE CONTROLE CENTRAL RESPIRATOIRE ET EN PARTICULIER SUR LA COMMANDE DES VAS ---- 331
III - LE VIEILLISSEMENT DU CONTROLE RESPIRATOIRE ET EN PARTICULIER DES VAS, DE LA MATURATION A LA SENESCENCE ---- 335
IV - L'INFLUENCE DES REGULATIONS RESPIRATOIRES ---- 339
1 - Sérotonine et tauopathie ---- *339*
2 - Implications du tonus excitateur hypercapnique ---- *341*
V - CONCLUSION ET PERSPECTIVES ---- 345

BIBLIOGRAPHIE ---- 347

Présentation Générale de la Thèse

Le travail de recherche présenté dans cette thèse concerne le contrôle nerveux de la respiration. Réalisé chez la souris ("sauvage" ou transgénique) *via* des approches multiples (génétiques, physiologiques, électrophysiologiques, biochimiques et immunohistochimiques), ce travail souligne l'importance des facteurs génétiques, maturationnels, environnementaux et liés au vieillissement dans la physiopathologie respiratoire.

Chez le mammifère, la respiration est, dès la naissance, indispensable à l'oxygénation du sang au niveau pulmonaire et donc à la survie. Le bon déroulement de l'acte respiratoire nécessite la contraction **rythmique et coordonnée** de plus d'une centaine de muscles, d'une part ceux de la cage thoracique pour provoquer les entrées / sorties d'air, et d'autre part ceux des voies aériennes supérieures (VAS) pour en contrôler le débit. De plus, l'amplitude et la fréquence de ces contractions musculaires doivent être en permanence **régulées et ajustées** aux conditions environnementales (teneur en CO_2 ou en O_2, altitude, température, etc.) et comportementales (sommeil, repos, stress, activité physique intense, etc.). Le réseau nerveux impliqué dans la rythmogenèse respiratoire et ses régulations doit donc impérativement se développer correctement pendant la période prénatale, mais aussi atteindre sa maturité postnatale et vieillir dans des conditions optimales, afin de maintenir l'homéostasie gazeuse sanguine durant toute la vie. Dans le chapitre « Introduction » de cette thèse, un état de l'art fait le point sur l'organisation du réseau nerveux respiratoire, sa maturation périnatale, ses principales régulations et plasticités, et enfin son vieillissement.

Au cours des deux dernières décennies, de nombreuses recherches ont concerné la rythmogenèse respiratoire chez le rongeur nouveau-né, en raison d'une part des problèmes posés par la Mort Subite du Nourrisson (0,5 cas pour 1000 naissances), et d'autre part des avantages offerts par de nouvelles approches *in vitro* qui facilitent l'étude du réseau néonatal du rongeur. Le contrôle nerveux des VAS a par contre bénéficié de moins d'intérêt. Pourtant, un dysfonctionnement des VAS peut conduire à diverses situations pathologiques graves. En premier lieu, les apnées obstructives : les muscles de la cage thoracique continuent à être actifs de façon rythmique mais un dysfonctionnement des VAS réduit, voire annule, le flux aérien et donc le renouvellement de l'oxygénation sanguine. Pendant le sommeil, des apnées obstructives trop fréquentes peuvent altérer l'oxygénation de tout l'organisme et notamment

du cerveau et du muscle cardiaque, et induire les symptômes caractéristiques du syndrome des apnées obstructives du sommeil (AOS) : fatigue dès l'éveil, perte de mémoire, endormissement diurne incontrôlable, problèmes cardio-vasculaires, etc. A des niveaux de gravité différents, les AOS concernent 2-3 % de la population mondiale (environ 200 millions de personnes), principalement les personnes âgées. D'autre part, les VAS constituent un carrefour anatomique pour des fonctions autres que la respiration telles la vocalisation, la déglutition, la toux, etc. Des dysfonctionnements des VAS peuvent avoir de nombreuses répercussions et contribuer aux déficits phonatoires, ou aux dysphagies comme les « fausses routes » récurrentes et pneumopathies associées qui surviennent fréquemment chez les personnes âgées, notamment celles souffrant de la maladie d'Alzheimer. La fréquence des AOS, l'évolution de la pyramide des âges et l'augmentation considérable du nombre de patients atteints par la maladie d'Alzheimer pourraient donc, dans les années à venir, susciter un regain d'intérêt pour l'étude des VAS et en faire un axe de recherche majeur.

Dans le chapitre « Résultats » de cette thèse, onze mémoires (huit publiés, deux soumis et un en préparation) apportent des informations nouvelles sur le contrôle nerveux de la respiration et des VAS, son vieillissement physiologique et pathologique, et l'influence complexe notamment du CO_2 et de la sérotonine (5-HT) pour la régulation respiratoire. Indubitablement, un point fort de cette thèse est la démonstration que des dysfonctionnements des VAS se développent avec l'âge chez des souris transgéniques qui sont des modèles reconnus de neuropathologies graves, d'une part le syndrome de Rett, une maladie neurodéveloppementale rare, et d'autre part les tauopathies neurodégénératives, dont la maladie d'Alzheimer est une des plus connues. Chez les souris « modèle Alzheimer », nous décrivons pour la première fois une altération avec l'âge des VAS et montrons qu'elle s'accompagne d'une atteinte de la phonation, ce qui n'est pas sans rappeler les troubles de la respiration et du langage que développent les patients atteints par la maladie d'Alzheimer. De plus, nous montrons qu'une anesthésie pendant la période pré-symptomatique induit prématurément non seulement une tauopathie des structures nerveuses contrôlant les VAS, mais altère également le fonctionnement des VAS chez ces jeunes souris « modèle Alzheimer ». Ce résultat conforte la prudence recommandée depuis peu par un consortium biomédical quant à l'anesthésie des patients âgés, qui pourrait avoir des effets néfastes pouvant aller jusqu'au déclenchement de la maladie d'Alzheimer. Finalement, nous identifions, chez la souris « modèle Alzheimer », des protocoles d'anesthésie moins à risque et des pistes thérapeutiques nouvelles.

A côté de ces résultats pionniers, d'autres ont été obtenus sur le rôle complexe de la sérotonine (5-HT) dans la régulation respiratoire, ainsi que sur celui de l'érythropoïétine (EPO). Nos résultats et un état de l'art (revue) rédigé en collaboration avec d'autres collègues mettent en exergue le rôle de la 5-HT dans les fonctionnements / dysfonctionnements du réseau respiratoire. D'une part, en comparant des souris "sauvages" provenant de deux souches génétiques différentes, nous suggérons que ces facteurs génétiques peuvent induire des spécificités du système 5-HT qui vont conférer au système respiratoire des différences phénotypiques, discernables avant même la naissance, et qui vont persister jusqu'à la vieillesse. D'autre part, nos résultats suggèrent que la prise de certains médicaments susceptibles d'altérer le système 5-HT de la mère pendant la gestation, peuvent affecter les réponses respiratoires du nouveau-né au CO_2, et contribuer à des troubles respiratoires facilitant la Mort Subite du Nourrisson. De plus, nous montrons que la tauopathie altère tardivement le métabolisme de la 5-HT des souris « modèle Alzheimer », ce qui induit des troubles respiratoires accrus peu de temps avant le décès. Ces résultats, mis en parallèle avec ceux obtenus précédemment chez la souris « modèle syndrome de Rett », révèlent que des altérations du système 5-HT peuvent contribuer à des déficits respiratoires létaux. Enfin, la 5-HT intervenant dans le sommeil, un lien pourrait exister entre dysfonctionnements 5-HT, dysfonctionnement des VAS et syndrome des AOS. La réponse ventilatoire à l'hypercapnie (RVHC) étant également un fil directeur de cette thèse, nous montrons que l'EPO désensibilise la RVHC par une action directe centrale et périphérique, et par une action indirecte *via* l'érythropoïèse qu'elle induit. Ces résultats sont d'une grande importance pour la compréhension des mécanismes menant au « mal chronique des montagnes ».

Finalement, un chapitre « Discussion générale » fait la synthèse de l'ensemble des résultats présentés dans cette thèse, en soulignant l'importance des facteurs génétiques dans la détermination du phénotype respiratoire, le rôle de la 5-HT et du gaz carbonique dans le contrôle nerveux respiratoire en général et dans celui des VAS en particulier, et en insistant sur divers aspects du vieillissement.

En conclusion, nos recherches chez la souris, "sauvage" ou transgénique, peuvent contribuer à l'amélioration de la compréhension des mécanismes nerveux permettant d'équilibrer l'apport en oxygène à l'organisme, ce qui est crucial pour son fonctionnement et sa survie. Nos recherches peuvent également avoir des retombées intéressantes dans le domaine de la santé, et particulièrement dans le cadre du vieillissement physiologique et pathologique du contrôle nerveux respiratoire. Finalement, il est très probable que nos

recherches sur le réseau nerveux qui élabore et régule la respiration, une activité motrice complexe mais relativement facile à enregistrer chez l'animal *in vivo*, puissent permettre de progresser dans la compréhension d'autres réseaux nerveux, plus difficiles à étudier, comme ceux liés à la cognition.

Liste des abréviations

5-HIAA	Acide 5-hydroxyindole acétique
5-HT	5-hydroxytryptamine
5-HTP	5-hydroxytryptophane
8-OH-DPAT	8-hydroxy-2-(di-n-propylamino)tetralin
V	Nerf trijumeau
VII	Nerf facial
IX	Nerf glossopharyngien
X	Nerf vague
XII	Nerf hypoglosse
Aß	ß-amyloïde
AMPK	Protéine kinase activée par l'adénosine monophosphate
APP	Protéine précurseur de l'amyloïde
ASIC	Canaux ioniques sensibles à l'acide
ATP	Adénosine triphosphate
"Aug"	Croissant
BACE-1	Enzyme 1 clivant l'APP sur son site bêta
BDNF	Facteur neurotrophique dérivé du cerveau
BötC	Complexe de Bötzinger
CC	Corps carotidiens
CCHS	Syndrome d'hypoventilation chronique congénitale
CDK5	Cyclin-dépendante kinase 5
CO_2	Dioxyde de carbone
"Con"	Constant
CPG	Générateur de patron moteur
CVR	Colonne ventrale respiratoire
DA	Dopamine
"Dec"	Décroissant
DFT	Démence frontotemporale
DHEA	Dehydroepiandrostérone
DLH	Acide DL-homocysteic

E	Jour embryonnaire
E1	Post-inspiration
E2	Expiration tardive
"Early"	Précoce
e-pF	Forme embryonnaire du RTN/pFRG
EPO	Erythropoïétine
GABA	Acide γ-aminobutyrique
GRD	Groupe respiratoire dorsal
GRP	Groupe respiratoire pontique
GRV	Groupe respiratoire ventral
GRVc	Groupe respiratoire ventral caudal
GRVr	Groupe respiratoire ventral rostral
GSK3ß	Glycogène synthase kinase 3 ß
HIF-1	Facteur induit par l'hypoxie 1
I	Inspiration
Iß	Cellules inspiratoires-ß
I_{ca}	Courant calcique
I_{CAN}	Courants cationiques non-spécifiques indépendants du voltage activés par le calcium
IGF	Facteur de croissance ressemblant à l'insuline
I_{NaP}	Courant produit par les canaux sodiques persistants
KF	Noyau de Kölliker-Fuse
Kir	Canaux potassiques rectifiants entrants
"Late"	Tardif
LC	Locus Cœruleus
L-DOPA	Dihydroxyphénylalanine
LPB	Noyau parabrachial latéral
LTF	Facilitation à long terme
MA	Maladie d'Alzheimer
MAOA	Monoamine oxydase A
MARK	Kinase régulant l'affinité des microtubules
MeCP2	Protéine 2 liée au méthyl-CpG
MPB	Noyau parabrachial médian
NA	Noyau ambigu

NADPH	Nicotinamide adénine dinucléotide phosphate
NK1	Neurokinine 1
NMDA	N-méthyl-D-aspartate
NMDARs	Récepteurs au NMDA
NO	Monoxyde d'azote
NRA	Noyau rétro-ambigu
NTS	Noyau du faisceau solitaire
O_2	Dioxygène
O-Glc-NAcylation	ß-N-acétylglucosamination O-liée
P	Jour post-natal
$PaCO_2$	Pression partielle artérielle en dioxyde de carbone
PAG	Substance grise périaqueducale
PaO_2	Pression partielle artérielle en dioxygène
PB	Complexe parabrachial
P-cells	Cellules "pompes"
pFRG	Groupe respiratoire parafacial
PP	Phosphatase protéique
PréBötC	Complexe de PréBötzinger
PSD95	Protéine de densité post-synaptique 95
pVHL	Protéine de Von Hippel-Lindau
RARs	Récepteurs à l'étirement pulmonaire à adaptation rapide
RRG	Réseau générateur du rythme respiratoire
RTN	Noyau rétrotrapézoïde
RVCH	Réponse ventilatoire à l'hypercapnie
RVH	Réponse ventilatoire à l'hypoxie
SARs	Récepteurs à l'étirement pulmonaire à adaptation lente
SERT	Transporteur membranaire de la 5-HT
SIDS	Syndrome de mort subite du nourrisson
SNC	Système nerveux central
SR	Syndrome de Rett
TASK	Canaux potassiques sensibles à l'acide TWIK-reliés
TH	Tyrosine hydroxylase
Tph	L-tryptophane hydroxylase
TTX	Tétrodotoxine

VAS	Voies aériennes supérieures
VEGF	Facteur de croissance vasculaire endothélial
Vglut2	Transporteur vésiculaire du glutamate de type 2
Vmat2	Transporteur vésiculaire des monoamines 2
WHBP	Préparation *in situ* cœur/tronc cérébral isolés perfusés

Introduction

Introduction générale : de l'oxygène à la respiration

La vie avec oxygène a débuté il y a environ 2,5 milliards d'années avec l'apparition d'organismes capables de transformer l'énergie solaire en énergie chimique de liaisons carbonées. Dans ce processus de photosynthèse, du dioxyde de carbone (CO_2) et de l'eau sont convertis en glucose, du dioxygène (O_2) étant également généré dans la réaction. Les organismes photosynthétiques ont prospéré et se sont multipliés, augmentant progressivement les concentrations en O_2 atmosphérique. Il y a environ 1,5 milliard d'années les organismes eucaryotes sont apparus, contenant des mitochondries, bactéries endosymbiotiques devenues organites subcellulaires dans lesquelles le pyruvate issu de la glycolyse est oxydé en CO_2 et eau, refermant ainsi le cycle énergétique (Wallin, 1926). Des équivalents réduits sont générés, qui vont céder des électrons à la chaîne respiratoire mitochondriale. Il en résulte la formation d'un gradient électrochimique de protons servant à resynthétiser l'adénosine triphosphate (ATP), dont l'hydrolyse est le principal vecteur énergétique des êtres vivants. La phosphorylation oxydative produit 18 fois plus d'ATP par mole de glucose que la glycolyse. Elle fournit ainsi l'énergie nécessaire au développement et au maintien d'organismes multicellulaires complexes. Les organismes métazoaires seraient apparus il y a environ 0,5 milliard d'années (Semenza, 2007). L'O_2 a donc permis l'évolution et le développement des organismes vivants via la respiration cellulaire.

Avec la complexification des organismes via la pluricellularité, la différenciation cellulaire et notamment l'apparition des cellules épithéliales, l'apport de l'O_2 aux cellules est devenu plus difficile avec des cloisonnements membranaires à franchir (Alberts et al., 2002). Ainsi les premiers organismes complexes sont apparus en milieu aquatique, avec un apport en O_2 par voie transcutanée, une deuxième forme de respiration. Il semble également que le système circulatoire, permettant un apport en O_2 plus efficace que par simple diffusion aux différents tissus de l'organisme, se soit mis en place de façon couplée au système nutritionnel car les premières branchies servaient à capter les nutriments dans l'eau par filtration (Farmer, 1999). Le sang fixait ainsi l'O_2 et relarguait le CO_2 au niveau cutané, tout en étant vecteur direct de nutriments *via* les branchies. Ce système définissait une condition adéquate pour l'apparition de nouvelles niches évolutives. Les branchies ont ensuite perdu leur fonction nutritionnelle et sont devenues les sites principaux d'échanges gazeux, la pompe buccale leur

assurant un mouvement unidirectionnel d'eau : c'est l'apparition du premier réseau générateur de rythme respiratoire (RRG) (Kinkead, 2009). Il y a plus de 400 millions d'années, les premiers poumons sont apparus dans le grade « poisson » (Roux, 2002). Une forte pression sélective en faveur d'un double organe respiratoire pulmonaire/branchial (respiration aérienne/aquatique) aurait existé au silurien (période de l'apparition des poumons), notamment à cause de la très faible teneur en O_2 des eaux stagnantes et/ou en faveur d'un apport direct d'O_2 au cœur (la respiration branchiale ne fait parvenir l'O_2 au cœur qu'après perfusion des tissus). Chez les poissons, cette pression sélective s'est inversée par la suite en raison des prédateurs aériens. Par contre la respiration aérienne pulmonaire s'est maintenue avec l'apparition des tétrapodes, premiers organismes passant du milieu aquatique au milieu terrestre, il y a environ 300 millions d'années. De ces tétrapodes descendent directement les amniotes, puis les mammifères.

Un fait évolutif marquant est le passage du couplage buccal entre acte moteur respiratoire et acte moteur nutritionnel chez les tétrapodes, à son découplage chez les amniotes. Les amphibiens, notamment étudiés pour leur similitude potentielle avec les tétrapodes, possèdent une ventilation buccale fonctionnant par surpression : l'air aspiré par la bouche est poussé dans les poumons par compression de la cavité buccale (Roux, 2002). Cette ventilation, très coûteuse en énergie, ne participe d'ailleurs pas à la totalité des échanges gazeux car les amphibiens possèdent une respiration cutanée importante et des échanges gazeux au niveau lingual. Chez les amniotes puis les mammifères, le passage à une respiration par dépression, selon le principe d'une pompe aspirante, a permis un gain énergétique considérable, tout en enlevant à la cavité buccale son rôle de pompe respiratoire (Roux, 2002). La commande nerveuse centrale de la pompe respiratoire qui transitait chez les amphibiens par les nerfs crâniens trijumeaux (V) et faciaux (VII) pour la pompe buccale et via les nerfs glossopharyngiens (IX) et vagues (X) pour la stabilisation des arches pharyngiennes, passe chez les amniotes par les nerfs spinaux phréniques et intercostaux (Kinkead, 2009). Cette dissociation entre la pompe respiratoire (qui devient thoracique) et la cavité buccale (qui ne sert plus qu'à l'acte nutritionnel) a conduit à l'émergence du carrefour oropharyngien. Ainsi, une commande nerveuse respiratoire est toujours transmise par les nerfs trijumeaux, vagues et hypoglosses (XII) chez les mammifères, mais aux voies aériennes supérieures (VAS) et pas à la pompe respiratoire. Les VAS deviennent alors le site d'une coordination cruciale entre actes moteurs de la respiration, de la déglutition ou encore de la vocalisation. C'est donc grâce à une dissociation entre une pompe respiratoire thoracique et

une valve oropharyngienne, que les mammifères ont acquis un système ventilatoire à la fois énergétiquement efficace et fonctionnellement plastique, permettant une grande variété de comportements moteurs. Dans cette optique, l'importance des VAS démontre à elle seule la nécessité d'appréhender l'acte respiratoire comme une entité physiologique complète, tant dans la **genèse** du rythme et du patron moteur que dans ses **régulations** et ses **interactions** avec d'autres comportements moteurs associés, et ce, que ce soit dans le cadre de sa **maturation** ou de son **vieillissement** physiologique ou pathologique.

Dans cette thèse, nous nous sommes intéressés à la neurophysiologie de l'acte moteur respiratoire du mammifère dans toute sa complexité phénotypique. En effet, nous avons appréhendé différents aspects fondamentaux de la régulation, de la maturation et du vieillissement des générateurs de rythme et de patron moteur respiratoire (CPG) chez la souris, en donnant une importance particulière à la coordination des VAS, afin de mieux cerner leur atteinte éventuelle dans deux pathologies, neurodéveloppementale et neurodégénérative : le Syndrome de Rett et les tauopathies (dont fait partie la Maladie d'Alzheimer), respectivement. C'est incontestablement dans le domaine des tauopathies et de la Maladie d'Alzheimer que cette thèse s'inscrit préférentiellement, apportant des données nouvelles sur l'atteinte pathologique des VAS chez un modèle animal reconnu.

L'objet de cette introduction de thèse sera d'accompagner le lecteur à travers la complexité de la neurophysiologie respiratoire, en essayant d'une part de faire objectivement le point des connaissances scientifiques actuelles, et d'autre part de situer les travaux de recherche de cette thèse parmi les différentes problématiques abordées. A cet effet, des « *nota bene »* seront imprimés en italique afin de souligner ponctuellement l'adéquation de cette thèse avec les grandes questions posées par la neurophysiologie respiratoire.

I - Neurophysiologie de l'acte moteur respiratoire du mammifère

Le mammifère possède une ventilation pulmonaire très efficace énergétiquement, car fonctionnant par dépression. En effet, lors de l'expansion de la cavité thoracique par contraction combinée du diaphragme et des muscles intercostaux externes, une dépression intra-pulmonaire aspire l'air extérieur venant de l'arbre trachéo-bronchique (cf. figure 1). Cette pompe respiratoire doit être coordonnée avec les VAS, qui jouent le rôle de valve par rétrécissement/élargissement de la lumière pharyngo-laryngienne, régulant ainsi le flux d'air parvenant aux poumons. Toute l'efficacité de la ventilation alvéolaire dépend donc de la contraction coordonnée des muscles de la pompe ventilatoire et de la valve (cf. figures 1 et 2).

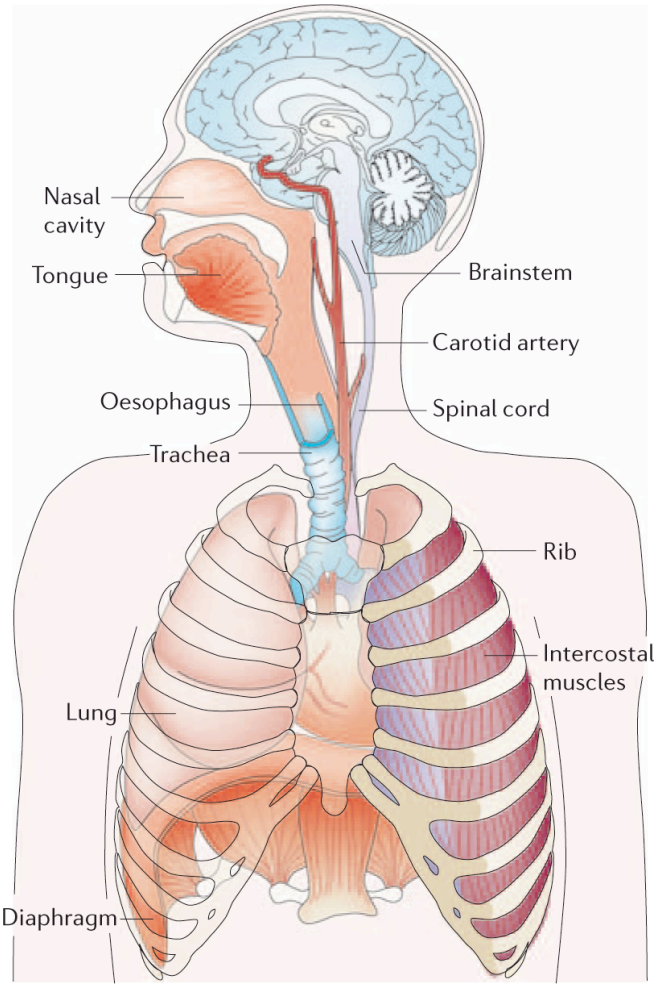

Figure 1 : anatomie générale de l'appareil respiratoire (*adapté de Feldman and Del Negro 2006*).

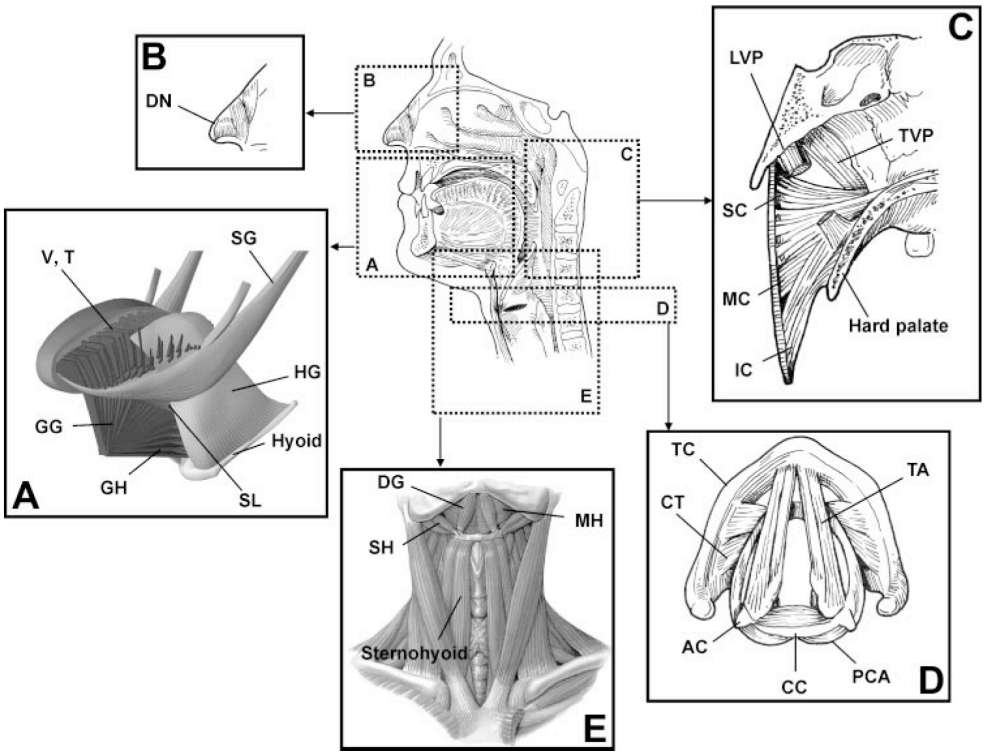

Figure 2 : muscles des voies aériennes supérieures, arrangés en régions anatomiques (rectangles) où le muscle exerce son effet mécanique principal. A : muscles extrinsèques (génioglosse (GG), styloglosse (SG), hyoglosse (HG)), et intrinsèques (verticalis (V), transversus (T), longitudinalis supérieur (SL)) de la langue ; géniohyoïdien (GH). B : muscles du vestibule nasal : dilatateur des narines (DN). C : muscles du voile du palais (levator veli palatini (LVP), tensor veli palatini (TVP)) et du pharynx (constricteur supérieur (SC), constricteur moyen (MC), constricteur inférieur (IC)). D : muscles du larynx : cricothyroïdien (CT), thyroaryténoïdien (TA), cricoaryténoïdien postérieur (PCA), cartilage aryténoïdien (AC), cartilage cricoïdien (CC), cartilage thyroïdien (TC). E : muscles de l'arche hyoïdienne : stylohyoïdien (ST), mylohyoïdien (MH), digastrique (DG). (*Adapté de Bailey and Fregosi 2006*).

1 - Modalités de décharges nerveuses respiratoires

La coordination pompe ventilatoire / valve est effectuée par une innervation complexe à la fois crânienne et cervicale, selon un cycle en trois étapes : inspiration (I), post-inspiration (ou expiration précoce, E1) et expiration tardive (E2) (cf. figure 3) (Richter, 1982).

1.1 - L'inspiration (I)

Le diaphragme, principal muscle inspiratoire de la pompe respiratoire, reçoit son innervation des nerfs phréniques dont les corps cellulaires se trouvent dans la moelle épinière, au niveau du quatrième espace cervical. Le patron de décharge du nerf phrénique est dit en « rampe », avec une augmentation progressive de l'énergie de la décharge au cours de la phase inspiratoire (cf. figure 3 D), ce qui est nécessaire pour lutter contre les résistances à l'expansion de la cage thoracique, croissantes au cours de l'inspiration. Les muscles intercostaux externes participent également à l'inspiration, dans une moindre mesure lors de la ventilation de repos, et de façon plus importante lorsque l'effort ventilatoire est augmenté comme lors d'un exercice physique. Les muscles intercostaux reçoivent leur innervation des motoneurons intercostaux, dont les corps cellulaires se trouvent dans la partie thoracique de la moelle épinière. Enfin, d'autres muscles, dits accessoires, peuvent intervenir dans l'inspiration forcée, comme le sterno-cléido-mastoïdien.

Pendant la phase inspiratoire, il est important que le diamètre de la lumière pharyngo-laryngienne soit maximal afin de limiter l'énergie dépensée par les muscles de la pompe ventilatoire. Pour maintenir ouvertes les VAS, il y a une protrusion de la langue principalement par contraction du muscle génioglosse, dont la commande passe par le nerf hypoglosse (XII), une abduction du pharynx dont la commande passe par le nerf glossopharyngien (IX), et surtout une ouverture de la glotte dont la commande passe par le nerf laryngé récurrent issu du nerf vague (X) (cf. figure 3 C). Cette commande d'ouverture des VAS, véhiculée par des nerfs crâniens, est cruciale, son altération pouvant mener à l'une des principales pathologies de la commande centrale respiratoire : les apnées obstructives du sommeil.

1.2 - La post-inspiration ou expiration précoce (E1)

Cette phase, souvent négligée, est pourtant d'une importance primordiale pour le comportement respiratoire et les activités qui y sont associées. En effet, elle est le lieu principal d'expression de comportements moteurs nécessitant un ajustement respiratoire tels la vocalisation, la déglutition, la toux ou encore le vomissement, son dysfonctionnement pouvant donc avoir des conséquences particulièrement néfastes (Gestreau et al., 1996, 2000, 2005; Roda et al., 2002; Bautista et al., 2010).

La post-inspiration est caractérisée par un relâchement des muscles inspiratoires de la pompe respiratoire, et une adduction du larynx.

Au niveau de la pompe ventilatoire, il peut persister une activité résiduelle post-inspiratoire sur le nerf phrénique (cf. figure 3 D), particulièrement chez les gros mammifères comme le chat, mais moindre chez les plus petits mammifères comme la souris (Paton, 1996a). Cette « queue » post-inspiratoire, en référence à sa forme, permettrait d'éviter un retour brutal à l'état de repos du diaphragme, susceptible d'induire un collapsus alvéolaire.

Au niveau de la valve, la post-inspiration se caractérise principalement par une adduction partielle des cordes vocales, induite par une décharge décroissante du nerf laryngé récurrent (cf. figure 3 C) qui commande la contraction des muscles latéraux cricoaryténoïdes, thyroaryténoïdes et interaryténoïdes. Cette adduction provoque une légère pression positive expiratoire contribuant également à éviter un collapsus alvéolaire et à maximiser le temps des échanges gazeux entre l'air inspiré et le sang (Donald Jr. Bartlett, 1986; Bautista et al., 2010). Le relâchement des muscles abducteurs du pharynx participe également à réduire le diamètre interne des VAS pendant la post-inspiration.

1.3 - L'expiration tardive (E2)

Au cours de la ventilation de repos, l'expiration tardive est une phase passive pour la pompe ventilatoire, mais en cas de forte demande métabolique et devant la nécessité d'augmenter les échanges gazeux alvéolo-capillaires, les muscles abdominaux (innervés par les nerfs intercostaux et lombaires) peuvent permettre une expiration active (cf. figure 3 D) (Iscoe, 1998). Au niveau de la valve, c'est essentiellement une constriction des muscles pharyngiens (innervés par la branche pharyngienne du nerf vague, X) qui réduit le diamètre interne des VAS, et permet la conservation d'un volume résiduel pulmonaire (Bianchi and Gestreau, 2009a).

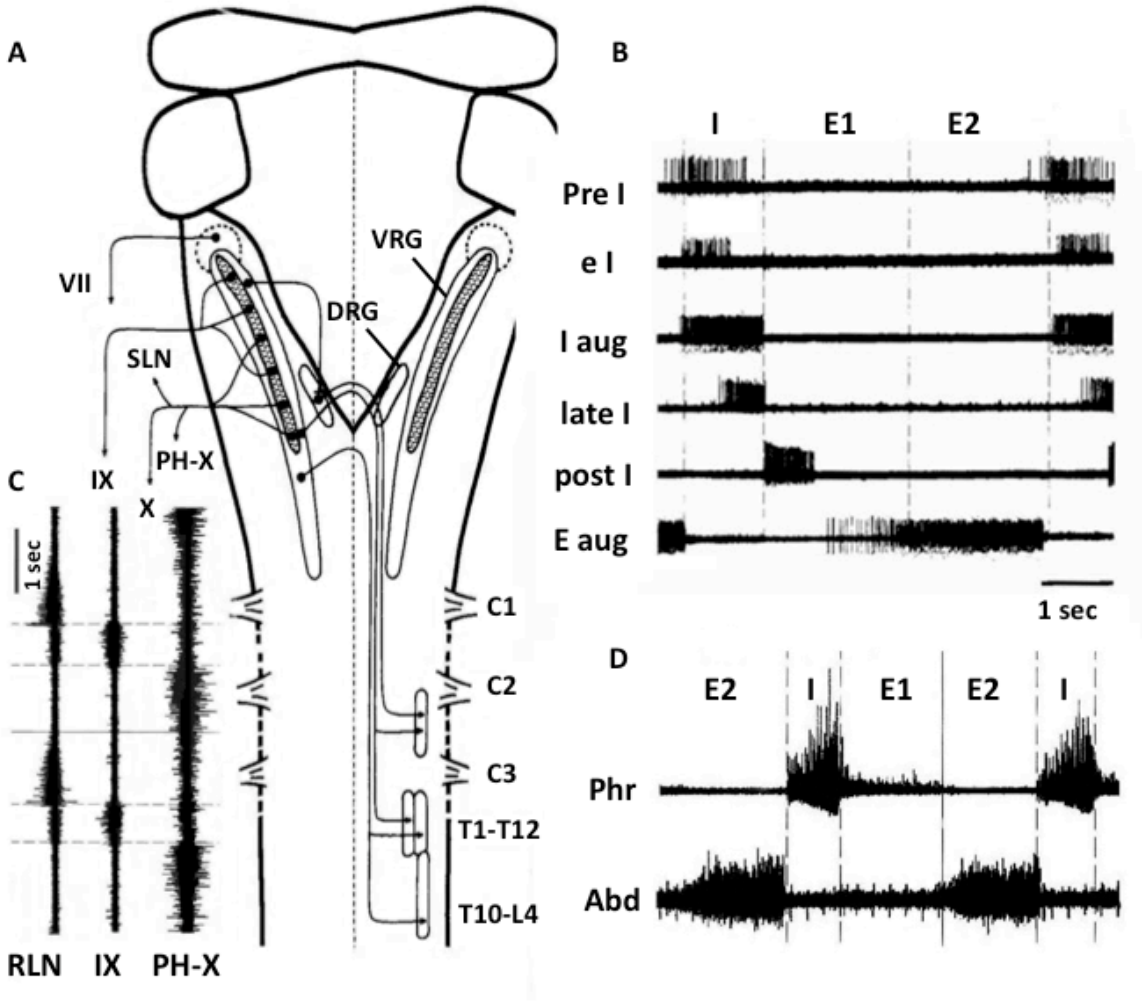

Figure 3 : A : vue dorsale du tronc cérébral représentant la localisation des neurones respiratoires dans le groupe respiratoire dorsal (DRG) et dans la colonne ventrale respiratoire (VRC), leurs projections axonales, et les nerfs crâniens innervant les muscles de la valve. Le cycle respiratoire progresse en trois phases : I inspiration ; E1 post-inspiration ou expiration précoce ; E2 expiration tardive. B : six patrons de décharges neuronales basiques sont enregistrés dans le DRG et la VRC. C : activités de décharge des nerfs crâniens ; D : activités de décharge des nerfs spinaux. Données obtenues chez le chat. Abréviations : Pre-I, pré-inspiratoire ; e-I, inspiratoire précoce ; I aug, inspiratoire croissant ; Late I, inspiratoire tardif ; Post I, post-inspiratoire ; E aug, expiratoire croissant ; Phr, nerf phrénique ; Abd, branche L1 du nerf lombaire ; RLN, nerf laryngé récurrent ; SLN, nerf laryngé supérieur ; VII, nerf facial ; IX, nerf glossopharyngien ; X, nerf vague ; PH-X, branche pharyngienne du X. (*adapté de Bianchi and Gestreau 2009*).

2 - Sites de projection axonale et modalités de décharges des neurones respiratoires

2.1 - Sites de projection axonale des neurones respiratoires

L'organisation temporelle en trois phases du cycle respiratoire du mammifère a été démontrée par l'analyse comparative des patrons de décharge des nerfs moteurs des différents muscles respiratoires (Richter, 1982; Bianchi et al., 1995; Hilaire and Pásaro, 2003), mais aussi par l'analyse de l'activité des motoneurones et interneurones respiratoires centraux identifiés par la technique de stimulation antidromique (Nakayama and Von Baumgarten, 1964; Merrill, 1970a). Cette technique a permis de diviser les neurones respiratoires en trois grandes catégories anatomiques et fonctionnelles selon leur projection axonale (Bianchi, 1969, 1971, 1974) :

- **Les neurones bulbospinaux** qui sont des neurones pré-moteurs, projetant leurs axones dans la moelle épinière vers les motoneurones respiratoires ;
- **Les neurones propriobulbaires** qui jouent le rôle d'interneurones au sein du réseau respiratoire du tronc cérébral ;
- **Les motoneurones crâniens**, qui commandent les muscles des VAS.

La caractérisation des neurones propriobulbaires s'est faite sur la base de résultats négatifs, c'est-à-dire le manque d'activation antidromique du neurone respiratoire après stimulation du nerf vague et de la moelle épinière (Bianchi and Gestreau, 2009a). D'autres techniques, comme celles de cross-corrélation (Hilaire and Monteau, 1976; Hilaire et al., 1984; Davies et al., 1985; Fedorko et al., 1989) et de moyennages déclenchés par les décharges neuronales (Cohen, 1979; Fedorko et al., 1983; Merrill and Lipski, 1987) ont permis d'analyser la connectivité entre les neurones respiratoires centraux et les motoneurones, ainsi que la connectivité inter-neuronale au sein du réseau respiratoire central, et d'apporter des informations sur la nature des projections (inhibitrices ou excitatrices) entre ces différents neurones respiratoires. Egalement, l'utilisation de traceurs rétrogrades (cheminant de la terminaison axonale vers le corps cellulaire) (Jack L. Feldman, 1986; Portillo and Pásaro, 1987, 1988; Grélot et al., 1989; Miller et al., 1989; Portillo et al., 1994) ou antérogrades (cheminant du corps cellulaire vers la terminaison axonale) (Yamada et al., 1988; Miller et al., 1989; Ellenberger et al., 1990; Núñez-Abades et al., 1991, 1993; Gaytán and Pásaro, 1998) a permis d'établir une cartographie des neurones respiratoires du tronc

cérébral ainsi que de leurs sites de projection axonale. L'utilisation de traceurs viraux (herpès ou rage) trans-synaptiques a permis de visualiser l'ensemble des régions bulbo-pontiques pouvant influencer directement ou indirectement l'activité des motoneurones phréniques (Dobbins and Feldman, 1994a; Gaytán et al., 2002a; Viemari et al., 2004a, 2004b) et hypoglosses (Ugolini, 1995). Enfin, une définition morphologique neuronale plus précise a été réalisée grâce à l'injection de marqueurs intracellulaires (Otake et al., 1987, 1988; Lipski and Martin-Body, 1987; Grélot et al., 1988; Sasaki et al., 1989; Zheng et al., 1991a).

2.2 - Modalités de décharges des neurones respiratoires

Une fois le lien anatomique et fonctionnel établi entre les neurones du CPG respiratoire et les motoneurones respiratoires, il convient de noter que l'organisation temporelle en trois phases du cycle respiratoire ne reflète que partiellement l'organisation des patrons de décharge des neurones à l'origine de la commande respiratoire. Une comparaison temporelle entre l'activité électrique extracellulaire des neurones du tronc cérébral du chat adulte anesthésié et les différentes phases respiratoires des décharges du nerf phrénique (pour l'inspiration), du nerf laryngé récurrent (pour la post-inspiration) et du nerf lombaire (pour l'expiration tardive), a permis d'identifier plusieurs catégories de neurones respiratoires (cf. figures 3B) (Jack L. Feldman, 1986; Bianchi et al., 1995; Bellingham, 1998). Ces neurones sont classés en 6 types en fonction de leur patron de décharge (croissant, « aug » ; décroissant, « dec » ; constant, « con ») et de la phase du cycle respiratoire pendant laquelle leur fréquence de décharge est maximale (I, E1 ou E2 ; de façon précoce, « early », ou tardive, « late ») :

- **Les neurones inspiratoires précoces (Early-I ou I-Dec)**, dont la fréquence de décharge décroit tout au long de l'inspiration ;
- **Les neurones inspiratoires (I-Aug)**, dont la fréquence de décharge est croissante au cours de l'inspiration, et qui présentent également une activité décroissante au cours de la post-inspiration ;
- **Les neurones inspiratoires tardifs (Late-I)**, qui sont actifs au cours de la transition entre inspiration et post-inspiration,
- **Les neurones post-inspiratoires (Post-I ou E-Dec ou Early-E)**, qui déchargent de façon décroissante pendant la post-inspiration ;
- **Les neurones expiratoires (E-Aug)**, dont la fréquence de décharge est croissante au cours de l'expiration tardive ;

- **Les neurones pré-inspiratoires (Pre-I)**, qui sont actifs au cours de la transition entre expiration tardive et inspiration.

En plus de ces neurones dits phasiques (qui émettent des potentiels d'action pendant une phase respiratoire donnée), des neurones toniques déchargent en continu tout au long du cycle respiratoire, avec une fréquence de décharge qui peut être modulée en fonction du cycle respiratoire, par exemple augmentée pendant l'inspiration ou pendant l'expiration tardive (St-John, 1998).

Le type de modalité de décharge neuronale ne permet pas de discriminer le caractère excitateur ou inhibiteur du neurone. De plus, même s'il existe une régionalisation anatomique préférentielle dans la typologie de décharge neuronale, on ne peut pas s'en servir pour discriminer les noyaux respiratoires entre eux (cf. figure 4) (Alheid and McCrimmon, 2008). Cette discrimination est le résultat de la synthèse des travaux scientifiques à la fois fonctionnels, anatomiques et biochimiques traitant du système respiratoire, et est perpétuellement discutée et réactualisée.

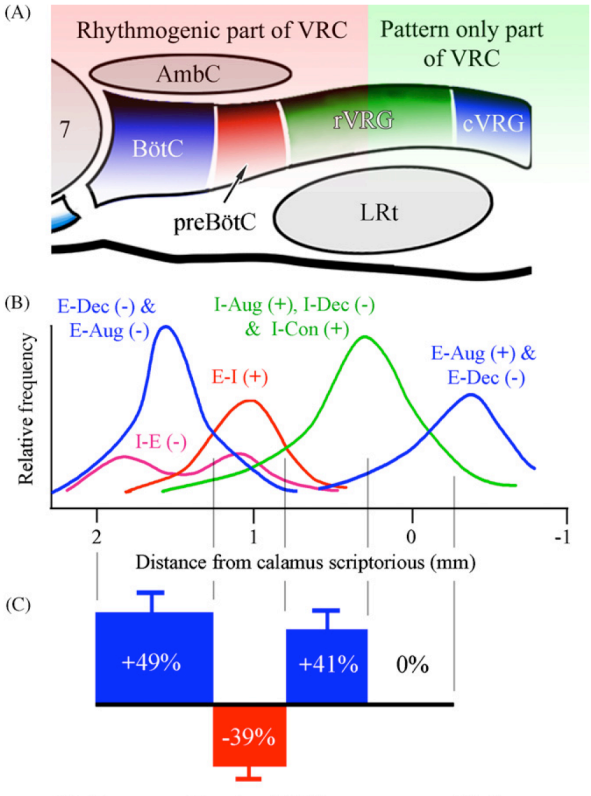

Figure 4 : distribution et fonctions comparées des neurones respiratoires du bulbe rachidien. A : Représentation des compartiments respiratoires dans la colonne ventrale respiratoire (VRC). Les régions en rose et vert indiquent une division approximative de la VRC en une partie rostrale contribuant à la genèse du rythme et du patron moteur respiratoire (rose), alors que la région plus caudale ne contribuerait qu'à la genèse du patron moteur respiratoire (vert). B : distribution relative des sous-types de neurones expiratoires et inspiratoires dans la VRC. On peut noter que la distribution du maximum de fréquence relative (normalisé par rapport aux neurones expiratoires du BötC) pour les sous-types particuliers de neurones correspond à des compartiments relativement bien définis de la VRC, mais que les limites montrées sur le dessin en (A) ne représentent pas de manière adéquate le dégradé réel de la distribution des différentes cellules le long de l'axe rostro-caudal de la VRC. C : effet sur la durée expiratoire (T_E) de la micro-stimulation du BötC, du PréBötC, et de la VRG rostrale par l'acide aminé excitateur acide DL-homocysteic (DLH). On peut noter que la stimulation du PréBötC cause une tachypnée (réduction du T_E) alors que la stimulation du BötC ou de la partie antérieure du VRG rostral produit une bradypnée (augmentation du T_E). La stimulation chimique de la portion postérieure de la VRG rostrale n'affecte pas le rythme respiratoire. (*Adapté de Alheid and McCrimmon 2008*).

3 - Anatomie du réseau respiratoire

Claudius Galenius, plus connu sous le nom de Galien, est généralement cité comme étant le premier à avoir remarqué, chez des gladiateurs de Pergamon dans l'Empire Romain (2e siècle), qu'une section de la moelle épinière sous le bulbe rachidien entraîne la mort par arrêt respiratoire (pour références, voir (Derenne et al., 1995)). Mais ce n'est qu'au 19e siècle qu'une régionalisation des centres respiratoires a été suggérée (LeGallois, 1812; Spyer, 2009), puis argumentée par des sections étagées du tronc cérébral (Flourens, 1842, 1851). Un travail beaucoup plus récent, mais reprenant le même paradigme expérimental de transsection du tronc cérébral, démontre l'importance de l'intégrité de l'ensemble du réseau respiratoire pour une genèse du cycle respiratoire en trois temps (cf. figures 5 et 6) (Smith et al., 2007). Le CPG respiratoire est ainsi habituellement décrit comme provenant d'une colonne bilatérale ponto-bulbaire (cf. figure 7), qui reçoit un grand nombre d'afférences modulant son activité.

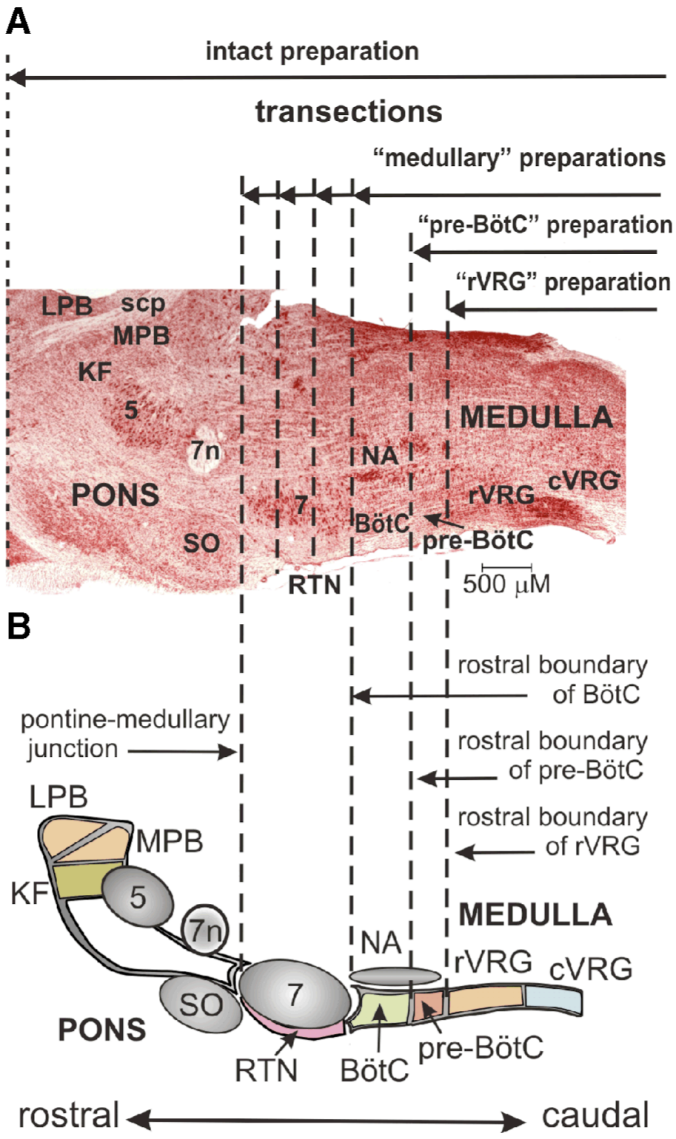

Figure 5 : A : sections parasagittales (coloration au rouge neutre) du tronc cérébral au niveau du noyau ambigu (NA), du VRG, du noyau facial (7), et du pont latéral. B : diagramme schématique montrant l'arrangement spatial des structures liées à la respiration. Les lignes verticales en pointillés indiquent plusieurs transsections expérimentales, qui séparent le niveau rostral de réduction des préparations (lignes horizontales solides avec des flèches). 5, noyau trigéminal ; 7n, nerf facial ; cVRG, VRG caudal ; KF, noyau de Kölliker-Fuse ; LPB, complexe parabrachial latéral ; MPB, complexe parabrachial médian ; RTN, noyau rétrotrapézoïde ; scp, pédoncule cérébelleux supérieur ; SO, olive supérieure. (*Adapté de Smith J. et al. 2007*).

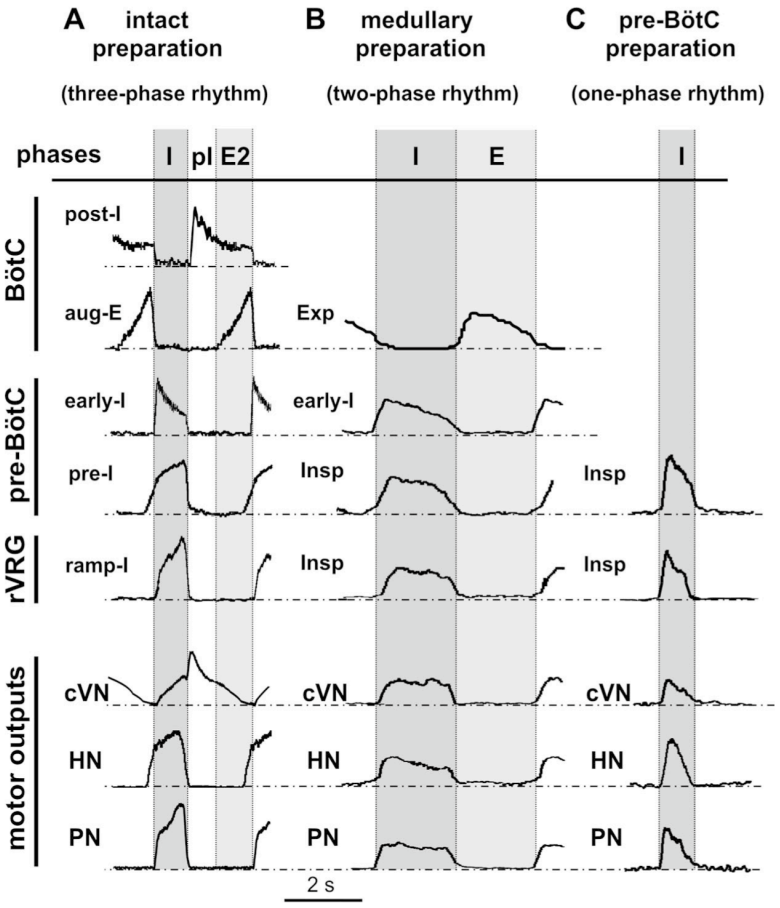

Figure 6 : patrons de décharges neuronales respiratoires enregistrées sur des préparations *in situ* "cœur tronc cérébral isolé perfusé" intactes et à différents niveaux de réductions, effectuées comme montrées sur la figure 5. A : enregistrement sur la préparation "intacte" ; phases inspiratoires (I), post-inspiratoires (pI) et expiratoires tardives (E2) sont présentes sur cette préparation intacte générant les 3 phases du cycle respiratoire. B : enregistrement sur la préparation "bulbaire" ("medullary") ; phases inspiratoires (I) et expiratoires (E) sont présentes sur cette préparation générant 2 phases respiratoires, la phase post-inspiratoire étant manquante. C : enregistrement sur la préparation "PréBötC" ("pre-BötC) ; seule une période inspiratoire (I) est enregistrée sur cette préparation. Nerfs moteurs : cVN, nerf vague cervical ; HN, nerf hypoglosse ; PN, nerf phrénique. (*Adapté de Smith et al. 2007*).

3.1 - Noyaux respiratoires pontiques

Une section ponto-bulbaire entraîne la disparition de l'activité respiratoire en 3 temps et l'apparition d'une activité respiratoire en 2 temps (inspiration et expiration), avec une phase inspiratoire dite apneustique, de longue durée et perdant sa forme de décharge en « rampe » pour une forme carrée (ceci est particulièrement vrai lorsque le réseau respiratoire est isolé de ses afférences pulmonaires, par exemple après bivagotomie) (cf. figures 5 et 6). Ainsi, la rythmogenèse respiratoire serait assurée au niveau bulbaire, mais les noyaux respiratoires pontiques joueraient un rôle essentiel dans le contrôle de la phase de transition respiratoire lors de la post-inspiration, impliquant tout particulièrement les VAS (Lumsden, 1923a, 1923b, 1923c; St-John, 1998; Okazaki et al., 2002; Alheid et al., 2004; Dutschmann and Herbert, 2006). Ces noyaux respiratoires pontiques sont également le relais de nombreuses

projections, par exemple celles venant des structures supérieures du cerveau pour la coordination de la respiration avec des activités comme la vocalisation (Smotherman et al., 2006; Subramanian et al., 2008; Subramanian and Holstege, 2010). Les noyaux respiratoires pontiques (ou groupe respiratoire pontique, GRP) incluent le noyau de Kölliker-Fuse (KF) et le complexe parabrachial (PB) (latéral, LPB, et médian, MPB), mais aussi les noyaux noradrénergiques A5 et A6 (Locus Cœruleus) (Hilaire et al., 2004).

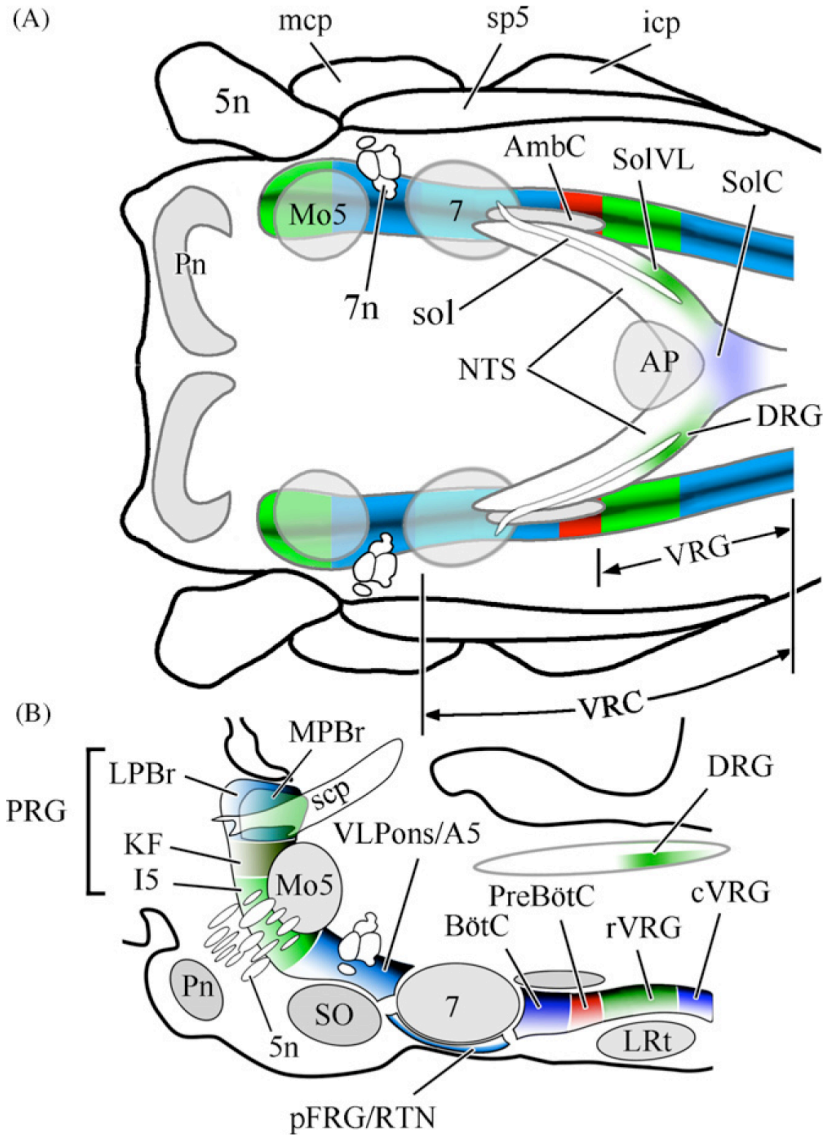

Figure 7 : régions liées à la respiration du rhombencéphale de rat représenté en vues horizontale (A) et sagittale (B). 5n, nerf trijumeau ; 7, noyau facial ; A5, groupe noradrénergique A5 ; AmbC, partie compacte du noyau ambigu ; AP, area postrema ; BötC, complexe de Bötzinger ; cVRG, groupe ventral respiratoire caudal ; DRG, groupe respiratoire dorsal ; I5, zone intertrigéminale ; icp, pédoncule inférieur cérébelleux ; KF, noyau de Kölliker-Fuse ; LPBr, complexe parabrachial latéral ; LRt, noyau réticulaire latéral ; mcp, pédoncule cérébelleux médian ; Mo5, noyau moteur du nerf trijumeau ; MPBr, complexe parabrachial latéral ; NTS, noyau du faisceau solitaire ; pFRG, groupe respiratoire parafacial ; Pn, noyau pontique basilaire ; preBötC, complexe de PréBötzinger ; PRG, groupe respiratoire pontique ; RTN, noyau rétrotrapézoïde ; rVRG, groupe respiratoire ventral rostral ; scp, pédoncule cérébelleux supérieur ; SO, olive supérieure ; sol, faisceau solitaire ; SolC, subdivision commissurale du noyau du faisceau solitaire ; SolVL, subdivision ventrolatérale du noyau du faisceau solitaire ; sp5, faisceau spinal trigéminal ; VLPons, région pontique ventrolatérale ; VRC, colonne ventrale respiratoire ; VRG, groupe respiratoire ventral. (*Adapté de Alheid and McCrimmon 2008*).

3.1.1 - Le noyau de Kölliker-Fuse (KF) et le complexe parabrachial (LPB et MPB)

Le KF et le PB, situés dans la partie dorsolatérale du pont, sont les constituants principaux du groupe respiratoire pontique, anciennement appelé « centre pneumotaxique ». Une grande variété de types de neurones respiratoires ont été décrits dans ces noyaux, incluant des phasiques inspiratoires (I, E-I, I-E) et expiratoires (E, E-Dec, E-Aug) (Song et al., 2006; Ezure and Tanaka, 2006), mais aussi des neurones toniques dont l'activité est modulée au cours du cycle respiratoire (Jiang et al., 2004; Ezure and Tanaka, 2006). Le KF est la source du plus grand nombre de projections vers la colonne ventrale respiratoire (CVR, cf. ci-après), avec des projections additionnelles vers le noyau du faisceau solitaire (NTS), les noyaux hypoglosses et faciaux, ainsi que des projections spinales vers les motoneurones phréniques (Dutschmann et al., 2004; Ezure and Tanaka, 2006; Yokota et al., 2007). Le KF est un noyau contenant un grand nombre de récepteurs de type N-méthyl-D-aspartate (NMDA), en particulier de la sous-unité NR1 (Zheng et al., 1998; Dutschmann and Herbert, 1998; Dutschmann et al., 1998; Guthmann and Herbert, 1999). Enfin, il existe un consensus sur un rôle potentiellement fondamental des noyaux pontiques dans l'intégration sensorimotrice (Song and Poon, 2004; Potts et al., 2005).

Nota Bene : la particularité neurochimique des neurones du KF, qui contiennent un grand nombre de récepteurs NMDA, nous a permis dans cette thèse de prévenir l'altération respiratoire induite par une anesthésie en période pré-symptomatique chez des souris modèles de tauopathie (souris Tau-P301L) (cf. partie résultats, chapitre 3, article 4).

3.1.2 - Les noyaux noradrénergiques A5 et A6

A5 et A6 sont deux noyaux noradrénergiques présents dans la partie ventrolatérale et dorsolatérale du pont, respectivement. Ils interviennent pour moduler le rythme respiratoire (Hilaire et al., 2004), mais sont également impliqués dans de nombreuses autres fonctions comme la régulation cardiovasculaire, la nociception, ou le système d'éveil (Sagen and Proudfit, 1986; Aston-Jones et al., 1986; Byrum and Guyenet, 1987; Murase et al., 1993; Berridge, 2008). Le noyau A5 projette sur le tractus intermédiolatéral de la moelle thoracique (Loewy et al., 1979) et sur le PB et le KF (Byrum and Guyenet, 1987), et reçoit des afférences cardiovasculaires venant de la région ventrolatérale du bulbe et du NTS (Guyenet, 1984;

Byrum and Guyenet, 1987). Le noyau A6, ou Locus Cœruleus, est le plus important noyau noradrénergique du cerveau, et contient 43% du nombre total de cellules noradrénergiques du cerveau de rat (Swanson and Hartman, 1975; Swanson, 1976; Moore and Bloom, 1979). Il émet des projections vers l'ensemble du système nerveux central (SNC), innervant notamment les structures supérieures du cerveau tels les noyaux thalamiques, l'hypothalamus, le néocortex, l'hippocampe, l'amygdale etc. (Ungerstedt, 1971; Kobayashi et al., 1974; Moore and Bloom, 1979), mais aussi la partie ventrolatérale de la moelle (Westlund et al., 1982, 1983), les cornes dorsales et ventrales de la moelle thoracique (Nygren and Olson, 1977) et le tractus intermédiolatéral de la moelle sacrée (Westlund et al., 1982).

3.2 - Noyaux respiratoires bulbaires

Les noyaux respiratoires bulbaires forment, à l'exception du groupe respiratoire dorsal, un continuum anatomique appelé colonne ventrale respiratoire (CVR) (cf. figure 7). Dans cette colonne est également identifié un sous-groupe, le groupe respiratoire ventral (GRV), qui représente la partie caudale de la CVR, contenant essentiellement des motoneurones crâniens et des pré-motoneurones bulbospinaux (cf. figure 7). La présence de cette colonne dans des préparations *in situ* ou *in vitro* suffit à la genèse d'un rythme respiratoire, même si ce dernier ne présente plus une activité de type triphasique (cf. figures 5 et 6). Fonctionnellement, il existe un débat récurrent dans la littérature sur la génération du rythme respiratoire, entre deux hypothèses selon lesquelles le rythme respiratoire serait issu 1) des propriétés membranaires particulières de certains neurones respiratoires, jouant le rôle de générateurs endogènes de rythme (Feldman and Del Negro, 2006a), ou 2) des propriétés synaptiques émergentes de réseau (St-John and Paton, 2004; St John, 2009). Nous apporterons en chapitre 2 de cette introduction de thèse un point de vue maturationnel sur ce débat. Toutefois, même s'il existe un chevauchement fonctionnel certain entre les différents noyaux constituant la CVR (cf. figure 4), il est possible de les discriminer par le cumul de leurs propriétés neurochimiques, transcriptomiques, protéomiques ainsi que leurs sites de projections axonales (Alheid and McCrimmon, 2008). Mais il faut admettre qu'il existe au sein même de la CVR une grande hétérogénéité neuronale qui sera présentée ci-dessous suivant un ordre rostro-caudal.

3.2.1 - Le groupe respiratoire parafacial (pFRG)

Onimaru et Homma ont été les premiers à décrire le pFRG *in vitro* chez le rat nouveau né, à partir de l'enregistrement de neurones Pre-I en position ventro-latérale par rapport au noyau facial (Onimaru and Homma, 1987). Ces neurones glutamatergiques sont souvent évoqués pour leur implication dans la rythmogenèse respiratoire (cf. chapitre 2) (Onimaru and Homma, 2003; Weston et al., 2004; Onimaru et al., 2006). Ils sont insensibles aux opioïdes (car ils ne possèdent pas de récepteurs μ aux opioïdes sur leurs membranes), ce qui les distingue des neurones du complexe de Pré-Bötzinger, qui serait le noyau potentiellement le plus impliqué dans la rythmogenèse respiratoire (Feldman and Del Negro, 2006a).

3.2.2 - Le noyau rétrotrapézoïde (RTN)

Le RTN a initialement été identifié suite à l'injection de marqueur rétrograde injecté dans le GRV chez le chat (Smith et al., 1989) et le rat (Pearce et al., 1989). Il est localisé en position ventro-médiane par rapport au noyau facial et médiane par rapport au pFRG. RTN et pFRG sont d'ailleurs souvent décrits comme étant deux groupes de neurones distincts fonctionnellement, mais se chevauchant, voire même colocalisés anatomiquement (Smith et al., 2009). Le RTN serait essentiellement impliqué dans la sensibilité chimique (chémosensibilité) au CO_2 et/ou au pH (cf. chapitre 3.2) (Mulkey et al., 2004a; Guyenet et al., 2010). Les neurones du RTN projettent vers la plupart des noyaux respiratoires de la CVR, vers le groupe respiratoire dorsal (GRD, cf. paragraphe 3.2.7) et vers le GRP (Connelly et al., 1989, 1990; Holtman et al., 1990; Ellenberger and Feldman, 1990; Gang et al., 1995; Rosin et al., 2006a). Le RTN reçoit des afférences en provenance du NTS, du GRV et du GRP, notamment des chémorécepteurs centraux et périphériques (via des relais synaptiques) et des neurones sérotoninergiques bulbaires et pontiques (Otake et al., 1992; Bodineau et al., 2000b; Takakura et al., 2006; Rosin et al., 2006; Mulkey et al., 2007a). La majeure partie des neurones du RTN sont actifs de manière tonique, avec ou sans modulation de leur décharge au cours du cycle respiratoire, et souvent avec un renforcement (ou l'apparition) d'une modulation respiratoire en condition d'hypercapnie ou d'acidose (Nattie et al., 1993; Bodineau et al., 2000b; Mulkey et al., 2004b; Guyenet et al., 2005b, 2005a). Enfin, les neurones du RTN expriment les récepteurs à la neurokinine 1 (NK1) et le facteur de transcription Phox2B (Nattie and Li, 2002a), ce dernier étant souvent utilisé comme marqueur

des neurones glutamatergiques du RTN (Stornetta et al., 2006; Dubreuil et al., 2008).

3.2.3 - Le complexe de Bötzinger

Le complexe de Bötzinger (BötC) contient principalement des neurones expiratoires (cf. figure 4), notamment E-Aug et E-Dec, de type glycinergique (inhibiteur) (Schreihofer et al., 1999; Ezure et al., 2003a). Le BötC projette sur les neurones bulbospinaux, les motoneurones phréniques et les motoneurones respiratoires crâniens, et le noyau facial et le RTN (Bianchi and Barillot, 1982; Tian et al., 1998; Ezure et al., 2003b; Rosin et al., 2006a). Chez le chat, les neurones GABAergiques (utilisant l'acide γ-aminobutyrique comme neurotransmetteur) du BötC projettent également sur le NTS (Livingston and Berger, 1989).

3.2.4 - Le complexe de PréBötzinger

Le complexe de PréBötzinger (PréBötC), situé en position caudale au complexe de Bötzinger dans la CVR, a été identifié comme un noyau essentiel pour la rythmogénèse respiratoire (Smith et al., 1991) (cf. chapitre 2). Il contient principalement des neurones propriobulbaires à décharge phasique, actifs dans la transition de phase entre l'expiration tardive et l'inspiration (cf. figure 4) (Dobbins and Feldman, 1994b; Sun et al., 1998; Guyenet and Wang, 2001; Gaytán et al., 2002b). Le premier type de neurones identifiés dans le PréBötC exprime à la fois des récepteurs à la NK1, au GABAB et aux opioïdes μ (Rekling et al., 1996; Gray et al., 1999). D'autres types de neurones du PréBötC ont ensuite été identifiés, exprimant à la fois les récepteurs à la NK1 et le transporteur vésiculaire de type 2 du glutamate (VGlut2) (Guyenet et al., 2002), ou encore les récepteurs à la NK1 et la somatostatine (Stornetta et al., 2003; Tan et al., 2008). Des populations de neurones inhibiteurs GABAergiques et glycinergiques sont aussi présentes dans le PréBötC (Kuwana et al., 2006; Winter et al., 2009).

3.2.5 - Les noyaux ambigu et para-ambigu

Le noyau ambigu, situé dorsalement par rapport aux BötC et PréBötC, contient les corps cellulaires des motoneurones laryngés et pharyngés innervant les VAS (Merrill, 1970b; Pásaro et al., 1981; Núñez-Abades et al., 1992). Le noyau para-ambigu contient des neurones bulbospinaux projetant sur les motoneurones phréniques (Onai and Miura, 1986).

3.2.6 - Le groupe respiratoire ventral

Le groupe respiratoire ventral (GRV) a été subdivisé en deux parties, une ventrale et une caudale (cf. figures 4, 5 et 7), selon la prééminence de neurones inspiratoires (partie rostrale) et expiratoires (partie caudale) (cf. figure 4). Les neurones bulbospinaux du GRV reçoivent de nombreuses afférences, notamment du PréBötC et du BötC, contribuant à la construction du patron de décharge caractéristique en « rampe » des neurones bulbospinaux inspiratoires et expiratoires (Alheid and McCrimmon, 2008; Smith et al., 2009).

- Groupe respiratoire ventral rostral (GRVr) : le GRVr contient les principaux neurones inspiratoires bulbospinaux excitateurs (glutamatergiques) qui projettent sur les motoneurones spinaux inspiratoires phréniques et intercostaux (Bianchi et al., 1995). Une sous-population rostrale de neurones du GRVr exprime le récepteur à la NK1, mais est différenciée des neurones du PréBötC par leur caractère bulbospinal, leur taille plus importante et leur patron de décharge I-Aug (Guyenet et al., 2002; Alheid et al., 2002).
- Groupe respiratoire ventral caudal (GRVc) : le GRVc, généralement assimilé au noyau rétroambigu, contient des neurones expiratoires bulbospinaux qui projettent caudalement sur les motoneurones expiratoires thoraciques et lombaires (Merrill, 1970b; Arita et al., 1987; Ezure, 1990; Zheng et al., 1991b). Il contient également des neurones bulbospinaux glycinergiques E-Dec, et des neurones propriobulbaires inhibiteurs, projetant rostralement sur les motoneurones crâniens du noyau ambigu (Schreihofer et al., 1999; Saito et al., 2002; Ezure et al., 2003a).

3.2.7 - Le noyau du faisceau solitaire et le groupe respiratoire dorsal

Le noyau du faisceau solitaire est situé dans la région dorsale du bulbe rachidien, il est médian rostralement à l'area postrema, et se latéralise caudalement à cette dernière (cf. figure

7). Les régions liées à la respiration sont celles latérales, situées caudalement à l'area postrema (Alheid and McCrimmon, 2008). Elles sont notamment le site principal de projection des afférences respiratoires sensorielles provenant des poumons et des chémorécepteurs périphériques, qui sont pour la plupart glutamatergiques (Sykes et al., 1997) et souvent associées à un co-transmetteur monoaminergique, purinergique, peptidergique ou volatile (Finley et al., 1992; Mizusawa et al., 1994; Gatti et al., 1995; Massari et al., 1996; Ichikawa et al., 2007). Des interneurones GABAergiques sont également présents dans cette région caudale du NTS, projetant au sein même du NTS (Kawai and Senba, 1999), ainsi que quelques neurones glycinergiques (Ezure and Tanaka, 2004). L'organisation fonctionnelle de la boucle sensitive passant par le NTS sera décrite plus précisément en chapitre 3, paragraphe 2.4 de cette introduction.

Il existe une sous-division ventro-latérale par rapport au NTS qui contient des neurones respiratoires constituant le groupe respiratoire dorsal (GRD) chez le chat (Bianchi, 1971; Berger, 1977; Grelot et al., 1988), mais l'existence du GRD reste controversée chez le rat et la souris. Le GRD du chat est composé de neurones bulbospinaux dont la majorité (50-80%) est inspiratoire, et dont les axones projettent vers les motoneurones phréniques (Bianchi, 1971; Berger, 1977; Grelot et al., 1988). Par contre chez le rat, des projections directes vers les motoneurones phréniques sont moins substantielles, ne représentant qu'environ 14% des neurones du GRD (de Castro et al., 1994). Récemment, des techniques d'imagerie par fluorescence voltage-sensible ont tout de même permis d'identifier des neurones inspiratoires dans le GRD de rat nouveau-né (Onimaru and Homma, 2005). Chez le chat, d'autres projections existent vers les niveaux C1-C2 de la moelle épinière, qui cibleraient des interneurones propriospinaux inspiratoires projetant sur les motoneurones phréniques (Lipski and Duffin, 1986).

II - Développement et maturation de la commande respiratoire

Le réseau central respiratoire a pour fonction principale de générer une commande respiratoire adaptée aux besoins énergétiques de l'organisme. De plus, il est sollicité pour la genèse de comportements moteurs couplés à la respiration, telles la vocalisation ou la déglutition. Mais son activité est en constante évolution en fonction de l'âge et du contexte environnemental. De nombreuses approches expérimentales existent pour étudier le réseau respiratoire, plus ou moins invasives et intégratives. Ces approches ne sont pas utilisables à tous les âges, notamment les préparations *in vitro* (préparation en bloc et tranche de tissu) qui ne sont ″viables″ qu'en période périnatale. De ces différentes techniques expérimentales et des résultats qu'elles ont permis d'obtenir, découlent différentes hypothèses sur la genèse du CPG respiratoire chez le mammifère adulte, dont aucune n'est encore complètement consensuelle. L'existence d'un centre rythmogénique chez l'adulte avec la participation de neurones générateurs endogènes de rythme, type "pacemaker", est notamment très contestée (St-John and Paton, 2004; Feldman and Del Negro, 2006b; St John, 2009). Le fait qu'il existe encore différentes théories sur la genèse du CPG respiratoire est inhérent à sa complexité fonctionnelle, et nous aborderons dans ce chapitre un point de vue maturationnel sur ce débat, sous-tendu par les différentes techniques expérimentales utilisées pour l'étude du réseau respiratoire.

1 - Embryogenèse d'oscillateurs couplés et respiration prénatale

Chez les mammifères, les mouvements respiratoires apparaissent dès le stade fœtal. Chez l'Homme (39 semaines de gestation), des mouvements abdominaux, puis thoraciques et enfin de liquide amniotique dans les cavités nasales sont détectables par ultrasons à partir de la 20^{e} semaine de gestation (Cosmi et al., 2003). Chez le rat (20 à 21 jours de gestation) et la souris (19 à 21 jours de gestation), des mouvements similaires ont été détectés par ultrasons dès le 15^{e} jour de gestation (Kobayashi et al., 2001), et par perfusion transplacentaire *ex utero* (Suzue, 1994). Des embryons de souris extériorisés par césarienne puis placés dans un pléthysmographe présentent des mouvements respiratoires dès E16,5 (jour embryonnaire

16,5) s'apparentant à des "gasps" (Viemari et al., 2003), forme de respiration monophasique dite de survie, de faible fréquence (environ 10 cyles par minute) et caractérisée par une inspiration très ample (ayant un patron moteur non adapté à la physiologie ventilatoire) (St John, 2009). Ces embryons ne survivent d'ailleurs pas à cette extériorisation. Par contre, à partir de E18,5, les embryons extériorisés développent en quelques minutes une respiration plus structurée et plus fréquente (environ 110 cycles/min) comparable à celle de nouveau-nés, et suffisante pour garantir la survie de ces "prématurés" sous réserve d'allaitement par la mère. Les techniques expérimentales *in vitro* (essentiellement la préparation dite "en bloc" ou "de Suzue" par rapport à son inventeur, et la tranche de tronc cérébral) ont permis d'identifier les mécanismes permettant la genèse et le développement périnatal de la commande centrale respiratoire, identifiant l'implication fonctionnelle de noyaux élémentaires à la rythmogenèse respiratoire, puis leur intégration dans un réseau plus complexe qui confère au système respiratoire la plasticité fonctionnelle nécessaire à la survie postnatale.

1.1 - Naissance du groupe respiratoire parafacial embryonnaire et du noyau de PréBötzinger, ou la recherche du « Nœud Vital »

Depuis Flourens en 1851 et sa définition du centre respiratoire comme « nœud vital » (Flourens, 1851), de nombreuses études ont cherché à réduire le réseau respiratoire à la plus petite entité possible pour le maintien d'une genèse de rythme. Lumsden, dans une série d'articles majeurs (Lumsden, 1923a, 1923b, 1923c), a ensuite identifié le bulbe rachidien comme étant à l'origine d'activités de type "gasps". Depuis, la diversité des approches expérimentales a permis un raffinement de cette localisation, conférant au couplage PréBötC / RTN/pFRG un rôle dans la rythmogenèse respiratoire.

Dès le stade E14,5, une activité rythmique à une fréquence de l'ordre de 10 cycles par minute est détectable au niveau de la forme embryonnaire du RTN/pFRG, appelée e-pF (on notera la possibilité que RTN et pFRG ne forment qu'un seul et même noyau mais à des âges différents) (Thoby-Brisson et al., 2009). Ces neurones expriment le récepteur à la NK1, le transporteur vésiculaire du glutamate de type 2 (Vglut2) et le facteur de transcription Phox2b, rappelant la description faite du RTN chez l'adulte (Nattie and Li, 2002a; Stornetta et al., 2006) et du pFRG chez le nouveau-né (Onimaru et al., 2008). En outre, ces neurones possèdent des propriétés dites "pacemaker", c'est-à-dire que leur potentiel de membrane peut présenter des oscillations autonomes résultant d'activations/inactivations cycliques de

conductances membranaires dépendantes du voltage. Ceci est dû à la présence de canaux sodiques persistants dans leurs membranes (générant un courant de type I_{NaP}). De plus, l'ajout de carbenoxolone, un inhibiteur des synapses électriques (jonctions communicantes, ou "gap junctions"), induit une perte de synchronisation des neurones du e-pF. L'activité rythmique du e-pF reposerait donc sur la synchronisation des neurones "pacemaker" par des synapses électriques. Cette activité est pré-inspiratoire, précédant celle du PréBötC. L'e-pF est justement qualifié d'embryonnaire car il n'existe aucune preuve de son existence chez le nouveau-né ou l'adulte. Cependant, une étude récente montre une forme de persistance de ce noyau chez l'adulte, qui pourrait représenter un oscillateur conditionnel actif uniquement lors d'expiration active pendant la phase d'expiration tardive (Pagliardini et al., 2011).

L'émergence d'activités rythmiques dites respiratoires au sein du PréBötC a lieu vers E15,5 (Thoby-Brisson et al., 2005), quelques heures après l'émergence du e-pF. Ces activités, également à la fréquence d'environ 10 cycles par minute, sont en phase avec l'activité inspiratoire des racines phréniques des préparations "en bloc", après extraction et perfusion du tronc cérébral et de la moelle épinière cervicale. Le PréBötC comprend plusieurs types fonctionnels de neurones, et notamment deux types de neurones "pacemaker", ceux dépendant d'une conductance membranaire sodique voltage-dépendante (I_{NaP}), et ceux qui requièrent des courants calciques (I_{ca}) et des courants cationiques non-spécifiques indépendants du voltage activés par le calcium (I_{CAN}) (Thoby-Brisson and Ramirez, 2001; Del Negro et al., 2002, 2005). Il existe plusieurs théories sur le mécanisme de genèse endogène d'activité électrique rythmique par le PréBötC dans les préparations *in vitro*. La théorie la plus récente et qui semble consensuelle postule l'existence d'un "group pacemaker" (Feldman and Del Negro, 2006b). Selon cette hypothèse, la genèse du rythme serait une propriété émergente du groupe de neurones composant le PréBötC, reposant sur les connections synaptiques récurrentes combinées aux propriétés membranaires individuelles intrinsèques de ces neurones. Dans ce cadre, des interconnections excitatrices entre les neurones du PréBötC initient un renforcement ("feedback") positif via des excitations récurrentes. Les courants I_{NaP} et I_{CAN} servent à amplifier la dépolarisation synaptique et génèrent alors des décharges résultant de l'activité électrique globale du noyau.

Thoby-Brisson et collaborateurs ont récemment démontré l'existence d'un couplage fonctionnel entre e-pF et PréBötC au stade prénatal *in vitro* (Thoby-Brisson et al., 2009), l'e-pF jouant un rôle essentiel dans l'entraînement du PréBötC. Ce couplage se retrouve *in vitro* en période postnatale entre pFRG et PréBötC, avec une activation successive du premier noyau en phase pré-inspiratoire, puis du deuxième noyau en phase inspiratoire, comme

montré sur la figure 8 (Onimaru and Homma, 2003). Toutefois, l'existence d'une activité dite respiratoire et autorythmique du pFRG et PréBötC n'a été démontrée que dans des modèles *in vitro*, et leur contribution fonctionnelle à la physiologie respiratoire *in vivo* est toujours fortement débattue dans la littérature.

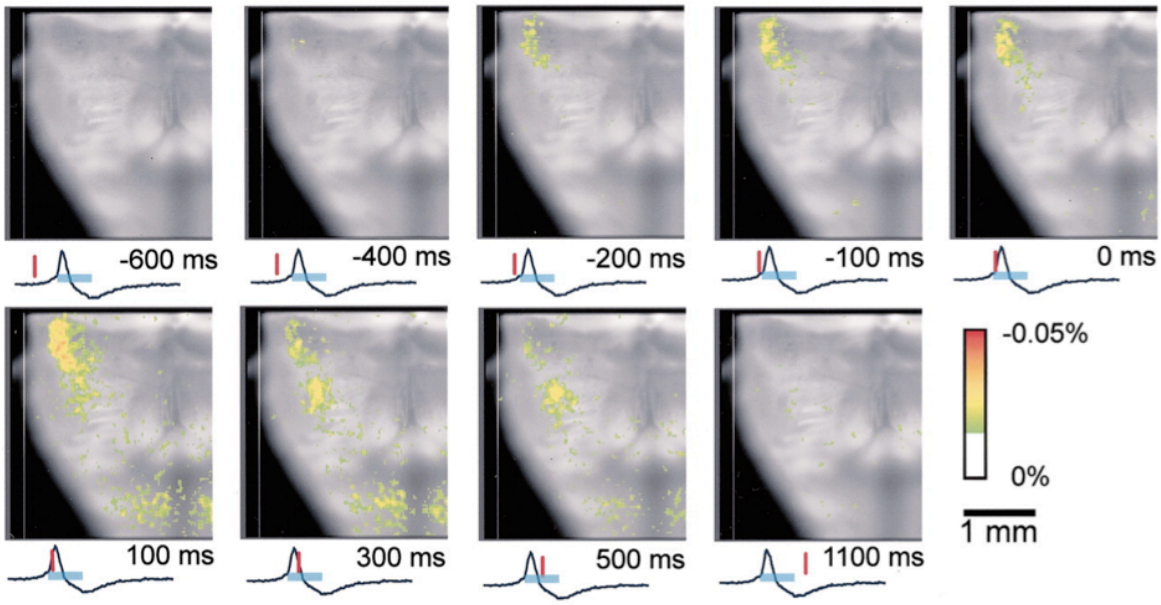

Figure 8 : patron d'activité spatiotemporel des neurones respiratoires observés par imagerie optique en période post-natale. Les images représentent la surface ventrale de la moitié droite du bulbe rachidien. Les nombres en bas à droite de chaque image annotent le temps par rapport au début de l'activité inspiratoire enregistrée sur la racine phrénique en C4. La trace sous chaque image représente l'activité enregistrée en C4 ; la phase inspiratoire est indiquée par la barre bleue. La barre rouge verticale montre le temps auquel l'image a été prise. On peut noter que le signal optique reflétant l'activité des neurones respiratoires apparaît dans le bulbe rostro-ventro-latéral, au niveau du pFRG, pendant la période pré-inspiratoire. Pendant la phase inspiratoire, le pic d'activité apparaît dans une zone plus caudale du bulbe rachidien ventrolatéral, au niveau du PréBötC. (*Adapté de Onimaru and Homma 2003*).

1.2 - Un « nœud vital » isolé suffisant pour générer du "gasp", mais pas de l'eupnée

L'eupnée est définie comme la respiration physiologique, celle qui implique l'activation séquentielle des muscles innervés par les nerfs crâniens et spinaux pendant les trois phases du cycle respiratoire (Duffin, 2003). Lors d'hypoxie sévère ou d'asphyxie, l'eupnée s'interrompt et un deuxième patron moteur respiratoire plus robuste apparaît, prenant le relais de l'eupnée : le "gasp". Caractérisé par une activité synchrone et décroissante des nerfs crâniens et spinaux, avec une activité expiratoire minimale, le "gasp" servirait de

mécanisme d'autoressuscitation, dans l'attente du ré-enclenchement éventuel de l'eupnée (Feldman, 1986; Bianchi et al., 1995; St-John, 1998; St-John and Paton, 2004).

En 1984, Suzue a introduit la préparation *in vitro* "en bloc" chez le rat nouveau-né (Suzue, 1984). Le principal avantage de cette technique est qu'elle préserve la genèse d'activités électriques rythmiques sur les racines nerveuses crâniennes et spinales associées à la respiration sur une préparation réduite, rendant plus aisés les enregistrements cellulaires et la pharmacologie centrale, très difficiles *in vivo*. Par contre, dès la première publication, Suzue a émis l'hypothèse que cette préparation serait génératrice de "gasps" et non d'eupnée (respiration physiologique). En effet, comme pendant le "gasp", (i) les décharges des nerfs crâniens et spinaux sont synchrones et décroissantes, (ii) ces nerfs ne présentent aucune activité ni post-inspiratoire ni expiratoire tardive entre les décharges inspiratoires, et (iii) le patron moteur de décharge des nerfs est peu modifié par l'ablation du pont. (Smith et al., 1990; St John, 1996, 2009). Egalement, ce type de décharge monophasique est retrouvé lors de transections du tronc cérébral ne conservant que le PréBötC comme présenté en figures 5 et 6 (Smith et al., 2007).

Une autre approche *in vitro* essentiellement réalisable en période périnatale, consiste à couper une tranche tangentielle de bulbe contenant à la fois le PréBötC, le noyau moteur hypoglosse et des racines nerveuses hypoglosses, pour enregistrer l'activité nerveuse produite sur ces racines. Cette préparation génère une activité rythmique de type "respiratoire", semblable à celle des préparations "en bloc", et il est probable que cette activité soit une forme de "gasp". Il est de toute façon très difficile d'extrapoler un type de patron moteur respiratoire seulement à partir de décharges nerveuses hypoglosses. En effet, à la fois chez le nouveau-né et chez le rat adulte, la décharge de l'hypoglosse peut être de type croissant ou décroissant en fonction de la préparation utilisée, voire même des deux types dans une même préparation (Leiter and St -John, 2004; Paton et al., 2006; Toppin et al., 2007). De plus, chez la souris adulte, ce nerf présente une activité décroissante prédominante à la fois en eupnée et en "gasp" (St John and Leiter, 2009). Les mécanismes de genèse de l'activité rythmique enregistrée en tranche ont été fortement liés à la décharge de neurones "pacemakers". Or, l'ajout de bloquants des conductances sodium persistantes I_{NaP} et/ou des conductances calciques I_{CAN} supprime la décharge sur l'hypoglosse en tranche fine, ou le patron moteur appelé "eupnéique" en tranche épaisse, mais n'élimine que le "gasp" et pas l'eupnée sur des préparations *in situ* ou *in vivo* (Paton et al., 2006; Paton and St-John, 2007; Ramirez and Garcia, 2007; St-John, 2008).

Il semblerait donc que les propriétés autorythmogènes du PréBötC notamment seraient

responsables de la genèse du "gasp", et qu'un « nœud vital » pour l'eupnée soit inexistant. De plus, les approches *in vitro* permettant d'appréhender les mécanismes de rythmogenèse endogène ne sont réalisables qu'en période périnatale, et donc sur un réseau respiratoire immature ne possédant pas encore toutes ses caractéristiques plastiques fonctionnelles. Chez l'animal adulte, plusieurs expériences visant à détruire le PréBötC ont induit des apnées transitoires, mais avec ensuite un retour d'activité respiratoire de type eupnéique (St-Jacques and St-John, 1999; Krause et al., 2009). D'autres études ont effectué des destructions de sous-types neuronaux du PréBötC, comme les neurones exprimant le récepteur à la NK1, ou les neurones somatostatinergiques, résultant dans le premier cas en une respiration ataxique, et dans le deuxième cas en une apnée de longue durée (Gray et al., 2001; Tan et al., 2008). Ces études réalisées en conditions aiguës ne précisent pas si un retour à une respiration eupnéique se fait après un certain temps.

1.3 - Vers une conciliation entre les deux grandes écoles de la rythmogenèse respiratoire ?

Les deux paragraphes précédents ont illustré, de manière volontairement appuyée, l'antagonisme conceptuel rencontré depuis plusieurs décennies dans la communauté scientifique s'intéressant à la rythmogenèse respiratoire. Ce débat est issu des deux grandes écoles de pensée, l'école « réseau » *in vivo* et l'école « pacemaker » *in vitro*. La première école de pensée, historiquement plus ancienne, soutient que la rythmogenèse respiratoire est une propriété émergente de réseau, principalement due à des inhibitions réciproques entre les neurones respiratoires, ce modèle étant soutenu par des expérimentations *in vivo* chez l'animal adulte (Richter, 1982; Bianchi et al., 1995; Haji et al., 2000; Ezure, 2004). La seconde école de pensée est apparue après la découverte *in vitro* de neurones respiratoires présentant des propriétés "pacemaker" endogènes au sein du PréBötC (Smith et al., 1991). L'antagonisme scientifique entre ces deux écoles a provoqué ces dernières années la conduite d'un nombre conséquent de travaux, visant à raffiner le concept de rythmogenèse respiratoire. Notamment, le rôle purement "pacemaker" de certains neurones pour leur contribution à la rythmogenèse a été revu, et comme présenté dans le paragraphe 1.1, la notion de "group pacemaker" a été proposée. De même, il n'existerait pas un oscillateur, mais deux oscillateurs couplés (Janczewski and Feldman, 2006; Pagliardini et al., 2011).

Il semblerait aujourd'hui qu'une forme de consensus apparaisse (même s'il persiste

certains irréductibles dans chaque école de pensée), considérant que la rythmogenèse respiratoire évolue avec la maturation, reposant fortement sur des oscillateurs en période prénatale, puis sur des oscillateurs intégrés et sous-jacents à l'âge adulte. Par ailleurs, le rôle des influences synaptiques inhibitrices est primordial au sein du réseau dans son intégralité, permettant notamment le couplage entre les deux oscillateurs (Iizuka, 1999).

Il est évident que dans la mesure du possible, l'étude du fonctionnement du CPG respiratoire *in vivo* est préférentielle, car elle en conserve la réalité physiologique. Mais les préparations *in vitro*, et en particulier la préparation "en bloc", ont tout de même contribué de manière majeure à l'avancée des connaissances sur la commande centrale respiratoire ces dernières années. Cette avancée des connaissances ne peut se faire que *via* des innovations expérimentales, qui seront forcément accompagnées d'inconvénients qu'il faut garder à l'esprit et chercher à atténuer, mais dont il ne faut surtout pas se priver car engendrant bien souvent de nouveaux paradigmes expérimentaux et conceptuels. Ainsi, un parallèle peut être fait avec la genèse de souris transgéniques, dont le rapport intérêts/inconvénients est parfois critiqué par les physiologistes, mais qui a permis des avancées considérables ces dernières années dans tous les domaines des sciences biologiques, et dont les techniques se sont raffinées avec notamment l'apparition des transgenèses conditionnelles (*via* le système Cre-lox) ce qui en diminue considérablement les faiblesses.

Nota Bene : dans cette thèse, nous nous sommes intéressés essentiellement à l'activité respiratoire eupnéique chez l'animal adulte étudié en condition in vivo, conservant au maximum l'intégrité (et la complexité) du réseau respiratoire (Duffin, 2003). Toutefois, nous avons également mis à profit les avantages uniques des préparations in situ et in vitro afin de simplifier la problématique et de pouvoir étudier certains mécanismes à différents stades maturationnels et à différents niveaux d'intégration.

2 - Maturation postnatale et "apprentissage" respiratoire

2.1 - Maturation postnatale du système respiratoire

Pour sa survie, un nouveau-né doit être capable à la fois de respirer et de se nourrir, ce qui suppose donc un CPG respiratoire suffisamment mature pour générer une commande nerveuse appropriée aux besoins énergétiques de l'organisme et coordonnée avec celle des autres CPG, déglutiteurs entre autres. Ainsi, les trois phases du cycle respiratoire nécessaires à la plasticité fonctionnelle de la respiration sont présentes dès sa naissance (Fung and St John, 1995; Dutschmann et al., 2000). Cependant, la maturation du CPG respiratoire se poursuit pendant la phase postnatale, dépendante d'interactions avec l'environnement et d'expériences qui vont permettre l'achèvement de son apprentissage respiratoire. A sa naissance, le nouveau-né passe d'un environnement placentaire normé, où les variations en O_2/CO_2/pH et nutriments sont tamponnées par l'organisme de la mère, à un environnement aérien changeant. Un fœtus, dans le placenta, est dans une situation de relative hypoxémie (avec une pression partielle artérielle en O_2, PaO_2, de 25-30 mmHg), parfois qualifiée de « mont Everest *in utero* » (Eastman, 1954), mais seulement relative car en fait adaptée à la consommation d'O_2 du fœtus et permettant le développement fœtal (Abu-Shaweesh, 2004). L'augmentation de PaO_2 à la naissance provoque notamment le "resetting" (forme de réinitialisation) des corps carotidiens, CC (Carroll, 2003), qui sont les principaux chémorécepteurs périphériques ajustant la commande respiratoire à la PaO_2 par une excitation tonique et modulable des centres respiratoires (cf. chapitre 3.2 pour une description de la chémosensibilité dans le système respiratoire). Ce "resetting" est caractérisé par un arrêt de l'excitation tonique des CC sur les centres respiratoires à la naissance, puis par sa reprise et son augmentation à la fois en normoxie et en hypoxie dans les quelques jours suivant la naissance (Blanco et al., 1984). Ce "resetting" est un exemple parmi d'autres de l'influence postnatale du nouvel environnement gazeux sur le système respiratoire.

L'influence postnatale des facteurs environnementaux se produit sur un réseau respiratoire fonctionnel mais encore immature, dont les caractéristiques électrochimiques, l'arborisation dendritique, les connections synaptiques ainsi que le nombre de neurones constituant par exemple le PréBötC ou les motoneurones commandant les différents muscles respiratoires, sont encore en évolution (Hilaire and Duron, 1999). Ainsi, alors que le développement prénatal du réseau respiratoire est sous fort contrôle génétique (avec des gènes

comme Kreisler, krox-20, hoxa1, Dbx1, Phox2b, Robo3, MafB etc. (Champagnat et al., 2011)), sa maturation postnatale est plutôt épigénétique. En effet, les expériences environnementales notamment gazeuses du nouveau-né vont modeler son réseau respiratoire et éventuellement laisser une empreinte pour le reste de sa vie. Par exemple, une hypoxie néonatale de 10 jours chez des rats perturbe la capacité de ces rats à s'acclimater à l'hypoxie à l'âge adulte, développant même des signes similaires au mal chronique des montagnes (Lumbroso and Joseph, 2009). Egalement, la période postnatale est le lieu d'expression de nombreuses pathologies respiratoires, comme le syndrome de mort subite du nourrisson (ou Sudden Infant Death Syndrome, SIDS). Première cause de mortalité d'enfants dans les pays industrialisés, le SIDS survient pendant le sommeil entre l'âge de 1 et 12 mois, serait causé par une défaillance transitoire, mais fatale, de la régulation respiratoire à l'hypoxie et/ou à l'hypercapnie, et serait lié à un défaut du système sérotoninergique (Kinney et al., 2009).

Après avoir vu dans le chapitre précédent (1) la mise en place prénatale du/des supposé(s) générateur(s) de rythme respiratoire, et avoir discuté leur contribution à l'eupnée, nous allons nous intéresser dans le paragraphe suivant (2.2) au rôle du pont dans la genèse de la post-inspiration.

2.2 - La post-inspiration, une phase cruciale du cycle respiratoire sous le contrôle du « centre pneumotaxique »

Le PréBötC isolé *in vitro* serait générateur de "gasp", ce qui n'exclut pas qu'il puisse jouer un rôle non négligeable pour la genèse de la phase inspiratoire pendant l'eupnée. Le BötC serait impliqué dans la phase expiratoire. Quant aux noyaux pontiques, ils semblent avoir un rôle considérable dans la phase post-inspiratoire de transition (cf. figures 5 et 6).

Lumsden fut le premier à remarquer qu'une section ponto-bulbaire créait un allongement important de la phase inspiratoire, avec un patron de décharge inspiratoire carré : l'apneuse (Lumsden, 1923a, 1923b, 1923c). Lumsden définit alors le pont comme étant le « centre pneumotaxique », ayant une influence sur l'arrêt de la phase inspiratoire. Le « centre pneumotaxique », appelé aujourd'hui groupe respiratoire pontique, comprend le noyau de Kölliker-Fuse (KF) et le complexe parabrachial (latéral, LPB, et médian, MPB). Pour étudier électrophysiologiquement l'influence de ces noyaux sur l'eupnée, il est nécessaire d'utiliser

des techniques expérimentales conservant l'intégrité du réseau respiratoire ponto-bulbaire. Trois techniques principales sont alors envisageables : l'animal anesthésié *in vivo*, l'animal non-anesthésié décérébré *in vivo*, et la préparation *in situ* cœur/tronc cérébral isolé perfusé (Working Heart Brainstem Preparation, WHBP) (Paton, 1996b, 1996a). La technique de WHBP possède des avantages majeurs, comme le fait que la préparation ne soit pas sous anesthésie, que les paramètres chimiques (O_2/CO_2/pH) soient normés expérimentalement, que les afférences périphériques chémosensibles soient maintenues, ou encore que l'accès au tronc cérébral soit aisé et permette de pratiquer des enregistrements cellulaires. Cette préparation présente une respiration de type eupnée, avec les trois phases du cycle respiratoire, et notamment si l'on sectionne le pont, on obtient un patron moteur apneustique (car les afférences pulmonaires ne sont plus présentes, la préparation étant paralysée et non ventilée). Egalement, cette technique a la particularité de mettre en exergue la décharge post-inspiratoire, notamment par rapport à l'animal anesthésié chez qui cette décharge est déprimée.

La phase post-inspiratoire est très importante pour la respiration, non seulement car elle permet de ralentir le flux aérien en début d'expiration et donc d'éviter un collapsus alvéolaire, mais aussi car elle est le lieu d'expression privilégié de la coordination entre respiration, vocalisation, déglutition, vomissement etc. (Paton et al., 1999; Shiba et al., 1999; Dutschmann et al., 2004; Gestreau et al., 2005; Bianchi and Gestreau, 2009b). Le début de la post-inspiration est caractérisé par un arrêt net de la phase inspiratoire, appelé "off-switch" inspiratoire, dont le mécanisme évolue avec la maturation postnatale. En effet, la commande centrale respiratoire est en permanence modulée par des afférences notamment pulmonaires (voir chapitre 3, paragraphe 2.4 de cette introduction pour une description plus détaillée), en l'occurrence des récepteurs à l'étirement pulmonaire. Ces récepteurs pulmonaires, activés par l'inflation des poumons lors de l'inspiration, projettent, via le nerf vague, sur le NTS, qui lui-même projette largement sur le KF et le PB (Loewy and Burton, 1978; Ricardo and Koh, 1978; Kubin et al., 2006). Cependant, l'influence des récepteurs à l'étirement pulmonaire pour l'"off-switch" inspiratoire est plus importante chez le nouveau-né que chez l'adulte, chez qui les mécanismes centraux semblent dominer (Mortola et al., 1984; Trippenbach, 1994). Le KF serait largement impliqué dans la genèse centrale de l'"off-switch" inspiratoire, et plus généralement dans la genèse de la phase post-inspiratoire. En effet, chez des animaux vagotomisés et donc privés d'afférences pulmonaires, des lésions ou suppressions pharmacologiques de la neurotransmission dans le KF causent l'apparition d'un patron moteur respiratoire apneustique (Richter, 1982; Morrison et al., 1994; St-John, 1998;

Dutschmann and Herbert, 2006; Smith et al., 2007), alors que la stimulation électrique du KF déclenche l'"off-switch" inspiratoire (Oku and Dick, 1992; Chamberlin and Saper, 1994; Dutschmann and Herbert, 1996, 2006; Okazaki et al., 2002). De plus, l'apnée causée par des lésions du KF est associée à une perte motrice de la phase post-inspiratoire, alors qu'une stimulation du KF entraîne une activité motrice post-inspiratoire prolongée (Dutschmann and Herbert, 2006). Ainsi, les récepteurs à l'étirement pulmonaire et le KF coordonnent la phase post-inspiratoire, avec une prédominance de chacun qui évolue avec la maturation.

La preuve la plus évidente de cet effet maturationnel sur la gestion de la phase post-inspiratoire a été apportée par une étude récente (Dutschmann et al., 2009). Il a été montré que la stimulation des récepteurs à l'étirement pulmonaire chez le rat nouveau-né (<P15) provoque le déclenchement stéréotypé de l'"off-switch" inspiratoire, alors que chez le rat juvénile (>P15), un ajustement progressif des paramètres respiratoires apparaît, menant à un "off-switch" inspiratoire anticipatoire, précédant la stimulation des récepteurs à l'étirement pulmonaire. De plus, le fait de bloquer les récepteurs NMDA dans le KF chez les rats juvéniles abolit l'"off-switch" inspiratoire anticipatoire, et rétablit un déclenchement stéréotypé par la stimulation des récepteurs à l'étirement pulmonaire. Il est donc supposé une forme de plasticité Hebbienne au sein du KF, où la répétition des stimulations du KF par les fibres des récepteurs à l'étirement pulmonaire via les projections du NTS provoquerait une forme d'"apprentissage" post-inspiratoire. Ce dernier confèrerait une plasticité accrue au système respiratoire, notamment pour l'intégration et le développement de coordinations complexes comme la respiration lors de l'exercice physique ou lors de la vocalisation (Dutschmann et al., 2004).

Au-delà de ce rôle crucial du groupe respiratoire pontique et surtout du KF pour la genèse de la post-inspiration, il a été montré qu'il existe des activités rythmiques endogènes dans le pont. Pendant l'eupnée, la branche mylohyoïde du nerf trijumeau, dont les corps cellulaires sont dans le pont, est active pendant la phase post-inspiratoire. Mais, après section ponto-bulbaire, il est possible d'enregistrer des décharges rythmiques spontanées sur le nerf mylohyoïde indépendantes des décharges du nerf phrénique (St John and Bledsoe, 1985; Huang and St John, 1988). Rien ne permet d'affirmer que les décharges rythmiques du nerf mylohyoïde après section ponto-bulbaire sont de type respiratoire (elles pourraient être masticatoires) (St-John and Paton, 2004). Cependant, elles démontrent qu'il est possible de faire apparaître expérimentalement une activité rythmique endogène dans une région respiratoire autre que bulbaire, ce qui donne encore plus de poids à la nécessité d'étudier le réseau respiratoire dans toute son intégrité pour l'analyse de l'eupnée.

3 - Le Syndrome de Rett, une pathologie neurodéveloppementale qui altère la respiration

Le Syndrome de Rett (SR) est une maladie rare, de type neurodéveloppemental, qui s'accompagne de troubles respiratoires sévères (voir plus loin). La période de maturation postnatale du réseau respiratoire semble critique pour la plasticité fonctionnelle du CPG respiratoire et tout particulièrement pour celle de la phase post-inspiratoire qui passe d'une activité réflexe induite par les retours afférents des récepteurs à l'étirement pulmonaire, à une activité générée centralement et régulée par les retours afférents. Cette maturation de la commande post-inspiratoire permettrait une interaction du réseau respiratoire plus fine avec d'autres commandes comme la déglutition ou la vocalisation (cf. chapitre 3.3). Ainsi, une pathologie neurodéveloppementale comme le SR peut perturber la maturation du système respiratoire, provoquer des altérations respiratoires dramatiques et altérer la coordination entre respiration, vocalisation et déglutition (Isaacs et al., 2003).

3.1 - Signes cliniques du syndrome de Rett et mutations du gène *MECP2*

En 1966, un pédiatre autrichien nommé Andreas Rett a décrit pour la première fois une pathologie de l'enfant qui ne sera reconnue que 17 ans plus tard par le corps médical et alors appelée syndrome de Rett (SR) (Rett, 1966; Hagberg et al., 1983). Le SR est une pathologie génétique liée au chromosome X qui ne permet pas aux garçons de survivre au-delà de l'âge de 1 an et qui, chez la femme, représente 2 à 3% de l'ensemble des cas de retard mental sévère et 10% des cas de retard mental profond (Armstrong, 1997).

Les patientes atteintes du SR ont un développement périnatal apparemment normal jusqu'à l'âge de 6-18 mois, incluant par exemple l'acquisition de la marche (Chahrour and Zoghbi, 2007). Ensuite, une cascade de symptômes se développe par étapes (cf. figure 9), l'un des premiers étant une décélération de la croissance crânienne, qui aboutit à une microcéphalie dès la 2ème année de vie. Le développement des patientes est alors ralenti, puis s'arrête et les acquisitions éventuelles comme la marche se perdent. Avec la progression du SR, les patientes perdent l'usage correct de leurs mains et développent des mouvements stéréotypés comme ceux de lavage, de battement ou encore de frottement. Les patientes présentent de nombreux symptômes autistiques, comme le retrait social, la perte d'expressions faciales, le manque de contact visuel etc. (Nomura, 2005). Egalement, les

patientes perdent leur coordination motrice et leur tonicité musculaire, présentent généralement une scoliose importante, et souffrent de crises d'épilepsie (Jian et al., 2006). Le système nerveux autonome est affecté par le SR, avec des troubles respiratoires sévères mais aussi une altération de la régulation cardiovasculaire et gastrointestinale (Katz et al., 2009). Environ 25% des décès des patientes atteintes du SR pourraient être dus à ces dysfonctionnements cardiorespiratoires (Kerr et al., 1997; Kerr and Julu, 1999).

L'origine génétique du SR a été découverte en 1999, au moins 95% des cas typiques de SR résultant d'une perte de fonction du gène codant pour la protéine 2 liée au méthyl-CpG (protéine MeCP2, gène *MECP2*), une protéine régulant l'expression d'autres gènes par la répression transcriptionnelle (Amir et al., 1999; Willard and Hendrich, 1999; Gura, 1999; Shahbazian et al., 2002; Klose and Bird, 2006). Un grand nombre de mutations du gène *MECP2* sont associées au SR, leur découverte ayant permis l'élaboration de modèles murins transgéniques qui reproduisent une grande partie du phénotype humain (Shahbazian et al., 2002; Chahrour and Zoghbi, 2007).

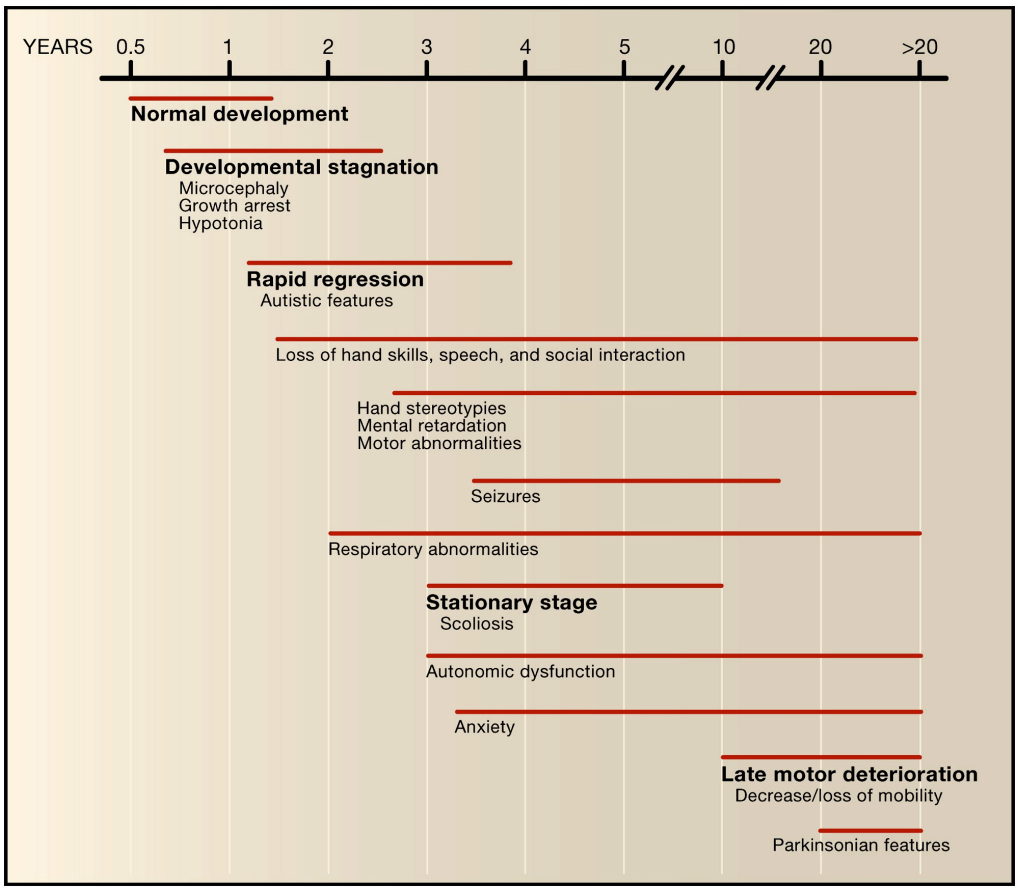

Figure 9 : début et progression du phénotype clinique du Syndrome de Rett.

3.2 - Syndrome de Rett et troubles respiratoires

Des troubles sévères de la respiration touchent toutes les patientes atteintes par le SR au cours de leur existence, avec des phases de respiration apneustique, et surtout des périodes d'hyperventilation et d'apnées qui pourraient être volontaires (blocage de la respiration) ou inconscientes (Elian and Rudolf, 1991; Julu et al., 2001; Cass et al., 2003; Weese-Mayer et al., 2006, 2008). Ces arythmies respiratoires sont intrigantes car elles dépendent de l'état de veille des patientes. La respiration est beaucoup moins altérée pendant le sommeil que pendant la veille, avec des périodes de régularité et de sévères anomalies du rythme en fonction du niveau d'éveil et d'excitation de la patiente (Kerr et al., 2001; Weese-Mayer et al., 2008; Katz et al., 2009). Cette relation entre altérations respiratoires et niveau d'éveil suggère que dans le SR, la rythmogenèse respiratoire n'est pas intrinsèquement altérée mais que les régulations respiratoires sont perturbées (Elian and Rudolf, 1991; Marcus et al., 1994; Katz et al., 2009).

Chez les souris transgéniques modèles de SR (plusieurs modèles existent, le plus répandu possédant une délétion exonique du gène *Mecp2*), les troubles respiratoires apparaissent vers P30, et de plus en plus d'apnées se développent avec l'âge, conduisant au décès vers l'âge de deux mois (Viemari et al., 2005b). L'analyse de la respiration de ces souris *in situ*, avec la technique de tronc cérébral-isolé-perfusé, a montré que la respiration erratique et les apnées sont principalement la conséquence d'une altération de la phase post-inspiratoire avec des fermetures prolongées de la glotte, ce qui pourrait être également la cause de la perte du langage et des altérations de la déglutition chez les patientes (Isaacs et al., 2003; Stettner et al., 2007, 2008). Des troubles neurochimiques complexes semblent être la cause de ces altérations respiratoires. Le système bioaminergique (cf. chapitre suivant) est particulièrement affecté à la fois chez les patientes et chez les souris modèles du SR (Nomura et al., 1985; Zoghbi et al., 1985, 1989; Dunn and MacLeod, 2001; Dunn, 2001; Ide et al., 2005; Viemari et al., 2005b; Ladas et al., 2009; Isoda et al., 2010; Panayotis et al., 2011). D'ailleurs, la désipramine, un inhibiteur de la recapture de la noradrénaline, améliore le phénotype respiratoire et prolonge la durée de vie des souris modèles du SR (Zanella et al., 2008; Roux et al., 2008). De même, le 8-hydroxy-2-(di-n-propylamino)tetralin (8-OH-DPAT), un agoniste des récepteurs 1A à la sérotonine, réduit les apnées, corrige l'irrégularité respiratoire et prolonge la survie des souris modèles du SR (Abdala et al., 2010). Egalement, d'autres neurotransmetteurs sont altérés par le SR, comme le Facteur Neurotrophique Dérivé du Cerveau (BDNF), présentant d'autres pistes potentielles de traitement des pathologies

respiratoires du SR (Wang et al., 2006; Ogier et al., 2007; Katz et al., 2009; Kline et al., 2010). Enfin, les découvertes les plus récentes concernent le système GABAergique, dont l'atteinte pourrait être responsable notamment du phénotype autistique associé au SR, et dont l'augmentation pharmacologique dans le cerveau des souris modèle du SR induit une amélioration marquée du phénotype respiratoire (Abdala et al., 2010; Voituron and Hilaire, 2011).

Nota Bene : dans cette thèse, nous montrons que les troubles respiratoires des souris modèle du SR peuvent être observés dès P15, donc en période pré-symptomatique, après un soupir spontané, et être provoqués transitoirement par une hypoxie ou une hypercapnie modérées, ce qui révèle l'importance des régulations du CPG respiratoire dans le déclenchement et le développement de la pathologie. Egalement, nous montrons que ces souris au cours de la phase terminale de la maladie présentent une grande proportion d'apnées obstructives, pendant lesquelles la pompe respiratoire lutte, inefficacement, contre la fermeture totale des VAS, ce qui peut précipiter le décès (cf. partie résultats, chapitre 1).

III - Régulations et plasticité respiratoires

Tout l'enjeu de la commande centrale respiratoire est de générer une respiration alvéolaire permettant le maintien de l'homéostasie gazeuse sanguine. Or la consommation énergétique de l'organisme fluctue énormément, avec les phases d'éveil et de sommeil, l'activité physique, le repos, l'altitude, la température, etc., provoquant des variations importantes et rapides du pH et des pressions partielles en O_2 et CO_2 sanguins. La respiration est une fonction physiologique très régulée, à la fois par des mécanismes centraux et périphériques, impliquant des régions anatomiques distinctes et des modes de transmissions variés.

1 - Les bioamines, modulateurs privilégiés de la respiration

Les bioamines, une famille de neurotransmetteurs comprenant les catécholamines et la sérotonine, régulent un grand nombre d'activités neurophysiologiques, des cycles veille/sommeil à la prise alimentaire, et sont également impliquées dans la maturation et la modulation du réseau respiratoire.

1.1 - Les catécholamines

Les neurotransmetteurs catécholaminergiques sont issus du même acide aminé, la L-tyrosine. La tyrosine hydroxylase (TH), l'enzyme dite limitante de la chaîne de synthèse des catécholamines (Nagatsu et al., 1964), permet la synthèse de dihydroxyphénylalanine (L-DOPA), à partir de laquelle seront créées successivement la dopamine, la noradrénaline et l'adrénaline via des catalyses enzymatiques. Parmi ces différents neurotransmetteurs, la noradrénaline jouerait un rôle primordial dans la modulation de la commande centrale respiratoire.

Les neurones catécholaminergiques du tronc cérébral sont regroupés en noyaux, 5 noradrénergiques (A1, A2, A5, A6 et A7) et 3 adrénergiques (C1, C2 et C3) (cf. figure 10). Chez le chat *in vivo*, l'adrénaline et la noradrénaline modulent la respiration de façon principalement inhibitrice, en agissant directement sur les neurones respiratoires bulbaires

(Champagnat et al., 1979). Cependant, l'influence des catécholamines sur la respiration a principalement été mise en évidence *in vitro*. Les noyaux pontiques A5 et A6 sont particulièrement impliqués dans cette modulation, exerçant un rôle opposé (Hilaire et al., 2004). En effet, le noyau A5 exerce une inhibition permanente sur la commande centrale respiratoire, via les récepteurs adrénergiques α2 bulbaires (Hilaire et al., 1989; Errchidi et al., 1990, 1991; Viemari et al., 2003; Hilaire, 2006). Cet effet inhibiteur de A5 est présent dès la période prénatale (Di Pasquale et al., 1992; Viemari et al., 2003), et perdure chez l'animal adulte. Les neurones A5 présentent une modulation respiratoire (principalement post-inspiratoire) dans leur patron de décharge (Guyenet et al., 1993) et leur activation ralentit le rythme respiratoire *in vivo* (Jodkowski et al., 1997; Dawid-Milner et al., 2001). A l'inverse, le noyau A6 (Locus Cœruleus) exerce un effet facilitateur sur la commande centrale respiratoire, via les récepteurs adrénergiques α1 bulbaires (Viemari et al., 2004a, 2005a; Viemari and Tryba, 2009). Par contre, cette facilitation n'est démontrée que chez le nouveau-né *in vitro*, même si chez l'adulte il est probable qu'elle se maintienne, les neurones de A6 étant synaptiquement connectés au réseau respiratoire adulte (Dobbins and Feldman, 1994b) et présentant une modulation respiratoire (inspiratoire et post-inspiratoire) dans leur patron de décharge (Guyenet et al., 1993). Au niveau du bulbe rachidien, A1/C1 exercerait également un effet facilitateur *in vitro* sur la commande centrale respiratoire, alors que A2/C2 serait impliqué dans la stabilisation du rythme respiratoire (Hilaire, 2006; Zanella et al., 2006; Viemari and Tryba, 2009).

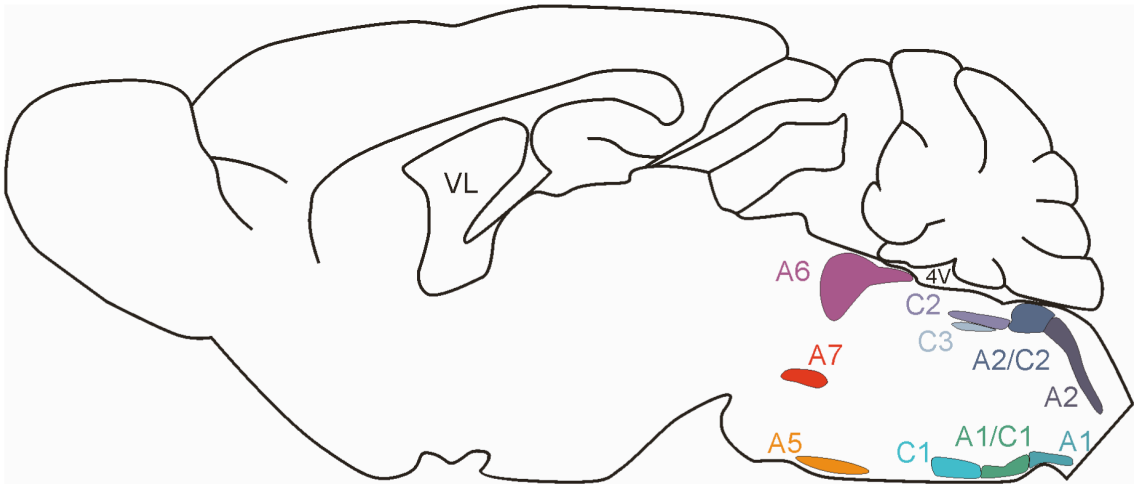

Figure 10 : Localisation des neurones catécholaminergiques du tronc cérébral de rat en vue sagittale. VL, ventricule latéral ; 4V, 4ème ventricule. (*Adapté de la thèse de Sébastien Zanella*).

Les noyaux catécholaminergiques ont ainsi un rôle majeur de frein ou d'accélérateur de la commande centrale respiratoire. Ces groupes sont également fortement impliqués dans la modulation respiratoire en réponse à un stimulus hypoxique ou hypercapnique, ce qui sera abordé en chapitre 3.2.

1.2 - La sérotonine

L'influence de la sérotonine (5-HT) sur la commande centrale respiratoire a fait l'objet notamment d'une revue présentée dans cette thèse (cf. partie résultats, chapitre 2, article 2). Le lecteur pourra se reporter à cette revue pour plus de détails sur le rôle de la 5-HT dans la physiologie et la pathologie respiratoires.

1.2.1 - Métabolisme de la 5-HT

La 5-HT (ou 5-hydroxytryptamine) a été initialement découverte dans le sang (Rapport et al., 1948), puis dans d'autres organes incluant le cerveau (Twarog and Page, 1953; Twarog, 1954; Amin et al., 1954). La synthèse de cette indolamine débute par la catalyse du L-tryptophane provenant de l'alimentation en 5-hydroxytryptophane (5-HTP), par la L-tryptophane hydroxylase (Tph) (cf. figure 11). Comme pour la TH dans la synthèse des catécholamines, la Tph est l'enzyme dite limitante de la chaîne de synthèse et dégradation de la 5-HT (Ichiyama et al., 1968). Ensuite, le 5-HTP est décarboxylé en 5-HT par la L-décarboxylase, enzyme également impliquée dans la décarboxylation de la L-DOPA lors de la synthèse des catécholamines. La 5-HT est alors stockée dans des vésicules synaptiques. Après sa libération et son action sur un grand nombre de récepteurs, la 5-HT est dégradée par la monoamine oxydase A (MAOA) en 5-hydroxyindole acétaldéhyde, lui-même dégradé par l'aldéhyde déshydrogénase en acide 5-hydroxyindole acétique (5-HIAA) qui est excrété dans l'urine. De plus, la 5-HT est aussi recapturée par le transporteur membranaire de la 5-HT SERT et emmagasinée dans des vésicules par le transporteur vésiculaire des monoamines Vmat2. La fluoxétine, un inhibiteur de la recapture de la 5-HT agissant sur SERT est un agent pharmacologique très utile pour augmenter les taux endogènes de 5-HT (cf. partie résultats, chapitre 2, article 3), qui est d'ailleurs le principe actif d'antidépresseurs tel le Prozac. On peut mesurer les taux de tryptophane, de 5-HT et de 5-HIAA dans le cerveau grâce à la technique de chromatographie liquide à haute pression (cf. partie résultats, chapitre 2 article 1,

et chapitre 3 article 2).

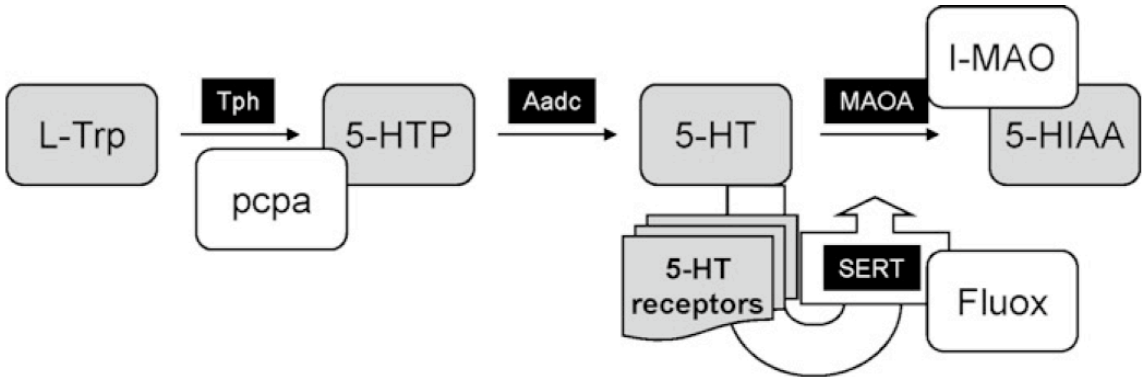

Figure 11 : représentation schématique du métabolisme de la sérotonine. Des agents pharmacologiques communs utilisés pour altérer le métabolisme de la sérotonine (5-HT) sont illustrés, comme la p-chlorophenylalanine (pcpa) qui bloque la synthèse de 5-HT, les inhibiteurs de la MAOA (I-MAO) qui bloquent la dégradation de la 5-HT, et l'antidépresseur fluoxétine (Fluox) qui bloque la recapture de la 5-HT. (*Adapté de Hilaire et al. 2010*).

1.2.2 - Anatomie du réseau sérotoninergique

Il existe actuellement 7 familles de récepteurs à la 5-HT, dont on distingue 15 sous-types de récepteurs ayant une structure et des propriétés pharmacologiques différentes. Les sous-types de récepteurs à la 5-HT forment d'ailleurs la plus grande famille de récepteurs aux neurotransmetteurs connue actuellement. La table 1 de l'article 2 en chapitre 2 de la partie résultats de cette thèse présente de manière approfondie ces différents sous-types de récepteurs. On notera 1) que tous les récepteurs à la 5-HT sont métabotropiques, couplés aux protéines G, à l'exception des récepteurs 5-HT_3 qui sont ionotropiques et 2) que la 5-HT peut aussi agir en dehors des synapses par des libérations des varicosités axonales "en passant", présentes dans presque tous les neurones sérotoninergiques (Leger et al., 2001; Moss et al., 2005).

La technique d'histochimie à fluorescence induite par le formaldéhyde a permis d'effectuer la première localisation des neurones 5-HT dans le système nerveux central de rat adulte (Dahlstrom and Fuxe, 1964). Des techniques plus récentes d'immunohistochimie ont augmenté la précision de la répartition anatomique des neurones 5-HT, même si l'organisation générale faite par Dahlstrom et Fuxe est toujours d'actualité (Steinbusch, 1981; Jacobs and Azmitia, 1992; Hornung, 2003). Les neurones 5-HT ont tous leurs corps cellulaires dans le tronc cérébral, dans des groupes distincts appelés les raphés (cf. figure 12).

Initialement définis caudo-rostralement de B1 à B9 (Dahlstrom and Fuxe, 1964), les raphés sont aujourd'hui plutôt identifiés par leur nom, les raphés pallidus, magnus et obscurus étant localisés dans le bulbe, le raphé pontin et la partie caudale du raphé dorsal étant dans le pont, et la partie rostrale du raphé dorsal ainsi que le raphé médian étant dans le mésencéphale. Les raphés reçoivent des afférences d'un grand nombre de structures du cerveau (Hermann et al., 1996, 1997), et notamment en ce qui concerne les structures neurovégétatives, venant de la substance grise périaqueducale (PAG), du noyau parabrachial (PB), du noyau de Kölliker-Fuse (KF) ou encore du noyau subcœruleus. Les neurones 5-HT projettent leurs axones sur l'ensemble du SNC, les raphés caudaux projetant principalement sur la moelle épinière et le bulbe, notamment sur les neurones de la colonne ventrale respiratoire et des groupes respiratoires pontiques, les raphés pontiques projetant sur le bulbe, les groupes respiratoires pontiques ainsi que le mésencéphale et des zones du cervelet, et les raphés mésencéphaliques projettent sur le diencéphale et le télencéphale (Steinbusch, 1981; Holtman et al., 1986, 1987; Holtman, 1988; Zhan et al., 1989; Smith et al., 1989; Connelly et al., 1989; Pilowsky et al., 1990; Voss et al., 1990; Jacobs and Azmitia, 1992; Manaker and Tischler, 1993; Jacobs and Fornal, 2000). Enfin, il est important de noter qu'il n'y a pas que des neurones 5-HT dans les raphés, on y trouve aussi des neurones notamment GABAergiques et glutamatergiques qui réguleraient l'activité des neurones 5-HT (Holmes et al., 1994; Monti, 2010a, 2010b).

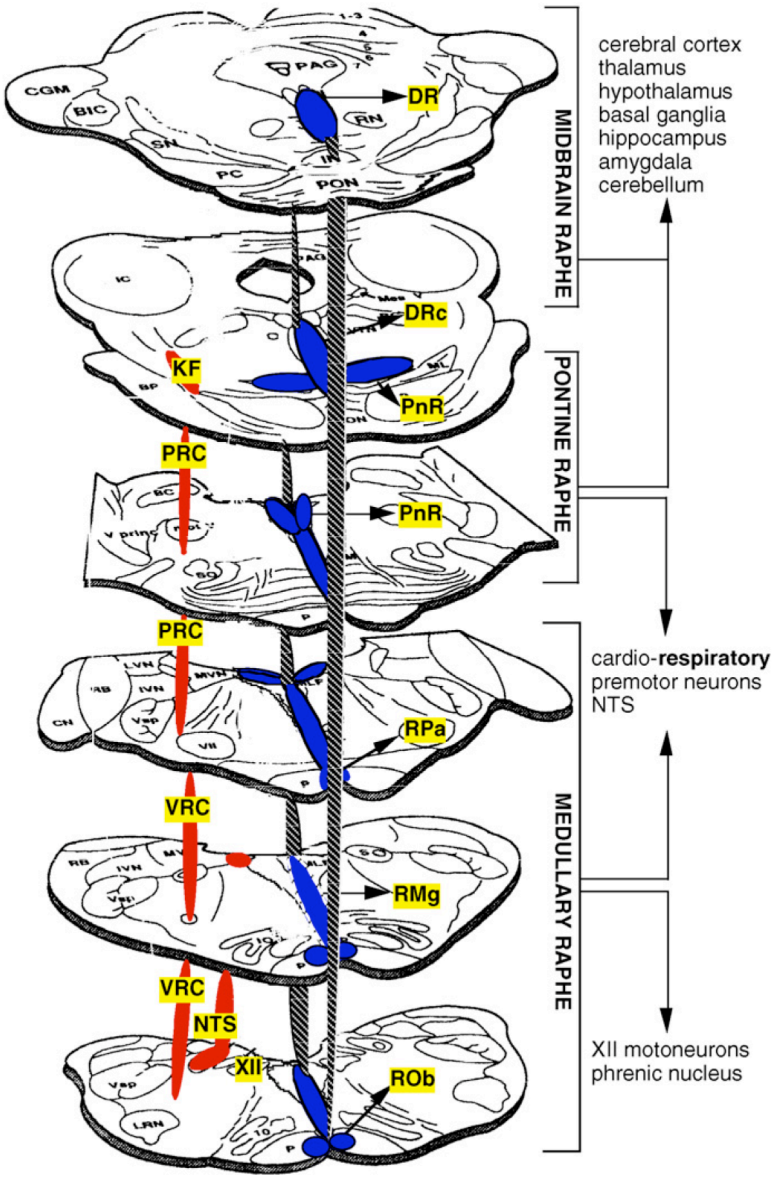

Figure 12 : distribution et connectivité des neurones sérotoninergiques dans le tronc cérébral. Les neurones synthétisant la 5-HT sont présents dans des groupes cellulaires distincts dans le tronc cérébral appelés les raphés. La ligne hachurée représente la structure en colonne des raphés le long de la ligne médiane. Les régions en rouge indiquent la colonne respiratoire. Rob, raphé obscurus ; RMg, raphé magnus ; RPa, raphé pallidus ; PnR, raphé pontin ; DRc, raphé caudal dorsal ; DR, raphé dorsal ; VRC, colonne ventrale respiratoire ; NTS, noyau du faisceau solitaire ; PRC, colonne pontique respiratoire ; KF, noyau de Kölliker-Fuse ; XII, noyau moteur de l'hypoglosse ; PAG, substance grise périaqueducale. (*Adapté de Hilaire et al. 2010*).

1.2.3 - Influence de la 5-HT sur le CPG respiratoire

Le rôle de la 5-HT dans le cerveau est difficile à appréhender. Jacobs et Fornal ont d'ailleurs écrit que la 5-HT est une « énigme », « virtuellement impliquée dans tout, mais responsable de rien » (Jacobs and Fornal, 2000). L'action de la 5-HT sur le système respiratoire a tout d'abord été démontrée comme agissant sur les structures périphériques envoyant des afférences sur le système respiratoire (principalement les corps carotidiens) (Reid and Rand, 1951; Douglas and Toh, 1953; Ginzel and Kottegoda, 1954). Une action centrale de la 5-HT sur les neurones respiratoires n'a pu être démontrée que plus tard, en

partie grâce aux approches *in vitro* qui permettent d'exclure tout effet périphérique (Fallert et al., 1979; Olson et al., 1979; McCrimmon and Lalley, 1982; Monteau et al., 1990; Morin et al., 1990a, 1992; Hilaire et al., 1993; Lalley et al., 1994, 1995, 1997). Une très grande diversité d'actions a été mise à jour, reflétant certainement encore mal l'importance du système sérotoninergique pour la respiration. *In vivo*, la 5-HT peut avoir un effet inhibiteur ou excitateur sur la fréquence respiratoire et même différentiel en fonction du type neuronal (Pre-I, I etc.), de la localisation des neurones, mais aussi du site d'injection (systémique, central, localisé sur certaines structures etc.), de la dose utilisée, du patron d'expression des différents sous-types de récepteurs, etc. (Fallert et al., 1979; Lalley et al., 1994, 1995, 1997; Manzke et al., 2003, 2008, 2009). Des expériences ont été menées *in vitro*, en particulier sur la préparation "en bloc", pour tenter de réduire la complexité du système. Il a été montré que la 5-HT facilite le réseau générateur du rythme respiratoire notamment via les récepteurs 5-HT_1 et les motoneurones phréniques via les récepteurs 5-HT_2 (Morin et al., 1990a, 1992; Lindsay and Feldman, 1993), et que les récepteurs 5-HT_{1B} localisés au niveau pré-synaptique modulent la transmission de la commande respiratoire aux motoneurones phréniques (Di Pasquale et al., 1997). Deux études ont également montré d'une part l'implication des récepteurs 5-HT_{4a} exprimés dans le PréBötC pour leur implication dans la dépression respiratoire induite par les opiacés (Manzke et al., 2003), et d'autre part l'abolition de cette dépression par une déphosphorylation de la sous-unité α3 des récepteurs à la glycine induite par l'activation des récepteurs 5-HT_{1A} (Manzke et al., 2010). Egalement, des propriétés "pacemaker" ont été montrées sur des neurones 5-HT, notamment du raphé dorsal, qui pourraient influencer la commande centrale respiratoire (Burlhis and Aghajanian, 1987; Aghajanian et al., 1990).

Cette thèse portant notamment sur l'atteinte de la coordination entre la pompe et la valve respiratoires, il est intéressant de noter que la 5-HT pourrait avoir des effets différents sur ces deux entités. En effet, la 5-HT appliquée *in vitro* sur la préparation "en bloc" potentialise l'activité inspiratoire du nerf phrénique alors qu'elle déprime celle du nerf hypoglosse, dépression passant par les récepteurs 5-HT_2 (Monteau et al., 1990, 1994; Morin et al., 1990b, 1992). Comme le nerf hypoglosse transmet entre autres la commande de protrusion de la langue pendant l'inspiration, facilitant le passage oral de l'air vers les VAS, la 5-HT pourrait ainsi être impliquée dans la formation d'apnées obstructives. Cette hypothèse a été confirmée *in vivo* : une augmentation de la 5-HT endogène déprime l'activité inspiratoire du muscle génioglosse, le protruseur de la langue (Morin et al., 1994), et un antagoniste aux récepteurs 5-HT_2 (le SR 46349B,) permet *in vitro* d'annuler l'effet dépresseur

sur l'hypoglosse (Monteau et al., 1994). Cependant, le système 5-HT est modulé au cours de la maturation, notamment pour l'expression de ses différents sous-types de récepteurs, mais aussi pour son rôle fonctionnel sur la respiration, passant d'un effet inhibiteur à un effet excitateur (Talley et al., 1997; Volgin et al., 2003; Hodges and Richerson, 2008a). L'hypoglosse exprime un nombre important de sous-types différents de récepteurs à la 5HT (Okabe et al., 1997; Fenik and Veasey, 2003), parmi lesquels les récepteurs 5-HT_2 (surtout 2A) semblent particulièrement importants pour sa modulation respiratoire (Schwarzacher et al., 2002; Zhan et al., 2002; Volgin et al., 2003). Chez l'animal adulte *in vivo*, l'injection d'antagonistes des récepteurs 5-HT_{2A} sur l'hypoglosse diminue fortement son activité respiratoire, alors que l'injection d'agonistes la potentialise (Fenik and Veasey, 2003; Brandes et al., 2006). Egalement, Besnard et collaborateurs ont montré *in vivo* sur le rat anesthésié que des agonistes aux récepteurs 5-HT_{1A} potentialisent l'activité du génioglosse, postulant qu'ils pourraient être utiles pour prévenir les apnées obstructives (Besnard et al., 2007, 2011). On notera cependant que ces auteurs ont aussi montré que des stimulations électriques à haute fréquence de la partie caudale du raphé pallidus induisent une tachypnée et une cessation de l'activité du muscle géniohyoïdien (Besnard et al., 2009), un muscle des VAS également innervé par l'hypoglosse. Ces résultats suggèrent donc que même chez l'adulte, la suractivation 5HT pourrait induire des apnées obstructives. Il est très difficile dans l'ensemble d'identifier les mécanismes d'actions exacts des divers agonistes et antagonistes 5HT pouvant agir à la fois en position pré et post-synaptique, pouvant moduler différentiellement chaque neurone et induire des cinétiques d'activations et/ou d'inhibitions peu maîtrisables.

L'altération du système sérotoninergique est fortement incriminée dans le Syndrome de Mort Subite du Nourrisson (SIDS) (Paterson et al., 2006, 2009; Duncan et al., 2010), et un défaut de maturation postnatale et de transition entre effet inhibiteur et excitateur de la 5HT sur l'hypoglosse pourrait contribuer au SIDS via l'occurrence d'apnées obstructives.

1.2.4 - Sérotonine et perspectives

Pour résumer, l'extrême complexité du réseau 5-HT, son grand nombre de récepteurs et ses actions multiples, sa très large arborisation anatomique, la multitude de techniques utilisées pour l'étudier etc., laissent encore de grandes interrogations. Par exemple, Besnard et collaborateurs ont montré que la stimulation à haute fréquence du raphé obscurus chez le rat anesthésié induit une apnée (Besnard et al., 2009), et Depuy et collaborateurs ont montré sur

la souris anesthésiée que la stimulation optogénétique (par les channelrhodopsin-2) du raphé obscurus induit une augmentation de la fréquence et de l'amplitude respiratoires (Depuy et al., 2011). Il se pourrait qu'il existe des différences inter-spécifiques des effets de la 5-HT sur le système respiratoire, comme le suggèrent les expériences réalisées chez le chat et le chien et conduisant à des résultats opposés (Douglas and Toh, 1953; Ginzel and Kottegoda, 1954), mais aussi que les protocoles expérimentaux ne soient pas encore assez spécifiques pour avoir la certitude du type de neurone, de récepteur 5-HT, de métabolite sérotoninergique manipulé et étudié.

Nota Bene : dans cette thèse, nous avons notamment poursuivi la dynamique de recherche sur les effets de la 5-HT sur le système respiratoire développée par Gérard Hilaire depuis de nombreuses années. Chez la souris, nous nous sommes particulièrement intéressés à la modulation sérotoninergique de la réponse à l'acidose du CPG respiratoire du nouveau-né (étude in vitro ; cf. partie résultats, chapitre 2, article 3), à l'influence de la 5-HT sur le phénotype respiratoire de deux souches de souris très utilisées pour les modèles transgéniques (étude in vivo ; cf. partie résultats, chapitre 2, article 1), et à l'altération du système sérotoninergique et à son implication potentielle pour la respiration pathologique d'un modèle murin de tauopathie (étude in vivo ; cf. partie résultats, chapitre 3, article 2).

2 - Chémosensibilité, réponses respiratoires à l'hypoxie et à l'hypercapnie, et réflexe de Hering-Breuer

La fonction première de la respiration alvéolaire est de maintenir l'homéostasie gazeuse sanguine, assurant avec le système circulatoire l'apport en O_2 aux cellules et l'excrétion du CO_2 produit. La consommation en O_2 peut varier considérablement ; chez l'Homme, elle est environ de 4 ml/min/kg au repos mais peut atteindre 35-40 ml/min/kg lors de l'exercice chez les individus non entraînés et jusqu'à 90-100 ml/min/kg chez des sportifs de haut niveau en sports d'endurance. Egalement, la pression partielle atmosphérique en O_2 n'est pas stable ; elle diminue exponentiellement avec l'altitude, réduisant les échanges alvéolo-capillaires en O_2 pour un même débit ventilatoire. Ces variations de consommation et de disponibilité en O_2 modifient les pressions partielles artério-veineuses en O_2 et CO_2 ainsi que le pH sanguin. En réponse à ces altérations de l'homéostasie gazeuse sanguine, le niveau d'activité du système respiratoire est régulé via des effecteurs périphériques et centraux.

La valeur physiologique de la pression partielle artérielle en O_2 (PaO_2) chez les mammifères est comprise entre 80 et 100 mmHg (Feldman, 1986; Gonzalez et al., 1994). Lorsque la PaO_2 diminue en dessous de 80 mmHg, la ventilation est augmentée en fonction du degré d'hypoxie et suivant plusieurs stades. En phase aigue, la réponse ventilatoire à l'hypoxie (RVH) se caractérise par une augmentation très importante de la ventilation, puis après quelques minutes, cette hyperventilation s'atténue mais reste toujours à un niveau supérieur aux valeurs pré-hypoxiques chez l'adulte, alors que chez le nouveau-né elle diminue sous les valeurs pré-hypoxiques (Teppema and Dahan, 2010). Cette diminution secondaire de la ventilation est appelée dépression ventilatoire relative ou "roll-off". Si l'hypoxie persiste, devenant une hypoxie chronique, il existe un troisième stade de RVH dans lequel la ventilation va de nouveau augmenter au-dessus des valeurs de ventilation du "roll-off", mais en dessous des valeurs maximales d'hyperventilation aiguë. Cette "re-augmentation" est expliquée par les processus d'acclimatation à l'hypoxie, qui induisent un remodelage biologique avec, par exemple, un tamponnage partiel de l'alcalose respiratoire induite par l'hyperventilation qui contribue à la diminution secondaire de la RVH. Une autre possibilité est l'expression accrue de nombreux gènes via le facteur de transcription HIF-1 (Facteur Induit par l'Hypoxie 1) et notamment celui de l'érythropoïétine (cf. paragraphe 2.3). Un plateau est atteint lors de cette acclimatation ventilatoire à l'hypoxie. En ce qui concerne la réponse ventilatoire à l'hypercapnie (RVHC), l'augmentation de la ventilation est très importante et ne possède pas de diminution marquée avec le temps, il n'existe pas de condition physiologique générant une hypercapnie chronique. On notera que le stimulus hypercapnique est supérieur au stimulus hypoxique dans l'activation respiratoire qu'il induit.

2.1 - Sensibilité périphérique à l'O_2, au CO_2 et au pH

Le réseau neuronal générant le CPG respiratoire est en permanence activé par des afférences toniques venant principalement des corps carotidiens (CC), mais aussi des corps aortiques et des corps neuroépithéliaux. Cette activation tonique périphérique représenterait plus de la moitié du tonus stimulant la respiration en condition eupnéique normoxique et normocapnique (Blain et al., 2009; Smith et al., 2010), et elle est modulée à la baisse ou à la hausse en fonction des concentrations artérielles en O_2 principalement, mais aussi, dans une moindre mesure, en CO_2 et en pH.

Les CC, dont la contribution à la respiration a été montrée dès 1930 (Heymans and

Bouckaert, 1930), sont situés à la bifurcation des artères carotides et sont un des organes les plus irrigués en sang (cf. figure 13) (López-Barneo et al., 2008). Leur parenchyme est organisé en glomeruli, où des groupes de cellules sont en contact étroit avec un dense réseau de capillaires. Les cellules principales des glomeruli des CC sont les cellules glomiques (ou cellules de type I), qui sont similaires à des neurones et sont les cellules chémosensibles connectées aux fibres afférentes du nerf de Hering (ou nerf du sinus carotidien), qui lui-même rejoint le nerf glossopharyngien. Ces afférences périphériques projettent directement dans le NTS, qui distribue ensuite l'information à des sites multiples généralement eux-mêmes chémosensibles comme le RTN, les raphés médullaires, le locus cœruleus, A1/C1 ou encore le PréBötC, notamment via des excitations glutamatergiques (Housley et al., 1987; Arango et al., 1988; Finley and Katz, 1992; Takakura et al., 2006b; Rosin et al., 2006a; Nuding et al., 2009; Nattie and Forster, 2010; Smith et al., 2010). Un deuxième type de cellules existe dans les CC, ce sont les cellules sustentaculaires (ou cellules de type II), similaires à des cellules gliales, qui jouent le rôle de cellules de soutien enveloppant les cellules glomiques, même si un rôle plus subtil n'est pas exclu.

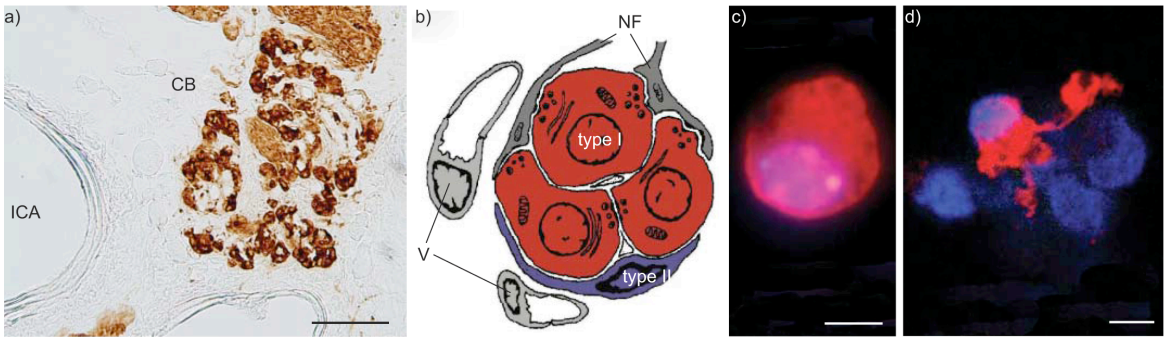

Figure 13 : organisation anatomique d'un corps carotidien (CC). a) : section histologique de la bifurcation carotidienne de souris marquée avec un anticorps dirigé contre la tyrosine hydroxylase (TH, couleur marron) ; CB, corps carotidien ; ICA, artère interne carotide. b) : représentation schématique d'un glomerulus de CC indiquant les cellules de type I et de type II, les vaisseaux sanguins (V) et les fibres nerveuses sensorielles afférentes (NF). c) : Apparence d'une cellule glomique de type I de rat positive au marquage TH. d) : apparence d'une cellule gliale de type II positive pour la protéine fibrillaire acidique (GFAP). Les noyaux cellulaires sont marqués avec le 4',6-diamidino-2-phenylindole. Barres d'échelle : 100 µm (a) et 5 µm (c et d). (*Adapté de López-Barneo et al. 2008*).

Lors d'une baisse de la PaO_2, l'excitation des fibres sensorielles du nerf de Héring par les cellules glomiques augmente, résultant en une hyperventilation (Biscoe et al., 1970; Vizek et al., 1987). Le ou plus probablement les mécanismes responsable(s) de la chémosensibilité des CC font débat (Teppema and Dahan, 2010). Les cellules glomiques expriment de

nombreux types de canaux potassiques, et notamment des canaux potassiques de fuite indépendants du voltage de la famille des domaines à deux pores, les canaux TASK-1 et -3 (canaux K^+ Sensibles à l'Acide TWIK-reliés) (Yamamoto et al., 2002; Buckler, 2007; Trapp et al., 2008). Ces canaux TASK contribuent au maintien du potentiel de membrane, leur fermeture bloquant l'efflux de K^+ et entraînant une dépolarisation de la membrane cellulaire. Le canal TASK-1 en particulier semble impliqué dans la chémosensibilité des CC (cf. figure 14) (Buckler, 2007; Trapp et al., 2008). Ce canal est sensible aux variations de pH et de concentrations en O_2. De plus, de nombreux candidats senseurs d'O_2 comme l'inhibition du métabolisme mitochondrial et la genèse accrue de radicaux libres de l'O_2, la NADPH oxydase (Nicotinamide Adénine Dinucléotide Phosphate), l'hème oxygénase 2 ou encore la voie de l'AMPK (protéine Kinase activée par l'Adénosine MonoPhosphate), concourent tous à la fermeture de canaux potassiques et notamment TASK-1 (Wyatt and Peers, 1995; Lahiri et al., 1999; Gonzalez et al., 2004, 2007; Wyatt and Buckler, 2004; Williams et al., 2004; Evans et al., 2005; Acker, 2005; Lee et al., 2006; Wyatt and Evans, 2007; Varas et al., 2007). La dépolarisation membranaire induite par la fermeture des canaux potassiques de fuite provoque un influx calcique dans les cellules glomiques via des canaux calciques voltage-dépendants (Long et al., 1993; Gonzalez et al., 1994; Lopez-Barneo et al., 2001; Rocher et al., 2005; Weir et al., 2005; López-Barneo et al., 2008). Il s'ensuit une libération vésiculaire synaptique d'ATP et d'acétylcholine notamment par les cellules glomiques, qui vont exciter les fibres afférentes du nerf de Hering (Nurse and Zhang, 2001; Prasad et al., 2001; Varas et al., 2003; Iturriaga and Alcayaga, 2004; Nurse, 2005; Reyes et al., 2007). L'information est ainsi transmise aux centres respiratoires via le NTS (cf. plus haut), mais ici encore il y a débat en ce qui concerne un effet hypoadditif ou hyperadditif de la chémosensibilité périphérique et de la chémosensibilité centrale (Smith et al., 2010).

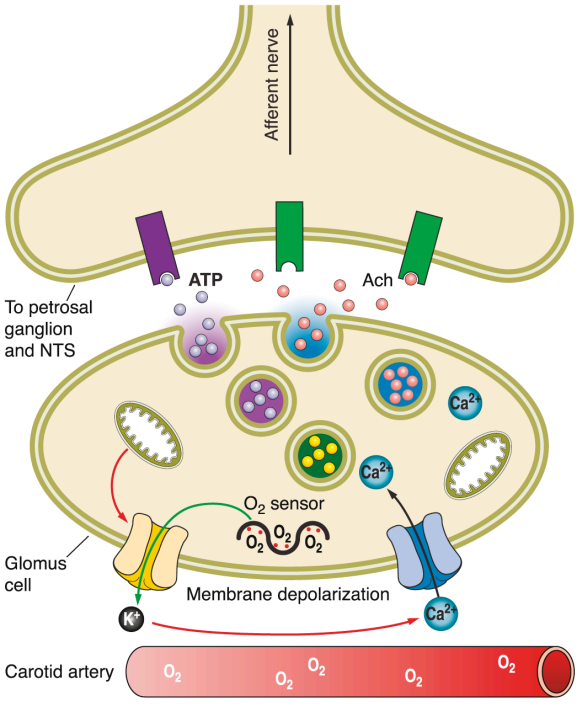

Figure 14 : cascade de transduction du signal des cellules sensibles à l'oxygène dans les corps carotidiens en hypoxie. (*Adapté de Teppema and Dahan 2010*).

2.2 - Sensibilité centrale à l'O_2, au CO_2 et au pH

2.2.1 - Sensibilité centrale à l'O_2

L'existence d'une sensibilité centrale à l'O_2 participant à la RVH, qui a longtemps été un sujet de débat, est relativement acceptée aujourd'hui. Il est généralement admis que la dépression ventilatoire relative suivant la phase initiale d'hyperventilation lors d'une hypoxie est due à la sensibilité centrale à l'O_2 et à son impact sur les centres respiratoires (Teppema and Dahan, 2010). Chez le chat et le rat anesthésiés et non-anesthésiés, l'hypoxie entraîne une dépression respiratoire après une chémodénervation des CC *via* une transsection bilatérale du nerf de Hering (Martin-Body et al., 1986; Fordyce, 1987; Javaheri et al., 1988; Bonora and Gautier, 1989; Ward et al., 1990; Melton et al., 1991; LaManna et al., 1996). Egalement, sur la préparation "en bloc" *in vitro*, qui ne conserve que le tronc cérébral et la moelle épinière rostrale, une diminution de la quantité d'O_2 dans le milieu de survie (hypoxie ou anoxie) provoque un ralentissement de la fréquence respiratoire enregistrée au niveau des racines phréniques, sans en modifier significativement l'amplitude (Kawai et al., 1995; Kato et al., 2000; Viemari et al., 2003; Voituron et al., 2006). Ces expériences montrent que les structures centrales du contrôle respiratoire répondent à l'hypoxie dans l'ensemble par une dépression respiratoire. Mais cela ne signifie pas que chaque neurone se comporte de la même manière. Globalement, une hypoxie cérébrale modérée provoque une dépression métabolique et une réduction de l'excitabilité neuronale (Teppema and Dahan, 2010). Toutefois, certains neurones se dépolarisent en hypoxie. Par exemple, les neurones inspiratoires du PréBötC sont excités en période d'hypoxie, ce qui a été montré à la fois *in vitro* sur des préparations "en tranche" et *in vivo* chez l'animal anesthésié (Telgkamp and Ramirez, 1999; Solomon et al., 2000; Thoby-Brisson and Ramirez, 2000). Au cours de la phase de dépression ventilatoire relative, une libération d'ATP au niveau de la surface ventrale du bulbe rachidien a été mesurée, exerçant un effet facilitateur notamment sur le PréBötC *via* l'activation des récepteurs métabotropiques (P2Y), et par conséquent atténuant la diminution de la ventilation (Gourine et al., 2005a; Lorier et al., 2007, 2008). Par ailleurs, cette particularité d'excitation des neurones inspiratoires du PréBötC en réponse à une hypoxie est considérée comme étant responsable de l'activité de "gasp" lors d'une hypoxie sévère.

La dépression ventilatoire d'origine centrale lors d'une hypoxie n'est pas seulement causée que par la dépression métabolique et la réduction de l'excitabilité neuronale. Les

neurones de la surface ventrale du bulbe rachidien et plus particulièrement le pFRG et le RTN sont à la fois des noyaux recevant les informations périphériques liées à la sensation de l'hypoxémie, et des noyaux sensibles aux variations physiologiques d'O_2 et impliqués dans la dépression ventilatoire relative (Sun and Reis, 1994; Bodineau et al., 2000a, 2000c; Voituron et al., 2006). Il a récemment été montré par Gestreau et collaborateurs que le canal TASK-2 est exprimé dans peu de noyaux du tronc cérébral, dont le RTN, et que les souris *Task2*$^{-/-}$ qui n'expriment pas ce canal ne présentent pas de dépression ventilatoire relative lors d'une hypoxie (Gestreau et al., 2010). La présence et l'action du canal TASK-2 dans le RTN lors d'une hypoxie représentent la première mécanistique moléculaire de sensibilité centrale à l'O_2 réellement établie. Mais il existe d'autres neurones sensibles à l'O_2, comme au niveau du NTS et de l'hypothalamus (Horn et al., 1999; Pascual et al., 2002; Voituron et al., 2005). Les neurones bioaminergiques sont aussi impliqués dans la sensibilité centrale à l'O_2. La RVH est atténuée voire absente *in vitro* chez les souris mutées pour les gènes *c-Ret* et *Phox2a*, chez qui les groupes catécholaminergiques A5 et A6 sont altérés (Viemari et al., 2004a, 2005a). D'ailleurs, le locus cœruleus (A6) est considéré comme un important modulateur inhibiteur de la RVH, *via* des mécanismes dépendants du monoxyde d'azote (NO) (Fabris et al., 1999, 2000; Teppema and Dahan, 2010). Les neurones sérotoninergiques sont cruciaux pour le couplage entre RVH et thermorégulation. Les souris *Lmx1b*$^{f/f/p}$, qui sont presque entièrement dépourvues de neurones sérotoninergiques, ont une RVH diminuée à 25°C, mais pas à 30°C (Hodges et al., 2008; Hodges and Richerson, 2008b). A l'inverse, les souris qui n'expriment pas le transporteur de la sérotonine 5-HTT, et qui présentent une quantité très importante de sérotonine dans leur liquide céphalorachidien, ont une RVH augmentée et une baisse de leur métabolisme en hypoxie exacerbée (Li and Nattie, 2008). Un autre mécanisme liant hypoxie et sérotonine est le phénomène de facilitation à long terme (LTF). Suite à des hypoxies intermittentes, c'est-à-dire des successions de périodes courtes d'hypoxies et de normo- ou d'hyperoxies, les décharges respiratoires des nerfs phréniques et hypoglosses sont augmentées. Cette forme de plasticité respiratoire appelée LTF est un mécanisme central dépendant de la sérotonine, car il est aboli par des antagonistes aux récepteurs de la sérotonine, une déplétion en sérotonine, ou une neurotoxocité sérotoninergique (Millhorn et al., 1980; Bach and Mitchell, 1996; Feldman et al., 2003). Des injections répétées de sérotonine dans la moelle épinière sont d'ailleurs suffisantes pour induire la LTF du nerf phrénique, même sans hypoxie. D'une manière générale, la LTF du nerf phrénique successive à des hypoxies intermittentes est considérée comme étant due à une libération de sérotonine et son action *via* les récepteurs 5-HT_2 et 5-HT_7, mais aussi à l'activation de la NADPH oxydase,

à une augmentation de la production de BDNF, de radicaux libres de l'oxygène et de VEGF (Facteur de Croissance Vasculaire Endothélial), menant à la facilitation de la transmission synaptique glutamatergique *via* notamment la phosphorylation des récepteurs NMDA (Baker et al., 2001; Baker-Herman and Mitchell, 2002; Feldman et al., 2003; Baker-Herman et al., 2004; Ling, 2008; MacFarlane et al., 2008, 2009; Teppema and Dahan, 2010; Hoffman and Mitchell, 2011; Dale-Nagle et al., 2011).

Nota Bene : dans cette thèse, nous avons souvent utilisé le stimulus hypoxique dans un objectif général d'étude de l'influence des régulations respiratoires, comme chez les souris Mecp2$^{-/y}$, un modèle murin du syndrome de Rett (cf. partie résultats, chapitre 1, article 1), chez les souris Tau-P301L, un modèle murin de tauopathie (cf. partie résultats, chapitre 3, article 2), et pour comparer le phénotype respiratoire des souches de souris FVB/N et C57Bl/6J (cf. partie résultats, chapitre 2, article 1).

2.2.2 - Sensibilité centrale au pH et au CO_2

Les variations de pression partielle artérielle en CO_2 ($PaCO_2$) représentent le tonus excitateur principal de la respiration, devant celui des variations d'O_2. La valeur physiologique de la $PaCO_2$ chez les mammifères se situe autour de 40 mmHg, et la ventilation double pour une augmentation de seulement 2 mmHg de la $PaCO_2$ (Nattie, 1999, 2000; Guyenet et al., 2010). La sensibilité au CO_2 et/ou au pH, appelée chémosensibilité, est majoritairement centrale, et son existence a été montrée dès 1954 (Leusen, 1954; Gautier and Bonora, 1979; Nattie, 1999). Cependant, on ne sait toujours pas aujourd'hui de manière irrévocable si la chémosensibilité centrale implique la sensation du CO_2 dissout ou du pH. Cette question a été l'objet d'un intense débat pendant de nombreuses années, débat qui s'est atténué ces dernières années autour de l'hypothèse la plus plausible au regard de la littérature, où le CO_2 stimulerait la respiration *via* le pH (Loeschcke, 1982; Nattie, 1999; Feldman et al., 2003; Guyenet et al., 2010). En effet, 1) l'hypercapnie diminue le pH du liquide céphalorachidien, 2) l'acidose métabolique et l'acidification topique du cerveau, en particulier au niveau du bulbe ventrolatéral, augmentent la respiration, et 3) *in vitro*, l'acidose métabolique active/inhibe les neurones et dépolarise certaines cellules gliales à un niveau comparable à celui produit par une augmentation de CO_2 provoquant le même changement de pH extracellulaire (Loeschcke, 1982; Eldridge et al., 1984; Arita et al., 1989; Nattie, 1999;

Wang et al., 2002b; Feldman et al., 2003; Putnam et al., 2004; Kawai et al., 2006; Guyenet et al., 2010). Cette incertitude sur le mode de stimulation du CO_2 et/ou du pH vient notamment du fait que les bases moléculaires de la chémosensibilité centrale ne sont pas encore connues. La première et la plus étudiée des hypothèses serait qu'un ou plusieurs canal(aux) ionique(s) jouerait(ent) le rôle de senseurs du pH. Par exemple, les canaux TASK étaient de très bons candidats, mais il ne ressort aucune altération majeure de la chémosensibilité centrale chez les souris n'exprimant pas ces canaux (Mulkey et al., 2007b; Gestreau et al., 2010). D'autres canaux, comme les canaux Kir (canaux potassiques rectifiants entrants), les canaux de la famille ASIC (canaux ioniques sensibles à l'acide), les canaux ionotropiques purinergiques (P2X) ou encore les canaux des jonctions communicantes, sont des candidats qui soit ont été écartés expérimentalement, soit n'ont pas encore été étudiés pour la chémosensibilité respiratoire (Mulkey et al., 2004a, 2007b; Vacher et al., 2008; Holzer, 2009; Ziemann et al., 2009; Guyenet et al., 2010). Au niveau cellulaire, la chémosensibilité centrale ne concernerait pas que les neurones, des données récentes impliquant fortement les cellules gliales et en particulier les astrocytes. Les astrocytes de la surface ventrale du bulbe rachidien, en particulier dans la région du RTN/pFRG, se dépolarisent en condition d'acidose par un influx calcique, et relarguent de l'ATP qui va exciter les neurones adjacents et stimuler la respiration (Gourine et al., 2005b, 2010; Ballanyi et al., 2010). Ces données corroborent l'idée de plus en plus acceptée que la glie n'est pas qu'un support structurel aux neurones, elle joue également un rôle fonctionnel. De plus, la localisation de la glie en tant qu'élément de la barrière hémato-encéphalique, à l'interface entre les vaisseaux sanguins et les neurones, et l'importance de la glie pour les régulations métaboliques dans le système nerveux, en font un acteur privilégié de la chémosensibilité centrale.

Même si les mécanismes moléculaires à la base de la chémosensibilité centrale ne sont pas encore clairement identifiés, les régions chémosensibles sont elles relativement bien caractérisées. La chémosensibilité est une fonction distribuée dans le cerveau, dont l'organisation hiérarchique est particulièrement débattue, et qui implique plusieurs phénotypes neuronaux (Coates et al., 1993; Nattie, 1999; Nattie and Li, 2001, 2002b, 2002a; Feldman et al., 2003; Nattie et al., 2004; Li and Nattie, 2006; Guyenet et al., 2010). Le groupe de neurones le plus étudié concernant la chémosensibilité centrale est le RTN. Les neurones du RTN répondent très vigoureusement à l'hypercapnie *in vivo* et à des variations physiologiques de pH *in vitro* (Li and Nattie, 2002; Mulkey et al., 2004a; Guyenet et al., 2005a; Fortuna et al., 2009; Marina et al., 2010). Cette chémosensibilité est intrinsèque au RTN, car elle persiste après blocage de la transmission synaptique avec la tétrodotoxine

(TTX), ou avec des cocktails de drogues bloquant la transmission glutamatergique, GABAergique, glycinergique et purinergique (Mulkey et al., 2004a, 2006). Egalement, l'activation des neurones du RTN par voie optogénétique produit une forte augmentation de la respiration, les neurones chémosensibles du RTN étant glutamatergiques (ils expriment le transporteur vésiculaire du glutamate 2) et fonctionnellement excitateurs projetant exclusivement sur le réseau respiratoire (au niveau du bulbe ventrolatéral, du pont dorsal, et de la portion ventrolatérale du NTS) (Mulkey et al., 2004a; Rosin et al., 2006; Abbott et al., 2009; Guyenet et al., 2010; Kanbar et al., 2010). Une autre évidence qui confère une importance particulière au RTN pour la chémosensibilité centrale est le Syndrome d'Hypoventilation Chronique Congénitale (CCHS), une pathologie humaine causée par une mutation du gène codant pour le facteur de transcription Phox2b (Amiel et al., 2009; Carroll et al., 2010). Les enfants humains atteints par le CCHS et les souris modèle de CCHS (souris *Phox2b*$^{27ala/+}$) souffrent d'hypoventilation sévère et d'un chémoréflexe extrêmement déprimé, présentant aussi des apnées importantes. Or la seule altération du tronc cérébral retrouvée chez les souris *Phox2b*$^{27ala/+}$ est une perte massive et sélective des neurones chémosensibles du RTN (Dubreuil et al., 2008, 2009a, 2009b). Le RTN est donc un noyau majeur de la chémosensibilité centrale, même s'il n'est pas l'unique noyau y participant.

En effet, les groupes bioaminergiques dans l'ensemble et particulièrement les groupes sérotoninergiques sont très impliqués dans la chémosensibilité centrale (Richerson, 2004; Hodges and Richerson, 2010). Contrairement au RTN dont la chémosensibilité est mature dès la naissance, la chémosensibilité des groupes sérotoninergiques commence vers P12 et est complètement mature après P20, ce qui corrèle d'ailleurs avec le développement de la RVHC *in vivo* (Wang and Richerson, 1999; Stunden et al., 2001; Davis et al., 2006; Hodges and Richerson, 2010). La localisation anatomique des neurones sérotoninergiques des raphés, que ce soit au niveau de la ligne médiane ou au niveau ventrolatéral du bulbe rachidien, leur confère une position parfaite pour la chémosensibilité car très proche d'artères importantes irriguant le cerveau et représentant donc un avantage dans la précision de la sensation des variations de CO_2 et/ou de pH sanguins (cf. figure 15) (Mitchell et al., 1963; Schlaefke et al., 1970; Bradley et al., 2002). Les neurones sérotoninergiques contribuent à une grande diversité d'actions liées au système d'éveil, d'excitation de l'organisme (Jacobs and Fornal, 1991, 2000; Jacobs and Azmitia, 1992). Mais tous ces neurones ne se comportent pas de la même manière, une sous-population étant chémosensible, avec 25% des neurones sérotoninergiques du raphé dorsal et 22% des neurones sérotoninergiques du bulbe qui ont une augmentation de leur fréquence de décharge pendant une hypercapnie, une réponse chémosensible significative

dès 3% de CO_2 inspiré (Veasey et al., 1995, 1997). Egalement, l'activation des neurones sérotoninergiques par l'hypercapnie est montrée par l'expression du proto-oncogène c-fos *in vivo* dans les raphés bulbaires, dont la localisation corrèle avec les sites de surface libérant de l'ATP lors d'une hypercapnie (cf. figure 15) (Larnicol et al., 1994; Haxhiu et al., 1996, 2001; Pete et al., 2002; Johnson et al., 2005; Gourine et al., 2005b). La destruction des neurones des raphés bulbaires par l'acide iboténique, et la destruction des neurones sérotoninergiques bulbaires avec la saporine ou la 5,7-dihydroxytryptamine, résultent en une forte diminution de la RVHC, souvent accompagnée d'une diminution de la ventilation de repos et dans le premier cas d'apnées (Mueller et al., 1985; Carruth et al., 1992; Dreshaj et al., 1998; Nattie et al., 2004; Hodges et al., 2004, 2005). Une évidence peut-être encore plus forte du rôle important des neurones sérotoninergiques pour la chémosensibilité vient du fait que les souris *Lmx1b*$^{f/f/p}$, qui ont une perte spécifique et quasi-totale (>99%) des neurones sérotoninergiques, présentent une réduction de plus de 50% de la RVHC (Zhao et al., 2006; Hodges et al., 2008).

Le RTN et les raphés sont les groupes chémosensibles les mieux caractérisés. Il est très probable qu'il y ait une interaction entre eux, en particulier des raphés vers le RTN (Guyenet et al., 2010). En outre, il est suggéré que le RTN jouerait un rôle primordial dans la chémosensibilité centrale dans les phases d'éveil, alors que les raphés seraient plutôt chémosensibles pendant les phases de sommeil ou d'anesthésie, même si certaines données tendent à montrer le contraire pour ces derniers (Veasey et al., 1995, 1997; Mitchell, 2004; Mulkey et al., 2004a; Hodges and Richerson, 2010). D'autres groupes de neurones participent à la chémosensibilité centrale, comme l'hypothalamus caudal, le noyau fastigial du cervelet, le NTS ou encore le locus cœruleus (Elam et al., 1981; Nielsen et al., 1986; Waldrop, 1991; Peano et al., 1992; Horn and Waldrop, 1994; Oyamada et al., 1998; Xu et al., 2001; Ballantyne and Scheid, 2001; Putnam, 2001; Nattie and Li, 2002b). Le locus cœruleus est d'ailleurs le troisième noyau dont la chémosensibilité est la plus avérée après le RTN et les raphés, des lésions du locus cœruleus réduisant RVHC (Ritucci et al., 2005; Li et al., 2008; Biancardi et al., 2008).

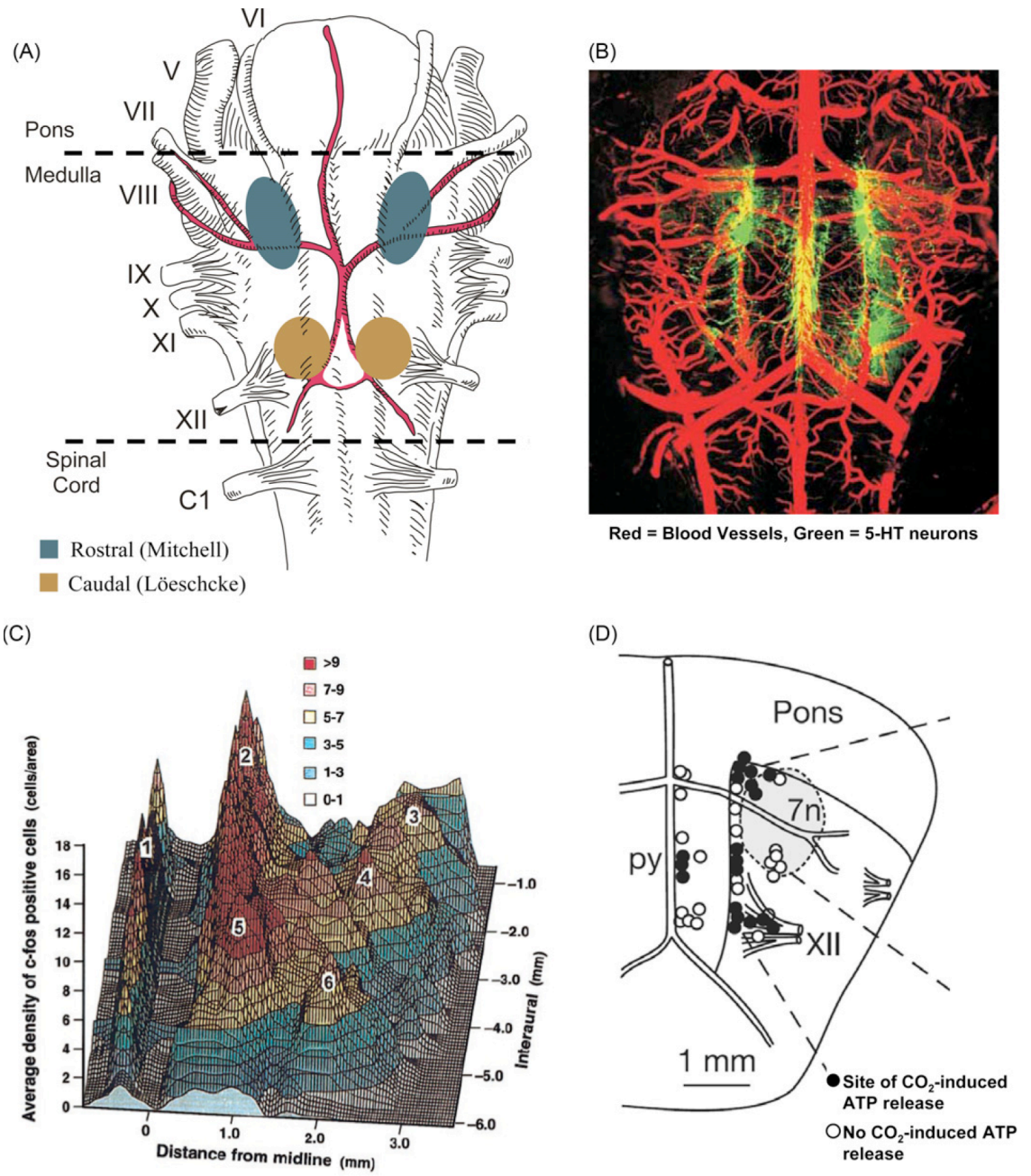

Figure 15 : (A) : schéma représentant les localisations estimées des zones chémosensibles rostrales (bleu) et caudales (orange) originellement décrites par Mitchell et Löeschcke, respectivement. (B) : images confocales des vaisseaux sanguins à la surface du tronc cérébral superposés sur la ligne médiane et sur la distribution ventrolatérale des neurones sérotoninergiques. On notera qu'en plus de ceux présents sur la ligne médiane, il y a également des zones ventrolatérales avec une grande densité de neurones sérotoninergiques, reproduisant les régions chémosensibles classiquement décrites. (C) : il y a des neurones positifs au c-fos sur la ligne médiane et sur la surface ventrolatérale du bulbe rachidien d'animaux exposés à une acidose hypercapnique progressive (5, 7, et 9% de CO_2) qui sont dans les mêmes régions que les neurones sérotoninergiques. (D) : schéma de la surface ventrale du bulbe rachidien indiquant les zones qui ont libéré (cercles pleins) ou n'ont pas libéré (cercles vides) de l'ATP lors d'une hypercapnie. Ces zones correspondent également à la localisation des neurones sérotoninergiques au niveau de la ligne médiane et de la surface ventrolatérale du bulbe rachidien. (*Adapté de Hodges and Richerson 2010*).

Nota Bene : dans cette thèse, nous nous sommes particulièrement intéressés à la RVHC et aux mécanismes altérant la chémosensibilité, comme l'augmentation endogène de la sérotonine in vitro (cf. partie résultats, chapitre 2, article 3) et l'influence de l'érythropoïétine (cf. paragraphe suivant et partie résultats, chapitre 2, article 4). De plus, nous avons souvent utilisé le stimulus hypercapnique dans un objectif général d'étude de l'influence des régulations de la commande respiratoire, comme chez les souris Mecp2$^{-/y}$, un modèle murin du syndrome de Rett (cf. partie résultats, chapitre 1, article 1), chez les souris Tau-P301L, un modèle murin de tauopathie (cf. partie résultats, chapitre 3, articles 1 et 2), et pour comparer le phénotype respiratoire des souches de souris FVB/N et C57Bl/6J (cf. partie résultats, chapitre 2, article 1).

2.3 - Erythropoïétine et réponse ventilatoire à l'hypoxie

En réponse à une hypoxie chronique, l'organisme s'acclimate en suivant deux grandes stratégies : 1) augmenter l'apport en O_2 aux tissus (notamment *via* l'augmentation des débits cardiaques et respiratoires pulmonaires, et une angiogénèse et une érythropoïèse accrues), et 2) diminuer les besoins énergétiques tissulaires en O_2 (notamment *via* une transition vers un métabolisme énergétique plus anaérobie). Cette acclimatation est principalement permise par l'augmentation de l'expression d'un facteur de transcription, HIF-1 (Facteur-1 Induit par l'Hypoxie) (Wang and Semenza, 1993; Semenza, 2001, 2007). HIF-1 est un hétérodimère constitué des sous-unités HIF-1α et HIF-1β, qui sont constitutivement exprimées. En condition normoxique, HIF-1α subit un processus permanent de synthèse puis de dégradation rapide, *via* la fixation de la protéine de Von Hippel-Lindau (pVHL) induisant l'ubiquitination puis la destruction de HIF-1α par le protéasome (Huang et al., 1998; Maxwell et al., 1999; Kamura et al., 2000; Jaakkola et al., 2001). En condition hypoxique, la protéine pVHL ne peut se fixer à HIF-1α, permettant la dimérisation de ce dernier avec HIF-1β pour former le facteur de transcription HIF-1. HIF-1 induit l'expression d'un grand nombre de gènes cibles, comme ceux codant pour le facteur VEGF (Facteur de Croissance Vasculaire Endothélial), pour les facteurs IGF (Facteur de Croissance ressemblant à l'Insuline), pour les enzymes de la glycolyse etc., le premier ayant été découvert étant le gène codant pour l'érythropoïétine (EPO) (Wang and Semenza, 1993; Bunn and Poyton, 1996; Semenza, 2002; Semenza et al., 2006; Kaluz et al., 2008).

L'EPO, une glycoprotéine appartenant à la famille des cytokines découverte en 1906

par Paul Carnot, est essentiellement connue pour son action érythropoïétique favorisant la différenciation des cellules souches de la moelle osseuse en érythrocytes (Hillman and Finch, 1971; Jelkmann, 2007). Lors d'une hypoxie, les kératinocytes synthétisent du monoxyde d'azote (NO), provoquant une vasodilatation cutanée qui augmente le flux sanguin périphérique mais diminue le flux sanguin rénal, diminuant ainsi l'apport en O_2, stabilisant le facteur HIF-1 et induisant la production d'EPO par les reins (Boutin et al., 2008). Mais l'EPO n'est pas synthétisée que par les reins, sa synthèse astrocytaire joue également un rôle prépondérant pour l'érythropoïèse suite à une hypoxie (Weidemann et al., 2009). Cet effet érythopoïétique induisant une polyglobulie et donc une augmentation de l'hématocrite (rapport entre les éléments figurés et le plasma sanguin) est un des effets les plus marquants et facilement analysables lors d'une hypoxie chronique. D'autres actions de l'EPO ont cependant été montrées récemment, avec en particulier un effet neuroprotecteur suite à des ischémies cérébrales comme lors d'accidents vasculaires cérébraux (Sakanaka et al., 1998; Digicaylioglu and Lipton, 2001; Leist et al., 2004; Rabie and Marti, 2008; Sanchez et al., 2009; Velly et al., 2010). En effet, le récepteur à l'EPO est présent dans un grand nombre de tissus, comme le cerveau, le cœur, les poumons, les testicules etc. (Gassmann et al., 2003; Sasaki, 2003; Jelkmann, 2007; Vogel and Gassmann, 2011).

Lors d'une hypoxie chronique, l'EPO participe à l'augmentation de l'apport en O_2 aux tissus par son effet érythropoïétique, mais également par une deuxième action sur le système respiratoire. En effet, l'EPO augmente la RVH chez la souris et chez l'Homme par une activation à la fois des CC et des neurones respiratoires du tronc cérébral (Soliz et al., 2005, 2007a; Gassmann and Soliz, 2009; Brugniaux et al., 2011). Le récepteur à l'EPO est présent dans de nombreux groupes respiratoires comme le PréBötC, le NTS ou encore les noyaux catécholaminergiques (Soliz et al., 2005). Egalement, il existe une expression cérébrale d'une forme soluble du récepteur à l'EPO, qui joue le rôle d'antagoniste non-compétitif de la liaison de l'EPO aux récepteurs membranaires. Le niveau d'expression de cette forme soluble du récepteur à l'EPO est diminué en hypoxie, et l'injection intra-cérébrale de la forme soluble pendant une hypoxie chronique abolit l'acclimatation ventilatoire à l'hypoxie (Soliz et al., 2007a). De plus, l'EPO modifie le métabolisme des catécholamines dans le tronc cérébral et dans les CC, augmentant la réponse à un stimulus hyperoxique (test de Dejours), et régulant de manière sexe-dépendante la RVH à la fois chez l'Homme et chez la souris (Soliz et al., 2007b, 2009).

Nota Bene : dans cette thèse, nous avons étudié l'impact de l'EPO sur la RVHC de la souris adulte, ce qui n'avait encore jamais été fait (cf. partie résultats, chapitre 2, article 4). Grâce à l'utilisation de souris transgéniques et d'approches pharmacologiques, nous montrons que l'EPO désensibilise la RVHC par une action directe à la fois centrale et périphérique, et par une action indirecte via la polyglobulie.

2.4 - Récepteurs à l'étirement pulmonaire et réflexe de Hering-Breuer

Les centres respiratoires ne sont pas influencés que par les paramètres gazeux et chimiques de l'organisme, la commande respiratoire est également régulée par des informations d'ordre mécanique. Dans les voies aériennes sous le larynx, trois catégories de récepteurs sont à l'origine de boucles réflexes qui protègent l'appareil respiratoire contre les lésions causées par une hyperinflation pulmonaire *via* le réflexe de Hering-Breuer, ou encore contre l'inhalation par exemple d'aliments *via* le réflexe de toux. Ces afférences participent également à la mise en forme du patron moteur respiratoire.

Les trois types de récepteurs sensoriels d'origine trachéo-broncho-pulmonaire sont (Bailey and Fregosi, 2006; Kubin et al., 2006; Widdicombe, 2006) :

- Les récepteurs à l'étirement pulmonaire à adaptation lente (SARs), qui sont principalement impliqués dans le réflexe de Hering-Breuer (cf. ci-après) et le contrôle du tonus du muscle lisse trachéo-bronchique (Schelegle, 2003) ;
- Les récepteurs à l'étirement pulmonaire à adaptation rapide (RARs), à l'origine entre autres du réflexe de toux (Widdicombe, 2003) ;
- Les fibres C broncho-pulmonaires qui répondent à une grande variété de stimuli, induisent une broncho-constriction et stimulent la sécrétion de mucus (Lee et al., 2003).

SARs et RARs sont des mécanorécepteurs innervés par des fibres afférentes de conduction rapide myélinisées. Les fibres C broncho-pulmonaires comprennent tous les autres récepteurs présents dans l'arbre trachéo-broncho-pulmonaire (par opposition aux SARs et RARs), et ont des axones à conduction lente non-myélinisés. Ces trois types d'afférences projettent *via* le nerf vague dans des régions distinctes du NTS, permettant notamment une grande spécificité dans les réflexes mis en jeu (Kubin et al., 2006). Les réponses induites par la stimulation des RARs et des fibres C broncho-pulmonaires sont moins bien caractérisées que celles induites par les SARs (Bailey and Fregosi, 2006). La stimulation des RARs et des

fibres C broncho-pulmonaires peut induire une respiration rapide et superficielle et des apnées. Toutefois, la plupart des réponses induites par la stimulation des RARs et des fibres C broncho-pulmonaires sont distinctes, l'activation des récepteurs des fibres C induisant des effets inhibiteurs (apnée ou bradypnée, hypotension et bradycardie), alors que la stimulation des RARs induit surtout des effets excitateurs (augmentation de l'amplitude respiratoire, tachypnée, toux) (Bailey and Fregosi, 2006). Les RARs ne sont pas stimulés que par l'étirement mécanique, ils sont également très sensibles aux irritants chimiques comme la fumée, l'ammoniac, ou la poussière. Les fibres C broncho-pulmonaires sont polymodales, et peuvent être stimulées par de grandes déformations mécaniques, des stimuli chimiques, une augmentation du volume du liquide intersticiel (œdème pulmonaire), ou une augmentation de la température.

Les expériences de Hering et Breuer en 1868 ont montré pour la première fois l'existence d'afférences vagales lors d'inflations et de déflations pulmonaires pour la régulation du CPG respiratoire (Breuer, 1868; Hering, 1868). Ensuite, en 1933, Adrian a montré que les SARs sont responsables du réflexe d'inflation, appelé aujourd'hui réflexe de Hering-Breuer (Adrian, 1933; Widdicombe, 2006). Le réflexe de Hering-Breuer est un réflexe inhibiteur qui survient en fin d'inspiration ou dans toute condition conduisant à une surinflation pulmonaire. A l'opposé, il existe le réflexe excito-inspiratoire de Hering-Breuer qui stimule l'inspiration lorsque les poumons sont vidés en deçà de leur volume de fin d'expiration physiologique. Ces réflexes sont supprimés par une vagotomie bilatérale, car ils ont pour origine les SARs dont les fibres afférentes transitent dans le nerf vague. Les fibres nerveuses issues des SARs projettent monosynaptiquement sur deux types de cellules dans le NTS ipsilatéral, les cellules "pompes" ou P-cells, et les cellules inspiratoires-ß (Iß) (Berger, 1977; Kubin et al., 2006). Ce sont les P-cells qui sont impliquées dans le réflexe de Hering-Breuer, ces cellules ayant une activité de décharge phasique (comme les SARs) qui suit les variations de volume pulmonaire. Les P-cells sont principalement des neurones inhibiteurs GABAergiques qui projettent dans le NTS controlatéral, et ipsilatéralement dans le noyau de Kölliker-Fuse (KF), le complexe parabrachial (PB), A5, et dans la colonne respiratoire ventrale (Ezure and Tanaka, 1996, 2004; Ezure et al., 1998, 2002). Le réflexe de Hering-Breuer joue un rôle prépondérant pour l'arrêt de l'inspiration et la transition vers la post-inspiration, et ce principalement durant la période de maturation du réseau respiratoire (cf. précédemment chapitre 2, paragraphe 2.2). Une autre condition physiologique dans laquelle le réflexe de Hering-Breuer intervient est le soupir. En effet, le soupir est une inspiration ample et prolongée qui servirait notamment à lutter contre l'atélectasie pulmonaire et à augmenter

l'oxygénation alvéolaire (Cherniack et al., 1981; Alvarez et al., 1993; Tomori et al., 1998; Patroniti et al., 2002; Yamauchi et al., 2008). Après un soupir on constate généralement une modification de la respiration en deux phases, la première étant une courte apnée, imputée au réflexe de Hering-Breuer, et la deuxième étant une bradypnée plutôt due à l'hyperoxygénation sanguine induite par le soupir. Il existe d'ailleurs une interaction entre les afférences des corps carotidiens et des SARs au niveau du NTS, qui serait linéaire et additive (Bajić et al., 1994).

Enfin, il existe des propriocepteurs au niveau de tous les muscles striés de l'appareil respiratoire qui participent à la coordination des mouvements respiratoires *via* la mise en jeu de boucles réflexes spinales (Hilaire et al., 1983).

Nota Bene : dans cette thèse, nous avons analysé la respiration post-soupir dans plusieurs études, notamment pour déterminer l'influence des régulations de la commande centrale respiratoire (en parallèle des tests hypoxiques et hypercapniques), et ce chez les souris Mecp2$^{-/y}$ en période pré-symptomatique (cf. partie résultats, chapitre 1, article 2), chez les souris Tau-P301L en période terminale (cf. partie résultats, chapitre 3, articles 2), et pour comparer le phénotype respiratoire des souches de souris FVB/N et C57Bl/6J (cf. partie résultats, chapitre 2, article 1).

3 - L'eupnée : physiologie d'un patron moteur indispensable à la plasticité fonctionnelle du réseau respiratoire

L'eupnée est caractérisée par son patron moteur tri-phasique, inspiration, post-inspiration et expiration. Alors que l'inspiration est une phase essentiellement respiratoire, la post-inspiration surtout mais aussi l'expiration tardive sont deux phases pendant lesquelles de nombreuses activités couplées à et/ou impliquant la respiration peuvent avoir lieu. Ces deux phases sont cruciales pour la plasticité fonctionnelle de la respiration notamment du mammifère, lui conférant des avantages évolutifs majeurs comme la capacité de mâcher tout en respirant, ou encore sa capacité performante de vocalisation. Dans ce contexte, il est très important de considérer l'acte moteur respiratoire dans toute sa complexité eupnéique et donc dans ses interactions avec ces actes moteurs associés.

3.1 - Plasticité fonctionnelle du réseau respiratoire

Les grandes avancées scientifiques dans le domaine des neurosciences ont souvent brisé des dogmes, démontrant par exemple que les neurotransmetteurs peuvent être libérés et avoir une action en dehors des synapses (Kukley et al., 2007), que les cellules gliales ont la capacité de générer des potentiels d'action (Karadottir et al., 2008) ou encore qu'il existe une neurogenèse chez l'Homme adulte (Sanai et al., 2004). Cette dernière découverte est directement liée à l'un des axes forts de recherche en neurosciences : la plasticité fonctionnelle du système nerveux central (qui a longtemps été présenté comme un système figé). Il a notamment été montré d'abord chez les invertébrés, puis chez les vertébrés, que les réseaux neuronaux générateurs de patrons moteurs (CPG) sont dynamiques et multifonctionnels (Schöner and Kelso, 1988; Ramirez and Pearson, 1988; Hooper and Moulins, 1990; Soffe, 1993; Meyrand et al., 1994; Marder and Calabrese, 1996; Destexhe and Marder, 2004). Le réseau respiratoire ne fait pas exception à cette règle, et c'est d'ailleurs une nécessité pour la coordination avec les activités motrices variées des VAS.

Au sein même du réseau respiratoire, nous avons vu précédemment qu'il peut être produit deux types d'activités respiratoires : une activité eupnéique et une activité de "gasp" notamment en fonction du niveau d'oxygénation (Paton et al., 2006). Le réseau respiratoire est également capable de produire un troisième type d'activité qui pourrait être un patron moteur intermédiaire entre eupnée et "gasp" : les soupirs (cf. ci-dessus paragraphe 2.4). Au-delà de ces activités intrinsèques à la respiration, le réseau respiratoire est fonctionnellement impliqué dans la genèse de patrons moteurs oro-pharyngés comme la déglutition, la toux ou encore le vomissement. Ces actes moteurs ont en commun un grand nombre de muscles (à la fois des VAS et du thorax), de nerfs (IX, X, XII, intercostaux etc.) et donc de motoneurones, mais aussi de prémotoneurones et d'interneurones. En effet, des neurones respiratoires du bulbe rachidien et du pont ont été identifiés comme impliqués également dans les décharges de CPG déglutiteurs, de toux ou de vomissement (Grélot et al., 1992; Gestreau et al., 1996, 1997, 2000, 2005; Roda et al., 2002; Poliacek et al., 2004, 2005; Jakus et al., 2008). Cependant, les mécanismes responsables de la reconfiguration fonctionnelle d'un même neurone au sein du réseau respiratoire et qui permettent sa contribution aux différents CPGs ne sont pas encore connus (Bianchi and Gestreau, 2009b).

3.2 - Un cas particulier, la vocalisation

Dans une des études présentées dans cette thèse, nous nous sommes particulièrement intéressés à une activité motrice couplée à la respiration et d'importance comportementale cruciale, la vocalisation (cf. partie résultats, chapitre 3, article 3). La vocalisation est un mécanisme qui sollicite une phase expiratoire active où les muscles abdominaux et intercostaux compriment l'air contenu dans les poumons afin de le pousser à travers les cordes vocales. La tension appliquée sur les cordes vocales notamment par le muscle laryngé crico-thyroïde provoque la production de sons par vibrations en modifiant la résistance au passage de l'air (Patrickson et al., 1991). Le ou les mécanismes neuronaux responsables de la genèse de la vocalisation sont encore débattus. En effet, la vocalisation est une fonction dont la complexité du patron moteur est directement impactée par le niveau d'évolution de l'organisme qui la produit. Au niveau des mammifères, il existe une hiérarchie, l'Homme possédant la plus grande diversité de zones cérébrales et de connexions entre ces zones impliquées dans la vocalisation, et donc la vocalisation la plus élaborée (Simonyan and Jürgens, 2003; Jürgens, 2009). Par exemple, il existerait chez l'Homme uniquement (pas même chez le primate non-humain) une voie directe entre le cortex moteur et le noyau ambigu (qui contient les motoneurones laryngés contrôlant les cordes vocales) qui serait impliquée dans le développement évolutif du langage (Kuypers, 1958; Iwatsubo et al., 1990; Simonyan and Jürgens, 2003). Les primates non-humains partagent avec l'Homme deux voies potentielles de genèse de la vocalisation : 1) une voie dite du cortex moteur contrôlant la genèse de vocalisation fine et apprise, et 2) une voie dite limbique contrôlant la promptitude à s'exprimer vocalement (cf. figure 16) (Dujardin and Jürgens, 2005, 2006; Jürgens, 2009). La voie du cortex moteur impliquerait une coordination complexe de nombreuses régions diencéphaliques et télencéphaliques, intégrée au niveau du cortex moteur, qui commanderait alors directement les interneurones de la réticulée bulbaire et notamment les prémotoneurones du noyau rétroambigu (caudal au noyau ambigu), ces derniers projetant sur les motoneurones laryngés du noyau ambigu (Holstege, 1989; Zhang et al., 1995; Vanderhorst et al., 2000a, 2000b; VanderHorst et al., 2001; Boers et al., 2002; Jürgens, 2002; Jürgens and Ehrenreich, 2007). Il n'y a, à notre connaissance, aucune démonstration que la voie du cortex moteur existe en dehors des primates. La voie limbique par contre est commune à tous les mammifères, et constitue un sujet d'étude en développement chez les rongeurs.

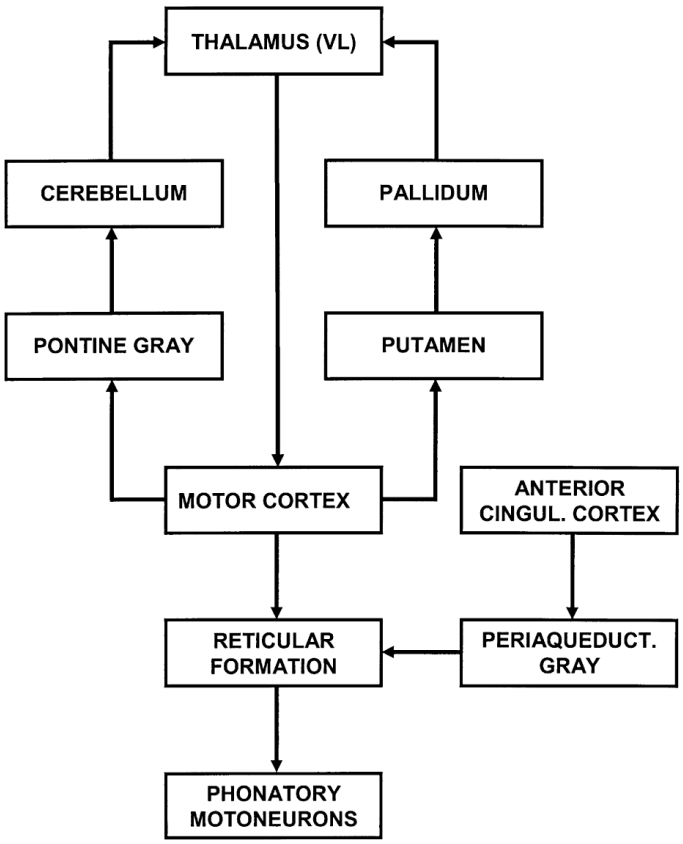

Figure 16 : schéma illustrant la relation anatomique entre divers structures impliquées dans le contrôle de la vocalisation. Représentation de la voie dite du cortex moteur, contrôlant la genèse de la vocalisation fine et apprise, et de la voie dite limbique, contrôlant la promptitude à s'exprimer vocalement. (*Adapté de Jürgens 2009*).

La voie limbique de vocalisation impliquerait le cortex cingulaire antérieur (ce qui n'a été montré que chez le primate non-humain, mais pas chez le rongeur, (Dujardin and Jürgens, 2005, 2006; Jürgens, 2009)), qui projette sur la substance grise périaqueducale (PAG), elle-même projetant sur la fin de la voie du cortex moteur, c'est-à-dire les structures bulbaires prémoto- et motoneuronales (Bandler and Carrive, 1988; Holstege, 1989; Carrive, 1993; Zhang et al., 1995; Holstege et al., 1997; Vanderhorst et al., 2000a, 2000b; VanderHorst et al., 2001; Jürgens, 2009; Sugiyama et al., 2010). Cette voie contrôlerait donc la promptitude à s'exprimer vocalement, c'est-à-dire toute vocalisation émotionnelle, de réaction. Dans cette voie limbique, la PAG possède un rôle central. La PAG est localisée autour de l'aqueduc cérébral dans le tegmentum mésencéphalique, et joue le rôle de carrefour central intégrant les afférences et efférences entre les structures supérieures du cerveau et le tronc cérébral, et donc entre structures de la conscience (émotions, douleur etc.) et systèmes autonomes (respiration, régulation cardiovasculaire, thermorégulation etc.). La PAG organise et coordonne le contrôle moteur des comportements de survie (le "fight or flight", l'immobilité de peur, la vocalisation, les comportements sexuels, la miction etc.), en modifiant à la fois les paramètres

neurovégétatifs et comportementaux (cf. figure 17) (Carrive, 1993; Lovick, 1993; Rossi et al., 1994; Behbehani, 1995; Graeff, 2004; Brandão et al., 2008; Subramanian et al., 2008; Holstege, 2010). La PAG est également suffisante en soi pour la production de vocalisation (et pas seulement de sons). En effet, des stimulations électriques et pharmacologiques (glutamate, histamine, antagonistes GABAergiques, agonistes cholinergiques), en particulier dans la partie caudale latérale et ventrolatérale de la PAG, induisent chez tous les mammifères de nombreuses vocalisations différentes, comme chez le chat le miaulement, le grondement, le feulement ou le ronronnement (Bandler and Carrive, 1988; Lu and Jürgens, 1993; Jürgens, 1994, 2009; Behbehani, 1995; Wang et al., 2002a). De plus, une lésion de la PAG entraîne le mutisme chez tous les animaux (Adametz and O'Leary, 1959; Skultety, 1962; Jürgens and Pratt, 1979), même l'Homme (Botez and Carp, 1968; Esposito et al., 1999). A l'inverse, la destruction du cortex cingulaire antérieur chez le primate non-humain et chez des patients humains entraîne des troubles de la vocalisation, caractérisés par une perte de contrôle volontaire et de motivation à parler, respectivement, mais conservant la capacité à répondre vocalement à des stimuli (ou à des questions chez l'Homme) (Sutton et al., 1974; Rubens, 1975; Jürgens and von Cramon, 1982).

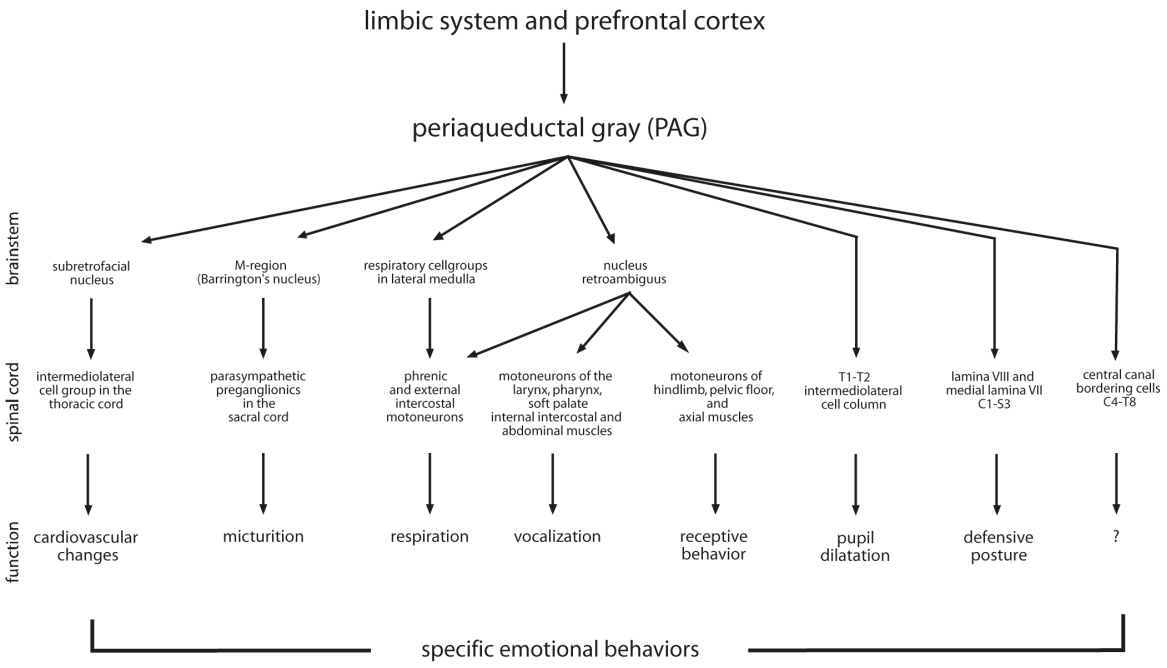

Figure 17 : diagramme montrant les différentes fonctions dans lesquelles intervient la PAG. Dans l'ensemble, ces fonctions sont nécessaires dans les activités et comportements nécessaires à la survie. (*Adapté de Subramanian et al. 2008*).

La PAG projette directement sur le noyau rétro-ambigu (NRA) pour le contrôle de la vocalisation, mais aussi pour son couplage avec la respiration (cf. figure 18). En effet, le NRA est un groupe de prémotoneurones qui projettent à la fois sur les motoneurones laryngés du noyau ambigu (contrôlant les muscles des VAS), sur les motoneurones phréniques, intercostaux ou encore abdominaux (contrôlant les muscles de la pompe respiratoire) (Holstege and Kuypers, 1982; Holstege, 1989; Miller et al., 1989; Vanderhorst and Holstege, 1997; Boers et al., 2002; Subramanian and Holstege, 2009). Le NRA possède une organisation anatomique somatotopique (tout comme la PAG d'ailleurs), et peut être comparé aux touches d'un piano : il ne contribue pas à la genèse des CPGs (respiratoire, de vocalisation, de toux etc.), mais il est le centre de projection et d'intégration des commandes des CPGs, renvoyant l'information vers les motoneurones, et constituant un réseau de neurones multifonctionnels par essence (Baekey et al., 2001; Shiba et al., 2007; Subramanian and Holstege, 2009, 2010). Pour la coordination de la vocalisation avec le CPG respiratoire, la PAG projette également sur le groupe respiratoire pontique (noyau de Kölliker-Fuse, KF, et surtout complexe parabrachial, PB), sur le NTS et sur le noyau rétrofacial (qui pourrait en fait être le RTN/pFRG) (Huang et al., 2000; Hayward et al., 2003, 2004; Zhang et al., 2005b, 2007; Smotherman et al., 2006; Subramanian et al., 2008). Cela permet l'intégration de la vocalisation dans le CPG respiratoire, et justement dans les phases post-inspiratoire et expiratoire tardive (active), coordonnées par le NTS/KF/PB (avec un rôle primordial du PB pour la vocalisation) et potentiellement le RTN/pFRG (cf. chapitres 2.1 et 2.2).

La souris est devenue un modèle très utilisé pour la recherche scientifique, notamment car elle est très perméable à la transgénèse. Le contrôle nerveux de la vocalisation chez la souris a cependant été peu étudié, la majeure partie des études se limitant à l'étude du comportement de vocalisation, enregistrant et analysant les paramètres de vocalisations. La souris vocalise principalement dans les gammes de fréquence ultra-sonores, jusqu'à 200 kHz chez le jeune et jusqu'à 100kHz chez l'adulte (Holy and Guo, 2005; Grimsley et al., 2011). Ces vocalisations sont émises lors des parades sexuelles, lors de comportements de peur (comme lorsque l'on expose les souris à l'odeur de l'urine de rat ou d'Homme), ou encore par les nouveaux-nés pour la relation mère/enfant et les comportement d'affection ou d'aversion (Holy and Guo, 2005; Landgraf et al., 2007; Scattoni et al., 2008; Wang et al., 2008; Scattoni et al., 2009, 2010; Hoffmann et al., 2009; Grimsley et al., 2011). Ce dernier point constitue d'ailleurs un outil de phénotypage comportemental dont l'utilisation est récente et en pleine croissance pour les troubles neurodéveloppementaux.

Toutes ces données comportementales suggèrent une importance primordiale de la voie limbique et en particulier de la PAG pour la vocalisation chez la souris, la vocalisation étant principalement émise en réaction, et pendant des comportements neurovégétatifs, de survie.

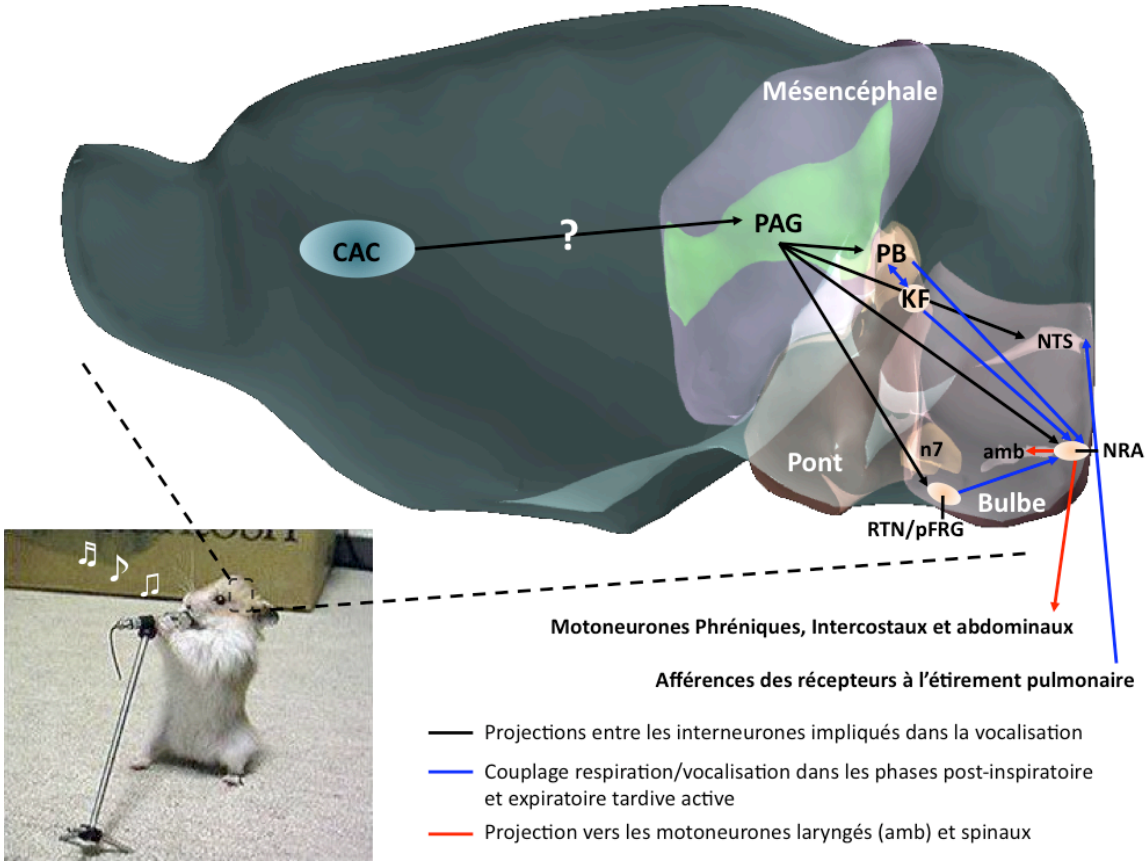

Figure 18 : schéma représentant la voie limbique de vocalisation chez le rongeur et son couplage anatomique avec le réseau respiratoire. amb, noyau ambigu ; CAC, cortex cingulaire antérieur ; KF, noyau de Kölliker-Fuse ; n7, noyau facial ; NRA, noyau rétroambigu ; NTS, noyau du faisceau solitaire ; PAG, substance grise périaqueducale ; PB, complexe parabrachial ; pFRG, groupe respiratoire parafacial ; RTN, noyau rétrotrapézoïde.

Nota Bene : dans cette thèse (chapitre 3 de la partie résultat), l'article 3 présente une étude de la vocalisation ultrasonore de souris sauvages et de souris transgéniques Tau-P301L, modèle reconnu de tauopathie. Pour la première fois, nous identifions une atteinte pathologique de la PAG et une atteinte fonctionnelle de la vocalisation qui révèle que ces souris peuvent être un modèle murin puissant pour l'étude des troubles progressifs de la vocalisation, similaires à ceux rencontrés chez le patient Alzheimer.

La plasticité fonctionnelle respiratoire est donc très complexe, intégrant de nombreuses activités comme la déglutition, la toux, la vocalisation etc. Cette plasticité est nécessaire car elle coordonne différentes activités motrices sollicitant les VAS et les muscles respiratoires, c'est donc une modification fonctionnelle intrinsèque du CPG respiratoire. Mais le CPG respiratoire peut aussi être modifié de manière extrinsèque, par son couplage avec d'autres CPGs. Notamment, il existe un couplage très fort entre la commande centrale respiratoire et la régulation centrale cardiovasculaire, comme le montrent les arythmies sinusales respiratoires et la modulation respiratoire sympathique (Potts et al., 2000; Grossman and Taylor, 2007; Simms et al., 2009, 2010; Dick et al., 2009). Ce couplage est essentiel pour coordonner les deux mécanismes permettant l'apport en O_2 aux cellules, la respiration alvéolaire et la circulation sanguine. Egalement, il existe un couplage central entre CPG respiratoire et locomoteur, impliquant très certainement le complexe parabrachial (Bramble and Carrier, 1983; Kawahara et al., 1989; Romaniuk et al., 1994; Morin and Viala, 2002). Ainsi, si l'on s'intéresse à l'eupnée au sens physiologique, il est important d'effectuer des études *in vivo* afin de conserver l'intégrité du système et particulièrement les plasticités intrinsèques et les couplages extrinsèques du CPG respiratoire.

IV - Physio/pathologie du vieillissement et respiration

1 - Théories du vieillissement

Le vieillissement est une notion difficile à appréhender. D'un point de vue sociétal, on distingue le "troisième âge" comme étant la catégorie de personnes dites âgées, cela étant souvent mis en parallèle avec un statut économique non-actif correspondant à la retraite. Mais d'un point de vue biologique, le vieillissement est plutôt appelé sénescence, correspondant aux modifications biologiques d'un organisme après sa maturité. Dans ce contexte, il est impossible de déterminer un âge à partir duquel on vieillit, car il existe une grande disparité dans la maturation de chaque organe, chaque sous-type cellulaire, et ce également en fonction des conditions de vie etc. Par exemple, le cristallin de notre œil commence à vieillir dès 10-15 ans, alors qu'à l'inverse les os de la hanche, qui sont les derniers à terminer leur processus d'ossification, terminent leur maturation vers 25 ans. Toutefois, ce vieillissement physiologique est à séparer du vieillissement pathologique, qui entraîne une perte prématurée de fonction. Pour le cristallin de l'œil par exemple, son opacification progressive provoque la cataracte en général aux alentours de 70 ans, induisant une perte de vision. En ce qui concerne les os, une dérégulation du processus permanent de remodelage osseux peut entraîner l'ostéoporose, menant à une fragilisation des os et des risques accrus de fracture, et ce rarement avant 60 ans.

Le flou qui entoure la notion biologique de vieillissement est sous-tendu par la méconnaissance des processus biologiques sous-jacents au vieillissement. Il existe de nombreuses hypothèses, que l'on peut diviser en deux groupes : les hypothèses stochastiques, où les processus de vieillissement se produisent au hasard et s'accumulent avec le temps, et les hypothèses non-stochastiques, où le vieillissement est inévitable, voire programmé. Certaines hypothèses sont génétiques, postulant l'existence de "gènes de mort", dont l'expression provoquerait une sénescence cellulaire, ou encore l'implication du raccourcissement des télomères à chaque division cellulaire, qui pourrait aller jusqu'à stopper la capacité de prolifération cellulaire (Harley et al., 1990; Finch and Tanzi, 1997; Blackburn,

2000; Guarente and Kenyon, 2000; Bryce et al., 2002). Ces différentes hypothèses génétiques pourraient contribuer ou expliquer la théorie de Hayflick, qui postule que les cellules ont un nombre fini de divisions possibles (Hayflick and Moorhead, 1961). La majorité des hypothèses sont cependant biochimiques. Par exemple, il est postulé que les espèces radicalaires (de l'oxygène principalement), qui sont des atomes ou molécules chez qui un électron est non apparié, provoqueraient en permanence des dommages sur les protéines, sur les membranes cellulaires, sur l'ADN, ce qui conduirait à une accumulation progressive de déchets et à la perte de fonction des cellules (Beckman and Ames, 1998; Finkel and Holbrook, 2000). Une autre hypothèse d'accumulation de déchets est celle du "cross-link", dans laquelle la glycation, ou liaison spontanée de molécules de glucose à des protéines, forme des agrégats protéiques conduisant à un dysfonctionnement cellulaire (Cerami, 1985). Egalement, les théories hormonales postulent que la décroissance de production d'hormones comme la testostérone, l'œstrogène, la mélatonine ou encore la dehydroepiandrostérone (DHEA) participe au déclin de l'organisme (Rudman et al., 1990; Oriander and Nader, 1996; Dollemore, 2006). Comme il serait illusoire de chercher à énumérer succintement toutes les hypothèses biologiques sur le vieillissement, nous recommandons au lecteur qui souhaiterait plus d'informations sur les mécanismes du vieillissement, le site internet du *National Institute on Aging* (http://www.nia.nih.gov/), l'organisme de recherche américain sur le vieillissement.

2 - Vieillissement du système respiratoire

Toutes les grandes fonctions physiologiques sont atteintes par le vieillissement : la vue et l'ouïe déclinent, les reins perdent de l'efficacité, les artères se raidissent etc. (Dollemore, 2006). Le système respiratoire ne déroge pas à cette règle. Cependant, alors que l'atteinte de l'appareil respiratoire par le vieillissement est très documentée, celle de la commande centrale respiratoire l'est très peu.

2.1 - Vieillissement de la pompe ventilatoire, poumons et cage thoracique

Avec l'âge, il y a une augmentation graduelle de calcification des côtes, particulièrement au niveau du cartilage antérieur près du sternum, menant à une rigidification progressive du thorax (cf. figure 19) (Levitzky, 1984; Janssens et al., 1999). Les muscles

respiratoires sont également affectés, avec une perte graduelle de force musculaire, expliquée principalement par une réduction de masse musculaire, mais aussi certainement par une perte de fibres musculaires de type "rapide" et une altération potentielle de la jonction neuromusculaire (Mizuno, 1991; Tolep and Kelsen, 1993; Enright et al., 1994; Tolep et al., 1995; Polkey et al., 1997; Janssens et al., 1999). Un autre paramètre important est la perte d'élasticité du tissu pulmonaire, qui serait certainement dû à un "cross-link" entre collagène et élastine. Cela entraîne un élargissement et une réduction de la profondeur des alvéoles pulmonaires, ce qui a pour effet de réduire très significativement la surface alvéolaire, un phénomène appelé "emphysème sénile" (Turner et al., 1968; Niewoehner et al., 1975; Verbeken et al., 1992; Kurozumi et al., 1994; Janssens et al., 1999).

Toutes ces modifications structurales conduisent à des modifications fonctionnelles de l'appareil respiratoire. Le volume résiduel (l'air restant dans les poumons suite à une expiration maximale) augmente avec l'âge à cause de la perte d'élasticité des poumons, phénomène appelé piégeage d'air ou "air trapping" (Turner et al., 1968; Crapo et al., 1982; Janssens et al., 1999). De même, la capacité vitale (le volume total d'air qui peut être expiré suite à une inspiration maximale) décline avec l'âge, et ce certainement à cause de l'augmentation graduelle de la rigidité thoracique et la perte de force des muscles respiratoires (cf. figure 19) (Schmidt et al., 1973; Knudson et al., 1976; Spirduso, 1995). Cependant, la capacité totale pulmonaire (le volume total d'air contenu dans les poumons suite à une inspiration maximale) ne change pas significativement avec l'âge, ce qui pourrait être dû à la réduction d'élasticité pulmonaire contrebalancée par l'augmentation de rigidité thoracique (Janssens et al., 1999). Le volume tidal (la quantité d'air échangée lors d'un cycle respiratoire normal, non forcé) semble diminuer avec l'âge, certainement à cause de l'augmentation de la rigidité thoracique et de la réduction de l'élasticité pulmonaire, et son coût énergétique est accru (Krumpe et al., 1985; Janssens et al., 1999). Par contre, les personnes âgées maintiennent un débit ventilatoire de repos comparable à celui de personnes jeunes, car leur fréquence respiratoire de repos est plus élevée (Krumpe et al., 1985; Janssens et al., 1999).

Malgré les altérations de l'appareil respiratoire dues au vieillissement citées ci-dessus, les échanges gazeux sont préservés chez les personnes âgées, la fonction première du système respiratoire étant donc maintenue (Delclaux et al., 1994; Guénard and Marthan, 1996). Par contre, ceci n'est valable que dans le cas d'un vieillissement sain, non pathologique, or de nombreuses maladies sont corrélées au vieillissement du système respiratoire, comme les troubles du sommeil dus aux apnées obstructives.

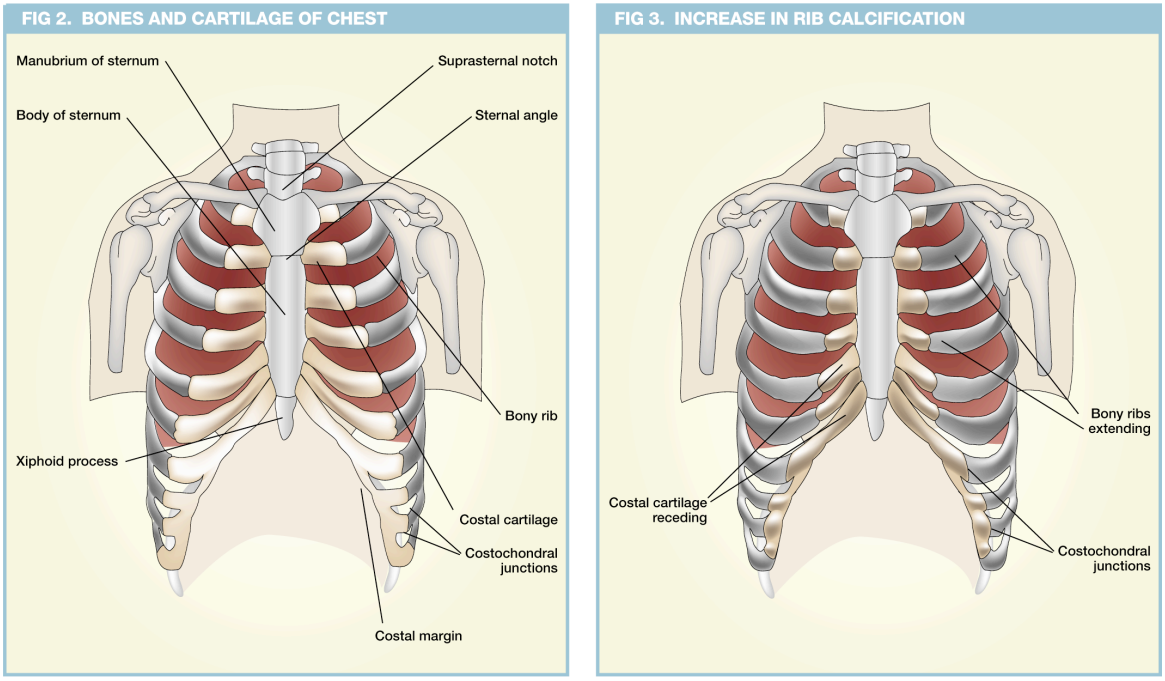

Figure 19 : schémas représentant les os (gris) et le cartilage (brun) de la cage thoracique chez un sujet jeune (FIG 2.) et chez un sujet âgé (FIG 3.). (*Adapté de Knight et al. 2008*).

2.2 - Vieillissement de la valve respiratoire, les voies aériennes supérieures

Le vieillissement est associé à des modifications des VAS, incluant des altérations structurelles et fonctionnelles comme pour la pompe ventilatoire. Des études montrent notamment que le vieillissement induit chez le rat une augmentation du nombre de fibres musculaires rapides et une baisse de l'endurance des muscles des VAS (génioglosse, sternohyoïdien et géniohyoïdien) (Van Lunteren et al., 1995; Oliven et al., 2001). De plus, chez l'Homme le diamètre des VAS diminue avec l'âge (Martin et al., 1997), et les VAS sont plus promptes à se collapser (Malhotra et al., 2006; Ray et al., 2008). Ces altérations semblent avoir peu d'incidence sur la respiration en état d'éveil, mais contribuent fortement à l'apparition d'apnées du sommeil chez la personne âgée (Schwab et al., 1995; Young et al., 2002; Malhotra et al., 2006).

Les apnées du sommeil sont généralement de type obstructif, c'est-à-dire provoquées par l'obstruction des VAS. L'origine centrale (altération de la commande nerveuse des VAS) ou périphérique (altérations notamment des muscles des VAS) est souvent débattue. Toutefois, les apnées du sommeil obstructives sont particulièrement associées à l'obésité et à

toute forme d'atteinte des VAS induisant une atonie musculaire et une propension accrue au collapsus. Un nombre croissant d'études montre que les apnées du sommeil obstructives augmentent très significativement avec l'âge, et ce indépendamment de l'index de masse corporelle, même si ce dernier est un facteur aggravant (Hla et al., 1994; Ware et al., 2000; Eikermann et al., 2007; Chung et al., 2009). Les apnées du sommeil liées à l'âge touchent également principalement les hommes (Young et al., 1993; Hla et al., 1994; Bixler et al., 1998, 2001; Ware et al., 2000). Ces apnées seraient majoritairement la conséquence des altérations structurelles et fonctionnelles des VAS citées précédemment, conduisant au collapsus des VAS. Cependant, certaines études tendent à montrer que l'altération de la capacité fonctionnelle musculaire des VAS chez les personnes âgées n'a pas une influence aussi marquée (Cantillon and Bradford, 2000), et que l'incidence des apnées du sommeil pourrait provenir d'une altération du contrôle nerveux (Ray et al., 2008).

Très peu d'études jusqu'à présent se sont intéressées au vieillissement de la commande centrale respiratoire, et la majorité d'entre elles concerne les motoneurones respiratoires plutôt que les interneurones à l'origine de la genèse du CPG respiratoire. Pourtant, le vieillissement induit entre autres une altération générale des systèmes bioaminergiques, et en particulier du système sérotoninergique, à la fois anatomique, morphologique, biochimique et métabolique (Morgan et al., 1987; Steinbusch et al., 1990; Van Luijtelaar et al., 1992; Ueda et al., 1998; Nishimura et al., 1998). Les atteintes principales du système sérotoninergique concernent le nombre de terminaisons sérotoninergiques, les concentrations en 5HT et ses métabolites, les densités en récepteurs 5HT, et les protéines de recapture de la 5HT, avec des variations considérables entre les différentes régions du système nerveux central (Van Luijtelaar et al., 1992; Ko et al., 1997). Les conséquences du vieillissement du système sérotoninergique sur la rythmogenèse respiratoire n'ont à notre connaissance pas encore été étudiées. Par contre, s'il y a bien un domaine du vieillissement de la commande respiratoire qui a été étudié, c'est l'altération de la facilitation à long terme (LTF) de l'hypoglosse dépendante de la 5HT (cf. chapitre 3, paragraphe 2.2.1 pour plus de détails sur la facilitation à long terme, et paragraphe 1.2.3 pour plus de détails sur l'action de la 5HT sur l'hypoglosse).

Cette altération, étudiée chez le rat, atteint principalement les mâles. Ainsi, une réduction du nombre de terminaisons 5HT et une altération de la morphologie des boutons synaptiques projetant sur l'hypoglosse sont décrites chez le rat mâle âgé (Behan and Brownfield, 1999; Behan et al., 2002). Les rates femelles présentent une augmentation des

récepteurs $5HT_{2A}$ sur l'hypoglosse avec l'âge, ce qui n'est pas le cas chez les mâles (Seebart et al., 2007). La LTF induite par des hypoxies intermittentes semble préservée avec l'âge sur le nerf phrénique, mais elle est annulée sur le nerf hypoglosse du rat mâle âgé et altérée sur le nerf hypoglosse de la rate femelle âgée (Zabka et al., 2001a, 2001b, 2003, 2005). L'atteinte particulière du rat mâle âgé serait due à ses hormones gonadales, et de même, le ratio progestérone sur œstradiol influence l'importance de la LTF à la fois de l'hypoglosse et du phrénique chez la rate femelle âgée (Zabka et al., 2003, 2005; Behan and Wenninger, 2008).

Comme les neurones 5-HT présentent une activité tonique et sont plus actifs pendant l'éveil que pendant le sommeil, la baisse de ce tonus excitateur sur les motoneurones de l'hypoglosse pourrait contribuer aux apnées du sommeil obstructives (Jacobs and Azmitia, 1992; Kubin et al., 1996). Egalement, la LTF pourrait être un mécanisme de protection en réponse à des hypoxies intermittentes, potentialisant l'activité nerveuse et facilitant l'activité respiratoire (Suratt et al., 1988; Babcock and Badr, 1998; Mitchell and Johnson, 2003; Morelli et al., 2004). La survenue des apnées du sommeil touche préférentiellement les hommes et les résultats décrits précédemment chez le rat pourraient expliquer cette différence de genre via l'altération du système sérotoninergique (Young et al., 1993; Hla et al., 1994; Bixler et al., 1998, 2001; Ware et al., 2000). Des apnées obstructives répétées altèrent le retour sensoriel du nerf vague et génèrent une LTF sur le nerf hypoglosse, mais cette LTF dépend des récepteurs adrénergiques α1 de l'hypoglosse (Tadjalli et al., 2010). Il serait intéressant d'étudier ce nouveau mécanisme dans le contexte des apnées obstructives de l'homme âgé, vu l'atteinte du système catécholaminergique lors du vieillissement.

2.3 - Vieillissement de la chémosensibilité

Le vieillissement provoque une dégénérescence des CC, induisant chez le rat une diminution du nombre et du volume des cellules glomiques (cellules de type I), une réduction du volume et de la fonction mitochondrials, ainsi qu'une réduction de la quantité et du "turnover" des catécholamines (Di Giulio et al., 2003; Pokorski et al., 2004; Conde et al., 2006). Chez le rat, la réponse des CC à une hypoxie diminue de moitié avec l'âge (Conde et al., 2006). Une dégénérescence avec l'âge des CC et en particulier des cellules glomiques existe aussi chez l'Homme (Heath, 1991). Egalement, l'Homme âgé présente une altération des contenus sanguins en dopamine (DA) et en dihydroxyphenylalanine (DOPA) suite à un test de réponse ventilatoire à l'hypoxie (Serebrovskaya et al., 2000).

De façon surprenante, aucune différence dans la réponse ventilatoire à l'hypoxie (RVH) ou à l'hypercapnie (RVHC) n'a été montrée chez le rat âgé par rapport au rat jeune, l'augmentation de ventilation étant surtout due à une augmentation de fréquence ventilatoire (Soulage et al., 2004; Wenninger et al., 2009; Pokorski and Antosiewicz, 2010). Chez l'Homme, beaucoup de travaux ont étudié l'impact du vieillissement sur la RVH et la RVHC, mais ces travaux ne permettent pas de tirer une conclusion définitive. Chez les personnes âgées, une partie des études montre une diminution de la RVH et de la RVHC (Kronenberg and Drage, 1973; Peterson et al., 1981; Brischetto et al., 1984; Mendez et al., 1996), d'autres ne signalent aucun changement (Ahmed et al., 1991; Smith et al., 2001; Pokorski and Marczak, 2003; Browne et al., 2003), et une étude montre même une augmentation de la RVH (Chapman and Cherniack, 1987). Les groupes d'âges étant relativement similaires (20-30 ans pour les individus jeunes, et 60-80 ans pour les individus âgés), la RVH et la RVHC ne seraient altérées que de façon marginale chez la personne âgée, ces résultats contrastant avec les données obtenues sur les CC. Plusieurs explications sont possibles, comme le fait que les études ont été réalisées chez des sujets âgés avant que leurs CC ne se dégradent, ou encore qu'une plasticité centrale compense la diminution de réponse des CC à l'hypoxie et à l'hypercapnie (par exemple un gain accentué dans les zones d'afférences des CC) (Smith et al., 2001; Pokorski et al., 2004; Teppema and Dahan, 2010).

Le vieillissement de l'appareil périphérique respiratoire a été très étudié, autant pour son altération structurelle que fonctionnelle, et l'augmentation des apnées du sommeil avec l'âge lui a d'ailleurs souvent été attribuée. Cependant, une origine centrale et non obstructive (par opposition à la diminution de LTF de l'hypoglosse avec l'âge) de ces apnées liées à l'âge est souvent mise en avant (Bixler et al., 1998; Browne et al., 2003). Or, à notre connaissance, une seule étude s'est intéressée à l'atteinte par le vieillissement du réseau central générant le CPG respiratoire : Mazzone et collaborateurs montrent une baisse d'expression des récepteurs à la NK1 dans le NTS de rats âgés, conduisant à la suppression de l'effet excitateur de l'injection de substance P dans le NTS sur la respiration (Mazzone and Geraghty, 1999). Il y a donc un manque cruel d'études concernant le vieillissement central du réseau respiratoire. Or, il est très probable que ce dernier soit touché par le vieillissement, les neurones respiratoires étant affectés comme toutes les autres cellules par les processus de sénescence (Dollemore, 2006). Le système déglutiteur est également particulièrement atteint par le vieillissement, atteinte qui pourrait avoir une origine centrale (Humbert and Robbins, 2008). Il est d'ailleurs fort probable que les activités les plus complexes, celles qui requièrent la plus grande plasticité fonctionnelle, soient les plus affectées par le vieillissement. L'étude de la

coordination de la respiration avec la déglutition ou avec la vocalisation, et par extension l'étude de la coordination entre pompe ventilatoire et VAS dans un contexte de vieillissement, semble donc être particulièrement importante.

Nota Bene : dans cette thèse, nous avons comparé l'influence du génotype de deux souches de souris sauvages sur le vieillissement respiratoire, étude qui n'a pu se faire que jusqu'à un an, en raison des contraintes de temps imposées par la réalisation d'une thèse (cf. chapitre résultats, chapitre 2, article 1). Nous avons également réalisé un certain nombre de travaux montrant l'atteinte pathologique de la commande des VAS et de la vocalisation chez un modèle murin de tauopathie (cf chapitre résultats, chapitre 3), pathologie liée au vieillissement décrite ci-après.

3 - Protéine tau et tauopathies

Au cours du vieillissement, les défenses immunitaires de l'organisme se détériorent, favorisant l'apparition de maladies infectieuses virales et bactériennes (Dollemore, 2006). Par ailleurs, le processus même de vieillissement peut provoquer l'apparition de pathologies dites neurodégénératives, notamment par l'accumulation de protéines dégradées. Parmi ces protéines, la protéine tau est responsable d'un grand nombre de pathologies, appelées tauopathies, parmi lesquelles la maladie d'Alzheimer.

3.1 - La protéine tau

3.1.1 - Biochimie de la protéine tau

La protéine tau est exprimée dans le système nerveux central et périphérique et, dans une moindre mesure, dans le cœur, les muscles squelettiques, les reins, les poumons, les testicules etc. (Gu et al., 1996). Tau est principalement présente dans les axones des neurones, mais aussi dans les compartiments somatodendritiques neuronaux et dans les oligodendrocytes (Trojanowski et al., 1989; Hirokawa et al., 1996; Tashiro et al., 1997; Aronov et al., 2001; Klein et al., 2002; Ittner et al., 2010). Tau contient 3 domaines principaux : un domaine de projection N-terminal, un domaine de liaison aux

microtubules, et un domaine C-terminal (Mandelkow et al., 1996; Ittner and Götz, 2011). Dans le cerveau humain, il existe 6 isoformes principales de la protéine tau, toutes issues du même gène et générées par des épissages alternatifs autour des domaines N-terminal et de liaison aux microtubules (cf. figure 20) (Goedert et al., 1989a; Wei and Andreadis, 1998). Les deux épissages alternatifs les plus prévalents autour du domaine de liaison aux microtubules sont appelés 3R et 4R, en référence au nombre de séquences répétées d'association aux microtubules qui sont exprimées (Goedert et al., 1989b; Jaworski et al., 2010).

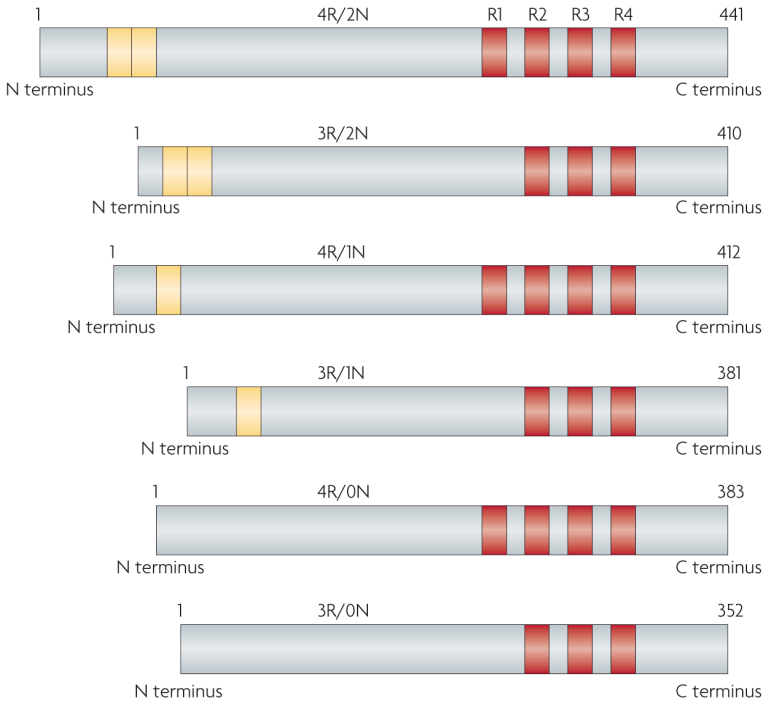

Figure 20 : domaines structurels des isoformes de protéines tau exprimées dans le cerveau de l'Homme adulte. Les différents domaines de liaison aux microtubules sont représentés en rouge, 3R ou 4R. La présence ou l'absence d'un ou deux inserts de 29 acides aminés, en jaune, participe également à la différenciation des isoformes de protéines tau. (*Adapté de Ballatore et al. 2007*).

Tau en conformation physiologique est une protéine intrinsèquement désordonnée, c'est-à-dire qu'elle n'a pas de structure tridimensionnelle stable, lui conférant une grande plasticité fonctionnelle (Morris et al., 2011). Tau possède 84 sites potentiels de phosphorylation, dont 45 sont des sérines, 35 des thréonines et 4 des tyrosines, représentant plus de 10^{11} combinaisons possibles de phosphorylation (Jaworski et al., 2010; Ittner and Götz, 2011). Malgré leur complexité, les différentes phosphorylations de tau ont été très étudiées en raison de leur rôle prépondérant pour la survenue de tauopathies (cf. plus loin). La protéine tau peut être modifiée post-translationnellement de nombreuses autres manières, par l'acétylation, la glycation, l'isomérisation, la nitration, la sumoylation, l'O-GlcNAcylation, l'ubiquitination etc., suggérant que tau est une protéine très régulée (Ledesma et al., 1994;

Arnold et al., 1996; Miyasaka et al., 2005; Dorval and Fraser, 2006; Cripps et al., 2006; Reyes et al., 2008; Min et al., 2010; Cohen et al., 2011).

3.1.2 - Fonctions de la protéine tau

Les microtubules, fibres constitutives du cytosquelette, sont des tubes polymériques polarisés et extrêmement dynamiques, formant une sorte de "tapis roulant" dans les axones et les dendrites. Des protéines motrices sont liées aux microtubules, et permettent les transports antéro et rétrogrades de cargos, comme des mitochondries ou des vésicules synaptiques, entre les terminaisons synaptiques et le corps cellulaire du neurone. Depuis 1975, la protéine tau est connue comme étant une protéine associée aux microtubules, participant à leur assemblage et à leur stabilité, tau étant principalement présente dans les axones en condition physiologique (Weingarten et al., 1975; Witman et al., 1976). Cette fonction est toujours la plus établie à l'heure actuelle, la protéine tau régulant même le transport axonal (Götz et al., 2006; Ittner and Götz, 2011). Tau peut interférer avec la liaison des protéines motrices aux microtubules, et il existe un gradient de concentration de tau le long de l'axone, les niveaux les plus concentrés étant les plus proches des synapses (Mandell and Banker, 1996; Ebneth et al., 1998; Dixit et al., 2008). Cette distribution pourrait faciliter le détachement des cargos de leurs protéines motrices près des terminaisons présynaptiques, augmentant l'efficacité du transport axonal (Dixit et al., 2008; Morris et al., 2011). Egalement, l'interaction physiologique tau/microtubule dépendrait de la formation d'homodimères de tau (Rosenberg et al., 2008). Ces homodimères pourraient être responsables de l'espacement entre les microtubules, nécessaire pour le transport des volumineux cargos par les protéines motrices (Jaworski et al., 2010). De plus, tau est en équilibre dynamique constant, se détachant et se liant aux microtubules par le jeu des phosphorylations/déphosphorylations *via* des kinases et des phosphatases, respectivement, ce qui serait nécessaire pour l'efficacité du transport axonal (cf. figure 21) (Roy et al., 2005; Ballatore et al., 2007). Tau peut aussi se lier aux filaments d'actine, participant à leur conformation en pelote, et pourrait connecter les microtubules aux filaments d'actine, renforçant d'autant plus la fonction cytosquelettique de cette protéine (Kotani et al., 1985; Farias et al., 2002; Yu and Rasenick, 2006; Fulga et al., 2007; He et al., 2009). On notera enfin que tau peut réguler la stabilité des microtubules par un mécanisme indépendant de sa liaison aux tubulines, car tau peut inhiber directement l'histone déacétylase 6, qui déacétyle les microtubules (Perez et al., 2009).

La protéine tau possède une grande plasticité fonctionnelle, ceci étant dû à sa structure intrinsèquement désordonnée, comme le montrent ses interactions multiples avec les microtubules citées précédemment, tau étant à la fois une protéine de liaison et une protéine de régulation. Mais la protéine tau possède d'autres rôles fonctionnels, qui sont de plus en plus étudiés. Notamment, tau peut jouer le rôle de protéine d'échafaudage, c'est-à-dire peut participer à la transduction du signal entre deux neurones en régulant les cascades de signalisation. Tau, présente dans les dendrites en petite quantité, interagit avec la protéine kinase FYN, facilitant le ciblage de FYN sur les sites post-synaptiques *in vivo*, où FYN va phosphoryler des récepteurs NMDA (NMDARs) induisant la formation d'un complexe entre NMDARs et la protéine de densité post-synaptique 95 (PSD95) (Lee et al., 1998; Salter and Kalia, 2004; Ittner et al., 2010; Ittner and Götz, 2011). Cette interaction NMDARs/PSD95 est importante pour les signaux d'excitotoxicité (Salter and Kalia, 2004). Tau pourrait aussi réguler des cascades de signalisation qui contrôlent l'extension des neurites, notamment via la facilitation de la signalisation de facteurs de croissance nerveux, ou encore de facteurs qui contrôlent le clivage de phospholipides, via sa liaison à la phospholipase C γ (Surridge and Burns, 1994; Brandt et al., 1995; Hwang et al., 1996; Dawson et al., 2001; Qiang et al., 2006; Morris et al., 2011). La protéine tau est également présente dans le noyau des cellules neuronales, où elle protège l'ADN contre un stress hyperthermique et facilite ensuite sa réparation (Loomis et al., 1990; Wang et al., 1993; Sultan et al., 2011). Enfin, tau serait impliquée dans la neurogenèse chez l'adulte, mais pas chez l'embryon (Hong et al., 2010; Morris et al., 2011).

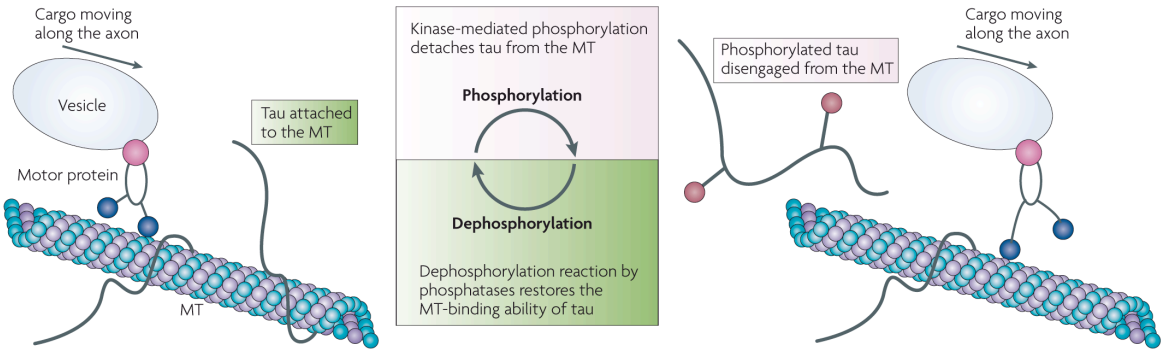

Figure 21 : l'équilibre dynamique de la liaison de tau aux microtubules (MT). Le niveau de phosphorylation de tau détermine si tau est liée aux MTs ou non. Bien que la présence de tau sur les MTs présente un obstacle physique pour les vésicules et autres cargos qui se déplacent le long de l'axone, l'association de tau aux MTs est essentielle pour l'intégrité de ces derniers. Ainsi, des cycles relativement fréquents d'association (provoquée par la déphosphorylation de tau) et de détachement (provoqué par la phosphorylation de tau) de tau par rapport aux MTs sont nécessaires au maintien d'un transport axonal efficace. (*Adapté de Ballatore et al. 2007*).

3.2 - Les tauopathies

Parmi toutes les modifications post-translationnelles que peut subir la protéine tau (cf. ci-dessus), son degré de phosphorylation a été l'objet d'un nombre considérable d'études ces dernières années pour son implication dans de nombreuses tauopathies, en particulier la maladie d'Alzheimer.

3.2.1 - La maladie d'Alzheimer

Plus de 35 millions de personnes dans le monde sont atteintes par la maladie d'Alzheimer (MA), pour environ 860 000 en France, un chiffre qui pourrait atteindre 1,3 million en 2020 (Ramaroson et al., 2003; Gallez, 2005; Helmer et al., 2006; Querfurth and LaFerla, 2010). En France, la prévalence des démences chez les plus de 75 ans atteint presque 18%, dont 80% sont dus à la MA (Ramaroson et al., 2003; Gallez, 2005). La MA est une maladie du vieillissement, le facteur de risque principal étant l'âge, et le risque de développer la maladie double tous les 5 ans après 65 ans (Hirtz et al., 2007; Querfurth and LaFerla, 2010). Avec l'augmentation de l'espérance de vie et le vieillissement de la population, les démences et la MA en particulier deviennent un enjeu sociétal majeur (Gallez, 2005).

La MA se caractérise principalement par une détérioration de la mémoire, suivie de l'altération graduelle des capacités de jugement, d'expression verbale, d'orientation etc. L'ordre séquentiel d'apparition de ces événements peut varier, même si les déficits de mémoire sont normalement la première et la plus dominante des altérations fonctionnelles (Roberta A Pagon, 1998; Götz et al., 2004). Les personnes atteintes par la MA meurent 3 à 9 ans après le diagnostic, généralement de malnutrition ou de pneumonie, le diagnostic représentant une des grandes difficultés et un des enjeux majeurs de la MA (Roberta A Pagon, 1998; Querfurth and LaFerla, 2010). En effet, les signes précoces de la MA ressemblent à ceux du vieillissement physiologique, et la MA n'est donc en général diagnostiquée que tardivement. Le diagnostic est difficile car il existe une très grande diversité de symptômes, ressemblant à d'autres pathologies neurodégénératives. Ce diagnostic se fait généralement grâce à des tests cognitifs (comme le test de Folstein, le test Codex etc.), auxquels peuvent s'ajouter des examens médicaux comme l'imagerie par résonance magnétique, la tomographie par émission de positons ou encore des dosages après prélèvement de liquide céphalo-rachidien (Ballard et al., 2011). Un élément fondamental du diagnostic est la recherche

d'atrophie cérébrale, qui est sévère dans la MA (Roberta A Pagon, 1998). La méthode pour établir le diagnostic a été révisée récemment après plusieurs consensus, qui proposent tous d'associer tests cognitifs et critères biologiques (Dubois et al., 2010; Albert et al., 2011; McKhann et al., 2011; Sperling et al., 2011). Il est toutefois important de noter qu'aucun de ces tests ne permet pour l'instant d'affirmer ou d'infirmer avec certitude la présence de la MA, seuls les examens anatomo-pathologiques *post-mortem* n'apportant que trop tardivement un diagnostic certain. Ces examens doivent confirmer la présence simultanée dans le cerveau de plaques ß-amyloïdes et d'agrégats neurofibrillaires, qui sont les caractéristiques fondamentales de la MA, comme décrites pour la première fois en 1907 par Alois Alzheimer lors de l'analyse des sections du cerveau d'un de ses patients, Auguste D. (Alzheimer et al., 1995). La MA est généralement vue comme une tauopathie secondaire, c'est-à-dire qu'elle est secondaire à l'apparition de pathologie ß-amyloïde.

3.2.1.1 - Les plaques ß-amyloïdes

La grande majorité des cas de MA sont sporadiques, c'est-à-dire qu'ils ne sont pas hérités génétiquement même si certains gènes peuvent être des facteurs de risque (dont le principal est *APOE4*). Seulement 0,1% des cas de MA sont familiaux, engendrés par des mutations des gènes codant pour la protéine précuseur de l'amyloïde (APP), ou pour les présénilines-1 et 2 (Bertram and Tanzi, 2005; Blennow et al., 2006). Egalement, les personnes atteintes de trisomie 21, qui portent un allèle additionnel d'APP, ont une fréquence accrue de développement de la MA (Bertram and Tanzi, 2005). Ces facteurs sont les principaux supports de l'hypothèse de la cascade amyloïde pour l'étiologie de la MA sporadique, hypothèse qui prédomine actuellement parmi un grand nombre d'autres (Hardy and Selkoe, 2002; Ittner and Götz, 2011) (pour une vue d'ensemble des différentes hypothèses pour la MA, cf. http://hypothesis.alzforum.org/swan/do!getHome.action).

Le terme amyloïde a été introduit pour décrire une classe hétérogène d'agrégats protéiques présentant une structure secondaire en feuillet bêta plissé, lui conférant une affinité pour le marqueur histochimique rouge congo (Götz et al., 2004). Les peptides ß-amyloïdes (Aß) sont des produits métaboliques naturels formés par l'association de 36 à 43 acides aminés ($Aß_{36}$ à $Aß_{43}$). Les peptides Aß sont dérivés de la protéolyse de l'APP par les actions enzymatiques séquentielles de l'enzyme 1 clivant l'APP sur son site bêta (BACE-1), une ß-sécrétase, et de la γ-sécrétase, un complexe protéique contenant la préséniline 1 dans son cœur catalytique (cf. figure 22) (Haass and Selkoe, 2007; Querfurth and LaFerla, 2010). Le site de

clivage par la γ-sécrétase est critique car il détermine la longueur du peptide généré, $Aß_{40}$ étant la forme la plus courante, et $Aß_{42}$ la moins courante mais la plus fibrillogène et la plus neurotoxique (Selkoe, 2001; Tanzi and Bertram, 2005). Aß s'accumule suite à un déséquilibre entre production et dégradation, et via l'agrégation des peptides, ce qui serait selon l'hypothèse de la cascade amyloïde le déclenchement de la MA. Les agrégations d'Aß sont spontanées, et coexistent sous des formes multiples, comme des oligomères (de 2 à 6 peptides), qui fusionnent en assemblages intermédiaires, ou les feuillets bêta plissés qui forment des fibres insolubles de plaques ß-amyloïdes (Klein et al., 2001; Kayed et al., 2003). Les oligomères solubles et les formes intermédiaires d'amyloïdes sont les formes les plus neurotoxiques d'Aß, les dimères et les trimères étant particulièrement toxiques pour les synapses (Walsh et al., 2005; Walsh and Selkoe, 2007). Les synapses sont les cibles premières de la toxicité d'Aß, et en particulier le compartiment post-synaptique, par des mécanismes d'excitotoxicité *via* les récepteurs NMDA (Selkoe, 2002; Ittner and Götz, 2011).

Dans la MA, Aß est lié à de nombreuses altérations, de l'inflammation aux dysfonctions mitochondriales, et est supposé être le déclencheur de la MA (Querfurth and LaFerla, 2010). La majorité des recherches médicales de ces dernières années sur la MA s'est concentrée sur la lutte contre les formes pathologiques d'Aß, conduisant à un grand nombre d'essais cliniques très prometteurs. Cependant, jusqu'à présent tous ces essais cliniques ont échoué, aggravant parfois la maladie, ce qui a contribué à un nouvel effort de recherche sur la tauopathie (Landhuis, 2011). De plus, dans la MA, la régionalisation et la progression de la tauopathie corrèlent temporellement et anatomiquement avec les dysfonctions neuronales et cognitives, ce qui n'est pas le cas pour la pathologie ß-amyloïde ; d'ailleurs, l'échelle d'évaluation post-mortem du niveau de progression de la MA la plus utilisée est fondée sur les agrégats neurofibrillaires de tau (échelle de "Braak and Braak") (Braak and Braak, 1991, 1995; Arriagada et al., 1992a, 1992b; Bierer et al., 1995; Ihara, 2001; Giannakopoulos et al., 2003; Duyckaerts et al., 2009).

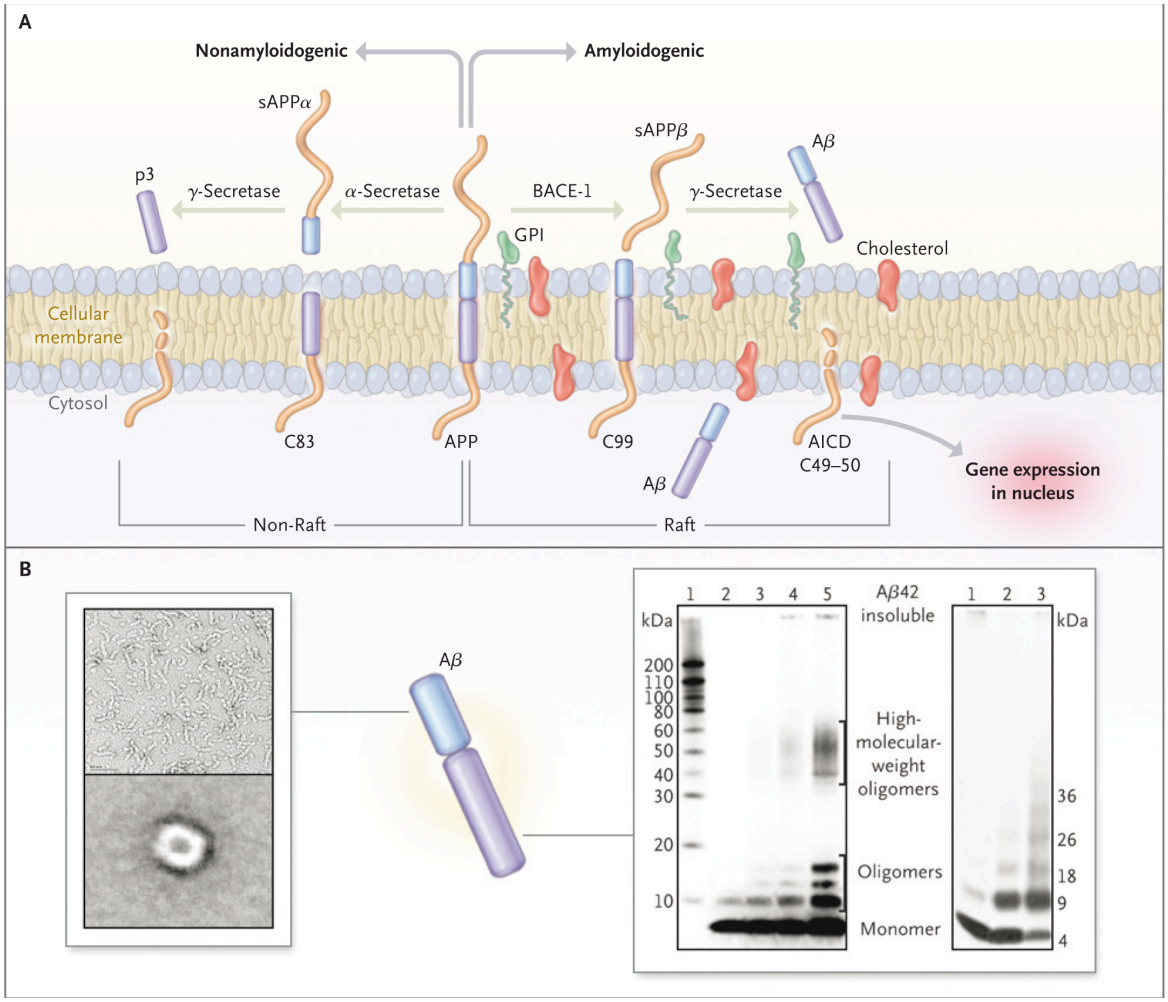

Figure 22 : A : dégradations de la protéine précurseur de l'amyloïde (APP). B : à gauche, agrégats intermédiaires protofibrillaires (en haut) et avec un profil annulaire ou similaire à un pore (en bas). A droite, l'association spontanée en oligomères de 2 à 14 monomères de peptides ß-amyloïde (Aß) est dépendante de leur concentration (immunoblot gauche) ; dans l'immunoblot de droite, l'oligomérisation est provoquée par des conditions oxidantes (ligne 2) et des conditions métalliques divalentes (ligne 3). Abréviations : AICD, domaine intracellulaire amyloïde ; BACE-1, enzyme 1 ß-sécrétase clivant l'APP sur son site bêta ; C83, fragment carboxy-terminal de 83 résidus ; GPI, protéine accrochée au glycophosphatidylinositol ; sAPPα, grand ectodomaine d'APP. (*Adapté de Querfurth and LaFerla 2010*).

3.2.1.2 - La neurodégénérescence induite par tau

La protéine tau possède de nombreuses fonctions, dont les altérations pourraient contribuer à la neuropathogenèse tauopatique de différentes manières. Ces altérations peuvent être regroupées en perte et gain de fonctions propres à la protéine tau, avec en plus des interactions avec Aß.

Perte de fonction de la protéine tau

La mutation du gène codant pour la protéine tau (*MAPT*) n'est pas responsable de la tauopathie dans la MA, que ce soit dans sa forme sporadique ou familiale. Par contre, la mutation de *MAPT* engendre des tauopathies primaires (cf. prochain paragraphe), comme la démence fronto-temporale (von Bergen et al., 2001; Goedert and Jakes, 2005). L'étude de la MA et des tauopathies en général a été révolutionnée par l'apparition de modèles transgéniques murins, réalisés pour la première fois en 1995 par l'expression spécifique neuronale (via le promoteur Thy-1) de l'isoforme humaine la plus longue de la protéine tau (Götz et al., 1995, 2004). Ensuite, de nombreux modèles murins transgéniques différents ont été générés, certains exprimant une forme mutante de protéine tau, comme la mutation P301L (Lewis et al., 2000; Terwel et al., 2005). La plupart de ces souris transgéniques, en particulier celles qui comprennent une mutation, sont caractérisées par la présence intraneuronale d'inclusions filamenteuses composées de protéines tau hyperphosphorylées qui est la caractéristique biochimique de la tauopathie (cf. figure 23) (Ballatore et al., 2007). Cet excès de phosphorylation de tau est la caractéristique invariable menant à la tauopathie, provoquant le détachement de tau des microtubules et une grande propension à l'agrégation (Grundke-Iqbal et al., 1986; Brion et al., 1986; Mandelkow and Mandelkow, 1998; Geschwind, 2003; Mazanetz and Fischer, 2007; Takashima, 2008). La perte de fonction de tau stabilisatrice des microtubules mène très probablement à une altération de la structure normale et des fonctions régulatrices du cytosquelette, compromettant le transport axonal et contribuant ainsi à des dysfonctions synaptiques et à la neurodégénérescence (Roy et al., 2005; Trojanowski et al., 2005). L'importance de cette perte de fonction de tau pour la neurodégénérescence a été validée par des études réalisées *in vivo*, montrant que le paclitaxel, une drogue stabilisatrice des microtubules, améliore le phénotype neurodégénératif de souris transgéniques modèles de la MA présentant la double pathologie tau et amyloïde (Zhang et al., 2005a). Toutefois, certaines données tendent à nuancer cette importance de la perte de fonction de tau. En effet, l'ablation de tau chez des souris "knockout" ($tau^{-/-}$) ne cause pas de mortalité prématurée ou de déficit neurologique majeur (Dawson et al., 2001; Roberson et al., 2007, 2011; Yuan et al., 2008), même si ces souris présentent certaines anomalies comportementales et structurelles au cours du vieillissement (Harada et al., 1994; Ikegami et al., 2000; Dawson et al., 2001). On notera qu'il est possible que d'autres protéines liées aux microtubules compensent la perte de la protéine tau ; il serait intéressant dans ce contexte d'étudier les effets du "knockdown" de tau chez la souris (dont les études sont en cours) (Morris et al., 2011).

Interactions avec Aß

La principale avancée apportée par les souris tau$^{-/-}$ est la démonstration que tau peut être l'acteur de la toxicité d'Aß (Ittner and Götz, 2011). *In vitro*, les neurones tau$^{-/-}$ sont protégés de la mort cellulaire induite par Aß (Rapoport et al., 2002). Cette protection a été retrouvée dans plusieurs études indépendantes *in vivo*, avec des modèles transgéniques d'APP différents (Roberson et al., 2007; Ittner et al., 2010; Vossel et al., 2010). Deux mécanismes principaux ont été avancés. Le premier montre que le "knockout" de tau protège les neurones contre l'excitotoxicité provoquée par Aß, prévenant également les déficits comportementaux (Roberson et al., 2007). Cette protection contre l'excitotoxicité chez les souris tau$^{-/-}$ est due à une localisation dendritique réduite de FYN, résultant en une interaction réduite des NMDARs avec PSD95 (cf. plus haut), et en conséquence diminuant l'excitotoxicité provoquée par Aß (Ittner et al., 2010). On notera que la présence dendritique de tau en faible quantité, dépend de son domaine de liaison aux microtubules ; des protéines tau tronquées n'ayant pas de domaine de liaison aux microtubules n'accèdent pas aux dendrites, protégeant ainsi contre l'excitotoxicité provoquée par Aß (Ittner et al., 2010). Cette protection peut également se faire en pertubant l'interaction entre NMDARs et PSD95 *via* un peptide thérapeutique (Ittner et al., 2010). Le deuxième mécanisme montre que la réduction de tau protège les neurones contre la perturbation du transport axonal des mitochondries et autres cargos induite par Aß (Vossel et al., 2010).

Tau et Aß peuvent également avoir des effets toxiques synergiques, agissant sur différentes parties d'un même système. En particulier, Aß provoque des dysfonctions mitochondriales et induit du stress oxydant, mécanismes pathologiques impliqués dans la neurodégénérescence (Querfurth and LaFerla, 2010). Chez des souris triple-transgéniques, exprimant à la fois des pathologies induites par tau et Aß, ces deux acteurs altèrent la respiration mitochondriale à des niveaux différents, le complexe 1 et le complexe 4 de la chaine respiratoire, respectivement (Rhein et al., 2009).

Les agrégats neurofibrillaires de tau corrèlent avec les atteintes anatomofonctionnelles de la MA, ce qui n'est pas le cas pour les plaques séniles d'Aß, ce qui confère aux espèces toxiques dérivées de tau un rôle prépondérant (Arriagada et al., 1992a, 1992b; Bierer et al., 1995; Ihara, 2001; Giannakopoulos et al., 2003; Duyckaerts et al., 2009). Selon l'hypothèse de la "cascade amyloïde", les espèces toxiques d'Aß déclencheraient la tauopathie. Cependant, les souris transgéniques pour APP, qui présentent de la neurotoxicité et des plaques séniles ß-amyloïdes, ne développent pas d'agrégats neurofibrillaires de tau (Jaworski et al., 2010). Au pire, la protéine tau murine endogène est phosphorylée dans les neurites

dystrophiques autour desquels se trouvent des plaques ß-amyloïdes (Moechars et al., 1999; Van Leuven, 2000; Van Dorpe et al., 2003). Mais cela peut être dû à la différence d'expression d'isoformes de la protéine tau entre la souris et l'Homme. En effet, lorsque des souris transgéniques pour APP sont croisées avec des souris transgéniques pour tau, la tauopathie est exacerbée, mais pas les plaques ß-amyloïdes (Lewis et al., 2001; Terwel et al., 2008). En outre, l'injection intracrânienne de fibrilles d'$Aß_{42}$ dans des souris transgéniques Tau-P301L aggrave et accélère la formation d'agrégats neurofibrillaires de tau (Götz et al., 2001). De plus, chez des souris triple transgéniques combinant les pathologies induites par tau et Aß, l'immunisation contre les plaques ß-amyloïdes réduit le niveau d'hyperphosphorylation de tau (Oddo et al., 2004). Il semble donc qu'Aß influence l'hyperphosphorylation des isoformes humaines de tau. Dans cette interaction entre Aß et la phosphorylation de tau, l'enzyme GSK3ß (Glycogène Synthase Kinase 3ß) peut jouer un rôle prépondérant (Muyllaert et al., 2006, 2008; Terwel et al., 2008).

Gains de fonctions de la protéine tau

Les tauopathies neurodégénératives sont caractérisées par la présence d'agrégats de protéines tau neurofibrillaires, en filaments droits ou pairés en hélices, en rubans torsadés ou toute autre conformation de tau phosphorylée de manière aberrante (Buée et al., 2000; Ballatore et al., 2007). En effet, en condition pathologique, l'équilibre de tau se liant aux microtubules est perturbé, résultant en une augmentation anormale du niveau de la fraction de tau libre dans le cytosole. Différentes kinases et phosphatases régulent le niveau de phosphorylation de tau, dont les principales sont GSK3α et ß (Glycogène Synthase Kinase 3), CDK5 (Cyclin-Dépendante Kinase 5) et MARK (Kinase Régulant l'Affinité des Microtubules) pour les kinases, et PP1 (Phosphatase Protéique 1), PP2A, PP2B et PP2C pour les phosphatases. L'activation ou l'inhibition de ces enzymes en condition pathologique participe au développement d'hyperphosphorylations de tau. En particulier, GSK3ß peut être activée par Aß, conduisant à un excès de phosphorylation de tau (Terwel et al., 2008). De manière surprenante, la surexpression de GSK3ß chez des souris transgéniques Tau-P301L conduit à une accélération et une aggravation de la tauopathie dans les structures supérieures du cerveau, alors que cela protège le tronc cérébral contre la tauopathie (Terwel et al., 2008). En effet, les souris Tau-P301L présentent normalement une tauopathie dense dans le tronc cérébral, qui pourrait expliquer la mortalité précoce de ces souris entre 9 et 11 mois, or la surexpression de GSK3ß chez ces souris leur redonne une durée de vie normale (Terwel et al., 2005, 2008). Un autre phénomène conduisant à l'hyperphosphorylation de tau est

l'hypothermie. Notamment, une anesthésie non contrôlée en température induit une hyperphosphorylation de tau, qui ne revient pas à la normale *a posteriori* chez des souris Tau-P301L, phosphorylation résultant principalement de l'inhibition de PP2A (Planel et al., 2007, 2008, 2009). D'une manière générale, plus les concentrations cytosoliques en protéines tau sont élevées et donc plus les protéines tau sont phosphorylées, plus il y a de chances que ces protéines se conforment en mauvais repliements ("misfolding"), augmentant leur propension à l'agrégation (Kuret et al., 2005; Jeganathan et al., 2008). Ensuite, de petits dépôts non fibrillaires de tau sont formés, qui vont eux-même devenir des filaments pairés en hélice puis des agrégats neurofibrillaires (Kuret et al., 2005; Ballatore et al., 2007).

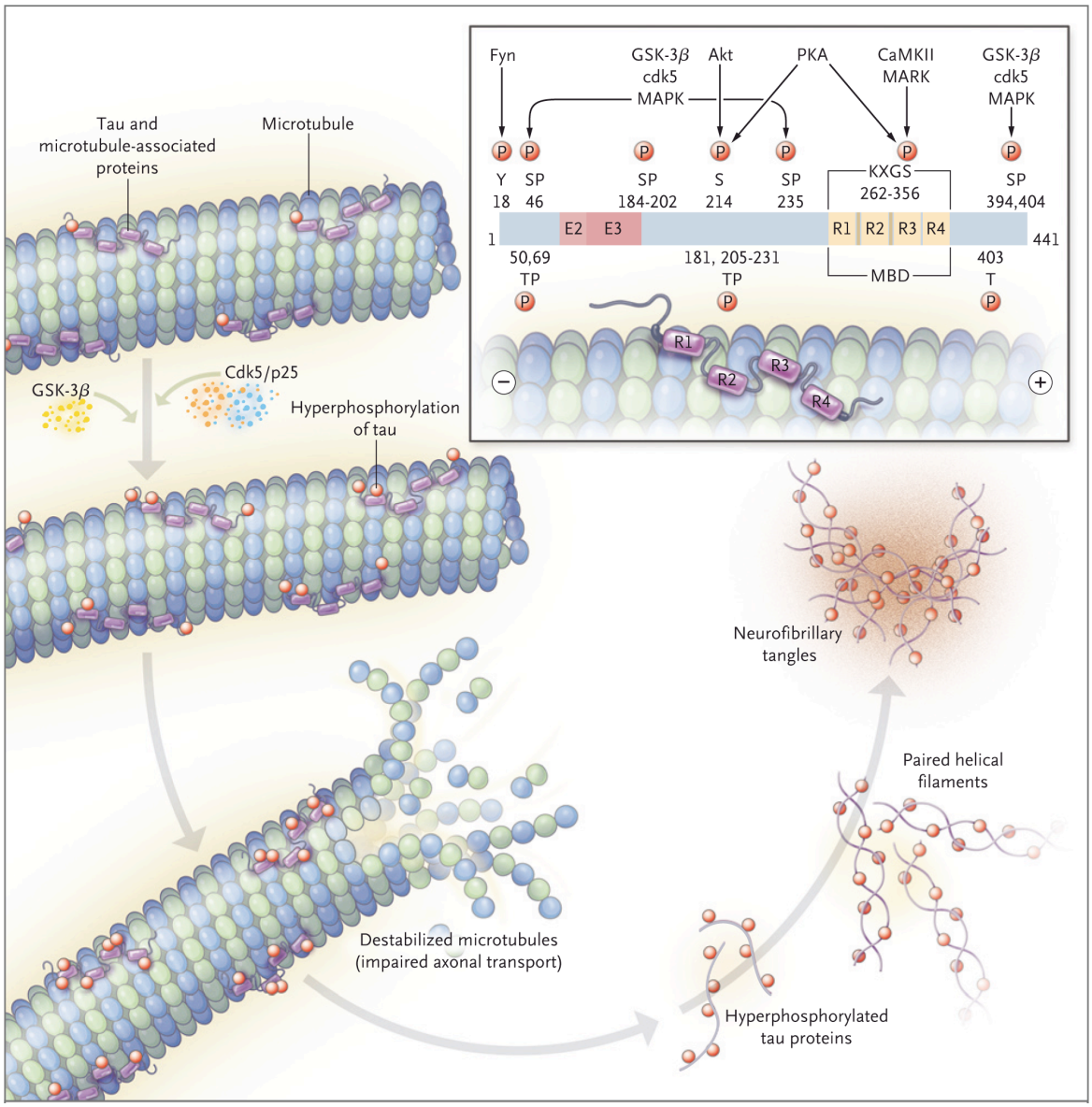

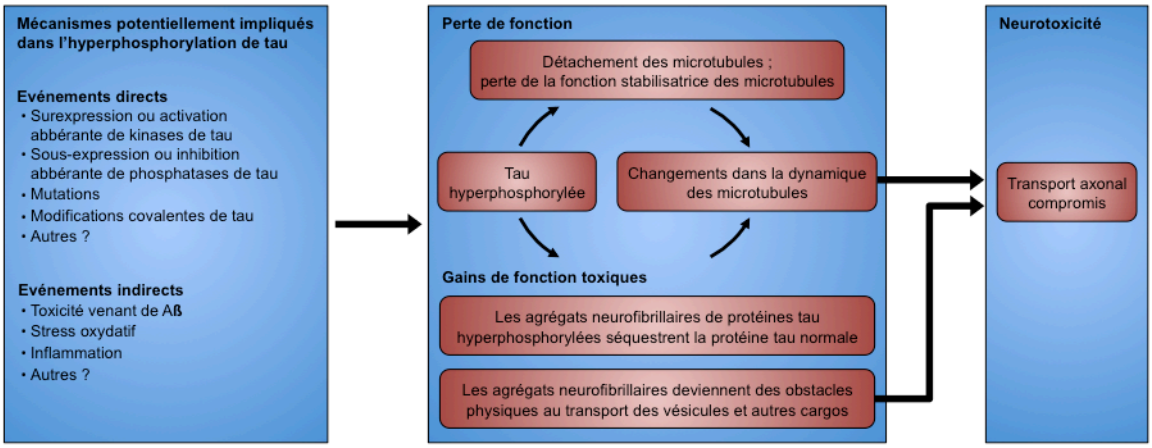

Figure 23 : fonctions et structures de la protéine tau. Des séquences à 4 répétitions (R1-R4) font le domaine d'association au microtubule (MBD). Les sites de phosphorylation (P en rouge) de tau sont sur ses résidus sérine (S), thréonine (T), proline (P), *via* la glycogène synthase kinase 3ß (GSK-3ß), la kinase cyclin-dépendante (cdk5) et sa sous-unité activatrice p25, la protéine kinase activée par le mitogène (MAPK), l'Akt, la protéine kinase FYN, la protéine kinase A (PKA), la proétine kinase calcium-calmoduline 2 (CaMKII), la kinase régulant l'affinité des microtubules (MARK). KXGS (pour lysine, un acide aminé inconnu ou autre, glycine, et sérine) est un motif cible. L'association de tau au microtubule induit son assemblage et sa stabilité. Des activités excessives des kinases, ou réduites des phosphatases, ou les deux, causent l'hyperphosphorylation de tau qui se détache des microtubules (ce qui déstabilise les microtubules), et s'agrège spontanément. (*Adapté de Querfurth and LaFerla 2010, et de Ballatore et al. 2007*).

Cette cascade menant à la formation des agrégats neurofibrillaires de tau est la caractéristique invariable des tauopathies, dans lesquelles la répartition anatomique des agrégats neurofibrillaires de tau corrèle avec les altérations fonctionnelles retrouvées (notamment atteinte de l'hippocampe et troubles de la mémoire), suggérant l'importance de gains de fonctions toxiques de tau pour la progression de la maladie. La majorité des stratégies thérapeutiques envisagées pour lutter contre la tauopathie (et actuellement en essais cliniques) visent à empêcher l'excès de phosphorylation de tau, notamment en inhibant GSK3ß *via* le lithium (Noble et al., 2005; Ballatore et al., 2007; Morris et al., 2011). Un autre mécanisme encore peu étudié est la ß-*N*-acétylglucosamination *O*-liée (O-GlcNAcylation) de la protéine tau, qui comme pour la phosphorylation est régulée enzymatiquement et est en équilibre dynamique constant (cf. figure 24) (Yuzwa and Vocadlo, 2009). L'O-GlcNAcylation de tau est en compétition avec la phosphorylation, et lorsque tau est hyperphosphorylée, elle est très peu O-GlcNAcylée (Liu et al., 2004; Yuzwa et al., 2008). Dans ce contexte, les agents pharmacologiques favorisant l'O-GlcNAcylation de tau, et en particulier les inhibiteurs de la O-GlcNAcase (l'enzyme clivant O-GlcNAc et protéine tau), représentent de futurs espoirs thérapeutiques (Yuzwa et al., 2008).

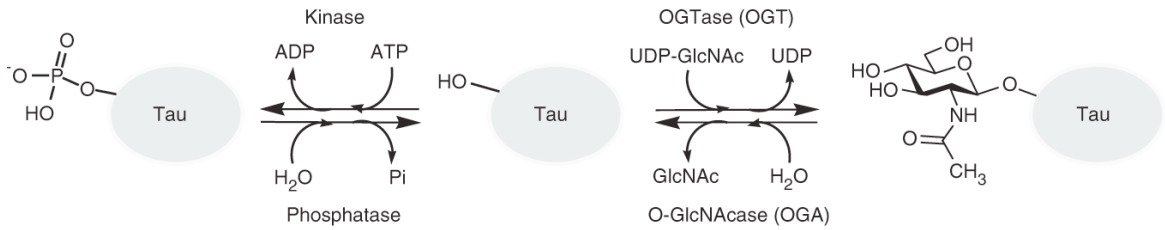

Figure 24 : la relation entre la phosphorylation et l'O-GlcNAcylation de tau est en équilibre dynamique. L'existence de résidus sérine ou thréonine qui sont connus pour être tous les deux phosphorylés et O-Glc-NAc-modifiés détermine que ce type de résidus peuvent exister dans un état parmi trois différents : phosphorylé, glycosylé ou en hydroxyle libre. La formation de ces états est régulée par les enzymes appropriées. (*Adapté de Yuzwa et al. 2008*).

Il est possible que l'effet toxique des agrégats neurofibrillaires soit dû à leur taille relativement large, s'accumulant à l'intérieur des neurones, et pouvant causer une altération physique directe des fonctions cellulaires comme le transport axonal (Ballatore et al., 2007). De plus, les agrégats neurofibrillaires de tau peuvent aussi contribuer à la progression de la pathologie en séquestrant plus de protéines tau avec d'autres protéines, renforçant et amplifiant la perte de fonction physiologique de tau. Cependant, cette importance des agrégats neurofibrillaires de tau pour la toxicité neuronale est de plus en plus remise en question. Chez une souris transgénique tau-P301L régulable, l'inhibition de la production de tau après la formation d'inclusions filamenteuses abolit leurs déficits comportementaux dans la piscine de Morris, alors que la formation des inclusions persiste (Santacruz et al., 2005). Dans ce même modèle, la réduction aigue de tau avec un traitement au bleu de méthylène améliore les scores de mémoire en corrélation avec la réduction de protéine tau soluble dans le cerveau, mais sans altérer le nombre ou la longueur des fibrilles de tau ou la quantité de tau Sarkosyl-insoluble (O'Leary et al., 2010). Dans un autre modèle de souris, exprimant un transgène de tau pro-agrégant et développant des pertes synaptiques, des déficits de mémoire et des altérations électrophysiologiques, on constate que l'arrêt expérimental d'expression du transgène réverse les déficits cités précédemment sans éliminer les agrégats insolubles de tau (Mocanu et al., 2008; Sydow et al., 2011). Ces données suggèrent que la toxicité de tau passerait peut-être par les espèces intermédiaires, avant la formation des agrégats insolubles. Ceci est soutenu par des études réalisées *in vivo* avec de l'imagerie bi-photonique sur les souris Tau-P301L régulables, qui montrent qu'il y a une activation de caspases dans les neurones précédant la formation d'agrégats neurofibrillaires de tau, et que ce signal pro-apoptotique ne mène pas à la mort cellulaire une fois les agrégats de tau formés malgré des altérations membranaires (de

Calignon et al., 2009, 2010). Egalement, le fait de diminuer le niveau de tau soluble réduit l'activation des caspases dans les neurones contenant des inclusions de tau, sans affecter le nombre et la taille de ces inclusions (de Calignon et al., 2010). Chez des souris transgéniques exprimant la mutation P301S de tau, des pertes synaptiques et une activation microgliale précèdent la formation des agrégats neurofibrillaires de tau (Yoshiyama et al., 2007). De plus, des études menées chez la drosophile confirment la toxicité des espèces solubles de tau, potentiellement les dimères (Feuillette et al., 2010). Dans l'ensemble, ces études suggèrent que les espèces de tau solubles seraient les plus toxiques, notamment les oligomères, qui ont été identifiés *in vitro* et *in vivo* à la fois chez des modèles murins et dans des cerveaux de personnes atteintes de MA (Maeda et al., 2007; Berger et al., 2007; Sahara et al., 2008).

La recherche sur la protéine tau a considérablement augmenté ces dernières années, principalement à cause de la progression alarmante de la MA. De nouveaux mécanismes sont découverts régulièrement, comme le fait que tau peut également avoir des effets toxiques depuis le milieu extracellulaire (Gómez-Ramos et al., 2006, 2008; Frost et al., 2009), ou encore que la tauopathie peut être transmise par l'injection d'extraits de cerveau pathologique dans un cerveau sain et se propager ensuite trans-synaptiquement (Clavaguera et al., 2009). On ne sait pas si la progression de la MA d'une région à une autre suit le même processus, même s'il est souvent admis que la mort neuronale induite par la tauopathie se fait de manière rétrograde (Braak and Braak, 1997). De plus, l'hyperphosphorylation de tau conduit à une inversion de la distribution cellulaire de la protéine tau, avec plus de protéine tau au niveau du soma et des dendrites du neurone atteint, ceci conduisant certainement aux effets délétères à la fois pré et post-synaptiques généralement observés (Hoover et al., 2010; Ittner and Götz, 2011). On notera que la majorité des recherches sur la tauopathie associées à la MA se fait sur des modèles murins transgéniques exprimant des formes mutantes de protéine tau humaine, mutations qui sont responsables de la démence frontotemporale et des autres tauopathies primaires, mais pas de la MA.

3.2.2 - La démence frontotemporale et les autres tauopathies

Les souris transgéniques Tau-P301L, exprimant la mutation P301L dans une isoforme de protéine tau humaine, sont un modèle de tauopathie très répandu notamment pour la recherche expérimentale sur la MA. Cette mutation absente dans la MA est présente dans la

démence frontotemporale (DFT) (Hutton et al., 1998).

Contrairement à la MA qui est principalement caractérisée par une perte de mémoire, la DFT débute avec des désordres comportementaux (comme la désinhibition, la perte de conscience de soi et des rapports sociaux), suivis par des symptômes affectifs, des troubles de la vocalisation et des problèmes de mémoire (comme pour la MA) (Götz et al., 2004). Un parkinsonisme tardif est commun, et une occurrence familiale est très fréquente (Groups TLaM, 1994; Neary et al., 1998). En général, une atrophie symétrique des lobes frontal et temporal est observée, avec fréquemment une altération dégénérative d'autres régions comme la substance noire (Wszolek et al., 1992). Il existe une forme familiale de DFT liée à des mutations du gène *MAPT* sur le chromosome 17, appelée DFTP-17 car entraînant systématiquement un parkinsonisme tardif (Froelich et al., 1997; Hutton et al., 1998; Spillantini et al., 1998).

La maladie de Pick est une forme extrême de DFT, mais difficile à différencier en clinique, car présentant les mêmes symptômes que la DFT classique. Toutefois, des lésions neuronales contenant de grandes densités de protéines tau dégénérées, appelées corps de Pick, sont retrouvées dans de nombreuses régions du cerveau (Brion et al., 1991; Hof et al., 1994). Une autre tauopathie, la paralysie supranucléaire progressive, nommée ainsi à cause de l'ophtalmoplégie supranucléaire qui la caractérise, affecte progressivement l'équilibre, la vue, la déglutition ou encore la parole, et cause des troubles du système autonome pour la régulation cardiovasculaire (Gutrecht, 1992; Litvan et al., 1996). Enfin, la dégénérescence corticobasale est une tauopathie qui touche principalement les régions sous-corticales puis corticales, avec un dysfonctionnement moteur asymétrique des membres supérieurs, une perte sensorielle corticale, une apraxie, des troubles du langage de type dysarthrie, des dysphagies etc. (Rebeiz et al., 1968; Rinne et al., 1994).

Dans l'ensemble, il n'existe pas de traitements autres que symptomatiques pour les tauopathies (comme pour la MA). Même si la tauopathie ne s'exprime pas de la même manière que dans la MA, on peut noter qu'il existe de nombreux symptômes similaires, les différences pouvant être dues pour la MA à la présence supplémentaire de plaques ß-amyloïdes. S'il est bien une caractéristique qui revient systématiquement dans les tauopathies, c'est l'atteinte fonctionnelle des VAS, notamment pour la déglutition et la vocalisation, qui est certainement la conséquence de l'atteinte du tronc cérébral par la tauopathie. Cependant, ces pistes n'ont été que très peu étudiées, malgré leur importance pour le développement de la pathologie, le handicap qu'elles induisent, et leur rôle prépondérant pour la mortalité.

3.3 - Structures et fonctions neurovégétatives dans la tauopathie

Dans les tauopathies en général, et surtout dans la MA, l'attention des médecins et des chercheurs se focalise principalement sur les altérations morphofonctionnelles des structures supérieures du cerveau, notamment l'hippocampe pour son rôle dans les processus mnésiques. Cependant, l'intégralité du SNC est atteinte par la tauopathie, le tronc cérébral ne faisant pas exception, cette atteinte variant tout de même en fonction du type de tauopathie.

Une étude longitudinale de grande envergure a montré qu'il existe une corrélation négative entre la qualité de la fonction respiratoire vers 50 ans et le risque de développer la MA (Guo et al., 2007). Egalement, lorsque des troubles nocturnes de la respiration sont présents chez des personnes atteintes de MA, l'appareillage imposant une pression positive d'air en continu réduit les apnées obstructives du sommeil et les altérations cognitives des patients (Ancoli-Israel et al., 2008; Cooke et al., 2009). Chez des personnes en période initiale de MA, une augmentation de la capacité cardiorespiratoire d'apport en oxygène est associée à une réduction de l'atrophie cérébrale (Burns et al., 2008). Enfin, la présence de la variante ε4 du gène codant pour l'Alipoprotéine E (*APOE4)*, qui est le facteur de risque génétique le plus connu et répandu pour la MA, est associée aux troubles nocturnes de la respiration (Kadotani et al., 2001; Bliwise, 2002). Ces études montrent dans l'ensemble qu'il existe un lien entre fonction respiratoire et MA, ou notamment qu'un défaut de fonction respiratoire peut aggraver la MA. Ceci est d'autant plus important qu'il est très probable que des hypoxies prolongées puissent provoquer la MA (Peers et al., 2007; Zhang et al., 2008). Comme pour les tauopathies citées ci-dessus, la principale cause de mortalité chez les personnes atteintes de MA est la dysphagie avec pneumonie d'aspiration (Kalia, 2003). De plus, les tauopathies sont souvent accompagnées par des troubles moteurs du langage (Hillert, 1999; Tolnay and Probst, 2002). Il est par conséquent très probable qu'il y ait une altération centrale des structures générant la commande de ces actes moteurs, affectant certainement la commande respiratoire.

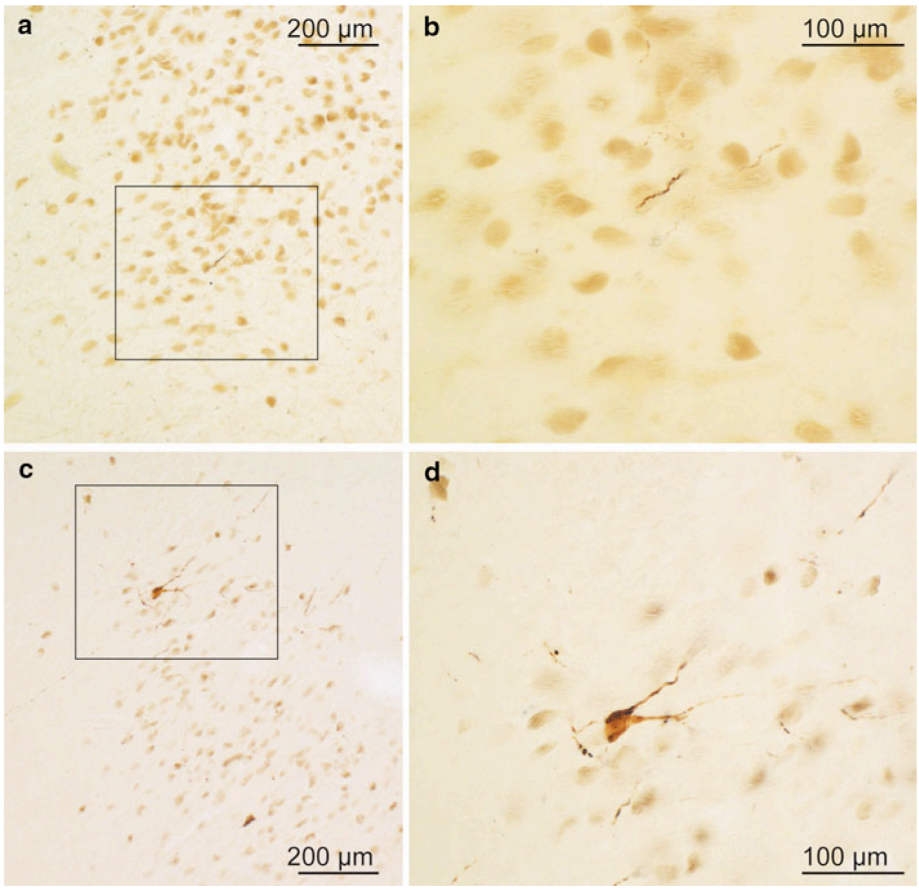

Figure 25 : séquence de formation pré-agrégat dans les cellules du locus cœruleus de jeunes garçons. Les sections de 100µm sont marquées avec l'anticorps AT8 marquant la protéine tau hyperphosphorylée, le marquage AT8 étant généralement reconnu comme un marqueur de tau à la limite entre physiologie et pathologie. **a** et **b** : un axone marqué par AT8 chez un garçon de 14 ans. **c** et **d** : marquage AT8 d'axones mais aussi du compartiment somatodendritique de neurones du locus cœruleus chez un garçon de 11 ans. **b** et **d** sont des agrandissements de **a** et **c**, respectivement. (*Adapté de Braak and Del Tredici 2011*).

Le tronc cérébral est atteint par la tauopathie, notamment les noyaux bioaminergiques. En particulier, les recherches en cours dans le domaine identifient le locus cœruleus (LC) comme un noyau d'une grande importance pour la MA : Le LC est atteint dans la MA, il dégénère et subit une perte neuronale, associée à une réduction de la densité de transporteurs de la noradrénaline (Mann et al., 1980; Bondareff et al., 1982; Haglund et al., 2006; Gulyás et al., 2010). Chez l'Homme atteint de MA, le LC est touché par la tauopathie dès les stades initiaux de la maladie (Grudzien et al., 2007) et il semblerait que le LC soit le premier noyau atteint par la tauopathie. En effet, le LC de jeunes garçons de 11 et 14 ans présente déjà des protéines tau hyperphosphorylées, dans la conformation précédant l'agrégation, marquées par l'anticorps AT8 (cf. figure 25) (Braak and Del Tredici, 2011a, 2011b). L'investigateur principal de ces études, M. Heiko Braak, dont l'échelle d'évaluation de la MA est une

référence, propose même que la MA débute dans le LC puis se propage par transmission transneuronale notamment de la tauopathie, ce qui est soutenu par de nombreuses autres études (German et al., 1992; Parvizi et al., 2001; Lyness et al., 2003; Zarow et al., 2003; Haglund et al., 2006; Grudzien et al., 2007; Sara, 2009; Grinberg et al., 2009; Simic et al., 2009; Braak and Del Tredici, 2011a, 2011b). Les projections très larges du LC permettraient la dissémination de la pathologie aux différentes régions du cerveau. Le système sérotoninergique est également touché dans la MA et les autres tauopathies, en particulier les raphés pontiques, présentant des pertes cellulaires dues à la pathologie et dans les phases initiales de la maladie, avec également des altérations des récepteurs et des transporteurs de la 5-HT (Halliday et al., 1992; Aletrino et al., 1992; Mössner et al., 2000; Rüb et al., 2000; Parvizi et al., 2001; Yang and Schmitt, 2001; Kovacs et al., 2003; Hendricksen et al., 2004; Kepe et al., 2006; Thomas et al., 2006; Grinberg et al., 2009; Simic et al., 2009). Comme pour le LC, l'atteinte du système sérotoninergique par la MA est très précoce, pourrait même être initiale avec le LC, et les projections très larges des neurones sérotoninergiques propageraient la pathologie et en particulier la tauopathie dans tout le système nerveux central. D'autres zones du tronc cérébral sont atteintes par la tauopathie, et notamment la substance grise périaqueducale (PAG), le complexe parabrachial (PB) et le noyau de Kölliker-Fuse (KF) (Parvizi et al., 1998, 2000; Rüb et al., 2001, 2002). A notre connaissance, rien n'indique dans la bibliographie que les noyaux respiratoires de la surface ventrale du bulbe rachidien soient touchés par la tauopathie et il semble que la tauopathie concerne principalement les noyaux respiratoires pontiques, ce qui peut avoir des conséquences graves notamment pour la gestion de la post-inspiration et des VAS, ce dernier point ayant été le sujet principal de cette thèse. En effet, jusqu'à présent et malgré les évidences d'interactions entre le système respiratoire et la tauopathie citées précédemment, l'effet de la tauopathie sur la genèse de la commande centrale respiratoire n'avait encore jamais été étudié. De plus, les souris Tau-P301L, modèle murin reconnu de tauopathie, meurent de façon prématurée et présentent une tauopathie dense mais régionalisée dans le tronc cérébral.

Nota Bene : nous avons eu la chance dans cette thèse de pouvoir analyser la commande respiratoire des souris Tau-P301L. En chapitre 3 de la partie résultats, nous montrons 1) que les souris Tau-P301L présentent un dysfonctionnement des VAS conduisant à une altération de la respiration et de la vocalisation, 2) que ce dysfonctionnement est certainement lié à l'atteinte par la tauopathie des noyaux pontiques respiratoires et notamment du KF mais aussi potentiellement du système 5-HT, et 3) que ce dysfonctionnement peut être déclenché précocement par une anesthésie hypothermiante.

Résultats

I - Syndrome de Rett et troubles respiratoires, études chez la souris *Mecp2*$^{-/y}$

Dans ce chapitre sont présentées les études que nous avons réalisées sur l'altération respiratoire présente chez les souris *Mecp2*$^{-/y}$, un modèle murin du Syndrome de Rett. Nous montrons tout d'abord que des altérations respiratoires peuvent survenir en période pré-symptomatique chez les souris *Mecp2*$^{-/y}$ après une hypoxie ou une hypercapnie modérée (1). Ensuite, nous montrons que la respiration post-soupir est également altérée durant la période pré-symptomatique chez les souris *Mecp2*$^{-/y}$, et que ces anomalies s'aggravent avec l'âge (2). Enfin, nous montrons qu'environ 40% des apnées des souris *Mecp2*$^{-/y}$ en période symptomatique sont des apnées obstructives, où les muscles de la cage thoracique forcent contre les voies aériennes supérieures qui sont obstruées (3).

1 - Défauts respiratoires précoces après une hypoxie ou une hypercapnie modérée chez un modèle murin du Syndrome de Rett

Voituron N., Zanella S., **Menuet C.**, Dutschmann M. & Hilaire G.
Publié dans *Respiratory Physiology & Neurobiology*, en 2009.

Résumé en français :

Le Syndrome de Rett (SR) est une maladie rare neurodéveloppementale causée par des mutations dans le gène du répresseur transcriptionnel methyl-CpG-binding protein 2 (MeCP2) et accompagnée par des symptômes complexes, incluant une respiration erratique et des apnées dramatiques. Chez des souris mâles dont le gène *Mecp2* a été muté (souris *Mecp2*$^{-/y}$), la respiration est normale à la naissance, mais elle devient altérée après le 30^{e} jour postnatal (P30), avec un rythme erratique et des apnées qui s'aggravent jusqu'à la mort aux alentours de P60. Utilisant la pléthysmographie, nous avons analysé la respiration de souris sauvages et *Mecp2*$^{-/y}$ non restreintes à P15, P25, et P30 en conditions d'air ambiant et d'expositions de courte durée à une hypoxie ou une hypercapnie modérée. Nous montrons que les souris *Mecp2*$^{-/y}$ qui ont une ventilation de repos normale présentent une réponse respiratoire à l'hypoxie exacerbée à P30, ainsi que des apnées et un rythme respiratoire erratique transitoires après une hypoxie et après une hypercapnie à P30, P25 et occasionnellement à P15. Des facteurs environnementaux peuvent donc induire des défauts respiratoires bien avant ceux attendus chez les souris *Mecp2*$^{-/y}$ et potentiellement chez les patientes RTT. Par conséquent, nous suggérons d'éviter l'exposition des jeunes patientes RTT à des situations environnementales où elles pourraient rencontrer une hypoxie ou une hypercapnie modérée.

Respiratory Physiology & Neurobiology 168 (2009) 109–118

Contents lists available at ScienceDirect

Respiratory Physiology & Neurobiology

journal homepage: www.elsevier.com/locate/resphysiol

Early breathing defects after moderate hypoxia or hypercapnia in a mouse model of Rett syndrome

Nicolas Voituron[1], Sébastien Zanella[1,2], Clément Menuet, Mathias Dutschmann[3], Gérard Hilaire*

Maturation, Plasticity, Physiology and Pathology of Respiration (mp3-resp team), Unité Mixte de Recherche 6231 CNRS, Faculté Saint-Jérôme, Service 362, 13397 Marseilles Cedex 20, France

ARTICLE INFO

Article history:
Accepted 29 May 2009

Keywords:
Hypoxia
Hypercapnia
Mecp2
Rett syndrome
Tidal volume

ABSTRACT

Rett syndrome (RTT) is a rare neurodevelopmental disease caused by mutations in the transcriptional repressor methyl-CpG-binding protein 2 (MeCP2) and accompanied by complex symptoms, including erratic breathing and life-threatening apnoeas. In *Mecp2*-deficient male mice (*Mecp2*$^{-/y}$), breathing is normal at birth but becomes altered after postnatal day 30 (P30), with erratic rhythm and apnoeas aggravating until death at around P60. Using plethysmography, we analyzed breathing of unrestrained wild type mice and *Mecp2*$^{-/y}$ at P15, P25 and P30 under air and under short-lasting exposure to moderate hypoxia or hypercapnia. In *Mecp2*$^{-/y}$ with normal resting ventilation, we report exacerbated respiratory responses to hypoxia at P30 and transient apnoeas with erratic rhythm after hypoxia and hypercapnia at P30, P25 and occasionally P15. Then environmental factors may induce breathing defects well before than expected in *Mecp2*$^{-/y}$ and possibly in RTT patients. We therefore suggest avoiding exposure of young RTT patients to environmental situations where they may encounter moderate hypoxia or hypercapnia.
© 2009 Elsevier B.V. All rights reserved.

1. Introduction

Rett syndrome (RTT) is a severe neurodevelopmental disease and the leading cause for genetic mental retardation in girls. After normal first postnatal months, RTT girls develop regression of acquisitions and different behavioural symptoms, including breathing defects with erratic rhythm and life-threatening apnoeas (Katz et al., 2009). RTT is caused by mutations in the X-linked gene that encodes methyl-CpG-binding protein 2 (MeCP2) and therefore MeCP2-deficient mice have been generated (Guy et al., 2001). After normal first postnatal weeks, males of *Mecp2*-deficient mice (*Mecp2*$^{-/y}$) develop symptoms reminiscent of RTT, with stiff, uncoordinated gait, reduced body movements and breathing defects (Guy et al., 2001; Viemari et al., 2005; Ogier et al., 2007; Katz et al., 2009). Although breathing of *Mecp2*$^{-/y}$ is normal at birth, rhythm irregularities and apnoeas develop after postnatal day 30 (P30). Then breathing becomes erratic, interrupted by severe apnoeas, leading to respiratory distress and premature death at around P60. Evidence exists that *Mecp2*$^{-/y}$ breathing defects are central in origin, reflecting dysfunctions of several systems implicated in the modulation and/or the production of the central respiratory drive such as the norepinephrine, serotonin, GABA, glutamate and BDNF systems (Katz et al., 2009).

From birth, the central respiratory drive must be permanently adapted to physiological needs. This means that the respiratory rhythm generator (RRG), possibly including the pre-Bötzinger Complex and the RTN/pFRG groups, and the central pattern generator, including neurons of the medullary ventral respiratory group (VRG) and pontine nuclei (Smith et al., 1991; Monteau and Hilaire, 1991; Bianchi et al., 1995; Hilaire and Duron, 1999) must permanently adjust their activity to environmental and behavioural changes to adequately secure rhythmic contractions of the respiratory muscles, normal air flow into/out of the lungs and correct blood oxygenation. This is achieved thanks to afferent inputs impinging on the respiratory network, such as those from the carotid body chemoceptors detecting peripheral blood hypoxia, those from brainstem neurons detecting central hypercapnia (Corcoran et al., 2009; Guyenet et al., 2009; Onimaru et al., 2009), those from vagal pulmonary receptors detecting lung inflations (Burnet and Hilaire, 1999), etc. MeCP2 loss may impair these respiratory reflexes, possibly inducing inadequate changes in respiratory frequency and/or amplitude in response to hypoxia and lung inflations. Indeed adult *Mecp2*$^{-/y}$ at P45 which already exhibit breathing defects, abnormally respond to hypoxia and vagal inputs (Bissonnette and Hilaire, 2008; Stettner et al., 2007; Roux et al., 2008).

* Corresponding author. Tel.: +33 491 28 81 72; fax: +33 491 28 83 97.
E-mail address: gerard.hilaire@univ-cezanne.fr (G. Hilaire).
[1] These two authors participate equally to the work.
[2] Present address: Seattle Children's Research Institute, Center for Neuroscience & University of Washington, Neurosurgery Department, Seattle, WA 98101, USA.
[3] Present address: Institute of Membrane and Systems Biology, Garstang Building, University of Leeds, Leeds LS2 9JT, UK.

1569-9048/$ – see front matter © 2009 Elsevier B.V. All rights reserved.
doi:10.1016/j.resp.2009.05.013

Here, we wondered whether the respiratory responses to hypoxia and hypercapnia were normal in young *Mecp2*$^{-/y}$ before the appearance of abnormal resting ventilation. We show exaggerated respiratory responses to hypoxia in *Mecp2*$^{-/y}$ at P30, an age when their breathing is still normal at rest. In addition for the first time, we show that imposing moderate hypoxia or hypercapnia to young *Mecp2*$^{-/y}$ transiently induces erratic breathing and apnoeas as early as at P30, P25 and even P15. Such early abnormal respiratory responses to moderate environmental challenges may contribute to the evolution of the disease in *Mecp2*$^{-/y}$, and eventually RTT girls.

2. Methods

Experiments were carried out in accordance with the European guidelines for the care and use of laboratory animals (Council Directive 86/6009/EEC) in mouse model for Rett Syndrome [strain B6.129P2(C)-*Mecp2*tm1–1Bird] (The Jackson Laboratory, Bar Harbor, ME). As reported previously (Viemari et al., 2005; Zanella et al., 2008), hemizygous mutant *Mecp2* males (*Mecp2*$^{-/y}$) were generated by crossing heterozygous knock-out females with wild type (WT) C57BL/6 males (Guy et al., 2001) and genotyped by routine PCR technique after the experiments.

In non-anesthetized, unrestrained and non-genotyped mice at postnatal day 15 (P15), P25, P30 and eventually P60, breathing was recorded using a constant flow whole-body plethysmograph (EMKA Technologies, Paris, France), with 200 ml animal chambers maintained 25 ± 0.5 °C and ventilated with air (600 ml min^{-1}). Twenty-five mice were studied (13 WT and 12 *Mecp2*$^{-/y}$). Before weaning, pups were housed together with their mother and eight males were first analyzed at P15. After weaning at P21, male littermates were housed together in identical cages where they had free access to food and water (three to four mice per cage). The mice previously analyzed at P15 were again analyzed at P25 and thereafter sacrificed for other purposes. Seventeen mice were not analyzed at P15 and P25 but were analyzed first at P30 and eventually at P60 when they survived. Two or three days before plethysmographic recordings, mice were habituated to stay in the plethysmograph chamber to reduce stress effect on breathing. Only periods of breathing without body movements were analyzed. To check the respiratory responses to hypoxia and hypercapnia, air was replaced by hypoxic (O_2, 10%) or hypercapnic (CO_2, 4%) gas mixture for short-lasting periods (5 min). Routinely, WT and *Mecp2*$^{-/y}$ were simultaneously recorded and subjected to the same environmental challenges. We measured the respiratory frequency (fR, in cycle per min, c min^{-1}), the tidal volume (V_T, μl) normalized as the ratio V_T divided by the body weight (V_T, μl g^{-1}), the minute ventilation (V_E, ml g^{-1} min^{-1}), the number of apnoeas per min > two normal respiratory cycles (apnoeas > 2Ttot) expressed as the Apnoea Index (AI) and the irregularity score (IS, variability in duration of respiratory cycles, see Viemari et al., 2005) during five successive periods. Measurements were performed during: (1) control period under air, prior to the challenge, (2 and 3) the 3rd min and the 5th min periods of the challenge, (4) the post-challenge period (after the end of the challenge when normoxia or normocapnia was restored in the plethysmographic chamber for 2 min), and (5) 10–15 min later.

Values are presented as mean ± standard error of the mean (S.E.M.). For all statistics, differences were considered significant when $p < 0.05$. The significance of difference between WT and *Mecp2*$^{-/y}$ values was determined by analysis of variance (ANOVA) followed by Fisher's PLSD (Post Hoc Least Squares Difference) correction. The significance of difference between control values and challenge values was determined by paired Student's *t*-test. The strength and significance of the linear relationship between two variables (AI vs. V_T and AI vs. fR) were analyzed using Pearson's correlation coefficient and R^2 values were given.

3. Results

We used plethysmography to record the breathing pattern of non-anesthetized, freely behaving WT and *Mecp2*$^{-/y}$ at P15, P25 and P30, either under air or hypoxic or hypercapnic mixtures. Young *Mecp2*$^{-/y}$ with a normal resting ventilation under air had altered respiratory responses to hypoxia and transiently had breathing defects after hypoxia and hypercapnia, well before than expected.

3.1. *Mecp2*$^{-/y}$ have a normal breathing pattern at P15, P25 and P30

As shown in Table 1, comparing the breathing pattern of young WT and *Mecp2*$^{-/y}$ did not reveal significant differences between WT and *Mecp2*$^{-/y}$ at P15, P25 and P30. Neither the respiratory frequency (fR), nor the Tidal Volume (V_T), nor the minute ventilation (V_E), nor the number of apnoeas > 2 mean respiratory cycles, i.e. the apnoea index (AI), nor the variability of the cycle duration expressed as the irregularity score (IS) were significantly different between WT and *Mecp2*$^{-/y}$ of matched ages. From P30 to P60 however half of *Mecp2*$^{-/y}$ developed respiratory distress and died. The breathing of five *Mecp2*$^{-/y}$ which survived at P60 and which was previously recorded at P30 is illustrated in Fig. 1A and B. The breathing pattern of *Mecp2*$^{-/y}$ drastically changed between P30 and P60. At P60, the cycle duration was highly irregular (IS = 46.0 ± 6.5), the fR significantly reduced (173 ± 9 c min^{-1}) and the number of apnoeas per min significantly elevated (AI = 9.5 ± 1.8). These five *Mecp2*$^{-/y}$ did not survive long and died few days later. All the above results were fully consistent with those previously published (Viemari et al., 2005; Zanella et al., 2008).

3.2. Young *Mecp2*$^{-/y}$ have abnormal respiratory responses to hypoxia

WT and *Mecp2*$^{-/y}$ at P30, P25 and P15 received a hypoxic mixture to breath for a short period (O_2 10%, 5 min). We compared the fR, V_T, V_E, AI and IS mean values during and just after the hypoxic challenges to control values prior to hypoxia.

At P30, WT ($n = 8$) and *Mecp2*$^{-/y}$ ($n = 9$) were subjected to hypoxia. V_E was increased in both genotypes but significant differences were observed between WT and *Mecp2*$^{-/y}$, with an exaggerated facilitation of V_E and occurrence of apnoeas after the hypoxic challenge in *Mecp2*$^{-/y}$ (see Table 2; Figs. 1C and 2). In WT, hypoxia classically induced the dual response already described (Vizek et al., 1987), with a significant V_E facilitation at the 3rd min of hypoxia and a reduced facilitation at the 5th min. At the 3rd min, V_E increased via significant increases in V_T and non-significant increases in fR. At the 5th min, the V_E facilitation ceased and V_T returned to control despite the persistence of hypoxia in the recording chamber. As already reported (Stettner et al., 2008), WT had a stable duration of respiratory cycles (weak IS), with a very few transient apnoeas (weak AI), when breathing air. During the 3rd and 5th min of hypoxia, IS was not significantly affected and AI was even significantly reduced. Finally, all the breathing parameters were in the control ranges during the post-hypoxic period.

In *Mecp2*$^{-/y}$ however hypoxia induced different changes in breathing parameters during the three studied periods, with larger increases of V_E, V_T and fR at the 3rd min than in WT, persisting facilitations of V_E, V_T and fR at the 5th min, and frequent apnoeas during the 2 min post-hypoxic period (Table 2; Figs. 1C, 2 and 3A). At the 3rd min, the V_E increase was significantly larger in *Mecp2*$^{-/y}$ than WT (1.9 ± 0.3 and 0.3 ± 0.1 ml g^{-1} min^{-1} above control V_E for *Mecp2*$^{-/y}$ and WT, respectively) via significantly larger increases of V_T and fR in *Mecp2*$^{-/y}$ than WT. At the 5th min, V_E remained significantly increased in *Mecp2*$^{-/y}$ (1.5 ± 0.2 ml g^{-1} min^{-1} above control V_E) via

Table 1
WT and *Mecp2*$^{-/y}$ have similar breathing parameters at P15, P25 and P30. In a given class of age (P15 or P25 or P30), no significant genotypic differences existed in respiratory frequency (fR), tidal volume (V_T), minute ventilation (V_E), apnoea index (AI) and irregularity score (IS) of WT and *Mecp2*$^{-/y}$ breathing air. Values were mean ± S.E.M. and statistical significance was set at $p < 0.05$.

	Genotype	P15 (4 WT and 4 *Mecp2*$^{-/y}$)	P25 (4 WT and 4 *Mecp2*$^{-/y}$)	P30 (10 WT and 9 *Mecp2*$^{-/y}$)
fR (c min^{-1})	WT	250 ± 12	231 ± 14	254 ± 17
	Mecp2$^{-/y}$	243 ± 3	198 ± 9	254 ± 9
V_T (μl g^{-1})	WT	4.5 ± 0.5	3.4 ± 0.7	10.0 ± 1.2
	Mecp2$^{-/y}$	4.0 ± 0.5	4.8 ± 0.4	11.4 ± 1.6
V_E (ml g^{-1} min^{-1})	WT	1.1 ± 0.1	0.8 ± 0.1	2.7 ± 0.5
	Mecp2$^{-/y}$	1.0 ± 0.1	1.0 ± 0.1	3.0 ± 0.5
AI (apnoea min^{-1})	WT	0.7 ± 0.2	0.6 ± 0.4	0.2 ± 0.1
	Mecp2$^{-/y}$	0.6 ± 0.2	1.5 ± 0.4	1.1 ± 0.7
IS	WT	14.4 ± 0.6	13.0 ± 1.8	11.7 ± 2.7
	Mecp2$^{-/y}$	17.0 ± 1.3	19.2 ± 3.0	13.6 ± 2.0

significant increases of V_T and fR (normal V_E, V_T and fR in WT). During the 2 min post-hypoxic period, fR was restored in *Mecp2*$^{-/y}$ but V_E remained significantly increased (1.9 ± 0.3 ml g^{-1} min^{-1} above control V_E) via increased V_T despite the restoration of normoxia within the plethysmographic recording chamber (Table 2 and Fig. 3A). In addition, all the tested *Mecp2*$^{-/y}$ had transient breathing defects during and after the hypoxic challenge (Table 2; Figs. 1C1–C2 and 2). Prior to hypoxia, *Mecp2*$^{-/y}$ had a stable duration of respiratory cycles (weak IS), with rare apnoeas (weak AI), similarly to WT. Whereas hypoxia did not affect IS and reduced AI in WT, hypoxia significantly increased IS and significantly increased AI in *Mecp2*$^{-/y}$ at the 3rd and 5th min. Surprisingly, IS and AI further increased after the end of the hypoxic challenge. During the 2 min post-hypoxic period, *Mecp2*$^{-/y}$ had a 3-fold increase of IS and a 10-fold increase of AI (>16 apnoeas per min) when compared to control prior to hypoxia. A full recovery of all breathing parameters occurred however 10–15 min later. Thus, despite normal resting ventilation, *Mecp2*$^{-/y}$ at P30 had an exaggerated facilitation of V_E under hypoxia and thereafter had breathing defects resembling to those they will produce at P60, a few days before death (Figs. 1B–C2 and 2B3).

At P25, WT ($n = 4$) and *Mecp2*$^{-/y}$ ($n = 4$) were subjected to similar hypoxic challenges (see Table S1 in Supplementary Material). No significant differences were observed during the 3rd and 5th min of hypoxia. In both genotypes, hypoxia significantly increased V_E, with a weaker facilitation of V_E at the 5th than the 3rd min. V_T was significantly increased by about 100% (Fig. 3A) whereas fR was non-significantly increased (<20%). During the 2 min post-hypoxic period however, differences were observed between WT and *Mecp2*$^{-/y}$, with a recovery of V_E in WT but not in *Mecp2*$^{-/y}$. At P25, as observed at P30, V_E of *Mecp2*$^{-/y}$ remained significantly larger than control during the post-hypoxic period, due to large V_T, till recovery 10–15 min later (Fig. 3A). In addition, hypoxia totally abolished apnoeas at the 5th min in WT whereas it increased AI and

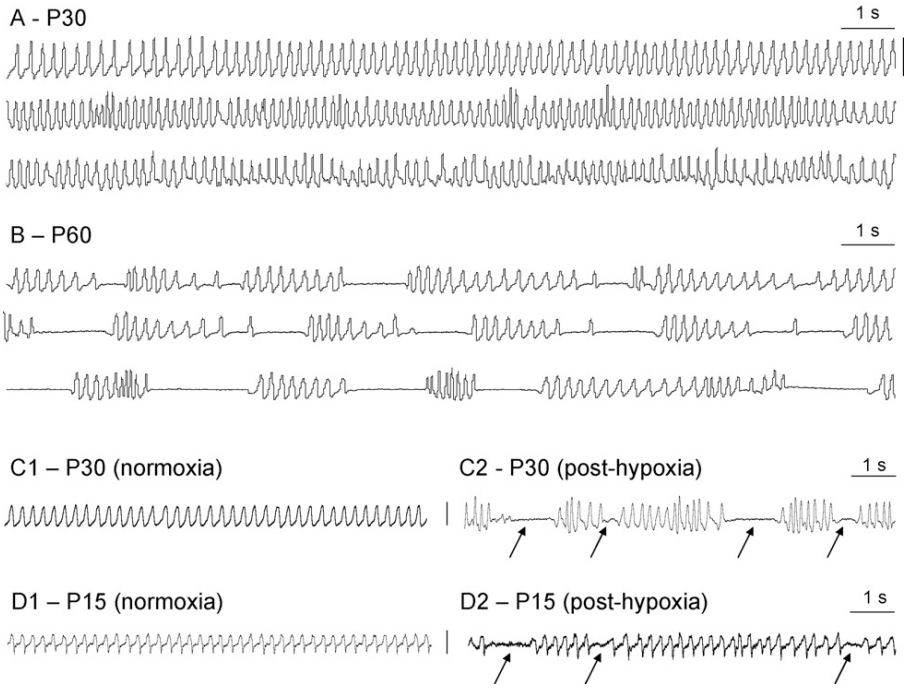

Fig. 1. Plethysmographic recordings of breathing in *Mecp2*$^{-/y}$. (A and B) Traces from the same three *Mecp2*$^{-/y}$ recorded under air at P30 (A) and P60 (B). Note the mice had a normal breathing at P30 but an erratic breathing at P60, with life-threatening apnoeas (traces are shown in the same order in (A) and (B)). (C) Traces from a *Mecp2*$^{-/y}$ at P30 recorded before (C1) and 2 min after (C2) hypoxic exposure (10% O_2, 5 min); note the occurrence of apnoeas (arrows) during the 2 min post-hypoxic period. (D) as in (C), but for another *Mecp2*$^{-/y}$ at P15 before (D1) and after (D2) hypoxic exposure; note the apnoeas (arrows). Calibration bar: 10 μl g^{-1} for (A), (C1), (C2), (D1) and (D2) ((B) non-calibrated).

Table 2
Effects of hypoxia on breathing parameters of WT and *Mecp2*$^{-/y}$ at P30. Comparison of respiratory frequency (fR), tidal volume (V_T), minute ventilation (V_E), apnoea index (AI) and irregularity score (IS) of WT and *Mecp2*$^{-/y}$ (n = 8 and 9, respectively) exposed to hypoxic challenge (O_2 10%, 5 min) at P30. Mean ± S.E.M. were calculated during control period under air prior to hypoxia, at the 3rd and 5th min of hypoxia, and under air at 2 min and 10–15 min after the end of the hypoxic challenge.

Age P30	Control (air)	Hypoxic challenge (O_2 10%, 5 min)		Post-challenge (air)	
		3rd min	5th min	2nd min	10–15 min
fR (c min^{-1})					
WT	220 ± 10	235 ± 8	213 ± 8	200 ± 10	223 ± 13
Mecp2$^{-/y}$	254 ± 12	293 ± 11*	291 ± 9*	269 ± 13	251 ± 10
V_T (µl g^{-1})					
WT	7.8 ± 0.5	8.7 ± 0.8*	8.2 ± 1.0	9.1 ± 1.5	7.9 ± 0.6
Mecp2$^{-/y}$	10.7 ± 1.2	16.3 ± 1.7*	13.9 ± 1.2*	17.5 ± 1.8*	9.3 ± 0.9
V_E (ml g^{-1} min^{-1})					
WT	1.7 ± 0.2	2.0 ± 0.2*	1.7 ± 0.2	1.9 ± 0.4	1.8 ± 0.2
Mecp2$^{-/y}$	2.8 ± 0.4	4.6 ± 0.4*	4.0 ± 0.3*	4.7 ± 0.5*	2.4 ± 0.3
AI (apnoea min^{-1})					
WT	1.0 ± 0.6	0.2 ± 0.2*	0.3 ± 0.3*	3.4 ± 2.8	0.0 ± 0.0
Mecp2$^{-/y}$	1.3 ± 0.7	2.7 ± 1.0*	5.6 ± 2.2*	16.4 ± 2.4*	1.4 ± 0.6
IS					
WT	11.7 ± 2.3	11.5 ± 0.9	12.3 ± 0.6	25.0 ± 9.1	6.2 ± 0.8*
Mecp2$^{-/y}$	15.2 ± 2.3	25.7 ± 1.6*	28.2 ± 3.1*	43.5 ± 4.9*	15.7 ± 2.3

* Indicate significant changes ($p < 0.05$) between the mean value at a given period when compared to control mean value prior to hypoxia.

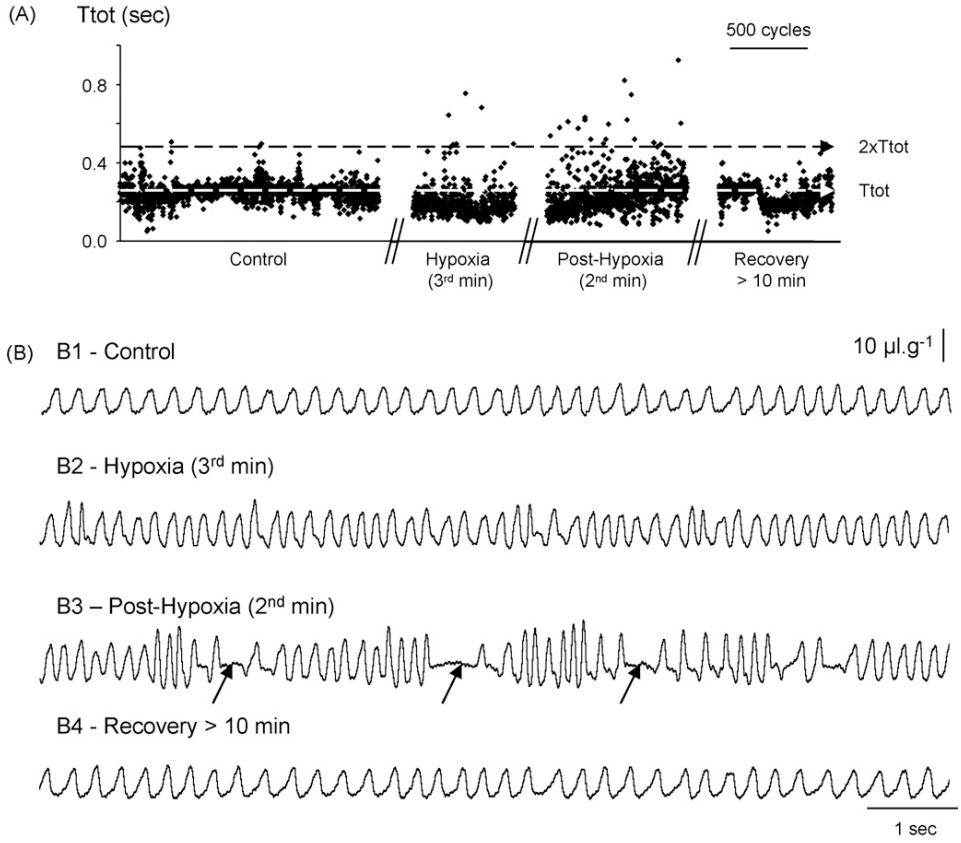

Fig. 2. Hypoxia induced apnoeas in young *Mecp2*$^{-/y}$ mice at P30. (A) Sequential plot of total respiratory cycle length (Ttot) values (in s) of consecutive respiratory cycles recorded in a *Mecp2*$^{-/y}$ mouse at P30 breathing air (control; about 1850 cycles), hypoxic mixture (3rd–5th min) and air (2nd–5th min and >10 min after the end of the hypoxic challenge), from the left to the right. White and black dotted lines indicate the mean-Ttot level and the 2× mean-Ttot level defined under control conditions, respectively. Apnoeas were considered to occur when expiratory duration >2 mean-Ttot. During control conditions, apnoeas are rare, with stable Ttot values, whereas they become frequent, with variable Ttot values, after hypoxia. (B) Plethysmographic traces from the same *Mecp2*$^{-/y}$ as in (A) when breathing air (B1, control), hypoxic mixture (B2, 3rd min) and air (B3, 2 min and B4, >10 min after the end of the hypoxic challenge). Note the apnoeas (arrow). Calibration bar: 10 µl g^{-1} for (B1), (B2), (B3) and (B4).

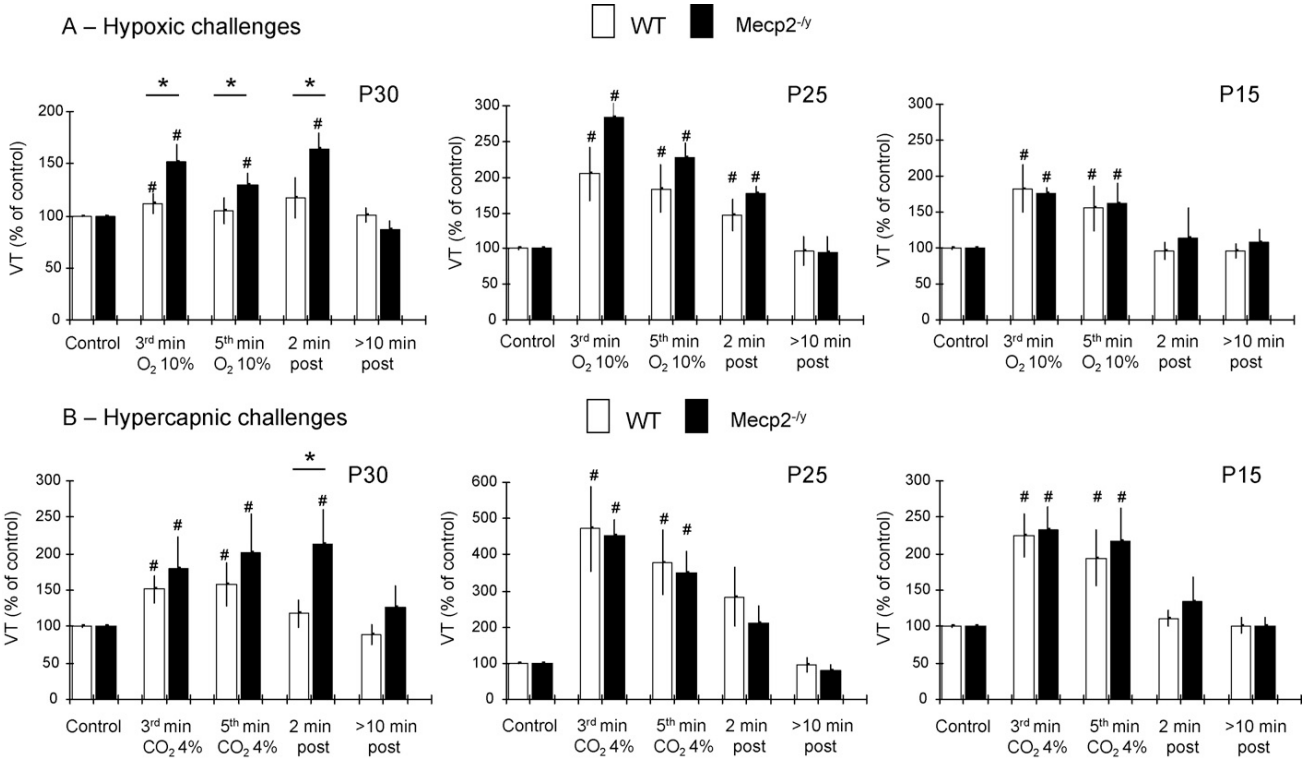

Fig. 3. V_T changes induced by hypoxic and hypercapnic challenges. Columns in histograms show V_T changes (mean ± S.E.M. expressed as % of control, 100%) in WT and *Mecp2*$^{-/y}$ (white and black columns, respectively) when exposed to hypoxia (O_2 10%, for 5 min) and hypercapnia (CO_2 4% for 5 min) at P30, P25 and P15. From the left to the right: control, 3rd min and 5th min of hypoxia, 2 min and 10–15 min after the challenge. * Indicate significant difference between WT and *Mecp2*$^{-/y}$; # indicate significant difference from control ($p < 0.05$).

IS by 3-fold in *Mecp2*$^{-/y}$. Full recovery of all breathing parameters was observed 10–15 min later.

At P15, exposure of WT ($n = 4$) and *Mecp2*$^{-/y}$ ($n = 4$) to hypoxia increased V_E at the 3rd and 5th min, with a weaker V_E facilitation at the 5th than the 3rd min (see Table S1 in supplementary data). The V_E changes were mainly due to marked increases in V_T (60–80%, Fig. 3A) and weak increases in fR (10–20%; not shown). No significant differences between WT and *Mecp2*$^{-/y}$ were observed in fR, V_T, V_E values during and after the hypoxic challenge. However, hypoxia did not affect IS in WT but significantly increased it at the 3rd, 5th min and 2 min post-challenge periods in *Mecp2*$^{-/y}$. In addition, hypoxia totally abolished apnoeas in all WT but induced frequent apnoeas in one out of four *Mecp2*$^{-/y}$ (AI = 6.6) during the post-hypoxic period (Fig. 1D1–D2).

3.3. Effects of imposed hypercapnia to young WT and *Mecp2*$^{-/y}$

We exposed WT and *Mecp2*$^{-/y}$ to moderate, short-lasting hypercapnic challenges (CO_2 4%, 5 min) at P30, P25 and P15 and analyzed the respiratory changes induced at the 3rd min, 5th min and 2 min post-hypercapnic periods.

At P30, hypercapnic challenges applied to WT ($n = 5$) and *Mecp2*$^{-/y}$ ($n = 4$) significantly increased V_E at the 3rd min and V_E further increased at the 5th min via both V_T and fR increases but no significant changes in IS and AI (Table 3). No significant differences between WT and *Mecp2*$^{-/y}$ were observed under hypercapnia (Fig. 3B) but significant differences occurred during the 2 min post-hypercapnic period. In WT, all the breathing parameters were in the control range but, in *Mecp2*$^{-/y}$, V_E and V_T remained significantly increased (normal fR was restored) despite the restoration of normocapnic conditions in the recording chamber (Fig. 3B). In addition, AI and IS were not significantly affected in WT whereas *Mecp2*$^{-/y}$ had frequent apnoeas (Table 3; Fig. 4) with significant increases of AI and IS (about 30-fold and 4-fold, respectively). *Mecp2*$^{-/y}$ recovered normal breathing parameters within 10–15 min. Thus, although the short-term responses to hypercapnia were similar in WT and *Mecp2*$^{-/y}$ at P30, significantly different post-effects were observed, with large V_T, erratic breathing and frequent apnoeas in *Mecp2*$^{-/y}$.

Mecp2$^{-/y}$ ($n = 4$) and WT ($n = 4$) mice were also studied at P25 and P15 (see Table S2 in supplementary data and Fig. 3). At P25, similarly to P30, hypercapnia significantly increased V_E in both WT and *Mecp2*$^{-/y}$ (5–6-fold increases), via increases of fR and V_T at the 3rd and 5th min. No significant differences between WT and *Mecp2*$^{-/y}$ were observed. During the 2 min post-hypercapnic period, V_T, fR and V_E fully recovered in both WT and *Mecp2*$^{-/y}$. Hypercapnia did not significantly affect AI and IS in WT but significantly increased AI by 10-fold in *Mecp2*$^{-/y}$. At P15, no significant differences were observed between WT and *Mecp2*$^{-/y}$: V_E increased during hypercapnia and recovered during the post-hypercapnic periods, and the numbed of apnoeas was not increased (surprisingly it was even significantly reduced during all periods in *Mecp2*$^{-/y}$ and during the 5th min in WT).

3.4. Hypoxia and hypercapnia induced transient apnoeas in young *Mecp2*$^{-/y}$

During the 2 min periods following the hypoxic and hypercapnic challenges, *Mecp2*$^{-/y}$, but not WT, transiently had breathing defects, with frequent apnoeas, variable duration of respiratory cycles and large V_T but normal fR. This was observed in all the studied *Mecp2*$^{-/y}$ at P30, all but one *Mecp2*$^{-/y}$ at P25 and in one *Mecp2*$^{-/y}$ at P15. It is worthy to note that both hypoxia and hypercapnia similarly induced apnoeas. Fig. 5A gathers individual AI

Table 3
Effects of hypercapnia on breathing parameters of WT and *Mecp2*$^{-/y}$ at P30. As for Table 2 but WT and *Mecp2*$^{-/y}$ (n = 5 and 4, respectively) were exposed to hypercapnic challenge (CO_2 4%, 5 min).

Age P30	Control (air)	Hypercapnic challenge (CO_2 4%, 5 min)		Post-challenge (Air)	
		3rd min	5th min	2nd min	10 min
fR (c min^{-1})					
WT	251 ± 29	324 ± 32*	333 ± 27*	238 ± 13	229 ± 5
Mecp2$^{-/y}$	253 ± 15	302 ± 24*	320 ± 33*	296 ± 17	264 ± 22
V_T (μl g^{-1})					
WT	11.5 ± 2.2	17.3 ± 2.1*	18.1 ± 3.3*	13.5 ± 2.2	10.2 ± 1.6
Mecp2$^{-/y}$	8.7 ± 2.2	15.6 ± 3.9*	17.4 ± 4.7*	18.5 ± 4.1*	10.9 ± 2.5
V_E (ml g^{-1} min^{-1})					
WT	3.1 ± 1.0	5.8 ± 1.2*	6.4 ± 1.6*	3.3 ± 0.7	2.3 ± 0.4
Mecp2$^{-/y}$	2.3 ± 0.6	4.9 ± 1.4*	6.0 ± 1.9*	5.5 ± 1.3*	3.0 ± 0.8
AI (apnoea min^{-1})					
WT	0.0 ± 0.0	1.7 ± 1.7	0.0 ± 0.0	0.3 ± 0.3	1.1 ± 0.9
Mecp2$^{-/y}$	0.4 ± 0.2	1.8 ± 1.2	1.0 ± 1.0	12.1 ± 3.5*	1.6 ± 1.5
IS					
WT	10.9 ± 3.5	14.6 ± 3.8	10.2 ± 2.6	19.0 ± 4.8	10.3 ± 2.7
Mecp2$^{-/y}$	11.0 ± 2.1	17.3 ± 1.9	12.1 ± 2.1	40.7 ± 7.4*	16.6 ± 4.6

* Indicate significant changes (p < 0.05) between the mean value at a given period when compared to control mean value prior to hypercapnia.

and V_T data measured during the 2 min post-challenge periods (both hypoxia and hypercapnia) from all the studied *Mecp2*$^{-/y}$ at all ages (P15, P25 and P30). Indeed, weak AI occurred when V_T was only slightly increased (V_T < 150% of control) whereas large AI occurred when V_T was markedly increased (V_T > 150% of control). A significant relationship was found between AI values and V_T increases when V_T increases were expressed as the difference between the post-challenge V_T and the control V_T, DiffV_T (AI = 1.421 × DiffV_T + 3.355; R^2 = 0.464; p < 0.0001). A significant relationship was also found when V_T increases were expressed as % of control V_T (AI = 0.069 × V_T% − 1.579; R^2 = 0.227; p < 0.02). On the other hand, AI values were neither dependent on V_T increases during the 5th min of challenges (R^2 = 0.051; Fig. 5B), nor dependent on fR changes during either the 2 min post-challenge period (R^2 = 0.032; Fig. 5C) or the 5th min of challenges (R^2 = 0.08; not shown).

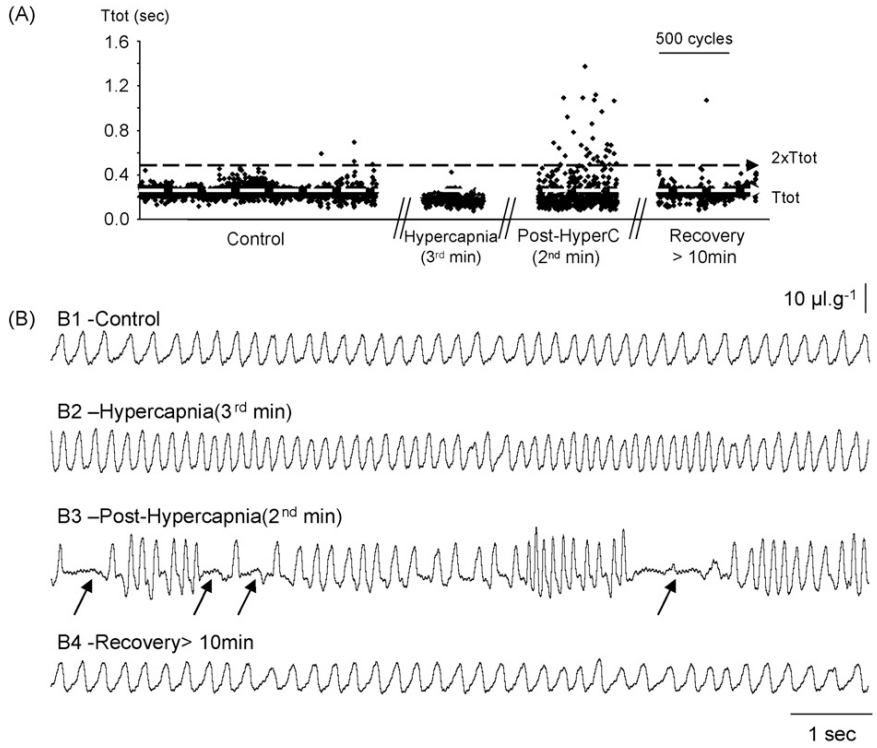

Fig. 4. Hypercapnia induced apnoeas in *Mecp2*$^{-/y}$ mice at P30. (A) Sequential plot of total respiratory cycle length (Ttot) values (in s) of consecutive respiratory cycles recorded in a *Mecp2*$^{-/y}$ mouse at P30 breathing air (control; about 1850 cycles), hypercapnic mixture (3rd–5th min) and air (2nd–5th min and >10 min after the end of the challenge), from the left to the right. White and black dotted lines indicate the mean-Ttot level and the 2× mean-Ttot level defined under control conditions, respectively. Ttot values are regular during control conditions. Note apnoeas after hypercapnia. (B) Plethysmographic traces from the same *Mecp2*$^{-/y}$ as in (A) when breathing air (B1, control), hypercapnic mixture (B2, 3rd min) and air (B3, 2 min and B4, >10 min after the end of the hypoxic challenge). Note the apnoeas (arrow). Calibration bar: 10 μl g^{-1} for (B1), (B2), (B3) and (B4).

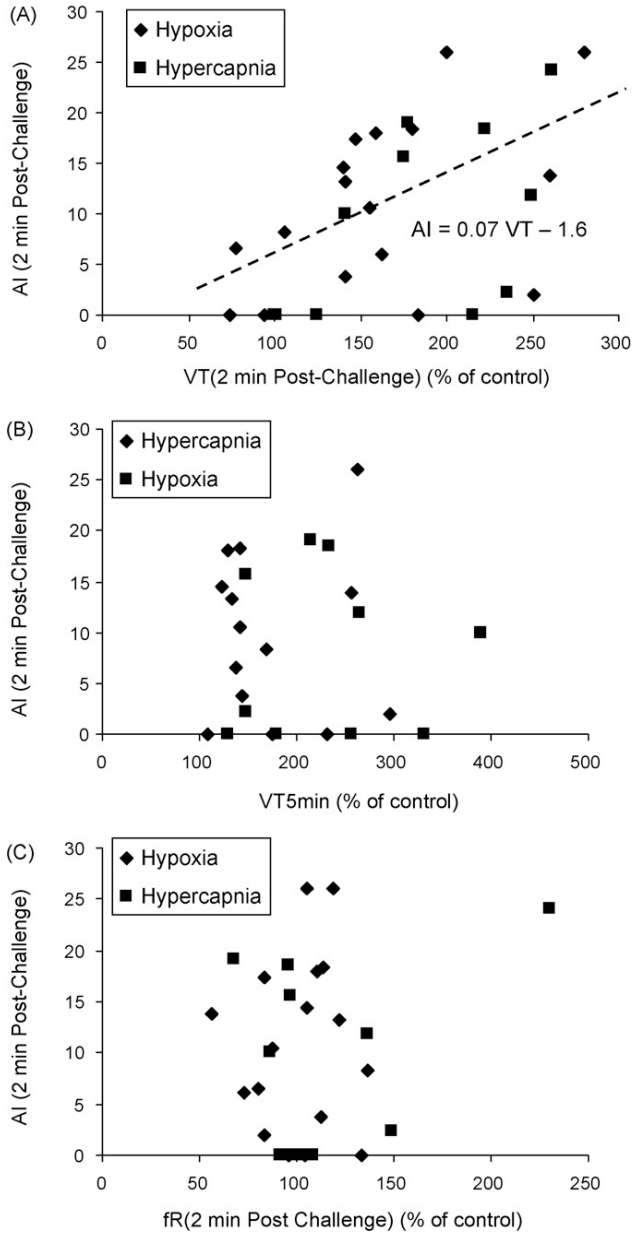

Fig. 5. The number of apnoeas is related to the V_T increase during the post-challenge periods in *Mecp2*$^{-/y}$ mice. *X*–*Y* plot showing the relationship between AI vs. V_T or AI vs. fR in different *Mecp2*$^{-/y}$ mice subjected to hypoxia or hypercapnia challenges at P15, P25 and P30. Analyzed variables were AI and V_T values measured during the 2 min post-challenge period (A), AI values during the 2 min post-challenge period and V_T values measured during the 5th min of challenges (B) and AI and fR values measured during the 2 min post-challenge period (C). Values are expressed in % of control. Note the significant relationship between AI and V_T values measured during the 2 min post-challenge period (A).

4. Discussion

As recently reviewed (Katz et al., 2009; Bissonnette and Hilaire, 2008; Ogier and Katz, 2008), MeCP2 loss in mice and humans induces breathing defects which develop with age and which likely originate from altered modulations of the brainstem respiratory network caused by earlier deficits of glutamate, GABA, BDNF and monoaminergic systems. Here for the first time, we report early anomalies in respiratory responses to hypoxia in young *Mecp2*$^{-/y}$ at an age when their resting ventilation is still normal. In addition, we reported occurrence of apnoeas after moderate hypoxia and hypercapnia in *Mecp2*$^{-/y}$ well before than expected. In mammals, survival requires not only a functional RRG to produce a robust respiratory rhythm but also adequate respiratory regulations to permanently adapt the RRG frequency and the strength of the VRG motor output to physiological needs. If respiratory regulations are altered, inadequate adaptation of the frequency and strength of the respiratory drive may alter blood oxygenation, and the resulting central hypoxia may affect the postnatal maturation and function of all the central neural networks, including the respiratory network. Then, our mouse results might help for understanding the mechanisms through which MeCP2 loss alters the functions of several central networks in young mice and RTT girls.

4.1. The short-term respiratory responses to hypoxia are abnormal in young *Mecp2*$^{-/y}$

The respiratory responses to hypoxia implicate first carotid body chemoceptors that rapidly detect peripheral blood hypoxia and activate relay neurons in the nucleus tractus solitarius (nTS), these latter in turn activate the central respiratory network to adapt the frequency and amplitude of respiratory movements and restore normoxia. If the restoration of normoxia is impaired then central hypoxia develops, that counterbalances the carotid body facilitation and reduces the respiratory facilitation (Vizek et al., 1987). The reduction of the respiratory facilitation may be viewed as a mean of sparing oxygen since over-activation of respiratory muscles is oxygen-consuming. Under our experimental conditions, hypoxia was imposed to mice and then persisted during the whole 5 min challenge despite the mouse respiratory efforts to compensate it. The dual facilitatory and depressing effects of hypoxia occurred at the 3rd and 5th min, respectively, in both WT and *Mecp2*$^{-/y}$ and at all ages but significant differences between WT and *Mecp2*$^{-/y}$ were observed at P30. At P30, the V_E increase at the 3rd min was larger in *Mecp2*$^{-/y}$ than WT and remained larger at the 5th min in *Mecp2*$^{-/y}$ than WT. It is worthy to note that the V_E facilitation mainly implicated V_T increases. In *Mecp2*$^{-/y}$, the large V_T at the 5th min is an inadequate response to hypoxia since it reflects a useless, intense work of respiratory muscles which aggravates the pre-existing central hypoxia.

In *Mecp2*$^{-/y}$ at P30, the exaggerated V_T responses to hypoxia may be due to increased responsiveness of carotid body, altered integrative processes within the nTS and/or altered responsiveness of the VRG neurons. GABA contributes to the hypoxic respiratory depression (Melton et al., 1990), and GABA receptors are expressed in the nTS and the VRG to modulate the effects of chemoceptor afferent inputs and the responsiveness of respiratory neurons, respectively (Pierrefiche et al., 1993; Suzuki et al., 1999). The reduced expression of GABA receptor subunits in the VRG area of *Mecp2*$^{-/y}$ mice at P7 (Medrihan et al., 2008) may contribute to their exaggerated V_T response at P30. NE is expressed within the carotid body (Joseph et al., 2002), modulates the transmission of carotid bodies inputs to nTS relay neurons (Zhang and Mifflin, 2007) and modulates the activity of the respiratory network (Hilaire et al., 2004; Viemari and Ramirez, 2006). NE endogenous levels in the brainstem of *Mecp2*$^{-/y}$ are reduced at P30 and even P14 (Viemari et al., 2005; Ide et al., 2005) as revealed by HPLC, and the NE reduction could have begun well before being detectable by HPLC. In addition, NE biosynthesis might be reduced within the carotid body of adult *Mecp2*$^{-/y}$ (Roux et al., 2008). Then the NE deficits of *Mecp2*$^{-/y}$ could also contribute to their exaggerated V_T responses to hypoxia. BDNF modulates the activity of nTS relay neurons by inhibiting postsynaptic glutamatergic AMPA receptors (Balkowiec et al., 2000). *Mecp2*$^{-/y}$ mice exhibit marked deficits in brain content of BDNF mRNA and protein after birth (Wang et al., 2006; Ogier et al., 2007; Chang et al., 2006), with marked deficits in the nTS. Finally, the exaggerated V_T responses to

hypoxia in *Mecp2*$^{-/y}$ at P30 may be due to early defects of BDNF, GABA and NE systems.

At P30, the exaggerated V_T facilitation by hypoxia of *Mecp2*$^{-/y}$ probably reflects a neurodevelopmental process since it was already present, although non-significant, at P25, and absent at P15. At P25 and P15, it is likely that the defects of BDNF, GABA and NE systems of *Mecp2*$^{-/y}$ are not severe enough to significantly affect the V_T responses to hypoxia. However hypoxia triggered apnoeas in all but one *Mecp2*$^{-/y}$ at P25 and in one *Mecp2*$^{-/y}$ at P15 (see below).

The respiratory responses to hypercapnia mainly implicate medullary neurons which detect CO_2/pH changes and in turn modulate the activity of the respiratory network. The central CO_2 chemoceptors are Phox2b expressing neurons of the RTN/pFRG and 5HT neurons of the raphe, which probably interact (Guyenet et al., 2008, 2009; Onimaru et al., 2009; Corcoran et al., 2009). Hypercapnia at P15, P25 and P30 increased V_E via both fR and V_T marked increases, without differences between WT and *Mecp2*$^{-/y}$. Since the V_E responses to hypercapnia are normal in *Mecp2*$^{-/y}$ at all tested ages, this means that the CO_2/pH chemosensitivity of the RTN/pFRG and raphe neurons is not significantly altered as well as the RRG and VRG responsiveness to these afferent central inputs. Even if levels of endogenous 5HT levels decrease in *Mecp2*, the decrease occurs lately, at P42 and P60, without 5HT neuron loss (Ide et al., 2005; Viemari et al., 2005, respectively). In addition it is worthy to note that the fR changes during hypercapnia are similar in WT and *Mecp2*$^{-/y}$ at all ages, confirming that the RRG function in *Mecp2*$^{-/y}$ is not drastically altered at these early ages, neither at rest (normal resting fR) nor under hypercapnia (normal fR increases).

4.2. Early occurrence of apnoeas in *Mecp2*$^{-/y}$ after hypoxic and hypercapnic challenges

After the end of environmental challenges, when mice were breathing air for 2 min, young *Mecp2*$^{-/y}$ produced an abnormal breathing pattern, with frequent apnoeas in all *Mecp2*$^{-/y}$ at P30, in all but one at P25, and in one at P15. Apnoeas were not expected to occur as early in *Mecp2*$^{-/y}$ where they were only reported after P30 (Viemari et al., 2005; Roux et al., 2007; Zanella et al., 2008).

The occurrence of apnoeas after both hypoxia and hypercapnia suggests that apnoeas do not specifically reflect nTS alterations since the nTS plays a crucial role in hypoxic but not hypercapnic responses. Post-challenge apnoeas do not reflect a marked, permanent dysfunction of the RRG since the RRG correctly functions at rest (same resting fR in WT and *Mecp2*$^{-/y}$) and correctly responds to hypercapnia (same fR increases in WT and *Mecp2*$^{-/y}$). In addition, post-challenge apnoeas followed periods of either normal fR (hypoxic challenges) or increased fR (hypercapnic challenges). The post-hypoxic and post-hypercapnic apnoeas share however one point in common: they occur during periods when the V_T is markedly increased (>150%). The significant relationship between AI values and V_T increases suggests that large V_T facilitate the occurrence of apnoeas. A simple explanation could be that large V_T over-activates the pulmonary stretch receptors, which in turn inhibit the RRG via the Hering–Breuer reflex, prolong the duration of expirations and facilitate the occurrence of apnoeas. This may fit well with the possible alteration of vagal regulation of breathing as reported in *Mecp2*$^{-/y}$ at P45 (Stettner et al., 2007). However a permanently reinforced Hering–Breuer inhibition in *Mecp2*$^{-/y}$ at P25 and P30 should have led to a significant reduction of the mean fR at rest or during the post-challenge period and this was not observed. In addition, this could hardly fit with the erratic occurrence of apnoeas. To be produced, a large V_T requires a sustained activation of phrenic and intercostal inspiratory motoneurons, i.e. a sustained activity of the VRG neurons driving them. During hypoxic periods imposed to induce a sustained activity of phrenic motoneurons, the level of glutamate within the VRG increases well above the control level (Richter et al., 1999). Glial cells play a major role in the elimination of glutamate excess to prevent synaptopathy and excitotoxic neuronal damage (Tilleux and Hermans, 2007; Schousboe et al., 2004; Danbolt, 2001). In RTT patients, the loss of MeCP2 occurs not only in neurons but also in glial cells (Ballas et al., 2009). In RTT mouse models, it has been shown that astrocytes dysfunction (Ballas et al., 2009) and that glutamine/glutamate ratios are abnormal, suggesting altered neurotransmitter recycling (Viola et al., 2007). Therefore, the loss of MeCP2 function in glial cells of *Mecp2*$^{-/y}$ might impair the elimination of glutamate excess in the VGR. Accumulation of glutamate within the VRG during and after the challenges may alter the elaboration of the respiratory motor output by the VRG as well as the synaptic pathways linking the VRG, RRG and RTN/pFRG, therefore contributing to large V_T, IS and AI. Indeed, local applications of glutamate receptors agonists in the VRG induces various, complex effects on frequency and amplitude of breathing, from silencing to enlarged phrenic discharges (Monnier et al., 2003; Chitravanshi and Sapru, 1999). An irreversible alteration of rhythmogenic mechanisms by glutamate excess cannot be definitively excluded but seems unlikely since the breathing defects of RTT patients weaken during sleep (Weese-Mayer et al., 2006, 2008) and those of *Mecp2*$^{-/y}$ are reduced by slight anaesthesia (Viemari et al., 2005), pharmacologic elevation of BDNF expression (Ogier et al., 2007) and pharmacological treatments targeting the NE system (Roux et al., 2007; Zanella et al., 2008). Nevertheless, drastic effects of glutamate excess, with synaptopathy and cytolytic neuronal damages within the central respiratory network, might develop during the late phase of the disease since treatments of *Mecp2*$^{-/y}$ improving breathing and prolonging life span cannot prevent premature death (Roux et al., 2007; Zanella et al., 2008).

As recently reviewed (Katz et al., 2009), loss of MeCP2 alters multiple neurochemical signaling mechanisms. Progressive deficits in BDNF, NE and 5-HT systems, eventually coupled with an altered elimination of glutamate excess by glial cells within the VRG may contribute to the early occurrence of apnoeas after occasional environmental challenges (P25), alteration of respiratory responses to hypoxia (P25–P30), alteration of respiratory rhythmogenesis (after P30), and finally in respiratory distress and death (around P60).

4.3. Repeated hypoxic challenges and evolution of the disease

Here we report that young *Mecp2*$^{-/y}$ retaining a normal resting ventilation have abnormal respiratory responses to hypoxia and transiently produce erratic breathing and apnoeas after only one hypoxic or hypercapnic environmental challenge. The environmental challenges we imposed on *Mecp2*$^{-/y}$ were moderate, short-lasting, and in the physiological range, but they transiently induced erratic rhythm and apnoeas for at least 2 min, and often more, in young *Mecp2*$^{-/y}$ which previously had a normal resting ventilation. These environmental challenges had no obvious deleterious effects on the evolution of the disease and *Mecp2*$^{-/y}$ recovered a normal breathing pattern within 10–15 min. That the environmental challenges may have significantly hastened and/or worsened the evolution of breathing defects when they were repetitively applied to *Mecp2*$^{-/y}$ cannot be excluded but requires further experiments for confirmation. In previous studies, the breathing of *Mecp2*$^{-/y}$ has been mainly studied after P30 (see Katz et al., 2009). Little is known yet about the breathing of young *Mecp2*$^{-/y}$ between P15 and P25, an intermediate developmental period between neonatal and adult ages when the vulnerability of the CNS to hypoxia is rapidly changing. During this crucial developmental period, inadequate adaptation to moderate environmental

challenges by the *Mecp2*$^{-/y}$ respiratory drive may alter blood oxygenation, leading to repeated intermittent central hypoxia, which may have drastic effects on the postnatal maturation and function of all the central neural networks, including the respiratory network. Thus, the abnormal respiratory responses to hypoxia reported herein may contribute to the evolution of the disease in *Mecp2*$^{-/y}$ and possibly RTT girls.

For RTT girls, no pharmacological treatments are available yet and approximately 25% of RTT patients may die prematurely of cardio-respiratory failure (Kerr et al., 1997; Laurvick et al., 2006; Katz et al., 2009). Based on our mouse results, we would recommend not subjecting young RTT girls to situations where they might repetitively experience moderate hypoxic challenges. Exposure to cigarette smoke could be an example, since inhalation of small amounts of CO may induce transient hypoxia. Rapid imposed altitude changes could be another, with fast transitions from seaside to mountain cities, where oxygen partial pressure in inspired air is significantly reduced. In addition, only partial compensation of the reduced atmospheric pressure is provided during most high altitude flights. Under such situations, RTT girls may be exposed to moderate hypoxia which might facilitate the early occurrence of apnoeas and accelerate the evolution of the disease.

Acknowledgements

This work was supported by the CNRS (FRE 2722, UMR 6153, UMR 6231; fellowship to MD), the "Université de la Méditerranée", the "Université Paul Cézanne", the French Ministry for Research (ACI NIC No. 054), the Rett Syndrome Research Foundation (fellowship 2007 for SZ) and the International Rett Syndrome Foundation (fellowship 2008–2009 for NV). This work is dedicated to all Rett patients that continue to suffer from severe breathing defects.

Appendix A. Supplementary data

Supplementary data associated with this article can be found at doi:10.1016/j.resp.2009.05.013.

References

Balkowiec, A., Kunze, D.L., Katz, D.M., 2000. Brain-derived neurotrophic factor acutely inhibits AMPA-mediated currents in developing sensory relay neurons. J. Neurosci. 20 (5), 1904–1911.
Ballas, N., Lioy, D.T., Grunseich, C., Mandel, G., 2009. Non-cell autonomous influence of MeCP2-deficient glia on neuronal dendritic morphology. Nat. Neurosci. 12 (3), 311–317.
Bianchi, A., Denavit-Saubié, M., Champagnat, J., 1995. Central control of breathing in mammals: neuronal circuitry, membrane properties, and neurotransmitters. Physiol. Rev. 75 (1), 1–45.
Bissonnette, J., Hilaire, G., 2008. Possible role of bioaminergic systems in the respiratory disorders of Rett syndrome. In: Gaultier, C. (Ed.), Genetic Basis for Respiratory Control Disorders. Springer Publishers, pp. 271–289.
Burnet, H., Hilaire, G., 1999. Pulmonary stretch receptor discharges and vagal regulation of respiration differ between two mouse strains. J. Physiol. 519, 581–590.
Chang, Q., Khare, G., Dani, V., Nelson, S., Jaenisch, R., 2006. The disease progression of Mecp2 mutant mice is affected by the level of BDNF expression. Neuron 49 (3), 341–348.
Chitravanshi, V.C., Sapru, H.N., 1999. Phrenic nerve responses to chemical stimulation of the subregions of ventral medullary respiratory neuronal group in the rat. Brain Res. 821 (2), 443–460.
Corcoran, A.E., Hodges, M.R., Wu, Y., Wang, W., Wylie, C.J., Deneris, E.S., Richerson, G.B., 2009. Medullary serotonin neurons and central CO_2 chemoreception. Resp. Physiol. Neurobiol. 168, 49–58.
Danbolt, N.C., 2001. Glutamate uptake. Prog. Neurobiol. 65 (1), 1–105.
Guy, J., Hendrich, B., Holmes, M., Martin, J.E., Bird, A., 2001. A mouse *Mecp2*-null mutation causes neurological symptoms that mimic Rett syndrome. Nat. Genet. 27, 322–326.
Guyenet, P.G., Stornetta, R.L., Bayliss, D.A., 2008. Retrotrapezoid nucleus and central chemoreception. J. Physiol. 586 (8), 2043–2048.
Guyenet, P.G., Bayliss, D.A., Stornetta, R.L., Fortuna, M.G., Abbott, S.B., Depuy, S.D., 2009. Retrotrapezoid nucleus, respiratory chemosensitivity and breathing automaticity. Resp. Physiol. Neurobiol. 168, 59–68.
Hilaire, G., Duron, B., 1999. Maturation of the mammalian respiratory system. Physiol. Rev. 79 (2), 325–360.
Hilaire, G., Viemari, J.C., Coulon, P., Simonneau, M., Bévengut, M., 2004. Modulation of the respiratory rhythm generator by the pontine noradrenergic A5 and A6 groups in rodents. Respir. Physiol. Neurobiol. 143, 187–197.
Ide, S., Itoh, M., Goto, Y., 2005. Defect in normal developmental increase of the brain biogenic amine concentrations in the mecp2-null mouse. Neurosci. Lett. 386 (1), 14–17.
Joseph, V., Soliz, J., Soria, R., Pequignot, J., Favier, R., Spielvogel, H., Pequignot, J.M., 2002. Dopaminergic metabolism in carotid bodies and high-altitude acclimatization in female rats. Am. J. Physiol. Regul. Integr. Comp. Physiol. 282 (3), R765–773.
Katz, D., Dutschmann, M., Ramirez, J.M., Hilaire, G., 2009. Breathing disorders in Rett syndrome: progressive neurochemical dysfunction in the respiratory network after birth. Resp. Physiol. Neurobiol. 168, 101–108.
Kerr, A.M., Armstrong, D.D., Prescott, R.J., Doyle, D., Kearney, D.L., 1997. Rett syndrome: analysis of deaths in the British survey. Eur. Child Adolesc. Psychiatry 6 (Suppl. 1), 71–74.
Laurvick, C.L., de Klerk, N., Bower, C., Christodoulou, J., Ravine, D., Ellaway, C., Williamson, S., Leonard, H., 2006. Rett syndrome in Australia: a review of the epidemiology. J. Pediatr. 148, 347–352.
Medrihan, L., Tantalaki, E., Aramuni, G., Sargsyan, V., Dudanova, I., Missler, M., Zhang, W., 2008. Early defects of GABAergic synapses in the brain stem of a MeCP2 mouse model of Rett syndrome. J. Neurophysiol. 99, 112–121.
Melton, J.E., Neubauer, J.A., Edelman, N.H., 1990. GABA antagonism reverses hypoxic respiratory depression in the cat. J. Appl. Physiol. 69, 1296–1301.
Monnier, A., Alheid, G.F., McCrimmon, D.R., 2003. Defining ventral medullary respiratory compartments with a glutamate receptor agonist in the rat. J. Physiol. 548, 859–874.
Monteau, R., Hilaire, G., 1991. Spinal respiratory motoneurons. Prog. Neurobiol. 37 (2), 83–144.
Ogier, M., Katz, D.M., 2008. Breathing dysfunction in Rett syndrome: Understanding epigenetic regulation of the respiratory network. Respir. Physiol. Neurobiol. 164 (1–2), 55–63.
Ogier, M., Wang, H., Hong, E., Wang, Q., Greenberg, M.E., Katz, D.M., 2007. Brain-derived neurotrophic factor expression and respiratory function improve after ampakine treatment in a mouse model of Rett syndrome. J. Neurosci. 27 (40), 10912–10917.
Onimaru, H., Ikeda, K., Kawakami, K., 2009. Phox2b, RTN/pFRG neurons and respiratory rhythmogenesis. Resp. Physiol. Neurobiol. 168, 13–18.
Pierrefiche, O., Foutz, A.S., Denavit-Saubié, M., 1993. Effects of GABAB receptor agonists and antagonists on the bulbar respiratory network in cat. Brain Res. 605, 77–84.
Richter, D.W., Schmidt-Garcon, P., Pierrefiche, O., Bischoff, A.M., Lalley, P.M., 1999. Neurotransmitters and neuromodulators controlling the hypoxic respiratory response in anaesthetized cats. J. Physiol. 514, 567–578.
Roux, J.C., Dura, E., Moncla, A., Mancini, J., Villard, L., 2007. Treatment with desipramine improves breathing and survival in a mouse model for Rett syndrome. Eur. J. Neurosci. 25, 1915–1922.
Roux, J.C., Dura, E., Villard, L., 2008. Tyrosine hydroxylase deficit in the chemoafferent and the sympathoadrenergic pathways of the Mecp2 deficient mouse. Neurosci. Lett. 447 (1), 82–86.
Smith, J., Ellenberger, H., Ballanyi, K., Richter, D., Feldman, J., 1991. Pre-Bötzinger complex: a brainstem region that may generate respiratory rhythm in mammals. Science 254 (5032), 726–729.
Stettner, G.M., Huppke, P., Brendel, C., Richter, D.W., Gärtner, J., Dutschmann, M., 2007. Breathing dysfunctions associated with impaired control of postinspiratory activity in Mecp2-/y knockout mice. J. Physiol. 579, 863–876.
Stettner, G.M., Zanella, S., Huppke, P., Gärtner, J., Hilaire, G., Dutschmann, M., 2008. Spontaneous central apneas occur in the C57BL/6J mouse strain. Respir. Physiol. Neurobiol. 160 (1), 21–27.
Schousboe, A., Sarup, A., Bak, L.K., Waagepetersen, H.S., Larsson, O.M., 2004. Role of astrocytic transport processes in glutamatergic and GABAergic neurotransmission. Neurochem. Int. 45 (4), 521–527.
Suzuki, M., Tetsuka, M., Endo, M., 1999. GABA(B) receptors in the nucleus tractus solitarii modulate the carotid chemoreceptor reflex in rats. Neurosci. Lett. 260, 21–24.
Tilleux, S., Hermans, E., 2007. Neuroinflammation and regulation of glial glutamate uptake in neurological disorders. J. Neurosci. Res. 85, 2059–2070.
Viemari, J.C., Ramirez, J.M., 2006. Norepinephrine differentially modulates different types of respiratory pacemaker and nonpacemaker neurons. J. Neurophysiol. 95 (4), 2070–2082.
Viemari, J.C., Roux, J.C., Tryba, A.K., Saywell, V., Bumet, H., Pena, F., Zanella, S., Bévengut, M., Barthelemy-Requin, M., Herzing, L.B., Moncla, A., Mancini, J., Ramirez, J.M., Villard, L., Hilaire, G., 2005. Mecp2 deficiency disrupts norepinephrine and respiratory systems in mice. J. Neurosci. 25, 11521–11530.
Viola, A., Saywell, V., Villard, L., Cozzone, P.J., Lutz, N.W., 2007. Metabolic fingerprints of altered brain growth, osmoregulation and neurotransmission in a Rett syndrome model. PLoS ONE 2, e157.
Vizek, M., Pickett, C.K., Weil, J.V., 1987. Biphasic ventilatory response of adult cats to sustained hypoxia has central origin. J. Appl. Physiol. 63 (4), 1658–1664.
Wang, H., Chan, S.A., Ogier, M., Hellard, D., Wang, Q., Smith, C., Katz, D.M., 2006. Dysregulation of brain-derived neurotrophic factor expression and neurosecretory function in Mecp2 null mice. J. Neurosci. 26 (42), 10911–10915.

Weese-Mayer, D.E., Lieske, S.P., Boothby, C.M., Kenny, A.S., Bennett, H.L., Silvestri, J.M., Ramirez, J.M., 2006. Autonomic nervous system dysregulation: breathing and heart rate perturbation during wakefulness in young girls with Rett syndrome. Pediatr. Res. 60, 443–449.
Weese-Mayer, D.E., Lieske, S.P., Boothby, C.M., Kenny, A.S., Bennett, H.L., Ramirez, J.M., 2008. Autonomic dysregulation in young girls with Rett syndrome during night time in-home recordings. Pediatr. Pulmonol. 43, 1045–1060.
Zanella, S., Mebarek, S., Lajard, A.M., Picard, N., Dutschmann, M., Hilaire, G., 2008. Oral treatment with desipramine improves breathing and life span in Rett syndrome mouse model. Respir. Physiol. Neurobiol. 160, 116–121.
Zhang, W., Mifflin, S.W., 2007. Modulation of synaptic transmission to second-order peripheral chemoreceptor neurons in caudal nucleus tractus solitarius by alpha1-adrenoreceptors. J. Pharmacol. Exp. Ther. 320 (2), 670–677.

2 - Anormalités précoces de la respiration post-soupir chez un modèle murin du Syndrome de Rett

Voituron N., Zanella S., **Menuet C.**, Lajard A.M., Dutschmann M. & Hilaire G.
Publié dans *Respiratory Physiology & Neurobiology*, en 2010.

Résumé en français :

Le Syndrome de Rett est une maladie neurodéveloppementale accompagnée par des symptômes complexes et très invalidants, incluant des altérations respiratoires. Parce que le Syndrome de Rett est causé par des mutations dans le gène du répresseur transcriptionnel methyl-CpG-binding protein 2 (MeCP2), des souris mutées pour ce gène (souris *Mecp2*$^{-/y}$) ont été générées comme modèle expérimental. Les souris mâles *Mecp2*$^{-/y}$ respirent normalement à la naissance mais montrent des réponses respiratoires à l'hypoxie et à l'hypercapnie anormales à partir du 25^{e} jour postnatal (P25). Après P30, les souris *Mecp2*$^{-/y}$ développent des symptômes respiratoires rappelant le Syndrome de Rett, qui s'aggravent jusqu'à la mort prématurée aux alentours de P60. Utilisant la pléthysmographie, nous avons analysé les soupirs et l'activité respiratoire post-soupir de souris mâles sauvages et *Mecp2*$^{-/y}$ non restreintes à partir de P15 et jusqu'à P60. Les soupirs sont de larges inspirations spontanées connus pour prévenir l'atelectasie pulmonaire et pour améliorer l'oxygénation alvéolaire. Toutefois, les souris *Mecp2*$^{-/y}$ montrent des anormalités précoces de la respiration post-soupir qui se développent dès P15, avec de longues apnées post-soupirs, un volume courant réduit quand l'eupnée reprend et un manque de bradypnée post-soupir, anormalités qui s'aggravent avec l'âge et qui contribuent potentiellement aux symptômes respiratoires successifs.

Respiratory Physiology & Neurobiology 170 (2010) 173–182

Contents lists available at ScienceDirect

Respiratory Physiology & Neurobiology

journal homepage: www.elsevier.com/locate/resphysiol

Early abnormalities of post-sigh breathing in a mouse model of Rett syndrome

N. Voituron, S. Zanella [1], C. Menuet, A.M. Lajard, M. Dutschmann [2], G. Hilaire *

Maturation, Plasticity, Physiology and Pathology of Respiration (mp3-resp team), Unité Mixte de Recherche 6231 CNRS, Faculté Saint-Jérôme, Service 362, 13397 Marseilles Cedex 20, France

ARTICLE INFO

Article history:
Accepted 21 December 2009

Keywords:
MeCP2
Breathing symptoms
Sigh
Post-sigh apnoea
Bradypnoea

ABSTRACT

Rett syndrome is a neurodevelopmental disease accompanied by complex, disabling symptoms, including breathing symptoms. Because Rett syndrome is caused by mutations in the transcriptional repressor methyl-CpG-binding protein 2 (MeCP2), *Mecp2*-deficient mice have been generated as experimental model. Males of *Mecp2*-deficient mice (*Mecp2*$^{-/y}$) breathe normally at birth but show abnormal respiratory responses to hypoxia and hypercapnia from postnatal day 25 (P25). After P30, *Mecp2*$^{-/y}$ mice develop breathing symptoms reminiscent of Rett syndrome, aggravating until premature death at around P60. Using plethysmography, we analyzed the sighs and the post-sigh breathing pattern of unrestrained wild type male mice (WT) and *Mecp2*$^{-/y}$ mice from P15 to P60. Sighs are spontaneous large inspirations known to prevent lung atelectasis and to improve alveolar oxygenation. However, *Mecp2*$^{-/y}$ mice show early abnormalities of post-sigh breathing, with long-lasting post-sigh apnoeas, reduced tidal volume when eupnoea resumes and lack of post-sigh bradypnoea which develop from P15, aggravate with age and possibly contribute to breathing symptoms to come.

© 2010 Elsevier B.V. All rights reserved.

1. Introduction

Rett syndrome (RTT) is a severe neurodevelopmental disease in which, after normal first postnatal months, affected girls develop complex symptoms including erratic breathing and life-threatening apnoeas (Katz et al., 2009). RTT is caused by mutations in the X-linked gene encoding methyl-CpG-binding protein 2 (MeCP2), and *Mecp2*-deficient mice have been generated as RTT model (Guy et al., 2001). Males of *Mecp2*-deficient mice (*Mecp2*$^{-/y}$) rapidly develop symptoms reminiscent of RTT, including breathing symptoms (Viemari et al., 2005). *Mecp2*$^{-/y}$ mice breathe normally at birth but display an erratic breathing pattern interrupted by severe apnoeas after postnatal day 30 (P30), aggravating with age to respiratory distress and premature death at around P60. The development of *Mecp2*$^{-/y}$ breathing symptoms reflects progressive dysfunction of the central respiratory network caused by early alterations of several neurochemical signalling systems including BDNF, norepinephrine (NE), serotonin (5HT), glutamate and GABA systems, known to contribute to the production or modulation of eupnoea (Katz et al., 2009). However, it has recently been reported (Voituron et al., 2009) that, before the appearance of permanent breathing symptoms, *Mecp2*$^{-/y}$ mice develop exacerbated respiratory responses to hypoxia and produce transient apnoeas with erratic rhythm after moderate hypoxic and hypercapnic challenges, which also may originate from earlier alterations of signalling systems.

In mammals, the central respiratory network not only generates eupnoea, the normal breathing activity, but also sighs, which are spontaneous, large inspirations which occur at a low frequency (about 0.5 sigh per min) and are followed by a brief apnoea (<1 s) and a long-lasting bradypnoea (about 10 s) (see Fig. 8 from Popa et al., 2005). *In vivo*, sighs play a crucial role in preventing lung atelectasis, maintaining lung compliance, restoring functional residual capacity and improving alveolar oxygenation (Poets et al., 1997; Patroniti et al., 2002; Qureshi et al., 2009). *In vitro*, the isolated respiratory network continues to produce fictive sighs and eupnoea which are primarily generated by the same set of medullary neurons in the Pre-Bötzinger Complex, with fictive sighs being followed by a brief post-sigh apnoea (Tryba et al., 2008). In *Mecp2*$^{-/y}$ mice, fictive sighs produced in P15–P21 slices appear normal but actual sighs produced in P45–P60 mice are often, but not always, followed by severe, long-lasting apnoeas (Viemari et al., 2005). Therefore, we used the non-invasive plethysmographic approach to analyze and compare the sighs and the post-sigh breathing patterns of maturing, unrestrained wild type male mice (WT) and *Mecp2*$^{-/y}$ mice. For the first time, we report early abnormalities of post-sigh breathing of *Mecp2*$^{-/y}$ mice, with sighs inducing long-lasting apnoeas and tidal volume reductions which develop at an age when their eupnoeic breathing is still normal. We suggest that the early abnormalities of post-sigh breathing observed in this recognized mouse

* Corresponding author. Tel.: +33 491 288 172; fax: +33 491 288 397.
E-mail address: gerard.hilaire@univ-cezanne.fr (G. Hilaire).
[1] Present address: Seattle Children's Research Institute, Center for Neuroscience & University of Washington, Neurosurgery Department, Seattle, WA 98101, USA.
[2] Present address: Institute of Membrane and Systems Biology, Garstang Building, University of Leeds, Leeds LS2 9JT, UK.

1569-9048/$ – see front matter © 2010 Elsevier B.V. All rights reserved.
doi:10.1016/j.resp.2009.12.009

model of RTT might be viewed as forerunner signs of breathing symptoms to come. We propose that the early abnormalities of post-sigh breathing pattern of *Mecp2*$^{-/y}$ mice might be caused by earlier GABA deficits which occur in the medulla of *Mecp2*$^{-/y}$ mice as early as P7 (Medrihan et al., 2008).

2. Methods

Experiments were carried out in accordance with the European guidelines for the care and use of laboratory animals (Council Directive 86/609/EEC) in mouse model for RTT [strain B6.129P2(C)-*Mecp2*tm1–1Bird] (The Jackson Laboratory, Bar Harbor, ME).

As reported previously (Viemari et al., 2005; Zanella et al., 2008; Voituron et al., 2009), hemizygous mutant *Mecp2* male mice (*Mecp2*$^{-/y}$) were generated by crossing heterozygous knock-out females with C57BL/6 male mice (Guy et al., 2001) and genotyped by routine PCR technique. Pups were housed with their mothers till weaning at P21 when male littermates were housed together in identical cages where they had free access to food and water (3–4 mice per cage). The breathing of non-anesthetized, unrestrained male mice was recorded using a constant flow whole-body plethysmograph (EMKA Technologies, Paris, France), with 200 ml animal chambers maintained 25 ± 0.5 °C and ventilated with air (600 ml/min). Two or three days before plethysmographic recordings, the mice were habituated to stay in the plethysmograph chamber to reduce stress effect on breathing. Routinely, the breathing of pairs of WT and *Mecp2*$^{-/y}$ mice of matched ages was simultaneously recorded. Data originated from 25 different mice (11 WT and 14 *Mecp2*$^{-/y}$) which were not systematically recorded at the different maturational ages, mice being occasionally used for other purposes. Recordings were performed during the pre-symptomatic period at P15 (n = 5 WT and 4 *Mecp2*$^{-/y}$), P25 (n = 4 WT and 4 *Mecp2*$^{-/y}$), and P30 (n = 4 WT and 4 *Mecp2*$^{-/y}$), and during the symptomatic period when breathing symptoms permanently occur in *Mecp2*$^{-/y}$, from P45 to P60 (n = 4 WT and 5 *Mecp2*$^{-/y}$). At least 10 sighs produced during a recording session by a given mouse at a given age were routinely analyzed.

In addition, we developed a home-made double-chamber plethysmograph to simultaneously record the respiratory chest movements and the resulting airflow in four other non-anesthetized *Mecp2*$^{-/y}$ mice during the symptomatic period at P55–P60. The double-chamber plethysmograph was built from two syringes, with the rubber piston separating the body chamber (50 ml) from the head chamber (20 ml). The piston was cut to make an adjustable neck collar, especially adapted to each mouse. Air-tightness between body and head chambers was verified by imposing small pressure changes in one chamber and checking the lack of pressure change in the other. The head chamber was connected to a constant flow pump to ensure proper and continuous flow of fresh air (200 ml/min). Body and head chambers were maintained at 25 ± 0.5 °C, connected to respective reference chambers and pressure recorders (EMKA Technologies, Paris, France). As for simple plethysmograph, the mice were habituated to stay in the double-chamber plethysmograph before recording sessions.

For plethysmographic experiments, spirograms were fed to an analog-to-digital converter (sampling frequency, 0.5 or 1 kHz), stored on a personal computer disk and analyzed via the Spike 2 interface and software (Cambridge Electronic Design, Cambridge, UK). Only periods of breathing without body movements were studied, during which the mean respiratory frequency (fR, expressed in respiratory cycles per minute), apnoea index (number of apnoeas > two respiratory cycles per minute) and tidal volume (V_T) were measured (Viemari et al., 2005; Zanella et al., 2008; Voituron et al., 2009). Because whole-body plethysmography did not allow suitable measurement of the actual V_T, V_T values were not expressed in absolute values but in relative values as the ratio of mean V_T produced after the sigh vs. mean V_T produced prior to the sigh. Thanks to Spike 2 software facilities, we averaged the inspirations produced during the 10 s pre-sigh period (control V_T = 100%) and those produced during the post-sigh period (expressed in % of control V_T). Three different types of sighs were distinguished in maturing WT and *Mecp2*$^{-/y}$ (see Fig. 1) and we used Chi-square test to compare the distribution of sigh types in the different age and genotype groups. To analyze the effect of sigh occurrence on the fR, we measured the fR every second during 30 s, the 10 s period preceding the sigh and the 20 s period following the sigh. For a given mouse, at least 10 peri-sigh periods were analyzed and data were averaged to obtain an individual Post-Sigh Time Histogram (PSTH) representative of mean fR changes (in Hz every second) prior to and after sigh occurrence for this mouse (Fig. 2). Mice of a given genotype (WT or *Mecp2*$^{-/y}$) and a given developmental age (P15, P25, P30, etc.) were grouped and their individual PSTH were pooled to built an averaged PSTH representative of the mean fR changes (expressed as % of control every second) prior to and after sigh for a given group of mice (Fig. 3). The significance of fR changes after the sigh was determined by the analysis of variance (ANOVA) followed by Fisher's PLSD correction to compare the mean fR in the second

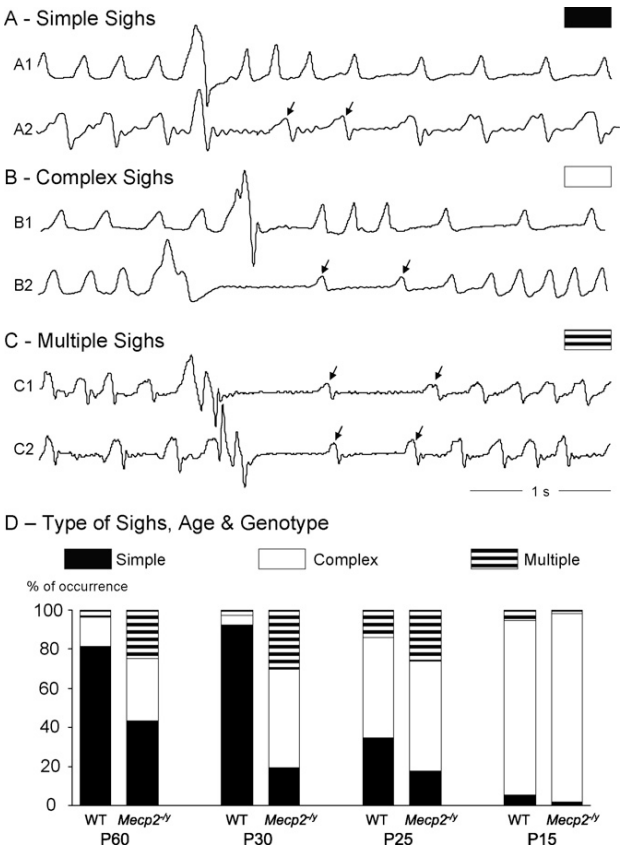

Fig. 1. Sigh patterns in maturing WT and *Mecp2*$^{-/y}$ mice. (A–C) Plethysmographic recordings in unrestrained maturing mice showing simple sighs (A) produced by WT (A1, at P60) and *Mecp2*$^{-/y}$ mice (A2, at P25), complex sighs (B) produced by WT (B1, at P60; same WT as in A1) and *Mecp2*$^{-/y}$ mice (B2, at P30) and multiple sighs (C) produced by *Mecp2*$^{-/y}$ mouse (at P25; same mouse in C1 and C2). In all figures, inspiration is shown upward. In *Mecp2*$^{-/y}$ mice, note that the three types of sighs induced long-lasting apnoeas followed by inspirations of reduced amplitude (oblique arrows). (D) Columns of the histogram show the partition in % of simple (black), complex (white) and multiple (hatched area) sighs in WT and *Mecp2*$^{-/y}$ mice (left and right columns, respectively) at the indicated developmental ages (100% = all types of sighs).

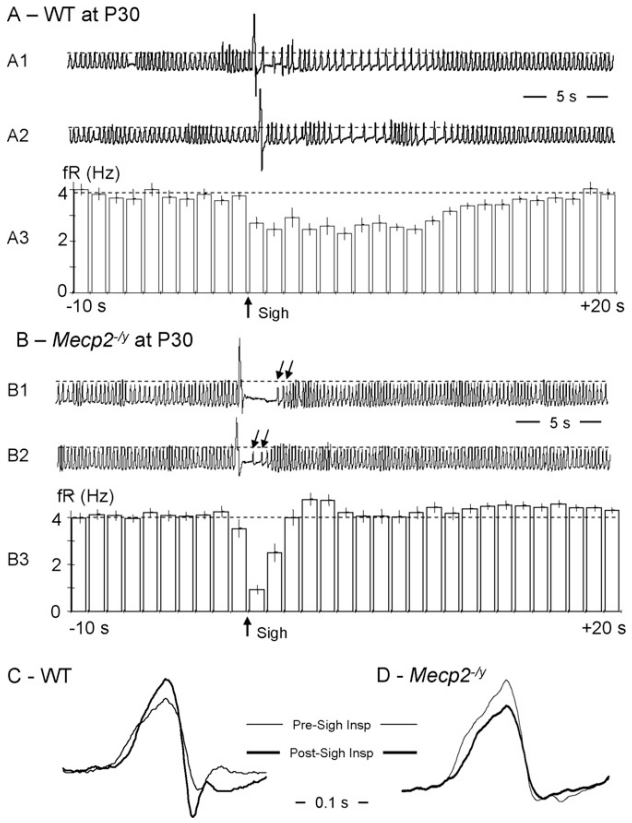

Fig. 2. Post-sigh breathing in WT and *Mecp2*$^{-/y}$ mice at P30. (A) WT at P30. The two plethysmographic traces (A1 and A2) show sighs recorded in the same WT mouse at P30. After the sighs, note the brief apnoea followed by the long-lasting bradypnoea with inspirations of increased amplitude (doted line: mean amplitude level prior to the sigh). (A3) Individual Post-Sigh Triggered Histogram (PSTH) built from 12 sighs recorded in the same mouse as above. Columns (and bars) of the histogram show the mean (and S.E.M.) respiratory frequency (fR, expressed in Hz) every second for a period extending from 10 s prior to the sigh (vertical arrow) to 20 s after the sigh (dotted line: mean fR during the 10 s pre-sigh period). (B), as in (A) but for a *Mecp2*$^{-/y}$ mouse at P30. The two plethysmographic traces (B1 and B2) and the individual PSTH (B3) show a marked post-sigh apnoea and a 1–2 s period of reduced fR after the sigh (vertical arrow). During the post-sigh period, note the lack of long-lasting bradypnoea and the reduced amplitude of inspirations when eupnoea resumed (oblique arrows). C-WT: averaging of inspirations produced by the WT mouse illustrated in A during 10 s periods either preceding the sigh (thin line, Pre-Sigh Insp) or following the sigh (large line, Post-Sigh Insp). Note that the Post-Sigh Insp trace peaks at higher values than the Pre-Sigh Insp trace. D-Mecp2: as in (C), but for the *Mecp2*$^{-/y}$ mouse illustrated in (B). The large line (Post-Sigh Insp) shows averaging of the first five inspirations produced after the sighs. Note that the Post-Sigh Insp trace is smaller than the Pre-Sigh Insp trace.

preceding the sigh ($fR_{-1\,s}$), in the second following the sigh ($fR_{1\,s}$) and in the 10 s period following the sigh ($fR_{1-10\,s}$) to the control fR measured during the 10 s period prior to the sigh. The durations of expirations preceding and following the sigh were measured and expressed in ms. During the sigh, the peak amplitudes reached by the spirogram during inspiration (Pk Insp; upward in figures) and expiration (Pk Exp; downward in figures) were measured for >10 sighs per mouse, averaged and Pk Exp was expressed as % of total sigh amplitude (Pk Insp + Pk Exp) for a given genotype at a given age. All data about the peri-sigh changes in fR ($fR_{-1\,s}$, $fR_{1\,s}$, $fR_{1-10\,s}$), post-sigh V_T changes, post-sigh apnoea duration, Pk Exp. vs. developmental ages were presented as mean ± standard error of the mean (S.E.M.) in Fig. 4 and differences were considered significant when $p < 0.05$.

For double-chamber plethysmographic experiments, chest respiratory movements and airflow were recorded and stored as reported above but no quantitative analysis were performed since these experiments were only programmed to qualitatively check the post-sigh breathing pattern in *Mecp2*$^{-/y}$ at P55–P60.

3. Results

Using plethysmography, we recorded the breathing of non-anesthetized WT and *Mecp2*$^{-/y}$ mice. As reported previously (Viemari et al., 2005; Zanella et al., 2008, Voituron et al., 2009), the breathing pattern of young *Mecp2*$^{-/y}$ was normal but became erratic, interrupted by frequent apnoeas at a few days after post-natal day 30 (P30), until respiratory distress and premature death at around P60. Here, we analyzed the pattern of sighs and the post-sigh changes in fR and V_T at different developmental stages, during the pre-symptomatic period from P15 to P30, and afterwards when breathing symptoms were permanently expressed in *Mecp2*$^{-/y}$ mice, from P45 to P60.

3.1. Pattern of sighs in maturing WT and *Mecp2*$^{-/y}$ mice

As illustrated in Fig. 1, sighs are large inspirations mobilizing a V_T twice of the control and occurring at a low frequency of approximately one sigh every 2 min. We distinguished three types of sighs: simple, complex and multiple sighs. Simple sighs appeared as augmented inspirations, with an extra-inspiration superimposed onto a normal, eupnoeic inspiration (Fig. 1A). Both normal and extra-inspirations were merged, forming a single inspiratory event. Complex sighs were characterized as a sigh on which a supplementary inspiration was grafted, either during the upward or the downward phase of the spirogram (Fig. 1B). Multiple sighs appeared as at least two subsequent sighs (Fig. 1C).

About 400 sighs were analyzed in 34 recordings from 25 mice aged from P15 to P60. The distribution of the three types of sighs was age- and genotype-dependent (Fig. 1D) as revealed by Chi-square analysis showing a significant difference in sigh types distribution between WT and *Mecp2*$^{-/y}$ mice at P30 and P60. At P15, the large majority of sighs were complex in both WT and *Mecp2*$^{-/y}$ (89% and 96%, respectively) whereas simple and multiple sighs were rare. At P25, complex sighs were still the most frequent form, but the occurrence of simple sighs increased. In WT mice, simple sigh were 2-fold more frequent than in *Mecp2*$^{-/y}$ mice (34% and 17%, respectively) whereas multiple sighs were 2-fold less frequent in WT than in *Mecp2*$^{-/y}$ mice (13% and 26%, respectively). However, these differences were not statistically significant at P25. At P30, simple sighs became significantly more frequent in WT than *Mecp2*$^{-/y}$ mice (92% and 19%, respectively) whereas complex sighs were significantly less frequent in WT than *Mecp2*$^{-/y}$ mice (5% and 51%, respectively). At P60, the difference in the distribution of sigh types persisted, with simple sighs significantly predominating in WT compared to *Mecp2*$^{-/y}$ mice (82% and 43%, respectively), whereas complex and multiple sigh forms were significantly less frequent in WT than *Mecp2*$^{-/y}$ mice (complex sighs: 15% and 32%; multiple sighs: 3% and 25%; for WT and *Mecp2*$^{-/y}$, respectively). Thus, during the postnatal development, the distribution of different sigh forms in *Mecp2*$^{-/y}$ mice was significantly affected prior to the appearance of breathing instability at rest. Statistical analysis of the breathing pattern (see below) following simple, complex and multiple sighs failed to reveal a significant relationship between the type of sigh and the resulting changes in breathing, i.e. simple, complex, and multiple sighs induced similar post-sigh breathing patterns at a given age and in a given genotype.

3.2. Post-sigh breathing pattern in WT and *Mecp2*$^{-/y}$ at P30

At P30, sighs occurred at a low frequency in four WT and four *Mecp2*$^{-/y}$ mice (0.37 ± 0.02 and 0.35 ± 0.02 sigh per min, respectively; ns). As shown in Fig. 2A for a given WT mouse, sighs

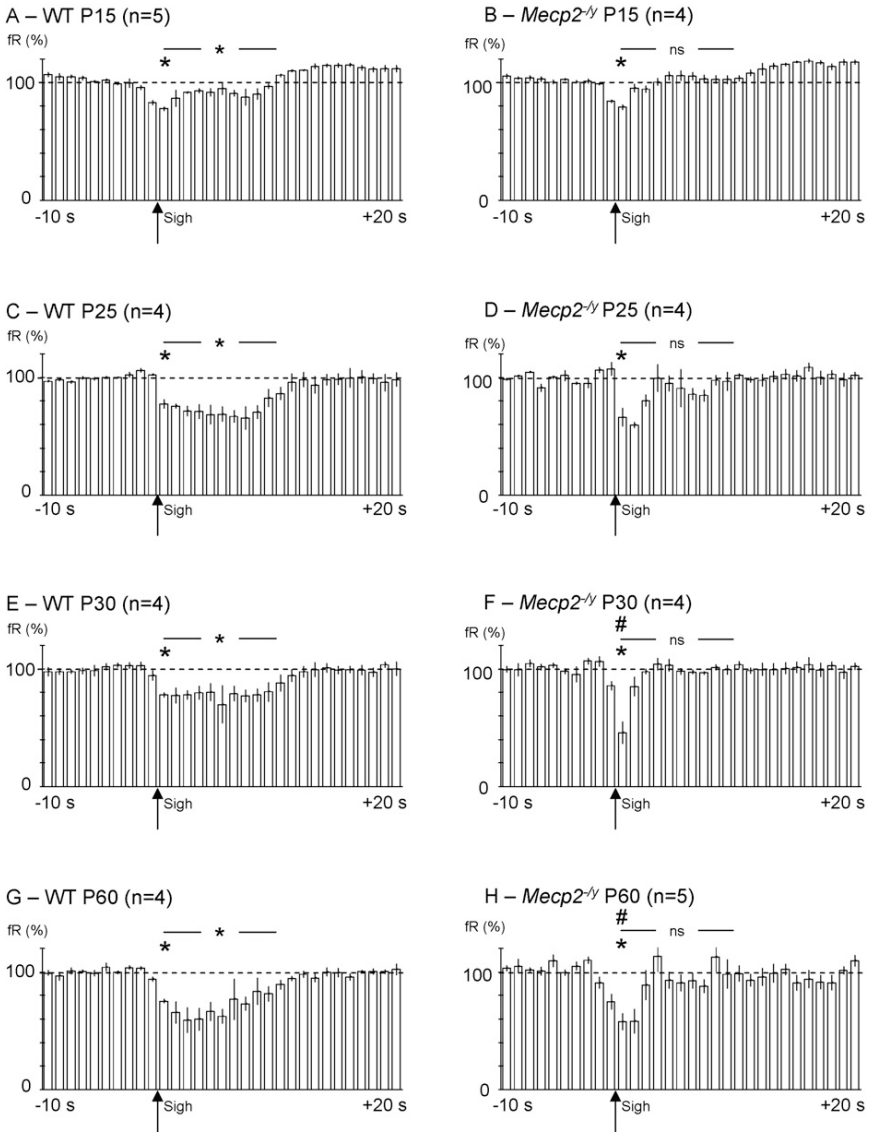

Fig. 3. Averaged PSTH showing the changes in respiratory frequency during the post-sigh period in WT and *Mecp2*$^{-/y}$ mice at different developmental ages. Each averaged PTSH was built from several individual PSTH obtained from mice of a given genotype (WT and *Mecp2*$^{-/y}$) and a given age (from P15 to P60). Genotype, age, and number of individual PSTH as indicated. Columns (and bars) in the averaged PTSH show the mean (and S.E.M.) changes in respiratory frequency (fR, expressed in % of the control fR measured during the 10 s pre-sigh period; 100%) every second for a period extending from 10 s prior to the sigh to 20 s after the sigh. After the sigh (vertical arrow), note the long-lasting bradypnoea in WT mice and the brief period of reduced fR in *Mecp2*$^{-/y}$ mice. The dotted lines indicate the fR control level (100%). Asterisks indicate a significant difference between $fR_{1\,s}$ and control fR. Thin lines with either centred asterisk or ns indicate a significant or non-significant difference, respectively, between $fR_{1-10\,s}$ and control fR. At P30 and P60, # indicates a significant difference between $fR_{1\,s}$ in WT and *Mecp2*$^{-/y}$.

affected the eupnoeic pattern. First, sighs induced an immediate, brief apnoea (444 ± 30 ms), reflecting a 2-fold increase in the expiratory duration, compared to baseline (196 ± 13 ms). Second, when breathing resumed after the brief post-sigh apnoea, the fR was reduced for about 10 s (Fig. 2A1). However in non-anesthetized, freely behaving mice, the post-sigh bradypnoea was not stereotyped but slightly fluctuated from sigh to sigh (compare traces in Fig. 2A1–A2). Therefore, we measured the fR during the peri-sigh period for at least 10 sighs to build an individual Post-Sigh Triggered Histogram (PSTH), which was representative for the fR changes in a given mouse. In the selected mouse, the individual PTSH confirmed a significant post-sigh bradypnoea of 10 s (Fig. 2A3). We similarly analyzed four WT at P30 and pooled individual PSTH to build a PSTH representative of the P30 WT group (Fig. 3E). The pooled PSTH confirmed that the mean fR was significantly reduced 1 s after the sigh ($fR_{1\,s}$ = 78 ± 2% of control fR) and remained significantly reduced for another 10 s ($fR_{1-10\,s}$ = 78 ± 1% of control). Third, when breathing resumed, inspirations were of larger amplitude during the post-sigh bradypnoea, with increased V_T compared to baseline V_T before the sigh (+23 ± 9%), as shown by individual plethysmographic traces (Fig. 2A1–A2) and averaged traces (Fig. 2C).

The four *Mecp2*$^{-/y}$ mice studied at P30 retained a normal breathing pattern at rest, but produced sighs with a different pattern than WT mice at P30. In WT mice, as shown in Fig. 2A for simple sighs and Fig. 4A for a complex sigh, the peak amplitudes of sighs during inspiration (Pk Insp) and expiration (Pk Exp) ranged the same values when expressed in % of total sigh amplitude (51 ± 3% and 49 ± 3% of total sigh amplitude for Pk Insp and Pk Exp, respectively; ns). In *Mecp2*$^{-/y}$ mice, sighs reached significant larger peak amplitudes during inspiration (Pk Insp = 71 ± 3% of total sigh amplitude) than

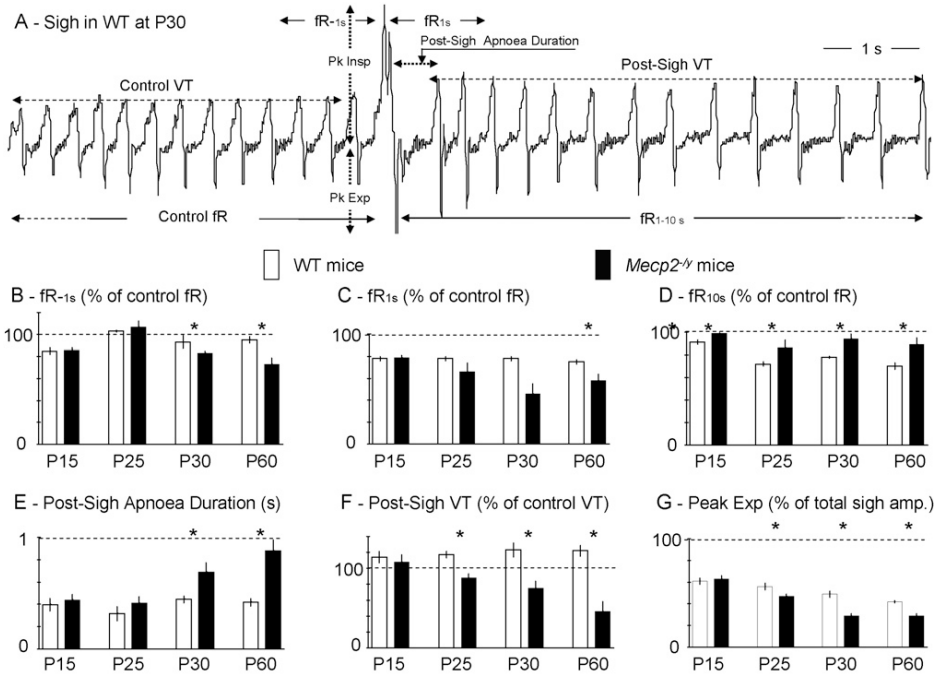

Fig. 4. Abnormalities in sighs and post-sigh breathing in WT and *Mecp2*$^{-/y}$ maturing mice. (A) Plethysmographic recording in WT mouse at P30 illustrating the different analyzed parameters: the control V_T and fR measured during the 10 s preceding the sigh, peak amplitudes of the inspiratory and expiratory components of the sigh (Pk Insp and Pk Exp, respectively), fR measured during the second preceding and following the sigh ($fR_{-1\,s}$ and $fR_{1\,s}$, respectively) and the 10 s period following the sigh ($fR_{1-10\,s}$), duration of the post-sigh apnoea and post-sigh V_T. (B) Columns (and bars) in the histogram show the mean (and S.E.M.) changes in fR (expressed in % of the control fR) during the second preceding the sigh in WT and *Mecp2*$^{-/y}$ mice (white and black columns, respectively) at the different developmental ages. Asterisks indicated a significant difference between genotypes. (C and D), as in (B) but for $fR_{1\,s}$ and $fR_{1-10\,s}$. (E–G) as in (B) but for the duration of post-sigh apnoea (expressed in second), the amplitude of post-sigh V_T (expressed in % of the control V_T) and the peak amplitude of the expiratory component of the sigh (Pk Exp, expressed in % of the total sigh amplitude).

during expiration (Pk Exp = 29 ± 2% of total sigh amplitude), weak Pk Exp values occurring after simple (Fig. 2B2), complex (Fig. 1B2 and Fig. 2B1) or multiple sighs (not shown). In addition, *Mecp2*$^{-/y}$ mice displayed an abnormal post-sigh breathing pattern. As shown in Fig. 2B1 and B2 for a given *Mecp2*$^{-/y}$ mouse, sighs induced marked post-sigh apnoeas but were not followed by long-lasting bradypnoeas with increased V_T. The mean duration of post-sigh apnoeas in four *Mecp2*$^{-/y}$ mice was 689 ± 83 ms, i.e. about 4-fold the baseline duration of expiration (176 ± 11 ms). Consequently, the mean fR was markedly reduced during the second following the sigh ($fR_{1\,s}$ = 46 ± 9% of control fR), a reduction significantly larger than that observed in WT (Fig. 4C). Second, when breathing resumed, baseline fR was restored within 1–3 s as illustrated by individual PSTH (Fig. 2B3) and averaged PSTH (Fig. 3F). During the 10 s post-sigh period, no significant bradypnoea occurred in *Mecp2*$^{-/y}$ mice ($fR_{1-10\,s}$ = 94 ± 4% of control), contrarily to WT (Fig. 4D). Interestingly, the mean fR during the second preceding the sigh was slightly but significantly decreased in *Mecp2*$^{-/y}$ mice ($fR_{-1\,s}$ = 83 ± 2% of control fR), a reduction not observed in WT at P30 (Fig. 4B). The $fR_{-1\,s}$ reduction was not caused by the occurrence of apnoea before the sigh but by a slowing of the rhythm. The mean V_T of inspirations produced during the 10 s post-sigh period was not significantly increased (−5 ± 11% of control). However, the first five post-sigh inspirations were of weaker amplitude than control pre-sigh inspirations, as illustrated by individual traces (Fig. 2B1 and B2) and confirmed by averaging (Fig. 2D), with a significant reduction of the mean V_T in the four studied *Mecp2*$^{-/y}$ mice (−25 ± 9% of control) (Fig. 4F). Thus, although *Mecp2*$^{-/y}$ mice did not display erratic breathing and frequent apnoeas at P30, their post-sigh breathing was already abnormal when compared to age matched WT mice, with a longer post-sigh apnoea followed by weakened inspirations.

3.3. Post-sigh breathing pattern in WT and *Mecp2*$^{-/y}$ younger than P30

In four WT and four *Mecp2*$^{-/y}$ mice at P25, sighs similarly occurred at a low frequency (0.38 ± 0.04 and 0.36 ± 0.04 sigh per min, respectively; ns). However, Pk Exp values were significantly larger in WT than *Mecp2*$^{-/y}$ (Pk Exp = 56 ± 3% and 42 ± 2% of total sigh amplitude, respectively) (Fig. 4G). *Mecp2*$^{-/y}$ mice already displayed an abnormal post-sigh breathing pattern as confirmed by individual traces (Fig. 5A and B) and pooled PSTH (Fig. 3C and D). A significant long-lasting bradypnoea occurred in WT mice ($fR_{1-10\,s}$ = 72 ± 2% of control) but not in *Mecp2*$^{-/y}$ mice ($fR_{1-10\,s}$ = 86 ± 7% of control) (Fig. 4D) and the mean V_T of post-sigh inspirations was significantly increased in WT (17 ± 4% of increase) but not in *Mecp2*$^{-/y}$ mice (+7 ± 12% of increase) where the mean amplitude of the first five inspirations was decreased by 12 ± 5% (Fig. 4F). There were no significant differences in the mean duration of post-sigh apnoeas of WT and *Mecp2*$^{-/y}$ mice (316 ± 64 and 407 ± 61 ms, respectively), nor in the reduction of the mean fR during the 1 s post-sigh period ($fR_{1\,s}$ = 78 ± 4 and 66 ± 8% of control, respectively), nor in the mean fR during the second preceding the sigh ($fR_{-1\,s}$ = 101 ± 1 and 104 ± 3% of control, respectively).

At P15, a comparison of sighs produced by four WT and five *Mecp2*$^{-/y}$ mice did not reveal significant differences in the frequency of sigh occurrence (0.35 ± 0.03 and 0.36 ± 0.04 sigh per min), the Pk Exp values (61 ± 3% and 63 ± 3% of total sigh amplitude), the mean duration of post-sigh apnoeas (396 ± 58 ms and 437 ± 52 ms, respectively), the mean V_T changes of post-sigh inspirations (14 ± 7% and 8 ± 9%). As illustrated in PSTH of Fig. 3A and B, the mean fR was reduced during the second following the sigh in both WT and *Mecp2*$^{-/y}$ mice ($fR_{1\,s}$ = 78 ± 2 and 79 ± 2% of control fR; ns). However, as shown in Figs. 3A, B and 4D, a slight but sig-

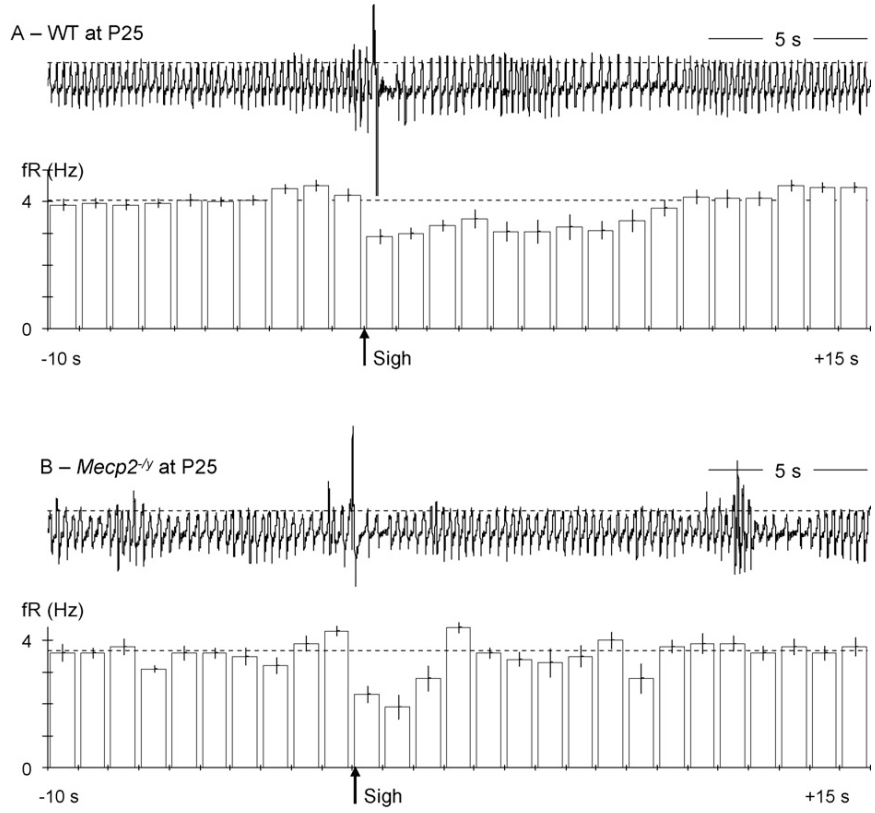

Fig. 5. Post-sigh breathing in WT and *Mecp2*$^{-/y}$ mice at P25. Plethysmographic traces and individual PSTH obtained from a given WT (A) and a given *Mecp2*$^{-/y}$ (B) at P25 (same organization than in Fig. 2). After the sigh (vertical arrow), note the long-lasting bradypnoea with inspirations of increased amplitude in WT (A) but not in *Mecp2*$^{-/y}$ mice (B).

nificant post-sigh bradypnoea occurred in WT but not in *Mecp2*$^{-/y}$ mice ($fR_{1-10\,s}$ = 91 ± 2 and 99 ± 3% of control, respectively).

3.4. Post-sigh breathing pattern in WT and Mecp2$^{-/y}$ older than P30

We studied the sigh and the post-sigh breathing pattern of five WT and eight *Mecp2*$^{-/y}$ mice at P45–P60 which all displayed obvious breathing symptoms with an erratic rhythm and severe apnoeas (Fig. 6). Sighs had significantly lower Pk Exp in *Mecp2*$^{-/y}$ than WT mice (29 ± 2 and 42 ± 1% of total sigh amplitude) (Fig. 4G). The frequency of sigh occurrence at P45–P60 compared to P30 was unchanged in WT mice (0.33 ± 0.02 sigh per min) but was significantly increased in *Mecp2*$^{-/y}$ mice (0.48 ± 0.07 sigh per min). Most apnoeas spontaneously occurred in *Mecp2*$^{-/y}$ mice, without being preceded by a sigh. We counted 577 spontaneous apnoeas and 45 sigh-induced apnoeas during 10 min periods in eight *Mecp2*$^{-/y}$ mice, revealing that post-sigh apnoeas corresponded to only 7% of the total number of apnoeas.

Because of the erratic breathing of *Mecp2*$^{-/y}$ at P45–P60, the post-sigh breathing pattern appeared variable. Sighs induced either long post-sigh apnoeas (Fig. 6A) or short post-sigh apnoeas (Fig. 6B–D) or occasionally had no obvious immediate effects (Fig. 6E). Nevertheless, the mean duration of post-sigh apnoeas was 2-fold increased in *Mecp2*$^{-/y}$ than WT mice (881 ± 97 and 428 ± 34 ms, respectively). As illustrated in Figs. 3E, F and 4B, the mean fR during the second preceding the sigh was significantly reduced in *Mecp2*$^{-/y}$ mice ($fR_{-1\,s}$ = 73 ± 6% of control fR) but not in WT mice ($fR_{-1\,s}$ = 95 ± 3% of control fR). The $fR_{-1\,s}$ reduction in *Mecp2*$^{-/y}$ mice reflected both the occurrence of pre-sigh apnoeas and slowing of the rhythm before the sigh. The mean fR during the second following the sigh was also significantly more reduced in *Mecp2*$^{-/y}$ than WT mice ($fR_{1\,s}$ = 58 ± 7% and 75 ± 2% of control, respectively), and thereafter no significant bradypnoea occurred in *Mecp2*$^{-/y}$ mice ($fR_{1-10\,s}$ = 89 ± 6%) whereas a bradypnoea persisted for 10 s in WT mice ($fR_{1-10\,s}$ = 70 ± 3%). The mean V_T during the 10 s post-sigh period was not significantly changed in *Mecp2*$^{-/y}$ (12 ± 27%) but was increased in WT mice (22 ± 7% of increase). However, the first five post-sigh inspirations in *Mecp2*$^{-/y}$ mice mobilized a significantly reduced V_T (46 ± 12% of control V_T; see Fig. 4F and arrows in Fig. 6B–D).

Because the function of upper airways is affected in *Mecp2*$^{-/y}$ mice at P45 (Stettner et al., 2007), we developed a double plethysmographic approach to simultaneously record chest respiratory movements and upper airway flow in aged *Mecp2*$^{-/y}$ mice and to further check the decrease in V_T during the post-sigh period. In four *Mecp2*$^{-/y}$ mice at P55–P60, we commonly observed marked reductions of both chest respiratory movements and airflow after the sigh (Fig. 7A–D). Interestingly, the weakest chest respiratory movements after the sigh failed to induce discernable upper airway flow during a post-sigh period, which lasted for 1–2 s (Fig. 7B and C) and occasionally longer (Fig. 7D). Thus, both simple and double plethysmographic approaches in *Mecp2*$^{-/y}$ mice older than P30 revealed that sighs severely disrupted the post-sigh breathing pattern, inducing long-lasting post-sigh apnoeas prolonged by a period of weak chest respiratory movements and reduced airflow, with the weakest chest movements failing to induce detectable airflow.

4. Discussion

Mecp2$^{-/y}$ mice display normal breathing at birth but show exacerbated respiratory responses to hypoxia and transient apnoeas

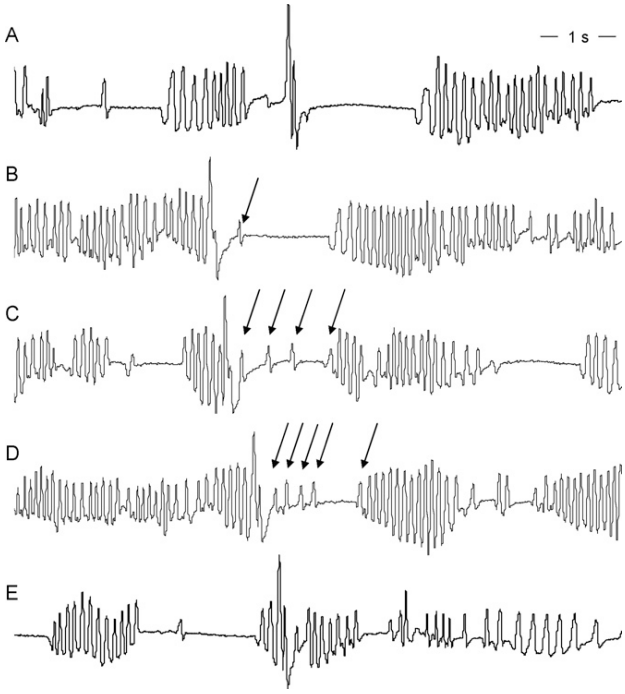

Fig. 6. Post-sigh breathing in *Mecp2*$^{-/y}$ mice at P60. (A–E) The five plethysmographic traces were recorded from a given *Mecp2*$^{-/y}$ mouse at P60. They show the variability of the post-sigh breathing pattern, with sighs inducing long apnoea (A), short apnoeas (B–D) and no obvious immediate effects on the erratic breathing rhythm (E). In (A), (C) and (E), note the erratic breathing pattern, with frequent spontaneous apnoeas occurring prior to the sighs and in (B), (C) and (D) the post-sigh inspirations of halved amplitude (oblique arrows).

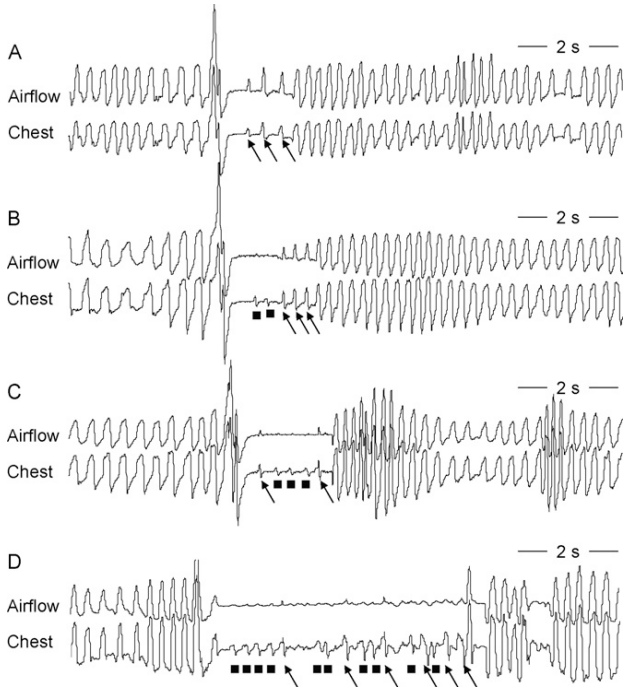

Fig. 7. Double-chamber plethysmographic approach reveals post-sigh reduction of airflow in *Mecp2*$^{-/y}$ mice at P55–P60. A double-chamber plethysmographic approach was used to simultaneously record chest respiratory movements and resulting airflow (lower and upper traces, respectively) in *Mecp2*$^{-/y}$ at P55 (A–C, same mouse) and P60 (D, other mouse; sigh truncated) which displayed severe breathing symptoms (not illustrated here). When eupnoea resumed after the sigh, the first chest respiratory movements and airflow produced by the *Mecp2*$^{-/y}$ mice were of reduced amplitude (oblique arrows). Note that the weakest chest respiratory movements failed to induce detectable airflow signal (black squares).

after moderate respiratory challenges from P25 (Voituron et al., 2009) and develop breathing symptoms reminiscent of RTT after P30 (Viemari et al., 2005), with possible upper airway dysfunctions at P45 (Stettner et al., 2007) and death around P60. Herein, we describe early abnormalities of the post-sigh breathing pattern of *Mecp2*$^{-/y}$ mice which develop from P15–P25 and aggravate thereafter. Although the early abnormalities of the post-sigh breathing (present study) and respiratory regulations (Voituron et al., 2009) of young *Mecp2*$^{-/y}$ mice are subtle and not sufficiently marked to significantly alter ventilation at rest, they might be viewed as indicators of later breathing symptoms. Thus, non-invasive recordings of breathing might permit earlier diagnosis of breathing symptoms in *Mecp2*$^{-/y}$ mice, and eventually in RTT patients. Below, we discuss the functional significance and the possible origin of early abnormalities of post-sigh breathing patterns in *Mecp2*$^{-/y}$ mice, suggesting they might be caused by earlier GABAergic deficits (Medrihan et al., 2008).

4.1. Functional significance of the abnormal post-sigh breathing of *Mecp2*$^{-/y}$ mice

Sighs are deep inspirations mobilizing a large V_T, which prevents lung atelectasis, restores functional residual capacity and improves alveolar oxygenation (Glogowska et al., 1972; Cherniack et al., 1981; Alvarez et al., 1993; Poets et al., 1997; Patroniti et al., 2002; Popa et al., 2005; Yamauchi et al., 2008). The sigh amplitude was twice normal inspirations in *Mecp2*$^{-/y}$ and WT mice but the peak expiratory component of the sigh was significantly weaker in *Mecp2*$^{-/y}$ than WT mice from P25. The reduction of sigh expiratory flow in *Mecp2*$^{-/y}$ mice probably originates from dysfunction of the upper airways already reported in *Mecp2*$^{-/y}$ mice at P45 (Stettner et al., 2007) and may be reminiscent of the breath-holding pattern of RTT patients (Katz et al., 2009).

In WT mice, sighs are followed by an immediate, brief post-sigh apnoea and a long-lasting bradypnoea (Popa et al., 2005). During the post-sigh bradypnoea, we show a previously undocumented V_T increase (but see Fig. 8 in Popa et al., 2005) which may contribute to maintain the minute ventilation during the post-sigh period, despite the bradypnoea. In *Mecp2*$^{-/y}$ mice, we report a longer post-sigh apnoea, a lack of bradypnoea with an increase in V_T, but a reduction in V_T when eupnoea resumes. These abnormalities of post-sigh breathing develop from P15, are marked at P25, during the pre-symptomatic period when *Mecp2*$^{-/y}$ still have a normal breathing at rest, and aggravate thereafter during the symptomatic period after P30. In *Mecp2*$^{-/y}$ mice, the reduction in V_T during the post-sigh period was first observed with simple plethysmography at P25, P30 and P60, and was confirmed with double-chamber plethysmography at P45–P60, showing that both chest respiratory movements and upper airway airflow were severely reduced during the post-sigh period. In addition, the weakest chest movements failed to induce detectable airflow, a result fully in agreement with upper airways dysfunction in *Mecp2*$^{-/y}$ mice at P45 (Stettner et al., 2007). When *Mecp2*$^{-/y}$ mice permanently express breathing symptoms, the frequency of sighs is increased. This increase may be the consequence of hypoxia and hypercapnia which are known to facilitate sigh occurrence (Glogowska et al., 1972; Cherniack et al., 1981). Thus, in *Mecp2*$^{-/y}$ mice, long-lasting post-sigh apnoeas followed by periods of reduced V_T may have deleterious effects on breathing, transiently and repetitively impairing blood oxygenation and possibly accelerating the progression of the disease.

4.2. Mechanisms underlying the post-sigh breathing pattern of WT

In WT mice, the brief post-sigh apnoea and the long-lasting bradypnoea with increased V_T originate from central and peripheral mechanisms, respectively. Eupnoea and sigh rhythms are primarily produced by the same set of respiratory neurons of the Pre-Bötzinger Complex, the isolated Pre-Bötzinger Complex generating the two rhythms (Smith et al., 1991; Lieske et al., 2000; Tryba et al., 2008). The fictive sighs produced *in vitro* are followed by a brief apnoea (<3 respiratory-like cycles), which likely corresponds to the brief post-sigh apnoea observed *in vivo*. The long-lasting bradypnoea observed *in vivo* (>30 respiratory cycles) has not been reported *in vitro* and probably implicates sensory afferent mediated mechanisms. *In vivo*, sighs are affected by peripheral afferent inputs from lungs and carotid bodies (Glogowska et al., 1972; Cherniack et al., 1981). The large V_T mobilized by the sigh activates the pulmonary stretch receptors, which in turn shortens inspiration via the Hering-Breuer reflex. In addition, the large V_T mobilized by the sigh improves blood oxygenation, which in turn reduces the stimulating drive from the carotid body chemoceptors. The cumulative effects of activation of lung inhibitory inputs and reduction of carotid body facilitatory inputs are highly likely the cause of the long-lasting changes in fR and V_T seen during the post-sigh period *in vivo*, but not *in vitro*.

Lung and carotid body afferent inputs synaptically target relay neurons within the nucleus tractus solitarius (nTS). The nTS has an important role in integrating respiratory afferent inputs, modulating breathing, and sending projections to medullary respiratory groups and pontine Kolliker-Fuse (KF) group (Yokota et al., 2008). The KF which also projects to the whole respiratory network modulates the Hering-Breuer reflex, upper airway function, coupling between breathing and sleep/wake states, cardiovascular regulations, swallowing, etc. (Siniaia et al., 2000; Stettner et al., 2007; Verner et al., 2008; Dutschmann and Herbert, 2006; Yokota et al., 2008; Kuna and Remmers, 1999; Núñez-Abades et al., 1990). Neither the nTS nor the KF are mature at birth (Vincent et al., 1996; Ohtake et al., 2000; Grabauskas and Bradley, 2001; Dutschmann et al., 2008; Kron et al., 2007, 2008; Tashiro et al., 2009), and their postnatal maturation may contribute to the development of the long-lasting bradypnoea in WT, from weak at P15 to well-established at P25. The nTS and KF postnatal maturation may also contribute to the changes in sigh pattern observed in maturing WT, from mostly multiple or complex sighs in young mice to simple sighs in adults. In humans, the sigh pattern similarly changes with age, from biphasic sighs in infants to simple sighs in adults (Qureshi et al., 2009). In *Mecp2*$^{-/y}$ mice however, multiple or complex sighs remain frequent in adults, and as discussed below, this might reflect alterations of nTS and KF functions although other explanations cannot be totally excluded.

4.3. Mechanisms underlying the abnormalities of the post-sigh breathing of *Mecp2*$^{-/y}$ mice

No obvious differences have been observed in fictive sighs produced in WT and *Mecp2*$^{-/y}$ slices at P14–P21 (Viemari et al., 2005). No significant differences have been observed in the sigh pattern and the post-sigh apnoea duration produced *in vivo* in WT and *Mecp2*$^{-/y}$ mice at P15 (present study). These two observations suggest that no major defects exist in the sigh generating mechanisms of young *Mecp2*$^{-/y}$ mice. However, in *Mecp2*$^{-/y}$ mice, the post-sigh bradypnoea is absent from P15, the post-sigh V_T is decreased from P25, and the post-sigh apnoea is prolonged from P30. As discussed above, the post-sigh bradypnoea with increased V_T of WT mice is caused by peripheral inputs to the brainstem respiratory network. In *Mecp2*$^{-/y}$ mice, the lack of bradypnoea and the reduced V_T may therefore reflect alterations of the central processes integrating peripheral inputs. *Mecp2*$^{-/y}$ mice display exacerbated respiratory responses to moderate hypoxia because of nTS defects (Voituron et al., 2009) and to lung afferents because of KF defects (Stettner et al., 2007). Altered responses of nTS and KF to afferent inputs in *Mecp2*$^{-/y}$ mice may therefore affect their post-sigh breathing pattern. For example, the large V_T mobilized during the sigh may induce a stronger inhibitory Hering-Breuer reflex in *Mecp2*$^{-/y}$ than WT mice (Stettner et al., 2007), which could explain both the long post-sigh apnoea and the V_T reduction when eupnoea resumes in *Mecp2*$^{-/y}$ mice. After the sigh, the long apnoea and the V_T reduction may lead to a transient, moderate hypoxia in *Mecp2*$^{-/y}$ mice, which could induce an exacerbated increase in fR (Voituron et al., 2009) impairing the bradypnoea.

In *Mecp2*$^{-/y}$ mice, dysfunctions of NE, 5HT, GABA, glutamate and BDNF signalling systems contribute to their exacerbated responses to hypoxia and the occurrence of transient apnoeas after moderate respiratory challenges at P25 and their severe breathing symptoms after P30 (Katz et al., 2009; Voituron et al., 2009). They could also affect post-sigh breathing but most systems are altered too late to initiate post-sigh breathing anomalies. The 5HT system affects the sigh pattern (Yamauchi et al., 2008; Saponjic et al., 2007; Popa et al., 2005) but dysfunctions late in *Mecp2*$^{-/y}$, after P30 (Viemari et al., 2005). BDNF deficits also occur too late in the medulla of *Mecp2*$^{-/y}$, by five weeks after birth (Ogier and Katz, 2008; Wang et al., 2006). NE deficits exist in the *Mecp2*$^{-/y}$ brain at P14 (Ide et al., 2005) but are significant in the *Mecp2*$^{-/y}$ medulla only at a later stage, at around P30 (Viemari et al., 2005). Glutamate exerts complex effects on sighs (Radulovacki et al., 2001; Lieske and Ramirez, 2006) and glutamatergic deficits occur in hippocampal neurons of P7–P14 *Mecp2*$^{-/y}$ (Chao et al., 2007). However, glutamate deficits in the medulla of *Mecp2*$^{-/y}$ mice have not been demonstrated.

The GABAergic transmission is specifically decreased in the medulla of *Mecp2*$^{-/y}$ mice as early as P7 (Medrihan et al., 2008) and insufficient GABA inhibition might underlie periodic and irregular breathing of old *Mecp2*-deficient female mice (Bissonnette and Knopp, 2008). GABA is the major inhibitory neurotransmitter in the CNS (Wong et al., 2003) and contributes to the modulation of both respiratory rhythm and upper airway flow (Melton et al., 1990; Pierrefiche et al., 1993; Suzuki et al., 1999; Ezure and Tanaka, 2004; Gallos et al., 2009; Sanchez et al., 2009). GABA receptors are expressed in the nTS where they modulate the respiratory responses to hypoxia (Suzuki et al., 1999, 2003, 2004) and lung inflation (Ezure and Tanaka, 2004). GABA nTS neurons project to the KF (Yokota et al., 2008) which modulates upper airway functions (Dutschmann and Herbert, 1998, 2006). KF dysfunctions in *Mecp2*$^{-/y}$ may result in upper airway problems (Stettner et al., 2007). Thus the early GABA deficits of *Mecp2*$^{-/y}$ mice at P7 may have a primary role in initiating abnormalities of post-sigh breathing from P15, while the other signalling systems which interact with the GABA system (Ciranna, 2006; Spedding and Gressens, 2008; Mora et al., 2008) possibly contribute to the evolution, but not the initiation, of post-sigh abnormalities.

However the abnormalities of the post-sigh breathing of *Mecp2*$^{-/y}$ mice may also have other origins. First, the responsiveness of carotid body chemoceptors and pulmonary stretch receptors might be altered in *Mecp2*$^{-/y}$ mice, but this has not been demonstrated yet. Second, the reduction of the peak expiratory flow of the sigh in *Mecp2*$^{-/y}$ mice may prolong the discharge of pulmonary stretch receptors during the post-sigh period, which may contribute to lengthen the post-sigh apnoea and to reduce the V_T when eupnoea resumes. Finally, the sigh and the brief post-sigh apnoea are centrally generated within the Pre-Bötzinger Complex (Tryba et al., 2008) and the GABA deficits of *Mecp2*$^{-/y}$ mice may directly alter the sigh generating system by unbalancing the ratio of excitatory vs. inhibitory synaptic transmission. Indeed, this may

happen in *Mecp2*$^{-/y}$ mice at P45–P60 where the eupneic rhythm is erratic and marked changes occur in sigh generation, with a fR reduction prior to the sigh. However in younger *Mecp2*$^{-/y}$ mice where eupneic rhythm and sigh generation are unaltered *in vitro* and *in vivo* (Viemari et al., 2005, and present study), the early GABA deficits unlikely alter the Pre-Bötzinger Complex whereas they may affect the KF and nTS regulation of post-sigh breathing.

4.4. The Rett syndrome and the neuro-archaeology theory

To conclude, analysing the breathing of unrestrained mice from P15 to P60 with non-invasive plethysmographic approaches has revealed early, subtle abnormalities of the post-sigh breathing of *Mecp2*$^{-/y}$ mice which develop from P15, during the pre-symptomatic period. The early abnormalities of post-sigh breathing in *Mecp2*$^{-/y}$ mice, a mouse model of RTT, may be indicators of more pronounced breathing symptoms later in development and might be caused by earlier GABA deficits, significant in the *Mecp2*$^{-/y}$ medulla as early as P7 (Medrihan et al., 2008).

The neuro-archaeology theory (Ben-Ari, 2008) proposes that "early- and late-onset neurological disorders as diverse as infantile epilepsies, mental retardation, dyslexia or, in certain conditions, even Huntington's and Alzheimer's disease might be, in part, born at early developmental stages before symptoms appear" and that "non-invasive recordings might unravel signatures of disorders to come, thereby permitting earlier diagnosis and potential treatment of neurological disorders". RTT girls, as *Mecp2*$^{-/y}$, develop breathing symptoms with age (Katz et al., 2009), have GABA defects in basal ganglia and frontal cortex (Blue et al., 1999a,b), and treatment with topiramate, a broad-spectrum drug with GABAergic effects, alleviates their breathing symptoms (Goyal et al., 2004). We do not know yet whether the RTT girls develop early abnormalities of their post-sigh breathing, but the non-invasive recording of their breathing could reveal it, which would permit earlier diagnosis and potential treatment of breathing symptoms, possibly via GABAergic agents.

Acknowledgments

This work was supported by the Rett Syndrome Research Foundation and the International Rett Syndrome Foundation (fellowship to NV and SZ, in 2007 and 2008–2009, respectively) and the CNRS (fellowship to MD in 2008).

References

Alvarez, J.E., Bodani, J., Fajardo, C.A., Kwiatkowski, K., Cates, D.B., Rigatto, H., 1993. Sighs and their relationship to apnea in the newborn infant. Biol. Neonate 63 (3), 139–146.
Ben-Ari, Y., 2008. Neuro-archaeology: pre-symptomatic architecture and signature of neurological disorders. Trends Neurosci. 31 (12), 626–636.
Bissonnette, J., Knopp, S., 2008. Insufficient GABA inhibition underlies periodic and irregular breathing in methyl-CpG-binding protein 2 (Mecp2) deficient mice. FASEB J. 22, 1232.12.
Blue, M.E., Naidu, S., Johnston, M.V., 1999a. Altered development of glutamate and GABA receptors in the basal ganglia of girls with Rett syndrome. Exp. Neurol. 156 (2), 345–352.
Blue, M.E., Naidu, S., Johnston, M.V., 1999b. Development of amino acid receptors in frontal cortex from girls with Rett syndrome. Ann. Neurol. 45 (4), 541–545.
Chao, H.T., Zoghbi, H.Y., Rosenmund, C., 2007. MeCP2 controls excitatory synaptic strength by regulating glutamatergic synapse number. Neuron 56 (1), 58–65.
Cherniack, N.S., Von Euler, C., Głogowska, M., Homma, I., 1981. Characteristics and rate of occurrence of spontaneous and provoked augmented breaths. Acta Physiol. Scand. 111 (3), 349–360.
Ciranna, L., 2006. Serotonin as a modulator of glutamate- and GABA-mediated neurotransmission: implications in physiological functions and in pathology. Curr. Neuropharmacol. 4 (2), 101–114.
Dutschmann, M., Herbert, H., 1998. NMDA and GABAA receptors in the rat Kolliker-Fuse area control cardiorespiratory responses evoked by trigeminal ethmoidal nerve stimulation. J. Physiol. 510 (3), 793–804.
Dutschmann, M., Herbert, H., 2006. The Kölliker-Fuse nucleus gates the postinspiratory phase of the respiratory cycle to control inspiratory off-switch and upper airway resistance in rat. Eur. J. Neurosci. 24 (4), 1071–1084.
Dutschmann, M., Mörschel, M., Reuter, J., Zhang, W., Gestreau, C., Stettner, G.M., Kron, M., 2008. Postnatal emergence of synaptic plasticity associated with dynamic adaptation of the respiratory motor pattern. Respir. Physiol. Neurobiol. 164 (1–2), 72–79.
Ezure, K., Tanaka, I., 2004. GABA, in some cases together with glycine, is used as the inhibitory transmitter by pump cells in the Hering-Breuer reflex pathway of the rat. Neuroscience 127 (2), 409–417.
Gallos, G., Gleason, N.R., Virag, L., Zhang, Y., Mizuta, K., Whittington, R.A., Emala, C.W., 2009. Endogenous gamma-aminobutyric acid modulates tonic guinea pig airway tone and propofol-induced airway smooth muscle relaxation. Anesthesiology 110 (4), 748–758.
Glogowska, M., Richardson, P.S., Widdicombe, J.G., Winning, A.J., 1972. The role of the vagus nerves, peripheral chemoreceptors and other afferent pathways in the genesis of augmented breaths in cats and rabbits. Respir. Physiol. 16 (2), 179–196.
Goyal, M., O'Riordan, M.A., Wiznitzer, M., 2004. Effect of topiramate on seizures and respiratory dysrhythmia in Rett syndrome. J. Child Neurol. 19 (8), 588–591.
Grabauskas, G., Bradley, R.M., 2001. Postnatal development of inhibitory synaptic transmission in the rostral nucleus of the solitary tract. J. Neurophysiol. 85 (5), 2203–2212.
Guy, J., Hendrich, B., Holmes, M., Martin, J.E., Bird, A., 2001. A mouse Mecp2-null mutation causes neurological symptoms that mimic Rett syndrome. Nat. Genet. 27, 322–326.
Ide, S., Itoh, M., Goto, Y., 2005. Defect in normal developmental increase of the brain biogenic amine concentrations in the *mecp2*-null mouse. Neurosci. Lett. 386, 14–17.
Katz, D.M., Dutschmann, M., Ramirez, J.M., Hilaire, G., 2009. Breathing disorders in Rett syndrome: progressive neurochemical dysfunction in the respiratory network after birth. Respir. Physiol. Neurobiol. 168 (1–2), 101–108.
Kron, M., Reuter, J., Gerhardt, E., Manzke, T., Zhang, W., Dutschmann, M., 2008. Emergence of brain-derived neurotrophic factor-induced postsynaptic potentiation of NMDA currents during the postnatal maturation of the Kolliker-Fuse nucleus of rat. J. Physiol. 586 (9), 2331–2343.
Kron, M., Zhang, W., Dutschmann, M., 2007. Developmental changes in the BDNF-induced modulation of inhibitory synaptic transmission in the Kölliker-Fuse nucleus of rat. Eur. J. Neurosci. 26 (12), 3449–3457.
Kuna, S.T., Remmers, J.E., 1999. Premotor input to hypoglossal motoneurons from Kölliker-Fuse neurons in decerebrate cats. Respir. Physiol. 117 (2–3), 85–95.
Lieske, S.P., Ramirez, J.M., 2006. Pattern-specific synaptic mechanisms in a multifunctional network. I. Effects of alterations in synapse strength. J. Neurophysiol. 95 (3), 1323–1333.
Lieske, S.P., Thoby-Brisson, M., Telgkamp, P., Ramirez, J.M., 2000. Reconfiguration of the neural network controlling multiple breathing patterns: eupnea, sighs and gasps. Nat. Neurosci. 3 (6), 600–607.
Medrihan, L., Tantalaki, E., Aramuni, G., Sargsyan, Y., Dudanova, I., Missler, M., Zhang, W., 2008. Early defects of GABAergic synapses in the brain stem of a MeCP2 mouse model of Rett syndrome. J. Neurophysiol. 99, 112–121.
Melton, J.E., Neubauer, J.A., Edelman, N.H., 1990. GABA antagonism reverses hypoxic respiratory depression in the cat. J. Appl. Physiol. 69 (4), 1296–1301.
Mora, F., Segovia, G., Del Arco, A., 2008. Glutamate-dopamine-GABA interactions in the aging basal ganglia. Brain Res. Rev. 58 (2), 340–353.
Núñez-Abades, P.A., Portillo, F., Pásaro, R., 1990. Characterisation of afferent projections to the nucleus ambiguus of the rat by means of fluorescent double labelling. J. Anat. 172, 1–15.
Ogier, M., Katz, D., 2008. Breathing dysfunction in Rett syndrome: understanding epigenetic regulation of the respiratory network. Respir. Physiol. Neurobiol. 164, 55–63.
Ohtake, P.J., Simakajornboon, N., Fehniger, M.D., Xue, Y.D., Gozal, D., 2000. N-methyl-D-aspartate receptor expression in the nucleus tractus solitarii and maturation of hypoxic ventilatory response in the rat. Am. J. Respir. Crit. Care Med. 162 (3), 1140–1147.
Patroniti, N., Foti, G., Cortinovis, B., Maggioni, E., Bigatello, L.M., Cereda, M., Pesenti, A., 2002. Sigh improves gas exchange and lung volume in patients with acute respiratory distress syndrome undergoing pressure support ventilation. Anesthesiology 96 (4), 788–794.
Pierrefiche, O., Foutz, A.S., Denavit-Saubié, M., 1993. Effects of GABAB receptor agonists and antagonists on the bulbar respiratory network in cat. Brain Res. 605 (1), 77–84.
Poets, C.F., Rau, G.A., Neuber, K., Gappa, M., Seidenberg, J., 1997. Determinants of lung volume in spontaneously breathing preterm infants. Am. J. Respir. Crit. Care Med. 155 (2), 649–653.
Popa, D., Léna, C., Fabre, V., Prenat, C., Gingrich, J., Escourrou, P., Hamon, M., Adrien, J., 2005. Contribution of 5-HT2 receptor subtypes to sleep-wakefulness and respiratory control, and functional adaptations in knock-out mice lacking 5-HT2A receptors. J. Neurosci. 25 (49), 11231–11238.
Qureshi, M., Khalil, M., Kwiatkowski, K., Alvaro, R.E., 2009. Morphology of sighs and their role in the control of breathing in preterm infants, term infants and adults. Neonatology 96 (1), 43–49.
Radulovacki, M., Pavlovic, S., Rakic, A., Janelidze, M., Shermulis, L., Carley, D.W., 2001. Riluzole suppresses post-sigh, but not spontaneous apnoeas during sleep in rats. J. Pharm. Pharmacol. 53 (11), 1555–1559.
Sanchez, A., Mustapic, S., Zuperku, E.J., Stucke, A.G., Hopp, F.A., Stuth, E.A., 2009. Role of inhibitory neurotransmission in the control of canine hypoglossal motoneuron activity in vivo. J. Neurophysiol. 101 (3), 1211–1221.

Saponjic, J., Radulovacki, M., Carley, D.W., 2007. Monoaminergic system lesions increase post-sigh respiratory pattern disturbance during sleep in rats. Physiol. Behav. 90 (1), 1–10.
Siniaia, M.S., Young, D.L., Poon, C.S., 2000. Habituation and desensitization of the Hering-Breuer reflex in rat. J. Physiol. 523 (2), 479–491.
Smith, J.C., Ellenberger, H.H., Ballanyi, K., Richter, D.W., Feldman, J.L., 1991. Pre-Bötzinger complex: a brainstem region that may generate respiratory rhythm in mammals. Science 254 (5032), 726–729.
Spedding, M., Gressens, P., 2008. Neurotrophins and cytokines in neuronal plasticity. Novartis Found Symp. 289, 222–233.
Stettner, G.M., Huppke, P., Brendel, C., Richter, D.W., Gärtner, J., Dutschmann, M., 2007. Breathing dysfunctions associated with impaired control of postinspiratory activity in Mecp2-/y knockout mice. J. Physiol. 579 (3), 863–876.
Suzuki, M., Nishina, M., Nakamura, S., Maruyama, K., 2003. Endogenous GABA in the commissural subnucleus of the NTS inhibits the carotid chemoreceptor reflex via GABA A receptors in rats. J. Neural. Transm. 110 (3), 211–218.
Suzuki, M., Nishina, M., Nakamura, S., Maruyama, K., 2004. Benzodiazepine-sensitive GABA(A) receptors in the commissural subnucleus of the NTS are involved in the carotid chemoreceptor reflex in rats. Auton. Neurosci. 110 (2), 108–113.
Suzuki, M., Tetsuka, M., Endo, M., 1999. GABA(B) receptors in the nucleus tractus solitarii modulate the carotid chemoreceptor reflex in rats. Neurosci. Lett. 260 (1), 21–24.
Tashiro, Y., Okada, T., Kawai, Y., 2009. Postnatal development of axosomatic synapses in the rat nucleus tractus solitarius: dorsal and ventral subnuclei differences. Neurosci. Lett. 450 (2), 217–220.
Tryba, A.K., Peña, F., Lieske, S.P., Viemari, J.C., Thoby-Brisson, M., Ramirez, J.M., 2008. Differential modulation of neural network and pacemaker activity underlying eupnea and sigh-breathing activities. J. Neurophysiol. 99, 2114–2125.
Verner, T.A., Pilowsky, P.M., Goodchild, A.K., 2008. Retrograde projections to a discrete apneic site in the midline medulla oblongata of the rat. Brain Res. 1208, 128–136.
Viemari, J.C., Roux, J.C., Tryba, A.K., Saywell, V., Burnet, H., Peña, F., Zanella, S., Bévengut, M., Barthelemy-Requin, M., Herzing, L.B., Moncla, A., Mancini, J., Ramirez, J.M., Villard, L., Hilaire, G., 2005. Mecp2 deficiency disrupts norepinephrine and respiratory systems in mice. J. Neurosci. 25, 11521–11530.
Vincent, A., Jean, A., Tell, F., 1996. Developmental study of N-methyl-D-aspartate-induced firing activity and whole-cell currents in nucleus tractus solitarii neurons. Eur. J. Neurosci. 8 (12), 2748–2752.
Voituron, N., Zanella, S., Menuet, C., Dutschmann, M., Hilaire, G., 2009. Early breathing defects after moderate hypoxia or hypercapnia in a mouse model of Rett syndrome. Respir. Physiol. Neurobiol. 168 (1–2), 109–118.
Wang, H., Chan, S.A., Ogier, M., Hellard, D., Wang, Q., Smith, C., Katz, D., 2006. Dysregulation of brain-derived neurotrophic factor expression and neurosecretory function in Mecp2 null mice. J. Neurosci. 26, 10911–10915.
Wong, C.G., Bottiglieri, T., Snead 3rd, O.C., 2003. GABA, gamma-hydroxybutyric acid, and neurological disease. Ann. Neurol. 54 (Suppl. 6), S3–S12.
Yamauchi, M., Ocak, H., Dostal, J., Jacono, F.J., Loparo, K.A., Strohl, K.P., 2008. Post-sigh breathing behavior and spontaneous pauses in the C57BL/6J (B6) mouse. Respir. Physiol. Neurobiol. 162 (2), 117–125.
Yokota, S., Tsumori, T., Oka, T., Nakamura, S., Yasui, Y., 2008. GABAergic neurons in the ventrolateral subnucleus of the nucleus tractus solitarius are in contact with Kölliker-Fuse nucleus neurons projecting to the rostral ventral respiratory group and phrenic nucleus in the rat. Brain Res. 1228, 113–126.
Zanella, S., Mebarek, S., Lajard, A.M., Picard, N., Dutschmann, M., Hilaire, G., 2008. Oral treatment with desipramine improves breathing and life span in Rett syndrome mouse model. Respir. Physiol. Neurobiol. 160 (1), 116–121.

3 - Définition physiologique de l'obstruction des voies aériennes supérieures chez un modèle murin du Syndrome de Rett

Voituron N., **Menuet C.**, Dutschmann M. & Hilaire G.
Publié dans *Respiratory Physiology & Neurobiology*, en 2010.

Résumé en français :

Le Syndrome de Rett est une maladie neurodéveloppementale accompagnée de symptômes respiratoires incluant des événements de blocages de la respiration, et est causé par des mutations dans le gène du répresseur transcriptionnel methyl-CpG-binding protein 2 (MeCP2). Les souris mâles dont le gène *Mecp2* a été muté (souris *Mecp2*$^{-/y}$) développent également des symptômes respiratoires, avec un rythme respiratoire erratique et des apnées dramatiques à partir du 30^{e} jour postnatal (P30), menant à une détresse respiratoire et à une mort prématurée aux alentours de P60. Nous avons investigué la fonction respiratoire de souris *Mecp2*$^{-/y}$ conscientes à P40-P60 en utilisant la pléthysmographie corps entier conventionnelle, la pléthysmographie double chambre et des enregistrements électromyographiques (EMG) thoraciques. La pléthysmographie double chambre a révélé une augmentation persistente de la charge de travail respiratoire avec des mouvements thoraciques augmentés, mais sans augmentation consécutive du volume courant, révélant ainsi un déséquilibre entre flux aérien et travail des muscles respiratoires. Des apnées avaient lieu avec une cessation des mouvements thoraciques et de la ventilation, mais certaines (40%) se développaient avec des décharges rythmiques persistant sur l'EMG thoracique ou des mouvements thoraciques sans flux aérien respiratoire, suggérant un effort respiratoire contre des voies aériennes obstruées. L'obstruction des voies aériennes était maintenue même quand le tonus excitateur respiratoire augmentait significativement, déclenchant d'importantes décharges sur l'EMG thoracique et de grands mouvements thoraciques. La pléthysmographie corps entier des souris *Mecp2*$^{-/y}$ a révélé des augmentations significatives des spirogrammes respiratoires, reflétant les mouvements thoraciques forcés contre les voies aériennes supérieures partiellement obstruées. Les décharges persistant sur l'EMG thoracique et les mouvements thoraciques rythmiques sans flux aérien respiratoire suggèrent que l'inactivation de la protéine MeCP2 altère les circuits neuronaux qui contrôlent les muscles abducteurs des

voies aériennes supérieures. Les blocages de la respiration observés chez les souris *Mecp2*$^{-/y}$ pourraient impliquer des troubles des circuits neuronaux du contrôle volontaire de la respiration.

Author's personal copy

Respiratory Physiology & Neurobiology 173 (2010) 146–156

Contents lists available at ScienceDirect

Respiratory Physiology & Neurobiology

journal homepage: www.elsevier.com/locate/resphysiol

Physiological definition of upper airway obstructions in mouse model for Rett syndrome

Nicolas Voituron[a], Clément Menuet[a], Mathias Dutschmann[a,b], Gérard Hilaire[a,*]

[a] Mp3-Respiration Team, Centre de Recherche en Neurobiologie et Neurophysiologie de Marseille (CRN2 M), Unité Mixte de Recherche 6231, CNRS - Université Aix-Marseille II & III, Faculté Saint Jérôme, 13397 Marseille Cedex 20, France
[b] Institute of Membrane and Systems Biology Garstang Building, University of Leeds, Leeds LS2 9JT, United Kingdom

ARTICLE INFO

Article history:
Accepted 19 July 2010

Keywords:
MeCP2
Upper airway
Obstructive apnoeas
Plethysmography
EMG

ABSTRACT

Rett syndrome is a neuro-developmental disease accompanied by breathing symptoms including breath-hold events, and is caused by mutation of the transcriptional repressor methyl-CpG-binding protein 2 (MeCP2). Males of *Mecp2*-deficient mice (*Mecp2*$^{-/y}$) also develop breathing symptoms, with erratic rhythm and life-threatening apnoeas from postnatal day 30 (P30), leading to respiratory distress and premature death at around P60. We investigated the respiratory function of conscious *Mecp2*$^{-/y}$ mice at P40–P60 using conventional whole-body plethysmography, double-chamber plethysmography and chest EMG recordings. Double-chamber plethysmography revealed a persistent increase in respiratory work-load with enlarged chest movements, but no subsequent increase of tidal volume thus revealing a mismatch between airflow and muscle work-load. Apnoeas occurred with cessation of both chest movements and ventilation, but some (40%) developed with persisting rhythmic chest EMG discharges or chest movements without respiratory airflow, suggesting respiratory efforts against obstructed airways. Airway obstruction was maintained even when the respiratory drive increased significantly, triggering large chest EMG discharges and movements. Whole-body plethysmography of *Mecp2*$^{-/y}$ mice revealed significant increases of spirograms, reflecting forced chest movements against partially obstructed airways. The persisting chest EMG discharges and rhythmic chest movements without respiratory airflow suggest that Mecp2 inactivation alters neural circuits controlling the upper airway dilator muscles. The observed breath-hold events in *Mecp2*$^{-/y}$ mice might imply disturbance of neural circuits attached to voluntary control of breathing.

© 2010 Elsevier B.V. All rights reserved.

1. Introduction

Breathing is a complex motor activity essential to lung ventilation and blood oxygenation. For survival, three different neural subsystems must function appropriately: (1) the medullary respiratory rhythm generator (RRG) (Feldman and Del Negro, 2006; Onimaru and Homma, 2003; Onimaru et al., 2009; Thoby-Brisson et al., 2009) producing inspiration and expiration, (2) the ponto-medullary central pattern generator (CPG) controlling the chest and upper airway motoneurons (Abdala et al., 2009; Dutschmann and Paton, 2002a; Smith et al., 2007) and, (3) the central and peripheral regulatory loops adapting the RRG and CPG drives to varying metabolic demands and behaviour. Prior to or at birth the main respiratory circuits are functional (Hilaire and Duron, 1999), but prominent postnatal maturational processes take place only until adolescence (Dutschmann et al., 2008, 2009).

Molecular genetic approaches have identified several genes crucial for RRG prenatal maturation and neonatal function in mice (Amiel et al., 2009; Baekey et al., 2009; Gaultier and Gallego, 2008; Gray, 2008; Onimaru et al., 2009). The role of methyl-CpG-binding protein 2 gene (MeCP2) is however different: MeCP2 does not contribute to the perinatal maturation of the RRG but contributes to its function in adults. MeCP2 mutations in girls with Rett syndrome (RTT) cause severe neuro-developmental disorder accompanied by breathing symptoms (Amir et al., 1999). After a seemingly normal period of postnatal development, RTT girls start to develop neurologic symptoms, including erratic respiratory rhythm, life-threatening apnoeas and breath-holdings (Katz et al., 2009). MeCP2 inactivation in mice also induces breathing symptoms (Katz et al.,

Abbreviations: AI, apnoea index; chestV_T, tidal volume measured from pressure changes in the chest chamber of the double-chamber plethysmograph; c-OA, centrally-mediated obstructive apnoea; CPG, central pattern generator; fR, respiratory frequency; headV_T, tidal volume measured from pressure changes in the head chamber of the double-chamber plethysmograph; Mecp2, methyl-CpG-binding protein 2; RRG, respiratory rhythm generator; RTT, Rett syndrome; Ttot, total respiratory cycle duration; V_T, tidal volume; wbV_T, tidal volume measured with whole-body plethysmography; WT, wild type.

* Corresponding author at: Mp3-Respiration Team, CRN2 M, UMR 6231, CNRS - Université Aix-Marseille II & III, Faculté Saint Jérôme, Service 362, 13397 Marseille Cedex 20, France. Tel.: +33 491 288172; fax: +33 491 288397.
E-mail address: gerard.hilaire@univ-cezanne.fr (G. Hilaire).

1569-9048/$ – see front matter © 2010 Elsevier B.V. All rights reserved.
doi:10.1016/j.resp.2010.07.006

Author's personal copy

Fig. 1. Breathing of a *Mecp2*$^{-/y}$ mouse recorded with whole-body plethysmography. Raw plethysmographic traces (inspiration upward in this and all following figures) recorded in the same *Mecp2*$^{-/y}$ mouse at postnatal day 30 (P30) and P60. Note the stable and regular breathing of the young *Mecp2*$^{-/y}$ mouse at P30 (A) and the erratic breathing at P60 (B), with four successive apnoeas, the three first labelled B1, B2 and B3 being displayed at larger time scale in B1, B2 and B3. Vertical arrows in B2 and B3 indicate small rhythmic events occurring during the apnoeic periods, suggesting the RRG was still driving the CPG which failed to induce normal breathing movements. Calibration bars for wbV_T: 10 $\mu L g^{-1}$.

2009; Viemari et al., 2005). *Mecp2*-deficient male (*Mecp2*$^{-/y}$) mice breathe normally from birth to P30 although they show subtle abnormalities of post-sigh breathing (Voituron et al., 2010) and respiratory responses to environmental challenges (Voituron et al., 2009). After P30, *Mecp2*$^{-/y}$ develop marked breathing symptoms, with an erratic respiratory rhythm and life-threatening apnoeas aggravating with age until respiratory distress and death occurs at around P60 (Viemari et al., 2005). The breathing symptoms of *Mecp2*$^{-/y}$ mice are thought to reflect RRG dysfunction caused by alterations of several neurochemical systems (Ide et al., 2005; Katz et al., 2009; Medrihan et al., 2008; Viemari et al., 2005). However, *in situ* studies in *Mecp2*$^{-/y}$ mice at P45 have revealed untimely discharges of laryngeal adductor (constrictor) muscles (Stettner et al., 2007). Since laryngeal motor dysfunction can cause pathological changes in upper airways resistance, we investigated the breathing pattern of *Mecp2*$^{-/y}$ mice from P40 to P60 via simultaneous examination of chest respiratory movements, airflow and chest electromyogram (EMG). We show that Mecp2 deficiency in mice leads to upper airway obstructions potentially involving CPG dysfunction.

2. Methods

Experiments were carried out in wild type (WT) and mouse model for RTT [strain B6.129P2(C)-*Mecp2*tm1–1Bird] (The Jackson Laboratory, Bar Harbor, ME) in accordance with the European guidelines for the care and use of laboratory animals (Council Directive 86/609/EEC). Hemizygous mutant *Mecp2* male mice (*Mecp2*$^{-/y}$) (Viemari et al., 2005; Voituron et al., 2009, 2010; Zanella et al., 2008) were generated by crossing heterozygous knock-out females with C57BL/6 male mice (Guy et al., 2001) and genotyped by routine PCR technique.

The breathing of unanesthetized, unrestrained male mice was recorded using a constant flow whole-body plethysmograph (EMKA Technologies, Paris, France), with 200 ml animal chambers ventilated with air (600 ml/min). Also the breathing of pairs of WT and *Mecp2*$^{-/y}$ mice of matched ages was simultaneously recorded. Recordings were performed during the P40–P60 period when breathing symptoms in *Mecp2*$^{-/y}$ persistently occur (n = 7 WT and 7 *Mecp2*$^{-/y}$ mice). We also used a double-chamber plethysmograph to simultaneously record the chest movement and lung ventilation in restrained, unanesthetized mice during P40 to P60 period (n = 7 WT and 8 *Mecp2*$^{-/y}$). As previously reported (Dutschmann et al., 2010; Voituron et al., 2010), the double-chamber plethysmograph was built from two syringes, with a rubber piston separating the body chamber (50 ml) from the head chamber (20 ml). The piston was cut to make an adjustable neck collar, individually adapted to each mouse. The head chamber was connected to a constant flow pump for continuous flow of fresh air (200 ml/min). Double-chamber plethysmography was used to simultaneously record the

Author's personal copy

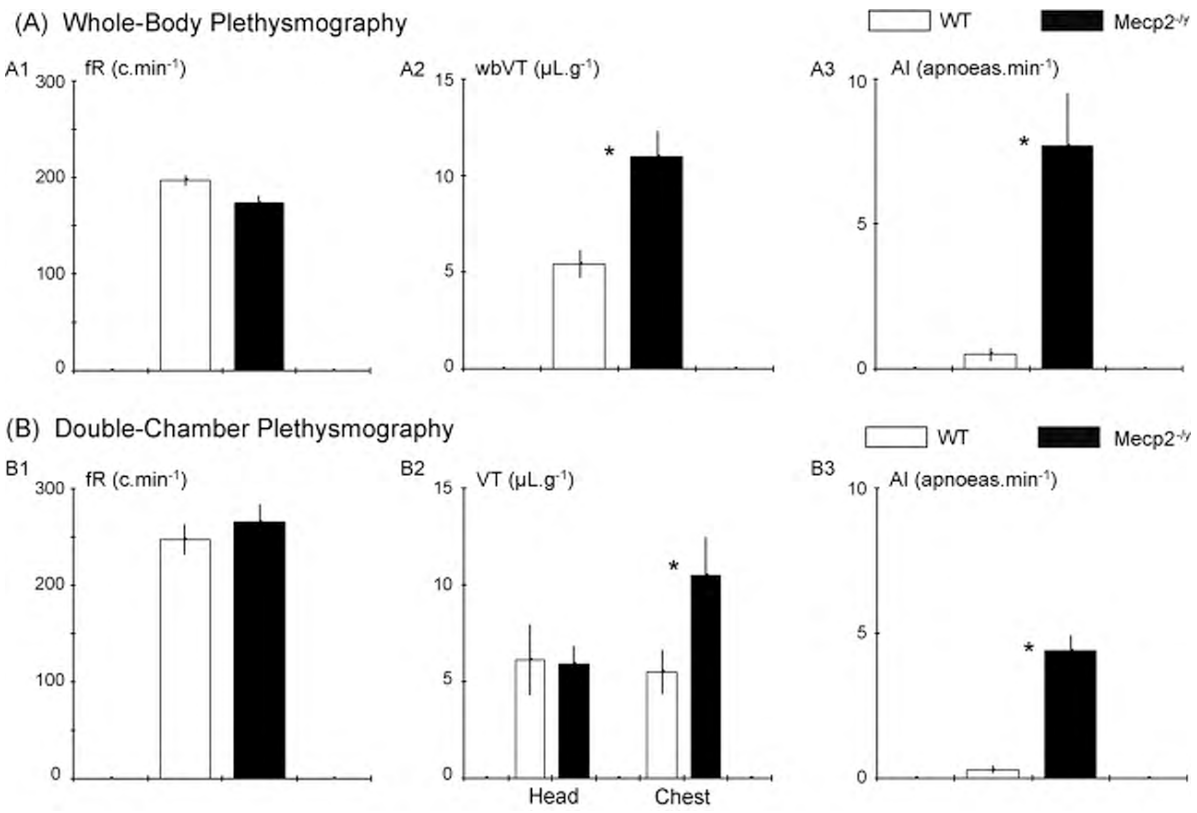

Fig. 2. Main breathing parameters recorded with whole-body plethysmography and double-plethysmography in *Mecp2*$^{-/y}$ and WT mice at P40–P60. Columns (and bars) show mean (and SEM) values for respiratory frequency (fR, in c min^{-1}), tidal volume (VT, in µL g^{-1}) and apnoea index (AI, in apnoea min^{-1}) for WT (white columns) and *Mecp2*$^{-/y}$ mice (black columns) aged P40–P60. (A) Values obtained with whole-body plethysmography show larger wbV$_T$ and AI in *Mecp2*$^{-/y}$ than WT mice. (B) Values obtained with double-plethysmography confirm larger AI in *Mecp2*$^{-/y}$ than WT mice (B3; apnoeas counted from chestV$_T$ signals) but gives larger fR values than whole-body plethysmography (B1). B2 shows mean values of headV$_T$ (two left hand columns) and chestV$_T$ (right hand columns). Mean headV$_T$ did not differ between *Mecp2*$^{-/y}$ and WT mice but mean chestV$_T$ was twice larger in *Mecp2*$^{-/y}$ than WT mice. Thus, large chest movements of *Mecp2*$^{-/y}$ mice induced an overestimate of wbV$_T$ with whole-body plethysmography. Asterisks indicate a significant difference between *Mecp2*$^{-/y}$ and WT mice.

respiratory pressure changes generated by the chest movements in the chest chamber and the resulting airflow in the head chamber. This enabled the identification of partial and/or total airway obstructions when the chest respiratory movement induced abnormally weak airflow and/or no airflow.

For whole-body and double-chamber plethysmography, chambers were maintained at 25 ± 0.5 °C, connected to reference chambers and pressure recorders (EMKA Technologies, Paris, France). Two or three days before recordings, the mice were habituated to stay in the plethysmograph chamber to reduce any stress. Spirograms were fed to an analog-to-digital converter (sampling frequency, 0.5 or 2.5 kHz), stored on a personal computer disk and analyzed via the Spike 2 interface and software (Cambridge Electronic Design, Cambridge, UK). Only periods of breathing without body movements were studied and mean respiratory frequency (fR, expressed in respiratory cycles per minute, c min^{-1}), total respiratory cycle duration (Ttot) and apnoea index (AI, number of apnoeas > two respiratory cycles per minute) were measured. The fR was measured exclusively during regular breathing periods. Apnoeas occurred during both regular and erratic breathing periods, but AI measurements were mainly undertaken during periods of erratic breathing when apnoeas were most frequent. Volume calibrations were performed (see Viemari et al., 2005; Voituron et al., 2009, 2010; Zanella et al., 2008) by injecting small amounts of air in the recording chambers (50–100 µL), enabling measurements of tidal volume (V$_T$; expressed in microliter per gram, µL g^{-1}) from spirograms of whole-body plethysmographic experiments (wbV$_T$) and from pressure changes in the chest chamber of double-chamber plethysmography experiments (chestV$_T$). Actual V$_T$ was measured from pressure changes in the head chamber of the double-chamber plethysmography experiments (headV$_T$). Large number of respiratory cycles (>100) was averaged (Spike 2 software) by using the peak of chestV$_T$ signal as trigger to build averaged curves showing the mean changes of headV$_T$ and chestV$_T$ vs. time. After averaging, the lags between chestV$_T$ and headV$_T$ averaged traces were measured at the beginning of inspiration estimated from chestV$_T$ increase and at the end of inspiration when chestV$_T$ reached its peak value. Averaged curves were expressed either as absolute values (µL g^{-1}) or as % changes of the peak to peak values (maximum–minimum). During periods of quiet breathing, the peak amplitudes of chestV$_T$ and headV$_T$ were measured on $n > 60$ respiratory cycles and Bravais–Pearson tests were performed to calculate the correlation coefficients between variables. All data (fR, Ttot, wbV$_T$, chestV$_T$, headV$_T$, etc.) were presented as mean ± standard error of the mean (SEM) and differences were considered significant when $p < 0.05$.

Six *Mecp2*$^{-/y}$ mice were deeply sedated with intraperitoneal injection of midazolam (5 mg kg^{-1}), a benzodiazepine of common clinical use for inducing sedation for short periods of time (Reves et al., 1985). Thin insulated cooper wires (100 µm diameter) were inserted in the external intercostals muscles (9th–10th spaces) and abdominal muscles (rectus abdominis). EMG signals were fed to

Author's personal copy

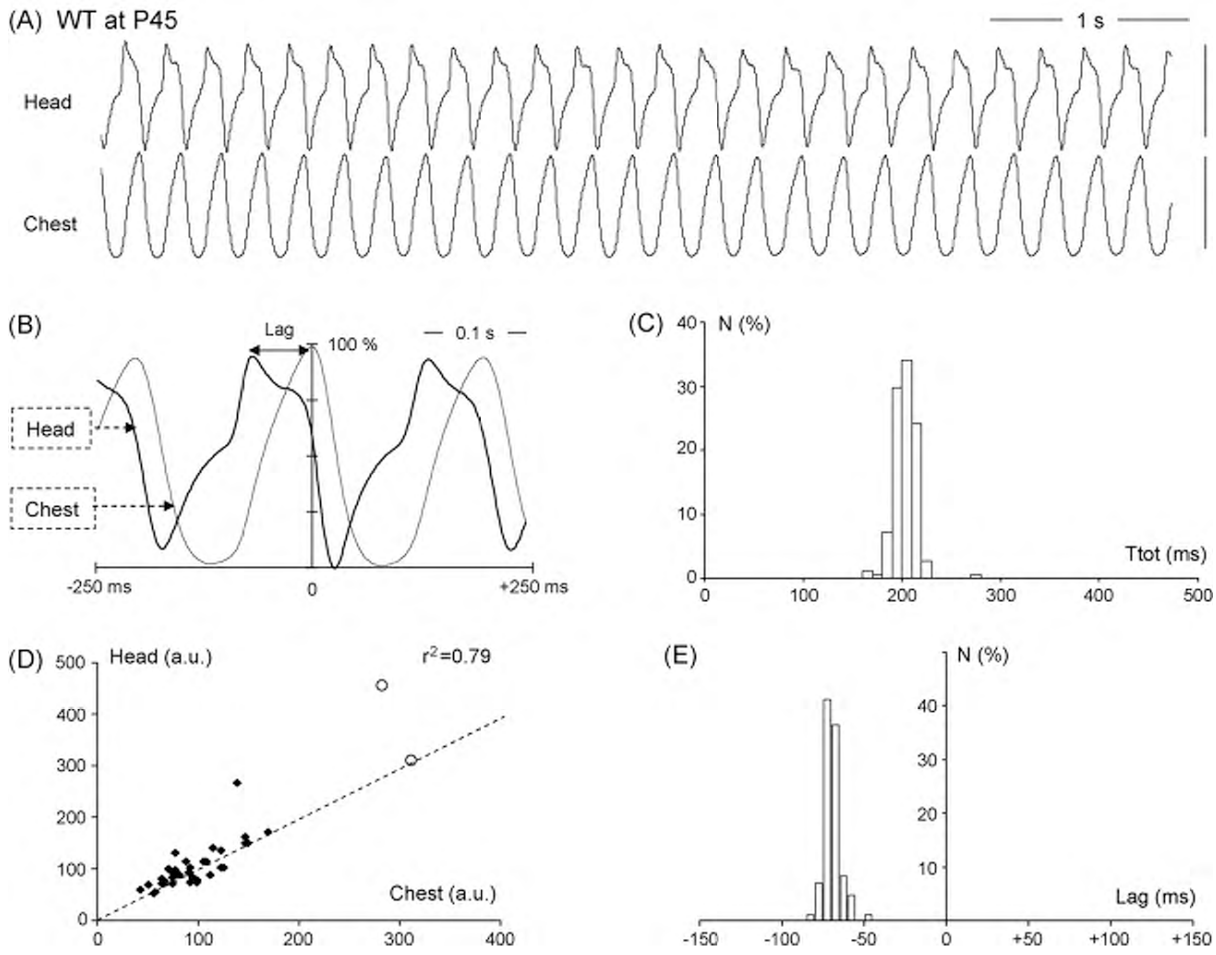

Fig. 3. Double-chamber plethysmography recordings of headV_T and chestV_T signals of WT mouse at P45. (A) Raw traces of headV_T and chestV_T signals (upper and lower traces, respectively) recorded with double-plethysmography in a P45 WT mouse (calibration bars for headV_T and chest V_T: 5 μL g^{-1}). (B) Averaged traces of head and chest signals triggered from the peak chestV_T signal; note the double head arrow indicating the mean time lag between the two peaks. Amplitudes are expressed in % of peak signals. (C) Distribution (in %) of respiratory cycle duration (Ttot) in 10 ms bins; note the tight Ttot partition. (D) Highly significant correlation between peak amplitudes expressed in arbitrary units (a.u.) of headV_T and chestV_T signals (the two open circles correspond to two sighs); the doted line indicates the line of identity for headV_T and chestV_T. (E) Frequency of occurrence (in %) of the lag (5 ms bins) measured between the peak values of head signal and chest signal (time zero in (B)); note the stability of the time lag between head vs. chest signal peaks.

filter, amplifier (Neurolog System) and integrated (time constant 100 ms). Thereafter the mice were placed in the plethysmograph and allowed to recover from sedation for about 30 min before starting the recording session.

3. Results

3.1. Breathing pattern of WT and Mecp2$^{-/y}$ mice recorded using whole-body (wb) plethysmography

Whole-body (wb) plethysmography was used to record breathing of conscious, unrestrained WT and *Mecp2*$^{-/y}$ mice aged from P40 to P60 ($n = 14$). Occasionally the same *Mecp2*$^{-/y}$ mouse was recorded twice, before (Fig. 1A) and during (Fig. 1B) the symptomatic period.

The breathing pattern of *Mecp2*$^{-/y}$ ($n = 7$) mice was significantly altered post-P40 when compared to seven WT mice (Fig. 2A). Although the mean respiratory frequency (fR) was not different between *Mecp2*$^{-/y}$ and WT mice (174 ± 7 and 197 ± 5 c min^{-1}, respectively), total cycle duration Ttot was more variable in *Mecp2*$^{-/y}$ than WT mice. As well, the apnoea index (AI, number of apnoeas per min) was significantly higher in *Mecp2*$^{-/y}$ than WT mice (7.7 ± 1.8 and 0.5 ± 0.2). In a given *Mecp2*$^{-/y}$ mouse, the tidal volume measured with whole-body plethysmography (wbV_T) was variable between individual inspirations, but the mean wbV_T was significantly larger in *Mecp2*$^{-/y}$ than WT mice (11.0 ± 1.3 and 5.4 ± 0.7 μL g^{-1}). This suggested that the CPG was generating a stronger respiratory drive in *Mecp2*$^{-/y}$ than WT mice. Most apnoeas in *Mecp2*$^{-/y}$ mice occurred with a total cessation of the respiratory signal (Fig. 1B1), suggesting RRG dysfunction. However, small and rhythmic events were occasionally observed during apnoeas (Fig. 1B2 and B3). Although rare (1–5 per 15 min), these events were found mostly in *Mecp2*$^{-/y}$ mice and revealing that weak respiratory movements could persist during some apnoeas.

3.2. Baseline breathing of WT and Mecp2$^{-/y}$ mice recorded with double-chamber plethysmography

In *Mecp2*$^{-/y}$ mice, the persistence of weak respiratory movements during some apnoeas and the large mean wbV_T were evident. We therefore used a double-plethysmography approach to simultaneously record the pressure changes induced by the

Author's personal copy

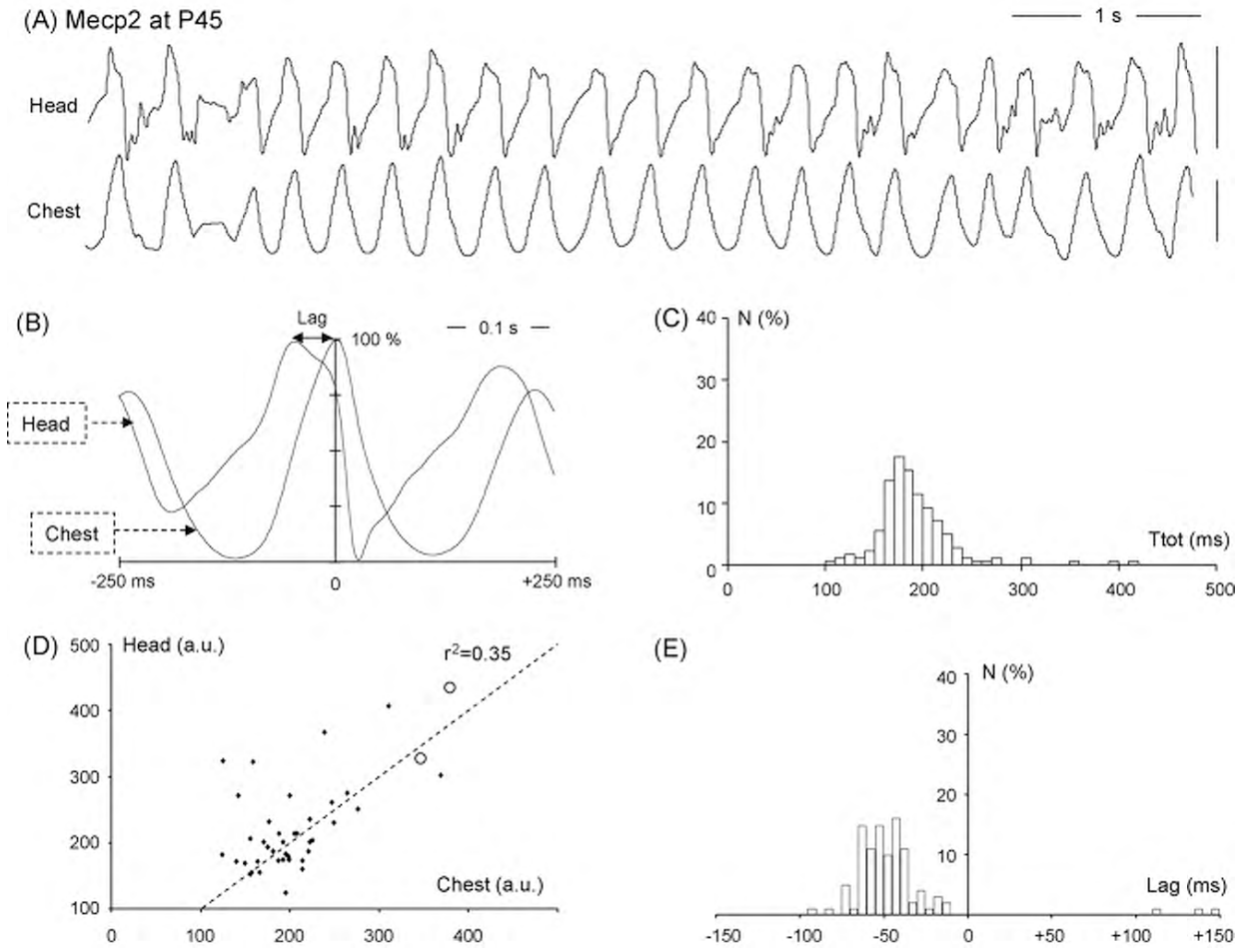

Fig. 4. Double-chamber plethysmography recordings of head and chest signals during a regular breathing period in *Mecp2*$^{-/y}$ mouse at P45. Same arrangement as in Fig. 3 but for a *Mecp2*$^{-/y}$ mouse at P45. (A) Raw traces of headV_T and chestV_T signals (upper and lower traces, respectively) recorded with double-plethysmography during a period of regular breathing in a *Mecp2*$^{-/y}$ mouse at P45 (calibration bars: 5 μL g^{-1} for head and chest signals). (B) Averaged traces of headV_T and chestV_T signals triggered from the peak chestV_T signal; note the double head arrow indicating the mean time lag between the two peaks. Amplitudes are expressed in % of signal peaks. (C) Distribution (in %) of respiratory cycle duration (Ttot) in 10 ms bins; note the variability of Ttot. (D) Correlation between peak amplitudes of headV_T and chestV_T signals (expressed in arbitrary units, a.u.; open circles, sighs); the doted line indicates the line of identity for headV_T and chestV_T. (E) Frequency of occurrence (in %) of the lag (5 ms bins) measured between the peak values of head signal and chest signal (time zero in (B)); note the variability of the lag, with a 50 ms precession of airflow peak vs. chest peak but lags could be short (10–15 ms) or long (80–90 ms).

chest respiratory movements in the chest chamber (chestV_T) and the pressure changes induced by ventilation in the head chamber (headV_T) (Dutschmann et al., 2010; Voituron et al., 2010).

With double-plethysmography (Fig. 2B), the mean fR measured in seven WT mice was significantly higher (247 ± 15 c min^{-1}) than that measured with whole-body plethysmography. Despite a 25% increase of the mean fR, WT mice retained a stable breathing pattern (Fig. 3A), a weak AI (0.3 ± 0.1) and a narrow distribution of Ttot values (Fig. 3C).

Analysis of raw (Fig. 3A) and averaged signals (Fig. 3B) showed synchronised changes in chestV_T and headV_T signals. At the beginning of inspiration, the chest inspiratory movement (detected from chestV_T) induced air inflow (detected from headV_T) with a 21 ± 4 ms delay, the chestV_T signal preceding the headV_T signal. While both signals increased during inspiration, the headV_T signal reached its maximum 46 ± 13 ms prior to the chestV_T signal (Fig. 3E). The mean values of chestV_T and headV_T peaks were not statistically different (6.1 ± 1.8 and 5.9 ± 0.9 μL g^{-1}, respectively) and thus yield a mean ratio of headV_T/chestV_T close to a value of one (1.12 ± 0.22).

With double-chamber plethysmography, *Mecp2*$^{-/y}$ mice (n = 8) showed periods of regular breathing (Fig. 4) intermingled with periods of erratic breathing with frequent apnoeas (Fig. 5). This led to a large mean value of AI (AI = 4.4 ± 0.5), not significantly different from that observed with whole-body plethysmography. During periods of regular breathing (Fig. 4A), Ttot was highly variable in *Mecp2*$^{-/y}$ mice (Fig. 4C) whereas it was stable in WT mice. The mean fR in *Mecp2*$^{-/y}$ mice (265 ± 19 c min^{-1}) was increased by 52% compared to the mean fR measured with whole-body plethysmography, an increase significantly larger than that observed in WT. No obvious differences in the shape and the time-course of headV_T and chestV_T signals between *Mecp2*$^{-/y}$ (Fig. 4B) and WT mice were seen from signal averaging. At the beginning of inspiration, chest movement induced air inflow with a 13 ± 5 ms delay. Subsequently, both signals increased, the headV_T signal reaching its maximum 21 ± 13 ms prior to the chestV_T signal (Fig. 4E). The lag between peaks of chestV_T and headV_T signals displayed a large breath to breath variability in *Mecp2*$^{-/y}$ mice (Fig. 4E) whereas it was stable in WT. However, the mean lags at the beginning of inspiration and at peak values were not significantly different between *Mecp2*$^{-/y}$ and WT mice. The major difference between *Mecp2*$^{-/y}$ and WT mice was a larger mean value of chestV_T peak in *Mecp2*$^{-/y}$ (10.5 ± 1.9 μL g^{-1}) than WT mice. Since the headV_T peak was not significantly larger in *Mecp2*$^{-/y}$ (5.9 ± 1.1 μL g^{-1}) than WT mice, the increased work of

Author's personal copy

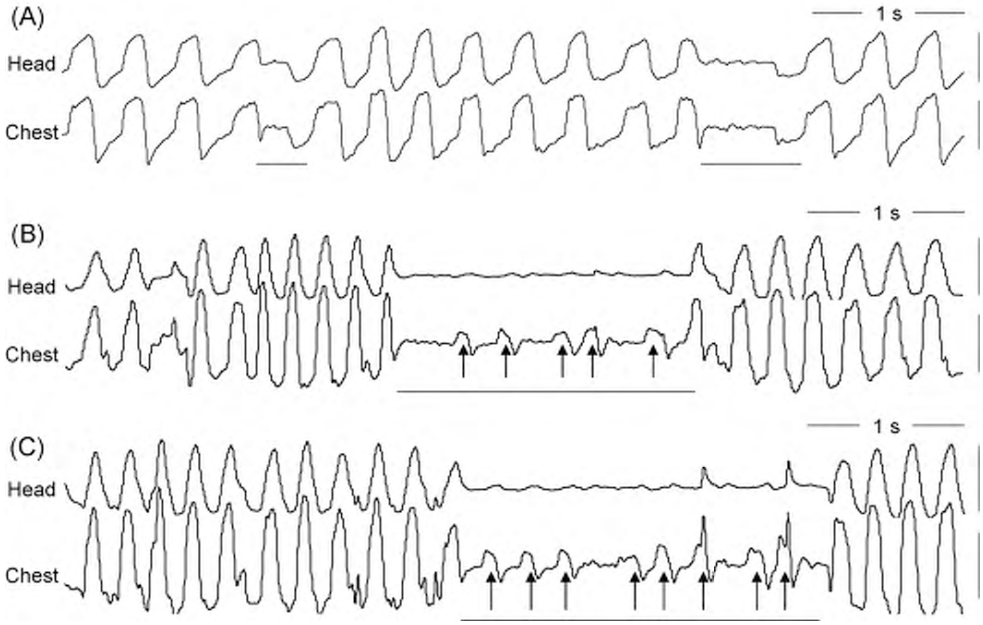

Fig. 5. Breathing and apnoeas in *Mecp2*$^{-/y}$ mice recorded with double-plethysmography. Raw traces of headV_T and chestV_T signals (upper and lower traces, respectively) recorded with double-plethysmography during periods of erratic breathing in *Mecp2*$^{-/y}$ mice (calibrations bars: 5 and 10 μL g^{-1} for headV_T and chestV_T signals, respectively). (A) Note the occurrence of two central apnoeas (horizontal line). (B and C) Show occurrence of obstructive apnoeas as attested by the lack of significant changes in headV_T signal meanwhile chest movements persisted as attested by chestV_T signals (vertical arrows). In (B), note the central apnoea that develops (no chest and head signals during >400 ms) prior to the appearance of the obstructive apnoea (no headV_T signal but persisting chest movements).

the chest pump in *Mecp2*$^{-/y}$ mice failed to produce a physiological increase in airflow. Indeed, the mean value of headV_T/chestV_T ratio was significantly lower in *Mecp2*$^{-/y}$ mice (0.57 ± 0.10) than WT mice.

3.3. Apnoeas of *Mecp2*$^{-/y}$ mice recorded with double-chamber plethysmography

During periods of erratic breathing, double-chamber plethysmography showed that *Mecp2*$^{-/y}$ mice produced two types of breathing arrest: (1) classic central apnoeas with no detectable headV_T and chestV_T signals suggesting total arrest of the RRG (Fig. 5A) and (2) possible centrally-mediated obstructive apnoeas (c-OA) with no headV_T signal but persisting rhythmic chestV_T signal (Fig. 5B and C). Central apnoeas were more frequent and shorter (about 60% and <1 s duration) than c-OA events (about 40% and >1 s duration). The c-OA with no headV_T signal but persisting rhythmic chestV_T signal were often followed by subsequent hyperventilation for a 1–2 s period, with increased fR, chestV_T and headV_T, possibly to compensate the hypoxia from the preceding apnoeic period. However, it has to be mentioned that the distinction between the two types of apnoeas was not always possible. Mixed types apnoeas were frequently observed in *Mecp2*$^{-/y}$ mice, with either central apnoeas leading to c-OA (Fig. 5B) or c-OA leading to central apnoeas (Fig. 6C). WT mice also occasionally produced a few transient apnoeas (also see Stettner et al., 2008) but these apnoeas were rare (Fig. 2B3) and of the central type, without chestVT and headV_T signals (data not shown).

Differences in post-sigh apnoea and breathing in WT and *Mecp2*$^{-/y}$ mice were previously reported (Voituron et al., 2010). In this study we confirm that sighs were followed by short-lasting post-sigh apnoeas (<1 s) in WT mice, with normal chestV_T and headV_T after breathing resumed (Fig. 6A). However in *Mecp2*$^{-/y}$ mice, sighs were followed by longer lasting post-sigh apnoeas (>1 s) and headV_T and chestV_T were of reduced amplitude when breathing resumed (triangles in Fig. 6B). In addition, post-sigh breathing activity occasionally showed c-OA, with hardly detectable headV_T despite the presence of clear chestV_T (arrows in Fig. 6C). These post-sigh c-OA were followed by a marked hyperventilation when breathing resumed.

3.4. *Mecp2*$^{-/y}$ mice exhibit chest EMG discharge during apnoeas

In order to investigate the mechanisms through which weak chestV_T were produced during c-OA periods (as attested by zeroed headV_T), six other symptomatic *Mecp2*$^{-/y}$ mice were deeply sedated with intraperitoneal injections of midazolam and were instrumented with EMG electrode implantation. As in the case of pentobarbiturates (Viemari et al., 2005), midazolam sedation transiently abolished breathing symptoms for one to 2 h, as attested by double-chamber recordings showing reduced fR (177 ± 24 c min^{-1}), stabilized Ttot and abolished apnoeas ($AI = 0.6 \pm 0.3$). However 2–3 h after sedation, breathing symptoms reappeared and four *Mecp2*$^{-/y}$ mice placed in the double-chamber plethysmography displayed a significant AI (3.3 ± 0.9). Chest EMG faithfully reflected chestV_T and headV_T signals during periods of normal breathing (Fig. 7A). However during erratic breathing periods, c-OA occurred with reduced chestV_T, hardly detectable headV_T, but persisting chest EMG with normal scope and amplitude (Fig. 7B). The same was observed during post-sigh apnoeas (Fig. 7C). During progression of c-OA, amplitude and frequency of chest EMG increased until they successfully initiated large chestV_T and significant headV_T. Thus, during c-OA periods attested by the lack of headV_T, the chest motoneurons continued to receive a central respiratory drive in *Mecp2*$^{-/y}$ mice.

Additionally, two other *Mecp2*$^{-/y}$ mice were instrumented for recording of both chest and abdominal EMGs to determine whether contractions of abdominal muscles contribute to c-OA. In these mice, the abdominal muscles remained quiescent during eupnoea as well as during short-lasting apnoeas (Fig. 8A). However, when long-lasting apnoeas developed with reduced chestV_T, no headV_T but with persisting chest EMG, the abdominal muscles

Author's personal copy

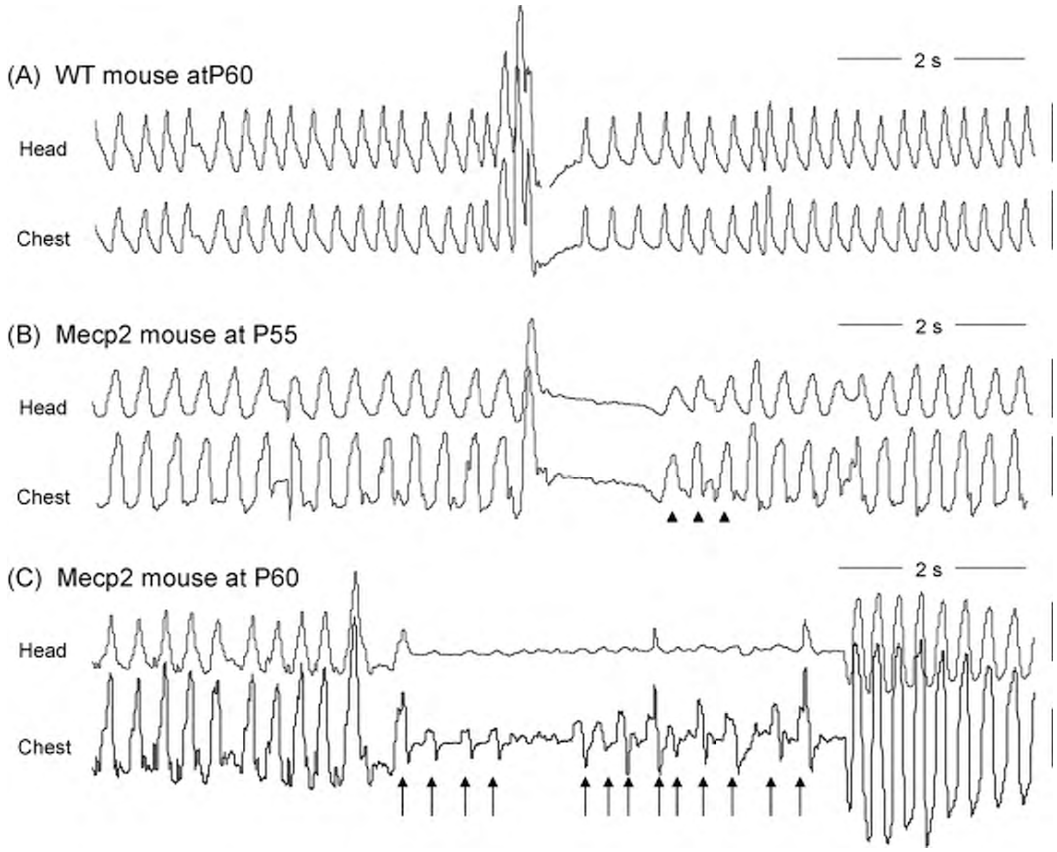

Fig. 6. Sighs recorded with double-plethysmography in *Mecp2*$^{-/y}$ and WT mice. Double-plethysmography traces show headV_T and chestV_T signals (upper and lower traces, respectively) and sighs produced by a WT mouse at P60 (A) and two *Mecp2*$^{-/y}$ mice at P55 and P60 (B and C, respectively). (A) Note the short-lasting (0.5 s) post-sigh apnoea and the normal amplitude of headV_T and chest V_T signals when breathing resumes. (B) Note the long-lasting (1.5 s) post-sigh apnoeas and the reduced headV_T and chestV_T during the first three inspirations when breathing resumes (triangles). (C) Note the long post-sigh apnoea (around 6 s) that occurred with persisting weak chestV_T signals (vertical arrows) without significant headV_T signals, the transient central apnoea (no vertical arrows) and the marked hyperventilation when breathing resumes. Calibration bars: headV_T 5 μL g^{-1} for A–C; chestV_T 5 μL g^{-1} for (A), 10 μL g^{-1} for (B and C).

were recruited at the end of the c-OA period (Fig. 8B and C). The abdominals fired tonically with reinforced discharges during expiration. Occasionally, the abdominal muscles were recruited when breathing resumed, firing during expiration (Fig. 8D). Therefore, the expiratory abdominal muscles do not initiate the c-OA period but could contribute to restore headV_T and ventilation. Lastly, we recorded chest EMG in two *Mecp2*$^{-/y}$ mice sedated with midazolam and placed in the whole-body plethysmograph in order to determine whether persistence of chest EMG without headV_T could be caused or facilitated by the neck collar and/or immobilization stress in the double-chamber plethysmography. With whole-body plethysmography, c-OA recordings were also obtained. This showed persistence of chest EMG during c-OA indicated by absence of wbV_T signals (data not shown).

4. Discussion

In *Mecp2*$^{-/y}$ mice which is a standardised mouse model for the study of RTT (Katz et al., 2009; Viemari et al., 2005), we report transient ventilatory arrests with persisting chest EMG discharge, revealing inspiratory efforts against obstructed airways. Our present *in vivo* data extend the previous *in situ* study (Stettner et al., 2007) showing that apnoeas of *Mecp2*$^{-/y}$ mice are linked to the tonic drive of laryngeal (constrictor) muscles. The occurrence of centrally-mediated obstructive apnoeas (c-OA) in symptomatic *Mecp2*$^{-/y}$ mice is fully consistent with breath-holding and frequent laryngeal and oropharyngeal problems in RTT patients (Budden et al., 1990; Morton et al., 1997a,b; Motil et al., 1999). Because c-OA and breath-holds significantly alter brain oxygenation and upper neural networks function, understanding their origin in *Mecp2*$^{-/y}$ mice is a critical step for RTT research.

4.1. Persisting airway dysfunction and transient centrally-mediated obstructive apnoeas (c-OA) in *Mecp2*$^{-/y}$ mice

During the symptomatic period, *Mecp2*$^{-/y}$ mice display regular breathing intermingled with periods of erratic breathing (Viemari et al., 2005; Voituron et al., 2009, 2010; Katz et al., 2009). During regular breathing periods, the ratio headV_T/chestV_T is halved in *Mecp2*$^{-/y}$ compared to WT mice. Large but inefficient chest movements in *Mecp2*$^{-/y}$ mice support the possibility of dysfunctional upper airways causing increased respiratory work during ventilation. The work-load and metabolic demands of such abnormal breathing is high, which might contribute to the weight loss of *Mecp2*$^{-/y}$ mice seen during ageing. During erratic breathing periods, double-chamber plethysmography shows transient arrest of ventilation with persisting chest EMG discharges, revealing c-OA in symptomatic *Mecp2*$^{-/y}$ mice. With whole-body plethysmography, such c-OA also occurred (Fig. 1B2 and B3 in the present report and Fig. 1 in Ogier and Katz, 2008) but could be classified as central apnoeas caused by RRG arrest. The c-OA commonly ends with a period of hyperventilation, increased fR and V_T, suggesting that res-

Author's personal copy

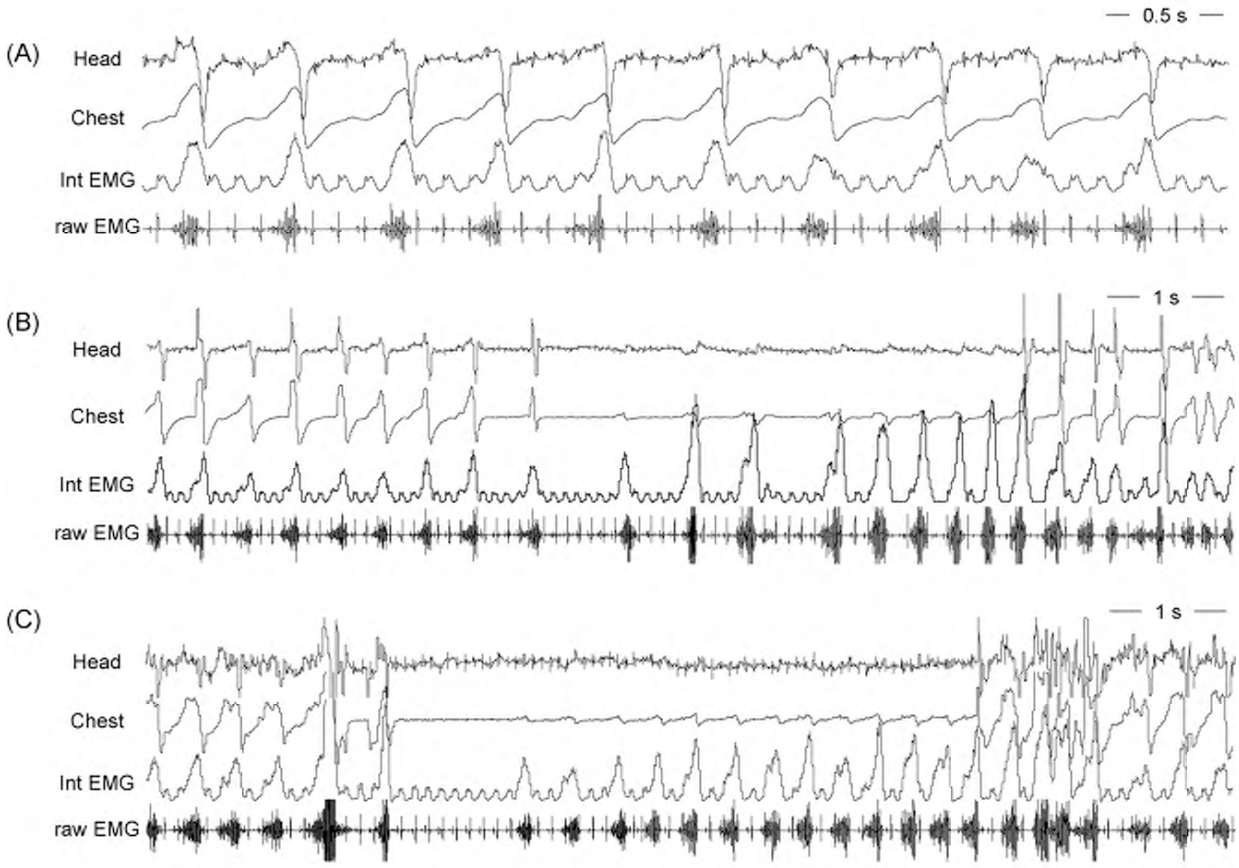

Fig. 7. Chest EMG discharges persisted during apnoeas in *Mecp2*$^{-/y}$ mouse at P55. Traces show head signal, chest signal, integrated and raw chest EMG discharges (from top to bottom) in a *Mecp2*$^{-/y}$ mouse at P55 during periods of stable (A) and erratic (B and C) breathing. (B and C) Long-lasting apnoeas during periods of erratic breathing occurred without significant headV_T signal (no ventilation) but weak chestV_T signals and maintained EMG discharges (note the amplitude of the integrated EMG). Apnoeas occurred without (B) and with (C) preceding sigh, respectively. In both (A) and (B), note the amplitudes of EMG discharges increased during apnoea until they became strong enough to restore ventilation.

piratory compensation for c-OA contributes to the highly variable breathing of *Mecp2*$^{-/y}$ mice. With whole-body plethysmography, such hyperventilations could also be attributed to RRG dysfunction. Compared to central apnoeas caused by RRG arrests, c-OAs are more damaging since the oxygen-consuming contractions of respiratory muscles trigger a rapid onset of asphyxia. In *Mecp2*$^{-/y}$ mice, c-OA occurred after normal breaths and after sighs. We have previously reported that the post-sigh apnoeas of *Mecp2*$^{-/y}$ mice are of long duration and followed by marked reduction of V_T when breathing resumes (Voituron et al., 2010). We now show strong chest EMG discharges during the post-sigh period occurring prior to the start of ventilation when breathing resumes. Thus it is clear that the long-lasting post-sigh apnoeas of *Mecp2*$^{-/y}$ mice are not caused by long-lasting arrests of the RRG but are due to CPG dysfunction.

4.2. Origins of centrally-mediated obstructive apnoeas in *Mecp2*$^{-/y}$ mice

To understand the origins of c-OA it is important to understand that breathing requires the co-ordinated contractions of two functionally different motor systems. Spinal motoneurons innervate the diaphragm and the chest wall muscles and the combined contractions of these muscles during inspiration produce airflow into the lungs while cranial motor neurons innervate the laryngeal and pharyngeal systems to control and adjust airflow. During inspiration, the co-activation of laryngeal and pharyngeal abductors (dilators) decreases upper airway resistance to support inhalation. During post-inspiration, the antagonistic laryngeal and pharyngeal adductors (constrictors) are activated and counteract recoil of the inflated lung, controlling strength and duration of expiratory airflow (Morschel and Dutschmann, 2009). The laryngo-pharyngeal motoneurons are multi-functional neurons contributing to eupnoeic breathing (expiratory airflow breaking), coughing, sneezing and respiratory-related upper airway behaviours underlying vocalization or swallowing (see Bianchi and Gestreau, 2009; Shiba et al., 1999). The pontine Kolliker-Fuse (KF) nucleus controls and gates the post-inspiratory laryngeal and pharyngeal adductor activity and plays a crucial role in coordinating the activity of motoneurons innervating the upper airway valve and chest wall. Importantly, a hyperexcitablility of KF neurons was detected in *Mecp2*$^{-/y}$ mice after the onset of severe breathing disorders (Stettner et al., 2007).

In previous studies, we discussed potential deficits or synaptic instability of the RRG of *Mecp2*$^{-/y}$ mice causing erratic respiratory rhythm (Viemari et al., 2005; Voituron et al., 2009, 2010). However, our current results provide a different picture suggesting that a large proportion of the apnoeas are not central apnoeas associated with arrest of the RRG. The occurrence of c-OAs shows the dysfunction of the CPG to co-ordinate and to modulate the diaphragm/chest wall and upper airway circuits in the *Mecp2*$^{-/y}$ mice. This fully supports the hypothesis of potential hyper-excitability within sensory

Author's personal copy

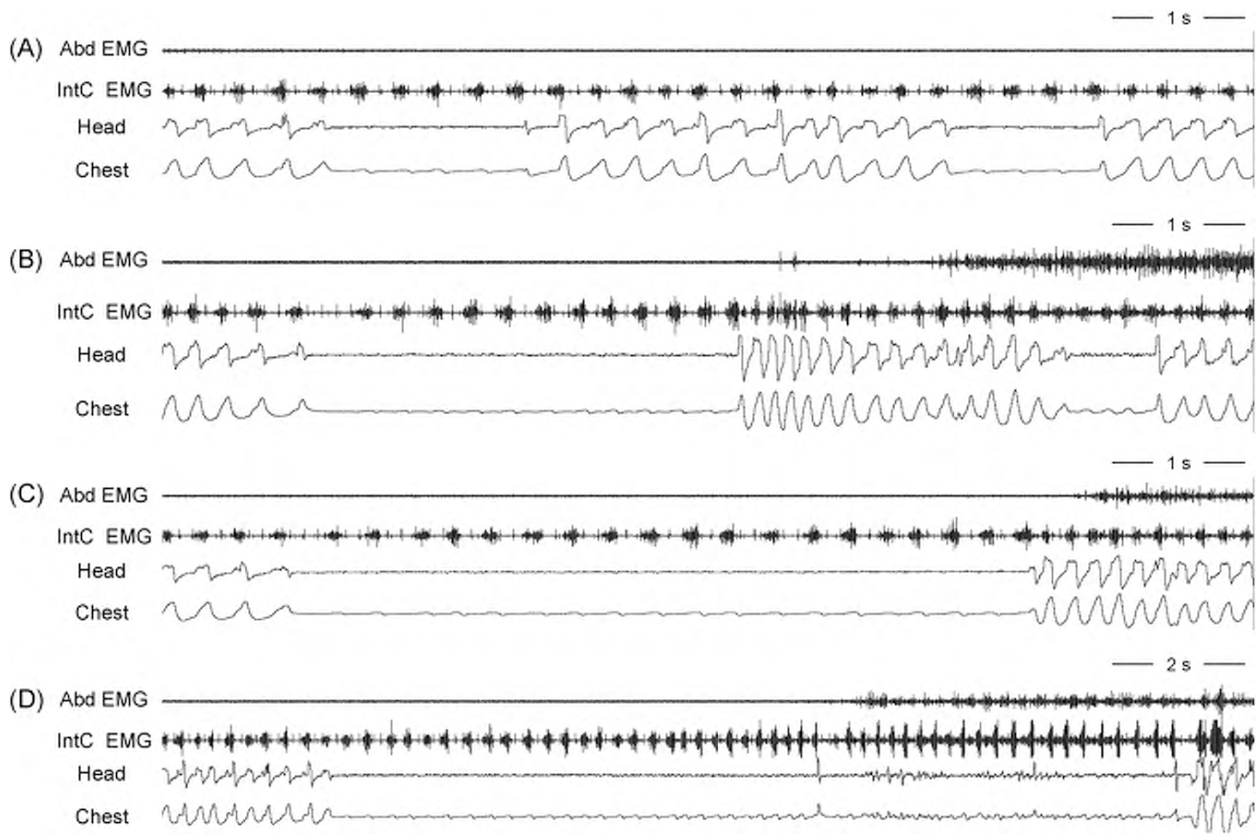

Fig. 8. Abdominal EMG discharges did not contribute to apnoeas in *Mecp2*$^{-/y}$ mouse at P45. Traces show abdominal EMG, chest EMG, headV_T and chestV_T (from top to bottom) in a *Mecp2*$^{-/y}$ mouse at P45. (A) Traces show two short-lasting apnoeas (1.3 and 1 s) with total arrest of ventilation (no headV_T signal), weak chestV_T signals but sustained EMG discharges. Note the silence of the abdominal muscle while the intercostal muscle was active during inspiration. (B–D) Show three long-lasting apnoeas (3, 5 and 12 s, respectively) without headV_T signal, but weak chestV_T signals and sustained EMG discharges. During apnoeas, the intercostal inspiratory discharges progressively increased until they became potent to restore significant headV_T signal with subsequent hyperventilation. Note that abdominal expiratory discharges were recruited either after (B and C) or at the end (D) of apnoeas.

relays and the KF (Stettner et al., 2007). The observed chest EMG discharge against obstructed airways is similar to what occurs during breath-hold diving (Angell-James et al., 1981; Dutschmann and Paton, 2002b). The diving apnoea is mediated within the KF and is modified by emotions (e.g. fear) or anticipation (Butler and Jones, 1997; McCulloch et al., 2010). This also raises the possibility of conscious control upper airway protective reflexes. The marked increase of fR in immobilized *Mecp2*$^{-/y}$ mice within the double-chamber plethysmography supports the view of strong emotional component impinging on breathing disorders in RTT. Since the CPGs are under permanent influence from the limbic system (Holstege et al., 1996), disturbances of these synaptic inputs may substantially contribute to breathing disorders.

4.3. Alteration of neurotransmitter systems linked to apnoeas in *Mecp2*$^{-/y}$ mice

Several neurochemical systems are altered in Mecp2 knock-out mice and RTT patients (Adachi et al., 2009; Ogier and Katz, 2008; Roux et al., 2009; Taneja et al., 2009; Viemari et al., 2005; Wu and Camarena, 2009). The GABAergic neurotransmission is amongst the first to be altered (Katz et al., 2009; Medrihan et al., 2008). As GABA inhibition contributes to the generation of the respiratory rhythm (Smith et al., 2009) and also shapes expiratory laryngeal discharge (Sun et al., 2008), GABA deficits in *Mecp2*$^{-/y}$ mice could affect both the RRG and CPG (Voituron et al., 2010). GABAergic neurotransmission is enhanced by benzodiazepine. Thus benzodiazepine treatment (present results) or GABA re-uptake inhibition (Abdala et al., 2010) could alleviate breathing symptoms and abolish c-OA of *Mecp2*$^{-/y}$ mice as evidenced by the case report of 6-year-old RTT patient treated with benzodiazepine (Kurihara et al., 2001).

4.4. Technical limitations

The use of whole-body plethysmography and double-chamber plethysmography both confirmed highly variable Ttot and frequent apnoeas in symptomatic *Mecp2*$^{-/y}$ mice. However, we measured abnormally large wbV_T in whole-body plethysmography. Whole-body plethysmography is a convenient method to measure the fR but not to measure the actual V_T since it measures the respiratory pressure changes caused by both airflow and chest movements. When airways and lung mechanics function correctly, whole-body plethysmography retrieves valid V_T values. However, as demonstrated in the present study in the case of airways obstruction, the animals increase their chest movements to compensate the high resistance of airway and whole-body plethysmography indicates a V_T increase but this increase in wbV_T only reflects increase of chest movements as confirmed by measurements of chestV_T and headV_T with double-chamber plethysmography.

Double-chamber plethysmography requires mouse immobilization and the stressful situation arising out of immobilization affects breathing behaviour. This leads to higher fR in immobilized mice in the double-chamber plethysmograph as compared to freely moving mice in the whole-body plethysmograph (Dutschmann et

Author's personal copy

al., 2010). The fR increase is two-fold higher in *Mecp2*$^{-/y}$ than WT immobilized mice, suggesting a generally high susceptibility to stress of *Mecp2*$^{-/y}$ mice (Fyffe et al., 2008; McGill et al., 2006; Perry et al., 1992). However, the immobilization stress is not the prime trigger for c-OA in *Mecp2*$^{-/y}$ mice. Firstly, c-OAs were recorded with whole-body plethysmography in freely moving mice. Secondly, rhythmic chest EMG discharges persisting during periods without ventilation were recorded in sedated *Mecp2*$^{-/y}$ mice placed either in whole-body or double-chamber plethysmographs. Thus, we have used whole-body plethysmography and double-chamber plethysmography as complementary approaches in order to lower methodological limitations. We have also used chest EMG recordings in combination with plethysmography to provide a satisfactory phenotyping of breathing activity of transgenic mice which are suspicious of respiratory disorders.

To conclude, the present study in symptomatic *Mecp2*$^{-/y}$ mice shows the occurrence centrally–mediated obstructive apnoeas, revealing that MeCP2 inactivation in mice alters not only the RRG but also the CPG. Indeed, the understanding of the complex breathing symptoms of RTT requires a strong integrative and collaborative research implicating different and complementary approaches.

Acknowledgments

The authors acknowledge the supports from the IRSF (NV 2008-2009 fellowship), NIH (MD), CNRS and Aix-Marseille University (mp3-respiration team) and the helpful scientific and editorial suggestions of Dr. Hari Subramanian.

References

Abdala, A.P., Dutschmann, M., Bissonnette, J.M., Paton, J.F., 2010. Suppression of expiratory activity in a mouse model of Rett syndrome follows blockade of GABA reuptake and activation of serotonin type 1a receptors. FASEB J. 24, 613.9.

Abdala, A.P., Rybak, I.A., Smith, J.C., Zoccal, D.B., Machado, B.H., St-John, W.M., Paton, J.F., 2009. Multiple pontomedullary mechanisms of respiratory rhythmogenesis. Respir. Physiol. Neurobiol. 168, 19–25.

Adachi, M., Autry, A.E., Covington 3rd, H.E., Monteggia, L.M., 2009. MeCP2-mediated transcription repression in the basolateral amygdala may underlie heightened anxiety in a mouse model of Rett syndrome. J. Neurosci. 29, 4218–4227.

Amiel, J., Dubreuil, V., Ramanantsoa, N., Fortin, G., Gallego, J., Brunet, J.F., Goridis, C., 2009. PHOX2B in respiratory control: lessons from congenital central hypoventilation syndrome and its mouse models. Respir. Physiol. Neurobiol. 168, 125–132.

Amir, R.E., Van den Veyver, I.B., Wan, M., Tran, C.Q., Francke, U., Zoghbi, H.Y., 1999. Rett syndrome is caused by mutations in X-linked MECP2, encoding methyl-CpG-binding protein 2. Nat. Genet. 23, 185–188.

Angell-James, J.E., Elsner, R., De Burgh Daly, M., 1981. Lung inflation: effects on heart rate, respiration, and vagal afferent activity in seals. Am. J. Physiol. 240, H190–H198.

Baekey, D.M., Feng, P., Decker, M.J., Strohl, K.P., 2009. Breathing and sleep: measurement methods, genetic influences, and developmental impacts. ILAR J. 50, 248–261.

Bianchi, A.L., Gestreau, C., 2009. The brainstem respiratory network: an overview of a half century of research. Respir. Physiol. Neurobiol. 168, 4–12.

Budden, S., Meek, M., Henighan, C., 1990. Communication and oral-motor function in Rett syndrome. Dev. Med. Child Neurol. 32, 51–55.

Butler, P.J., Jones, D.R., 1997. Physiology of diving of birds and mammals. Physiol. Rev. 77, 837–899.

Dutschmann, M., Paton, J.F., 2002a. Inhibitory synaptic mechanisms regulating upper airway patency. Respir. Physiol. Neurobiol. 131, 57–63.

Dutschmann, M., Paton, J.F., 2002b. Influence of nasotrigeminal afferents on medullary respiratory neurones and upper airway patency in the rat. Pflugers Arch. 444, 227–235.

Dutschmann, M., Morschel, M., Reuter, J., Zhang, W., Gestreau, C., Stettner, G.M., Kron, M., 2008. Postnatal emergence of synaptic plasticity associated with dynamic adaptation of the respiratory motor pattern. Respir. Physiol. Neurobiol. 164, 72–79.

Dutschmann, M., Morschel, M., Rybak, I.A., Dick, T.E., 2009. Learning to breathe: control of the inspiratory-expiratory phase transition shifts from sensory- to central-dominated during postnatal development in rats. J. Physiol. 587, 4931–4948.

Dutschmann, M., Menuet, C., Stettner, G.M., Gestreau, C., Borghgraef, P., Devijver, H., Gielis, L., Hilaire, G., Van Leuven, F., 2010. Upper airway dysfunction of Tau-P301L mice correlates with tauopathy in midbrain and ponto-medullary brainstem nuclei. J. Neurosci. 30, 1810–1821.

Feldman, J.L., Del Negro, C.A., 2006. Looking for inspiration: new perspectives on respiratory rhythm. Nat. Rev. Neurosci. 7, 232–242.

Fyffe, S.L., Neul, J.L., Samaco, R.C., Chao, H.T., Ben-Shachar, S., Moretti, P., McGill, B.E., Goulding, E.H., Sullivan, E., Tecott, L.H., Zoghbi, H.Y., 2008. Deletion of Mecp2 in Sim1-expressing neurons reveals a critical role for MeCP2 in feeding behavior, aggression, and the response to stress. Neuron 59, 947–958.

Gaultier, C., Gallego, J., 2008. Neural control of breathing: insights from genetic mouse models. J. Appl. Physiol. 104, 1522–1530.

Gray, P.A., 2008. Transcription factors and the genetic organization of brain stem respiratory neurons. J. Appl. Physiol. 104, 1513–1521.

Guy, J., Hendrich, B., Holmes, M., Martin, J.E., Bird, A., 2001. A mouse Mecp2-null mutation causes neurological symptoms that mimic Rett syndrome. Nat. Genet. 27, 322–326.

Hilaire, G., Duron, B., 1999. Maturation of the mammalian respiratory system. Physiol. Rev. 79, 325–360.

Holstege, G., Bandler, R., Saper, C.B., 1996. The emotional motor system. Prog. Brain Res. 107, 3–6.

Ide, S., Itoh, M., Goto, Y., 2005. Defect in normal developmental increase of the brain biogenic amine concentrations in the mecp2-null mouse. Neurosci. Lett. 386, 14–17.

Katz, D.M., Dutschmann, M., Ramirez, J.M., Hilaire, G., 2009. Breathing disorders in Rett syndrome: progressive neurochemical dysfunction in the respiratory network after birth. Respir. Physiol. Neurobiol. 168, 101–108.

Kurihara, M., Kumagai, K., Nakae, Y., 2001. Effect of diazepam on apnea attacks in a 6-year-old girl with Rett syndrome: a polysomnographic study. No To Hattatsu 33, 58–62.

McCulloch, P.F., Dinovo, K.M., Connolly, T.M., 2010. The cardiovascular and endocrine responses to voluntary and forced diving in trained and untrained rats. Am. J. Physiol. Regul. Integr. Comp. Physiol. 298, R224–R234.

McGill, B.E., Bundle, S.F., Yaylaoglu, M.B., Carson, J.P., Thaller, C., Zoghbi, H.Y., 2006. Enhanced anxiety and stress-induced corticosterone release are associated with increased Crh expression in a mouse model of Rett syndrome. Proc. Natl. Acad. Sci. U.S.A. 103, 18267–18272.

Medrihan, L., Tantalaki, E., Aramuni, G., Sargsyan, V., Dudanova, I., Missler, M., Zhang, W., 2008. Early defects of GABAergic synapses in the brain stem of a MeCP2 mouse model of Rett syndrome. J. Neurophysiol. 99, 112–121.

Morschel, M., Dutschmann, M., 2009. Pontine respiratory activity involved in inspiratory/expiratory phase transition. Philos. Trans. R. Soc. Lond. B: Biol. Sci. 364, 2517–2526.

Morton, R.E., Bonas, R., Minford, J., Kerr, A., Ellis, R.E., 1997a. Feeding ability in Rett syndrome. Dev. Med. Child Neurol. 39, 331–335.

Morton, R.E., Bonas, R., Minford, J., Tarrant, S.C., Ellis, R.E., 1997b. Respiration patterns during feeding in Rett syndrome. Dev. Med. Child Neurol. 39, 607–613.

Motil, K.J., Schultz, R.J., Browning, K., Trautwein, L., Glaze, D.G., 1999. Oropharyngeal dysfunction and gastroesophageal dysmotility are present in girls and women with Rett syndrome. J. Pediatr. Gastroenterol. Nutr. 29, 31–37.

Ogier, M., Katz, D.M., 2008. Breathing dysfunction in Rett syndrome: understanding epigenetic regulation of the respiratory network. Respir. Physiol. Neurobiol. 164, 55–63.

Onimaru, H., Homma, I., 2003. A novel functional neuron group for respiratory rhythm generation in the ventral medulla. J. Neurosci. 23, 1478–1486.

Onimaru, H., Ikeda, K., Kawakami, K., 2009. Phox2b, RTN/pFRG neurons and respiratory rhythmogenesis. Respir. Physiol. Neurobiol. 168, 13–18.

Perry, A., Sarlo-McGarvey, N., Factor, D.C., 1992. Stress and family functioning in parents of girls with Rett syndrome. J. Autism Dev. Disord. 22, 235–248.

Reves, J.G., Fragen, R.J., Vinik, H.R., Greenblatt, D.J., 1985. Midazolam: pharmacology and uses. Anesthesiology 62, 310–324.

Roux, J.C., Panayotis, N., Dura, E., Villard, L., 2009. Progressive noradrenergic deficits in the locus coeruleus of Mecp2 deficient mice. J. Neurosci. Res..

Shiba, K., Satoh, I., Kobayashi, N., Hayashi, F., 1999. Multifunctional laryngeal motoneurons: an intracellular study in the cat. J. Neurosci. 19, 2717–2727.

Smith, J.C., Abdala, A.P., Koizumi, H., Rybak, I.A., Paton, J.F., 2007. Spatial and functional architecture of the mammalian brain stem respiratory network: a hierarchy of three oscillatory mechanisms. J. Neurophysiol. 98, 3370–3387.

Smith, J.C., Abdala, A.P., Rybak, I.A., Paton, J.F., 2009. Structural and functional architecture of respiratory networks in the mammalian brainstem. Philos. Trans. R. Soc. Lond. B: Biol. Sci. 364, 2577–2587.

Stettner, G.M., Huppke, P., Brendel, C., Richter, D.W., Gartner, J., Dutschmann, M., 2007. Breathing dysfunctions associated with impaired control of postinspiratory activity in *Mecp2*$^{-/y}$ knockout mice. J. Physiol. 579, 863–876.

Stettner, G.M., Zanella, S., Huppke, P., Gartner, J., Hilaire, G., Dutschmann, M., 2008. Spontaneous central apneas occur in the C57BL/6J mouse strain. Respir. Physiol. Neurobiol. 160, 21–27.

Sun, Q.J., Berkowitz, R.G., Pilowsky, P.M., 2008. GABA A mediated inhibition and post-inspiratory pattern of laryngeal constrictor motoneurons in rat. Respir. Physiol. Neurobiol. 162, 41–47.

Taneja, P., Ogier, M., Brooks-Harris, G., Schmid, D.A., Katz, D.M., Nelson, S.B., 2009. Pathophysiology of locus ceruleus neurons in a mouse model of Rett syndrome. J. Neurosci. 29, 12187–12195.

Thoby-Brisson, M., Karlen, M., Wu, N., Charnay, P., Champagnat, J., Fortin, G., 2009. Genetic identification of an embryonic parafacial oscillator coupling to the pre-Botzinger complex. Nat. Neurosci. 12, 1028–1035.

Viemari, J.C., Roux, J.C., Tryba, A.K., Saywell, V., Burnet, H., Pena, F., Zanella, S., Bevengut, M., Barthelemy-Requin, M., Herzing, L.B., Moncla, A., Mancini, J., Ramirez, J.M., Villard, L., Hilaire, G., 2005. Mecp2 deficiency disrupts norepinephrine and respiratory systems in mice. J. Neurosci. 25, 11521–11530.

Author's personal copy

Voituron, N., Zanella, S., Menuet, C., Dutschmann, M., Hilaire, G., 2009. Early breathing defects after moderate hypoxia or hypercapnia in a mouse model of Rett syndrome. Respir. Physiol. Neurobiol. 168, 109–118.
Voituron, N., Zanella, S., Menuet, C., Lajard, A.M., Dutschmann, M., Hilaire, G., 2010. Early abnormalities of post-sigh breathing in a mouse model of Rett syndrome. Respir. Physiol. Neurobiol. 170, 173–182.
Wu, S.H., Camarena, V., 2009. MeCP2 function in the basolateral amygdala in Rett syndrome. J. Neurosci. 29, 9941–9942.
Zanella, S., Mebarek, S., Lajard, A.M., Picard, N., Dutschmann, M., Hilaire, G., 2008. Oral treatment with desipramine improves breathing and life span in Rett syndrome mouse model. Respir. Physiol. Neurobiol. 160, 116–121.

II - Etudes des régulations respiratoires induites par le CO_2 et la sérotonine

Dans ce chapitre sont présentées des études dans lesquelles nous nous sommes intéressés aux régulations respiratoires, et en particulier au principal tonus excitateur de la respiration, le CO_2, aux composés pharmacologiques qui modifient la réponse ventilatoire à l'hypercapnie (RVHC) comme la sérotonine et l'érythropoïétine (EPO), et au rôle de la sérotonine pour la fonction et la dysfonction respiratoires, notamment au cours du vieillissement. Nous montrons que deux souches de souris sauvages très utilisées pour la transgénèse, les souris C57Bl/6J et les souris FVB/N, présentent des différences respiratoires tout au long de la vie avec une fragilité respiratoire chez les souris C57Bl/6J et à l'inverse une robustesse respiratoire chez les souris FVB/N, et que ces différences phénotypiques peuvent être expliquées par des différences du métabolisme sérotoninergique (1). Ensuite, nous avons effectué une revue de questions concernant le rôle de la sérotonine pour la fonction respiratoire et pour les pathologies qui y sont associées (2). Dans l'article suivant, nous présentons des résultats obtenus chez la souris nouveau-née *in vitro*, chez qui la fluoxétine, un inhibiteur de la recapture de la sérotonine présent dans les antidépresseurs comme le Prozac, annule la réponse respiratoire à l'acidose (3). Enfin, nous montrons chez des souris transgéniques et sauvages que la surexpression d'EPO diminue la RVHC par une action directe à la fois au niveau périphérique et au niveau central, et par une action indirecte *via* l'érythropoïèse (4).

1 - Les différences de métabolisme sérotoninergique contribuent potentiellement aux différences de phénotype respiratoire des souris FVB/N et C57Bl/6J

Menuet C., Kourdougli N., Hilaire G. & Voituron N.
Publié dans *The Journal of Applied Physiology*, en 2011.

Résumé en français :

La propension des souris pour la manipulation génétique a permis la production de souris mutantes avec des défauts respiratoires similaires à ceux provoqués par divers syndromes respiratoires. Comme les souches de souris C57Bl/6J et FVB/N sont souvent utilisées comme fonds génétiques pour la production de souris transgéniques, nous avons comparé leurs activités respiratoires à partir de la naissance. A la naissance, des approches *in vivo* et *in vitro* ont révélé un rythme respiratoire robuste chez les souris FVB/N, mais pas chez les souris C57Bl/6J. Avec l'âge, cette différence de robustesse du rythme respiratoire a persisté, et des différences ont été observées entre les souches de souris en volume courant, débit ventilatoire, régulations respiratoires, et paramètres des gaz du sang. Comme la sérotonine affecte la maturation et la fonction du réseau respiratoire dans le tronc cérébral, nous avons examiné le métabolisme sérotoninergique dans le tronc cérébral des souris nouveau-nées et âgées C57Bl/6J et FVB/N. Des différences du métabolisme sérotoninergique entre ces deux souches de souris ont été observées aux deux âges testés. Nous en concluons que des différences de métabolisme sérotoninergique peuvent potentiellement contribuer aux différences de phénotype respiratoire des souris FVB/N et C57Bl/6J.

J Appl Physiol 110: 1572–1581, 2011.
First published March 17, 2011; doi:10.1152/japplphysiol.00117.2011.

Differences in serotoninergic metabolism possibly contribute to differences in breathing phenotype of FVB/N and C57BL/6J mice

Clément Menuet, Nazim Kourdougli, Gérard Hilaire, and Nicolas Voituron

Centre de Recherche en Neurobiologie, Neurophysiologie de Marseille, UMR 6231 Centre National de la Recherche Scientifique, MP3-Respiration Team, Faculté des Sciences et Techniques Saint Jérôme, Université Aix-Marseille II et III, Marseille, France

Submitted 27 January 2011; accepted in final form 15 March 2011

Menuet C, Kourdougli N, Hilaire G, Voituron N. Differences in serotoninergic metabolism possibly contribute to differences in breathing phenotype of FVB/N and C57BL/6J mice. *J Appl Physiol* 110: 1572–1581, 2011. First published March 17, 2011; doi:10.1152/japplphysiol.00117.2011.—Mouse readiness for gene manipulation allowed the production of mutants with breathing defects reminiscent of breathing syndromes. As C57BL/6J and FVB/N inbred strains were often used as background strains for producing mutants, we compared their breathing pattern from birth onwards. At birth, in vivo and in vitro approaches revealed robust respiratory rhythm in FVB/N, but not C57BL/6J, neonates. With aging, rhythm robustness difference persisted, and interstrain differences in tidal volume, minute ventilation, breathing regulations, and blood-gas parameters were observed. As serotonin affected maturation and function of the medullary respiratory network, we examined the serotoninergic metabolism in the medulla of C57BL/6J and FVB/N neonates and aged mice. Interstrain differences in serotoninergic metabolism were observed at both ages. We conclude that differences in serotoninergic metabolism possibly contribute to differences in breathing phenotype of FVB/N and C57BL/6J mice.

maturation; background strain; transgenic mice; respiratory rhythmogenesis; respiratory regulations

FROM BIRTH ONWARDS, THE NEONATAL mammal must be able to breath and adapt its breathing to behavior and environment, which requires correct function and regulations of the medullary respiratory rhythm generator (RRG). In infants, RRG dysfunctions contribute to distinct syndromes, such as congenital central hypoventilation syndrome (2), sudden infant death syndrome (38), Prader-Willi syndrome (63), and Rett syndrome (30). In aged persons, sleep-disordered breathing and upper airway dysfunctions develop, emerging as risk factors for cardiovascular morbidity (32) and Alzheimer disease (6, 12, 15, 23). RRG dysfunctions remain poorly understood in humans, but mouse readiness for genetic manipulation has allowed the identification of crucial genes for RRG (5) and the production of mutant models for congenital central hypoventilation syndrome, Prader-Willi syndrome and Rett syndrome (1, 2, 55, 58, 59, 64), sleep-disordered breathing (45), and Alzheimer disease (18).

The C57BL/6J and FVB/N inbred strains are often used as background strains to produce mutant models, and the mutant phenotype may be, at least partly, affected by the background strain phenotype. The breathing phenotype of young adults of the C57BL/6J strain has been studied and compared with that of other strains (26, 43, 48–52, 62). However, the breathing phenotype of FVB/N mice has not been extensively documented. In addition, the breathing phenotype of FVB/N and C57BL/6J mice has never been compared at distinct developmental ages. Here, we examined their breathing phenotype from birth up to 1 yr. Using in vitro electrophysiology and in vivo plethysmography, we found interstrain differences in respiratory rhythm robustness, breathing parameters, and breathing regulations. As the neuromodulator/neurotransmitter serotonin (5-HT) is known to affect maturation and function of all central networks, including the RRG (7, 9, 10, 21, 27, 39, 54), we have examined the 5-HT metabolism in the medulla of FVB/N and C57BL/6J neonates and aged mice. For the first time, we found interstrain differences in 5-HT metabolism that could contribute to interstrain differences in breathing. Those interstrain differences in 5-HT and breathing systems have to be taken into account when analyzing the phenotype of mutants produced from FVB/N or C57BL/6J strains.

METHODS

Experiments were performed on 169 mice aged from embryonic *day 18* to postnatal (P) *day 360* (P360) from FVB/N ($n = 82$) and C57BL/6J ($n = 87$) strains (Charles River laboratories, France), in accordance with national legislation (JO 87–848) and European Communities Council Directive of 22 September 2010 (2010/63/EU). Permit numbers A13–505 and 13–426 for C. Menuet and N. Voituron, respectively were approved by Direction Départementale de la Protection des Populations, Préfecture des Bouches du Rhône, France. No follow-up study was performed, and different mice were studied at different ages. All methods and analyses have already been reported in detail elsewhere (14, 18, 55–59).

In Vitro Recordings

In vitro experiments were performed in en bloc preparations at either P1 or embryonic *day 18.5* (14, 57). After cold anesthesia, the medulla and cervical spinal cord were dissected out, placed ventral side upward in a 2-ml recording chamber, and superfused with artificial cerebrospinal fluid bubbled with carbogen (in mM: 129.0 NaCl, 3.35 KCl, 1.26 $CaCl_2$, 1.15 $MgCl_2$, 21.0 $NaHCO_3$, 0.58 NaH_2PO_4, and 30.00 glucose; pH 7.4; 4 ml/min, 27°C). The activity of phrenic motoneuron axons of the C_4 ventral root was recorded and integrated, and the phrenic burst (PB) frequency was used to define the activity of the RRG. We analyzed the PB frequency [expressed in cycles per minute (c/min)], the apnea index (AI) (expressed in number of PB cycles/min $>$ 2 mean PB cycles), and the irregularity score (IS) of the PB cycle period (55).

Address for reprint requests and other correspondence: N. Voituron, Laboratoire Réponses Cellulaires et Fonctionnelles à l'Hypoxie, EA 2363, UFR Santé, Médecine, Biologie Humaine, Université Paris 13, 74 rue Marcel Cachin, Bureau 128, 93017 BOBIGNY Cedex, France (e-mail: nicolas.voituron@univ-paris13.fr).

8750-7587/11 Copyright © 2011 the American Physiological Society

Downloaded from jap.physiology.org on June 11, 2011

In Vivo Recordings

From birth up to P360, the breathing activity of conscious mice was recorded using noninvasive plethysmographic approaches at 32°C for neonates and 25°C for adults. Before recordings, the mice were habituated to stay in the plethysmograph chamber to reduce stress. Only periods of breathing without body movements were studied. We used a home-made plethysmograph built from a 20-ml syringe, ventilated with air (200 ml/min) at P1, and a constant-flow plethysmograph (EMKA Technologies, Paris, France) with 200-ml animal chamber ventilated with air (600 ml/min) at older ages. A double-chamber plethysmograph was also used in aged mice to simultaneously record the respiratory pressure changes generated by the chest movements in the chest chamber and the resulting airflow in the head chamber (18, 56, 59).

Spirograms were stored and analyzed (Spike 2; Cambridge Electronic Design, Cambridge, UK) to calculate the mean respiratory frequency (Rf; expressed in respiratory c/min), tidal volume normalized by the body weight (V_T, μl/g), minute ventilation normalized by the body weight ($\dot{V}_E$, $ml \cdot g^{-1} \cdot min^{-1}$, with $\dot{V}_E = Rf \times V_T/1{,}000$), the AI defined as the number of apneas per minute > 2 normal respiratory cycles, and the IS. For V_T measurements, volume calibrations were performed by injecting small amounts of air in the recording chambers (50–100 μl). As previously reported and discussed (18, 56), whole body plethysmography may lead to relative uncertainty of V_T measurements, especially during upper airway dysfunction, with production of enlarged chest respiratory movements to compensate airway narrowing. Therefore, we also used double-chamber plethysmography to examine possible upper airway dysfunction in adult mice. We simultaneously recorded the spirograms generated by the chest movements in the chest chamber (chest V_T) and the resulting airflow in the head chamber (head V_T) and calculated the ratio of head V_T to chest V_T (head V_T/chest V_T), with a ratio significantly < 1 being indicative of upper airway dysfunction (18, 56).

We analyzed the effect of imposed hypoxic and hypercapnic challenges by first recording breathing under normal air for 20 min and thereafter under hypoxic (O_2, 10%) or hypercapnic (CO_2, 4%) gas mixture for a 5-min period (58). Changes in Rf, V_T, and $\dot{V}_E$ induced by hypoxia or hypercapnia were expressed as increment of control values measured before challenges. We analyzed the effect of sigh on the Rf by measuring the Rf every second during the 10-s period preceding the sigh (control period) and the 20-s period following the sigh, and expressing Rf every second in percentage of the mean Rf during the control period (59). For a given mouse, at least seven perisigh periods were analyzed, and data were averaged to obtain an individual postsigh time histogram representative of mean Rf changes before and after the sigh. The individual postsigh time histograms of different C57BL/6J and FVB/N mice were pooled to build an averaged histogram representative of a given strain.

Biochemical Analysis of Blood-Gas Parameters

Values of pH, P_{O_2}, and P_{CO_2} levels (Torr) and hematocrit (%) were measured in venous mixed-blood samples of nonanesthetized C57BL/6J and FVB/N aged mice. After tail blood vessel dilatation with water at 40–42°C and small incision at the tip of the tail, 100-μl blood samples were collected in plastic capillaries with electrolyte-balanced heparin (Radiometer, 70 IU heparin/ml) and analyzed with ABL 80 Flex analyzer (Radiometer). Due to blood sample volumes, measurements could not be performed in neonates.

Biochemical Analysis of Brain Stem Serotoninergic System

As previously reported (55), the medulla was quickly removed after decapitation and kept at −80°C until measurements. Medullary contents in 5-HT, its precursor L-tryptophan (L-Trp), and its main 5-HT metabolite 5-hydroxy-indol acid acetic (5-HIAA) from the monoamine oxydase A (MAOA) degradation pathway were measured with high-pressure liquid chromatography separation and electrochemical detection (Waters System: pump P510, electrochemical detector EC2465; Atlantis column DC18; mobile phase: citric acid, 50 mM; orthophosphoric acid, 50 mM; sodium octane sulfonic acid, 0.112 mM; EDTA, 0.06 mM; methanol, 5%; NaCl, 2 mM; pH 2.95). Contents were expressed in nanograms per medulla.

Statistical Analysis

Values are given as means ± SE. Statistical comparisons were performed using Student's unpaired *t*-test (C57BL/6J VS. FVB/N mice) or Student's paired *t*-test (double-chamber plethysmography). Differences were regarded as significant if $P < 0.05$. In Table 1, significant and nonsignificant differences are indicated as $*P < 0.05$, $**P < 0.01$, $***P < 0.001$, and nonsignificant (NS), respectively.

RESULTS

Distinct Breathing and Serotoninergic Phenotypes in FVB/N and C57BL/6J Neonates

In vivo study of breathing. At P1, whole body plethysmography revealed obvious interstrain differences in the breathing phenotype of conscious, unrestrained FVB/N ($n = 8$) and C57BL/6J ($n = 8$) neonates (Table 1), with robust respiratory rhythm in FVB/N vs. unstable in C57BL/6J neonates (Fig. 1*A*). The duration of consecutive respiratory cycles was stable in FVB/N, but highly variable in C57BL/6J neonates, with significant fivefold lower IS in FVB/N than C57BL/6J neonates (Fig. 2*A*). In addition, transient apneas were rare in FVB/N, but highly frequent in C57BL/6J neonates, with significant 14-fold lower AI in FVB/N than C57BL/6J neonates. Neonates from both strains had similar V_T, but the Rf was significantly twofold higher in FVB/N than C57BL/6J neonates, leading to significantly higher $\dot{V}_E$ in FVB/N than C57BL/6J neonates. Then C57BL/6J compared with FVB/N neonates had lower Rf, lower $\dot{V}_E$, and unstable breathing pattern at P1.

In vitro study of respiratory-like activity. To examine the origins of the interstrain differences in breathing pattern, in vitro experiments were conducted at P1 using medullary preparations, where the neonatal RRG continued to produce rhythmic PB after total isolation from upper structures and periphery (Fig. 3*A*). No obvious interstrain difference was observed in the PB amplitude, and the PB frequency was found slightly but nonsignificantly higher in FVB/N ($n = 8$) than C57BL/6J ($n = 14$) preparations (10.1 ± 0.8 and 8.8 ± 0.8 c/min, respectively, NS). However, the PB rhythm was robust in FVB/N, but highly unstable in C57BL/6J preparations, with significantly lower IS in FVB/N than C57BL/6J preparations (39 ± 7 and 73 ± 6, respectively, $P < 0.01$) and AI (0.02 ± 0.01 and 0.38 ± 0.15, respectively, $P < 0.05$). This revealed an inherent instability of the RRG of C57BL/6J neonates. We then examined whether the RRG instability of C57BL/6J neonates was prenatal in origin by conducting in vitro experiments at gestational *day 18.5*, 1 day before birth (data not shown). The isolated RRG of C57BL/6J embryos ($n = 5$) produced rhythmic PB with high IS (69 ± 20) and AI (7.2 ± 0.3). Thus the breathing instability observed in vivo in C57BL/6J neonates originated, at least in part, from a prenatal instability of their RRG.

Different 5-HT Metabolisms in C57BL/6J and FVB/N Neonatal Medullas

Given that endogenous 5-HT affected the RRG maturation and function (7, 27), we analyzed the 5-HT metabolism in the

Downloaded from jap.physiology.org on June 11, 2011

Table 1. *Breathing parameters of neonatal, young and aged C57BL/6J and FVB/N mice*

Age/Strain	*N*	Rf, c/min	V_T, μl/g	$\dot{V}_E$, ml·g^{-1}·min^{-1}	AI, apneas/min	IS
P1		***	NS	***	***	**
C57Bl6	8	94 ± 8	10.0 ± 0.6	0.96 ± 0.11	5.62 ± 0.59	54.5 ± 9.1
FVBN	8	213 ± 15	10.0 ± 0.4	2.11 ± 0.14	0.44 ± 0.19	11.1 ± 0.8
P30		**	NS	NS	NS	NS
C57Bl6	10	245 ± 17	10.0 ± 1.2	2.68 ± 0.54	0.20 ± 0.10	11.7 ± 2.7
FVBN	8	184 ± 11	9.8 ± 0.9	1.65 ± 0.15	0.30 ± 0.11	8.0 ± 0.7
P120		**	NS	NS	***	*
C57Bl6	9	192 ± 4	6.7 ± 0.8	1.30 ± 0.17	0.48 ± 0.08	11.7 ± 0.8
FVBN	10	171 ± 6	6.4 ± 0.5	1.10 ± 0.11	0.01 ± 0.01	8.3 ± 1.2
P240		NS	***	*	*	**
C57Bl6	8	146 ± 18	2.7 ± 0.6	0.45 ± 0.15	0.83 ± 0.31	18.3 ± 3.3
FVBN	14	148 ± 5	5.6 ± 0.4	0.85 ± 0.08	0.04 ± 0.03	8.5 ± 1.2
P360		NS	***	***	*	NS
C57Bl6	10	128 ± 8	2.6 ± 0.2	0.33 ± 0.03	0.23 ± 0.07	10.3 ± 1.4
FVBN	9	139 ± 3	5.4 ± 0.5	0.75 ± 0.08	0.05 ± 0.03	7.6 ± 0.6

Values are means ± SE of respiratory frequency [Rf; cycles/min (c/min)], tidal volume (V_T; μl/g), minute ventilation ($\dot{V}_E$; ml·g^{-1}·min^{-1}), apnea index (AI; apneas/min), and irregularity score (IS) of conscious, unrestrained FVB/N and C57Bl/6J mice at a given class of age, from postnatal *day 1* (P1) up to P360, with *N* indicating the number of studied animals. Significant differences between mean values at a given class of age (unpaired Student's *t*-test) are indicated by $*P < 0.05$, $**P < 0.01$, and $***P < 0.001$ (NS, nonsignificant). Note the significant interstrain difference in breathing phenotype of C57BL/6J and FVB/N neonates (P1) and aged mice (P240 and P360).

medulla of C57BL/6J ($n = 10$) and FVB/N ($n = 10$) neonates by measuring contents of 5-HT, its main catabolite 5-HIAA, and its precursor L-Trp. At P1, we found similar 5-HT contents in both strains (0.19 ± 0.03 and 0.18 ± 0.03 ng/medulla, NS) but twofold higher L-Trp contents in FVB/N than C57BL/6J neonates (33 ± 4 and 18 ± 2 ng/medulla, $P < 0.001$), and threefold weaker 5-HIAA contents in FVB/N than C57BL/6J neonates (0.15 ± 0.02 and 0.57 ± 0.05 ng/medulla, $P < 0.001$), leading to a significantly threefold higher 5-HT-to-5-HIAA ratio (5-HT/5-HIAA) in FVB/N than C57BL/6J neonates (1.28 ± 0.22 and 0.35 ± 0.06, $P < 0.001$). We then examined whether the 5-HT/5-HIAA of C57BL/6J mice was already weak before birth. In C57BL/6J embryos at gestational *day 16.5*, we found a 5-HT/5-HIAA not significantly different (0.32 ± 0.01) from that of neonates. Then the faster turnover of the neuromodulator/neurotransmitter 5-HT in C57BL/6J than FVB/N medullas could differently affect the prenatal maturation and neonatal function of the RRG.

Alleviated Breathing Phenotypic Differences in C57BL/6J and FVB/N Young Adults

To examine whether the differences in robustness of the neonatal RRG persisted with aging, plethysmographic recordings were performed in young and aged adult mice (this and next paragraphs, respectively). In young adults, the marked difference in breathing parameters was alleviated (Table 1). At P30, the Rf of FVB/N young adults ($n = 8$) was slightly reduced compared with that of FVB/N neonates, whereas the Rf of C57BL/6J young adults ($n = 10$) was significantly increased compared with that of C57BL/6J neonates. This reduced the interstrain difference in Rf, although the mean Rf was slightly but significantly lower in FVB/N than C57BL/6J mice. Neither V_T nor $\dot{V}_E$ differed between strains, and the rhythm robustness was improved in C57BL/6J mice, with similar weak IS and AI in C57BL/6J and FVB/N mice. Three months later (P120), Rf, V_T, and $\dot{V}_E$ were decreased in both strains, and no interstrain differences in breathing pattern were obvious, even if Rf, AI, and IS were slightly but significantly lower in FVB/N ($n = 10$) than C57BL/6J ($n = 9$) mice. Then the breathing phenotypic differences between C57BL/6J and FVB/N mice were alleviated during the P30–P120 period.

Marked Breathing Phenotypic Differences in C57BL/6J and FVB/N Aged Mice

We thereafter analyzed the breathing pattern of aged C57BL/6J and FVB/N mice at P240 and P360 (Table 1). At P240 (Figs. 1*B* and 2*B*), the Rf was similarly reduced in both strains, but the respiratory rhythm remained robust in FVB/N ($n = 14$), but not in C57BL/6J ($n = 8$) mice. C57BL/6J compared with FVB/N mice had significantly higher IS and AI, and their V_T was drastically reduced, leading to a significant reduction of $\dot{V}_E$. At P360, the same significant interstrain differences in rhythm robustness, V_T, and $\dot{V}_E$ were observed.

As C57BL/6J compared with FVB/N mice had significantly reduced V_T and $\dot{V}_E$ at P240, we examined whether this differently affected their blood parameters. Although less indicative than arterial blood samples, venous mixed-blood samples obtained via a relatively noninvasive way from tails of C57BL/6J ($n = 6$) and FVB/N ($n = 8$) conscious mice at P240 revealed interstrain differences. The mixed-venous blood P_{O_2} was similar in both strains (50 ± 6 and 61 ± 5 Torr, NS), but the mixed-venous blood pH was significantly higher in FVB/N than C57BL/6J mice (7.19 ± 0.03 and 7.10 ± 0.04, respectively, $P < 0.05$), and, correspondingly, the mixed-venous blood P_{CO_2} was significantly lower in FVB/N than C57BL/6J mice (54 ± 5 and 69 ± 6 Torr, respectively, $P < 0.05$). Hematocrit was significantly lower in FVB/N than C57BL/6J mice (44 ± 2 and 49 ± 1%, respectively, $P < 0.05$).

Possible Origins of V_T Reduction in C57BL/6J vs. FVB/N Aged Mice

From birth up to 1 yr, the $\dot{V}_E$ developmental changes were fairly different in FVB/N and C57BL/6J mice, with a monotonous decrease of $\dot{V}_E$ in FVB/N mice (maximal $\dot{V}_E$ at birth and progressive decrease with age) vs. bell-shaped changes of $\dot{V}_E$ in C57BL/6J mice (weak at birth, marked but transient increase

Downloaded from jap.physiology.org on June 11, 2011

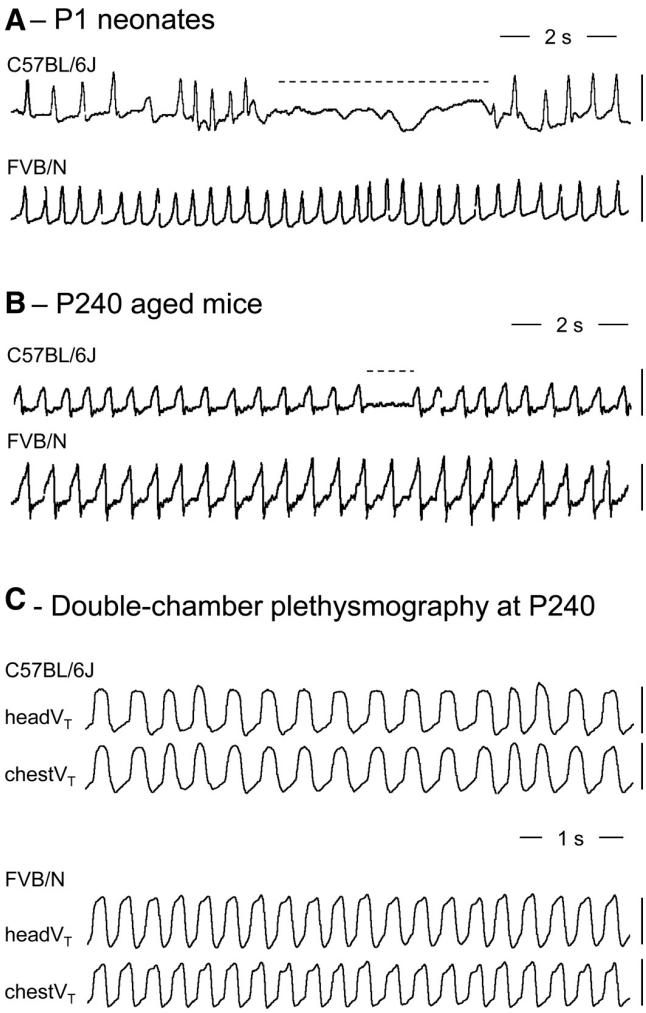

Fig. 1. Plethysmographic recordings of in vivo breathing in C57BL/6J and FVB/N mice. *A*: at postnatal *day 1* (P1), whole body plethysmography revealed unstable vs. robust respiratory rhythm in C57BL/6J (*top* trace) and FVB/N (*bottom* trace) neonates, respectively. Note the long-lasting apnea in the C57BL/6J neonate (horizontal dotted line). *B*: at postnatal *day 240* (P240), whole body plethysmography revealed the persistence of apneas in C57BL/6J (*top* trace; horizontal dotted line: apnea) vs. robust rhythm in FVB/N aged mice (*bottom* trace). In addition, the tidal volume (VT) was weaker in C57BL/6J than FVB/N mice. *C*: double-chamber plethysmography recordings were performed in C57BL/6J (*top* dual traces) and FVB/N (*bottom* dual traces) mice at P240 to simultaneously record the chest respiratory movements (chest VT) and the resulting airflow changes (head VT); recordings did not reveal upper airway dysfunction in both strains. Horizontal bars, time scale as indicated. Vertical bars, VT calibrations: *A* for P1 neonates, 10 μl/g; *B* for P240 mice, 5 μl/g; *C* for P240 mice, arbitrary units.

at P30–P120, and decrease at P240–P360) mainly caused by a stepped, drastic decrease of VT between P120 and P240. Such VT decrease deserved further examination, and we, therefore, analyzed upper airway function, breathing regulations, and 5-HT metabolism in FVB/N and C57BL/6J mice at P240.

Lack of Upper Airway Dysfunction in C57BL/6J and FVB/N Aged Mice

Whole body plethysmography may detect false VT values in case of airways dysfunction (18, 56). To examine whether the VT reduction at P240 observed with whole body plethysmography in C57BL/6J mice was actual or reflected airway dysfunction, we used double-chamber plethysmography. This allowed the simultaneous recordings of chest breathing movements (chest VT) and resulting airflow (head VT) and calculation of the head VT/chest VT. A reduced head VT/chest VT was reported to be the sign of upper airway dysfunction, with mouse producing enlarged chest movements to ventilate against partly obstructed airways. Double-chamber plethysmography in C57BL/6J mice did not reveal significant decreases in the head VT/chest VT from P30 to P240 (1.12 ± 0.22, $n = 7$, and 0.90 ± 0.15, $n = 7$, respectively, NS). As no upper airway dysfunction developed with age in C57BL/6J mice, then an actual reduction of VT occurred at P240. Double-chamber plethysmography in FVB/N mice at P30 ($n = 8$) and P240 ($n = 6$) similarly showed no reduction of the head VT/chest VT between P30 and P240.

Differences in VT Responses to O_2 and CO_2 Drive in C57BL/6J and FVB/N Aged Mice

To examine whether the VT reduction of C57BL/6J mice at P240 reflected a weak sensitivity of their respiratory centers to O_2 and CO_2 chemosensory drives, FVB/N and C57BL/6J mice were subjected to identical hypoxic (10% O_2, 5 min) or hypercapnic (4% CO_2, 5 min) challenges at P240. As illustrated in Fig. 4, hypoxia or hypercapnia significantly increased Rf, VT, and $\dot{V}_E$ in both strains, but the responses were larger in FVB/N than C57BL/6J mice. Hypoxia induced a nonsignificant larger increment of Rf in FVB/N ($n = 10$) than C57BL/6J ($n = 8$) mice (56 ± 22 and 28 ± 13 c/min, respectively, NS), a significant fourfold larger increment of VT in FVB/N than C57BL/6J mice (9.2 ± 1.9 and 2.2 ± 0.9 μl/g, respectively, $P < 0.01$), and, therefore, a significant sixfold larger increment of $\dot{V}_E$ in FVB/N than C57BL/6J mice (2.5 ± 0.5 and 0.4 ± 0.2 $ml \cdot g^{-1} \cdot min^{-1}$, respectively, $P < 0.01$). Hypercapnia similarly increased Rf in FVB/N ($n = 10$) and C57BL/6J ($n = 8$) mice (94 ± 8 and 89 ± 25 c/min, respectively, NS), but induced a significant threefold larger increment of VT in FVB/N than C57BL/6J mice (14.1 ± 1.5 and 4.0 ± 1.1 μl/g, respectively, $P < 0.001$), and, therefore, of $\dot{V}_E$ in FVB/N than C57BL/6J mice (3.9 ± 0.4 and 1.3 ± 0.4 $ml \cdot g^{-1} \cdot min^{-1}$, respectively, $P < 0.001$). Then C57BL/6J aged mice were less sensitive to chemical drives than FVB/N aged mice, and the weak sensitivity to chemical drives of C57BL/6J mice was highly likely contributing to their reduced VT under basal conditions.

Different Postsigh Pattern in C57BL/6J vs. FVB/N Aged Mice

As previously reported (59), sighs are deep inspirations that spontaneously occur at a low frequency (about 0.5 sigh/min) and overinflate the lungs, which prevents lung atelectasis, restores functional residual capacity, and transiently improves alveolar oxygenation. The sigh-induced overinflation of the lungs first induces a brief Rf reduction, reflecting the overactivation of pulmonary stretch receptors (Hering-Breuer reflex) and, second, induces a long-lasting bradypnea, reflecting the improvement of alveolar oxygenation (chemosensory reflex). Then the Rf changes during the post-sigh period reflected the Hering-Breuer and chemosensory regulations in conscious, unrestrained mice (59). In FVB/N ($n = 14$) and C57BL/6J

Downloaded from jap.physiology.org on June 11, 2011

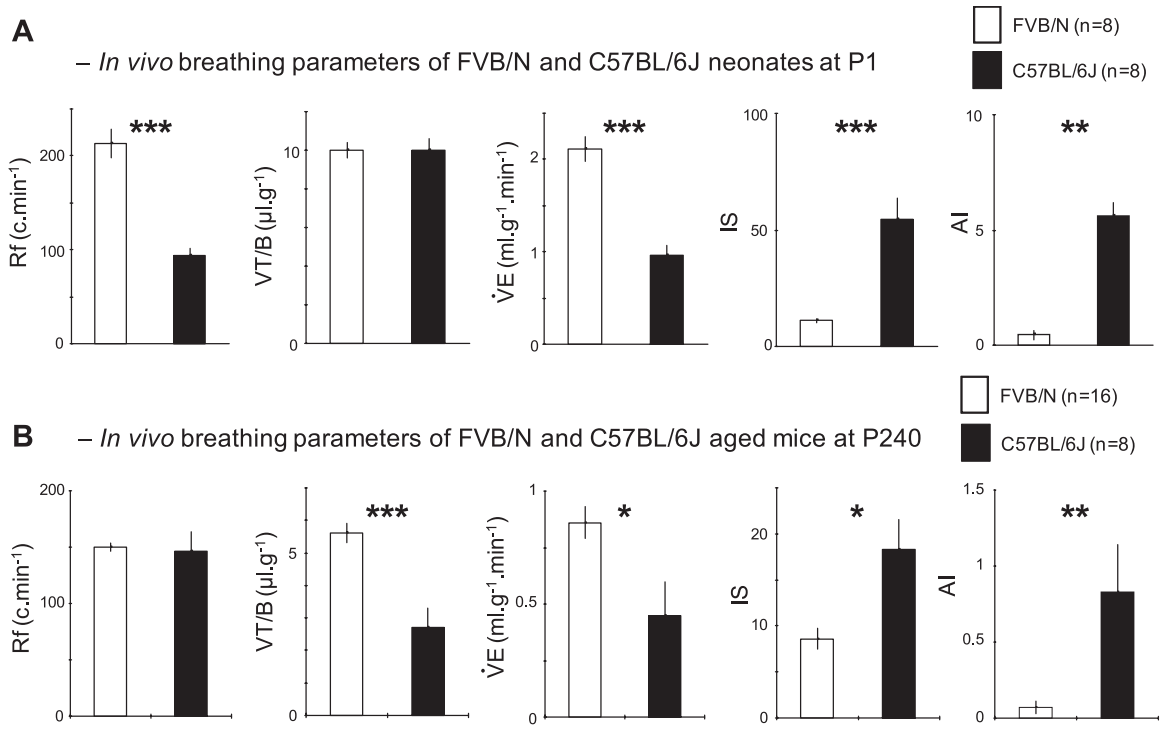

Fig. 2. Interstrain differences in breathing of C57BL/6J and FVB/N mice. Bars in histograms indicate mean (and SE) values of respiratory frequency [Rf; in cycle/min (c/min)], V_T normalized by body weight (V_T/B; in µl/g), minute ventilation ($\dot{V}_E$; in ml·g^{-1}·min^{-1}), irregularity score (IS), and apnea index (AI; in apneas/min) for C57BL/6J (solid bars) and FVB/N (open bars) mice from whole body plethysmography recordings performed at P1 (*A*) and at P240 (*B*). Significant difference between mean values: *$P < 0.05$, **$P < 0.01$, and ***$P < 0.001$. Both at P1 and P240, note that AI and IS were significantly larger in C57BL/6J than FVB/N mice, attesting for a more unstable breathing, and that $\dot{V}_E$ was significantly weaker in C57BL/6J than FVB/N mice, revealing hypoventilation of C57BL/6J mice caused by low Rf in neonates and low V_T in old adults.

($n = 8$) mice at P240, we compared the postsigh Rf to the control Rf before the sigh (100%). The Rf was first depressed during the second following the sigh in both strains (Fig. 5), but significantly less in FVB/N (79 ± 3% of the control) than C57BL/6J mice (58 ± 5% of the control), suggesting a stronger Hering-Breuer inhibitory reflex in C57BL/6J than FVB/N mice. Thereafter, a long-lasting post-sigh bradypnea developed in both strains, but the mean Rf during the following 5 s was significantly more reduced in FVB/N (57 ± 2% of the control) than C57BL/6J mice (72 ± 3% of the control), suggesting a weaker responsiveness to sigh-induced improvement of O_2 in C57BL/6J than FVB/N mice. Then differences in lung and chemosensory regulations of breathing existed between FVB/N and C57BL/6J mice.

Differences in Brain Stem 5-HT Metabolism of C57BL/6J vs. FVB/N Aged Mice

As 5-HT was shown to contribute to respiratory function and dysfunctions in adult mice (14, 27), we analyzed the 5-HT metabolism of C57BL/6J ($n = 7$) and FVB/N ($n = 7$) mice at P240. No significant differences were observed in medullary contents of the L-Trp precursor (10 ± 1 and 12 ± 3 ng/medulla, NS) and the 5-HIAA catabolite (1.39 ± 0.09 and 1.79 ± 0.26 ng/medulla, NS), but the 5-HT contents were significantly higher in the medulla of FVB/N than C57BL/6J mice (3.26 ± 0.22 and 2.19 ± 0.18 ng/medulla, respectively, $P < 0.01$). Therefore, the 5-HT/5-HIAA was significantly higher in the medulla of FVB/N than C57BL/6J mice (2.36 ± 0.13 and 1.35 ± 0.19, respectively, $P < 0.001$), revealing again differences in 5-HT metabolism that possibly contributed to breathing differences.

DISCUSSION

For the first time, we report phenotypic differences in 5-HT and breathing systems of FVB/N and C57BL/6J mice from birth onwards. Given that 5-HT affects maturation and function of all central networks (21), including the respiratory network (7, 9, 27, 54), then interstrain differences in 5-HT metabolism may contribute to interstrain differences in breathing. As FVB/N and C57BL/6J strains are often used as background strain for producing mutants, and as the background phenotype may affect the mutant phenotype, the 5-HT and breathing differences between FVB/N and C57BL/6J strains should be taken into account for analyzing the mutant phenotype.

RRG Robustness vs. RRG Instability: Possible Role of 5-HT

From birth onwards, robustness vs. instability characterizes the RRG of FVB/N and C57BL/6J mice, respectively. The RRG instability of C57BL/6J mice is, at least partly, central and prenatal in origins, as the isolated RRG of C57BL/6J embryos produces an unstable rhythm. The RRG is composed of two coupled, interacting networks that form and are active before birth: the pre-Bötzinger complex and the retrotrapezoid nucleus/parafacial respiratory group (53). The RRG function relies on pacemaker and synaptic properties (60) and on several

Downloaded from jap.physiology.org on June 11, 2011

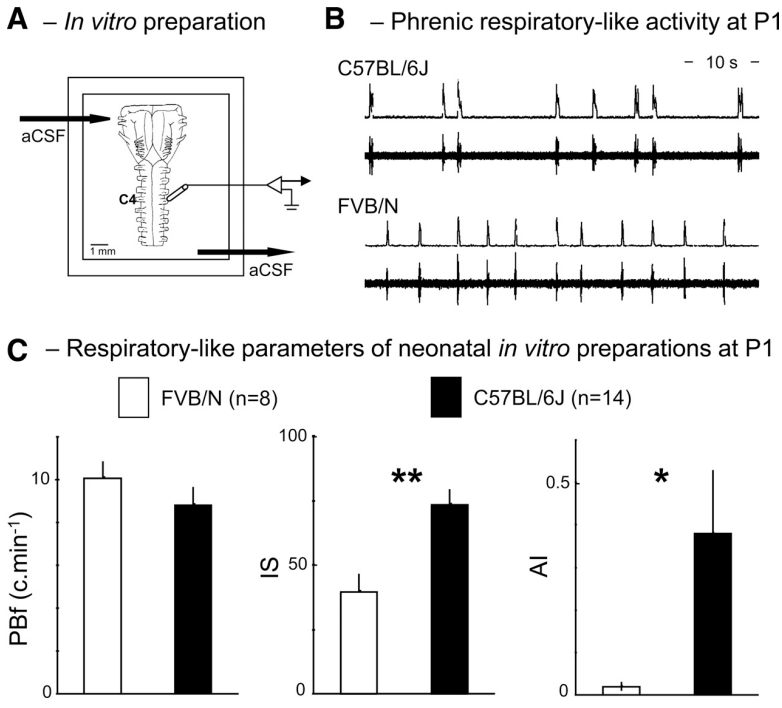

Fig. 3. Interstrain differences in respiratory-like activity of C57BL/6J and FVB/N in vitro preparations. *A*: schematic view of in vitro medullary preparations used to study the respiratory-like activity produced by the isolated respiratory rhythm generator (RRG) of neonatal mice. aCSF, artificial cerebrospinal fluid. *B*: raw and integrated phrenic bursts (*bottom* and *top* traces, respectively) recorded on C_4 ventral roots of FVB/N and C57BL/6J (*bottom* and *top* paired traces, respectively) neonatal preparations at P1. Note the rhythm instability in the C57BL/6J vs. FVB/N preparations. *C*: bars in histograms indicate mean (and SE) values of phrenic burst frequency (PBf; in c/min), IS, and AI (in apneas/min) for C57BL/6J (solid bars) and FVB/N (open bars) neonatal preparations. Significant difference between mean values of IS and AI: $*P < 0.05$, and $**P < 0.01$.

genes whose expression is crucial for neonatal survival (2, 4, 8, 14). It also relies on 5-HT afferent inputs from raphe neurons (27), affecting the RRG perinatal maturation and neonatal function (7, 9, 17, 21, 27, 64). The different 5-HT/5HIAA in C57BL/6J and FVB/N neonates reveal differences in 5-HT metabolism, which may differentially affect RRG maturation and function at birth, but also induce long-lasting sequels in adults. Although differences in 5-HT metabolism have not been previously documented in FVB/N and C57BL/6J mice, they have already been described in C57BL/6J and BALBc adults, with lower 5-HT levels in C57BL/6J (16).

RRG instability has been commonly reported in mutant mice where genetic manipulations have altered 5-HT systems. In MAOA-null mice, the lack of 5-HT degradation by MAOA induces excess of 5-HT, altered wiring of the respiratory network, unstable breathing in neonates, and frequent apneas in adults (7, 9, 31, 46). In Necdin-null mice, the 5-HT and RRG systems dysfunction at birth, and unstable respiratory rhythm with frequent apneas persists in adults, despite 5-HT metabolism restoration (64). In Mecp2-null mice, the 5-HT and RRG systems correctly function in neonates, but dysfunction in adults, leading to erratic rhythm, severe apneas, and premature

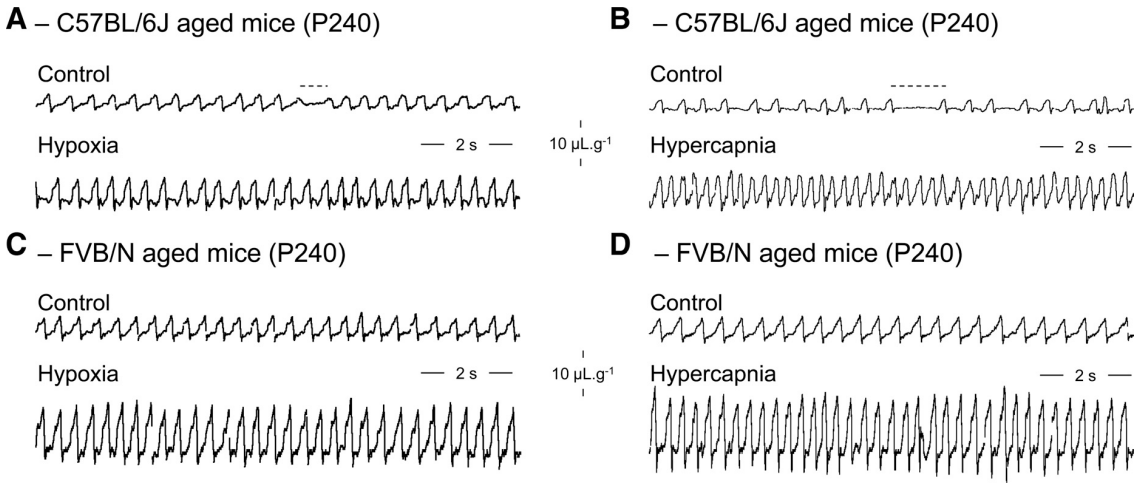

Fig. 4. Breathing responses to hypoxic or hypercapnic challenges in C57BL/6J and FVB/N aged mice at P240. Traces show plethymographic recordings obtained in C57BL/6J (*A* and *B*) and FVB/N (*C* and *D*) mice at P240 when breathing normal air (Control; *top* traces) or gas mixtures (*bottom* traces) containing low concentration of O_2 (10%; Hypoxia) or high concentration of CO_2 (4%; Hypercapnia) for 5 min. Horizontal dotted lines indicate apneas in C57BL/6J mice under air. Note the marked V_T increases in FVB/N mice compared with C57BL/6J mice.

Downloaded from jap.physiology.org on June 11, 2011

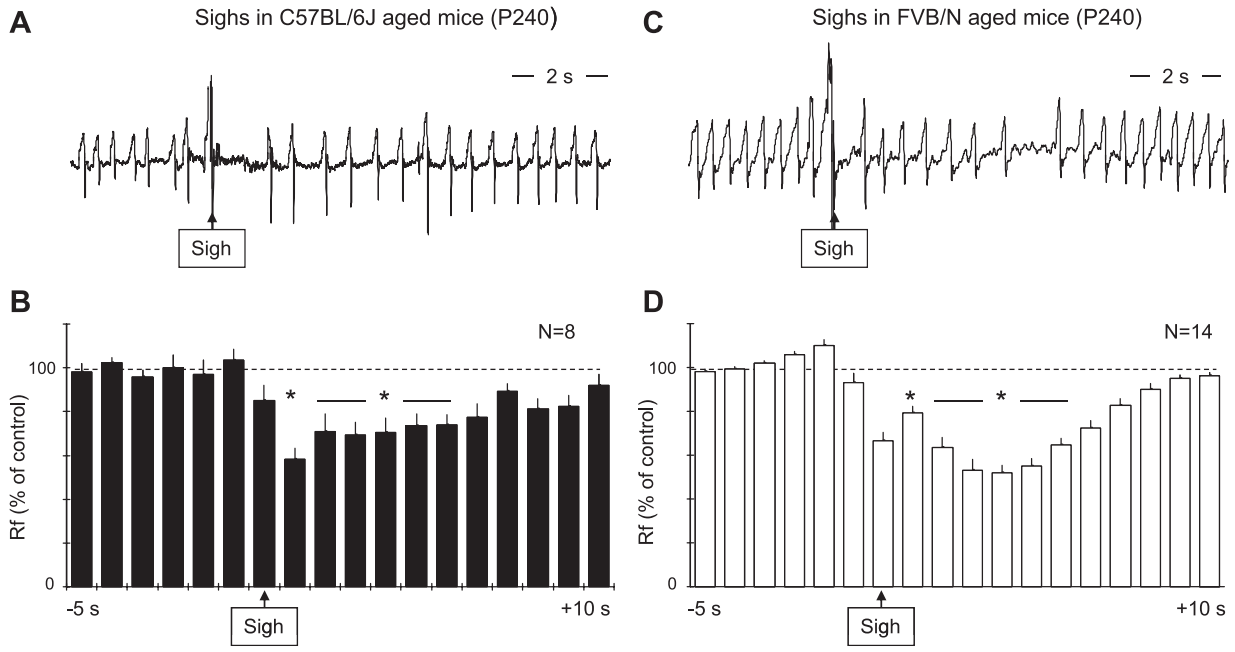

Fig. 5. Postsigh changes in Rf in C57BL/6J and FVB/N aged mice at P240. *A*: traces show plethymographic recordings during a sigh (arrow) in a given C57BL/6J mouse. *B*: bars in histogram show the mean (and SE) changes in Rf every second (expressed in %control Rf during the 10-s period before the sigh; horizontal dotted line indicates 100% of control Rf) from 5 s before the sigh up to 10 s after the sigh. The histogram shown in *B* was averaged from individual histograms built from 8 distinct C57BL/6J mice aged P240 (at least 7 sighs for each mouse). Note that the sigh induced, first, a brief, marked reduction of Rf in the first postsigh second, and, second, a long-lasting bradypnea that developed during the following seconds. *C* and *D*: as above, but for FVB/N mice ($n = 14$). In *B* and *D* averaged histograms, *significant difference between postsigh Rf changes compared with control Rf before the sigh. Note that the Rf was more reduced during the first second following the sigh in C57BL/6J than FVB/N mice, but that the long-lasting bradypnea was less pronounced in C57BL/6J than FVB/N mice.

death (55). In mutant mice lacking 5-HT_{2A} receptors, a role of 5-HT in sleep apneas has been suggested (42). In mutant mice with 5-HT defects and also in C57BL/6J mice, the RRG instability is affected by 5-HT treatments (1, 7, 46, 48, 49, 64). Indeed, differences in 5-HT metabolism of FVB/N and C57BL/6J mice may contribute to differences in RRG robustness from birth onwards.

Differences in Breathing Regulations: Possible Role of 5-HT

Aged C57BL/6J mice compared with aged FVB/N mice show reduced V_T and $\dot{V}_E$, with reduced pH and increased P_{CO_2} in mixed-venous blood. Double-chamber plethysmography reveals that the weak V_T of C57BL/6J mice is not due to upper airway dysfunctions (18, 56). The weak V_T of C57BL/6J mice might reflect age-related alteration of respiratory effectors. Lung parenchyma and diaphragm contractile properties degrade with age in rodents, but during the senescent period (28, 29), not as early as P240. The weak V_T of C57BL/6J mice more likely reflects altered breathing regulations that impair correct adjustments of the central respiratory drive to physiological needs. In C57BL/6J mice, the marked reduction of Rf just after the sigh suggests a potent respiratory inhibition from pulmonary stretch receptors, whereas their weak postsigh bradypnea confirms weak sensitivity/responsiveness to chemical inputs (59), consistently with weak V_T increments during respiratory challenges. Interstrain differences in sensitivity of pulmonary stretch receptors to lung inflation have already been reported between OF1 and C3H/J adults (11), as well as interstrain differences in carotid body size and breathing responses to hypoxia between DBA/2J and A/J mice (61).

Both retrotrapezoid nucleus/parafacial respiratory group and 5-HT systems contribute to breathing regulations (20, 24, 25, 27, 36, 37, 39, 47, 65). In C57BL/6J neonates, fluoxetine-induced alteration of the 5-HT metabolism abolishes the RRG response to acidosis (57). In C57BL/6J but not A/J mice, a periodic breathing occurs after hypoxic challenges (26), persists after pretreatment with nitric oxide agent (43), but is abolished by pretreatment with the 5-HT_{1A} receptor agonist buspirone (62). In MAOA-null adults, the genetically induced alteration of 5-HT metabolism reduces the resting V_T, the response to hypoxia, and the response to lung inflations, these defects being alleviated after 5-HT treatments (10). In Necdin-null neonates, the altered 5-HT metabolism blunts their breathing responses to hypercapnia and hypoxia (64). In addition, maternal dietary tryptophan deficiency affects the 5-HT system of rat pups and, in turn, alters their breathing pattern and ventilatory responses to hypercapnia (40). Then differences in 5-HT metabolism between FVB/N and C57BL/6J mice may differently affect not only RRG robustness, but also resting ventilation and breathing regulations.

The P30–P120 Intermediate Period

The 5-HT/5-HIAA at P1 and P240 is lower in C57BL/6J than FVB/N medulla. At P1, the low precursor and the high catabolite contents in C57BL/6J medulla are consistent with a faster turnover of 5-HT in C57BL/6J than FVB/N neonates. At P240, although the precursor content is similar in the two strains, the low 5-HT and the high catabolite contents in C57BL/6J medulla also support a fast turnover of 5-HT.

Downloaded from jap.physiology.org on June 11, 2011

However, further experiments are required to examine the genetic and molecular origins of the interstrain difference in 5-HT metabolism at P1 and P240. From P30 to P120, after the postnatal maturational period during which pups learn to breathe and to manage with peripheral and upper brain inputs (19), FVB/N and C57BL/6J mice display a rather similar breathing pattern, even if slight, but significant, differences persist in Rf, AI, and IS. During this period, the breathing improvement in C57BL/6J mice may be related to postnatal changes in 5-HT metabolism, as those reported in multiple nuclei of rats (34). In C57BL/6J mice, our laboratory previously reported, but did not comment on, weak 5-HT/5HIAA (0.27) at P2, but large 5-HT/5HIAA (1.98) at P30 (64). Such increase in 5-HT/5-HIAA from P2 to P30 reveals changes in the 5-HT metabolism of C57BL/6J mice, which correlates well with their breathing improvement at P30–P120. Interestingly, the inactivation of the 5-HT transporter has age-related effects on the $\dot{V}_E$ of mutant mice: no effect at P8, reduction at P15, and increase at 5–6 mo (33, 41), which further suggests a complex link between 5-HT and respiratory systems. However, besides 5-HT inputs, the mature RRG receives a plethora of inputs, including those from upper structures, to adapt its activity to mood, motor activity, temperature, etc. FVB/N mice are more anxious, more active, and have a slightly higher central temperature than C57BL/6J mice (44), and this may also contribute to breathing differences, although the 5-HT system affects anxiety, motor activity, and thermoregulation.

As the distinct brain stem raphe nuclei differ in terms of rostrocaudal projections, targeted structures, and modulated functions, it may be important to further examine which mechanisms and raphe nuclei sustain the 5-HT and breathing differences between FVB/N and C57BL/6 mice.

Selecting the Background Strain for Producing Mutant Models

Both FVB/N and C57BL/6J strains are suitable for producing mutants, but their distinct 5-HT and breathing phenotypes may affect the mutant phenotype. On the one hand, the inherent RRG instability of the C57BL/6J background may worsen the mutant breathing phenotype. Teashirt3 inactivation on the C57BL/6J background is 100% lethal for heterozygous neonates (13), whereas Teashirt3 inactivation on the CD1 background allows survival of 50% of heterozygotes (14). Necdin inactivation induces breathing defects, with more severe neonatal lethality on C57BL/6J than 129/SvEv backgrounds (22, 35). Hoxa5 inactivation induces more severe respiratory distress and lethality in C57BL/6J than 129/SvEv backgrounds (3). On the other hand, the RRG robustness of the FVB/N background may mitigate genetically induced breathing defects, facilitate mutant survival over the postnatal period, and allow the study of breathing defects with late onset. Tau-P301L mice, a possible mutant model for Alzheimer disease produced on FVB/N background, develop upper airway dysfunctions only late, after 8 mo of age (18); the breathing defect could have been sooner and more severe on C57BL/6J background. Mecp2-null mice, a mutant model for Rett syndrome produced on C57BL/6J background, develop early and lethal apneas (55); the breathing defect could have been later and less severe on an FVB/N background. As reviewed, 5-HT may affect central network maturation (21), respiratory function and dysfunction (27), postnatal body growth, vegetative control, and adult behaviors (54). Although FVB/N and C57BL/6J strains are frequently used for producing mutants, other strains are also used. Whatever the used strains are, 5-HT and breathing phenotypic differences must be taken into account for studying mutants, as they could affect mutant phenotype, exaggerating or masking breathing symptoms, as well as other defects.

GRANTS

This work was supported by UMR 6231 (Centre National de la Recherche Scientifique, University Aix-Marseille II & III). N. Voituron was supported by Agence Nationale de la Recherche Prageder (Fellowship 2010).

DISCLOSURES

No conflicts of interest, financial or otherwise, are declared by the author(s).

REFERENCES

1. **Abdala AP, Dutschmann M, Bissonnette JM, Paton JF.** Correction of respiratory disorders in a mouse model of Rett syndrome. *Proc Natl Acad Sci U S A* 107: 18208–18213, 2010.
2. **Amiel J, Dubreuil V, Ramanantsoa N, Fortin G, Gallego J, Brunet JF, Goridis C.** PHOX2B in respiratory control: lessons from congenital central hypoventilation syndrome and its mouse models. *Respir Physiol Neurobiol* 168: 125–132, 2009.
3. **Aubin J, Lemieux M, Tremblay M, Behringer RR, Jeannotte L.** Transcriptional interferences at the Hoxa4/Hoxa5 locus: importance of correct Hoxa5 expression for the proper specification of the axial skeleton. *Dev Dyn* 212: 141–156, 1998.
4. **Blanchi B, Kelly LM, Viemari JC, Lafon I, Burnet H, Bevengut M, Tillmanns S, Daniel L, Graf T, Hilaire G, Sieweke MH.** MafB deficiency causes defective respiratory rhythmogenesis and fatal central apnea at birth. *Nat Neurosci* 6: 1091–1100, 2003.
5. **Blanchi B, Sieweke MH.** Mutations of brainstem transcription factors and central respiratory disorders. *Trends Mol Med* 11: 23–30, 2005.
6. **Bliwise DL.** Sleep apnea, APOE4 and Alzheimer's disease 20 years and counting? *J Psychosom Res* 53: 539–546, 2002.
7. **Bou-Flores C, Lajard AM, Monteau R, De ME, Seif I, Lanoir J, Hilaire G.** Abnormal phrenic motoneuron activity and morphology in neonatal monoamine oxidase A-deficient transgenic mice: possible role of a serotonin excess. *J Neurosci* 20: 4646–4656, 2000.
8. **Bouvier J, Thoby-Brisson M, Renier N, Dubreuil V, Ericson J, Champagnat J, Pierani A, Chedotal A, Fortin G.** Hindbrain interneurons and axon guidance signaling critical for breathing. *Nat Neurosci* 13: 1066–1074, 2010.
9. **Bras H, Gaytan SP, Portalier P, Zanella S, Pasaro R, Coulon P, Hilaire G.** Prenatal activation of 5-HT2A receptor induces expression of 5-HT1B receptor in phrenic motoneurons and alters the organization of their premotor network in newborn mice. *Eur J Neurosci* 28: 1097–1107, 2008.
10. **Burnet H, Bevengut M, Chakri F, Bou-Flores C, Coulon P, Gaytan S, Pasaro R, Hilaire G.** Altered respiratory activity and respiratory regulations in adult monoamine oxidase A-deficient mice. *J Neurosci* 21: 5212–5221, 2001.
11. **Burnet H, Hilaire G.** Pulmonary stretch receptor discharges and vagal regulation of respiration differ between two mouse strains. *J Physiol* 519: 581–590, 1999.
12. **Burns JM, Cronk BB, Anderson HS, Donnelly JE, Thomas GP, Harsha A, Brooks WM, Swerdlow RH.** Cardiorespiratory fitness and brain atrophy in early Alzheimer disease. *Neurology* 71: 210–216, 2008.
13. **Caubit X, Lye CM, Martin E, Core N, Long DA, Vola C, Jenkins D, Garratt AN, Skaer H, Woolf AS, Fasano L.** Teashirt 3 is necessary for ureteral smooth muscle differentiation downstream of SHH and BMP4. *Development* 135: 3301–3310, 2008.
14. **Caubit X, Thoby-Brisson M, Voituron N, Filippi P, Bevengut M, Faralli H, Zanella S, Fortin G, Hilaire G, Fasano L.** Teashirt 3 regulates development of neurons involved in both respiratory rhythm and airflow control. *J Neurosci* 30: 9465–9476, 2010.

Downloaded from jap.physiology.org on June 11, 2011

15. **Cooke JR, Ayalon L, Palmer BW, Loredo JS, Corey-Bloom J, Natarajan L, Liu L, Ancoli-Israel S.** Sustained use of CPAP slows deterioration of cognition, sleep, and mood in patients with Alzheimer's disease and obstructive sleep apnea: a preliminary study. *J Clin Sleep Med* 5: 305–309, 2009.
16. **Daszuta A, Barrit MC, Faudon M, Gambarelli F.** Comparison of brain serotoninergic systems in C57BL and BALBc mice during development. *J Physiol (Paris)* 77: 315–318, 1981.
17. **Di Pasquale E, Monteau R, Hilaire G.** Endogenous serotonin modulates the fetal respiratory rhythm: an in vitro study in the rat. *Brain Res Dev Brain Res* 80: 222–232, 1994.
18. **Dutschmann M, Menuet C, Stettner GM, Gestreau C, Borghgraef P, Devijver H, Gielis L, Hilaire G, Van Leuven F.** Upper airway dysfunction of Tau-P301L mice correlates with tauopathy in midbrain and pontomedullary brainstem nuclei. *J Neurosci* 30: 1810–1821, 2010.
19. **Dutschmann M, Morschel M, Rybak IA, Dick TE.** Learning to breathe: control of the inspiratory-expiratory phase transition shifts from sensory- to central-dominated during postnatal development in rats. *J Physiol* 587: 4931–4948, 2009.
20. **Gargaglioni LH, Coimbra NC, Branco LG.** The nucleus raphe magnus modulates hypoxia-induced hyperventilation but not anapyrexia in rats. *Neurosci Lett* 347: 121–125, 2003.
21. **Gaspar P, Cases O, Maroteaux L.** The developmental role of serotonin: news from mouse molecular genetics. *Nat Rev Neurosci* 4: 1002–1012, 2003.
22. **Gerard M, Hernandez L, Wevrick R, Stewart CL.** Disruption of the mouse necdin gene results in early post-natal lethality. *Nat Genet* 23: 199–202, 1999.
23. **Guo X, Waern M, Sjögren K, Lissner L, Bengtsson C, Björkelund C, Ostling S, Gustafson D, Skoog I.** Midlife respiratory function and incidence of Alzheimer's disease: a 29-year longitudinal study in women. *Neurobiol Aging* 28: 343–350, 2007.
24. **Guyenet PG, Bayliss DA, Stornetta RL, Fortuna MG, Abbott SB, DePuy SD.** Retrotrapezoid nucleus, respiratory chemosensitivity and breathing automaticity. *Respir Physiol Neurobiol* 168: 59–68, 2009.
25. **Guyenet PG, Stornetta RL, Bayliss DA.** Central respiratory chemoreception. *J Comp Neurol* 518: 3883–3906, 2010.
26. **Han F, Subramanian S, Price ER, Nadeau J, Ströhl KP.** Periodic breathing in the mouse. *J Appl Physiol* 92: 1133–1140, 2002.
27. **Hilaire G, Voituron N, Menuet C, Ichiyama RM, Subramanian HH, Dutschmann M.** The role of serotonin in respiratory function and dysfunction. *Respir Physiol Neurobiol* 174: 76–88, 2010.
28. **Huang K, Rabold R, Schofield B, Mitzner W, Tankersley CG.** Age-dependent changes of airway and lung parenchyma in C57BL/6J mice. *J Appl Physiol* 102: 200–206, 2007.
29. **Imagita H, Yamano S, Tobimatsu Y, Miyata H.** Age-related changes in contraction and relaxation of rat diaphragm. *Biomed Res* 30: 337–342, 2009.
30. **Katz DM, Dutschmann M, Ramirez JM, Hilaire G.** Breathing disorders in Rett syndrome: progressive neurochemical dysfunction in the respiratory network after birth. *Respir Physiol Neurobiol* 168: 101–108, 2009.
31. **Lajard AM, Bou C, Monteau R, Hilaire G.** Serotonin levels are abnormally elevated in the fetus of the monoamine oxidase-A-deficient transgenic mouse. *Neurosci Lett* 261: 41–44, 1999.
32. **Lavie P, Lavie L.** Cardiovascular morbidity and mortality in obstructive sleep apnea. *Curr Pharm Des* 14: 3466–3473, 2008.
33. **Li A, Nattie E.** Serotonin transporter knockout mice have a reduced ventilatory response to hypercapnia (predominantly in males) but not to hypoxia. *J Physiol* 586: 2321–2329, 2008.
34. **Liu Q, Wong-Riley MT.** Postnatal changes in tryptophan hydroxylase and serotonin transporter immunoreactivity in multiple brainstem nuclei of the rat: implications for a sensitive period. *J Comp Neurol* 518: 1082–1097, 2010.
35. **Muscatelli F, Abrous DN, Massacrier A, Boccaccio I, Le Moal M, Cau P, Cremer H.** Disruption of the mouse Necdin gene results in hypothalamic and behavioral alterations reminiscent of the human Prader-Willi syndrome. *Hum Mol Genet* 9: 3101–3110, 2000.
36. **Nucci TB, Branco LG, Gargaglioni LH.** 5-HT1A, but not 5-HT2 and 5-HT7, receptors in the nucleus raphe magnus modulate hypoxia-induced hyperpnoea. *Acta Physiol (Oxf)* 193: 403–414, 2008.
37. **Nucci TB, Dias MB, Branco LG, Gargaglioni LH.** Ionotropic glutamatergic receptors in the rostral medullary raphe modulate hypoxia and hypercapnia-induced hyperpnea. *Respir Physiol Neurobiol* 175: 105–111, 2011.
38. **Paterson DS, Hilaire G, Weese-Mayer DE.** Medullary serotonin defects and respiratory dysfunction in sudden infant death syndrome. *Respir Physiol Neurobiol* 168: 133–143, 2009.
39. **Pena F, Ramirez JM.** Endogenous activation of serotonin-2A receptors is required for respiratory rhythm generation in vitro. *J Neurosci* 22: 11055–11064, 2002.
40. **Penatti EM, Barina AE, Raju S, Li A, Kinney HC, Commons KG, Nattie EE.** Maternal dietary tryptophan deficiency alters cardiorespiratory control in rat pups. *J Appl Physiol* 110: 318–328, 2011.
41. **Penatti E, Barina A, Schram K, Li A, Nattie E.** Serotonin transporter null male mouse pups have lower ventilation in air and 5% CO_2 at postnatal ages P15 and P25. *Respir Physiol Neurobiol.* In Press.
42. **Popa D, Lena C, Fabre V, Prenat C, Gingrich J, Escourrou P, Hamon M, Adrien J.** Contribution of 5-HT2 receptor subtypes to sleep-wakefulness and respiratory control, and functional adaptations in knock-out mice lacking 5-HT2A receptors. *J Neurosci* 25: 11231–11238, 2005.
43. **Price ER, Han F, Dick TE, Ströhl KP.** 7-Nitroindazole and posthypoxic ventilatory behavior in the A/J and C57BL/6J mouse strains. *J Appl Physiol* 95: 1097–1104, 2003.
44. **Pugh PL, Ahmed SF, Smith MI, Upton N, Hunter AJ.** A behavioural characterisation of the FVB/N mouse strain. *Behav Brain Res* 155: 283–289, 2004.
45. **Real C, Popa D, Seif I, Callebert J, Launay JM, Adrien J, Escourrou P.** Sleep apneas are increased in mice lacking monoamine oxidase A. *Sleep* 30: 1295–1302, 2007.
46. **Real C, Seif I, Adrien J, Escourrou P.** Ondansetron and fluoxetine reduce sleep apnea in mice lacking monoamine oxidase A. *Respir Physiol Neurobiol* 168: 230–238, 2009.
47. **Richerson GB.** Serotonergic neurons as carbon dioxide sensors that maintain pH homeostasis. *Nat Rev Neurosci* 5: 449–461, 2004.
48. **Stettner GM, Zanella S, Hilaire G, Dutschmann M.** 8-OH-DPAT suppresses spontaneous central apneas in the C57BL/6J mouse strain. *Respir Physiol Neurobiol* 161: 10–15, 2008.
49. **Stettner GM, Zanella S, Huppke P, Gärtner J, Hilaire G, Dutschmann M.** Spontaneous central apneas occur in the C57BL/6J mouse strain. *Respir Physiol Neurobiol* 160: 21–27, 2008.
50. **Tankersley CG.** Selected contribution: variation in acute hypoxic ventilatory response is linked to mouse chromosome 9. *J Appl Physiol* 90: 1615–1622, 2001.
51. **Tankersley CG, Elston RC, Schnell AH.** Genetic determinants of acute hypoxic ventilation: patterns of inheritance in mice. *J Appl Physiol* 88: 2310–2318, 2000.
52. **Tankersley CG, Fitzgerald RS, Levitt RC, Mitzner WA, Ewart SL, Kleeberger SR.** Genetic control of differential baseline breathing pattern. *J Appl Physiol* 82: 874–881, 1997.
53. **Thoby-Brisson M, Karlen M, Wu N, Charnay P, Champagnat J, Fortin G.** Genetic identification of an embryonic parafacial oscillator coupling to the preBotzinger complex. *Nat Neurosci* 12: 1028–1035, 2009.
54. **Trowbridge S, Narboux-Neme N, Gaspar P.** Genetic models of serotonin (5-HT) depletion: what do they tell us about the developmental role of 5-HT? *Anat Rec (Hoboken).* In press.
55. **Viemari JC, Roux JC, Tryba AK, Saywell V, Burnet H, Pena F, Zanella S, Bevengut M, Barthelemy-Requin M, Herzing LB, Moncla A, Mancini J, Ramirez JM, Villard L, Hilaire G.** Mecp2 deficiency disrupts norepinephrine and respiratory systems in mice. *J Neurosci* 25: 11521–11530, 2005.
56. **Voituron N, Menuet C, Dutschmann M, Hilaire G.** Physiological definition of upper airway obstructions in mouse model for Rett syndrome. *Respir Physiol Neurobiol* 173: 146–156, 2010.
57. **Voituron N, Shvarev Y, Menuet C, Bevengut M, Fasano C, Vigneault E, El Mestikawy S, Hilaire G.** Fluoxetine treatment abolishes the in vitro respiratory response to acidosis in neonatal mice. *PLoS One* 5: e13644, 2010.
58. **Voituron N, Zanella S, Menuet C, Dutschmann M, Hilaire G.** Early breathing defects after moderate hypoxia or hypercapnia in a mouse model of Rett syndrome. *Respir Physiol Neurobiol* 168: 109–118, 2009.
59. **Voituron N, Zanella S, Menuet C, Lajard AM, Dutschmann M, Hilaire G.** Early abnormalities of post-sigh breathing in a mouse model of Rett syndrome. *Respir Physiol Neurobiol* 170: 173–182, 2010.
60. **Wittmeier S, Song G, Duffin J, Poon CS.** Pacemakers handshake synchronization mechanism of mammalian respiratory rhythmogenesis. *Proc Natl Acad Sci U S A* 105: 18000–18005, 2008.
61. **Yamaguchi S, Balbir A, Schofield B, Coram J, Tankersley CG, Fitzgerald RS, O'Donnell CP, Shirahata M.** Structural and functional

Downloaded from jap.physiology.org on June 11, 2011

differences of the carotid body between DBA/2J and A/J strains of mice. *J Appl Physiol* 94: 1536–1542, 2003.

62. **Yamauchi M, Dostal J, Kimura H, Ströhl KP.** Effects of buspirone on posthypoxic ventilatory behavior in the C57BL/6J and A/J mouse strains. *J Appl Physiol* 105: 518–526, 2008.
63. **Zanella S, Tauber M, Muscatelli F.** Breathing deficits of the Prader-Willi syndrome. *Respir Physiol Neurobiol* 168: 119–124, 2009.
64. **Zanella S, Watrin F, Mebarek S, Marly F, Roussel M, Gire C, Diene G, Tauber M, Muscatelli F, Hilaire G.** Necdin plays a role in the serotonergic modulation of the mouse respiratory network: implication for Prader-Willi syndrome. *J Neurosci* 28: 1745–1755, 2008.
65. **Zhang Z, Xu F, Zhang C, Liang X.** Opioid mu-receptors in medullary raphe region affect the hypoxic ventilation in anesthetized rats. *Respir Physiol Neurobiol* 168: 281–288, 2009.

Downloaded from jap.physiology.org on June 11, 2011

2 - Le rôle de la sérotonine dans la fonction et la dysfonction respiratoires

Hilaire G., Voituron N., **Menuet C.**, Ichiyama R.M., Subramanian H.H. & Dutschmann M.

Publié dans *Respiratory Physiology & Neurobiology*, en 2010.

Résumé en français :

La sérotonine (5-HT) est un neuromodulateur-transmetteur qui influence la fonction globale du cerveau. Des découvertes passées et présentes illustrent un rôle proéminent de la 5-HT pour la modulation des circuits autonomes ponto-bulbaires. La 5-HT est également impliquée dans le contrôle de processus neurotrophiques pendant le développement pré- et postnatal des circuits neuronaux. Les implications fonctionnelles de la 5-HT sont particulièrement illustrées par les altérations du système sérotoninergique, vues dans une grande variété de désordres neurologiques. Cet article est une revue du rôle de la 5-HT dans le développement et le contrôle du réseau respiratoire dans le tronc cérébral ponto-bulbaire. Cette revue examine de manière approfondie le rôle de la 5-HT dans des désordres respiratoires qui se produisent à différentes étapes de la vie, et en particulier, les maladies neurodéveloppementales néonatales comme le Syndrome de Rett, la Mort Subite du Nourrisson et le Syndrome de Prader-Willi, ainsi que les maladies de l'adulte comme les apnées du sommeil et les désordres mentaux liés à la neurodégénérescence.

Respiratory Physiology & Neurobiology 174 (2010) 76–88

Contents lists available at ScienceDirect

Respiratory Physiology & Neurobiology

journal homepage: www.elsevier.com/locate/resphysiol

Review

The role of serotonin in respiratory function and dysfunction☆

Gérard Hilaire[a], Nicolas Voituron[a], Clément Menuet[a], Ronaldo M. Ichiyama[b], Hari H. Subramanian[b], Mathias Dutschmann[b,*]

[a] Mp3-respiration team, Centre de Recherche en Neurobiologie et Neurophysiologie de Marseille (CRN2 M), Unité Mixte de Recherche 6231, CNRS - Université Aix-Marseille II & III, Faculté Saint Jérôme 13397 Marseille Cedex 20, France
[b] Institute of Membrane and Systems Biology, Garstang Building, University of Leeds, Leeds LS2 9JT, United Kingdom

ARTICLE INFO

Article history:
Accepted 20 August 2010

Keywords:
5-HT
Respiratory rhythm
Neurodegeneration
Development
Respiratory disorders

ABSTRACT

Serotonin (5-HT) is a neuromodulator–transmitter influencing global brain function. Past and present findings illustrate a prominent role for 5-HT in the modulation of ponto-medullary autonomic circuits. 5-HT is also involved in the control of neurotrophic processes during pre- and postnatal development of neural circuits. The functional implications of 5-HT are particularly illustrated in the alterations to the serotonergic system, as seen in a wide range of neurological disorders. This article reviews the role of 5-HT in the development and control of respiratory networks in the ponto-medullary brainstem. The review further examines the role of 5-HT in breathing disorders occurring at different stages of life, in particular, the neonatal neurodevelopmental diseases such as Rett, sudden infant death and Prader–Willi syndromes, adult diseases such as sleep apnoea and mental illness linked to neurodegeneration.
Crown Copyright © 2010 Published by Elsevier B.V. All rights reserved.

1. Introduction

In the 1930s, the Italian pharmacologist Vitorio Erspamer became interested in the amine substances that are involved in smooth muscle constriction in the intestinal tracts of a variety of species including rabbits, frogs and mollusks. While studying the enterochromaffin cells of the gut, Erspamer discovered an unknown indole and named it enteramine (Erspamer and Vialli, 1937). The structure of the same indole via investigation of the blood serum was determined to be 5-hydroxytryptamine (Rapport et al., 1948). However, at a time when the theory of 'neurotransmitters' itself was controversial, it was Twarog working with Page at the Cleveland Clinic, who showed that the same substance which they named as serotonin or 5-hydroxytryptamine (5-HT) was actually found in the brain (Twarog and Page, 1953; Twarog, 1954). Finally, the emergence of 5-HT as an important chemical constituent of the central nervous system (CNS) was demonstrated by Woolley (1963), who made the best case for the participation of 5-HT in brain development, function and mental illness. In this review, we describe the role of 5-HT on breathing control in mammals. It is presently thought that the serotonergic neurons and receptors play a powerful role in setting the 'gain' of motor systems. This review will focus on the serotonergic neuronal network in the brainstem and the various pre and post-synaptic 5-HT receptors (5-HTR) that are implicated in both respiratory motor function as well as dysfunction. While it is not possible to isolate the respiratory system from the cardiovascular system (particularly when discussing the effect of 5-HT), owing to limitations of space, this review will focus mainly on breathing control. Regarding the role of 5-HT on cardiovascular function, we recommend the readers to see recent reviews by Ramage and Villalón (2008), Nalivaiko and Sgoifo (2009) and Minson et al. (1990).

2. 5-HT synthesis and neurotransmission mechanisms

5-HT is a ubiquitous neurotransmitter that is synthesized from L-tryptophan by L-tryptophan hydroxylase (Tph), a marker of 5-HT neurons, first into 5-hydroxy-tryptophan (5-HTP) and then into 5-HT (by aromatic L-amino acid decarboxylase (AaDc, see Fig. 1)) (see Gaspar, 2004; Gaspar et al., 2003). After its release, 5-HT acts on a plethora of 5-HTR and is degraded into 5-hydroxyindolacetic acid (5-HIAA) by monoamine oxydase A (MAOA) in the synaptic cleft. In addition, 5-HT is also recaptured by the 5-HT membrane transporter (SERT) and stored in vesicles by the vesicular monoamine transporter (Vmat2). Tph, the initial and rate-limiting enzyme in 5-HT biosynthesis, is irreversibly inactivated by nitric oxide (Kuhn and Arthur, 1996, 1997) and inhibited by hypoxia (Rahman and Thomas, 2009; Poncet et al., 1997; Hedner et al., 1978). This deserves to be noted as a reduction of 5-HT biosynthesis may contribute, at least in part, to the complex effects of nitric oxide or hypoxia.

☆ This paper is part of a special issue entitled "Central cardiorespiratory regulation: physiology and pathology", guest-edited by Thomas E. Dick and Paul M. Pilowsky.

* Corresponding author. Tel.: +44 113 3432593; fax: +44 113 3434228.
E-mail address: M.dutschmann@leeds.ac.uk (M. Dutschmann).

1569-9048/$ – see front matter. Crown Copyright © 2010 Published by Elsevier B.V. All rights reserved.
doi:10.1016/j.resp.2010.08.017

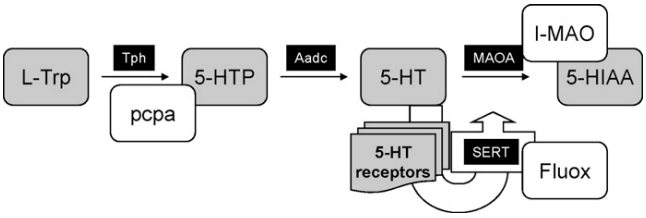

Fig. 1. Schematic illustration of 5-HT biosynthesis and neurotransmission. L-tryptophan (L-Trp) is transformed in 5-hydroxytryptophan (5-HTP) by the enzyme tryptophan hydroxylase (Tph) and subsequently into serotonin (5-HT) by the enzyme aromatic L-amino acid decarboxylase (Aadc). In normal conditions, the rate-limiting step of the 5-HT biosynthesis is Tph and not Aadc. After 5-HT release re-uptake is mediated via the serotonin transporter (SERT) and is degraded in 5-hydroxy-indol acetic acid (5-HIAA) by the enzyme monoamine oxydase A (MAOA). Common pharmacological tools used to alter the 5-HT biosynthesis such as p-chlorophenylalanine (pcpa) which blocks 5-HT synthesis, MAOA inhibitors (I-MAOA) which block the degradation and the antidepressant fluoxetine which blocks 5-HT re-uptake are also illustrated.

Gaddum and Picarelli (1957) proposed first the existence of two types of 5-HTR subtypes, which they termed M and D. Since then, it has become evident from the pharmacological, electrophysiological and DNA-cloning experiments that the serotonergic system comprises of multiple 5-HTRs. In fact, the 5-HTR subtypes cloned to date represent the largest known neurotransmitter receptor families. These subtypes are expressed in distinct, but often overlapping patterns (Palacios et al., 1990), coupled to different transmembrane signaling mechanisms (Table 1). The currently accepted classification scheme (Hoyer et al., 1994) proposes seven sub-families of 5-HTR: the 5-HT_{1A}R coupled to G_i proteins, the 5-HT_2R coupled to G_Q proteins, the gated ion channel 5-HT_3R, and the heterogeneous groups of 5-HT_4R–5-HT_7R. In particular, the $5HT_{1A}$R are also known to be located at pre-synapses to provide auto-inhibition and fine tuning of serotonergic activity. Moreover, 5-HT may act via non-synaptic mechanisms via 5-HT "en passant" release from varicosities. Varicose axonal arborizations are found in almost every 5-HT immunoreactive fibers in the CNS (Leger et al., 2001) indicating possible non-synaptic action of 5-HT in almost every brain area. Serotonergic neurotransmission via hitherto identified 5-HTRs modulate the activity of brainstem cardio-respiratory circuits (Table 1).

2.1. Location of serotonergic neurons in the brain

5-HT content was first related to specific neuronal elements in the brain based on lesion and sub-cellular fractionation studies (see Cooper et al., 1991). The direct examination of 5-HT containing cellular processes became possible via the application of formaldehyde-induced fluorescence histochemistry (known as the Falck and Hillarp method; Falck, 1962; Falck et al., 1962). Despite this application, the mapping of 5-HT cells was slow (as compared to say, the mapping of catecholamine) because the 5-HT fluorophore develops less efficiently and also fades rapidly under fluorescent microscopy (see Cooper et al., 1991). In the recent years, the mapping of 5-HT in the brain has greatly improved through combined application of immunohistochemistry (via both direct purification of tryptophan hydroxylase as well as 5-HT), of orthograde axoplasmic transport of radiolabelled amino acids microinjected into identified 5-HT cells via fluorescence histochemistry and via retrograde isolation of 5-HT neurons from suspected terminal fields. It should be specially mentioned here that the basic organization of 5-HT cells originally described by Dahlström and Fuxe (1964) stands to this day. As a result of subsequent extensive studies in the last decade, a good map of 5-HT neurons in the brain has been developed (Steinbusch, 1981; Steinbusch et al., 1981; Steinbusch and Mulder, 1984; Tork and Hornung, 1990; Jacobs and Azmitia, 1992; Hornung, 2003). 5-HT cells are found exclusively in the brainstem in distinct cell groups classified as the raphe (Fig. 2). The dorsal raphe nuclei and superior central nucleus are located in the midbrain, the pontine raphe nuclei and inferior central nucleus in the pons, while the caudal raphe, namely the raphe pallidus, raphe magnus and raphe obscurus are located in the medulla. Immunocytochemical localization of 5-HT has also identified 5-HT reactive neurons in the area postrema, in the caudal locus coeruleus, around the interpeduncular nucleus and in the parapyramidal region of the ventral medulla (Steinbusch and Mulder, 1984).

2.2. Afferent inputs and projections of serotonergic neurons in the brain

The brainstem raphe nuclei receive afferents from a large number of brain structures (Hermann et al., 1996, 1997). Significantly, these projections include inputs to the nucleus raphe magnus,

Table 1
Serotonin receptors found in the brainstem cardio-respiratory networks.

Subtype	Signalling cascades	Physiological effects	Localization	Cardiorespiratory sites	Central function
$5HT_{1A}$	$G_{i/o}$ proteins	Increase K^+ conductance	Pre- and post-synaptic	Raphe nuclei hypoglossal nuclei ponto-medullary networks	Inhibit cell firing depresses excitability of respiratory neurons
$5HT_{1B}$	$G_{i/o}$ proteins	Increase K^+ conductance	Pre- and post-synaptic	Raphe nuclei	Inhibit cell firing neurotransmitter release control
$5HT_{1D}$	$G_{i/o}$ proteins	Increase K^+ conductance	Axon terminals of both 5HT and non-5HT neurons	Dorsal raphe midbrain PAG	Behavioral breathing control?
$5HT_{1E/1F}$	$G_{i/o}$ proteins	Unknown	Unidentified	Unidentified	Not known
$5HT_{2A/2B/2C}$	$G_{q/11}$ proteins	Decrease K^+ conductance	Unidentified	Ponto-medullary networks (2A/2B)	Neuronal excitation
$5HT_3$	Ionotropic	Gating of K^+, Na^+	Somato-dendritic/sub-cellular?	NTS area prostrema dorsal motor nucleus of vagus	Neuronal excitation vomitting reflex
$5HT_4$	G_s proteins	Decrease K^+ conductance	Post-synaptic	Pre-Botzinger complex	Neuronal excitation neurotransmitter release control
$5HT_5$	$G_{i/o}$ or G_s proteins	Unknown	Unidentified	Unidentified	Not known
$5HT_6$	G_s proteins	Unknown	Post-synaptic in higher brains	Unidentified	Not known
$5HT_7$	G_s proteins	Decrease K^+ conductance	Unidentified	Dorsal raphe pre-Botzinger complex	Neuronal excitation

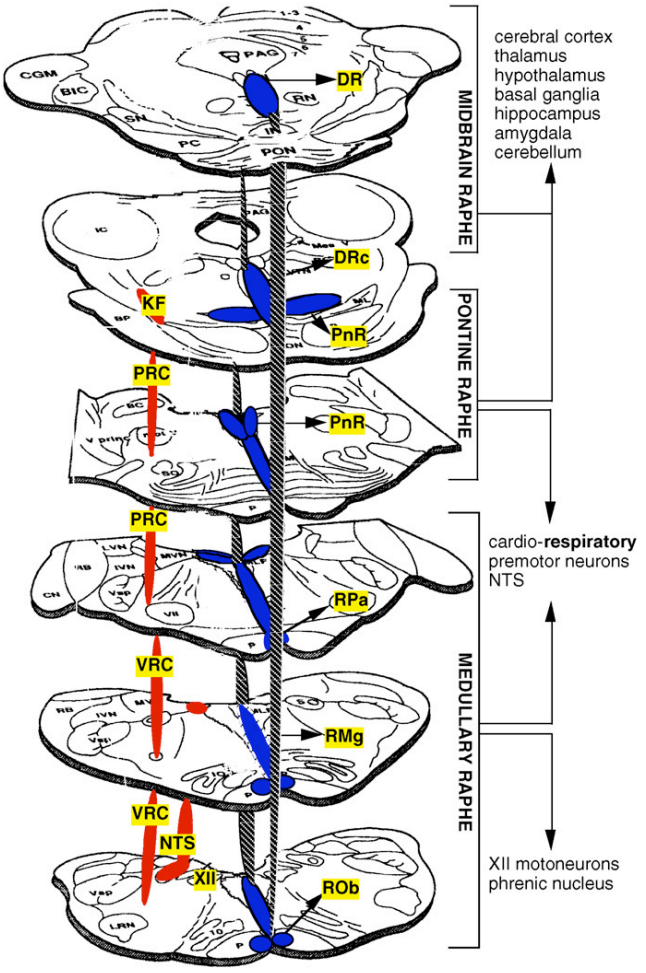

Fig. 2. Distribution and connectivity of serotonin neurons in the brainstem. Neurons synthesizing 5-HT are found in distinct cell groups called as the raphe in the brainstem. These cells form a column along the midline extending from the caudal medulla to the midbrain. The raphé neurons project to virtually all regions of the neuraxis. The hashed line is intended to elucidate the columnar structure of the raphe system along the midline. The red regions indicate the respiratory columns. Rob: raphe obscurus; RMg: raphe magnus; RPa: raphe pallidus; PnR: pontine raphe nuclei; DRc: caudal dorsal raphe; DR: dorsal raphe; VRC: ventral respiratory column; NTS: nucleus tractus solitari; PRC: pontine respiratory column; KF: Kölliker-Fuse; XII: hypoglossal motor nuclei; PAG: periaqueductal gray.

nucleus raphe pallidus and the dorsal raphe from the prelimbic, infralimbic and precentral cortices, dorsal hypothalamic area, the midbrain periaqueductal gray, pre-optic area, bed nucleus of the stria terminalis, amygdala, parabrachial nucleus, Kölliker-Fuse and the subcoerulus area in the pons. The caudal raphe receives a small number of projections from the insular and perirhinal cortices, the periaqueductal gray and the pontine reticular nuclei. The brainstem 5-HT cell groups project virtually to all areas of the brain (Steinbusch and Mulder, 1984). The caudal raphe projects mainly to the medulla and the spinal cord, the pontine raphe projects both to the medulla along the ventral and dorsal tegmental field, the pontine respiratory column and the Kölliker-Fuse nucleus (KF), as well as to the midbrain and cerebellar areas, while the dorsal raphe in the midbrain provides extensive 5-HT innervation of the telencephalon and the diencephalon. In particular, the caudal raphe (raphe pallidus, raphe magnus and raphe obscurus) cell projections have been well identified (and are of special interest as they modulate brainstem cardio-respiratory output). They project extensively to the pontine and ventral respiratory columns (PRC and VRC), in particular to the parabrachial area, KF, nucleus ambiguous (NA), retrotrapezoid nucleus (RTN), Botzinger (BotC) and preBotzinger (PreBotC) regions, hypoglossal motor nucleus in the medulla and phrenic nucleus in the cervical spinal cord (Steinbusch, 1981; Steinbusch et al., 1981; Steinbusch and Mulder, 1984; Holtman et al., 1986, 1987; Holtman, 1988; Connely et al., 1989; Smith et al., 1989; Zhan et al., 1989; Pilowsky et al., 1990; Voss et al., 1990; Jacobs and Azmitia, 1992; Manaker and Tischler, 1993). In general, the serotonergic termination fields tend to overlap, this may be because many investigations used electrolytic or chemical lesions to study cell projections. This can also interrupt fibers of passage. Also, in the past, attempts to localize 5-HT terminals relied mainly on the 5-HT analogue uptakes, 5-HT selective toxins or radiolabelling of 5-HT. These techniques depend heavily on the specificity of the uptake processes. Hence, for discrete mapping of the 5-HT neuronal terminations more orthograde and retrograde studies are required. The main projections of the serotonergic cell groups to the brainstem cardio-respiratory nuclei are summarized in Fig. 2.

2.3. Role of 5-HT in the modulation of respiratory rhythm and motor pattern

Reid and Rand (1951) were perhaps the first to note the direct involvement of 5-HT in the central regulation of breathing. They reported that intravenous injection of 5-HT causes apnea in the cat. A follow-up study extended these findings showing that small amounts of 5-HT injected into the carotid sinus region induced a brief apnea followed by respiratory stimulation and a fall in blood pressure (Ginzel and Kottegoda, 1954). Similar experiments attempted in dogs (Douglan and Toh, 1953) reported the contrary. In dogs, intravenous injection of 5-HT caused stimulation of breathing. Interestingly, in their experiments (Douglan and Toh, 1953) while intra-arterial injection of 5-HT did not cause any respiratory effect, direct injections into the heart (either into the right auricle or left ventricle) or into the carotid body region caused a respiratory increase. Vagotomy, however, did not influence the respiratory increase caused by intravenous 5-HT injection. Combined, these two studies showed that there could be a species difference in the respiratory responses to 5-HT (Page, 1952; Page and McCubbin, 1953; Schneider and Yonkman, 1954). However, denervation of carotid sinus abolished the respiratory (and cardiovascular) effects originally induced via intravenous injection. Hence, a general consensus evolved that 5-HT acts either on the chemo or baroreceptors and that they may not be centrally mediated. This was corroborated by evidence obtained in humans at that time (Page and McCubbin, 1953; Michelson et al., 1958; Parks et al., 1960) that respiratory changes due to intravenous injection of 5-HT were due to a direct action of the drug on the receptors located on the arterial side of systemic circulation.

Subsequently, several studies (Olsen et al., 1979; McCrimmon and Lalley, 1982; Dempsey et al., 1987; Morin et al., 1990; Monteau and Hillaire, 1991; Lindsay and Feldman, 1993) established that 5-HT is an important neuromodulator of breathing. Perhaps a definitive role for the direct action of 5-HT on the CNS was demonstrated by Fallert et al. (1979) where microelectrophoretic application of 5-HT directly on the medullary respiratory neurons changed the neuronal activity pattern. They showed that while neurons showing inspiratory–expiratory phase spanning (IE cells) were excited following 5-HT microinjection, other inspiratory neurons became inhibited. Lalley et al. (1994a) reported that the 5-HT agonists 5-MeODMT had a differential action on the respiratory system depending upon the dose and route of administration. For example, small dosage of 5-MeODMT intravenously injected increased the discharge frequency of inspiratory and expiratory neurons while larger dosage iontophoretically administered onto respiratory neu-

rons caused acute hyperpolarization and reduced action potential discharges. Another study (Lalley et al., 1995) reported that iontophoresis of α-Me-5-HT a 5-HT_2R agonist depolarized membrane potential and increased the frequency of action potentials in most of the ventrolateral medullary respiratory neurons and in particular the E2 and postinspiratory neurons. Later investigations showed that depression of expiratory neural discharges arising from stimulation of the raphe obscurus involved both pre-and post-synaptic 5-HT_{1A}R (Lalley et al., 1997). Recent studies from Richter's laboratory has revealed that the inhibitory or excitatory effects of systemic 5-HT administration strongly depend on the expression profile of 5-HTR on specific populations of respiratory neurons (Manzke et al., 2008, 2009). In particular, the expression of G_i coupled 5-HT_{1A}R on glycinergic interneurones within the ventral respiratory column (VRC) could explain the paradoxical excitatory effect of the putative inhibitory 5-HTR subtype (Manzke et al., 2009).

Despite *in vivo* investigations generalizing the excitatory or inhibitory effects of 5-HT on medullary respiratory neurons, the precise pre-synaptic action which induces either excitation or inhibition as well as the selective post-synaptic modulation that fine tunes the responses of respiratory neurons to various neurotransmitters are yet to be elucidated. Owing to the highly diversified effect of the 5-HT system on respiratory neurons, its direct impact on the medullary respiratory rhythm generator has still not been fully defined. In this regard investigations undertaken on highly reduced *in vitro* preparations have started to provide emerging principles of 5-HT action. Of significance are investigations conducted using *in vitro* models by Morin et al. (1990, 1992) and Lindsay and Feldman (1993). Morin et al. (1990) used an *in vitro* brainstem-spinal cord preparation of the newborn rat to study the central effects of 5-HT. They reported that 5-HT facilitates the respiratory rhythm generating networks in the medulla via 5-HT_{1R} and the motoneurons through 5-HT_2R. In a follow-up study Di Pasquale et al. (1992) reported a landmark finding that 5-HT acts at the medullary level and its effect is due to its specificity on the rostral VRC areas and not due to any diffuse action on all medullary respiratory centers, although the A5 area in the caudal pons may also contribute. In addition, spinal 5-HT_{1B}R located at the pre-synaptic level modulates the transmission of the central drive to phrenic motoneurons (Di Pasquale et al., 1997). Further studies examined the effect of 5-HT on both hypoglossal and phrenic motoneurons (Morin et al., 1992; Lindsay and Feldman, 1993). While 5-HT depressed hypoglossal activity (Morin et al., 1992), its influence increased phrenic motoneuronal activity (Morin et al., 1992; Lindsay and Feldman, 1993) with several cells firing tonically even during expiration. The *in vitro* studies also allowed for a selective analysis of the influence of 5-HT on central respiratory activity during pre- and postnatal development (for details see below). For example, three different effects of 5-HT via medullary 5-HT_{1A}R, spinal 5-HT_{2A}R and spinal 5-HT_{1B}R modulating the frequency and amplitude of the phrenic motoneuron discharge in neonatal rats (Fig. 3) have been confirmed in neonatal mice (Bou-Flores et al., 2000).

Intrinsic ionic mechanisms (for example calcium activated potassium conductance) regulate the firing of serotonergic neurons (Burlhis and Aghajanian, 1987; see Aghajanian et al., 1990). A recent study (Rockhill et al., 2009) has found that that spontaneous activity propagation in the mouse midbrain originates from the midline serotonergic cell bodies during early embroyonic stage. These findings suggest that 5-HT cells may possess tonic pacemaker properties, which may in turn be modulated by two neurotransmitters: (1) norepinephrine acting through adrenergic receptors and (2) 5-HT acting through somatodendritic 5-HT_{1A} autoreceptors. While norepinephrine action excites the pacemaker, 5-HT action is inhibitory (see Aghajanian et al., 1990). Thus, the coupling of raphe nuclei serotonergic pacemakers to medullary respiratory rhythm generators should be explored in the future.

2.4. Serotonergic neurotransmission in the control of blood gas homeostasis, body temperature and circulation

Besides the neuromodulatory role of 5-HT in shaping and modulating central respiratory function (for details see Section 2.4), 5-HT also plays a prominent role in other autonomic circuits linked to breathing. Of particular interest is the 5-HT control of CO_2/pH homeostasis. Although it is commonly admitted that the RTN/pFRG neurons have a crucial role in mediating ventilatory responses to CO_2/pH changes (Guyenet et al., 2009; Onimaru et al., 2009), 5-HT neurons also contribute to the central chemosensitivity (Corcoran et al., 2009; Richerson, 2004; Hodges and Richerson, 2010). 5-HT neurons located in close proximity to arteries entering the brainstem, may detect changes in arterial CO_2 and thus contribute to the adaptation of the central respiratory drive to environmental changes. In *in vitro* preparations 5-HT neurons have been shown to be intrinsically chemosensitive. 5-HT cells increase their firing rate in response to hypercapnia and focal acidosis of the raphe nuclei *in vivo* (Bernard et al., 1996; Nattie and Li, 2001; Feldman et al., 2003) while specific lesions of raphe 5-HT neurons reduce the respiratory response to hypercapnia (Nattie et al., 2004; Dias et al., 2007). In the chemosensitive RTN/pFRG area, SERT and 5-HTR expressions have been reported, revealing a dense 5-HT innervation that possibly constitutes the anatomical substrate for 5-HT-dependent control of RTN/pFRG chemoceptors (Liu and Wong-Riley, 2010; Mulkey et al., 2007; Rosin et al., 2006). Further, the ventilatory response to hypercapnia is reduced in SERT knock-out mice, especially in males (Li and Nattie, 2008). As well, lmx1b and Pet-1 knock-out mice causing near-complete deletion of serotonergic neurons in the brain have altered respiratory responses to CO_2/pH (Erickson et al., 2007; Hodges et al., 2008). CO_2/pH related changes in transgenic mice are potentially also due to compensatory mechanisms occurring during ontogeny and thus may not relate solely to the absence of 5-HT.

5-HT also plays an important role in arterial oxygen sensing of carotid body chemoceptors (see Prabhakar et al., 2006). In MAOA-KO mice, the excess of 5-HT decreases the ventilatory responses to hypoxia (Burnet et al., 2001), suggesting that the excessive 5-HT affects the responsiveness of the central respiratory network to hypoxia. However, microdialysis of the 5-HT_{1A}R agonist 8-OHDPAT in the medullary raphe does not affect the ventilatory responses to hypoxia (Taylor et al., 2005). Perhaps the impaired ventilatory responses to hypoxia of MAOA-KO mice originates from an effect of the excessive 5-HT on the responsiveness of carotid bodies chemoceptors to hypoxia and/or on the central relay of peripheral hypoxic inputs. The latter possibility is more likely as hypoxia induces a release of 5-HT in the NTS area, possibly contributing to the early ventilatory response to hypoxia (Kanamaru and Homma, 2009). Nevertheless, it was also shown that 5-HT is dynamically released within the medullary VRC during the hypoxic respiratory depression (Richter et al., 1999).

The raphé nuclei play a major role in thermoregulation (Blessing and Nalivaiko, 2000; Morrison et al., 2008; McAllen et al., 2010) which is also substantiated via the use of transgenic mouse line Lmx1b, lacking almost all central 5-HT neurons. The Lmx1b mice become rapidly hypothermic when exposed to cold environment because of impaired shivering and non-shivering thermogenesis, although they retain normal thermosensory perception and heat conservation (Hodges et al., 2008). In these mice, mild cold stress compromises ventilatory control as a result of defective thermogenesis (Hodges and Richerson, 2008, 2010). In the dorsolateral pons, the lateral parabrachial nucleus may be pivotal in processing central chemoreceptor inputs and cutaneous thermoreceptor inputs,

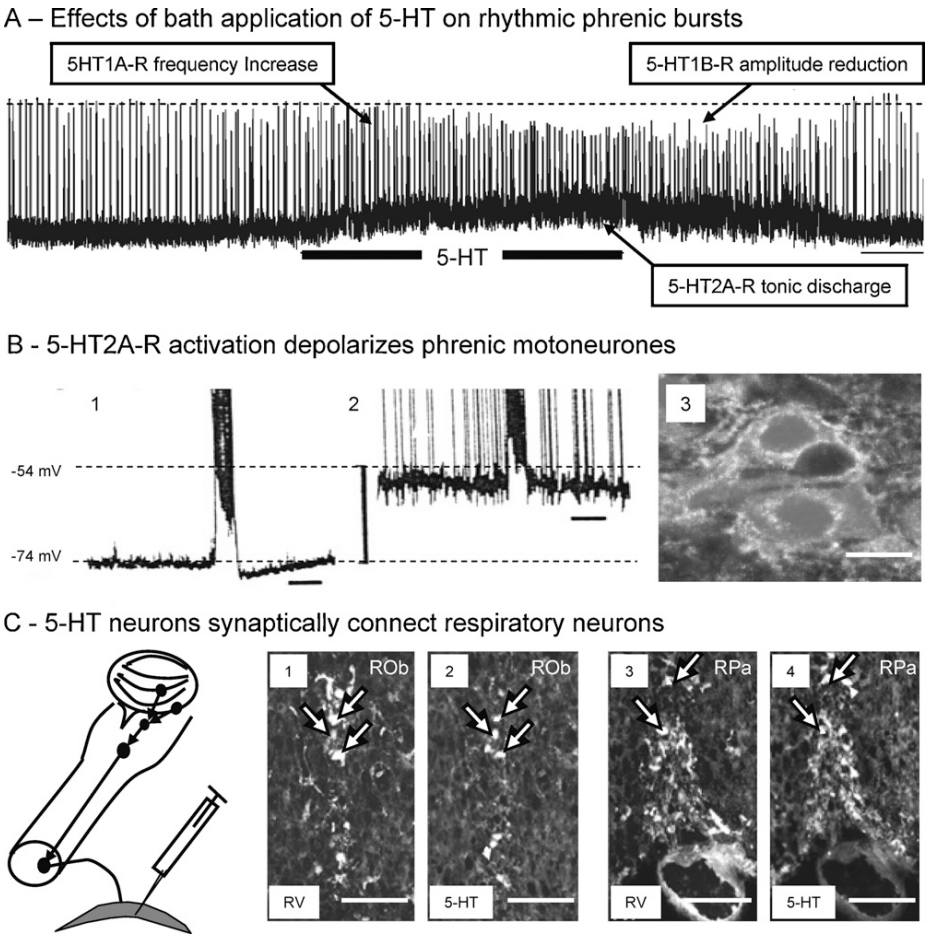

Fig. 3. 5-HT modulation of neonatal respiratory activity.
A) Traces showing *in vitro* phrenic bursts recorded from *en bloc* preparations of neonatal mice and changes evoked following bath application of 25 μM 5-HT (horizontal bar). Note that 5-HT application induced complex effects characterized by an increase in phrenic burst frequency (due to activation of medullary 5-HT_{1A}R), a tonic discharge of motoneurons (due to activation of spinal 5-HT_{2A}R) and a reduction in phrenic burst amplitude (due to a possible pre-synaptic activation of spinal 5-HT_{1B}R). Scale bar: 1 min (see Bou-Flores et al., 2000).
B) 5-HT_{2A}R activation depolarizes phrenic motoneurons. Intracellular recording of a phrenic motoneuron before (B1) and after 5-HT application (B2). 5-HT induced a 20 mV depolarization and a tonic firing of the motoneuron (time scale: 1 s; spikes truncated). B3: Immunohistochemistry reveals that neonatal phrenic motoneurons (retrogradely labelled with rhodamine) widely express 5-HT_{2A}R (white dots). Calibration bar: 20 μm. (see also Bras et al., 2008).
C) 5-HT neurons synaptically coupled with respiratory neurons. Schematic drawing illustrates medullary neurons that project to phrenic motoneurons in neonatal mice after rabies virus (RV) inoculated in the diaphragm at P1. After RV inoculation in the diaphragm, RV progressively infected neurons controlling phrenic motoneuronal output. Thirty hours after inoculation phrenic motoneurons were labeled. After 36 h neurons in the VRC revealed labeling and after 42 h infected neurons were observed in histochemically identified 5-HT neurons of the raphe nuclei obscurus (1–2) and pallidus (3–4). These experiments illustrate the synaptic connectivity of raphe 5-HT neurons with phrenic premotor neurons in the VRC. Calibration bars: 100 μm. (also see Zanella et al., 2008).

with 5-HT inputs contributing to gate the spino-parabrachial thermoafferent pathway for an optimal interaction of respiratory and thermal regulation (Poon, 2009).

3. 5-HT and respiratory disorders

To understand respiratory dysfunction connected with 5-HT it is important to examine the role of 5-HT during prenatal development of neuronal circuits because many respiratory disorders are of neurodevelopmental origin (see Section 3.2). 5-HT neurons are amongst the earliest to be expressed during embryogenesis. They develop from embryonic days 10–12 (E10–12) in mice and ring the first month of gestation in primates (Gaspar et al., 2003; Gaspar, 2004). They are generated in rhombomeres r1–r3 and r5–r7 caudal to the midbrain–hindbrain organizer under the control of the fibroblast growth factors 4 and 8 (Fgf4 and Fgf8) and sonic hedgehog (Shh) from precursors in the ventricular zone (Fig. 4). The combined action of the secreted positional markers Shh, Fgf4 and Fgf8 defines the dorso–ventral positioning of 5-HT somata within the CNS. Nkx2.2, downstream of Shh, could be implicated in the specification of the caudal 5-HT neurons, probably in conjunction with Gata3.

In post-mitotic neurons, the 5-HT phenotype is determined by a sequence of genes such as Pet1, Lmx1b, Nkx2.2, Mash1, Gata2, Gata3, and Phox2b forming a transcriptional network (Fig. 4) specifying the differentiation of 5-HT neurons (Alenina et al., 2006). It is interesting to note that Phox2b, a crucial gene for the production of enzymes for catecholamine biosynthesis, also plays a pivotal role in the selection between a motoneuron and a 5-HT neuronal fate (Pattyn et al., 2003).

During development, expression of Lmx1b precedes Pet1. Lmx1b knock-out mice lack all central 5-HT neurons (Ding et al., 2003) whereas Pet1 knock-out mice have a loss of 70–80% of central 5-HT neurons (Hendricks et al., 1999, 2003). In Lmx1b conditional knock-out mice in which Lmx1b was only deleted in Pet1-expressing 5-HT neurons, the initial generation of central 5-

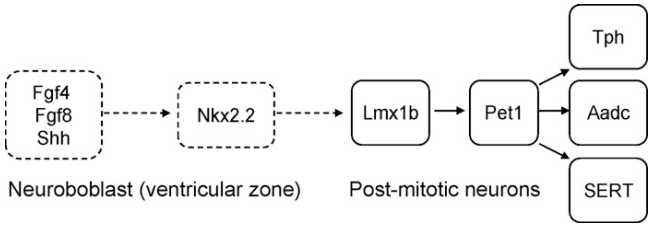

Fig. 4. Genetic determination and genesis of 5-HT neurons.
During the early embryogenesis 5-HT neurons are generated from ventricular zone precursors controlled by fibroblast growth factors 4 and 8 (Fgf4 and Fgf8) and sonic hedgehog (Shh). In post-mitotic neurons, a complex network of genes such as Pet1, Lmx1b, Nkx2.2, Mash1, Gata2, Gata3, and Phox2b will determine the important proteins for 5-HT biosynthesis and neurotransmission such as Tph, Aadc, SERT (for details see Fig. 1).

HT neurons is normal and the mice survive, although they lack almost all central 5-HT neurons at later stages of development (Zhao et al., 2006). Thus, Lmx1 and Pet1 contribute to establishing the enzymatic machinery required for the production of 5-HT (Zhao et al., 2006). Two isoforms of Tph exist that produce 5-HT in the periphery (Tph1) and CNS (Tph2) (Nakamura and Hasegawa, 2007). Pet1 expression is strictly limited to the raphe nuclei and appears 1 day before the 5-HT neurons can be identified as it contributes to the formation of Tph and SERT. SERT and Vmat2 may be expressed in glutamatergic neuronal subpopulations which may take-up and store 5-HT released from neighbouring 5-HT terminals, even though they do not express Tph and do not synthesize 5-HT (Lebrand et al., 1996, 1998). This is mostly the case in developing thalamic neurons of neonatal rodents (Lebrand et al., 1996, 1998) and in the locus coeruleus, the medial and lateral parabrachial, and KF of adult cats where 5-HT containing neurons have been reported (Léger et al., 1979).

As discussed previously (see Gaspar et al., 2003; Gaspar, 2004; Nakamura and Hasegawa, 2007; Kinney et al., 2007), the early expressed 5-HT neurons affect via 5-HT release, several developmental processes such as cell division, migration, differentiation and synaptogenesis. From this view-point it is possible to suggest that 5-HT contributes to the formation and function of all the central networks. As early as E11.5 when rhombomeric segmentation disappears in mice, 5-HT neurons of the developing midline raphe system and 5-HT_{2A}R already play a role in initiating and propagating spontaneous, rhythmic and synchronous activity throughout the hindbrain (Hunt et al., 2005). It cannot be excluded that these early (E11.5) 5-HT-related rhythmic events which occur at a slow rate (about two cycles per minute) contribute to the emergence of the embryonic respiratory rhythm a few days later; first at the level of the embryonic parafacial group (E14.5) and one day later at the Pre-Bötzinger complex level (Thoby-Brisson et al., 2009; Fortin and Thoby-Brisson, 2009). Hence, 5-HT may play a role in the maturation of central networks, including the brainstem respiratory network and the respiratory rhythm generator. In MAOA-deficient mice (Cases, 1996), the lack of MAOA degradation of 5-HT results in excess of endogenous 5-HT, with levels of 5-HT during the foetal and neonatal periods 5–10-fold higher than in control mice (Lajard et al., 1999). This perinatal excess of 5-HT is not lethal, but alters behaviour of MAOA-deficient mice (Cases, 1996) and the formation of several neuronal networks. The excess of 5-HT in MAOA-deficient mice affects the formation of somatosensory maps (Cases et al., 1996), retinal projections to the dorsal lateral geniculate nucleus (Upton et al., 1999), spinal locomotor network (Cazalets et al., 2000) and brainstem respiratory network (Bou-Flores et al., 2000). Excessive 5-HT in MAOA-deficient mice alters the organization of the distal dendritic tree of phrenic motoneurons, the expression of 5-HT_{1A}R and 5-HT_{1B}R and the synaptic organization of the medullary respiratory neurons (Bou-Flores et al., 2000; Lanoir et al., 2006; Bras et al., 2008). Indeed, transient alterations in 5-HT homeostasis during development may modify the wiring of network connections and may permanently affect behaviours (Nakamura and Hasegawa, 2007) and as well, the 5-HTR expression. 5-HTRs are expressed early in embryonic life and are dynamically regulated during the perinatal development by 5-HT availability, the latter being regulated via SERT. SERT is the primary target for widely used antidepressants.

3.1. Neurodevelopmental disorders linked to 5-HT system alterations

Identified alterations of the 5-HT system play a major role in dysfunctions of the central respiratory network associated with neurodevelopmental disorders. This review is focused on the Rett Syndrome (RTT; Katz et al., 2009) and the Prader–Willi Syndrome (PWS; Zanella et al., 2008, 2009) as prime examples for neurodevelopmental diseases while others such as congenital central hypoventilation syndrome are reviewed elsewhere (see Amiel et al., 2009). Finally, despite the lack of an understanding of gene mutation(s) underlying sudden infant death syndrome (SIDS) we review it under the section of neurodevelopmental disorders concerning breathing as 5-HT may play a critical role in the onset of SIDS.

3.1.1. Rett syndrome

Rett syndrome (RTT) (OMIM312750) is a neurodevelopmental disease with low prevalence (see Katz et al., 2009) where infants, after an apparently normal perinatal period, enter a stage of regression and develop neurologic symptoms involving respiratory deficits. This includes erratic respiratory rhythm and life-threatening apnoeas. RTT mainly concerns girls and approximately 25% of RTT patients may die prematurely from cardio-respiratory failure. RTT results from mutations in the gene encoding methyl-CpG-binding protein 2 (Mecp2), one of many of methyl-binding proteins that regulate gene expression by repressing transcription at methylated promoters.

Breathing abnormalities are amongst the essential criteria prescribed for the diagnosis of RTT. The respiratory symptoms are more severe during wakefulness than sleep (Weese-Mayer et al., 2006, 2008) and are exacerbated by emotions and behavioural arousal. As mutations in MECP2 are responsible for most cases of RTT, mouse models have been generated in which Mecp2 is either deleted, mutated or overexpressed. Several mouse models for RTT are now available, presenting breathing defects reminiscent of RTT. In $Mecp2^{-/y}$ mice, with extended exonic deletion of the Mecp2 gene, breathing pattern is normal from birth to P30 although they show subtle abnormalities of post-sigh breathing (Voituron et al., 2010a) and respiratory responses to environmental challenges (Voituron et al., 2009). After P30 $Mecp2^{-/y}$ develops breathing symptoms, with an erratic rhythm and life-threatening apnoeas aggravating with age until respiratory distress and death occurs at about P60 (Viemari et al., 2005). *In situ* studies using a perfused brainstem preparation revealed that apnoeas at P45 correlate with discharges of laryngeal adductor motor output causing upper airway closure (Stettner et al., 2007). These findings indicated that apnoeas in $Mecp2^{-/y}$ could be interpreted as breath-hold. Recent data from our labs have now confirmed the occurrence of active breath-holds in $Mecp2^{-/y}$ *in vivo* (Voituron et al., 2010b).

The breathing symptoms of $Mecp2^{-/y}$ mice are thought to reflect respiratory dysfunction caused by alterations in several neurochemical systems, including the 5-HT system (Katz et al., 2009). In $Mecp2^{-/y}$ mice, the number of 5-HT neurons is normal but HPLC measurements have revealed reduced levels of 5-HT in the brain and the medulla. In addition, comparison of mRNAs encoding 5-HT metabolic enzymes, 5-HTR subtypes and the 5-HT transporter in

respiratory-related areas of WT and Mecp2$^{-/y}$ mice has revealed significant decreases in mutant mice by P40 (Manzke et al., 2008). As the alterations of the 5-HT system are detected at a rather late developmental stage, they are unlikely linked to initiating the breathing deficits but they may still contribute to the expression of breathing instability.

3.1.2. Prader–Willi syndrome

Prader–Willi syndrome (PWS) (OMIM 176270) is a rarely occurring (prevalence 1/25000) multi-genetic and neurodevelopmental disorder (Zanella et al., 2009). PWS patients develop complex neurologic deficits that advance with age. Amongst the first deficit is a marked neonatal hypotonia leading to feeding problems followed by hyperphagia at later stages leading to obesity during childhood. In addition, hypothalamic dysfunction results in growth hormone deficiency, hypogonadism, dysautonomy, learning disabilities, behavioral and psychiatric problems. PWS patients also display breathing disorders, including frequent sleep apnoeas and attenuated ventilatory response to hypoxia and hypercapnia (Nixon and Brouillette, 2002; Festen et al., 2006). Since these breathing disorders appear well before obesity, and it is hypothetised that the deficits are present at birth (Zanella et al., 2008).

PWS is caused by the loss of the paternal expression of several genes of the 15q11-q13 family. Among several mutant mice generated as model for PWS, *Necdin* deficient mice (*Ndn*-KO) display respiratory disorders similar to that seen in PWS (but not obesity) (Zanella et al., 2008). This suggests that the human *Necdin* gene may be responsible for the breathing symptoms associated with PWS.

In vivo and *in vitro* approaches revealed dysfunctions of the central respiratory network of *Ndn*-KO. First, *in vivo* plethysmography at P2 reveals that *Nd*n-ko neonates (compared to WT littermates) have a highly variable respiratory rhythm, frequent apnoeas and attenuated responses to hypoxia and hypercapnia. Secondly, the isolated respiratory network of Ndn-ko neonates (compared to WT littermates) produce a variable respiratory rhythm, frequent apnoeas, weak response to hypoxia and a paradoxical reduction of the respiratory rhythm under 5-HT application. The central respiratory network of neonatal *Ndn*-KO mice does not seem to work appropriately at birth, consistent with results obtained in *Ndn*-ko foetuses (Ren et al., 2003). In mice, the Necdin allele is expressed in the maturing CNS as early as E10.5, with a peak expression between P0 and P4. *Ndn* mRNA is expressed in the cortex, the hypothalamus and several brainstem respiratory networks, such as the NTS, the hypoglossal motor nucleus and the VRC, but not in the pre-Bötzinger complex or the RTN/pFRG areas. Interestingly, high levels of *Ndn* mRNA (Lee et al., 2003) and proteins have been detected in most 5-HT neurons examined in the medulla (Zanella et al., 2008). Using Rabies Virus to retrogradely label the respiratory network after inoculation into the diaphragm revealed that 5-HT neurons expressing *Necdin* were synaptically connected to the medullary respiratory network controlling the diaphragm. The number of 5-HT neurons in WT and *Ndn*-KO neonates does not reveal a significant difference, revealing that Ndn is not crucial for 5-HT neurons maturation and survival. However, 5-HT concentrations in the medulla of WT and Necdin-KO neonates are more than 50% increased in *Ndn*-KO compared to WT (Zanella et al., 2008). These findings suggest that excess in endogenous 5-HT in *Ndn*-KO mice alters the maturation of the central respiratory network, leading to persistent anomalies in respiratory rhythmogenesis and regulation. The same may occur in PWS patients and is supported by evidence of abnormal levels of 5-HT metabolites in the cerebrospinal fluid and abnormal MAOA activity in platelets (Akefeldt et al., 1998). In addition, treatments targeting 5-HT systems have been used in PWS patients and have shown significant alleviation of some symptoms but nothing is known about the effects of 5-HT treatment on breathing symptoms of PWS patients (Goldstone, 2004).

3.1.3. Sudden infant death syndrome (SIDS)

SIDS is defined as the sudden and unexpected death of an infant (<12 months) that remains unexplained despite a complete autopsy and post-mortem examination. SIDS is the leading cause of infant death in industrialized countries, with twice as many boys than girls and the peak incidence occurring at 2–4 months. SIDS is of multi-origin and its actual neurogenic cause remains unknown. However, a recent review (see Paterson et al., 2009) proposes that prenatal alterations of the maturing 5-HT system weaken the robustness of the neonatal respiratory system, which increases the risk of SIDS. The commonly accepted hypothesis is that SIDS occurs when three factors simultaneously impinge on the infant: (1) an underlying vulnerability, (2) a developmental window (the 2–4 months critical period), and (3) several environmental factors heightening the infant vulnerability (e.g. face-down sleeping position, bed sharing, warm environment, prenatal exposure to drugs, nicotine, alcohol). A consensus has been reached that infant vulnerability may be related to an altered respiratory control during sleep, possibly including reduced chemoreceptor sensitivity, abnormal rhythmogenesis causing failure to initiate inspiration and/or gasping. A common scenario is that SIDS is facilitated by hypercapnia/hypoxia from re-breathing exhaled air as a result of sleeping in the face-down position in a warm bedroom. However, the precise nature of the trigger(s) for SIDS remains unknown.

Post-mortem examination have revealed that an important subset of SIDS infants (approximately 70% of studied cases) have abnormalities of different 5-HT markers in the brainstem (Paterson et al., 2006, 2009; Duncan et al., 2010). As the 5-HT system affects maturation and function of the respiratory network, as well as sleep and thermoregulation, such 5-HT anomalies may induce alterations/dysfunctions of the respiratory system, which may contribute to SIDS during the critical developmental window in conjunction with environmental stressors. A pioneering study reported abnormal levels of 5-HT metabolites found in the cerebrospinal fluids of SIDS infants (Caroff et al., 1992). Since then multiple abnormalities of the 5-HT system have been observed in SIDS victims, such as an increased number of 5-HT neurons, reduced expression of 5-HT$_{1A}$R and 5-HT$_{2A}$R, reduced 5-HT binding, abnormal Tph expression, reduced brain 5-HT levels and altered 5-HT turnover (Paterson et al., 2009). As in rodents, 5-HT neurons in humans are expressed early in embryogenesis, as early as the 7th gestational week (Kinney et al., 2007). Post-mortem tract-tracing reveal that human 5-HT neurons send axonal projections to brainstem respiratory-related areas such as the NTS and the hypoglossal motor nucleus, where the presence of SERT, 5-HT$_{1A}$R, and 5-HT$_{2A}$R binding sites have been demonstrated. In addition, NK1-positive neurons in the putative PreBötzC area of infants express 5-HT$_{1A}$R and 5-HT$_{2A}$R (see Fig. 3 in Paterson et al., 2009). Consistent with the developmental role of 5-HT in central respiratory networks, SIDS can be linked to mal-development of 5-HT circuits during the early foetal life, which may become fatal later after birth.

Recent studies have screened for the genetic basis of 5-HT anomalies that may play a role in SIDS. First, significant differences in genotype distribution and allele frequency of the SERT promoter gene were found in a Japanese SIDS and control infants groups, with more frequent L and XL alleles in SIDS infants (Narita et al., 2001). As the L allele induces a more efficient 5-HT re-uptake than the S allele, 5-HT availability at the synaptic cleft and 5-HT modulation of the respiratory network might be reduced in SIDS victims. SERT gene anomalies in SIDS cases are also observed in other ethnic groups (Weese-Mayer et al., 2003a,b). PHOX2B is an important gene for the production of essential enzymes for catecholamine biosynthesis and for the selection between motoneuron

and 5-HT neuronal fate in the embryonic CNS. A study (Rand et al., 2006) suggests a potential relationship between the 5HT system, PHOX2B, and SIDS. However, genetic variations of genes for the 5-HT_{1AR} and 5-HT_{2AR} were reported unlikely to be responsible for the 5-HT system alterations observed in SIDS victims (Morley et al., 2008; Rand et al., 2009). Thus, significant changes in 5-HT_{1AR} and 5-HT_{2AR} expression observed in SIDS victims could be a secondary effect in a global autonomic circuit instability. On the other hand, genetically induced over-expression of 5-HT_{1AR} in mice induce sporadic bradycardia and hypothermia, frequently progressing to death, suggesting that excessive 5-HT auto-inhibition and altered 5-HT homeostasis are risk factors for SIDS (Audero et al., 2008). In addition, besides 5-HT deficits, catecholaminergic deficits may occur, altering the noradrenergic modulation of the respiratory network and therefore increasing SIDS risks (Hilaire, 2006).

3.2. Respiratory dysfunction connected to alteration of 5-HT system with unclear genetic background

Here we summarize the implication of 5-HT in breathing disorders which are not explicitly linked to a genetic cause and show onset during different stages of life. Examples of these disease types include breathing abnormalities linked to neurodegenerative diseases (e.g. dementia), sleep apnoea syndromes and panic disorders. Importantly, all these diseases may have a genetic pre-disposition and with the disease onset and expression influenced by epigenetics. However these genetic/epigenetic factors are not yet well understood.

3.2.1. Sleep apnoea syndrome (SAS)

As already outlined the 5-HT system is a potent modulator of neuronal circuits that control breathing. However, 5-HT has also strong implication in the regulation of the sleep-wake cycle (Popa et al., 2005). Alterations of the 5-HT system that affect both respiration and sleep may contribute to SAS. In fact compelling experimental evidence has accumulated supporting a crucial role of the 5-HT system in the generation of apnoeic events.

First, subjecting anaesthetized neonatal rats to intraperitoneal injection of L-tryptophan, which activates the 5-HT biosynthesis, increases 5-HT levels and induces transient apnoeas. Some of these apnoeas showed airways obstructions (Hilaire et al., 1993). Application of 5-HT or other serotonergic drugs to the IVth ventricle in decerebrated kittens also induces apnoeas (Khater-Boidin et al., 1996). Also, transgenic mice lacking 5-HT_{2A}R showed increased incidence for SAS (Popa et al., 2005). Finally, increasing 5-HT levels in WT mice by pharmacological blockade of the 5-HT degradation also increased the number of sleep apnoeas (Real et al., 2007). MAOA-KO mice linked to excess of 5-HT display frequent apnoeas and their numbers can be reduced by treatment to block 5-HT biosynthesis (Real et al., 2007) or by enhancing 5-HT (Real et al., 2009). C57/BL6 mice spontaneously produce transient breath-holds characterized by glottal closure (Stettner et al., 2008a) and the incidence of these active breath-holds could be decreased with application of the 5-HT_{1A}R agonist 8-OH DPAT (Stettner et al., 2008b).

In humans most of the sleep apnoeas are considered to be obstructive sleep apneas (OSA). This specific type of sleep apnoea is caused by a decreased tone of the upper airway muscles during sleep. In connection with predisposing factors such as unfavourable upper airway anatomy and obesity, upper airway atonia can cause physical obstruction to respiratory airflow thus leading to repetitive apnoeas during sleep. OSA is now recognized as a major disorder and an important cause of medical morbidity and mortality affecting millions of people worldwide. For example OSA is considered to be the most common respiratory disorder in adults and concerns >20 million people in the USA alone (Lavie and Lavie, 2008). OSAs have pre-dispositions to hypertension, cardiovascular disease, stroke, and even sexual dysfunction. Pharmacological management of sleep apnoea remains a major problem (see Abad and Guilleminault, 2006) and modulation and stabilization of the 5-HT system is a prime target. Studies of control subjects and medically healthy recreational users of "ecstasy" (a popular recreational drug and a selective brain 5-HT neurotoxin) suggest that brain 5-HT dysfunction may play a causal role in the pathophysiology of sleep apnoeas (McCann et al., 2009). Another clinical study involving SAS patients and healthy controls in Chinese Han population has suggested that SERT gene may be involved in susceptibility to SAS (Yue et al., 2008).

3.2.2. Neurodegenerative disease

Neurodegenerative diseases and dementia are characterized by cognitive, behavioural and emotional deficits. However, despite breathing dysfunction being a major problem in these neurodegenerative diseases and dementia, respiratory deficits receive less attention compared to the loss of memory. In fact Subramanian et al. (2008) have suggested that the elimination of the midbrain periaqueductal gray (PAG) control of brainstem respiratory networks may contribute to the animals (and humans) inability to express emotions as seen in very many neurodegenerative behavioural disorders. Thus, it could well be that breathing dysfunction may play a major role in cognitive, behavioural and emotional impairments.

In fact dementia patients suffer from sleep-disordered breathing, with the common cascade of repeated transient apnoea and hypoxemia, disrupted sleep, day-time fatigue along with decreased cognitive abilities (Bliwise, 2002, 2004; Cooke et al., 2006). Possible links between sleep-disordered breathing and dementia are supported by the advent of mental impairment in persons suffering from sleep-disordered breathing and subsequent cognitive improvement with continuous positive airway pressure treatment (Cooke et al., 2009a,b). The development of dementia in persons retaining a good respiratory function at midlife has been found to be low (Guo et al., 2007). The correlation between cardio-respiratory fitness and reduced brain atrophy in dementia patients has also been reported (Burns et al., 2008). These findings reveal that respiratory disorders may not be a secondary factor as commonly assumed in dementia.

More direct evidence for neurodegeneration of brainstem respiratory networks is provided by the finding of tauopathy in monoaminergic nuclei (Parvizi et al., 2001), raphe nuclei (Rüb et al., 2000; Grinberg et al., 2009), pontine parabrachial nuclei (Rüb et al., 2001) and medullary reticular formation (Attems et al., 2007). A recent study from our laboratories showed for the first time that tauopathy in the above mentioned brain-areas is also found in the transgenic mouse line Tau-P301L (Dutschmann et al., 2010). In this specific mouse line, tauopathy was most prevalent in the pontine respiratory group (e.g. parabrachial nuclei) and midbrain periaqueductal grey, which are involved in supra-medullary respiratory control and specifically in upper airway patency and upper airway related behaviours (Dutschmann et al., 2004; Gestreau et al., 2005; Subramanian et al., 2008). Dense *tauopathy* was also observed in the medullary raphe nuclei providing the main source of 5-HT mediated modulation of central breathing circuits, while the primary pattern and rhythm generating nuclei of the VRC were largely devoid of tauopathy (Dutschmann et al., 2010). This selective pattern of tauopathy is also reflected in the breathing phenotype of the animals. Upper airway dysfunction affects the laryngeal airflow control particularly during increased chemical drive in the respiratory network in response to hypercapnia (Dutschmann et al., 2010). The identified activation of the laryngeal adductors during the inspiratory phase may not only impair airflow and oxygen uptake but also other important upper airway behaviours such as vocal-

isation or swallowing which were not tested in the study. Upper airway disorders are common features in various forms of dementias. For instance, progressive aphasia is a frontotemporal dementia associated with downstream motor speech deficits (Hillert, 1999). In addition, laryngeal adductors are essential for laryngeal closure during swallowing preventing aspiration of food or fluids into the lungs. Dysphagia and aspiration pneumonia belong to the most serious and common complications in dementia patients (Kalia, 2003).

Amongst neurodegenerative diseases multiple systems atrophy (MSA) is most closely linked to cardio-respiratory function. MSA is linked to severe autonomic failure leading to sudden death. Hallmarks of MSA amongst endocrine and cardiovascular disturbances are OSA and laryngeal stridor (Benarroch, 2002, 2007). Autopsy of MSA victims show changes in the various catchelomaniergic cell groups and brainstem raphe nuclei (Benarroch et al., 2004, 2007). These changes in the serotonergic system could directly relate to the upper airway phenotype, since experimental evidence shows that serotonergic inputs from the medullary raphe facilitate activity of inspiratory laryngeal abductor motoneurons (Berkowitz et al., 2005; Sun et al., 2002). Thus, loss of serotonergic inputs to laryngeal motorneurones of nucleus ambiguus could explain the sleep related upper airway disorders not only in MSA but also dementia patients.

Disease related alteration of the 5-HT system may also contribute to behavioural symptoms (Rüb et al., 2000; Grinberg et al., 2009) in dementia. Autopsy of dementia patients reveals normal numbers of 5-HT neurons in the dorsal raphe nuclei (Hendricksen et al., 2004) but abnormal density of 5-HT_{1A} and 5-HT_{2A}R (Yeung et al., in press) in pons and medulla. In the cortex of AD patients 5-HT_{1A}R alteration was found in correlation with aggressive behaviours (Lai et al., 2003) and a reduced density of 5-HT_4R expression connected to hyperphagia (Tsang et al., 2010). The reduced density of 5-HT_{2A}R found post-mortem in patients was confirmed in the anterior cingulate cortex of a small sample of living patients with Alzheimer's disease (AD), although 5-HT_{2A}R binding was found normal (Santhosh et al., 2009). Also, a reduction of SERT binding was observed in the cortex of dementia patients by PET, consistently with a 5-HT dysfunction affecting higher centers of cognition and emotion (Ouchi et al., 2009).

Certain SERT inhibitors and drugs targeting 5-HTR have been tested in neurodegenerative diseases (Lauterbach et al., 2010; Neugroschl and Sano, 2010). However, no conclusive data on effective treatment of behavioural symptoms in dementia are published and potential effects of SERT inhibitors on upper airway dysfunction or sleep apnoea are not tested as yet.

3.2.3. Mental disorders linked to disturbed breathing: a role for 5-HT

Amongst a variety of mental disorders the panic disorder is considered most directly to be linked to an aberration in the control of respiration (Klein, 1993; Nardi et al., 2009). Contrary to other anxiety related disorders panic disorder is often characterized by respiratory symptoms, such as hyperventilation and shortness of breath (Nardi et al., 2009). Moreover, patients with panic disorder were reported to show increased respiratory variability between panic attacks (Gorman et al., 1988; Martinez et al., 2001) even during sleep (Stein et al., 1995). Interestingly, patients also display hypersensitivity to CO_2 (Papp et al., 1993). Whether the breathing abnormalities are causal to specific changes in neuronal circuits sensitive to CO_2 (potentially including the medullary raphe) remains undetermined. Evidence that changes in the 5-HT system may be indirectly implicated in the breathing abnormality arise from the established finding that long-term treatment with 5-HT reuptake inhibitors can alleviate panic attacks. However, direct evidence of pathological changes in 5-HT system from autopsy is not yet available and to our knowledge an animal model for panic disorder is not currently established.

4. Therapeutic use of serotonergic drugs in central respiratory dysfunction

The targeted use of serotonergic drugs to treat centrally mediated respiratory disorders is sparse. The use of the 5-HT_{1A}R agonist buspirone was successful in the treatment of severe apneusis occurring in a child after ponto-medullary surgery (Wilken et al., 1997). Further, it has been shown that breathing stabilizes in a RTT patient after buspirone administration (Andaku et al., 2005). The use of 5-$HT_{2/3}$R antagonist significantly reduces the apnoea index in sleep apnoea patients but also reveals sedation and weight-gain as unwarranted side effects (Carley et al., 2007). A recent placebo controlled clinical trial completely failed to show effective treatment of respiratory abnormality in panic disorder (Coryell and Rickels, 2009).

Besides the largely unsatisfactory results in clinical trials, experimental evidence proposes interesting future avenues for the use of serotonergic drugs in central respiratory disturbance and failure. For example, 5-HT_4R and 5-HT_{1A}R agonists have been shown to compensate central respiratory disturbances including apneusis or apnoeic periods in the experimental settings (El-Khatib et al., 2003; Lalley et al., 1994a,b; Manzke et al., 2003, 2009; Sahibzada et al., 2000; Stettner et al., 2008a,b; Wilken et al., 1997; Yamauchi et al., 2008; Guenther et al., 2009). Specifically 5-HT_4R and 5-HT_{1A}R agonists may have a broader applicability in the treatment of opioid mediated respiratory arrest. Opioids are currently the most powerful analgesics available to treat pain but their use is limited by side effects including the risk of fatal apnoea. Recent evidence provided by Diethelm Richter's group suggest that 5-HT_4R or 5-HT_{1A}R mediated recovery of μ-opioid receptor evoked respiratory depression or even total arrest (Manzke et al., 2003, 2009). The use of a 5-HT_{1A}R agonist has been shown to evoke breathing recovery following opioid induced respiratory depression in awake rodents (Dutschmann et al., 2009). However it needs to be mentioned that preliminary test in humans failed to produce similar beneficial effect on opioid evoked respiratory depression (Lötsch et al., 2005; Oertel et al., 2007).

In summary, the discrepancies between promising effect of serotonergic drugs on various central breathing instabilities as seen in animal models and the comparable results as seen in human trials remain. One reason for the unpredictability of serotonergic drug treatment is related to pronounced pre-synaptic autoinhibitory mechanism, which fine tunes afferent synaptic inputs to 5-HT neurons. For instance the block of 5-HT re-uptake can lead to increased activation of pre-synaptic 5HT_{1A}R of the raphe nuclei by endogenous 5-HT. This in turn suppresses synaptic drive to 5HT neurons consequently reducing 5-HT release in central nervous system. Therefore a drug aiming to potentiate the action the 5-HT system does not produce the warranted net-effect in the brain. Future breakthroughs in drug design may help to tailor serotonergic drugs to specifically target respiratory disorder with minimal impact on other physiological systems.

5. Conclusion

Compelling experimental evidence shows that the 5-HT plays a crucial role in the central control of breathing. Disease-related alterations of 5-HT system (linked to genetic and/or environmental factors) induce severe breathing disorders occurring at different stages in life, ranging form the early postnatal period with SIDS, neurodevelopmental disorders and to neurodegenerative disease in the elderly and ageing. The wide range of neurologic diseases

correlate to several differential mechanisms through which 5-HT may affect the respiratory system. There is much to be deciphered on the precise mechanism through which 5HT mediates respiratory function (and dysfunction) and the future is bright and forthcoming.

Acknowledgments

This study was supported by NHLBI (Cluster Grant R33HL087377, M.D., and H.H.S.) and the Agence National de la Recherche (NV 2009-2010 fellowship to N.V.)

References

Abad, V.C., Guilleminault, C., 2006. Pharmacological management of sleep apnoea. Expert Opin. Pharmacother. 7, 11–23.
Aghajanian, G.K., Sprouse, J.S., Sheldon, P., Rasmussen, K., 1990. Electrophysiology of the central serotonin system: receptor subtypes and transducer mechanisms. Ann. N. Y. Acad. Sci. 600, 93–103.
Akefeldt, A., Ekman, R., Gillberg, C., Månsson, J.E., 1998. Cerebrospinal fluid monoamines in Prader-Willi syndrome. Biol. Psychiatry 44, 1321–1328.
Alenina, N., Bashammakh, S., Bader, M., 2006. Specification and differentiation of serotonergic neurons. Stem Cell Rev. 2, 5–10.
Amiel, J., Dubreuil, V., Ramanantsoa, N., Fortin, G., Gallego, J., Brunet, J.F., Goridis, C., 2009. PHOX2B in respiratory control: lessons from congenital central hypoventilation syndrome and its mouse models. Respir. Physiol. Neurobiol. 168, 125–132.
Andaku, D.K., Mercadante, M.T., Schwartzman, J.S., 2005. Buspirone in Rett syndrome respiratory dysfunction. Brain Dev. 27, 437–438.
Attems, J., Quass, M., Jellinger, K.A., 2007. Tau and alpha-synuclein brainstem pathology in Alzheimer disease: relation with extrapyramidal signs. Acta Neuropathol. 113, 53–62.
Audero, E., Coppi, E., Mlinar, B., Rossetti, T., Caprioli, A., Banchaabouchi, M.A., Corradetti, R., Gross, C., 2008. Sporadic autonomic dysregulation and death associated with excessive serotonin autoinhibition. Science 321 (5885), 130–1333.
Benarroch, E.E., 2002. New findings on the neuropathology of multiple system atrophy. Auton. Neurosci. 96, 59–62.
Benarroch, E.E., Schmeichel, A.M., Low, P.A., Parisi, J.E., 2004. Involvement of medullary serotonergic groups in multiple system atrophy. Ann. Neurol. 55, 418–422.
Benarroch, E.E., 2007. Brainstem respiratory control: substrates of respiratory failure of multiple system atrophy. Mov. Disord. 22, 155–161.
Benarroch, E.E., Schmeichel, A.M., Sandroni, P., Parisi, J.E., Low, P.A., 2007. Rostral raphe involvement in Lewy body dementia and multiple system atrophy. Acta Neuropathol. 114, 213–220.
Berkowitz, R.G., Sun, Q.J., Goodchild, A.K., Pilowsky, P.M., 2005. Serotonin inputs to laryngeal constrictor motoneurons in the rat. Laryngoscope 115, 105–109.
Bernard, D.G., Li, A., Nattie, E.E., 1996. Evidence for central chemoreception in the midline raphé. J. Appl. Physiol. 80, 108–115.
Blessing, W.W., Nalivaiko, E., 2000. Regional blood flow and nociceptive stimuli in rabbits: patterning by medullary raphe, not ventrolateral medulla. J. Physiol. 524, 279–292.
Bliwise, D.L., 2002. Sleep apnea, APOE4 and Alzheimer's disease 20 years and counting? J. Psychosom. Res. 53, 539–546.
Bliwise, D.L., 2004. Sleep disorders in Alzheimer's disease and other dementias. Clin. Cornerstone 6 (Suppl. 1A), S16–S28.
Bou-Flores, C., Lajard, A.M., Monteau, R., De Maeyer, E., Seif, I., Lanoir, J., Hilaire, G., 2000. Abnormal phrenic motoneuron activity and morphology in neonatal monoamine oxidase A-deficient transgenic mice: possible role of a serotonin excess. J. Neurosci. 20, 4646–4656.
Bras, H., Gaytán, S.P., Portalier, P., Zanella, S., Pásaro, R., Coulon, P., Hilaire, G., 2008. Prenatal activation of 5-HT2A receptor induces expression of 5-HT1B receptor in phrenic motoneurons and alters the organization of their premotor network in newborn mice. Eur. J. Neurosci. 28 (6), 1097–1107.
Burlhis, T.M., Aghajanian, G.K., 1987. Pacemaker potentials of serotonergic dorsal raphe neurons: contribution of a low-threshold Ca2+ conductance. Synapse 1, 582–588.
Burnet, H., Bevengut, M., Chakri, F., Bou-Flores, C., Coulon, P., Gaytan, S., Pasaro, R., Hilaire, G., 2001. Altered respiratory activity and respiratory regulations in adult monoamine oxidase A-deficient mice. J. Neurosci. 21 (14), 5212–5221.
Burns, J.M., Cronk, B.B., Anderson, H.S., Donnelly, J.E., Thomas, G.P., Harsha, A., Brooks, W.M., Swerdlow, R.H., 2008. Cardiorespiratory fitness and brain atrophy in early Alzheimer disease. Neurology 71, 210–216.
Carley, D.W., Olopade, C., Ruigt, G.S., Radulovacki, M., 2007. Efficacy of mirtazapine in obstructive sleep apnea syndrome. Sleep 30, 35–41.
Caroff, J., Girin, E., Alix, D., Cann-Moisan, C., Sizun, J., Barthelemy, L., 1992. Neurotransmission and sudden infant death. Study of cerebrospinal fluid. C R Acad. Sci. III 314 (10), 451–454.
Cases, O., Seif, I., Grimsby, J., Gaspar, P., Chen, K., Pournin, S., Müller, U., Aguet, M., Babinet, C., Shih, J.C., Cases, O., Vitalis, T., Seif, I., De Maeyer, E., Sotelo, C., Gaspar, P., 1996. Lack of barrels in the somatosensory cortex of monoamine oxidase A-deficient mice: role of a serotonin excess during the critical period. Neuron 16, 297–307.
Cazalets, J.R., Gardette, M., Hilaire, G., 2000. Locomotor network maturation is transiently delayed in the MAOA-deficient mouse. J. Neurophysiol. 83, 2468–2470.
Connely, C.A., Elllenberger, H.H., Feldman, J.L., 1989. Are there serotonergic projections from raphe and retrotrapezoid nuclei to the ventral respiratory group in the rat? Neurosci. Lett. 105, 30–40.
Cooke, J.R., Liu, L., Natarajan, L., He, F., Marler, M., Loredo, J.S., Corey-Bloom, J., Palmer, B.W., Greenfield, D., Ancoli-Israel, S., 2006. The effect of sleep-disordered breathing on stages of sleep in patients with Alzheimer's disease. Behav. Sleep Med. 4, 219–227.
Cooke, J.R., Ayalon, L., Palmer, B.W., Loredo, J.S., Corey-Bloom, J., Natarajan, L., Liu, L., Ancoli-Israel, S., 2009a. Sustained use of CPAP slows deterioration of cognition, sleep, and mood in patients with Alzheimer's disease and obstructive sleep apnea: a preliminary study. J. Clin. Sleep Med. 5, 305–309.
Cooke, J.R., Ancoli-Israel, S., Liu, L., Loredo, J.S., Natarajan, L., Palmer, B.S., He, F., Corey-Bloom, J., 2009b. Continuous positive airway pressure deepens sleep in patients with Alzheimer's disease and obstructive sleep apnea. Sleep Med. 10 (10), 1101–1106.
Cooper, J.R., Bloom, F.E., Roth, R.H., 1991. The Biochemical Basis of Neuropharmacology. Ox Uni Press, Oxford.
Corcoran, A.E., Hodges, M.R., Wu, Y., Wang, W., Wylie, C.J., Deneris, E.S., Richerson, G.B., 2009. Medullary serotonin neurons and central CO2 chemoreception. Respir. Physiol. Neurobiol. 168, 49–58.
Coryell, W., Rickels, H., 2009. Effects of escitalopram on anxiety and respiratory responses to carbon dioxide inhalation in subjects at high risk for panic disorder: a placebo-controlled, crossover study. J. Clin. Psychopharmacol. 29, 174–178.
Dahlström, A., Fuxe, K., 1964. Evidence for the existence of monoamine-containing neurons in the central nervous system. I. Demonstration of monoamines in the cell bodies of brain stem neurons. Acta Physiol. Scand. 62 (Suppl. 232), 1–55.
Dempsey, J.A., Olsen, E.B., Skatrud, J.B., 1987. Hormones and neurochemicals in the regulation of breathing. In: Fishman, A.P., Cherniak, N.S., Widdicombe, J.G., Geiger, S.R. (Eds.), The Handbook of Physiology – The Respiratory System II. APS, Washington DC, pp. 181–221, Chapter 7.
Di Pasquale, E., Morin, D., Monteau, R., Hilaire, G., 1992. Serotonergic modulation of the respiratory rhythm generator at birth: an in vitro study in the rat. Neurosci. Lett. 143, 91–95.
Di Pasquale, E., Lindsay, A., Feldman, J.L., Monteau, R., Hilaire, G., 1997. Serotonergic inhibition of phrenic motoneuron activity: an in vitro study in neonatal rat. Neurosci. Lett. 230, 29–32.
Dias, M.B., Nucci, T.B., Margatho, L.O., Antunes-Rodrigues, J., Gargaglioni, L.H., Branco, L.G., 2007. Raphe magnus nucleus is involved in ventilatory but not hypothermic response to CO2. J. Appl. Physiol. 103 (5), 1780–1788.
Ding, Y.Q., Marklund, U., Yuan, W., Yin, J., Wegman, L., Ericson, J., Deneris, E., Johnson, R.L., Chen, Z.F., 2003. Lmx1b is essential for the development of serotonergic neurons. Nat. Neurosci. 6 (9), 933–938.
Douglan, W.W., Toh, C.C., 1953. The respiratory stimulamnt action of 5-Hydroxytryptamine (serotonin) in the dog. J. Physiol. 120, 311–318.
Duncan, J.R., Paterson, D.S., Hoffman, J.M., Mokler, D.J., Borenstein, N.S., Belliveau, R.A., Krous, H.F., Haas, E.A., Stanley, C., Nattie, E.E., Trachtenberg, F.L., Kinney, H.C., 2010. Brainstem serotonergic deficiency in sudden infant death syndrome. JAMA 303, 430–437.
Dutschmann, M., Mörschel, M., Kron, M., Herbert, H., 2004. Development of adaptive behaviour of the respiratory network: implications for the pontine Kolliker-Fuse nucleus. Respir. Physiol. Neurobiol. 143, 155–165.
Dutschmann, M., Waki, H., Manzke, T., Simms, A.E., Pickering, A.E., Richter, D.W., Paton, J.F., 2009. The potency of different serotonergic agonists in counteracting opioid evoked cardiorespiratory disturbances. Philos. Trans. R Soc. Lond. B Biol. Sci. 364, 2611–2623.
Dutschmann, M., Menuet, C., Stettner, G.M., Gestreau, C., Borghgraef, P., Devijver, H., Gielis, L., Hilaire, G., Van Leuven, F., 2010. Upper airway dysfunction of Tau-P301L mice correlates with tauopathy in midbrain and ponto-medullary brainstem nuclei. J. Neurosci. 30, 1810–1821.
El-Khatib, M.F., Kiwan, R.A., Jamaleddine, G.W., 2003. Buspirone treatment for apneustic breathing in brain stem infarct. Respir. Care 48, 956–958.
Erickson, J.T., Shafer, G., Rossetti, M.D., Wilson, C.G., Deneris, E.S., 2007. Arrest of 5HT neuron differentiation delays respiratory maturation and impairs neonatal homeostatic responses to environmental challenges. Respir. Physiol. Neurobiol. 159, 85–101.
Erspamer, V., Vialli, M., 1937. Ricerche sul secreto delle cellule enterocromaffini. Boll. d Soc. Med-chir Pavia. 51, 357–363.
Falck, B., 1962. Observations on the possibilities of the cellular localization of monoamines by a fluorescence method. Acta Physiol. Scand. 56 (Suppl. 197), 1–25.
Falck, B., Hillarp, N.A., Thieme, G., Torp, A., 1962. Fluorescence of catechol amines and related compounds condensed with formaldehyde. J. Histochem. Cytochem. 10, 348–354.
Fallert, M., Böhmer, G., Dinse, H.R., Sommer, T.J., Bittner, A., 1979. Microelectrophoretic application of putative neurotransmitters onto various types of bulbar respiratory neurons. Arch. Ital. Biol. 117, 1–12.
Feldman, J.L., Mitchell, G.S., Nattie, E.E., 2003. Breathing: rhythmicity, plasticity, chemosensitivity. Annu. Rev. Neurosci. 26, 239–266.
Festen, D.A., de Weerd, A.W., van den Bossche, R.A., Joosten, K., Hoeve, H., Hokken-Koelega, A.C., 2006. Sleep-related breathing disorders in prepubertal children with Prader-Willi syndrome and effects of growth hormone treatment. J. Clin. Endocrinol. Metab. 91 (12), 4911–4915.
Fortin, G., Thoby-Brisson, M., 2009. Embryonic emergence of the respiratory rhythm generator. Respir. Physiol. Neurobiol. 168, 86–91.

Gaddum, J.H., Picarelli, Z.P., 1957. Two kinds of tryptamine receptors. Br. J. Pharmacol. 12, 323–328.
Gaspar, P., Cases, O., Maroteaux, L., 2003. The developmental role of serotonin: news from mouse molecular genetics. Nat. Rev. Neurosci. 4 (12), 1002–1012.
Gaspar, P., 2004. Genetic models to understand how 5-HT acts during development. J. Soc. Biol. 198, 18–21.
Gestreau, C., Dutschmann, M., Obled, S., Bianchi, A.L., 2005. Activation of XII motoneurons and premotor neurons during various oropharyngeal behaviors. Respir. Physiol. Neurobiol. 147, 159–176.
Ginzel, K.H., Kottegoda, S.R., 1954. The action of 5-hydroxytryptamine and tryptamine on aortic and carotid sinus receptors in the cat. J. Physiol. 123, 277–288.
Goldstone, A.P., 2004. Prader-Willi syndrome: advances in genetics, pathophysiology and treatment. Trends Endocrinol. Metab. 15, 12–20.
Gorman, J.M., Fyer, M.R., Goetz, R., Askanazi, J., Liebowitz, M.R., Fyer, A.J., Kinney, J., Klein, D.F., 1988. Ventilatory physiology of patients with panic disorder. Arch. Gen. Psychiatry 45, 31–39.
Grinberg, L.T., Rüb, U., Ferretti, R.E., Nitrini, R., Farfel, J.M., Polichiso, L., Gierga, K., Jacob-Filho, W., Heinsen, H., Brazilian Brain Bank Study Group, 2009. The dorsal raphe nucleus shows phospho-tau neurofibrillary changes before the transentorhinal region in Alzheimer's disease. A precocious onset? Neuropathol. Appl. Neurobiol. 35, 406–416.
Guenther, U., Manzke, T., Wrigge, H., Dutschmann, M., Zinserling, J., Putensen, C., Hoeft, A., 2009. The counteraction of opioid-induced ventilatory depression by the serotonin 1A-agonist 8-OH-DPAT does not antagonize antinociception in rats in situ and in vivo. Anesth. Analg. 108, 1169–1176.
Guo, X., Waern, M., Sjögren, K., Lissner, L., Bengtsson, C., Björkelund, C., Ostling, S., Gustafson, D., Skoog, I., 2007. Midlife respiratory function and incidence of Alzheimer's disease: a 29-year longitudinal study in women. Neurobiol. Aging 28, 343–350.
Guyenet, P.G., Bayliss, D.A., Stornetta, R.L., Fortuna, M.G., Abbott, S.B., DePuy, S.D., 2009. Retrotrapezoid nucleus, respiratory chemosensitivity and breathing automaticity. Respir. Physiol. Neurobiol. 168, 59–68.
Hedner, T., Lundborg, P., Engel, J., 1978. Effect of hypoxia on monoamine synthesis in brains of developing rats. III. Various O2 levels. Biol. Neonate 34, 55–60.
Hendricks, T., Francis, N., Fyodorov, D., Deneris, E.S., 1999. The ETS domain factor Pet-1 is an early and precise marker of central serotonin neurons and interacts with a conserved element in serotonergic genes. J. Neurosci. 19 (23), 10348–10356.
Hendricks, T.J., Fyodorov, D.V., Wegman, L.J., Lelutiu, N.B., Pehek, E.A., Yamamoto, B., Silver, J., Weeber, E.J., Sweatt, J.D., Deneris, E.S., 2003. Pet-1 ETS gene plays a critical role in 5-HT neuron development and is required for normal anxiety-like and aggressive behavior. Neuron 37, 233–247.
Hendricksen, M., Thomas, A.J., Ferrier, I.N., Ince, P., O'Brien, J.T., 2004. Neuropathological study of the dorsal raphe nuclei in late-life depression and Alzheimer's disease with and without depression. Am. J. Psychiatry 161 (6), 1096–1102.
Hermann, D.M., Luppi, P.H., Peyron, C., Hinckel, P., Jouvet, M., 1996. Forebrain projections of the rostral nucleus raphe magnus shown by iontophoretic application of choleratoxin b in rats. Neurosci. Lett. 216, 151–154.
Hermann, D.M., Luppi, P.H., Peyron, C., Hinckel, P., Jouvet, M., 1997. Afferent projections to the rat nuclei raphe magnus, raphe pallidus and reticularis gigantocellularis pars alpha demonstrated by iontophoretic application of choleratoxin (subunit b). J. Chem. Neuroanat. 13, 1–21.
Hilaire, G., Morin, D., Lajard, A.M., Monteau, R., 1993. Changes in serotonin metabolism may elicit obstructive apnoea in the newborn rat. J. Physiol. 466, 367–381.
Hilaire, G., 2006. Endogenous noradrenaline affects the maturation and function of the respiratory network: possible implication for SIDS. Auton. Neurosci. 126–127, 320–331.
Hillert, D., 1999. On processing lexical meanings in aphasia and Alzheimer's disease: some (re)considerations. Brain Lang. 69, 95–118.
Hodges, M.R., Richerson, G.B., 2008. Interaction between defects in ventilatory and thermoregulatory control in mice lacking 5-HT neurons. Respir. Physiol. Neurobiol. 164, 350–357.
Hodges, M.R., Tattersall, G.J., Harris, M.B., McEvoy, S.D., Richerson, D.N., Deneris, E.S., Johnson, R.L., Chen, Z.F., Richerson, G.B., 2008. Defects in breathing and thermoregulation in mice with near-complete absence of central serotonin neurons. J. Neurosci. 28 (10), 2495–2505.
Hodges, M.R., Richerson, G.B., 2010. The role of medullary 5-HT (5-HT) neurons in respiratory control: contributions to eupneic ventilation, CO2 chemoreception, and thermoregulation. J. Appl. Physiol. 108 (5), 1425–1432.
Holtman Jr., J.R., Dick, T.E., Berjer, A.J., 1986. Involvement of serotonin in the excitation of phrenic motoneurons evoked by stimulation of raphe obscurus. J. Neurosci. 6, 1185–1193.
Holtman Jr., J.R., Dick, T.E., Berjer, A.J., 1987. Serotonin mediated excitation of recurrent laryngeal and phrenic motoneurons evoked by stimulation of raphe obscurus. Brain Res. 417, 12–20.
Holtman Jr., J.R., 1988. Immunohistochemical localization of serotonin and substance P containing fibers around respiratory muscle motoneurons in the nucleus ambiguss of the cat. Neuroscience 26, 169–178.
Hornung, J.P., 2003. The human raphe nuclei and the serotonergic system. J. Chem. Neuroanat. 26, 331–343.
Hoyer, D., Clarke, D.E., Fozard, J.R., Harting, P.R., Martin, G.R., Mylecharane, E.J., Saxena, P.R., Humphrey, P.P.A., 1994. VII International union of pharmacology classification of receptors for 5-hydroxytryptamine. Pharmacol. Rev. 46, 157–203.
Hunt, P.N., McCabe, A.K., Bosma, M.M., 2005. Midline serotonergic neurones contribute to widespread synchronized activity in embryonic mouse hindbrain. J. Physiol. 566, 807–819.
Jacobs, B.L., Azmitia, E.C., 1992. Structure and function of the brain serotonin system. Physiol. Rev. 72, 165–229.
Kalia, M., 2003. Dysphagia and aspiration pneumonia in patients with Alzheimer's disease. Metabolism 52 (Suppl. 2), 36–38.
Kanamaru, M., Homma, I., 2009. Dorsomedial medullary 5-HT2 receptors mediate immediate onset of initial hyperventilation, airway dilation, and ventilatory decline during hypoxia in mice. Am. J. Physiol. Regul. Integr. Comp. Physiol. 297, R34–R41.
Katz, D.M., Dutschmann, M., Ramirez, J.M., Hilaire, G., 2009. Breathing disorders in Rett syndrome: progressive neurochemical dysfunction in the respiratory network after birth. Respir. Physiol. Neurobiol. 168, 101–108.
Khater-Boidin, J., Rose, D., Duron, B., 1996. Central effects of 5-HT on activity of respiratory and hypoglossally innervated muscles in newborn kittens. J. Physiol. 495, 255–265.
Kinney, H.C., Belliveau, R.A., Trachtenberg, F.L., Rava, L.A., Paterson, D.S., 2007. The development of the medullary serotonergic system in early human life. Auton. Neurosci. 132, 81–102.
Klein, D.F., 1993. False suffocation alarms, spontaneous panics, and related conditions. An integrative hypothesis. Arch. Gen. Psychiatry 50, 306–317.
Kuhn, D.M., Arthur Jr., R.E., 1996. Inactivation of brain tryptophan hydroxylase by nitric oxide. J. Neurochem. 67 (3), 1072–1077.
Kuhn, D.M., Arthur Jr., R.E., 1997. Inactivation of tryptophan hydroxylase by nitric oxide: enhancement by tetrahydrobiopterin. J. Neurochem. 68 (4), 1495–1502.
Lai, M.K., Tsang, S.W., Francis, P.T., Esiri, M.M., Keene, J., Hope, T., Chen, C.P., 2003. Reduced 5-HT 5-HT1A receptor binding in the temporal cortex correlates with aggressive behavior in Alzheimer disease. Brain Res. 974, 82–87.
Lajard, A.M., Bou, C., Monteau, R., Hilaire, G., 1999. Serotonin levels are abnormally elevated in the fetus of the monoamine oxidase-A-deficient transgenic mouse. Neurosci. Lett. 261, 41–44.
Lalley, P.M., Bischoff, A.M., Richter, D.W., 1994a. 5-HT-1A receptor-mediated modulation of medullary expiratory neurones in the cat. J. Physiol. 476, 117–130.
Lalley, P.M., Bischoff, A.M., Richter, D.W., 1994b. Serotonin 1A-receptor activation suppresses respiratory apneusis in the cat. Neurosci. Lett. 172, 59–62.
Lalley, P.M., Bischoff, A.M., Schwarzacher, S.W., Richter, D.W., 1995. 5-HT2 receptor-controlled modulation of medullary respiratory neurones in the cat. J. Physiol. 487, 653–661.
Lalley, P.M., Benacka, R., Bischoff, A.M., Richter, D.W., 1997. Nucleus raphe obscurus evokes 5-HT-1A receptor-mediated modulation of respiratory neurons. Brain Res. 747, 156–159.
Lanoir, J., Hilaire, G., Seif, I., 2006. Reduced density of functional 5-HT1A receptors in the brain, medulla and spinal cord of monoamine oxidase-A knockout mouse neonates. J. Comp. Neurol. 495 (5), 607–623.
Lauterbach, E.C., Victoroff, J., Coburn, K.L., Shillcutt, S.D., Doonan, S.M., Mendez, M.F., 2010. Psychopharmacological neuroprotection in neurodegenerative disease: assessing the preclinical data. J. Neuropsychiatry Clin. Neurosci. 22, 8–18.
Lavie, P., Lavie, L., 2008. Cardiovascular morbidity and mortality in obstructive sleep apnea. Curr. Pharm. Des. 14 (32), 3466–3473.
Lebrand, C., Cases, O., Adelbrecht, C., Doye, A., Alvarez, C., El Mestikawy, S., Seif, I., Gaspar, P., 1996. Transient uptake and storage of 5-HT in developing thalamic neurons. Neuron 17, 823–835.
Lebrand, C., Cases, O., Wehrleï, R., Blakely, R.D., Edwards, R.H., Gaspar, P., 1998. Transient developmental expression of monoamine transporters in the rodent forebrain. J. Comp. Neurol. 401, 506–524.
Lee, S., Walker, C.L., Wevrick, R., 2003. Prader-Willi syndrome transcripts are expressed in phenotypically significant regions of the developing mouse brain. Gene Expr. Patterns 3 (5), 599–609.
Léger, L., Wiklund, L., Descarries, L., Persson, M., 1979. Description of an indolaminergic cell component in the cat locus coeruleus: a fluorescence histochemical and radioautographic study. Brain Res. 168, 43–56.
Leger, L., Charnay, Y., Hof, P.R., Bouras, C., Cespuglio, R., 2001. Anatomical distribution of serotonin-containing neurons and axons in the central nervous system of the cat. J. Comp. Neurol. 433, 157–182.
Li, A., Nattie, E.E., 2008. Serotonin transporter knockout mice have a reduced ventilatory response to hypercapnia (predominantly in males) but not to hypoxia. J. Physiol. 586, 2321–2329.
Lindsay, A.D., Feldman, J.L., 1993. Modulation of respiratory activity of neonatal rat phrenic motoneurones by serotonin. J. Physiol. 461, 213–233.
Liu, Q., Wong-Riley, M.T., 2010. Postnatal changes in tryptophan hydroxylase and serotonin transporter immunoreactivity in multiple brainstem nuclei of the rat: implications for a sensitive period. J. Comp. Neurol. 518, 1082–1097.
Lötsch, J., Skarke, C., Schneider, A., Hummel, T., Geisslinger, G., 2005. The 5-hydroxytryptamine 4 receptor agonist mosapride does not antagonize morphine-induced respiratory depression. Clin. Pharmacol. Ther. 78, 278–287.
Manaker, S., Tischler, L.J., 1993. Origin of serotonergic afferents to the hypoglossal nucleus in the rat. J. Comp. Neurol. 334, 466–476.
Manzke, T., Guenther, U., Ponimaskin, E.G., Haller, M., Dutschmann, M., Schwarzacher, S., Richter, D.W., 2003. 5-HT4(a) receptors avert opioid-induced breathing depression without loss of analgesia. Science 301, 226–229.
Manzke, T., Bidon, O., Dutschmann, M., Richter, D.W., 2008. Mecp2-deficiency causes developmental changes in the serotonergic system. Acta Physiol. 192, PT03–PT05.
Manzke, T., Dutschmann, M., Schlaf, G., Morschel, M., Koch, U.R., Ponimaskin, E., Bidon, O., Lalley, P.M., Richter, D.W., 2009. Serotonin targets inhibitory synapses

to induce modulation of network functions. Philos. Trans. R Soc. Lond. B Biol. Sci. 364, 2589–2602.
Martinez, J.M., Kent, J.M., Coplan, J.D., Browne, S.T., Papp, L.A., Sullivan, G.M., Kleber, M., Perepletchikova, F., Fyer, A.J., Klein, D.F., Gorman, J.M., 2001. Respiratory variability in panic disorder. Depress. Anxiety 14, 232–237.
McAllen, R.M., Tanaka, M., Ootsuka, Y., McKinley, M.J., 2010. Multiple thermoregulatory effectors with independent central controls. Eur. J. Appl. Physiol. 109, 27–33.
McCann, U.D., Sgambati, F.P., Schwartz, A.R., Ricaurte, G.A., 2009. Sleep apnea in young abstinent recreational MDMA ("ecstasy") consumers. Neurology 73 (23), 2011–2017.
McCrimmon, D.R., Lalley, P.M., 1982. Inhibition of respiratory neural discharges by clonidine and 5-hydroxytryptamine. J. Pharmacol. Exp. Ther. 2222, 771–777.
Michelson, A.L., Hollander, W., Lowell, F.C., 1958. The effect of 5-Hydroxytryptamine on the respiration of non-asthmatic and asthmatic subjects. J. Lab. Clin. Med. 51, 57–62.
Minson, J., Chalmers, J., Drolet, G., Kapoor, V., Llewellyn-Smith, I., Mills, E., Morris, M., Pilowsky, P., 1990. Central serotonergic mechanisms in cardiovascular regulation. Cardiovasc. Drugs Ther. 4 (Suppl. 1), 27–32.
Monteau, R., Hillaire, G., 1991. Spinal respiratory motoneurons. Prog. Neurobiol. 37, 83–144.
Morin, D., Hennequin, S., Monteau, R., Hilaire, G., 1990. Serotonergic influences on central respiratory activity: an in vitro study in the newborn rat. Brain Res. 535, 281–287.
Morin, D., Monteau, R., Hilaire, G., 1992. Compared effects of serotonin on cervical and hypoglossal inspiratory activities: an in vitro study in the newborn rat. J. Physiol. 451, 605–629.
Morley, M.E., Rand, C.M., Berry-Kravis, E.M., Zhou, L., Fan, W., Weese-Mayer, D.E., 2008. Genetic variation in the HTR1A gene and sudden infant death syndrome. Am. J. Med. Genet. A 146 (7), 930–933.
Morrison, S.F., Nakamura, K., Madden, C.J., 2008. Central control of thermogenesis in mammals. Exp. Physiol. 93 (7), 773–797.
Mulkey, D.K., Rosin, D.L., West, G., Takakura, A.C., Moreira, T.S., Bayliss, D.A., Guyenet, P.G., 2007. Serotonergic neurons activate chemosensitive retrotrapezoid nucleus neurons by a pH-independent mechanism. J. Neurosci. 27, 14128–14138.
Nakamura, K., Hasegawa, H., 2007. Developmental role of tryptophan hydroxylase in the nervous system. Mol. Neurobiol. 35, 45–54.
Nalivaiko, E., Sgoifo, A., 2009. Central 5-HT receptors in cardiovascular control during stress. Neurosci. Biobehav. Rev. 33, 95–106.
Nardi, A.E., Freire, R.C., Zin, W.A., 2009. Panic disorder and control of breathing. Respir. Physiol. Neurobiol. 167, 133–143.
Narita, N., Narita, M., Takashima, S., Nakayama, M., Nagai, T., Okado, N., 2001. Serotonin transporter gene variation is a risk factor for sudden infant death syndrome in the Japanese population. Pediatrics 107 (4), 690–692.
Nattie, E.E., Li, A., 2001. CO2 dialysis in the medullary raphe of the rat increases ventilation in sleep. J. Appl. Physiol. 90 (4), 1247–1257.
Nattie, E.E., Li, A., Richerson, G.B., Lappi, D.A., 2004. Medullary serotonergic neurones and adjacent neurones that express neurokinin-1 receptors are both involved in chemoreception in vivo. J. Physiol. 556, 235–253.
Neugroschl, J., Sano, M., 2010. Current treatment and recent clinical research in Alzheimer's disease. Mt. Sinai J. Med. 77, 3–16.
Nixon, G.M., Brouillette, R.T., 2002. Sleep and breathing in Prader-Willi syndrome. Pediatr. Pulmonol. 34, 209–217.
Oertel, B.G., Schneider, A., Rohrbacher, M., Schmidt, H., Tegeder, I., Geisslinger, G., Lötsch, J., 2007. The partial 5-hydroxytryptamine1A receptor agonist buspirone does not antagonize morphine-induced respiratory depression in humans. Clin. Pharmacol. Ther. 81, 59–68.
Olsen, E.B., Dempsey, J.A., McCrimmon, D.R., 1979. Serotonin and the control of ventilation in awake rats. J. Clin. Invest. 64, 689–693.
Onimaru, H., Ikeda, K., Kawakami, K., 2009. Phox2b, RTN/pFRG neurons and respiratory rhythmogenesis. Respir. Physiol. Neurobiol. 168, 13–18.
Ouchi, Y., Yoshikawa, E., Futatsubashi, M., Yagi, S., Ueki, T., Nakamura, K., 2009. Altered brain 5-HT transporter and associated glucose metabolism in Alzheimer disease. J. Nucl. Med. 50 (8), 1260–1266.
Page, I.H., 1952. The vascular action of natural serotonin 5 and 7-hydroxytryptamine and tryptamine. J. Pharmacol. 105, 58–73.
Page, I.H., McCubbin, J.W., 1953. The variable arterial pressure responses to serotonin and laboratory animals and man. Circ. Res. 1, 354–362.
Palacios, J.M., Waeber, C., Hoyer, D., Mengod, D., 1990. Distribution of serotonin receptors. Ann. N. Y. Acad. Sci. 600, 36–52.
Papp, L.A., Klein, D.F., Gorman, J.M., 1993. Carbon dioxide hypersensitivity, hyperventilation, and panic disorder. Am. J. Psychiatry 150, 1149–1157.
Parks, V.J., Sandison, A.G., Skinner, S.L., Whelan, R.F., 1960. The stimulation of respiration by 5-hydroxytryptamine in man. J. Physiol. 151, 342–351.
Parvizi, J., Van Hoesen, G.W., Damasio, A., 2001. The selective vulnerability of brainstem nuclei to Alzheimer's disease. Ann. Neurol. 49, 53–66.
Paterson, D.S., Trachtenberg, F.L., Thompson, E.G., Belliveau, R.A., Beggs, A.H., Darnall, R., Chadwick, A.E., Krous, H.F., Kinney, H.C., 2006. Multiple serotonergic brainstem abnormalities in sudden infant death syndrome. JAMA 296 (17), 2124–2132.
Paterson, D.S., Hilaire, G., Weese-Mayer, D.E., 2009. Medullary serotonin defects and respiratory dysfunction in sudden infant death syndrome. Respir. Physiol. Neurobiol. 168, 133–143.
Pattyn, A., Vallstedt, A., Dias, J.M., Samad, O.A., Krumlauf, R., Rijli, F.M., Brunet, J.F., Ericson, J., 2003. Coordinated temporal and spatial control of motor neuron and serotonergic neuron generation from a common pool of CNS progenitors. Genes Dev. 17 (6), 729–737.
Pilowsky, P.M., de Castro, D., Llewellyn-Smith, I., Lipski, J., Voss, M.D., 1990. Serotonin immunoreacive boutons make synapses with feline phrenic motoneurons. J. Neurosci. 10, 1091–1098.
Poncet, L., Denoroy, L., Dalmaz, Y., Pequignot, J.M., 1997. Activity of tryptophan hydroxylase and content of indolamines in discrete brain regions after a long-term hypoxic exposure in the rat. Brain Res. 765, 122–128.
Poon, C.S., 2009. Optimal interaction of respiratory and thermal regulation at rest and during exercise: role of a 5-HT-gated spinoparabrachial thermoafferent pathway. Respir. Physiol. Neurobiol. 169, 234–242.
Popa, D., Léna, C., Fabre, V., Prenat, C., Gingrich, J., Escourrou, P., Hamon, M., Adrien, J., 2005. Contribution of 5-HT2 receptor subtypes to sleep-wakefulness and respiratory control, and functional adaptations in knock-out mice lacking 5-HT2A receptors. J. Neurosci. 25 (49), 11231–11238.
Prabhakar, N.R., Peng, Y.J., Yuan, G., Kumar, G.K., 2006. Reactive oxygen species facilitate oxygen sensing. Novartis Found. Symp. 272, 95–99.
Rahman, M.S., Thomas, P., 2009. Molecular cloning, characterization and expression of two tryptophan hydroxylase (TPH-1 and TPH-2) genes in the hypothalamus of Atlantic croaker: down-regulation after chronic exposure to hypoxia. Neuroscience 158, 751–765.
Ramage, A.G., Villalón, C.M., 2008. 5-hydroxytryptamine and cardiovascular regulation. Trends Pharmacol. Sci. 29 (9), 472–481.
Rand, C.M., Weese-Mayer, D.E., Zhou, L., Maher, B.S., Cooper, M.E., Marazita, M.L., Berry-Kravis, E.M., 2006. Sudden infant death syndrome: case-control frequency differences in paired like homeobox Phox2B gene. Am. J. Med. Genet. A 140 (15), 1687–1691.
Rand, C.M., Berry-Kravis, E.M., Fan, W., Weese-Mayer, D.E., 2009. HTR2A variation and sudden infant death syndrome: a case-control analysis. Acta Paediatr. 98, 58–61.
Rapport, M.M., Green, A.A., Page, I.H., 1948. Crystalline serotonin. Science 108, 329–330.
Real, C., Popa, D., Seif, I., Callebert, J., Launay, J.M., Adrien, J., Escourrou, P., 2007. Sleep apneas are increased in mice lacking monoamine oxidase A. Sleep 30 (10), 1295–1302.
Real, C., Seif, I., Adrien, J., Escourrou, P., 2009. Ondansetron and fluoxetine reduce sleep apnea in mice lacking monoamine oxidase. Respir. Physiol. Neurobiol. 168, 230–238.
Reid, G., Rand, M., 1951. Physiological actions of the partially purified neurons serum vasoconstrictor (serotonin). Aust. J. Exp. Biol. Med. Sci. 29, 401–415.
Ren, J., Lee, S., Pagliardini, S., Gérard, M., Stewart, C.L., Greer, J.J., Wevrick, R., 2003. Absence of Ndn, encoding the Prader-Willi syndrome-deleted gene necdin, results in congenital deficiency of central respiratory drive in neonatal mice. J. Neurosci. 23 (5), 1569–1573.
Richerson, G.B., 2004. Serotonergic neurons as carbon dioxide sensors that maintain pH homeostasis. Nat. Rev. Neurosci. 5 (6), 449–461.
Richter, D.W., Schmidt-Garcon, P., Pierrefiche, O., Bischoff, A.M., Lalley, P.M., 1999. Neurotransmitters and neuromodulators controlling the hypoxic respiratory response in anaesthetized cats. J. Physiol. 514, 567–578.
Rockhill, W., Kirkman, J.L., Bosma, M.M., 2009. Spontaneous activity in the developing mouse midbrain driven by an external pacemaker. Dev. Neurobiol. 69, 689–704.
Rosin, D.L., Chang, D.A., Guyenet, P.G., 2006. Afferent and efferent connections of the rat retrotrapezoid nucleus. J. Comp. Neurol. 499, 64–89.
Rüb, U., Del Tredici, K., Schultz, C., Thal, D.R., Braak, E., Braak, H., 2000. The evolution of Alzheimer's disease-related cytoskeletal pathology in the human raphe nuclei. Neuropathol. Appl. Neurobiol. 26 (6), 553–567.
Rüb, U., Del Tredici, K., Schultz, C., Thal, D.R., Braak, E., Braak, H., 2001. The autonomic higher order processing nuclei of the lower brain stem are among the early targets of the Alzheimer's disease-related cytoskeletal pathology. Acta Neuropathol. 101 (6), 555–564.
Sahibzada, N., Ferreira, M., Wasserman, A.M., Taveira-DaSilva, A.M., Gillis, R.A., 2000. Reversal of morphine-induced apnea in the anesthetized rat by drugs that activate 5-hydroxytryptamine(1A) receptors. J. Pharmacol. Exp. Ther. 292, 704–713.
Santhosh, L., Estok, K.M., Vogel, R.S., Tamagnan, G.D., Baldwin, R.M., Mitsis, E.M., Macavoy, M.G., Staley, J.K., van Dyck, C.H., 2009. Regional distribution and behavioral correlates of 5-HT(2A) receptors in Alzheimer's disease with [(18)F]deuteroaltanserin and PET. Psychiatry Res. 173 (3), 212–217.
Schneider, J.A., Yonkman, F.F., 1954. Species differences in the respiratory cardiovascular response to serotonin (5-hydroxytryptamine). J. Pharmacol. 111, 84–98.
Smith, J.C., Morrison, D.E., Ellengerger, H.H., Otto, M.R., Feldman, J.L., 1989. Brainstem projections to the major respiratory neuron populations in the medulla of the cat. J. Comp. Neurol. 281, 69–96.
Stein, M.B., Millar, T.W., Larsen, D.K., Kryger, H., 1995. Irregular breathing during sleep in patients with panic disorder. Am. J. Psychiatry 152, 1168–1173.
Steinbusch, H.W., 1981. Distribution of serotonin-immunoreactivity in the central nervous system of the rat-cell bodies and terminals. Neuroscience 6, 557–618.
Steinbusch, H.W., Mulder, A.H., 1984. Serotonin immunoreactive neurons and their projections in the CNS. In: Bjorklund, A., Hokferl, Kuhar, M. (Eds.), Handbook of Chemical Neuroanatomy. Classical Transmitters and Transmitter Receptors in the CNS, Vol. 3, Part II. Elsevier Science, New York.
Steinbusch, H.W., Verhofstad, A.A., Penke, B., Varga, J., Joosten, H.W., 1981. Immunohistochemical characterization of monoamine-containing neurons in the central nervous system by antibodies to serotonin and noradrenalin. A study in the rat and the lamprey (lampetra fluviatilis). Acta Histochem. Suppl. 24, 107–122.

Stettner, G.M., Huppke, P., Brendel, C., Richter, D.W., Gärtner, J., Dutschmann, M., 2007. Breathing dysfunctions associated with impaired control of postinspiratory activity in Mecp2−/y knockout mice. J. Physiol. 579, 863–876.
Stettner, G.M., Zanella, S., Huppke, P., Gärtner, J., Hilaire, G., Dutschmann, M., 2008a. Spontaneous central apneas occur in the C57BL/6J mouse strain. Respir. Physiol. Neurobiol. 160, 21–27.
Stettner, G.M., Zanella, S., Hilaire, G., Dutschmann, M., 2008b. 8-OH-DPAT suppresses spontaneous central apneas in the C57BL/6J mouse strain. Respir. Physiol. Neurobiol. 161, 10–15.
Subramanian, H.H., Balnave, R.J., Holstege, G., 2008. The midbrain periaqueductal gray control of respiration. J. Neurosci. 28 (47), 12274–12283.
Sun, Q.J., Berkowitz, R.G., Goodchild, A.K., Pilowsky, P.M., 2002. Serotonin inputs to inspiratory laryngeal motoneurons in the rat. J. Comp. Neurol. 451, 91–98.
Taylor, N.C., Li, A., Nattie, E.E., 2005. Medullary serotonergic neurones modulate the ventilatory response to hypercapnia, but not hypoxia in conscious rats. J. Physiol. 566, 543–557.
Thoby-Brisson, M., Karlén, M., Wu, N., Charnay, P., Champagnat, J., Fortin, G., 2009. Genetic identification of an embryonic parafacial oscillator coupling to the pre-Bötzinger complex. Nat. Neurosci. 12 (8), 1028–1035.
Tork, I., Hornung, J.P., 1990. Raphe nuclei and the serotonergic system. In: Paxinos (Ed.), The Human Nervous System. Academic Press, San Diego, CA, pp. 1001–1022.
Tsang, S.W., Keene, J., Hope, T., Spence, I., Francis, P.T., Wong, P.T., Chen, C.P., Lai, M.K., 2010. A 5-HTergic basis for hyperphagic eating changes in Alzheimer's disease. J. Neurol. Sci. 288, 151–155.
Twarog, B.M., Page, I.H., 1953. Serotonin content of some mammalian tissues and urine and a method for its determination. Am. J. Physiol. 175, 157–161.
Twarog, B.M., 1954. Responses of a molluscan smooth muscle to acetylcholine and 5-hydroxytryptamine. J. Cell. Comp. Physiol. 44, 141–163.
Upton, A.L., Salichon, N., Lebrand, C., Ravary, A., Blakely, R., Seif, I., Gaspar, P., 1999. Excess of serotonin (5-HT) alters the segregation of ispilateral and contralateral retinal projections in monoamine oxidase A knock-out mice: possible role of 5-HT uptake in retinal ganglion cells during development. J. Neurosci. 19 (16), 7007–7024.
Viemari, J.C., Roux, J.C., Tryba, A.K., Saywell, V., Burnet, H., Peña, F., Zanella, S., Bévengut, M., Barthelemy-Requin, M., Herzing, L.B., Moncla, A., Mancini, J., Ramirez, J.M., Villard, L., Hilaire, G., 2005. Mecp2 deficiency disrupts norepinephrine and respiratory systems in mice. J. Neurosci. 25 (50), 11521–11530.
Voituron, N., Zanella, S., Menuet, C., Dutschmann, M., Hilaire, G., 2009. Early breathing defects after moderate hypoxia or hypercapnia in a mouse model of Rett syndrome. Respir. Physiol. Neurobiol. 168, 109–118.
Voituron, N., Zanella, S., Menuet, C., Lajard, A.M., Dutschmann, M., Hilaire, G., 2010a. Early abnormalities of post-sigh breathing in a mouse model of Rett syndrome. Respir. Physiol. Neurobiol. 170, 173–182.
Voituron, N., Zanella, S., Menuet, C., Dutschmann, M., Hilaire, G., 2010b. Physiological definition of upper airway obstructions in mouse model for Rett Syndrome. Respir. Physiol. Neurobiol., doi:10.1016/j.resp.2010.07.006.
Voss, M.D., de Castro, D., Lipski, J., Pilowsky, P.M., Jiang, C., 1990. Serotonin immunoreactive boutons form close appositions with respiratory neurons of the dorsal respiratory group in the cat. J. Comp. Neurol. 295, 208–218.
Weese-Mayer, D.E., Berry-Kravis, E.M., Maher, B.S., Silvestri, J.M., Curran, M.E., Marazita, M.L., 2003a. Sudden infant death syndrome: association with a promoter polymorphism of the serotonin transporter gene. Am. J. Med. Genet. 117A, 268–274.
Weese-Mayer, D.E., Zhou, L., Berry-Kravis, E.M., Maher, B.S., Silvestri, J.M., Marazita, M.L., 2003b. Association of the serotonin transporter gene with sudden infant death syndrome: a haplotype analysis. Am. J. Med. Genet. 122A, 238–245.
Weese-Mayer, D.E., Lieske, S.P., Boothby, C.M., Kenny, A.S., Bennett, H.L., Silvestri, J.M., Ramirez, J.M., 2006. Autonomic nervous system dysregulation: breathing and heart rate perturbation during wakefulness in young girls with Rett syndrome. Pediatr. Res. 60 (4), 443–449.
Weese-Mayer, D.E., Lieske, S.P., Boothby, C.M., Kenny, A.S., Bennett, H.L., Ramirez, J.M., 2008. Autonomic dysregulation in young girls with Rett Syndrome during nighttime in-home recordings. Pediatr. Pulmonol. 43 (11), 1045–1060.
Wilken, B., Lalley, P.M., Bischoff, A.M., Christen, H.J., Behnke, J., Hanefeld, F., Richter, D.W., 1997. Treatment of apneustic respiratory disturbance with a serotonin-receptor agonist. J. Pediatr. 130, 89–94.
Woolley, D.W., 1963. The Biochemical Bases of Psychoses or the Serotonin Hypothesis about Mental Illness. John Wiley and Sons, Inc., New York, NY.
Yamauchi, M., Ocak, H., Dostal, J., Jacono, F.J., Loparo, K.A., Strohl, K.P., 2008. Postsigh breathing behavior and spontaneous pauses in the C57BL/6J (B6) mouse. Respir. Physiol. Neurobiol. 162, 117–125.
Yeung, L.Y., Kung, H.F., Yew, D.T., 2010. Localization of 5-HT1A and 5-HT2A positive cells in the brainstems of control age-matched and Alzheimer individuals. Age (Dordr), in press.
Yue, W., Liu, H., Zhang, J., Zhang, X., Wang, X., Liu, T., Liu, P., Hao, W., 2008. Association study of 5-HT transporter gene polymorphisms with obstructive sleep apnea syndrome in Chinese Han population. Sleep 31 (11), 1535–1541.
Zanella, S., Watrin, F., Mebarek, S., Marly, F., Roussel, M., Gire, C., Diene, G., Tauber, M., Muscatelli, F., Hilaire, G., 2008. Necdin plays a role in the serotonergic modulation of the mouse respiratory network: implication for Prader-Willi syndrome. J. Neurosci. 28 (7), 1745–1755.
Zanella, S., Tauber, M., Muscatelli, F., 2009. Breathing deficits of the Prader-Willi syndrome. Respir. Physiol. Neurobiol. 168, 119–124.
Zhan, W.Z., Ellenberger, H.H., Feldman, J.L., 1989. Monoaminergic and GABAergic terminations in the phrenic nucleus of rat identified by immunohistochemical labelling. Neuroscience 31, 105–113.
Zhao, Z.Q., Scott, M., Chiechio, S., Wang, J.S., Renner, K.J., Gereau 4th, R.W., Johnson, R.L., Deneris, E.S., Chen, Z.F., 2006. Lmx1b is required for maintenance of central serotonergic neurons and mice lacking central serotonergic system exhibit normal locomotor activity. J. Neurosci. 26 (49), 12781–12788.

3 - Le traitement à la fluoxétine abolit la réponse respiratoire à l'acidose *in vitro* chez la souris nouveau-née

Voituron N., Shvarev Y., **Menuet C.**, Bevengut M., Fasano C., Vigneault E., El Mestikawy S. & Hilaire G.
Publié dans *Plos One*, en 2010.

Résumé en français :

Pour maintenir l'homéostasie du pH, le réseau respiratoire central doit en permanence ajuster son activité rythmique motrice à l'environnement et aux comportements de l'organisme. Chez les nouveau-nés, il est généralement admis que les groupes de neurones du noyau rétrotrapézoïde/groupe respiratoire parafacial de la surface ventrale du bulbe rachidien jouent un rôle primordial dans la réponse respiratoire à l'acidose, même si le système sérotoninergique pourrait également contribuer à cette réponse. Utilisant la préparation de bulbe rachidien *en bloc* de souris nouveau-nées, nous avons montré pour la première fois que la réponse respiratoire à l'acidose est abolie après un pré-traitement avec la fluoxétine (25-50 µM, 20 min), un bloqueur du transporteur de la sérotonine communément utilisé comme antidépresseur. Utilisant de l'hybridation *in situ* des mRNA, et de l'immunohistologie, nous avons également montré que les expressions du mRNA du transporteur de la sérotonine, et des neurones contenant de la sérotonine, se font dans la zone contenant le RTN/pFRG des souris nouveau-nées. Ces résultats révèlent que le système sérotoninergique joue un rôle essentiel pour l'homéostasie du pH. Même s'ils ont été obtenus sur de la souris nouveau-née *in vitro*, ces résultats suggèrent que des drogues ciblant le système sérotoninergique devraient être utilisées avec prudence chez les enfants, chez les femmes enceintes et chez les mères qui allaitent.

Fluoxetine Treatment Abolishes the *In Vitro* Respiratory Response to Acidosis in Neonatal Mice

Nicolas Voituron[1], Yuri Shvarev[1,2,3], Clément Menuet[1], Michelle Bevengut[1], Caroline Fasano[4], Erika Vigneault[4], Salah El Mestikawy[4,5,6,7], Gérard Hilaire[1]*

1 Maturation, Plasticité, Physiologie et Pathologie de la Respiration, Unité Mixte de Recherche 6231, Centre National de la Recherche Scientifique - Université de la Méditerranée - Université Paul Cézanne, Marseille, France, **2** Department of Woman and Child Health, Karolinska Institute, Stockholm, Sweden, **3** Institute of Cytology and Genetics, Siberian Division of the Russian Academy of Sciences, Novosibirsk, Russia, **4** Department of Psychiatry, Douglas Hospital Research Center, McGill University, Québec, Canada, **5** Unité 952, Institut National de la Santé et de la Recherche Médicale, Paris, France, **6** Unité Mixte de Recherche 7224, Centre National de la Recherche Scientifique, Paris, France, **7** Université Pierre et Marie Curie, Paris, France

Abstract

Background: To secure pH homeostasis, the central respiratory network must permanently adapt its rhythmic motor drive to environment and behaviour. In neonates, it is commonly admitted that the retrotrapezoid/parafacial respiratory group of neurons of the ventral medulla plays the primary role in the respiratory response to acidosis, although the serotonergic system may also contribute to this response.

Methodology/Principal Findings: Using *en bloc* medullary preparations from neonatal mice, we have shown for the first time that the respiratory response to acidosis is abolished after pre-treatment with the serotonin-transporter blocker fluoxetine (25–50 μM, 20 min), a commonly used antidepressant. Using mRNA *in situ* hybridization and immunohistology, we have also shown the expression of the serotonin transporter mRNA and serotonin-containing neurons in the vicinity of the RTN/pFRG of neonatal mice.

Conclusions: These results reveal that the serotonergic system plays a pivotal role in pH homeostasis. Although obtained *in vitro* in neonatal mice, they suggest that drugs targeting the serotonergic system should be used with caution in infants, pregnant women and breastfeeding mothers.

Citation: Voituron N, Shvarev Y, Menuet C, Bevengut M, Fasano C, et al. (2010) Fluoxetine Treatment Abolishes the *In Vitro* Respiratory Response to Acidosis in Neonatal Mice. PLoS ONE 5(10): e13644. doi:10.1371/journal.pone.0013644

Editor: Rory Edward Morty, University of Giessen Lung Center, Germany

Received June 18, 2010; **Accepted** September 24, 2010; **Published** October 26, 2010

Copyright: © 2010 Voituron et al. This is an open-access article distributed under the terms of the Creative Commons Attribution License, which permits unrestricted use, distribution, and reproduction in any medium, provided the original author and source are credited.

Funding: NV was supported by an International Rett Syndrome Foundation grant and Agence Nationale de la Recherche Prageder, YS by a Paul Cezanne University fellowship. The funders had no role in study design, data collection and analysis, decision to publish, or preparation of the manuscript.

Competing Interests: The authors have declared that no competing interests exist.

* E-mail: gerard.hilaire@univ-cezanne.fr

Introduction

From birth onwards, the neonatal mammal must be able to breathe and adapt its breathing activity to environmental changes and behaviors. Therefore a correct function of the ponto-medullary respiratory network is required at birth, not only for the elaboration of the respiratory rhythm but also for its adaptation to physiological needs. In neonates, the respiratory rhythm generator (RRG) is composed of two coupled, interacting networks: the preBötzinger complex (preBötC) which contains the primary rhythm generating neurons in brainstem slices [1,2] and the parafacial respiratory group (pFRG). The pFRG neurons express the transcription factor Phox2b, display a pre-inspiratory discharge and play a major role in detecting CO2/pH changes and adjusting the RRG activity in neonatal and juvenile animals [3,4]. In embryos, organized rhythmic activities emerge in the preBötC and pFRG as early as at embryonic day 15.5 and 14.5, respectively [5–7]. After birth, the embryonic pFRG forms the retrotrapezoid nucleus (RTN) with Phox2b glutamatergic neurons detecting changes in CO2/pH, receiving peripheral inputs from carotid bodies chemoreceptors, and controlling the respiratory network [8–10]. The RTN/pFRG neurons are severely depleted in transgenic mouse model of the Central Congenital Hypoventilation Syndrome, a rare disease defined by the lack of CO2/pH responsiveness and RRG automaticity during sleep [11].

Although the RTN/pFRG neurons have a crucial role in ventilatory responses to CO2/pH changes in neonates, the serotonin (5-HT) neurons also contribute to the maintenance of blood gas homeostasis [12–14]. As recently reviewed, the 5-HT neurons are involved in respiratory function and dysfunction [14], they synaptically contact the RRG [15], modulate the activity of the maturing RRG [16], are intrinsically chemosensitive *in vitro*, are stimulated by hypercapnia *in vivo*, and their disruption alters the ventilatory response to CO2/pH changes [12,17,18]. In a transgenic mouse model of Prader-Willi syndrome, a rare disease with complex symptoms including frequent apnoeas during sleep and blunted ventilatory responses to CO2/pH, the medullary 5-HT levels are abnormally increased at birth and the ventilatory responses to CO2/pH reduced [15]. In addition, an altered 5HT system and insufficient ventilatory responses to CO2/pH and/or hypoxia during sleep might contribute to sudden infant death syndrome (SIDS), the main cause of death in infants in industrialized countries [14,18–21].

The present work aimed at a further elucidation of the role of endogenous 5-HT in the RRG response to CO2/pH in neonatal mice. Using *en bloc* medullary preparations where the isolated RRG still functions *in vitro* and responds to CO2/pH changes, we show that a pre-treatment with fluoxetine, a blocker of the serotonin transporter (SERT) and 5-HT re-uptake, abolishes the RRG responses to CO2/pH. Using mRNA hybridization and immunohistology, we also report SERT mRNA expression and a few 5-HT neurons in the vicinity of the RTN/pFRG area. As fluoxetine is a commonly used antidepressant known to increase endogenous levels of 5-HT [22], we suggest a cautious use of pharmacological treatments targeting the 5HT system in infants, pregnant women and breastfeeding mothers.

Materials and Methods

Ethics Statement

The experiments were performed on neonatal mice (n = 48) born from C57BL6 mice (Charles River Laboratories; l'Arbresle, France) housed with food and water ad libitum and were conducted in agreement with the European Communities Council Directive (86/609/EEC) (permit number 13–426 to Nicolas Voituron; approved by Direction Départementale des Services Vétérinaires - Préfecture des Bouches du Rhône, France).

Surgery and electrophysiology

The medulla and cervical cord of neonatal mice (n = 42; postnatal days 1–3) were dissected, placed in a 2 ml *in vitro* recording chamber and superfused (>2 ml per min) with artificial cerebro-spinal fluid (aCSF), as reported previously [15]. Under these conditions, the isolated RRG continued to function, producing rhythmic bursts on phrenic roots for long periods of time. The 4th cervical ventral root containing the axons of phrenic motoneurons was sucked in a glass micropipette. Its electrical activity was filtered (100–3000 Hz), amplified (×5000), integrated (time constant 100 ms), digitized and stored (1 Khz; Spike 2 data system; Cambridge Electronic Design, UK).

As reported previously [7,23], two different aCSF, bubbled with carbogene and maintained at 27°C, were used: a normal aCSF (pH = 7.4) and an acidified aCSF (pH = 7.1), and pH values were regularly measured (pHmeter P107, Consort, Bioblock Scientific). The composition of the normal aCSF, also termed below aCSF(7.4), was (in mM): 129.0 NaCl, 3.35 KCl, 21.0 NaHCO3, 1.26 CaCl2, 1.15 MgCl2, 0.58 NaH2PO4, and 30.0 D-glucose. The composition of the acidified aCSF, also termed below aCSF(7.1), was similar but NaHCO3 was reduced to 10.0 mM [7,23]. This protocol already used by us [7] and others [23] to impose reproducible acidosis to en bloc medullary preparations without bubbling gases containing higher levels of CO_2 and lower levels of O_2 in the superfusate, was used to examine the direct effects of acidosis on the activity produced by the isolated respiratory network. In a first set of experiments, the RRG response to acidosis was analyzed by subjecting preparations to 5 or 10 min application of aCSF(7.1). In a second set of experiments, the effect of pre-treating the preparations with aCSF(7.4) containing fluoxetine (10 µM or 50 µM; 20 min) was investigated on the RRG response to acidosis. Fluoxetine is a well-known antidepressant of common clinical use that blocks the serotonin transporter (SERT), the blockade of the 5-HT reuptake increasing the 5-HT endogenous levels and potentiating the 5-HT effects at the synaptic cleft [22]. After fluoxetine pre-treatment, the RRG response to acidosis was investigated by subjecting the preparations to aCSF(7.1) containing the same amount of fluoxetine for 5 min. In a third set of experiments, the RRG response to acidosis was investigated after pre-treatment with aCSF(7.4) containing 5-HT (1 µM or 5 µM; 20 min) to mimic the effect of fluoxetine by increasing the extracellular level of 5-HT. After 5-HT pre-treatment, the RRG response to acidosis was analyzed by subjecting the preparations to aCSF(7.1) containing the same amount of 5-HT for 5 min. All drugs were purchased from Sigma (Sigma-Aldrich, Saint-Quentin Fallavier, France) and dissolved in aCSF.

For each individual experiment (n = 42), the phrenic burst frequency (PBf) was measured every min. The 5 min period under aCSF(7.4) prior to any drug application was used to define the control PBf (100%) and the changes in PBf induced by application of the modified aCSF were expressed in % of control PBf. Standardized experiments were repeated on different preparations from different litters and only one trial was performed per preparation. The mean changes in PBf were averaged min after min from different preparations and the results were given as mean ± SEM. As in previous reports [15,16,24,25], the figures present the mean PBf changes as % of the control PBf, whereas the statistical analysis of the changes in PBf was performed on absolute values (cycle per min, c.min^{-1}) using a student's paired *t*-test to compare the PBf during acidosis to the mean PBf calculated during the five min prior to the acidosis tests. The level of statistical significance was set at $p<0.05$.

SERT mRNA expression and 5-HT neurons analysis

To analyze SERT mRNA expression in neonatal mice (n = 3), brains were dissected at postnatal day 6 and frozen in isopentane at −30°C. Sections (10 µm) were prepared with a cryostat at −20°C, thaw-mounted on glass slides and stored at −80°C until usage. Regional mRNA hybridization *in situ* for the SERT sequences (*Mus musculus*, accession numbers: NM_010484.2) was performed as already described [26] with the following antisens oligonucleotide:

5′- GGAGGAGATGAGGTAGTAGAGCGCCCAGGCTA-TG-3′,

5′- GAACAGGAGAAACAGAGGGCTGATGGCCACCC-AG-3′,

5′-CTCAGCAGGTGACGTGGAATGGAGTGTCCAGG-TG-3′,

5′- AGAACCAAGACACGACGACGGCCTCGATGAGA-GC -3′

and 5′- CCCACACCCCTGTCTCCAAGAGTTTCTGCCA-GTTGG-3′, using Helios oligo design software (http://www.heliosbioscience.com, Helios Biosciences, France) [26]. Negative controls were performed using labeled sense oligonucleotides. In brief, oligonucleotides were labeled with [^{35}S]-dATP, using terminal transferase (Amersham Biosciences, UK), to a specific activity of 5×10^8 dpm/µg. Sections were covered with 100 µl of an hybridization of Helios medium [26] and $3–5\times10^5$ dpm of each labeled oligonucleotide. Samples were incubated overnight at 42°C, washed and exposed to BAS-TR Fuji Imaging screens (Fuji Film Photo Co., Tokyo, Japan) for 4–5 days. Screens were then scanned with a Fuji Bioimaging Analyzer BAS-5000 (Fuji Film Photo Co., Tokyo, Japan).

To analyze 5-HT neurons expression, brainstems were dissected at postnatal day 3 (n = 3) and fixed in 4% paraformaldehyde dissolved in phosphate-buffered saline (PBS; 0.1 M phosphate buffer at pH 7.4+0.15 M NaCl). Free-floating serial coronal sections (70 µm thickness; vibroslicer Campden Instruments, Longhborough, UK) were first incubated for 30 min at room temperature in a blocking solution (BS) containing 1% normal goat serum and 0.3% w/v Triton X-100 in PBS, followed by overnight incubation at 4°C in an anti-5HT antibody (Sigma),

diluted 1:1,000 in BS. After rinsing in PBS, the sections were incubated for 4 hours at room temperature in a goat anti-mouse IgG Rhodamine-conjugated (Jackson ImmunoResearch, West Grove, PA), diluted 1:200 in PBS containing 1% normal goat serum, rinsed again, and incubated overnight at 4°C in a mouse PAP complex (Sigma), diluted 1:100 in PBS. On the following day, the sections were first rinsed and pre-treated for 20 min in a cobalt (0.5%) solution and rinsed; then the PAP complex was developed with 3, 3′-diaminobenzidine (DAB 0.04%) and hydrogen peroxide (0.01%). After rinsing in cold PBS, the sections were mounted on gelatin-chromalin coated slides, dried overnight, stained with neutral red (1% in H_2O), dehydrated in a graded series of ethanol (70%, 80%, 95%, and 100%), cleared in xylene, coverslipped with DPX, investigated in transmitted light, and photographed.

Results

The isolated RRG generated rhythmic phrenic bursts with stable amplitude and frequency (Fig. 1A) and the mean PBf under aCSF(7.4) containing no drugs (10.0 ± 0.7 c.min^{-1}; n = 42) was fully consistent with previously reported values [15].

Acidosis increases the PBf of en bloc medullary preparations

To analyze the PBf changes induced by acidosis, we measured the control PBf every min in twelve preparations superfused with aCSF(7.4) for at least 20 min followed by superfusion with aCSF(7.1) for five min. As shown in Fig. 1B, the mean PBF did not change in the first two min of acidosis, after which it significantly increased to reach 133 ± 8% of the control PBf during

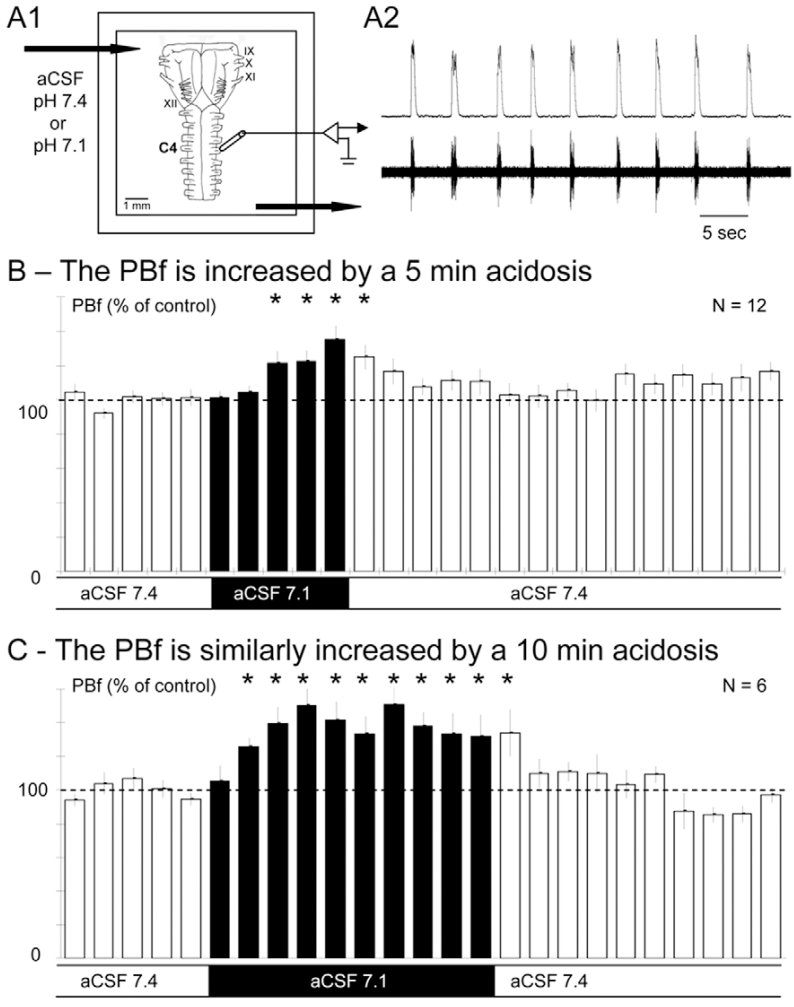

Figure 1. Acidosis increases the phrenic burst frequency of en bloc medullary preparations. A – Schematic presentation of the *en bloc* preparation of neonatal mice (A1) and example of raw and integrated phrenic bursts (bottom and top traces, respectively) produced by the isolated respiratory rhythm generator (RRG) on the C4 ventral roots of *en bloc* preparations (A2). B – Columns of the histogram show the mean (and SEM) phrenic burst frequency (PBf; expressed as % of the control PBf) measured every min (one column = 1 min) in 12 *en bloc* preparations when the control aCSF(7.4) (white columns) superfusing the preparations was replaced by aCSF(7.1) for 5 min (black columns). Note that acidosis significantly increased the PBf (asterisks indicate a $p<0.05$ statistical difference). C- As in B but aCSF(7.1) application for 10 min to 6 other preparations. Note that the PBf reached a plateau from the 5th to the 10th min of aCSF(7.1) application.
doi:10.1371/journal.pone.0013644.g001

the last min of acidosis. When superfusion with aCSF(7.4) was resumed, the PBf recovered control values within two min. In a second set of experiments, six other preparations were also subjected to aCSF(7.1) but the application was maintained for ten min instead of five min to know whether longer period of acidosis induced more marked changes in the PBf (Fig. 1C). The PBf did not significantly change in the first min of acidosis, slightly but significantly increased at the 2nd min, reached 142±10% at the 5th min and thereafter remained at a plateau until the 10th min of acidosis (132±13% of control) when superfusion with aCSF(7.4) was resumed, the PBf returning to control values.

Neither five nor ten min of acidosis significantly affected the mean amplitude of the integrated PB (data not shown). As five and ten min of acidosis similarly increased the PBf, data corresponding to the PBf changes induced by the first five min of acidosis in the two types of experiments (five and ten min of acidosis) were pooled together. On the whole sample of 18 preparations, acidosis always increased the PBf. It had no significant effects on the mean PBf during the first min, weakly but significantly increased it from the second min (112±4%) and raised the PBf up to 137±6% of the control at the 5th min. No significant relationship was found between the PBf increment induced by acidosis at the 5th min and the control PBf prior to acidosis ($r = 0.312$; $df = 16$; $p > 0.1$). In addition, no significant difference was observed between the mean PBf increment induced by acidosis at the 5th min in preparations displaying the highest (13.1±0.6 $c.min^{-1}$, $n = 5$) vs. the lowest (5.9±0.2 $c.min^{-1}$, $n = 5$) control PBf (mean PBf increment: 3.7±1.4 $c.min^{-1}$ and 2.3±0.7 $c.min^{-1}$, respectively; $P > 0.2$). Therefore, acidosis increased the PBf in all the preparations, even when the control PBf was high. Because the five-min application of acidified aCSF was more likely to reflect the physiological breathing responses to transient blood acidosis than the ten-min application, we only tested below the PBf changes induced by five min of acidosis.

Excess of 5HT abolishes the PBf response to acidosis

In a second set of experiments, preparations were subjected to pre-treatment with aCSF containing fluoxetine, a well-known SERT blocker known to increase 5-HT endogenous levels [22], prior to investigating the PBf responses to acidosis. As applications of fluoxetine at large concentration (100 μM) were reported to double the mean PBf [16], we used weaker concentrations to avoid marked increases of the resting PBf. Indeed, pre-treatments with fluoxetine at 10 μM ($n = 6$) and 50 μM ($n = 4$) did not significantly affect the resting PBf at either concentrations and therefore data were pooled ($n = 10$). As shown in Fig. 2A, subjecting the preparations to aCSF(7.4) containing fluoxetine for 20 min did not significantly increase the mean PBf during the last five min of

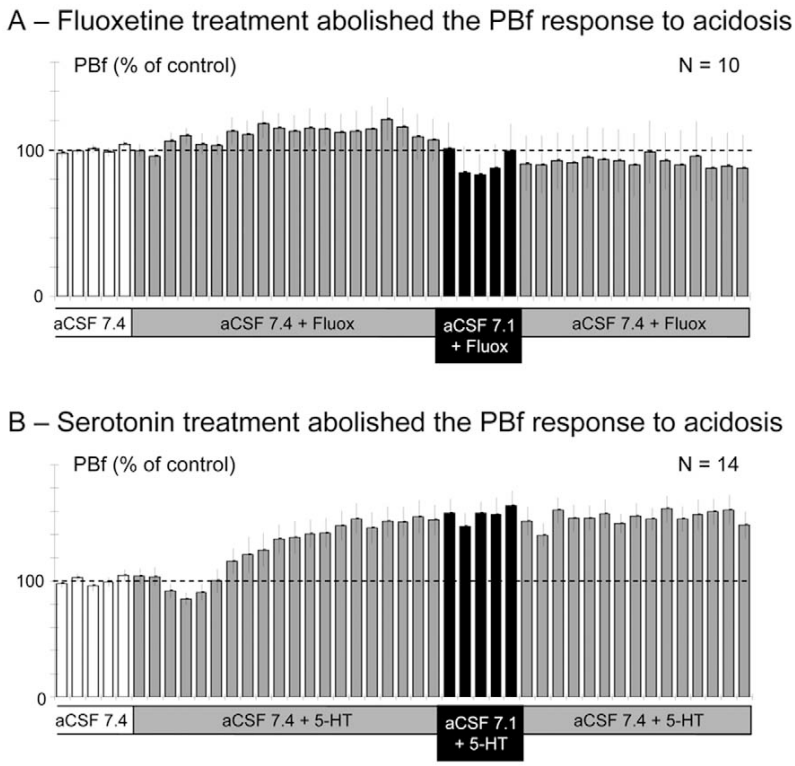

Figure 2. Fluoxetine and serotonin pre-treatments abolish the increase of phrenic burst frequency induced by acidosis. A - Columns of the histogram show the mean (and SEM) PBf (expressed as % of the control PBf) measured every min (one column = 1 min) in 10 preparations when the control aCSF(7.4) (white columns) superfusing the preparations was first replaced by aCSF(7.4) containing fluoxetine (10–25 μM) for 20 min to block the serotonin transporter SERT (grey columns) and thereafter by aCSF(7.1) containing the same amount of fluoxetine for 5 min (black columns). Note that pre-treatment with fluoxetine did not significantly increase the PBf but abolished the PBf increase under acidosis. **B** - PBf changes (expressed as % of control) every min (one column) but for 14 preparations superfused with control aCSF(7.4) (white columns), aCSF(7.4) containing serotonin, 5-HT (1–5 μM) for 20 min (grey columns) and thereafter aCSF(7.1) containing the same amount of 5-HT for 5 min (black columns). Note that pre-treatment with 5-HT significantly increased the PBf by about 50% and, similarly to fluoxetine treatment, abolished the PBf increase under acidosis.

doi:10.1371/journal.pone.0013644.g002

fluoxetine (113±6% of the control; p>0.1). Then, to investigate the effect of fluoxetine pre-treatment on the PBf response to acidosis, the aCSF(7.4) containing fluoxetine was replaced by aCSF(7.1) containing the same amount of fluoxetine for 5 min. Acidosis slightly but non-significantly decreased the PBf, the PBf being similar to control at the 5th min. Thus, pre-treating *en bloc* medullary preparations with the SERT blocker fluoxetine abolished the PBf response to acidosis.

To mimic the fluoxetine-induced increase of 5-HT levels, fourteen other preparations were subjected to aCSF(7.4) containing weak concentrations of exogenous 5-HT for 20 min. Two different concentrations of 5-HT were used, 1 μM (n = 7) and 5 μM (n = 7). After 20 min of application, they both slowly and significantly increased the PBf by around 50% and similarly altered the PBf response to acidosis; therefore data were pooled (n = 14). As shown in Figure 2B, aCSF(7.4) containing 5-HT slowly and significantly increased the PBf up to a plateau at 151±6% of the control during the five last min of 5-HT pre-treatment. Thereafter, applying aCSF(7.1) containing the same amount of 5-HT for 5 min to 14 preparations either reduced the PBf (83±7% of control; n = 6) or increased it (130±10% of control; n = 8). On the whole sample (n = 14), acidosis after 5-HT pre-treatment did not significantly affect the PBf at the 5th min (112±9% of control; p>0.1). No significant relationship was found between the PBf responses to acidosis and the control PBf either prior to ($r = -0.174$; df = 12; p>0.1) or after 5-HT pre-treatment ($r = -0.346$; df = 12; p>0.1). In addition, no significant difference was observed between the PBf response to acidosis in preparations displaying the highest (22.7±2.4 c.min^{-1}; n = 5) vs. the lowest (12.2±0.7 c.min^{-1}; n = 6) PBf under 5-HT (mean PBf response: 0.2±0.9 c.min^{-1} and 1.4±1.6 c.min^{-1}, respectively; P>0.2).Then, exposure of preparations to exogenous 5-HT abolished the PBf response to acidosis, even when the PBf was moderately increased by 5-HT exposure.

SERT mRNA expression and 5-HT neurons in the RTN/pFRG area

To decipher the mechanisms through which the SERT blocker fluoxetine abolished the PBf response to acidosis, we examined possible fluoxetine targets with *in situ* hybridization for SERT mRNA in 10 μm medullary sections of three neonatal mice. We identified the brainstem section level from observation of adjacent sections stained with Cresyl Violet. As previously [7], we defined the RTN/pFRG area as located below the caudal part of the facial motor nucleus (n7), rostral to the appearance of the nucleus ambiguous. SERT mRNA was constantly found expressed in three distinct ventral spots of medullary sections cut at the RTN/pFRG level (Fig. 3A). First, SERT mRNA expression formed a median, large and heavily stained triangle, possibly delimiting the raphe magnus (Rm in Fig. 3). Second, SERT mRNA expression was also found at a more lateral spot, about 500 μm from the midline, just lateral to the pyramidal tract (py), in an area possibly corresponding to the para-pyramidal subgroup of 5-HT neurons (ppy in Fig. 3). Third, a distinct and small spot of SERT mRNA was observed 200–300 μm laterals from the ppy, ventral to the medial part of the facial nucleus (n7). This small lateral spot was observed in the three studied neonatal mice (arrows in Fig. 3).

The SERT mRNA spot in the vicinity of the RTN/pFRG of neonatal mice was consistent with the dense 5-HT innervation to the RTN/pFRG described in rats [27–29]. However, as SERT mRNA expression could only originate from 5-HT somata and not 5-HT terminals, we used antibody against 5-HT to seek for 5-HT-containing neurons in sections passing at the RTN/pFRG level. We clearly identified three distinct groups of 5-HT neurons (Fig. 3B1) forming the medial raphe magnus, the lateral ppy column and a lateral group of a few scattered 5-HT neurons. The latter 5-HT-containing neurons were located very close to the ventral surface and medial to the n7 (Fig. 3B2, B3) and were highly likely at the origin of the most lateral SERT mRNA spot found in the vicinity of the RTN/pFRG area.

Asides from the RTN/pFRG area, our *in situ* hybridization studies revealed a very dense expression of SERT mRNA in all the median raphe nuclei and all along the ppy column of 5-HT neurons. At the caudal medullary level, SERT mRNA expression was also found in the respiratory-related areas of the ventro-lateral medulla, below the nucleus ambiguous, but not in the dorsal medulla (data not shown).

Discussion

In neonatal mice, we report that the PBf response to acidosis is abolished by pre-treatment with the SERT blocker fluoxetine and that SERT mRNA and 5-HT neurons are found in the vicinity of the RTN/pFRG area. These new results are of main importance since they argue for a pivotal role of the 5-HT system in the PBf response to acidosis and suggest that altered 5-HT metabolism in infants may affect the breathing response to acidosis.

Basic aspects of the PBf responses to acidosis

In medullary preparations of neonatal mice, acidosis increases the PBf by about 40% without affecting the phrenic burst amplitude, in agreement with previous reports in neonatal rats [30] and foetal mice [7]. Compelling evidence exist that the neonatal RTN/pFRG plays a main role in the PBf response to acidosis [3,4,8–10]. However, the one min latency of the PBf response appears to be long since the RTN/pFRG chemoreceptors are close to the ventral surface and rapidly detect CO2/pH changes [28]. The RRG responds in a few seconds when the RTN/pFRG neurons are stimulated by direct photo-activation *in vivo* [31] or direct CO2/pH stimulation *in vitro* [32]. The kinetics of the PBf responses to acidified aCSF applications have not been previously documented in details but latencies in a min range are commonly illustrated [30,33,34]. Aside the superficial RTN/pFRG chemoreceptors, several groups of chemoreceptors are described in discrete brainstem areas, such as the pontine catecholaminergic A5 and A6 areas, the ventrolateral medulla and the raphe areas [33,35]. Indeed, the 5-HT neurons play a crucial role in respiratory function and dysfunction [14]: they are intrinsically chemosensitive [12], synaptically contact the respiratory neurons [15] and exert a facilitatory modulation on the RRG via a release of endogenous 5HT and activation of 5-HT1A receptors [16,36]. Although some 5-HT neurons are very close to the ventral surface of the medulla, most are located deeper in the brainstem than the superficial RTN/pFRG chemoreceptors and may require a longer latency to detect acidosis. As five and ten min acidosis applications similarly affect the PBf, we speculate that the PBf response to acidosis we have analyzed reflects the integrated response of the whole medullary chemosensitive system rather than the solely response of superficial RTN/pFRG chemoreceptors.

Basic aspects of the fluoxetine abolition of the PBf response to acidosis

Fluoxetine blocks SERT and increases the 5-HT endogenous level and the 5-HT availability at the synaptic cleft [22,37]. Correlatively, fluoxetine potentiates the facilitation of the RRG by endogenous 5-HT, doubling the resting PBf when applied at 100 μM [16]. Herein applying fluoxetine at weaker concentrations did not significantly increase the PBf but totally abolished the PBf

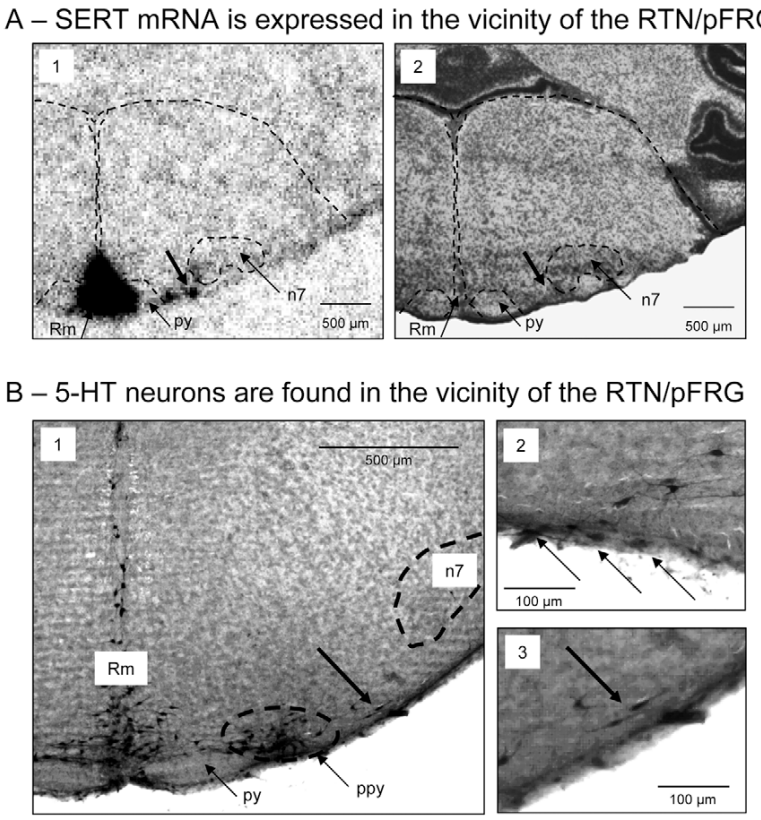

Figure 3. SERT mRNA and 5-HT-containing neurons in the vicinity of the RTN/pFRG of neonatal mice. A: Two serial coronal sections passing through the RTN/PFRG area of a neonatal mouse show SERT mRNA expression (A1) and Cresyl Violet staining (A2). Anatomical limits drawn from A2 Cresyl Violet section have been superimposed on A1 section (dotted line). Note SERT mRNA is expressed in three areas, the median Raphe Magnus (Rm), the para-pyramidal group (ppy) lateral to the pyramid tract (py) and a lateral spot (arrow) located in a medio-ventral position from the facial motor nucleus (n7), as defined from Cresyl Violet staining (in A2). B- 5-HT neurons in the RTN/pFRG area of a neonatal mouse. Note 5-HT neurons in the median raphe magnus (Rm), the parapyramidal group (ppy, doted circle) lateral to the pyramidal tract (py) and the lateral spot (arrow in B1) in the medio-ventral location of the facial nucleus (n7). In B2 and B3, note the superficial location of some 5-HT neurons (arrows). B3 is an enlargement of B1.
doi:10.1371/journal.pone.0013644.g003

response to acidosis. Mimicking the fluoxetine-induced increase in 5-HT levels with exogenous 5-HT application significantly increased the PBf and also totally abolished the PBf response. The abolition of the PBf response by 5-HT applications was unlikely caused by the increased resting PBf since no significant relationship was found between the resting PBf and the magnitude of the PBf response to acidosis under normal aCSF as well as under aCSF containing 5-HT.

Our histological results in neonatal mice show SERT mRNA expression in all areas known to contain 5-HT neurons as well as in the vicinity of the RTN/pFRG area where we also report 5-HT-containing neurons. In the RTN/pFRG of neonatal rats, SERT immunoreactivity and 5-HT receptors expression has been reported, such a dense 5-HT innervation forming a possible anatomical substrate for 5HT-dependent control of RTN/pFRG chemoreceptors [27–29]. In neonatal mice, the neurons expressing the SERT mRNA and containing 5-HT in the vicinity of the RTN/pFRG area may be viewed as a lateral subcluster of 5-HT neurons from the ppy column but it cannot be excluded that they are not actual 5-HT neurons. During development, SERT expression can transiently occur in some glutamatergic non-5-HT neurons allowing them to take up and store 5-HT released from neighbouring terminals [38]. Further experiments are required to examine whether the SERT-expressing and 5-HT-containing neurons in the vicinity of the RTN/pFRG area are actual 5-HT neurons able to synthesize 5-HT or glutamatergic RTN/pFRG neurons expressing SERT and up-taking 5-HT. Nevertheless, fluoxetine blockade of 5-HT uptake may affect the 5-HT levels, the pH response of brainstem chemoreceptors and the RRG activity and responsiveness. Application of 5-HT to RTN/pFRG chemoreceptors increases their baseline level but not the magnitude of their response to pH [28]. Thus, the abolition of the PBf responses to acidosis by fluoxetine cannot be simply explained by a decreased chemosensitivity of RTN/pFRG neurons and it possibly reflects more complex, 5-HT dependent mechanisms affecting the whole chemosensitive system.

Within the maturing CNS, endogenous 5-HT acts through a plethora of receptors subtypes to modulate maturational processes, synaptic mechanisms and neuronal excitability [14,38]. Similarly 5-HT exerts multiple effects on the neonatal respiratory network, facilitating the RRG via 5-HT1A receptors, depolarizing and firing the phrenic motoneurons via 5-HT2A receptors and reducing the transmission of the respiratory drive to motoneurons via 5-HT1B receptors [14,16,24,25,36,39]. An excess of endog-

enous 5-HT affects the expression of 5-HT1A receptors, the RRG modulation by 5-HT [36,40] and may also affect non-5HT systems known to modulate the RRG such as the catecholaminergic system [41,42]. In addition, 5-HT may affect the gap junction coupling. Gap junction coupling occurs between cultured chemoreceptors [43] as well as between chemoreceptors of discrete brainstem areas such as the locus coeruleus [44], the raphe [45] and the RTN/pFRG [46]. Frequent gap junctions contribute to the synchronous firing of raphe neurons [45] and may lead the brainstem chemoreceptors to behave as a syncytium [47]. Blockade of gap junctions reduces the *in vivo* RTN/pFRG chemosensitivity [48] and the *in vitro* resting PBf [49]. Interestingly, the gap junction coupling is reduced by excess of 5-HT [50,51]. We therefore speculate that the fluoxetine-induced excess of 5-HT reduces the gap junction coupling between brainstem chemoreceptors and that a disorganized chemoreceptor drive to the RRG during acidosis may affect the PBf response.

Thus, the fluoxetine-induced excess of 5-HT may directly (via the 5-HT system) and indirectly (via other neurotransmitter systems) affect the RRG responsiveness to acidosis as well as the elaboration of the chemoreceptor drive. Although further experiments are required to decipher these different, non-exclusive mechanisms, data from several lines of transgenic mice further support a link between 5-HT and RRG response to CO2/pH. Indeed, genetically-induced alterations of the 5-HT system in mice affect the RRG responses to CO2/pH, as reported in SERT knockout mice [37,52] and lmx1b and Pet-1 knockout mice [53,54]. In mouse model for Prader-Willi syndrome, a rare disease with blunted breathing responses to CO2/pH, neonates have excess of 5-HT in the medulla and reduced breathing response to CO2/pH [15]. In mouse model for the Central Congenital Hypoventilation Syndrome, the respiratory responses to pH are abolished, the number of 5-HT neurons is normal but nothing has been reported about 5-HT metabolism yet [11].

Translational aspects of 5-HT and breathing responses to acidosis in infants

SIDS, the main cause of infant death in industrialized countries, might result from developmental abnormality of the 5-HT system leading to altered breathing responses to CO2/pH during sleep [18–21]. Alterations of 5-HT metabolism, number of 5-HT neurons, SERT expression and 5-HT receptors expression have been reported in SIDS and a subset of SIDS infants has genetic polymorphisms impacting the 5-HT system [14,18–20]. Although our results have been obtained *in vitro* and in neonatal mice, they may be of some values for infants. Indeed, they are fully consistent with 5-HT metabolism anomalies altering breathing response to CO2/pH and increasing SIDS risks.

SERT is the primary target for widely used antidepressants. Depression concerns up to 2–3% of the pregnant women population and mothers are often subjected to treatment with SERT inhibitors, which may indirectly affect the foetuses via placental transfer and the infants via breastfeeding, resulting to clinical manifestations in 30% of the neonates, including breathing symptoms [55]. As it cannot be excluded that fluoxetine treatment of the mother depresses the infant breathing response to CO2/pH, we suggest that antidepressants targeting the 5-HT system are used with caution during pregnancy and breastfeeding period, with careful follow-up of infants exposed to these agents.

Author Contributions

Conceived and designed the experiments: SEM GH. Performed the experiments: NV YS CM MB CF EV. Analyzed the data: NV YS CM. Wrote the paper: NV GH.

References

1. Smith JC, Ellenberger HH, Ballanyi K, Richter DW, Feldman JL (1991) Pre-Botzinger complex: a brainstem region that may generate respiratory rhythm in mammals. Science 254: 726–729.
2. Blanchi B, Kelly LM, Viemari JC, Lafon I, Burnet H, et al. (2003) MafB deficiency causes defective respiratory rhythmogenesis and fatal central apnea at birth. Nat Neurosci 6: 1091–1100.
3. Onimaru H, Ikeda K, Kawakami K (2009) Phox2b, RTN/pFRG neurons and respiratory rhythmogenesis. Respir Physiol Neurobiol 168: 13–18.
4. Onimaru H, Ikeda K, Kawakami K (2008) CO2-sensitive preinspiratory neurons of the parafacial respiratory group express Phox2b in the neonatal rat. J Neurosci 28: 12845–12850.
5. Fortin G, Thoby-Brisson M (2009) Embryonic emergence of the respiratory rhythm generator. Respir Physiol Neurobiol 168: 86–91.
6. Thoby-Brisson M, Karlen M, Wu N, Charnay P, Champagnat J, et al. (2009) Genetic identification of an embryonic parafacial oscillator coupling to the preBotzinger complex. Nat Neurosci 12: 1028–1035.
7. Caubit X, Thoby-Brisson M, Voituron N, Filippi P, Bévengut M, et al. (2010) Teashirt3 regulates development of neurons involved in both respiratory rhythm and airflow control. J Neurosci In Press.
8. Stornetta RL, Moreira TS, Takakura AC, Kang BJ, Chang DA, et al. (2006) Expression of Phox2b by Brainstem Neurons Involved in Chemosensory Integration in the Adult Rat. J Neurosci 26: 10305–10314.
9. Guyenet PG, Bayliss DA, Stornetta RL, Fortuna MG, Abbott SB, et al. (2009) Retrotrapezoid nucleus, respiratory chemosensitivity and breathing automaticity. Respir Physiol Neurobiol 168: 59–68.
10. Guyenet PG, Mulkey DK (2010) Retrotrapezoid nucleus and parafacial respiratory group. Respir Physiol Neurobiol in press.
11. Amiel J, Dubreuil V, Ramanantsoa N, Fortin G, Gallego J, et al. (2009) PHOX2B in respiratory control: lessons from congenital central hypoventilation syndrome and its mouse models. Respir Physiol Neurobiol 168: 125–132.
12. Corcoran AE, Hodges MR, Wu Y, Wang W, Wylie CJ, et al. (2009) Medullary serotonin neurons and central CO2 chemoreception. Respir Physiol Neurobiol 168: 49–58.
13. Richerson GB (2004) Serotonergic neurons as carbon dioxide sensors that maintain pH homeostasis. Nat Rev Neurosci 5: 449–461.
14. Hilaire G, Voituron N, Menuet C, Ichiyama RM, Subramanian HH, et al. (2010) The role of serotonin in respiratory function and dysfunction. Respir Physiol Neurobiol.
15. Zanella S, Watrin F, Mebarek S, Marly F, Roussel M, et al. (2008) Necdin plays a role in the serotonergic modulation of the mouse respiratory network: implication for Prader-Willi syndrome. J Neurosci 28: 1745–1755.
16. Di Pasquale E, Monteau R, Hilaire G (1994) Endogenous serotonin modulates the fetal respiratory rhythm: an in vitro study in the rat. Brain Res Dev Brain Res 80: 222–232.
17. Hodges MR, Richerson GB (2010) Medullary serotonin neurons and their roles in central respiratory chemoreception. Respir Physiol Neurobiol in press.
18. Kinney HC, Richerson GB, Dymecki SM, Darnall RA, Nattie EE (2009) The brainstem and serotonin in the sudden infant death syndrome. Annu Rev Pathol 4: 517–550.
19. Paterson DS, Trachtenberg FL, Thompson EG, Belliveau RA, Beggs AH, et al. (2006) Multiple serotonergic brainstem abnormalities in sudden infant death syndrome. JAMA 296: 2124–2132.
20. Paterson DS, Hilaire G, Weese-Mayer DE (2009) Medullary serotonin defects and respiratory dysfunction in sudden infant death syndrome. Respir Physiol Neurobiol 168: 133–143.
21. Duncan JR, Paterson DS, Hoffman JM, Mokler DJ, Borenstein NS, et al. (2010) Brainstem serotonergic deficiency in sudden infant death syndrome. JAMA 303: 430–437.
22. Rudnick G (2006) Structure/function relationships in serotonin transporter: new insights from the structure of a bacterial transporter. Handb Exp Pharmacol. pp 59–73.
23. Okada Y, Masumiya H, Tamura Y, Oku Y (2007) Respiratory and metabolic acidosis differentially affect the respiratory neuronal network in the ventral medulla of neonatal rats. Eur J Neurosci 26: 2834–2843.
24. Di Pasquale E, Lindsay A, Feldman J, Monteau R, Hilaire G (1997) Serotonergic inhibition of phrenic motoneuron activity: an in vitro study in neonatal rat. Neurosci Lett 230: 29–32.
25. Di Pasquale E, Morin D, Monteau R, Hilaire G (1992) Serotonergic modulation of the respiratory rhythm generator at birth: an in vitro study in the rat. Neurosci Lett 143: 91–95.
26. Gras C, Amilhon B, Lepicard EM, Poirel O, Vinatier J, et al. (2008) The vesicular glutamate transporter VGLUT3 synergizes striatal acetylcholine tone. Nat Neurosci 11: 292–300.
27. Liu Q, Wong-Riley MT (2010) Postnatal changes in tryptophan hydroxylase and serotonin transporter immunoreactivity in multiple brainstem nuclei of the rat: implications for a sensitive period. J Comp Neurol 518: 1082–1097.

28. Mulkey DK, Rosin DL, West G, Takakura AC, Moreira TS, et al. (2007) Serotonergic Neurons Activate Chemosensitive Retrotrapezoid Nucleus Neurons by a pH-Independent Mechanism. J Neurosci 27: 14128–14138.
29. Rosin DL, Chang DA, Guyenet PG (2006) Afferent and efferent connections of the rat retrotrapezoid nucleus. J Comp Neurol 499: 64–89.
30. Kawai A, Ballantyne D, Muckenhoff K, Scheid P (1996) Chemosensitive medullary neurones in the brainstem—spinal cord preparation of the neonatal rat. J Physiol 492(Pt 1): 277–292.
31. Abbott SB, Stornetta RL, Fortuna MG, DePuy SD, West GH, et al. (2009) Photostimulation of retrotrapezoid nucleus phox2b-expressing neurons in vivo produces long-lasting activation of breathing in rats. J Neurosci 29: 5806–5819.
32. Issa FG, Remmers JE (1992) Identification of a subsurface area in the ventral medulla sensitive to local changes in PCO2. J Appl Physiol 72: 439–446.
33. Oyamada Y, Ballantyne D, Muckenhoff K, Scheid P (1998) Respiration-modulated membrane potential and chemosensitivity of locus coeruleus neurones in the in vitro brainstem-spinal cord of the neonatal rat. J Physiol 513(Pt 2): 381–398.
34. Ritucci NA, Erlichman JS, Leiter JC, Putnam RW (2005) Response of membrane potential and intracellular pH to hypercapnia in neurons and astrocytes from rat retrotrapezoid nucleus. Am J Physiol Regul Integr Comp Physiol 289: R851–R861.
35. Erlichman JS, Boyer AC, Reagan P, Putnam RW, Ritucci NA, et al. (2009) Chemosensory responses to CO2 in multiple brain stem nuclei determined using a voltage-sensitive dye in brain slices from rats. J Neurophysiol 102: 1577–1590.
36. Bou-Flores C, Lajard AM, Monteau R, De Meyer E, Seif I, et al. (2000) Abnormal phrenic motoneuron activity and morphology in neonatal monoamine oxidase A-deficient transgenic mice: possible role of a serotonin excess. J Neurosci 20: 4646–4656.
37. Kim DK, Tolliver TJ, Huang SJ, Martin BJ, Andrews AM, et al. (2005) Altered serotonin synthesis, turnover and dynamic regulation in multiple brain regions of mice lacking the serotonin transporter. Neuropharmacology 49: 798–810.
38. Gaspar P, Cases O, Maroteaux L (2003) The developmental role of serotonin: news from mouse molecular genetics. Nat Rev Neurosci 4: 1002–1012.
39. Hilaire G, Bou C, Monteau R (1997) Serotonergic modulation of central respiratory activity in the neonatal mouse: an in vitro study. Eur J Pharmacol 329: 115–120.
40. Lanoir J, Hilaire G, Seif I (2006) Reduced density of functional 5-HT1A receptors in the brain, medulla and spinal cord of monoamine oxidase-A knockout mouse neonates. J Comp Neurol 495: 607–623.
41. Hilaire G, Viemari JC, Coulon P, Simonneau M, Bevengut M (2004) Modulation of the respiratory rhythm generator by the pontine noradrenergic A5 and A6 groups in rodents. Respir Physiol Neurobiol 143: 187–197.
42. Zanella S, Roux JC, Viemari JC, Hilaire G (2006) Possible modulation of the mouse respiratory rhythm generator by A1/C1 neurones. Respir Physiol Neurobiol 153: 126–138.
43. Yang L, Su J, Zhang X, Jiang C (2008) Hypercapnia modulates synaptic interaction of cultured brainstem neurons. Respiratory Physiology & Neurobiology 160: 147–159.
44. Nichols NL, Hartzler LK, Conrad SC, Dean JB, Putnam RW (2008) Intrinsic chemosensitivity of individual nucleus tractus solitarius (NTS) and locus coeruleus (LC) neurons from neonatal rats. Adv Exp Med Biol 605: 348–352.
45. Stezhka VV, Lovick TA (1995) Dye coupling between dorsal raphe neurones. Exp Brain Res 105: 383–390.
46. Erlichman JS, Leiter JC (2010) Glia modulation of the extracellular milieu as a factor in central CO2 chemosensitivity and respiratory control. J Appl Physiol 108: 1803–1811.
47. Nattie E (1999) CO2, brainstem chemoreceptors and breathing. Prog Neurobiol 59: 299–331.
48. Hewitt A, Barrie R, Graham M, Bogus K, Leiter JC, et al. (2004) Ventilatory effects of gap junction blockade in the RTN in awake rats. Am J Physiol Regul Integr Comp Physiol 287: R1407–R1418.
49. Bou-Flores C, Berger AJ (2001) Gap Junctions and Inhibitory Synapses Modulate Inspiratory Motoneuron Synchronization. J Neurophysiol 85: 1543–1551.
50. Rorig B, Sutor B (1996) Serotonin regulates gap junction coupling in the developing rat somatosensory cortex. Eur J Neurosci 8: 1685–1695.
51. Moss BL, Fuller AD, Sahley CL, Burrell BD (2005) Serotonin modulates axo-axonal coupling between neurons critical for learning in the leech. J Neurophysiol 94: 2575–2589.
52. Li A, Nattie E (2008) Serotonin transporter knockout mice have a reduced ventilatory response to hypercapnia (predominantly in males) but not to hypoxia. J Physiol 586: 2321–2329.
53. Erickson JT, Shafer G, Rossetti MD, Wilson CG, Deneris ES (2007) Arrest of 5HT neuron differentiation delays respiratory maturation and impairs neonatal homeostatic responses to environmental challenges. Respir Physiol Neurobiol 159: 85–101.
54. Hodges MR, Tattersall GJ, Harris MB, McEvoy SD, Richerson DN, et al. (2008) Defects in breathing and thermoregulation in mice with near-complete absence of central serotonin neurons. J Neurosci 28: 2495–2505.
55. Belik J (2008) Fetal and neonatal effects of maternal drug treatment for depression. Semin Perinatol 32: 350–354.

4 - L'érythrocytose excessive et des hauts niveaux d'érythropoïétine dans le sang et dans le cerveau diminuent la réponse ventilatoire à l'hypercapnie chez la souris

Menuet C., Khemiri H., de la Poëze d'Harambure T., Gassmann M., Hilaire G., Gestreau C.* & Soliz J.*
*Ces auteurs ont contribué de manière égale au travail.
Soumis à *The Journal of Physiology (London)*.

Résumé en français :

L'érythropoïétine (EPO), sécrétée dans le plasma et dans le cerveau, interagit avec les structures périphériques et centrales pour augmenter la réponse ventilatoire à l'hypoxie. Cet effet a été attribué à la présence des récepteurs à l'EPO dans les centres respiratoires du tronc cérébral et dans les corps carotidiens. Comme les chémorécepteurs centraux et périphériques sont sensibles aux changements de PCO_2, nous avons testé l'hypothèse selon laquelle l'EPO modulerait la réponse ventilatoire à l'hypercapnie (RVHC). La ventilation de base et la RVHC ont été évaluées en pléthysmographie et en électrophysiologie *in vivo* chez deux souches de souris transgéniques surexprimant constitutivement l'EPO humaine dans le cerveau seulement (Tg21) ou dans le cerveau et dans le plasma (Tg6), et ont été comparées à celles de souris sauvages (WT). De plus, l'hématocrite (Htc) des souris WT ou Tg6 a été augmenté de manière aiguë par l'injection d'une protéine récente stimulant l'érythropoïèse (NESP ; WT-NESP) ou baissé par application de phénylhydrazine (un agent pharmacologique qui induit une hémolyse, PHZ ; Tg6-PHZ), respectivement. Les résultats ont montré que les souris Tg6 et Tg21 présentent une RVHC plus faible que les souris WT. Egalement, la RVHC était réduite chez les souris WT-NESP alors qu'elle était augmentée chez les souris Tg6-PHZ. Nous concluons que l'augmentation des niveaux d'EPO dans le plasma et dans le cerveau, mais aussi l'érythrocytose excessive, diminuent la RVHC. Ces résultats pourraient être importants pour mieux comprendre les désordres respiratoires se produisant en altitude.

Excessive erythrocytosis and high levels of erythropoietin in blood and brain blunt the hypercapnic ventilatory response in mice

Clément Menuet[1], Hanan Khemiri[1], Théodora de la Poëze d'Harambure[1], Max Gassmann[2], Gérard Hilaire[1], Christian Gestreau[1]* & Jorge Soliz[1,2]*

1: Maturation, Plasticity, Physiology and Pathology of Respiration (mp3-resp team), Unité Mixte de Recherche 6231 CNRS, Université d'Aix-Marseille II et III, Service 362, 13397 Marseille Cedex 20, France.
2: Institute of Veterinary Physiology, Vetsuisse Faculty, and Zurich Center for Integrative Human Physiology (ZIHP), University of Zurich, Winterthurerstrasse 260, CH-8057 Zurich, Switzerland
** These senior authors contributed equally to this work*

Keywords: carbon dioxide, ventilatory control, brainstem respiratory centres, carotid bodies
Running title: Blunted ventilatory response to CO_2 in mice overexpressing erythropoietin
Total words number: 5030

Corresponding author
Jorge Soliz, PhD
Prof. sous octroi
Département de Pédiatrie, Université Laval
Centre de Recherche, HSFA, D0-717
10, rue de l'Espinay
Québec (Qc), Canada, G1L 3L5
Tel : (418) 525 4444 # 53946
Fax: (418) 525 4195
E-mail: jorge.soliz@crchuq.ulaval.ca

Abstract

Erythopoietin (Epo), secreted in plasma and brain, interacts with central and peripheral structures to increase the ventilatory response to hypoxia. This effect has been attributed to the presence of Epo receptors in both brainstem respiratory centres and carotid bodies. Since central as well as peripheral chemoreceptors also sense changes in PCO_2, we tested the hypothesis that Epo modulates the hypercapnic ventilatory response (HCVR). Baseline ventilation and HCVR were evaluated by plethysmography and *in vivo* electrophysiology in two transgenic mouse lines constitutively overexpressing human Epo in brain only (Tg21) or in brain and plasma (Tg6), and compared to those of wild type (WT) mice. Further, the haematocrit (Htc) levels of WT or Tg6 mice were acutely elevated by injection of the novel erythropoiesis-stimulating protein (NESP; WT-NESP) or reduced by application of the haemolysis-inducing compound phenylhydrazine (PHZ; Tg6-PHZ), respectively. The results showed that Tg6 and Tg21 mice had a lower HCVR than WT mice. Also, HCVR was reduced in WT-NESP whereas it was increased in Tg6-PHZ. We conclude that increased levels of Epo in plasma and brain, as well as excessive erythrocytosis blunt the HCVR. These findings may be relevant to better understand respiratory disorders such as those occurring at high altitude.

(200 words)

Abbreviations AUC, area under the curve; CMS, chronic mountain sickness; EMG_{EIC}, external intercostal muscles electromyogram; Epo, erythropoietin; EpoR, erythropoietin receptor; Hct, haematocrit; Hb, haemoglobin; HCVR, hypercapnic ventilatory response; NESP, aranesp; PHZ, phenylhydrazine hydrochloride; R_f, respiratory frequency; Tg6-PHZ, Tg6 mice spleenectomized and treated with PHZ; Tg6-SHAM, sham operated Tg6 mice; V_E, minute ventilation; VNA, vagus nerve activity; V_T, tidal volume; WT, wild type; WT-NESP, WT mice treated with NESP; WT-Tg6, WT controls for Tg6 mice; WT-Tg21, WT controls for Tg21 mice.

Introduction

Erythropoietin (Epo) is a glycoprotein hormone that plays an essential role in erythropoiesis (Maurer *et al.* 2002; Kilic *et al.* 2005a and 2005b). It is also a cytokine characterized by low expression and activity under normal conditions but one that is rapidly up-regulated during such stressful conditions as hypoxia (Haroon *et al.* 2003; Muller-Ehmsen *et al.* 2005), tumor growth (Farrell & Lee, 2004) and trauma (Jelkmann, 2005). Epo is produced by the peritubular capillary endothelial cells in the kidney and liver, and its basal level is upregulated when the arterial PO_2 (PaO_2) decreases below normal levels, as occurs at sufficiently high altitudes.

The erythropoietic function of Epo was recognized more than 100 years ago (Jelkmann, 2007), and is the basis for its extensive use in clinics for the treatment of patients after chemotherapy (Kassem & Yassin, 2010) or in need of repeated blood transfusions as a result of such anemia-related illnesses as chronic kidney disease (Leon-Velarde *et al.* 1998; Kato, 2010).

During the last decade, however, Epo and its receptor (EpoR) have been detected in many tissues, including brain, heart, lungs and testis, suggesting that EPO has a much broader field of action than previously recognized. In particular, Epo in brain plays an important role in the response to stroke (Marti *et al.* 2000), multiple sclerosis (Sattler *et al.* 2004), schizophrenia (Ehrenreich *et al.* 2004), trauma (Grasso *et al.* 2007), epilepsy (Kondo *et al.* 2009) and retinopathy (Romagnoli *et al.* 2000).

Several studies from our laboratory have helped to characterize the effects of Epo on breathing. In mice, Epo increases the ventilatory response to hypoxia by activating brainstem respiratory neurons and cells of the carotid body (Soliz *et al.* 2005 and 2007a). Indeed, by using transgenic mice specifically overexpressing Epo in the nervous system, we demonstrated that Epo enhances the ventilatory response and acclimatization to acute and chronic hypoxia (Soliz *et al.* 2005). Epo also increases the hypoxic ventilatory response in humans (Gassmann & Soliz, 2009). Immunohistochemical analysis revealed that EpoR is expressed in mice brainstem nuclei involved in respiratory control (pre-Bötzinger complex, nucleus tractus solitarii and medullary catecholaminergic nuclei), as well as in carotid bodies (Soliz *et al.* 2005). Although these results demonstrate that Epo contributes significantly to oxygen homeostasis, the potential role of Epo in modulating the ventilatory response to changes in $PaCO_2$ has never been explored. Assessing this role may be relevant because hypoxia-mediated hyperventilation increases the elimination of CO_2 that *per se* exerts a powerful drive to breathe (Feldman *et al.* 2003; Guyenet *et al.* 2010). Knowing that carotid bodies as well as multiple sites in the brainstem detect changes in $PaCO_2$ (Mulkey *et al.* 2004; Richerson, 2004; Trapp *et al.* 2008; Nattie & Li, 2009; Gestreau *et al.* 2010; Gourine *et al.* 2010; Guyenet *et al.* 2010), and that EpoR are present in both peripheral and central chemosensitive structures (see above), we reasoned that increased Epo levels may influence the activity of chemoreceptors during hypercapnia and modulate the hypercapnic ventilatory response (HCVR). To test this hypothesis, we studied two transgenic mouse lines showing enhanced level of Epo in brain only (Tg21) and in brain and plasma (Tg6),

and compared their baseline ventilations and responses to CO_2 inhalation to those of wildtype (WT) mice. The HCVR of Tg6 and Tg21 was decreased, suggesting that both plasma and brain overexpression of Epo, as well as excessive erythrocythosis, blunt the HCVR. We discuss potential mechanisms consistent with our findings and their relevance in understanding respiratory disorders at low and high altitude, such as obstructive sleep apnoea and chronic mountain sickness.

Methods

Experiments were performed in accordance with French national legislation (JO 87-848) and European Communities Council Directive (22 September 2010, 2010/63/EU, 74). Permit numbers A13-505 and 13-227 for C. Menuet and C. Gestreau, respectively, were delivered by Direction Départementale de la Protection des Populations, Préfecture des Bouches du Rhône, France. This study also conformed to the standards required by *The Journal of Physiology* (Drummond, 2009).

Transgenic animals

Transgenic mouse lines overexpressing Epo were generated by microinjection of human Epo cDNA driven by the human platelet-derived growth factor (PDGF) β-chain promoter into the pronuclei of fertilized oocytes derived from B6C3 hybrid mice (Ruschitzka *et al.* 2000). One resulting transgenic mouse line TgN(PDGFBEPO)321ZbZ (Tg6) showed increased Epo levels in plasma (12 fold *vs* WT control animals) and brain (26 fold *vs* WT), accompanied by a doubled haematocrit (Hct) (Wagner *et al.* 2001; Heinicke *et al.* 2006) and increased (25.3 ± 0.7 g dl^{-1}) haemoglobin (Hb) concentration. This erythrocytotic line was backcrossed to C57Bl/6 mice for more than 12 generations by mating hemizygous males to WT C57Bl/6 females. Half of the offspring were hemizygous for the transgene while the other half were WT and thus used as controls (WT-Tg6). The second transgenic mouse line termed TgN(PDGFBEPO)322ZbZ (Tg21) was generated as Tg6 and was bred to homozygosity in a C57Bl/6 background and showed increased Epo levels in brain only (4 fold *vs* WT) (Wiessner *et al.*

2001). Both WT (WT-Tg21) and Tg21 animals presented normal Hct and Hb concentration (15.4 ± 0.5 g dl^{-1}). Knowing that aged Tg6 mice display organ degeneration (Heinicke *et al.* 2006), we used exclusively transgenic (18 Tg6 and 13 Tg21) and WT (17 WT-Tg6 and 14 WT-Tg21) male mice of 2-3 months of age in our experiments.

Determination of ventilation by plethysmography

Ventilation of conscious mice was recorded using non-invasive whole-body plethysmography as previously described (Soliz *et al.* 2005; Menuet *et al.* 2011). Before recordings, the mice were habituated to the plethysmograph chamber to reduce stress. Only periods of breathing without body movements were studied. We used a constant flow plethysmograph (EMKA Technologies, Paris, France) with 200 ml animal chamber ventilated with air (600 ml min^{-1}). Spirograms were stored and analyzed (Spike 2; Cambridge Electronic Design, Cambridge, UK) to calculate the mean respiratory frequency (R_f, expressed in cycles per minute), the tidal volume normalized by the body weight (V_T, µl g^{-1}), and the minute ventilation normalized by the body weight (V_E, ml g^{-1} min^{-1}, with $V_E = R_f \times V_T / 1000$). For V_T measurements, calibrations were performed by injecting a small volume (100 µl) of air into the recording chamber. We analyzed the effect of imposed hypercapnic challenge by first recording ventilation during inhalation of room air for 20 min and then during inhalation of a hypercapnic mixture (4% CO_2, 21% O_2, balance N_2) for 5 min period (Menuet *et al.* 2011). Since hypercapnia usually induces transient agitation, only recordings during the last 3 minutes of the hypercapnic challenge were analyzed.

Analysis of respiratory parameters by *in vivo* electrophysiology

To further assess the HCVR of WT and transgenic animals, electrophysiological recordings were obtained from anaesthetised animals.

Anaesthesia. Mice were put in an induction chamber flushed with 3% isoflurane in air. Volatile anaesthesia was maintained via a face mask by reducing the inspired isoflurane concentration to 1.5-2.0 %. Body temperature was maintained at 37°C using a temperature-controlled heating pad.

Surgery and electrophysiological recordings. A pair of copper electrodes was implanted in an external intercostal muscle to record electromyographic inspiratory activity (EMG_{EIC}). The cervical vagus nerve was dissected free from surrounding tissue and mounted on coiled bipolar silver electrodes to record vagal nerve activity (VNA). The raw respiratory activities (EMG_{EIC} and VNA) were amplified (gain 5-20 K), filtered (band pass 0.1-3 kHz), and moving averages obtained (leaky integrator with 100 ms time constant). Both raw and integrated signals were digitized (sampling frequency 6 kHz) and stored on computer for off-line analyses (Spike 2; Cambridge Electronic Design, Cambridge, UK).

Experimental paradigm. Fifteen minutes after completion of surgery, all mice had stable heart rate and R*f*. Signals were then recorded for 3 minutes under basal condition (control period). Subsequently, mice were exposed for 3 minutes to a normoxic hypercapnic gas mixture (7% CO_2, 21% O_2, balance N_2). Immediately after this first hypercapnic challenge, signals were then recorded for 5 min (recovery period). Once cardiorespiratory activity returned to basal values, signals were again recorded for 3 minutes

(control period) before exposure of mice for 3 minutes to a second hypercapnic challenge with a second more hypercapnic gas mixture (12% CO_2, 21% O_2, balance N_2). Once room air was re-established, respiratory signals were recorded for additional 5 minutes (recovery period). This protocol was chosen based on preliminary data showing dose-dependent increases in ventilatory responses of anaesthetised mice.

Data Analysis. Duration (expressed in seconds), peak amplitude and area under the curve (AUC, expressed in arbitrary units) of respiratory bursts were measured from the integrated signals. For each animal, the values were first measured during control periods and compared with data obtained during the 3 minutes of the hypercapnic challenges. Changes in peak amplitude and AUC of integrated EMG_{EIC} and VNA were expressed as percentage of control values. We did not measure R*f* in this set of experiments since it is depressed under anaesthesia and was already measured in awake mice using plethysmography. At the end of the experiments, blood samples were collected from the heart to measure Epo levels in plasma. Rats were killed by injection (0.5 ml, intracardiac) of a euthanizing agent (T-61, Intervet S.A., Beaucouzé, France).

Pharmacological experiments

We used pharmacological treatments in WT and transgenic mice in order to assess the different factors contributing to the reduction of the HCVR. We followed the same protocol as previously described by Schuler and colleagues (Schuler *et al.* 2010). Each pharmacological protocol was followed by plethysmographic assessment of the HCVR of the mice.

Aranesp-treatment of WT-Tg6 mice (WT-NESP). To examine the effect of excessive erythrocytosis on the HCVR, the Hct of WT-Tg6 mice was increased using s.c. injections of Aranesp (darbopoietin alfa, Amgen; 12.5 µg kg^{-1}) twice a week. At least 10 days of treatment were necessary to reach a high level of Hct, as observed from blood samples taken from the tail vein of the animals and Hct measurements after centrifugation.

Splenectomy and phenylhydrazine-treatment of Tg6 mice (Tg6-PHZ). Massive erythropoiesis occurs in the spleen of Tg6 animals (Ruschitzka *et al*. 2000). In order to decrease the Hct level, splenectomy of 6 week old Tg6 mice was first performed using a left side abdominal laparatomy (Vogel *et al.* 2003; Gassmann *et al*., 2003; Schuler *et al.* 2010). Once Tg6 mice were 10 weeks old, their Hct was reduced to normal range levels (40-45%) by s.c. administration of freshly prepared phenylhydrazine hydrochloride (PHZ; Sigma, P6926, Switzerland) that causes chemical haemolysis (Lim *et al.* 1998; Vannucchi *et al.* 2001). Animals received one PHZ injection (1.2 mg 10 g^{-1} body weight) every 2 days for 6 days. Blood samples were taken from the tail veins of the animals, and Hct was measured by centrifugation. A group of sham-operated Tg6 animals (Tg6-SHAM) was used as controls.

Quantification of plasma Epo

Blood samples were drawn by cardiac puncture into heparinized Ependorff tubes and plasma was collected after centrifugation at 18,000 g. Protein concentrations of plasma were determined by the Bradford protein assay (Bio-Rad, Hercules, CA, USA). Subsequently, Epo levels were quantified using an ^{125}I-Epo-based radioimmunoassay (RIA) (Amersham, Zurich, Switzerland),

according to previously published protocols (Kilic *et al.* 2005a). The lower detection limit of our RIA was 4 $U.l^{-1}$, and the intra-assay/inter-assay variances were < 2% and < 6%, respectively.

Statistical analysis

Analysis was performed using Statview software (Abacus Concepts, Berkeley, CA), and values expressed as means ± SD. A one-way ANOVA followed by a post-hoc PLSD (Protected Least Significant Difference of Fisher) test was used to analyse data from plethysmography and plasma Epo measurements when comparisons were done between more than two groups. Repeated measures ANOVA were used to compare data obtained with electrophysiology. Student *t*-tests were used to analyse data from plethysmography and Hct measurements in which only two groups were compared. Regression analyses were also performed to analyse correlation between V_E and Hct or plasma Epo concentration. Differences were considered significant when $p<0.05$.

4. RESULTS

Decreased HCVR in awake Tg6 mice

Minute ventilation (V_E), tidal volume (V_T) and respiratory frequency (R_f) were evaluated in unrestrained WT-Tg6 (n=8) and Tg6 mice (n=11), the latter showing constitutive overexpression of Epo (in brain and plasma) and excessive erythrocythosis. The Tg6 group consisted of both Tg6-SHAM (n=5) and Tg6 (n=6) mice, since their ventilatory parameters were similar under both normocapnic (V_T, R_f and V_E, p=0.73, 0.36, and 0.49 respectively) and hypercapnic (V_T, R_f and V_E, p=0.3, 0.24 and 0.75 respectively) conditions. Neither V_E nor ventilatory pattern (R_f and V_T) differed between WT-Tg6 and Tg6 mice exposed to normoxic normocapnic environment (room air) (Fig. 1). Exposure to normoxic hypercapnia (21% O_2, 4% CO_2 for 5 minutes) triggered a strong ventilatory response in both groups. However, compared to control values, V_E was greater ($p<0.001$) in WT-Tg6 than in Tg6 mice (12.8 ± 1.7 vs 5.0 ± 0.7, respectively) (Fig. 1A). Overall, the HCVR of Tg6 mice was blunted by 60% due to a significant decrease in both R_f ($p<0.01$; Fig. 1B) and V_T ($p<0.001$; Fig.1C).

Decreased intercostal and vagal respiratory activities in anaesthetised Tg6 mice exposed to hypercapnia

Respiratory drive to both laryngeal and thoracic muscles was evaluated from vagal nerve activity (VNA) and external intercostal muscle discharge (EMG_{EIC}) in isoflurane-anethetized mice. Mean duration, peak amplitude and AUC of integrated signals were measured in Tg6 (n=7) and WT-Tg6 mice (n=9) (Fig.

2). When mice were exposed to 7% CO_2, there was no difference between strains in duration of EMG_{EIC} or VNA (Fig. 2A). However, the AUC of both respiratory signals measured during the HCVR was significantly greater in WT-Tg6 compared to Tg6 mice ($p<0.05$ and $p<0.01$ for EMG_{EIC} and VNA, respectively) (Fig. 2A). This difference was mainly attributable to changes in peak amplitude of the respiratory signals ($p<0.01$ for EMG_{EIC} and VNA) (Fig. 2A). The mean amplitude and AUC of VNA measured during recovery in Tg6 mice remained significantly elevated ($p<0.05$ for both parameters). Similar results were obtained when animals were exposed to 12% CO_2 except that the evoked HCVR in the two groups were greater than those observed with 7% CO_2 (Fig. 2B). These data demonstrate that Tg6 mice harbouring increased Epo (in brain and plasma) and a nearly double Hct have a decreased HCVR at high and even very high percentages of CO_2 inhalation.

Excessive erythrocytosis contributes to the decreased HCVR

The novel erythropoiesis stimulating agent Aranesp (NESP) and treatment with the haemolytic agent phenylhydrazine (PHZ) were used to manipulate Hct values in WT and Tg mice (Schuler *et al*., 2010). NESP significantly increased the Hct of WT-Tg6 mice (WT-NESP, n=6) and PHZ effectively reduced the Hct of Tg6 mice (Tg6-PHZ, n=7) to normal values (Fig. 3A). Subsequent evaluation of ventilatory parameters showed that WT-NESP mice with increased Hct (Fig. 3A) had a significantly reduced HCVR (Fig. 3B-C). In contrast, The HCVR of Tg6-PHZ animals with reduced Hct (Fig. 3A) did not increase compared to Tg6 mice (Fig. 3B-C). There was a significant linear correlation ($r^2=0.987$; $p<0.001$) between HCVR and Hct in WT-Tg6, WT-NESP

and Tg6 mice (Fig. 3B), suggesting that decreases in the HCVR are associated with increases in Hct.

Increased plasma Epo blunts the HCVR

Treatments with either NESP or PHZ altered not only the Hct but also the levels of plasma Epo. Indeed, both WT-Tg6 animals injected with NESP (WT-NESP) and Tg6 mice injected with PHZ (Tg6-PHZ) had significant increases in plasma Epo concentrations (Fig. 4A). We interpret the increased levels of plasma Epo in Tg6-PHZ mice as a probable consequence of hypoxemia due to the haemolytic action of PHZ. The correlation observed between the HCVR and plasma Epo concentration was analysed using data from WT-Tg6, WT-NESP, Tg6 and Tg6-PHZ mice (Fig. 4B); a highly significant logarithmic correlation (r^2=0.923, $p<0.001$) was found (Fig. 4B), suggesting that an increase in plasma Epo contributes to decrease the HCVR.

Increased level of cerebral Epo decreases the HCVR

Next, a second strain of transgenic mice (Tg21) was used to analyse the effect of cerebral Epo on the HCVR. Tg21 mice overexpress Epo in brain only and show normal levels of plasma Epo and Hct (Wiessner *et al.* 2001). Compared to WT-Tg21 mice, the TG21 mice had a significantly ($p<0.05$) reduced V_E in response to CO_2 (Fig. 5A). This reduction was mainly attributable to a significant reduction in R*f* (Fig. 5B) since the two strains had similar VT values (Fig. 5C). In agreement with these data, our electrophysiological measurements revealed significant decreases in vagal and intercostal respiratory activities in Tg21 mice exposed to 7% (Fig. 6A) and

12% CO_2 (Fig. 6B), compared with the gradual increase in HCVR in WT-Tg21 mice (Fig. 6A-B). The lower HCVR of Tg21 mice was mainly due to significant decreases in peak amplitude and AUC of both vagal and intercostal discharges (Fig. 6A-B). The duration of VNA differed significantly ($p<0.05$) between WT-Tg21 and Tg21 mice exposed to 12% CO2 (Fig. 6B). The amplitude, duration and/or AUC of the respiratory signals did not recover similarly between the two groups of animals (Fig. 6A-B), probably due to changes in magnitude of the HCVR.

DISCUSSION

In the present study, we examined the effects of high Epo levels and excessive erythrocythosis on the respiratory responses to hypercapnia in a transgenic mouse line (Tg6) showing constitutive high levels of Epo in brain (26 fold *vs* WT) and plasma (12 fold *vs* WT) and high Hct (Wiessner *et al.* 2001). Our results show for the first time strong evidence that overexpression of Epo decreases the HCVR. In addition, data obtained after treatment of WT-Tg6 mice with NESP as well as injection of PHZ in transgenic Tg6 mice, suggest also that at the peripheral level both excessive erythrocythosis and increased Epo concentration in plasma reduce the HCVR. In addition, the use of a second strain of transgenic mice (Tg21) that overexpress Epo exclusively in brain (4 fold *vs* WT) allowed us to discriminate central *vs* peripheral effects of Epo on HCVR. Our data indicate that Epo overexpression in brain decreases the HCVR. This central effect of Epo could be mediated by a decreased sensitivity to CO_2 of brainstem chemoreceptors.

Decreased HCVR due to excessive erythrocytosis

In this study, we observed that excessive erythrocytosis blunted the HCVR. It is now clear that this desensitization is due to both direct and indirect effects of Epo. Our data show that there is a strong, inverse linear relationship between the Hct and the HCVR of WT-Tg6, WT-Tg6 with increased Hct level (WT-NESP) and Tg6 mice. Elevation of red blood cells increases the level of carbonic anhydrase, the enzyme catalyzing the reversible hydration of CO_2 into bicarbonate and protons (Lindskog *et al*. 1993). Since inhibition of carbonic anhydrase, for instance with acetazolamide, induces tissue acidosis

and increases ventilation (Maren, 1977; Coates *et al.* 1991), we suggest that an elevation of carbonic anhydrase increases the buffering capacity of blood, thus lowering the CO_2/pH chemical drive on respiratory centres. In addition, a higher Hct would confer a higher capacity to form carboxy-haemoglobin, increasing CO_2 elimination by pulmonary gas exchange and lowering plasma CO_2. This may decrease the peripheral and/or central chemosensitivity to CO_2.

The contributions of these indirect mechanisms related to excessive erythrocytosis are further supported by the decreased basal ventilation of WT-NESP mice. However, data from Tg6 mice with Hct values restored to a normal level (Tg6-PHZ) are below the linear correlation between Hct and HCVR, suggesting the contribution of additional parameters.

Decreased HCVR due to increased plasma [Epo]

Spleenectomy and phenylhydrazine treatment in Tg6 mice (Tg6-PHZ) restored Hct to normal but not the HCVR. Interestingly, Tg6-PHZ as well as WT-NESP mice had increased levels of plasma Epo, indeed a significant negative correlation was observed between the ventilatory responses to CO_2 and plasma [Epo] measured in all mice. These results strongly suggest that high plasma [Epo] blunts the HCVR. The mechanisms remain speculative. Under physiological conditions, an intact blood-brain-barrier excludes large glycosylated molecules such as Epo (Marti *et al.*, 1997; Buemi *et al.*, 2000). Moreover, when high doses of Epo (5000 U/l or higher) are administered systemically, only about 1% of the Epo crosses the blood-brain-barrier (Banks *et al.*, 2004; Marti, 2004; Xenocostas *et al.*, 2005; Statler *et al.*, 2007). Thus,

high plasma Epo concentration may not be able to affect central chemoreceptors. By contrast, the impact of plasma Epo on carotid bodies cannot be ignored. Indeed, Epo receptors are expressed in glomus cells (Soliz *et al.*, 2005; Lam *et al.*, 2009), and plasma Epo modulates the ventilatory response to hypoxia by interacting with carotid chemoreceptors (Soliz *et al.* 2005 and 2007b; Gassmann *et al.* 2010). Further studies are needed to determine how Epo in carotid bodies interacts with O_2 and CO_2 sensitive channels and/or neurotransmitters.

Decreased HCVR due to increased brain [Epo]

Centrally-produced Epo also acts directly on brainstem respiratory centers to modulate the ventilatory response to hypoxia and Epo receptors are present in medullary structures that control breathing *(Soliz et al.* 2005, 2007b and 2009; *Gassmann et al. 2010*). These data suggest that in addition to the peripheral effects of Epo discussed above, Epo may also blunt the HCVR via a central action.

Comparisons of data from Tg6 and Tg21 mice

Tg21 mice overexpress Epo only in brain and show normal haematological parameters (Wiessner *et al.* 2001). Our plethysmography and electrophysiology results revealed that these mice display a decreased HCVR, consistent with the idea that Epo directly modulates the central respiratory drive during hypercapnia. Moreover, the decrease of ventilation in response to hypercapnia found in Tg21 mice was less pronounced than that observed in Tg6 mice. This difference may be explained by additive peripheral

and central effects of Epo in Tg6 mice, or by the fact that Tg6 mice show a higher overexpression of central Epo (26 fold *vs* WT) compared to Tg21 animals (4 fold *vs* WT) (Wiessner *et al.* 2001).

In our experiments, two different *in vivo* strategies were used to assess the HCVR in Tg6 and Tg21 mice. Plethysmography enables recording of ventilation in unrestrained, non-anaesthetised mice. This useful technique, however, provides only a global measure of ventilation and sometimes detects artifactual increases in V_T (Dutschmann *et al.* 2010; Voituron *et al.* 2010). Effective ventilation requires the coordinated activity of upper airway muscles (regulation of resistance) and pump muscles (flow generation) (Bianchi & Gestreau, 2009). Therefore, we further assessed the ventilatory response of mice using electrophysiological approaches under anaesthesia to describe the effects of Epo on cranial and spinal respiratory motor outputs. Our results revealed that the decreased HCVR of Tg6 and Tg21 mice is associated with a lower drive to both ventilatory “pump” (external intercostal muscle electromyogram) and “valve” (vagal nerve activity) muscles.

Putative mechanism of Epo-induced central desensitization to hypercapnia

Our results suggest that Epo acts directly on brainstem respiratory centres to modulate the HCVR. Therefore, Epo may target one or more central chemosensitive structures that are widely distributed throughout the brainstem (Richerson, 2004; Nattie & Li, 2009; Guyenet *et al.* 2010). Among them, the retrotrapezoid nucleus (RTN) is thought to be a key component of CO_2/pH chemosensitivity (Mulkey *et al.* 2004; Guyenet *et al.* 2010). Interestingly, a

recent study showed that RTN neurons express TASK2 channels responsible for an acid-sensitive background K^+ current, and that mutant Task2$^{-/-}$ mice have an increased ventilatory response to hypoxia as well as decreased sensitivity to hypercapnia (Gestreau *et al.* 2010). The similarity between respiratory phenotypes of Tg6/Tg21 and Task2$^{-/-}$ mice suggests that RTN neurons may be a direct target of Epo. In addition, Epo modulation of the ventilatory response to hypoxia is correlated with a lower and higher catecholamine turnover in the medulla and pons, respectively (Soliz *et al.* 2005). As catecholaminergic groups also represent CO_2/pH chemosensitive areas (Haxhiu *et al.* 1996; Li *et al.* 2008; Kanbar *et al.* 2011), these nuclei represent other putative mediators of the Epo-induced hypercapnic desensitization.

Alternatively, astrocytes also mediate a CO_2/pH chemosensitive drive to respiration (Gourine *et al.* 2010). Astrocytes are the main sources of Epo in the brain (Masuda *et al.* 1994; Marti *et al.* 1996; Weidemann *et al.* 2009) and express Epo receptors (Nagai *et al.* 2001; Buemi *et al.* 2003). Central Epo could thus act in an autocrine/paracrine manner in chemosensitive areas on both astrocytes and neurons. In addition, high numbers of Epo receptors are found in astrocytic endfeet around brain capillaries that could be bound by circulating Epo (Marti, 2004). The latter mechanisms may explain the greater blunting of the HCVR in Tg6 compared to Tg21 mice.

Conclusions and perspectives

Our results show for the first time that Epo decreases the HCVR via both peripheral and central effects. We are convinced that this has major

implications for a better understanding of the pathophysiology of chronic mountain sickness (CMS), a condition in which high altitude residents affected by this disease develop a blunted ventilatory response to hypoxia, inducing severe and persistent hypoxemia leading to increased Epo production, excessive erythrocytosis, pulmonary hypertension, right heart failure and death (Monge & Whittembury, 1976; Leon-Velarde *et al.* 2010). Patients with CMS have greater end-tidal $PaCO_2$s and lower pHs compared to control high altitude dwellers (Fatemian *et al.* 2003; Leon-Velarde *et al.* 2010), and hypoventilation in CMS patients is associated to reduced central chemosensitivity to CO_2 (Hurtado, 1960; Fatemian *et al.* 2003; Leon-Velarde & Richalet, 2006). We propose that Epo plays a crucial role in the development of CMS, not only by inducing a pathological level of Hct, but also by reducing the respiratory drive due to blunted CO_2/pH chemosensitivity, contributing to hypoventilation and thus hypoxemia.

6. AUTHOR CONTRIBUTION

C.M., C.G. and J.S. contributed to the conception and design of the experiments. C.M., H.K., T.P.H., C.G. and J.S. collected and analysed the data, and C.M., C.G. and J.S. interpreted them. C.M., C.G. and J.S. wrote the article. M.G. and G.H. revised the article critically and funded the project. All authors approved the final version of the manuscript. All experiments were performed in CRN2M UMR 6231 CNRS, Univ. Aix-Marseille II and III, Marseille, France.

7. ACKNOWLEDGMENTS

The authors thank Dr. Steve Iscoe for his appraisal of the manuscript and editorial assistance. Some of the equipment used in this study was funded by grants from Ville de Marseille and Conseil Régional Provence Alpes Côte d'Azur (PACA) to C.G. Part of this study has been financed by the Roche Foundation for Anemia Research (RoFAR), the European Respiratory Society (ERS) and the Swiss National Science Foundation, to M.G.

8. REFERENCES

Banks WA, Jumbe NL, Farrell CL, Niehoff ML & Heatherington AC (2004). Passage of erythropoietic agents across the blood-brain barrier: a comparison of human and murine erythropoietin and the analog darbepoetin alfa. *Eur J Pharmacol* **505,** 93-101.

Bianchi AL & Gestreau C (2009). The brainstem respiratory network: an overview of a half century of research. *Respir Physiol Neurobiol* **168**, 4-12.

Buemi M, Allegra A, Corica F, Floccari F, D'Avella D, Aloisi C, Calapai G, Iacopino G & Frisina N (2000). Intravenous recombinant erythropoietin does not lead to an increase in cerebrospinal fluid erythropoietin concentration. *Nephrol Dial Transplant* **15,** 422-423.

Buemi M, Cavallaro E, Floccari F, Sturiale A, Aloisi C, Trimarchi M, Corica F & Frisina N (2003). The pleiotropic effects of erythropoietin in the central nervous system. *J Neuropathol Exp Neurol* **62,** 228-236.

Coates EL, Li AH & Nattie EE (1991). Acetazolamide on the ventral medulla of the cat increases phrenic output and delays the ventilatory response to CO2. *J Physiol* **441**, 433-51.

Drummond GB (2009). Reporting ethical matters in *The Journal of Physiology*: standards and advice. J Physiol 587, 713-719.

Dutschmann M, Menuet C, Stettner GM, Gestreau C, Borghgraef P, Devijver H, Gielis L, Hilaire G & Van Leuven F (2010). Upper airway dysfunction of Tau-P301L mice correlates with tauopathy in midbrain and ponto-medullary brainstem nuclei. *J Neurosci* **30**, 1810-21.

Ehrenreich H, Degner D, Meller J, Brines M, Behe M, Hasselblatt M, Woldt H, Falkai P, Knerlich F, Jacob S, von Ahsen N, Maier W, Bruck W, Ruther E, Cerami A, Becker W & Siren AL (2004). Erythropoietin: a candidate compound for neuroprotection in schizophrenia. *Mol Psychiatry* **9,** 42-54.

Farrell F & Lee A (2004). The erythropoietin receptor and its expression in tumor cells and other tissues. *Oncologist* **9 Suppl 5,** 18-30.

Fatemian M, Nieuwenhuijs DJ, Teppema LJ, Meinesz S, van der Mey AG, Dahan A & Robbins PA (2003). The respiratory response to carbon dioxide in humans with unilateral and bilateral resections of the carotid bodies. *J Physiol* **549,** 965-973.

Feldman JL, Mitchell GS & Nattie EE (2003). Breathing: rhythmicity, plasticity, chemosensitivity. *Annu Rev Neurosci* **26**, 239-66.

Gassmann M, Manini A, Stallmach T, Saam B, Kuhn G, Grenacher B, Bogdanova AY & Vogel J (2008). Abortion in mice with excessive erythrocytosis is due to impaired arteriogenesis of the uterine arcade. *Biol Reprod* **78,** 1049-1057.

Gassmann M, Pfistner C, Doan VD, Vogel J & Soliz J (2010). Impaired ventilatory acclimatization to hypoxia in female mice overexpressing erythropoietin: unexpected deleterious effect of estradiol in carotid bodies. *Am J Physiol Regul Integr Comp Physiol* **299,** R1511-1520.

Gassmann M & Soliz J (2009). Erythropoietin modulates the neural control of hypoxic ventilation. *Cell Mol Life Sci* **22,** 3575-3582.

Gestreau C, Heitzmann D, Thomas J, Dubreuil V, Bandulik S, Reichold M, Bendahhou S, Pierson P, Sterner C, Peyronnet-Roux J, Benfriha C, Tegtmeier I, Ehnes H, Georgieff M, Lesage F, Brunet JF, Goridis C, Warth R & Barhanin J (2010). Task2 potassium channels set central respiratory CO2 and O2 sensitivity. *Proc Natl Acad Sci U S A* **107**, 2325-30.

Gourine AV, Kasymov V, Marina N, Tang F, Figueiredo MF, Lane S, Teschemacher AG, Spyer KM, Deisseroth K & Kasparov S (2010). Astrocytes control breathing through pH-dependent release of ATP. *Science* **329**, 571-5.

Grasso G, Sfacteria A, Meli F, Fodale V, Buemi M & Iacopino DG (2007). Neuroprotection by erythropoietin administration after experimental traumatic brain injury. *Brain Res* **1182,** 99-105.

Guyenet PG, Stornetta RL & Bayliss DA (2010). Central respiratory chemoreception. *J Comp Neurol* **518**, 3883-906.

Haroon ZA, Amin K, Jiang X & Arcasoy MO (2003). A novel role for erythropoietin during fibrin-induced wound-healing response. *Am J Pathol* **163,** 993-1000.

Haxhiu MA, Yung K, Erokwu B & Cherniack NS (1996). CO2-induced c-fos expression in the CNS catecholaminergic neurons. *Respir Physiol* **105**, 35-45.

Heinicke K, Baum O, Ogunshola OO, Vogel J, Stallmach T, Wolfer DP, Keller S, Weber K, Wagner PD, Gassmann M & Djonov V (2006). Excessive erythrocytosis in adult mice overexpressing erythropoietin leads to hepatic, renal, neuronal, and muscular degeneration. *Am J Physiol Regul Integr Comp Physiol* **291,** R947-956.

Hurtado A (1960). Some clinical aspects of life at high altitudes. *Ann Intern Med* **53,** 247-258.

Jelkmann W (2005). Effects of erythropoietin on brain function. *Curr Pharm Biotechnol* **6,** 65-79.

Jelkmann W (2007). Erythropoietin after a century of research: younger than ever. *European journal of haematology* **78,** 183-205.

Kanbar R, Depuy SD, West GH, Stornetta RL & Guyenet PG (2011). Regulation of visceral sympathetic tone by A5 noradrenergic neurons in rodents. *J Physiol* **589**, 903-17.

Kassem LA & Yassin NA (2010). Role of erythropoeitin in prevention of chemotherapy-induced peripheral neuropathy. *Pak J Biol Sci* **13,** 577-587.

Kato A (2010). Increased hepcidin-25 and erythropoietin responsiveness in patients with cardio-renal anemia syndrome. *Future Cardiol* **6,** 769-771.

Kilic E, Kilic U, Soliz J, Bassetti CL, Gassmann M & Hermann DM (2005a). Brain-derived erythropoietin protects from focal cerebral ischemia by dual activation of ERK-1/-2 and Akt pathways. *Faseb J* **19,** 2026-2028.

Kilic U, Kilic E, Soliz J, Bassetti CI, Gassmann M & Hermann DM (2005b). Erythropoietin protects from axotomy-induced degeneration of retinal ganglion cells by activating ERK-1/-2. *Faseb J* **19,** 249-251.

Kondo A, Shingo T, Yasuhara T, Kuramoto S, Kameda M, Kikuchi Y, Matsui T, Miyoshi Y, Agari T, Borlongan CV & Date I (2009). Erythropoietin exerts anti-epileptic effects with the suppression of aberrant new cell formation in the dentate gyrus and upregulation of neuropeptide Y in seizure model of rats. *Brain Res* **1296,** 127-136.

Lam SY, Tipoe GL & Fung ML (2009). Upregulation of erythropoietin and its receptor expression in the rat carotid body during chronic and intermittent hypoxia. *Adv Exp Med Biol* **648,** 207-214.

Leon-Velarde F & Richalet JP (2006). Respiratory control in residents at high altitude: physiology and pathophysiology. *High Alt Med Biol* **7,** 125-137.

Leon-Velarde F, Richalet JP, Chavez JC, Kacimi R, Rivera-Chira M, Palacios JA & Clark D (1998). Inter and intra-species-related differences in the regulation of the cardiac autonomic system. *Comp Biochem Physiol B Biochem Mol Biol* **119,** 819-823.

Leon-Velarde F, Villafuerte FC & Richalet JP (2010). Chronic mountain sickness and the heart. *Prog Cardiovasc Dis* **52,** 540-549.

Li A, Emond L & Nattie E (2008). Brainstem catecholaminergic neurons modulate both respiratory and cardiovascular function. *Adv Exp Med Biol* **605**, 371-6.

Lim SK, Kim H, Lim SK, bin Ali A, Lim YK, Wang Y, Chong SM, Costantini F & Baumman H (1998). Increased susceptibility in Hp knockout mice during acute hemolysis. *Blood* **92**, 1870-7.

Lindskog S (1993). Structure and mechanism of carbonic anhydrase. *Pharmacol Ther* **74**, 1-20.

Maren TH (1977). Use of inhibitors in physiological studies of carbonic anhydrase. *Am J Physiol* **232**, F291-7.

Marti HH (2004). Erythropoietin and the hypoxic brain. *J Exp Biol* **207,** 3233-3242.

Marti HH, Bernaudin M, Petit E & Bauer C (2000). Neuroprotection and Angiogenesis: Dual Role of Erythropoietin in Brain Ischemia. *News Physiol Sci* **15,** 225-229.

Marti HH, Gassmann M, Wenger RH, Kvietikova I, Morganti-Kossmann MC, Kossmann T, Trentz O & Bauer C (1997). Detection of erythropoietin in human liquor: intrinsic erythropoietin production in the brain. *Kidney Int* **51,** 416-418.

Marti HH, Wenger RH, Rivas LA, Straumann U, Digicaylioglu M, Henn V, Yonekawa Y, Bauer C & Gassmann M (1996). Erythropoietin gene expression in human, monkey and murine brain. *Eur J Neurosci* **8,** 666-676.

Masuda S, Okano M, Yamagishi K, Nagao M, Ueda M & Sasaki R (1994). A novel site of erythropoietin production. Oxygen-dependent production in cultured rat astrocytes. *J Biol Chem* **269,** 19488-19493.

Maurer MH, Frietsch T, Waschke KF, Kuschinsky W, Gassmann M & Schneider A (2002). Cerebral transcriptome analysis of transgenic mice overexpressing erythropoietin. *Neurosci Lett* **327,** 181-184.

Menuet C, Kourdougli N, Hilaire G & Voituron N (2011). Differences in serotoninergic metabolism possibly contribute to differences in breathing phenotype of FVB/N and C57BL/6J mice. *J Appl Physiol*; DOI: 10.1152/japplphysiol.00117.2011.

Monge CC & Whittembury J (1976). Chronic mountain sickness. *Johns Hopkins Med J* **139 SUPPL,** 87-89.

Mulkey DK, Stornetta RL, Weston MC, Simmons JR, Parker A, Bayliss DA & Guyenet PG (2004). Respiratory control by ventral surface chemoreceptor neurons in rats. *Nat Neurosci* **7**, 1360-9.

Muller-Ehmsen J, Schmidt A, Krausgrill B, Schwinger RH & Bloch W (2006). Role of Erythropoetin for Angiogenesis and Vasculogenesis - from Embryonic Development through Adulthood. *Am J Physiol Heart Circ Physiol* **290**, H331-40.

Nagai A, Nakagawa E, Choi HB, Hatori K, Kobayashi S & Kim SU (2001). Erythropoietin and erythropoietin receptors in human CNS neurons, astrocytes, microglia, and oligodendrocytes grown in culture. *J Neuropathol Exp Neurol* **60,** 386-392.

Nattie E & Li A (2009). Central chemoreception is a complex system function that involves multiple brain stem sites. *J Appl Physiol* **106**, 1464-6.

Richerson GB (2004). Serotonergic neurons as carbon dioxide sensors that maintain pH homeostasis. *Nat Rev Neurosci* **5**, 449-61.

Romagnoli C, Zecca E, Gallini F, Girlando P & Zuppa AA (2000). Do recombinant human erythropoietin and iron supplementation increase the risk of retinopathy of prematurity? *Eur J Pediatr* **159,** 627-628.

Ruschitzka FT, Wenger RH, Stallmach T, Quaschning T, de Wit C, Wagner K, Labugger R, Kelm M, Noll G, Rulicke T, Shaw S, Lindberg RL, Rodenwaldt B, Lutz H, Bauer C, Luscher TF & Gassmann M (2000). Nitric oxide prevents cardiovascular disease and determines survival in polyglobulic mice overexpressing erythropoietin. *Proc Natl Acad Sci U S A* **97,** 11609-11613.

Sattler MB, Merkler D, Maier K, Stadelmann C, Ehrenreich H, Bahr M & Diem R (2004). Neuroprotective effects and intracellular signaling pathways of erythropoietin in a rat model of multiple sclerosis. *Cell Death Differ* **11 Suppl 2,** S181-192.

Schuler B, Arras M, Keller S, Rettich A, Lundby C, Vogel J & Gassmann M (2010). Optimal hematocrit for maximal exercise performance in acute and

chronic erythropoietin-treated mice. *Proc Natl Acad Sci U S A* **107,** 419-423.

Soliz J, Joseph V, Soulage C, Becskei C, Vogel J, Pequignot JM, Ogunshola O & Gassmann M (2005). Erythropoietin regulates hypoxic ventilation in mice by interacting with brainstem and carotid bodies. *J Physiol* **568,** 559-571.

Soliz J, Gassmann M & Joseph V (2007a). Downregulation of soluble erythropoietin receptor in the mouse brain is required for the ventilatory acclimatization to hypoxia. *J Physiol* **583.1,** 329-336.

Soliz J, Soulage C, Hermann DM & Gassmann M (2007b). Acute and chronic exposure to hypoxia alters ventilatory pattern but not minute ventilation of mice overexpressing erythropoietin. *Am J Physiol Regul Integr Comp Physiol* **293,** R1702-R1710.

Soliz J, Thomsen J, Soulage C, Lundby C & Gassmann M (2009). Sex-dependent regulation of hypoxic ventilation in mouse and man is mediated by erythropoietin. *Am J Physiol Regul Integr Comp Physiol* **296,** R1837-1846.

Statler PA, McPherson RJ, Bauer LA, Kellert BA & Juul SE (2007). Pharmacokinetics of high-dose recombinant erythropoietin in plasma and brain of neonatal rats. *Pediatr Res* **61,** 671-675.

Trapp S, Aller MI, Wisden W & Gourine AV (2008). A role for TASK-1 (KCNK3) channels in the chemosensory control of breathing. *J Neurosci* **28**, 8844-50.

Vannucchi AM, Bianchi L, Cellai C, Paoletti F, Carrai V, Calzolari A, Centurione L, Lorenzini R, Carta C, Alfani E, Sanchez M, Migliaccio G & Migliaccio AR (2001). Accentuated response to phenylhydrazine and erythropoietin in mice genetically impaired for their GATA-1 expression (GATA-1(low) mice). *Blood* **97**, 3040-50.

Vogel J, Kiessling I, Heinicke K, Stallmach T, Ossent P, Vogel O, Aulmann M, Frietsch T, Schmid-Schonbein H, Kuschinsky W & Gassmann M (2003). Transgenic mice overexpressing erythropoietin adapt to excessive erythrocytosis by regulating blood viscosity. *Blood* **102,** 2278-2284.

Voituron N, Menuet C, Dutschmann M & Hilaire G (2010). Physiological definition of upper airway obstructions in mouse model for Rett syndrome. *Respir Physiol Neurobiol* **173**, 146-56.

Wagner KF, Katschinski DM, Hasegawa J, Schumacher D, Meller B, Gembruch U, Schramm U, Jelkmann W, Gassmann M & Fandrey J (2001). Chronic inborn erythrocytosis leads to cardiac dysfunction and premature death in mice overexpressing erythropoietin. *Blood* **97,** 536-542.

Weidemann A, Kerdiles YM, Knaup KX, Rafie CA, Boutin AT, Stockmann C, Takeda N, Scadeng M, Shih AY, Haase VH, Simon MC, Kleinfeld D & Johnson RS (2009). The glial cell response is an essential component of hypoxia-induced erythropoiesis in mice. *J Clin Invest* **119,** 3373-3383.

Wiessner C, Allegrini PR, Ekatodramis D, Jewell UR, Stallmach T & Gassmann M. (2001). Increased cerebral infarct volumes in polyglobulic mice overexpressing erythropoietin. *J Cereb Blood Flow Metab* **21,** 857-864.

Xenocostas A, Cheung WK, Farrell F, Zakszewski C, Kelley M, Lutynski A, Crump M, Lipton JH, Kiss TL, Lau CY & Messner HA (2005). The pharmacokinetics of erythropoietin in the cerebrospinal fluid after intravenous administration of recombinant human erythropoietin. *Eur J Clin Pharmacol* **61,** 189-195.

9. FIGURES AND LEGENDS

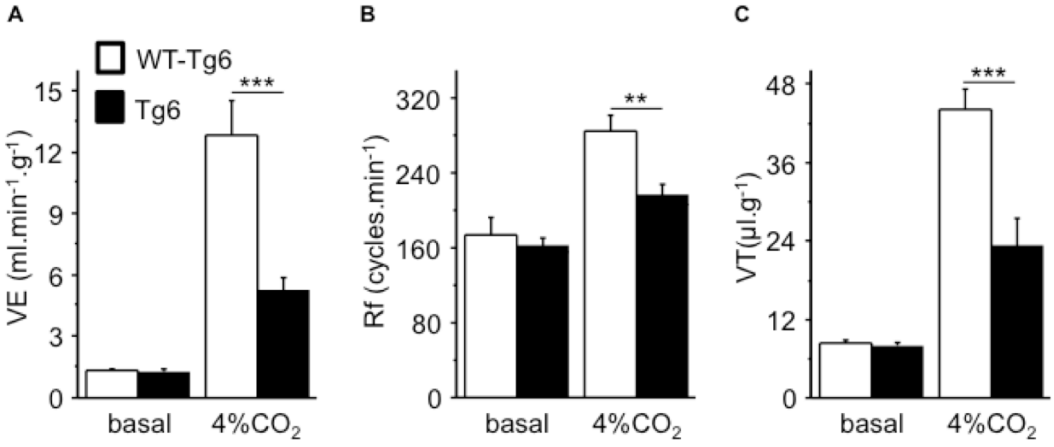

Figure 1. Minute ventilation (V_E, A), mean respiratory frequency (Rf, B) and tidal volume (V_T, C) for eucapnic (room air or basal) and hypercapnic (4% CO_2) breathing in awake control (WT-Tg6) and mutant (Tg6) mice.

**P<0.01, ***P<0.001: difference compared within hypercapnic breathing.

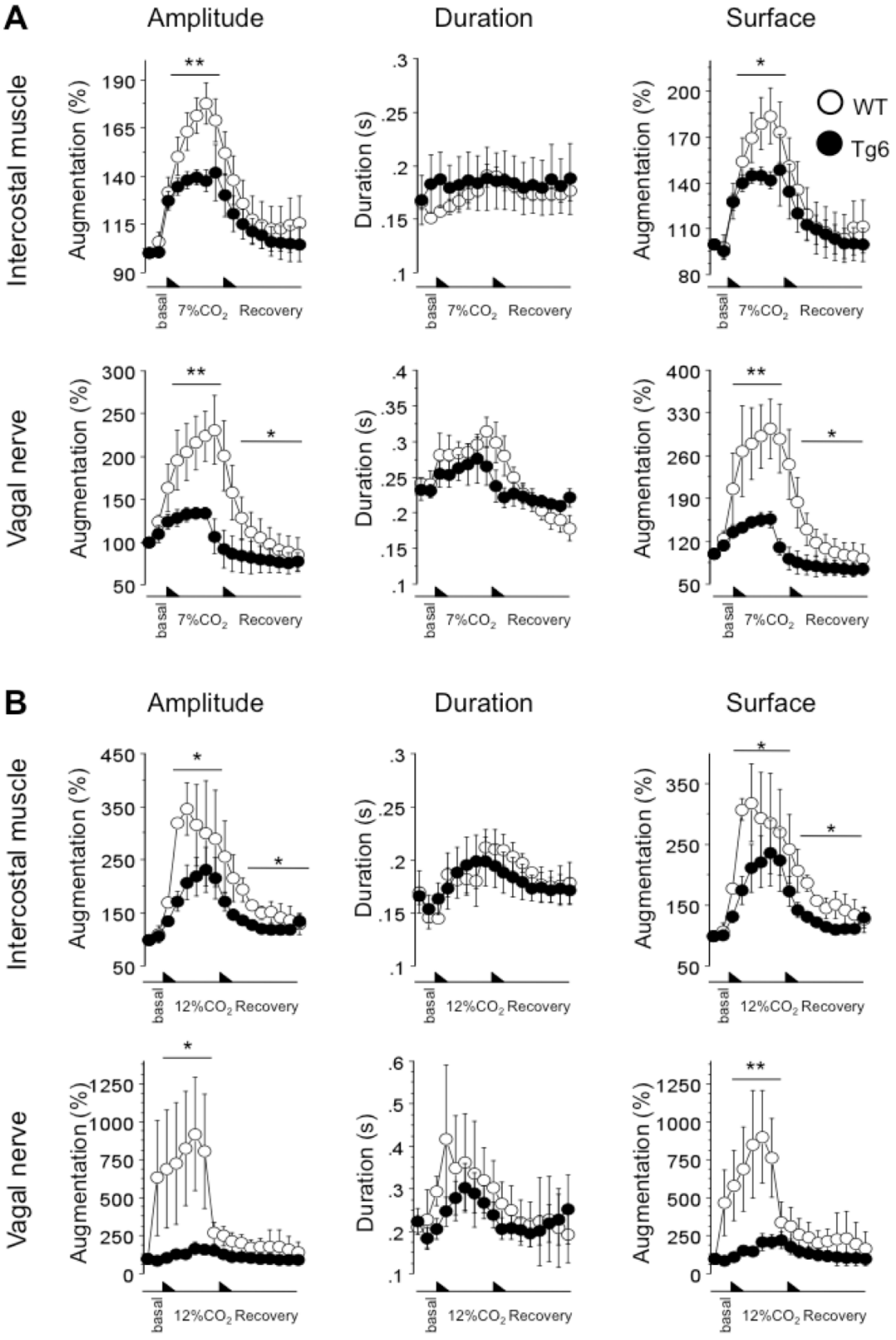

Figure 2. Changes in intercostal muscle and vagal nerve discharges in anaesthetized control (WT-Tg6) and mutant (Tg6) mice during breathing

under basal, hypercapnic (7% CO_2, A; 12% CO_2, B) and recovery conditions.

*P<0.05, **P<0.01: difference comparison within hypercapnic breathing or recovery period.

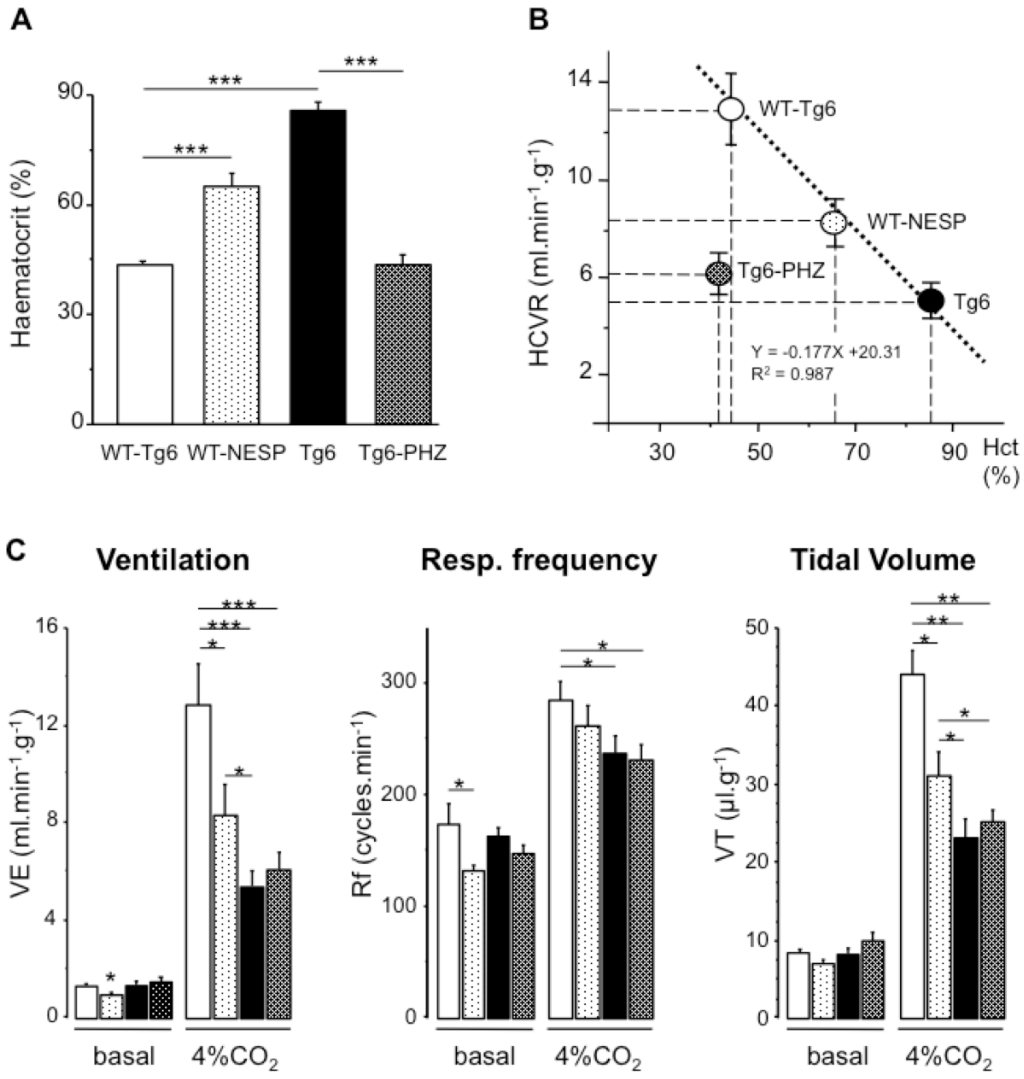

Figure 3. Levels of haematocrit (A), relation between changes in hypercapnic ventilatory responses (HCVR) and changes in haematocrit (Hct, B), and comparison of minute ventilation (V_E), respiratory frequency (Rf) and tidal volume (V_T) during basal breathing and

hypercapnia (CO_2 4%) in control (WT-Tg6), control treated with aranesp (WT-NESP), Tg6 and Tg6 mice after splenectomy and phenylhydrazine (Tg6-PHZ).

***P<0.001 in A: difference comparison between two groups.

*P<0.05 in C: difference comparison within basal condition (room air) denoting lower VE of WT-NESP mice vs the other three groups of mice, and lower Rf of WT-NESP vs WT-Tg6 group.

*P<0.05, **P<0.01, ***P<0.001: difference comparison within hypercapnic breathing between two groups.

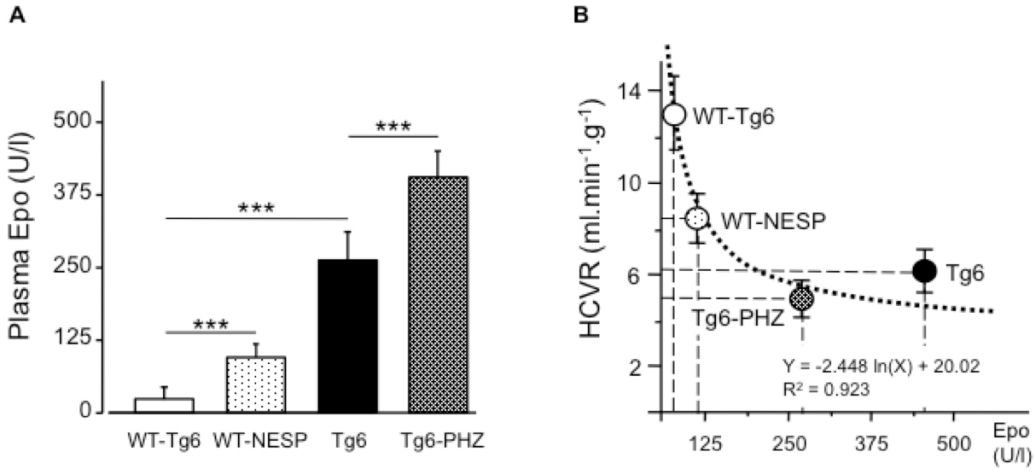

Figure 4. Concentration of erythropoietin in plasma (Plasma Epo, A) and relation between changes in hypercapnic ventilatory responses (HCVR) and changes in concentration of Epo in plasma (Epo, B) in control (WT-Tg6), control treated with aranesp (WT-NESP), Tg6 and Tg6 mice after splenectomy and phenylhydrazine (Tg6-PHZ).

***P<0.001: difference comparison between two groups.

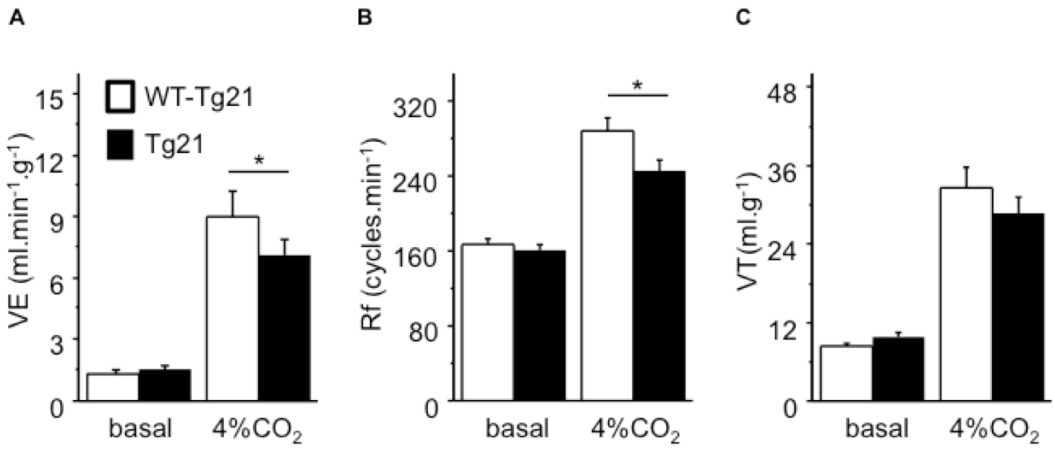

Figure 5. Minute ventilation (V_E, A), mean respiratory frequency (Rf, B) and tidal volume (V_T, C) for eucapnic (room air or basal) and hypercapnic (4% CO_2) breathing in awake control (WT-Tg21) and mutant (Tg21) mice.

*P<0.05: difference comparison within hypercapnic breathing.

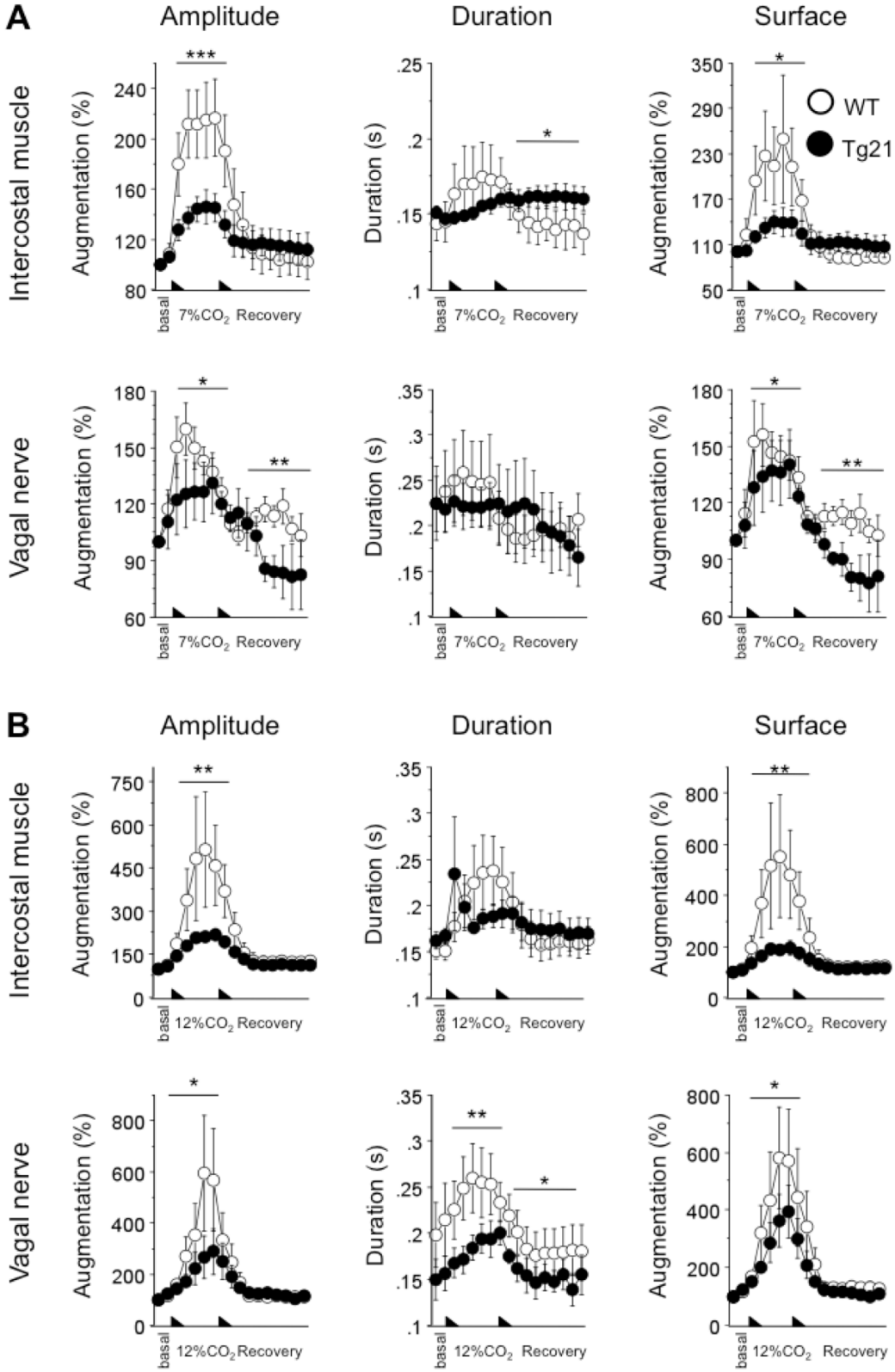

Figure 6. Changes in intercostal muscle and vagal nerve discharges in anaesthetized control (WT-Tg21) and mutant (Tg21) mice during

breathing under basal, hypercapnic (7% CO_2, A; 12% CO_2, B) and recovery conditions.

*P<0.05, **P<0.01, ***P<0.001: difference comparison within hypercapnic breathing or recovery period between groups.

III - Tauopathie et troubles respiratoires, études chez les souris Tau-P301L

Dans ce chapitre sont présentées des études réalisées sur un modèle murin de tauopathie, les souris Tau-P301L. Nous montrons tout d'abord que ces souris présentent une altération du fonctionnement des voies aériennes supérieures en période symptomatique (7-8 mois), qui est corrélée à la tauopathie présente dans certains noyaux du tronc cérébral et notamment dans le noyau de Kölliker-Fuse (3.1). Ensuite, nous montrons que les souris Tau-P301L en période terminale de la pathologie, quelques semaines avant leur mort prématurée, subissent une aggravation de leurs symptômes respiratoires avec l'apparition d'une altération du rythme et des régulations respiratoires, qui peuvent être causées par la progression de la tauopathie dans les raphés et l'altération du métabolisme sérotoninergique, en plus de l'aggravation des troubles des voies aériennes supérieures déjà existants (3.2). Dans le troisième article présent dans ce chapitre, nous montrons que les souris Tau-P301L âgées, contrairement aux souris Tau-P301L jeunes, présentent une altération de la vocalisation ultrasonore, qui est corrélée à une baisse de leur flux expiratoire et à la présence de tauopathie marquée dans les noyaux qui contrôlent la vocalisation et son couplage avec la respiration (substance grise périaqueducale, noyau de Kölliker-Fuse, noyau rétroambigu) (3.3). Enfin, nous avons réalisé une étude qui met en exergue les risques liés à l'anesthésie à l'isoflurane, cette dernière déclenchant en période pré-symptomatique chez les souris Tau-P301L la tauopathie du tronc cérébral et l'altération du fonctionnement des voies aériennes supérieure, et ce certainement *via* des mécanismes impliquant les récepteurs NMDA. Toutefois, nous montrons que certains protocoles d'anesthésie permettent d'empêcher la survenue de ces altérations (3.4).

1 - La dysfonction des voies aériennes supérieures des souris Tau-P301L corrèle avec la tauopathie dans les noyaux mésencéphaliques et ponto-bulbaires du tronc cérébral

Dutschmann M.*, **Menuet C.***, Stettner G.M.*, Gestreau C., Borghgraef P., Devijver H., Gielis L., Hilaire G. & Van Leuven F.
*Ces auteurs ont contribué de manière égale au travail.
Publié dans *The Journal of Neuroscience*, en 2010.

Résumé en français :

La tauopathie est caractérisée par l'hyperphosphorylation de la protéine tau, une protéine associée aux microtubules, hyperphosphorylation qui mène à la formation et à l'accumulation d'agrégats intracellulaires neurofibrillaires et de filaments du neuropile. Quelques tauopathies primaires sont liées à des mutations dans le gène *MAPT* qui code pour la protéine tau, mais la plupart sont sporadiques et de causes inconnues. Ainsi, dans la maladie d'Alzheimer, la tauopathie secondaire la plus fréquente, ni la cause ni les mécanismes pathologiques et leurs répercutions ne sont compris. Des souris transgéniques exprimant la forme mutante de tau Tau-P301L souffrent de déficits cognitifs et moteurs et meurent prématurément de cause inconnue. Ici, l'électrophysiologie *in situ* chez des souris Tau-P301L symptomatiques (âgées de 7-8 mois) a révélé une réduction de la décharge post-inspiratoire qui contrôle les muscles constricteurs du larynx. Sous un tonus excitateur élevé (hypercapnie), la décharge post-inspiratoire était presque abolie, alors que la décharge inspiratoire laryngée était augmentée de manière disproportionnée. Ce dernier résultat suggère un passage de l'activité constrictrice post-inspiratoire laryngée en inspiration. La pléthysmographie double chambre *in vivo* des souris Tau-P301L a montré une réduction significative du flux aérien respiratoire et une augmentation significative des mouvements thoraciques au cours de la respiration de base, phénomènes amplifiés en hypercapnie, confirmant une augmentation significative des résistances à l'inspiration. Une analyse histologique a démontré la présence de protéine tau hyperphosphorylée dans des noyaux du tronc cérébral, directement ou indirectement impliqués dans le contrôle moteur des voies aériennes supérieures (i.e., le noyau de Kölliker-Fuse, la substance grise périaqueducale, et les noyaux réticulaires intermédiaires). A l'inverse, les souris jeunes Tau-P301L n'ont pas présenté de désordres de la respiration ou de tauopathie dans le tronc cérébral. Par

conséquent, chez les souris Tau-P301L vieillissantes, la dysfonction progressive des voies aériennes supérieures est liée à la tauopathie progressive retrouvée dans des circuits neuronaux bien identifiés. Comme les patients atteints de tauopathie souffrent de dysfonctions des voies aériennes supérieures, les souris Tau-P301L peuvent servir de modèle expérimental pour étudier les dysfonctions synaptiques spécifiques de cette maladie dans des circuits neuronaux fonctionnels bien définis.

1810 • The Journal of Neuroscience, February 3, 2010 • 30(5):1810–1821

Neurobiology of Disease

Upper Airway Dysfunction of Tau-P301L Mice Correlates with Tauopathy in Midbrain and Ponto-Medullary Brainstem Nuclei

Mathias Dutschmann,[1,2]* Clement Menuet,[3]* Georg M. Stettner,[4]* Christian Gestreau,[3] Peter Borghgraef,[5] Herman Devijver,[5] Lies Gielis,[5] Gerard Hilaire,[3] and Fred Van Leuven[5]

[1]Institute of Membrane and Systems Biology, University of Leeds, Leeds LS2 9JT, United Kingdom, [2]Bernstein Center for Computational Neurosciences, D-37073 Göttingen, Germany, [3]MP3–Respiration, Centre de Recherche de Neurobiologie–Neurophysiologie de Marseille, Unité Mixte de Recherche Centre National de la Recherche Scientifique 6231, Faculté Saint Jérôme, 13397 Marseille, France, [4]Department of Pediatrics and Pediatric Neurology, University Medicine Göttingen, Georg August University, D-37075 Göttingen, Germany, and [5]Experimental Genetics Group, Department of Human Genetics, Katholieke Universiteit Leuven, B-3000 Leuven, Belgium

Tauopathy comprises hyperphosphorylation of the microtubule-associated protein tau, causing intracellular aggregation and accumulation as neurofibrillary tangles and neuropil treads. Some primary tauopathies are linked to mutations in the *MAPT* gene coding for protein tau, but most are sporadic with unknown causes. Also, in Alzheimer's disease, the most frequent secondary tauopathy, neither the cause nor the pathological mechanisms and repercussions are understood. Transgenic mice expressing mutant Tau-P301L suffer cognitive and motor defects and die prematurely from unknown causes. Here, *in situ* electrophysiology in symptomatic Tau-P301L mice (7–8 months of age) revealed reduced postinspiratory discharges of laryngeal motor outputs that control laryngeal constrictor muscles. Under high chemical drive (hypercapnia), postinspiratory discharge was nearly abolished, whereas laryngeal inspiratory discharge was increased disproportionally. The latter may suggest a shift of postinspiratory laryngeal constrictor activity into inspiration. *In vivo* double-chamber plethysmography of Tau-P301L mice showed significantly reduced respiratory airflow but significantly increased chest movements during baseline breathing, but particularly in hypercapnia, confirming a significant increase in inspiratory resistive load. Histological analysis demonstrated hyperphosphorylated tau in brainstem nuclei, directly or indirectly involved in upper airway motor control (i.e., the Kölliker–Fuse, periaqueductal gray, and intermediate reticular nuclei). In contrast, young Tau-P301L mice did not show breathing disorders or brainstem tauopathy. Consequently, in aging Tau-P301L mice, progressive upper airway dysfunction is linked to progressive tauopathy in identified neural circuits. Because patients with tauopathy suffer from upper airway dysfunction, the Tau-P301L mice can serve as an experimental model to study disease-specific synaptic dysfunction in well defined functional neural circuits.

Introduction

Neurodegenerative diseases, with Alzheimer's disease (AD) as a prime example, are inherently associated with tauopathy, pathologically demonstrated postmortem as neurofibrillary tangles (NFTs) and neuropil treads. In AD, the mainstream hypothesis holds amyloid peptides, cleaved from the amyloid precursor protein, as the primary pathological cause. Neither the connection to phosphorylation of protein tau nor the contributions of tauopathy to the clinical symptoms are understood in molecular and pathological detail (Terwel et al., 2002; Janus, 2008; Takashima, 2008; Denk and Wade-Martins, 2009). Because amyloid pathology is not observed as a separate entity, the associated tauopathy in AD should contribute to the neurodegeneration and clinical problems. In this context, we developed an experimental model for tauopathy (i.e., Tau-P301L transgenic mice) (Terwel et al., 2005, 2008) that we have studied here specifically for autonomic functions that become compromised by the developing tauopathy with aging.

Protein tau functions in the assembly and stabilization of microtubuli in neurons, a process regulated mainly by phosphorylation in adult brain (Andorfer and Davies, 2000; Buée et al., 2000; Goedert and Jakes, 2005). In frontotemporal dementia with parkinsonism, mutations in the tau gene on chromosome 17 are closely associated with disease and with accumulation of hyperphosphorylated tau as NFTs, diagnostic for all tauopathies, including AD (Goedert and Jakes, 2005). In patients and transgenic mice, tauopathy correlates well with memory impairment (Tatebayashi et al., 2002). Conversely, hyperphosphorylation of tau at later stages was often associated with premature death in transgenic animals (Lewis et al., 2001; Oddo et al., 2003; Götz et al., 2004; Terwel et al., 2005, 2008).

Received Oct. 23, 2009; revised Nov. 27, 2009; accepted Dec. 4, 2009.

This work was supported by the Bernstein Center for Computational Neurosciences, Göttingen, Grant 01GQ0432 (M.D.) and by Fonds Wetenschappelijk Onderzoek–Vlaanderen, Katholieke Universiteit (KU) Leuven Research Fund, and KU Leuven R&D. We are most grateful to Peter Davies (Litwin-Zucker Center for Research on Alzheimer's Disease, Feinstein Institute for Medical Research, Manhasset NY) and Eugeen Van Mechelen (Innogenetics, Gent, Belgium) for generously providing us with antibodies.

*M.D., C.M., and G.M.S. contributed equally to this work.

Correspondence should be addressed to Dr. Mathias Dutschmann, Institute for Membrane and Systems Biology, University of Leeds, Leeds LS2 9JT, UK. E-mail: m.dutschmann@leeds.ac.uk.

DOI:10.1523/JNEUROSCI.5261-09.2010

Copyright © 2010 the authors 0270-6474/10/301810-12$15.00/0

Tau-P301L transgenic mice progressively develop severe neuronal tauopathy in midbrain and brainstem, and neurological symptoms start around age 6–7 months (Terwel et al., 2005). The mice become progressively lethargic and motor impaired, lose weight, and die of unknown causes, most at age 9–10 months (Terwel et al., 2005, 2008).

Because of these well known motor defects of Tau-P301L mice (Terwel et al., 2005, 2008), we investigated the impact of the brainstem tauopathy on breathing as a vital motor function at 3 and 7–8 months of age (i.e., before and at symptomatic ages, respectively). Analysis of the respiratory motor pattern using *in situ* approaches (Paton, 1996; Stettner et al., 2007) and *in vivo* plethysmography revealed increased inspiratory resistive load in Tau-P301L mice potentially because of laryngeal constrictor activation during inspiration. The observed dysregulation of upper airway resistance during the breathing cycle correlates with the expression of hyperphosphorylated protein tau in brainstem upper airway premotor populations [i.e., Kölliker–Fuse (KF) and intermediate reticular nuclei]. At 3 months of age, Tau-P301L mice neither showed alteration in the breathing pattern nor tauopathy in vital brainstem circuits. The identified tau-laden neuron clusters in various midbrain and brainstem areas are anatomically linked directly to the observed upper airway dysfunction. They further suggest disturbances in other autonomic functions, ranging from the regulation of the sleep–wake cycle to the mediation of defensive behavior, all to be explored in detail.

Materials and Methods

The experimental procedures were performed in accordance with European and national guidelines for care and use of laboratory animals and were approved by the local ethical committees.

Animals. Unless indicated otherwise, male Tau-P301L transgenic mice in the FVB/N genetic background (3 and 7–8 months of age) were studied and compared with age- and sex-matched FVB/N nontransgenic mice (Terwel et al., 2005, 2008). In these transgenic mice, the longest human tau isoform bearing the P301L mutation (tau-4R/2N-P301L) is expressed under control of the mouse *thy1* gene promoter aiming for neuron-specific expression starting in the third postnatal week (Terwel et al., 2005).

Transgenic mice used were homozygous for the Tau-P301L transgene and were genotyped by PCR with forward primer specific for the mouse *thy1* gene promoter and reversed primer specific for human tau cDNA (Terwel et al., 2005).

In vivo *single- and double-chamber plethysmography.* The breathing pattern of 64 mice has been studied *in vivo* thanks to two different noninvasive plethysmographic approaches. As reported previously (Viemari et al., 2005; Zanella et al., 2008), breathing was recorded from 40 unrestrained, conscious mice [$n = 16$ wild type (WT) and $n = 12$ Tau-P301L, 7–8 months of age; mean weight, 29.5 ± 0.9 g; $n = 6$ WT and $n = 6$ Tau-P301L, 3 months of age; mean weight, 28.1 ± 0.7 g] using a standard whole-body flow plethysmograph (EMKA Technologies) in which a constant flow pump connected to the animal chamber ensures proper and continuous inflow of fresh air (600 ml/min) or of a hypercapnic gas mixture (CO_2, 4%). The animal and reference chambers (volume, 200 ml) were maintained at 25 ± 0.5°C (temperature sensor Checktemp 1; Hanna Instruments). The spirogram, reflecting the strength of the mouse respiratory movement, was obtained by recording the pressure difference between the two chambers. The signal was amplified, filtered (DC, 50 Hz), fed to an analog-to-digital converter (sampling frequency, 1 kHz), and stored on a PC disk via the Spike 2 interface and software (Cambridge Electronic Design). To avoid stress, the mice were habituated to the plethysmograph by putting them in the chamber 2 d before the recording during 2 h. The next day, only those recording periods were analyzed during which the animals were quiet (i.e., without major limb, body, and head movements). Routinely, breathing of four mice was simultaneously recorded in the four-chamber plethysmograph, allowing comparison between WT and Tau-P301L mice placed in identical conditions. The mouse temperature was monitored before and after recording sessions (Infrared thermosensor S 01500; Technimed). Temperature did not change during the recording session, and no significant differences were observed in WT versus Tau-P301L mice. The mean respiratory frequency (fR) [expressed in cycle per minute (c min^{-1})], durations of inspiratory (T_I) and expiratory (T_E) periods (expressed in milliseconds), and spirogram amplitude (SA) were measured during 10–20 min baseline and during 5 min hypercapnic challenges. Because plethysmographic recordings do not provide absolute information about actual tidal volumes, SA values were expressed in arbitrary units (a.u.). In addition, the apnea index (AI) [i.e., the number of long-lasting apneas (>2 respiratory cycles) per minute] and the irregularity score (IS) of successive respiratory cycles (>200 cycles) were calculated as reported previously (Zanella et al., 2008) to check whether the respiratory rhythmogenic mechanisms were altered in Tau-P301L mice.

A double-chamber plethysmograph was developed to separately record the respiratory chest movements and respiratory airflow in 24 other conscious mice ($n = 6$ WT, $n = 6$ Tau-P301L, 7–8 months of age; $n = 6$ WT, $n = 6$ Tau-P301L, 3 months of age). The double-chamber plethysmograph was built from two 50 ml syringes, with a rubber collar separating the body chamber (50 ml) from the head chamber (20 ml). Air tightness between body and head chambers was verified by imposing small pressure changes in one chamber and checking the lack of pressure changes in the other. The head chamber was connected to a constant flow pump to ensure proper and continuous flow of either fresh air (200 ml/min) or hypercapnic gas mixture (CO_2, 4% in air). Body and head chambers were connected to respective reference chambers, all maintained at 25 ± 0.5°C, and pressure changes were recorded by pressure gauges (EMKA Technologies) to measure spirogram amplitude from the chest and the airflow (chest SA and airflow SA). In contrast to single-chamber analysis, double-chamber recordings are more stressful, and the mice were habituated to the double-chamber plethysmograph before actual recordings were made, according the same protocol described above.

In situ *working heart–brainstem preparation.* Experiments were performed using the arterially perfused working heart–brainstem preparation (Paton, 1996). Mice ($n = 4$ WT; $n = 6$ Tau-P301L; 8 months of age) were anesthetized deeply in a saturated atmosphere of isoflurane (1-chloro-2,2,2-trifluoroethyl-difluoromethylether) (Abbott). Once the animal failed to respond to noxious pinch to the tail or a hindpaw, it was transected below the diaphragm, transferred into ice-cooled (5°C) artificial CSF (aCSF) gassed with carbogen (95% O_2 and 5% CO_2), decerebrated at the precollicular level, and cerebellectomized. The lungs were removed. The left phrenic nerve was separated and cut at the level of the diaphragm. The descending aorta was isolated from the ventral surface of the spinal column. The right vagal nerve was also dissected and prepared for recording.

These initial procedures took ~15 min. The preparation was then transferred to a recording chamber. The descending aorta was cannulated and perfused using a peristaltic pump (Watson-Marlow) with carbogen-gassed aCSF at 31°C containing Ficoll (1.25%; Sigma-Aldrich) to maintain colloid-osmotic pressure. The perfusate contained the following (in mM): 125 NaCl, 3 KCl, 1.25 KH_2PO_4, 2.5 $CaCl_2$, 1.25 $MgSO_4$, 25 $NaHCO_3$, 10 D-glucose, and 1.25% Ficoll. The osmolarity of the perfusate was 300 ± 10 mosmol L^{-1}, and the pH was 7.35 ± 0.05 by gassing with carbogen. The perfusate was filtered and passed through bubble traps to remove gas bubbles. The perfusate leaking from the preparation was collected and recirculated after reoxygenation. Cardiac activity returned within seconds, and rhythmic contractions of respiratory muscles within a few minutes after onset of reperfusion. Respiratory-related movements were abolished by vecuronium bromide (0.3 μg ml^{-1}; Inresa).

After paralysis, phrenic nerve activity (PNA) was primarily used to fine-tune the preparations by adjusting the flow rate (10–22 ml min^{-1}) and perfusion pressure (40–70 mmHg). For measurement of aorta perfusion pressure, a double lumen catheter was used and connected to a pressure transducer. During the tuning, the flow rates were individually adjusted to fulfill the following criteria: reappearance of a clearly identi-

fiable respiratory pattern, rhythmic respiratory motor discharges of at least 40 bursts/min, and maintenance of the respiratory pattern for at least 30 min before starting any experiments or data analysis. To test the respiratory response to hypercapnia, the perfusate was gassed with carbogen containing 12% CO_2 for 1 min.

Nerve recordings. Respiratory motor nerve activities were recorded simultaneously from the phrenic and central vagus nerve in all preparations. The suction electrodes were connected to differential amplifiers (Neurolog 100). Nerve activity was amplified and filtered (8 Hz to 3 kHz; Neurolog modules 104 and 125). All data were digitized using a MacLab 8s interface and stored on a computer using Chart software (version 5.2; ADInstruments). Respiratory motor nerve activity was integrated (time constant, 100 ms). The electrocardiogram was recorded simultaneously with the PNA but not analyzed in present study.

Data analysis. Using the PNA and central vagal nerve activity (cVNA) recordings, we analyzed the duration of the following respiratory parameters: total respiratory cycle length (T_{tot}), time of inspiration (T_i), postinspiration (T_π), and late expiration (T_{e2}). In contrast to cat *in vivo* investigations, PNA recording does not display a clearly identifiable postinspiratory activity in mice. Therefore, we classified the entire expiratory interval as T_e (including T_π and T_{e2}). T_π and T_{e2} were identified and measured from the cVNA. The inspiratory cVNA coincided with the PNA. The duration of the expiratory cVNA was defined as T_π and the phase with absent cVNA in the late expiration as T_{e2}. To quantify changes in the discharge strength inspiratory and postinspiratory cVNA (I-VNA and PI-VNA, respectively), we measured the surface area of the integrated signals. Since the cVNA showed prominent changes in its discharge pattern, a more detailed analysis was performed on the timing of the peak amplitude of the integrated cVNA. Peak cVNA amplitude was demonstrated in numerous publications to coincide with the activation of laryngeal adductor muscles (for review, see Dutschmann and Paton, 2002a). We determined the inspiratory off-switch from the abrupt cessation of PNA and used it as reference point ($T = 0$) to comparatively analyze the occurrence of VNA peak amplitude in inspiration or early expiration. A negative latency of cVNA peak thereby reflects its occurrence in expiration, and a positive latency, its occurrence during inspiration (see Fig. 3).

Finally, we focused the present study on respiratory dysfunctions in Tau-P301L mice; thus, cardiovascular parameters such as ECG or perfusion pressure were not analyzed.

Statistics. Data analysis was performed with the Statistica 7.1 software package (StatSoft). All results are presented as mean ± SEM. Respiratory parameters of WT and Tau-P301L preparations were compared using the two-sided unpaired (differences between WT and Tau-P301L) or paired (differences between normocapnia and hypercapnia) Student *t* test in the case of normally distributed data and using the Mann–Whitney *U* test in the case of non-normally distributed data. A value of $p < 0.05$ was considered to be significant.

Mouse brain immunohistochemistry. Mice were anesthetized (Nembutal; 120 mg/kg, i.p.) for transcardiac perfusion with ice-cold saline (2 ml/min, 2 min). Brain and spinal cord were removed, fixed overnight in 4% paraformaldehyde in PBS at 4°C, and stored in 0.1% sodium azide in PBS at 4°C until sectioning. Coronal vibratome sections of 40 μm were cut from brain, brainstem, and spinal cord. Immunohistochemistry was performed essentially as described previously (Terwel et al., 2005, 2008). After rinsing in PBS, sections were treated for 15 min with 1.5% H_2O_2 in 50% methanol/PBS to eliminate endogenous peroxidase activity. Nonspecific binding sites were blocked by incubation in 10% fetal calf serum, 0.1% Triton X-100 in PBS (blocking buffer). The sections were incubated with primary monoclonal antibodies AT8 (mouse anti-AT8, 0.2 μg/ml) (Terwel et al., 2005) or PG5 (mouse anti-PG5, 1/5000) (Andorfer and Davies, 2000) in blocking buffer at 4°C overnight. After rinsing in blocking buffer, sections were incubated for 1 h with the secondary goat anti-mouse IgG antiserum (1:500 in blocking buffer) (Dako). Sections were rinsed in PBS and incubated in 50 mM Tris·HCl, pH 7.6, for 5 min, before enzymatic staining with 3,3′-diaminobenzidine (0.5 mg/ml), 0.3% H_2O_2 in 50 mM Tris·HCl, pH 7.6. Sections were counterstained with hematoxylin, before dehydration by passage through a graded series of ethanol solutions. After delipidation in xylol, the sections were mounted for microscopic analysis.

We analyzed continuous series of between 90 and 100 sections (20 μm; WT, $n = 3$; Tau-P301L, $n = 7$) from the caudal medulla oblongata to rostral end of the superior colliculus in the midbrain. In addition, sections of cervical and thoracic spinal cord segments containing respiratory motor neurons were analyzed (Tau-P301L, $n = 2$; WT, $n = 1$).

The expression of phospho-epitopes of protein tau, defined by monoclonal antibodies AT8 and PG5, was analyzed in brainstem and midbrain ($n = 7$; $n = 5$, respectively) series of adjacent sections from Tau-P301L mice at symptomatic age (8 months) and compared with young mice (3 months of age). The tauopathy pattern in brainstem and midbrain nuclei is expressed on a relative score (i.e., Ø, no expression; and scores + to +++ refer to 1–5, 5–20, and 20–50 positive neurons per 10^4 μm^2). It is important to note that brainstem and midbrain from young Tau-P301L mice (3 months of age) and from WT mice at ages 3 and 8 months did not show any accumulation of hyperphosphorylated Tau into tau aggregates, let alone NFTs. Faint staining for AT8 but not PG5 could be observed in some midbrain and brainstem areas (e.g., reticular formation). Consequently, statistical analysis of NFT expression in Tau-P301L versus WT mice or during development is per se highly significant and therefore not reported.

Results

Abnormal breathing pattern of 7- to 8-month-old Tau-P301L mice (*in vivo* approach)

The premature death of Tau-P301L mice at age 9–10 months is preceded by generalized motor deficiency starting around age 7–8 months. Here, we analyzed Tau-P301L mice for breathing disorders as potential cause of the premature death in this transgenic mouse line, extensively characterized previously for forebrain tauopathy and cognition (Terwel et al., 2005, 2008; Boekhoorn et al., 2006).

First, we used a standard whole-body plethysmograph to record breathing in unrestrained, conscious WT and Tau-P301L mice (Fig. 1*A*) under normocapnic conditions (air breathing) and during moderate hypercapnic challenges (5 min; 4% CO_2 in air). Analyzing breathing parameters under normocapnia during periods when mice were quiet, not moving revealed no significant differences between young WT and Tau-P301L mice (3 months of age) but significant abnormalities in 7- to 8-month-old Tau-P301L mice (Fig. 1).

In young WT ($n = 6$) and Tau-P301L ($n = 6$) mice under normocapnia, the mean respiratory frequency (fR = 174 ± 9 vs 179 ± 10 c min^{-1}; NS) and mean durations of inspiratory (T_I = 144 ± 20 vs 130 ± 10 ms; NS) and expiratory (T_E = 207 ± 10 vs 207 ± 10 ms; NS) periods did not significantly differ. In addition, the spirogram amplitudes were not statistically different (SA = 6.6 ± 0.9 vs 6.6 ± 0.5 a.u.; NS) (Fig. 1*D1*), as well as the mean apnea index (AI = 0.1 ± 0.1 vs 0.1 ± 0.2; NS) and the mean irregularity score (IS = 10.3 ± 1.5 vs 6.7 ± 0.8; NS). When subjected to moderate hypercapnia, similar breathing changes were observed in WT and Tau-P301L mice: both types of mice significantly increased fR and SA to reach similar mean values (fR = 254 ± 10 vs 246 ± 8 c min^{-1}; NS; SA = 18.5 ± 0.9 vs 17.4 ± 0.9 a.u.; NS) (Fig. 1*D1*).

In 7- to 8-month-old WT ($n = 16$) and Tau-P301L ($n = 12$) mice under normocapnia, no differences were observed in the mean fR (150 ± 4 vs 155 ± 4 c min^{-1}; NS), T_I (148 ± 5 vs 139 ± 9 ms; NS), T_E (258 ± 10 vs 251 ± 8 ms; NS), AI (0.1 ± 0.1 and 0.1 ± 0.1; NS), and IS (8.6 ± 1.1 and 10.6 ± 1.1; NS). However, the mean SA was significantly higher in Tau-P301L than WT mice (9.5 ± 0.9 vs 5.6 ± 0.3 a.u.; $p < 0.005$) (Fig. 1*B1*,*C1*,*D2*). When subjected to moderate hypercapnia, old WT ($n = 10$) and Tau-P301L ($n = 12$) mice increased their fR by ~50% to reach

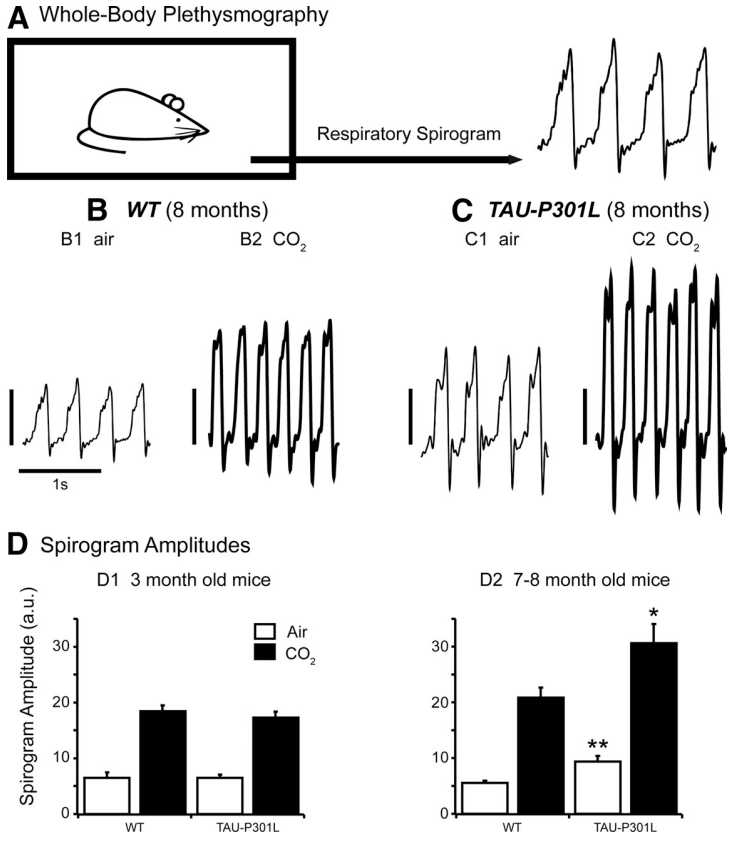

Figure 1. Whole-body plethysmographic recordings in unrestrained, conscious WT and Tau-P301L mice. ***A***, Schematic representation of the experimental setup used to record breathing in unrestrained, conscious mouse placed in a 200 ml recording chamber (to be compared with the experimental setup illustrated in Fig. 2*A*, in which the mouse is restrained). ***B***, ***C***, Individual traces show spirograms (inspiration upward) recorded from 8-month-old WT (***B***) and Tau-P301L (***C***) mice placed under control (***B1***, ***C1***) (air; room air, 0.03% CO_2) and hypercapnic (***B2***, ***C2***) (CO_2; 4% CO_2 in air, 5 min) breathing conditions. SA values are expressed in arbitrary units (vertical calibration bars: 5 a.u. for ***B1*** and ***C1***; 10 a.u. for ***B2*** and ***C2***); note the increased SA under hypercapnic conditions in ***B2*** and ***C2***. ***D***, The bars in the histograms show the mean SA (and SEM) from 6 WT and 6 Tau-P301L mice at 3 months of age (***D1***) and from 16 WT and 12 Tau-P301L mice at 7–8 months of age (***D2***). Note that the mean SA did not significantly differ in young WT versus Tau-P301L mice placed under identical breathing conditions (in ***D1***; either air or CO_2), whereas the mean SA was significantly larger in Tau-P301L versus WT old mice under air (***D2***; $*p < 0.01$) and CO_2 (***D2***; $**p < 0.05$) breathing conditions. In all groups, hypercapnia significantly increased mean SA when compared with air.

similar mean fR values (240 ± 10 vs 252 ± 4 c min^{-1}; NS), but Tau-P301L mice had a significantly shorter TI than WT (91 ± 2 vs 105 ± 5 ms, respectively; $p < 0.05$) and retained a significantly larger SA than WT (30.7 ± 3.6 vs 20.9 ± 1.7 a.u.; $p < 0.05$) (Fig. 1*B2*,*C2*,*D2*).

We developed a double-plethysmographic approach to simultaneously record the chest respiratory movements and the resulting airflow in conscious old mice at 7–8 months of age (Fig. 2*A*) because SA gained from simple plethysmographic recordings does not provide absolute information about actual tidal volumes. Consequently, the increased SA observed in old Tau-P301L mice could be related to an increase of respiratory movements potentially caused by increase of upper airway resistance. Indeed, compared with old WT mice ($n = 6$), old Tau-P301L mice ($n = 6$) showed significantly weaker airflow SA (123 ± 12 vs 84 ± 11 a.u.; $p < 0.05$) but significantly larger chest SA (42 ± 5 vs 99 ± 5 a.u.; $p < 0.001$) (Fig. 2*B–D*). Therefore, the ratio of airflow/chest SA was more than threefold larger in WT than Tau-P301L mice (3.1 ± 0.4 vs 0.9 ± 0.1, respectively; $p < 0.01$) (Fig. 2*D3*). Neither fR (252 ± 13 vs 247 ± 7 c min^{-1}; NS) nor T_I (123 ± 6 vs 112 ± 2 ms; NS) nor T_E (115 ± 7 vs 132 ± 7 ms; NS) differed significantly between WT versus Tau-P301L mice. In both strains, the baseline fR measured with double plethysmography was significantly higher than that previously measured with simple plethysmography. The increase of fR probably reflected the immobilization stress caused by the restrained double-chamber plethysmography. The fR appeared elevated close to the physiological maximum, because hypercapnia did not further increase the fR in both genotypes. However, hypercapnia differently affected the chest and airflow SA of old WT and Tau-P301L mice (Fig. 2*D1*,*D2*). In old WT mice, hypercapnia increased both airflow and chest SA by ~50%, and the ratio airflow/chest SA under hypercapnia (3.2 ± 0.5) was not statistically different from the ratio under normocapnia (Fig. 2*D3*). In old Tau-P301L mice, hypercapnia had opposite effects on airflow and chest SA, further depressing the airflow SA by 27% (61 ± 10 a.u.; $p < 0.001$) and further increasing the chest SA by 31% (130 ± 9 a.u.; $p < 0.001$). Therefore, the ratio airflow/chest SA of old Tau-P301L mice, which was already weak under normocapnia, was further reduced under hypercapnia (0.5 ± 0.1 a.u.; $p < 0.01$) (Fig. 2*D3*). The observed mismatch between airflow and chest SA in old Tau-P301L during both normocapnia and hypercapnia provides strong evidence for an increased work load of inspiratory pump muscles (e.g., diaphragm) against a potentially constricted upper airway, resulting in a significantly reduced airflow.

In young WT ($n = 6$) and Tau-P301L ($n = 6$) mice, double-chamber plethysmographic approach revealed identical ratio airflow/chest SA during normocapnia (1.1 ± 0.2 vs 1.1 ± 0.1 a.u.; NS) and during hypercapnia (1.1 ± 0.1 vs 1.1 ± 0.1 a.u.; NS). However, under the experimental condition of restrained double plethysmography, the mean fR was found significantly higher in Tau-P301L than WT mice (256 ± 11 vs 204 ± 8 c min^{-1}, respectively; $p < 0.05$), a result possibly suggesting a greater sensitivity to immobilization stress in Tau-P301L than WT mice.

Pathophysiological changes of respiratory-related upper airway activity in 7- to 8-month-old Tau-P301L mice (*in situ* approach)

We analyzed the three-phase motor pattern (inspiration, I; postinspiration, PI; late expiration, l-E) of breathing in WT ($n = 4$) and Tau-P301L mice ($n = 6$) to reveal significant differences in the respiratory motor pattern determined from PNA and cVNA (Fig. 3). Experimental baseline condition (5% CO_2) revealed a significant shortening of the expiratory interval (T_E, postinspiration plus late expiration) because of a significant reduction of postinspiratory phase duration (T_{PI}, 383 ± 177 vs 141 ± 39 ms; $p < 0.05$) and integrated PI-cVNA in Tau-P301L mice (33.5 ± 16.5 vs 3.5 ± 1.5 $\mu V * 100$ ms; $p < 0.05$). No significant differences in inspiratory duration (T_I, 357 ± 93 vs 479 ± 87 ms; NS) and integrated I-VNA (16.7 ± 8.0 vs 8.4 ± 2.6 $\mu V * 100$ ms; NS),

late expiratory phase duration (359 ± 77 vs 485 ± 145 ms; NS) were observed between WT and Tau-P301L mice. The phrenic burst frequency was also the same in Tau-P301L and WT mice (54.6 ± 11 vs 54.6 ± 18 c min^{-1}; NS). The significantly reduced postinspiratory motor discharge in Tau-P301L mice was further depressed when excitatory drive and arousal in the ponto-medullary respiratory network was enhanced with hypercapnic challenge evoked by gassing the perfusate with 12% CO_2 (Fig. 3*C*,*D*). In WT mice, an enhanced integrated I-VNA (16.7 ± 8.0 to 29.1 ± 18.5 μV * 100 ms) was observed, whereas PI-VNA remained constant compared with baseline (33.5 ± 16.5 vs 28.4 ± 14.4 μV * 100 ms). In contrast, in mutant Tau-P301L mice, a massive increase in integrated I-VNA (8.4 ± 2.6 to 40.0 ± 11.3 μV * 100 ms; $p < 0.05$) compared with baseline was observed, whereas integrated PI-VNA was almost abolished (3.5 ± 1.5 vs 0.6 ± 0.15 μV * 100 ms; $p < 0.05$).

The peak discharge of cVNA occurs physiologically in the transition from inspiration to expiration and is tightly linked to the activation of laryngeal adductor muscles, which breaks the expiratory airflow and counteracts elastic lung recoil after lung inflation (for review, see Dutschmann and Paton, 2002a). To further classify the changes in cVNA, we analyzed the occurrence of peak cVNA in relation to the inspiratory off-switch determined from the abrupt cessation of PNA (Fig. 3*E*). The cVNA peak discharge in WT always occurred with the termination of the inspiratory PNA discharge in normocapnia (5% CO_2) and hypercapnia (12% CO_2), thus matching the physiological role of expiratory airflow breaking. In contrast, in Tau-P301L mice, cVNA peak discharge occurred during the late inspiratory phase in normocapnia and was shifted deeper into the inspiratory phase during hypercapnia (Fig. 3*E*). The shift of the peak discharge of cVNA in Tau-P301L mice suggested paradoxical laryngeal constrictor activation during inspiration causing pathological inspiratory flow obstruction (Dutschmann and Paton 2002a,b). Therefore, *in situ* preparations of 7- to 8-month-old Tau-P301L mice revealed a paradoxical discharge pattern in laryngeal motor nerves, which could explain the upper airway dysfunction and breathing abnormalities suggested by the plethysmographic approaches.

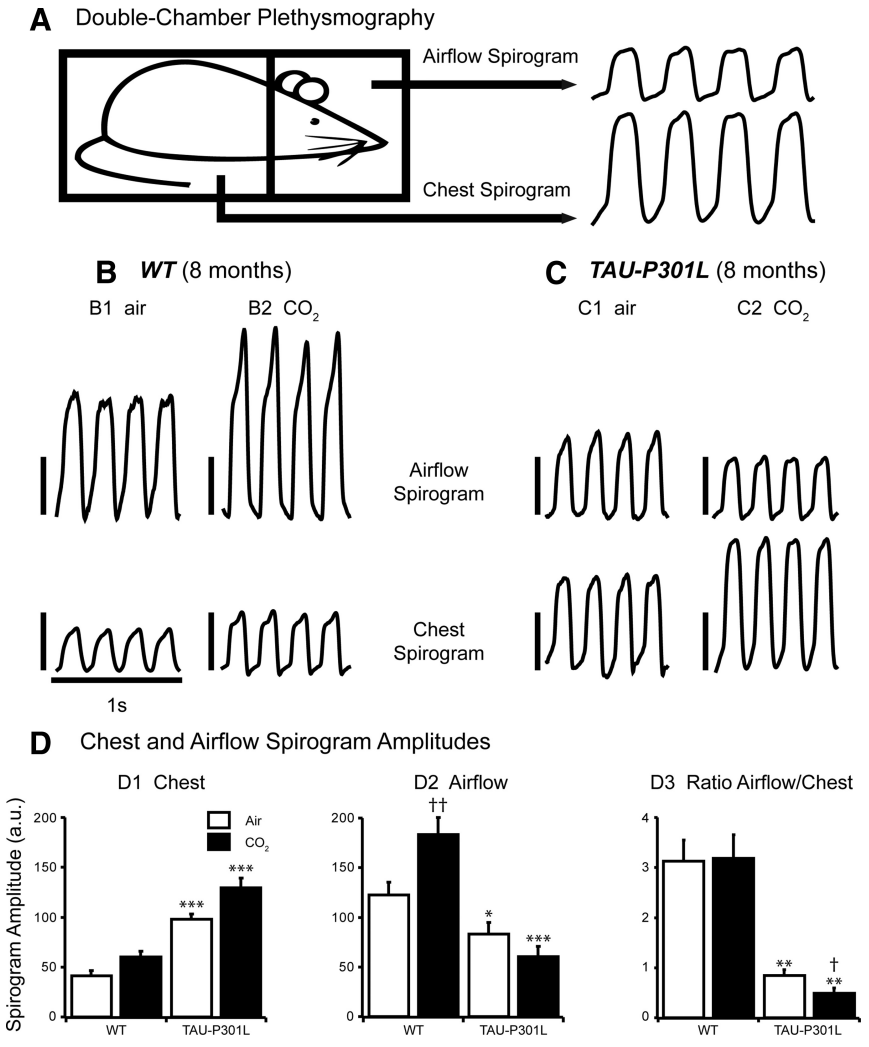

Figure 2. Double-chamber plethysmographic recordings in conscious WT and Tau-P301L mice. ***A***, Schematic representation of the experimental setup used for simultaneous recordings of chest and airflow spirograms in conscious but restrained mouse placed in a 50 ml recording chamber (to be compared with the experimental setup illustrated in Fig. 1*A*, in which the mouse is not restrained). ***B***, ***C***, Individual traces show chest and airflow spirograms (inspiration upward) recorded from 8-month-old WT (***B***) and Tau-P301L (***C***) mice placed under control (***B1***, ***C1***) (air; room air, 0.03% CO_2) and hypercapnic (***B2***, ***C2***) (CO_2; 4% CO_2 in air, 5 min) breathing conditions. SA values are expressed in arbitrary units (vertical calibration bars, 50 a.u.). Note that hypercapnia increased both chest SA and airflow SA in the WT mouse (***B***), whereas hypercapnia increased chest SA but reduced airflow SA in the Tau-P301L mouse (***C***). ***D***, The bars in the histograms show the mean (and SEM) values of chest SA (***D1***), airflow SA (***D2***), and ratio airflow versus chest SA (***D3***) obtained from double-plethysmographic recordings in 7- to 8-month-old WT ($n = 6$) and Tau-P301L ($n = 6$) mice placed under control (air, white bars) and hypercapnic (CO_2, black bars) breathing conditions. The asterisk (*) indicated a significant difference between WT and Tau-P301L mice placed under identical breathing conditions (either air or CO_2) (*$p < 0.05$; **$p < 0.01$; ***$p < 0.001$). The dagger (†) indicated a significant difference in control versus hypercapnic conditions between either paired WT or paired Tau-P301L mice ($^{\dagger}p < 0.05$; $^{\dagger\dagger}p < 0.01$). Note chest SA was significantly larger in Tau-P301L than WT mice under both breathing conditions (***D1***), whereas airflow SA was significantly smaller in Tau-P301L than WT mice under both breathing conditions (***D2***). ***D3*** shows that the ratio airflow/chest SA was significantly lower in Tau-P301L than WT mice under air and was further lowered by hypercapnia.

Another difference between WT and Tau-P301L mice was observed in the response to hypercapnia. WT mice showed a physiological response with a subtle increase in PNA burst frequency from 55.1 ± 3.5 to 61.8 ± 7.4 c min^{-1} (NS) and significant increase in PNA peak discharge from 124 ± 19 to 184 ± 34 μV ($p < 0.05$). In contrast, Tau-P301L mice responded with a significant decrease in PNA burst frequency from 56.1 ± 4.8 to 37.9 ± 4.8 c min^{-1} ($p < 0.05$) (Fig. 3) accompanied by an increase in PNA peak discharge from 75 ± 19 to 139 ± 34 μV ($p < 0.05$).

Expression pattern of phosphorylated Tau in brainstem

Tau-P301L mice develop a clinical phenotype around age 7–8 months involving a progressive motor deficiency, most easily identified by hindlimb and later forelimb clasping. The mice die prematurely around age 9–10 months and none survive for >12

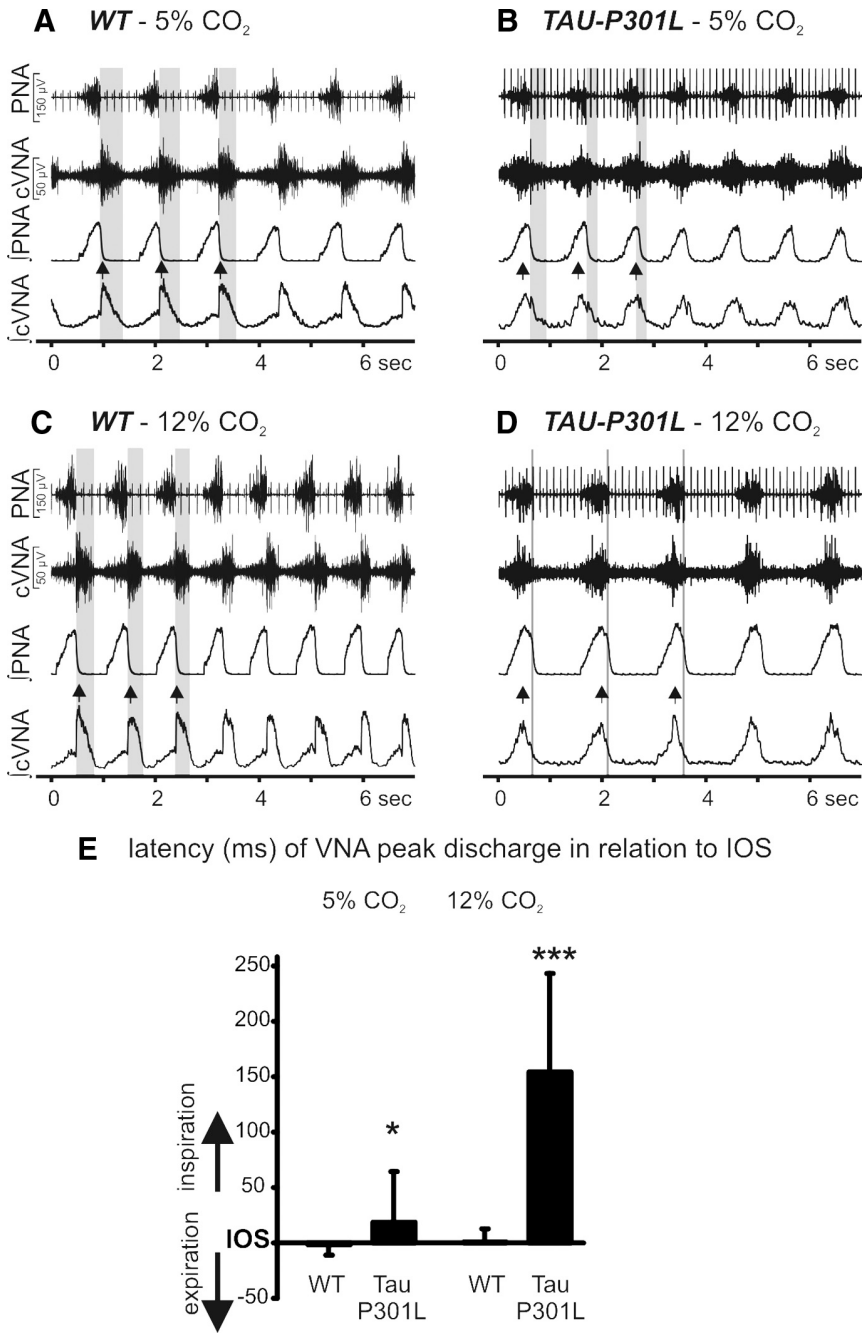

Figure 3. *In situ* recordings of the respiratory motor pattern from WT and Tau-P301L mice. ***A–D***, Recordings of inspiratory phrenic and inspiratory/postinspiratory vagal nerve activity (PNA; cVNA) of WT (***A***) and Tau-P301L mice (***B***) under control condition, 5% CO_2 in perfusate and hypercapnic conditions 12% CO_2 in perfusate (***C***, ***D***). The gray-shaded areas highlight the reduced postinspiratory activity in Tau-P301L mice. Postinspiratory activity was virtually absent, whereas inspiratory-related cVNA discharge was disproportionally increased. For additional details and statistical analysis, see text. The double arrowheads in the integrated signals (***A–D***) illustrate cVNA peak discharge in coincidence with inspiratory PNA. Group data for the occurrence of cVNA peak discharge during the respiratory cycle are illustrated in ***E*** (*$p < 0.05$, ***$p < 0.001$). IOS, Inspiratory off-switch.

months of age (supplemental Fig. 1*A*, available at www.jneurosci.org as supplemental material) (Terwel et al., 2005, 2008). The lethality correlates with significant brainstem tauopathy, exemplified by the number of MC1-positive neurons (supplemental Fig. 1*B*, available at www.jneurosci.org as supplemental material). MC1 is a monoclonal antibody that defines a conformational form of Tau that is typical for tauopathy, including AD (Weaver et al., 2000). Although the initial analysis suggested that the premature death of Tau-P301L mice relates to brainstem tauopathy, neither the precise location of Tau aggregates in the brainstem nor their physiological consequences have been investigated previously.

In the present study, we performed detailed histochemical analysis of the expression of protein Tau phospho-epitopes AT8 and PG5, widely accepted as pretangle and pathological epitopes, respectively (Figs. 4–7). Accumulated hyperphosphorylated Tau and tau aggregates were revealed in very distinct patterns in the brainstem and midbrain substructures of mutant Tau-P301L mice at age 7–8 months (summarized in Table 1, Fig. 4). Immunohistochemistry revealed typically stained somata in specific brain nuclei, whereas in some brain nuclei also labeling of putative nerve terminals was detected (for details, see below). Staining for epitope AT8 was more pronounced in all analyzed brain areas compared with PG5 and MC1 epitopes, which fits the definition of the AT8 epitope as "pretangle" (i.e., on the borderline between physiology and pathology) (Terwel et al., 2005, 2008, and references therein). Tauopathy was completely absent in the CNS of nontransgenic mice at any age (data not shown) and in brain of young Tau-P301L mice, analyzed here and previously (Terwel et al., 2005, 2008; Boekhoorn et al., 2006).

Tauopathy in the pontine Kölliker–Fuse nucleus

Closely correlating with the upper airway phenotype of Tau-P301L mice was the accumulation of hyperphosphorylated tau and tau aggregates in the KF of Tau-P301L mice at age 7–8 months (Fig. 4*A*,*B*). The KF nucleus is known to specifically gate postinspiratory laryngeal adductor activity in the respiratory motor pattern of rodents (Dutschmann and Herbert, 2006). In addition, at age 3 months, no indications for tauopathy were observed in the KF of Tau-P301L mice (Fig. 4*C*,*D*). Because of the complete absence of tauopathy in WT mice, quantification of tauopathy-positive neurons was performed only on the intermediate part of the KF in Tau-P301L mice at age 8 months. For the analysis, the presence of the external and internal lateral subnuclei of the lateral parabrachial complex was used as landmark. In Tau-P301L mice (8 months of age; $n = 5$), we found an average of 24 ± 5 KF neurons per 10^4 μm^2 that expressed Tau phospho-epitope AT8, whereas the density of neuronal expression of the PG5 epitope was lower (20 ± 7 per 10^4 μm^2).

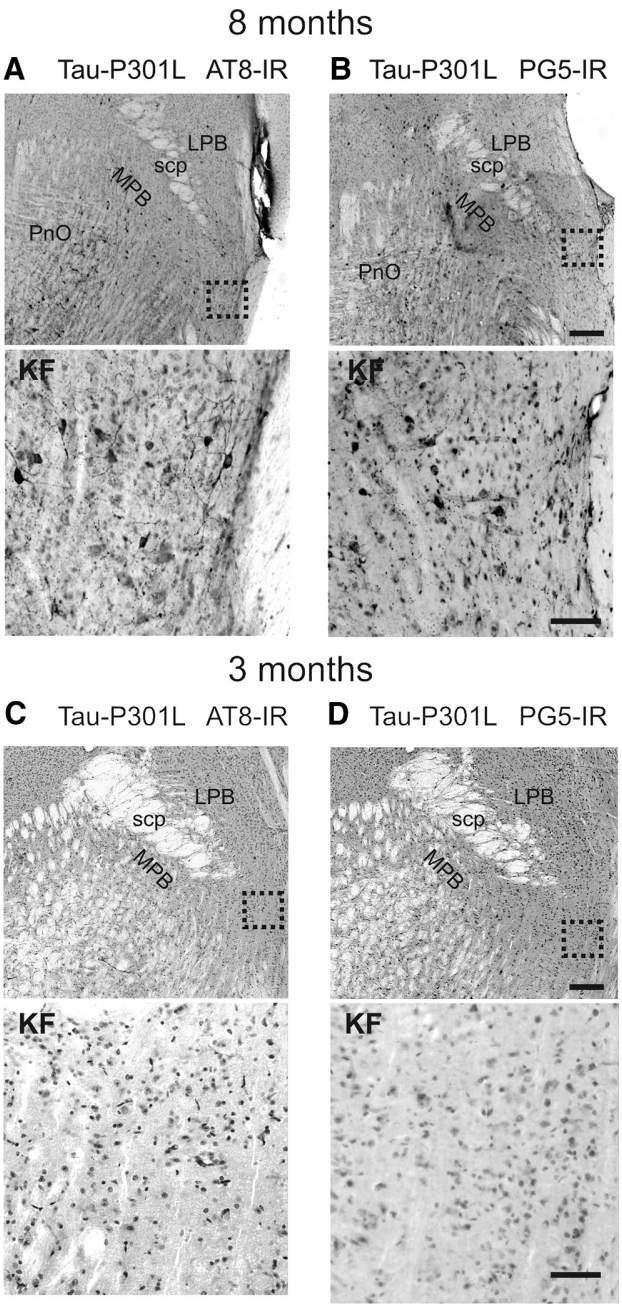

Figure 4. Tauopathy in the Kölliker–Fuse nucleus. The photomicrographs in ***A–D*** illustrate staining for phospho-epitopes AT8 and PG5 in the KF nucleus at 8 and 3 months of age. Scale bars: low magnification, 300 μm; high magnification, 50 μm. Abbreviations: LPB, Lateral parabrachial nuclei; MPB, medial parabrachial nucleus; PnO, pontine reticular nucleus, oral part; scp, superior cerebellar peduncle.

Tauopathy in midbrain and ponto-medullary nuclei in old Tau-P301L mice

Both phospho-epitopes on protein tau defined by Mab AT8 and PG5 showed a strongly overlapping expression pattern in the midbrain, ponto-medullary brainstem (Fig. 5). In contrast, these and other Tau phospho-epitopes were completely absent in CNS of WT mice (Terwel et al., 2005, 2008). The intensity of the tauopathy in Tau-P301L mice was scored on a relative scale, based on the counted number of neurons expressing the indicated tau phospho-epitopes (for details, see Materials and Methods).

Table 1. Summary of the relative density of tauopathy, based on phospho-tau epitopes AT8 and PG5, within neurons of brainstem and midbrain nuclei

Brain nuclei	Wild type AT8/PG5	Tau-P301L AT8	Tau-P301L PG5
Nuclei of the medullary and pontine reticular formation			
LRt	Ø	+	++
CVLM	Ø	Ø	Ø
Gi	Ø	+++	
RVLM	Ø	Ø	Ø
C1	Ø	Ø/+	Ø
Pre-BötC	Ø	Ø	Ø
BötC	Ø	Ø/+	Ø/+
pFRG/RTN	Ø	Ø	Ø
A5	Ø	+	+
PnC	Ø	+++	+++
ITR	Ø	+	Ø/+
KF	Ø	++	++
LPB	Ø	Ø/+	Ø/+
MPB	Ø	Ø/+	Ø/+
PnO	Ø	+++	+++
IRt	Ø	+++	+++
NRA	Ø	Ø/+	Ø/+
Nuclei of the arousal system			
RPa	Ø	+	+
ROb	Ø	+++	+++
RMg	Ø	++	++
Dorsal raphe	Ø	Ø	Ø
LC	Ø	++	+
Cranial motor nuclei			
Amb	Ø	Ø/+	Ø/+
Mo5	Ø	Ø/+	Ø/+
7N	Ø	Ø/+	+
10N	Ø	Ø/+	Ø
12N	Ø	+	+
Cerebellum			
Deep	Ø	+++	++
Other cerebellar nuclei	Ø	Ø	Ø
Midbrain nuclei			
PAG	Ø	+++	+++
Visceral and somatic sensory relay nuclei			
Sp5C	Ø	Ø	Ø
Sp5O	Ø	Ø	Ø
Sp5I	Ø	Ø/+	
SolVL	Ø	+ (only terminals)	+
SolM	Ø	+	Ø/+
SolC	Ø	Ø/+	Ø/+
Cu	Ø	++	+
IO	Ø	Ø/+	Ø/+
LSO	Ø	Ø/+	Ø
IC	Ø	Ø	Ø
NC	Ø	Ø	Ø
Ve	Ø	++	+
Cervical and thoracic spinal cord			
Dorsal horn	Ø	Ø	Ø
Ventral horn	Ø	+++/++	++

+++, Very dense; ++, dense; +, moderate; Ø, no tauopathy. For details, see Materials and Methods. Abbreviations (Paxinos and Franklin, 2001) in alphabetical order are as follows: 7N, facial nucleus; 10N, dorsal motor nucleus of vagus; 12N, hypoglossal nucleus; A5, A5 noradrenaline cells; Amb, ambiguus nucleus; BötC, Bötzinger complex; C1, C1 adrenaline cells; Cu, cuneate nucleus; CVLM, caudal ventrolateral medulla oblongata; Deep, lateral and interposed cerebellar nucleus; Gi, gigantocellular reticular nucleus; IC, inferior colliculus; IO, inferior olive; IRt, intermediate reticular nucleus; ITR, intertrigeminal region; KF, Kölliker–Fuse nucleus; LC, locus ceruleus; LPB, lateral parabrachial nuclei; LRt, spinal trigeminal nucleus, caudal part; LSO, lateral superior olive; Mo5, motor trigeminal nucleus; MPB, medial parabrachial nucleus; NC, cochlear nucleus; NRA, nucleus retroambiguus; PAG, periaqueductal gray; pFRG/RTN, parafacial respiratory group/retro trapezoid nucleus; PnC, pontine reticular nucleus, caudal part; PnO, pontine reticular nucleus, oral part; pre-BötC, pre-Bötzinger complex; RMg, raphe magnus nucleus; Rob, raphe obscurus nucleus; RPa, raphe pallidus nucleus; RVLM, rostral ventrolateral medulla oblongata; SolC, nucleus of the solitary tract, commissural part; SolM, nucleus of the solitary tract, medial part; SolVL, nucleus of the solitary tract, ventrolateral part; Sp5C, spinal trigeminal nucleus, caudal part; Sp5I, spinal trigeminal nucleus, interpolar part; Sp5O, spinal trigeminal nucleus, oral part; Ve, vestibular nuclei.

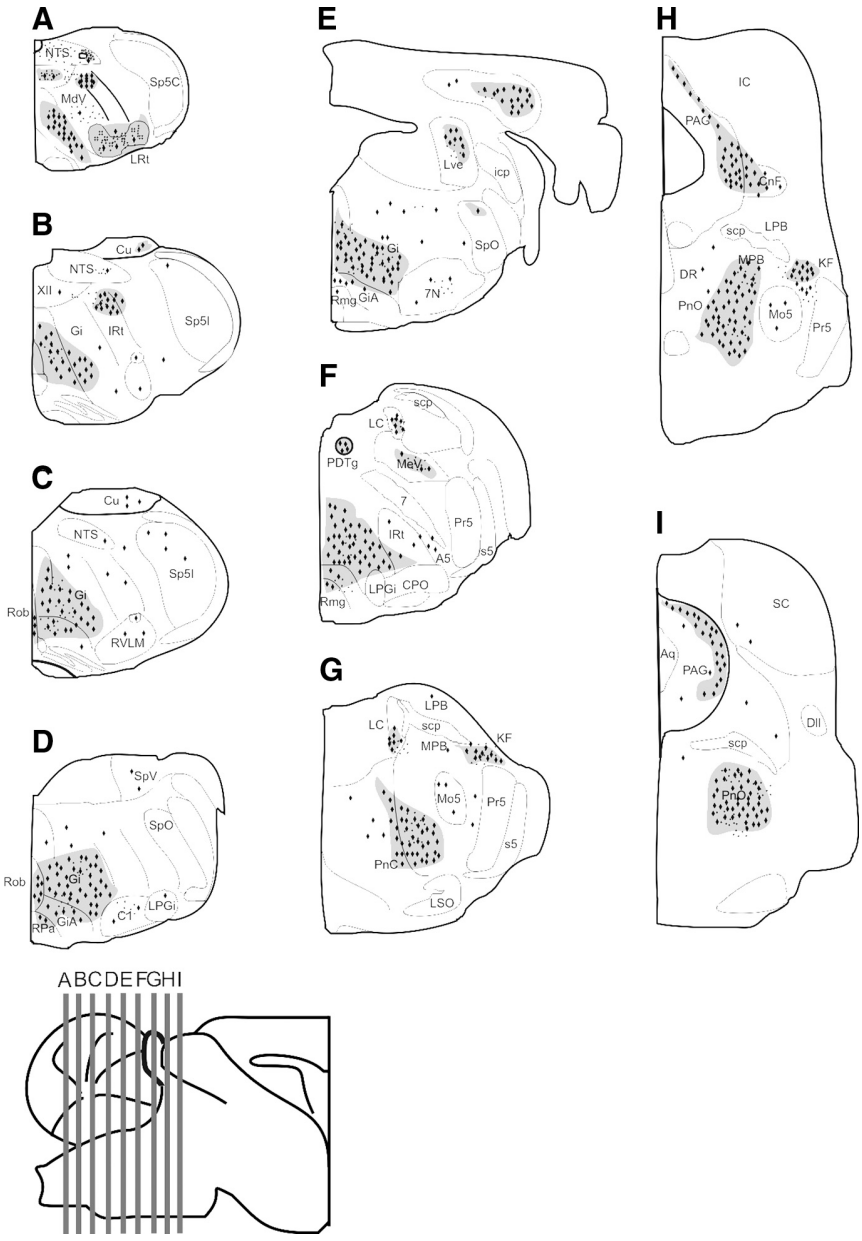

Figure 5. Relative intensity of tauopathy in brainstem and midbrain nuclei by immunohistochemistry with phospho-tau epitopes AT8 and PG5. Schematic rendering of the location of tauopathy [i.e., neurons containing NFTs within the caudal midbrain and ponto-medullary brainstem]. ***A–I***, Sections from the caudal medulla oblongata to the caudal midbrain. The gray-shaded areas with black diamonds (NFTs) and points (AT8- and PG-5-IR staining of terminal-like structures) symbolize dense staining. 7, Facial nerve; 7N, facial nucleus; XII, hypoglossal nucleus; A5, A5 noradrenaline cells; Aq, aqueduct; C1, C1 adrenaline cells; Cu, cuneate nucleus; Dll, dorsal nucleus of the lateral lemniscus; PDTg, posterodorsal tegmental nucleus; DR, dorsal raphe nucleus; Gi, gigantocellular reticular nucleus; IC, inferior colliculus; IRt, intermediate reticular nucleus; KF, Kölliker–Fuse nucleus; LC, locus ceruleus; LPB, lateral parabrachial nuclei, LRt, spinal trigeminal nucleus, caudal part; LSO, lateral superior olive; Mo5, motor trigeminal nucleus; MPB, medial parabrachial nucleus; PAG, periaqueductal gray; PnC, pontine reticular nucleus, caudal part; PnO, pontine reticular nucleus, oral part; Pr5, principal trigeminal nucleus; RMg, raphe magnus nucleus; ROb, raphe obscurus nucleus; RPa, raphe pallidus nucleus; RVLM, rostral ventrolateral medulla oblongata; scp, superior cerebellar peduncle; SolC, nucleus of the solitary tract, commissural part; SolM, nucleus of the solitary tract, medial part; SolVL, nucleus of the solitary tract, ventrolateral part; Sp5C, spinal trigeminal nucleus, caudal part; Sp5I, spinal trigeminal nucleus, interpolar part; Sp5O, spinal trigeminal nucleus, oral part; LVe, lateral vestibular nucleus.

Midbrain

Tauopathy was most prominently present in the midbrain intermediate and caudal periaqueductal gray (PAG). Dense clusters of neurons containing tau aggregates were observed within the dorsal, dorsolateral, lateral, and ventrolateral columns of the PAG (Figs. 5*H*,*I*, 6*A*,*B*).

Ponto-medullary reticular formation

Tauopathy was dense in the oral and caudal parts of pontine reticular nucleus (PnO; PnC). Whereas expression in the PnO was more dorsal (Figs. 5*H*,*I*, 7*A*,*B*), staining in the PnC was predominantly in the ventral aspects involving reticular giant neurons (Fig. 5*F*). Heavily attained were the posterodorsal tegmental nucleus (PDTg) (Fig. 5*F*), the Kölliker–Fuse nuclei (KF) (Figs. 4, 5*G*,*H*) of the parabrachial complex (PB), whereas staining in the lateral or medial nuclei (LBP; MPB) was rare (Table 1). Some cells were labeled in the intertrigeminal region (ITR) and at the level of the A5 noradrenergic cell group (Fig. 5*F*). At the medullary level, AT8 and PG5 stained neurons predominantly in the mediolateral reticular formation, involving strongly the gigantocellular reticular nucleus (Gi) (Fig. 5*C*,*D*). Another particular dense cluster of tauopathy was observed in the dorsal intermediate reticular nucleus (IRt) (Figs. 5*A*,*B*, 6*C*,*D*). Finally, some somata were labeled in the lateral reticular nucleus, whereas moderate-to-dense labeling was evident in putative nerve terminals in this nucleus (Fig. 5*A*). Tauopathy was rare in the "classical" cardiorespiratory autonomic centers of the medulla oblongata [i.e., the caudal and rostral ventro-lateral medulla oblongata (CVLM; RVLM) including the parafacial respiratory group/retro trapezoid nucleus (pFRG/RTN), pre-Bötzinger (pre-BötC), Bötzinger complex (BötC), or nucleus retroambiguus (NRA) tauopathy was sparse] (Fig. 5*B–D*, Table 1).

Ponto-medullary arousal system

Dense tauopathy-laden neurons were evident in key nuclei of the ponto-medullary reticular arousal system. In the pons, a dense cluster of AT8- and PG5-positive neurons was located in the locus ceruleus (Figs. 5*F*, 7*C*,*D*), whereas the dorsal raphe nuclei were devoid of staining. In the medullary raphe nuclei, AT8- and PG5-labeled cells were most dominant in the raphe obscurus (Rob) (Figs. 5*C–E*, 7*E*,*F*) and raphe magnus (RMg), whereas in the raphe pallidus (RPa) fewer neurons were stained.

Cranial motor nuclei

In cranial motor nuclei such as the nucleus ambiguus (Amb), trigeminal motor nucleus (Mo5), facial vagal and hypoglossal motor nuclei (7N, 10N, 12N), tauopathy was generally sparse, although moderate labeling of putative nerve terminals was observed in the Mo5, 7N, and 12N (Fig. 5, Table 1). In only one Tau-P301L animal, dense staining for PG5 was observed in the 7N and 12N nuclei.

Visceral and somatic relay nuclei
In the caudal, interpolar, and oral part of the spinal trigeminal nucleus (Sp5C, Sp5I, Sp5O), tauopathy was absent, only occasionally evident in Sp5l (Fig. 5*B*,*C*). In the commissural, medial, and ventrolateral parts of the nucleus of the solitary tract (SolC, SolM, SolVL), moderate staining was observed in the SolM, whereas labeled terminal-like structures were observed in the SolVL (Fig. 5*A*,*B*). Medullary and pontine nuclei of the auditory system such as the cochlear nucleus (NC), lateral superior olive (LSO), and inferior colliculus (IC) were devoid of tauopathy. In contrast, tauopathy was dense in the vestibular and cuneate nuclei, whereas it was absent in the inferior olive (Table 1).

Cerebellum and spinal cord
The cerebellum of Tau-P301L mice was completely devoid of tauopathy, as described previously (Terwel et al., 2005, 2008). A dense cluster of tau-laden neurons was identified in deep cerebellar nuclei such as the lateral and interposed cerebellar nucleus (Table 1). At the level of the cervical and thoracic spinal cord, dense tauopathy, defined by AT8 or PG5 staining, was observed in the ventral horn (Table 1). It is important to note that the spinal cord at these levels contains crucial populations of respiratory motor neurons innervating the diaphragm and intercostal muscles. In contrast, the sensory relays in the dorsal horn showed no obvious tauopathy (Table 1).

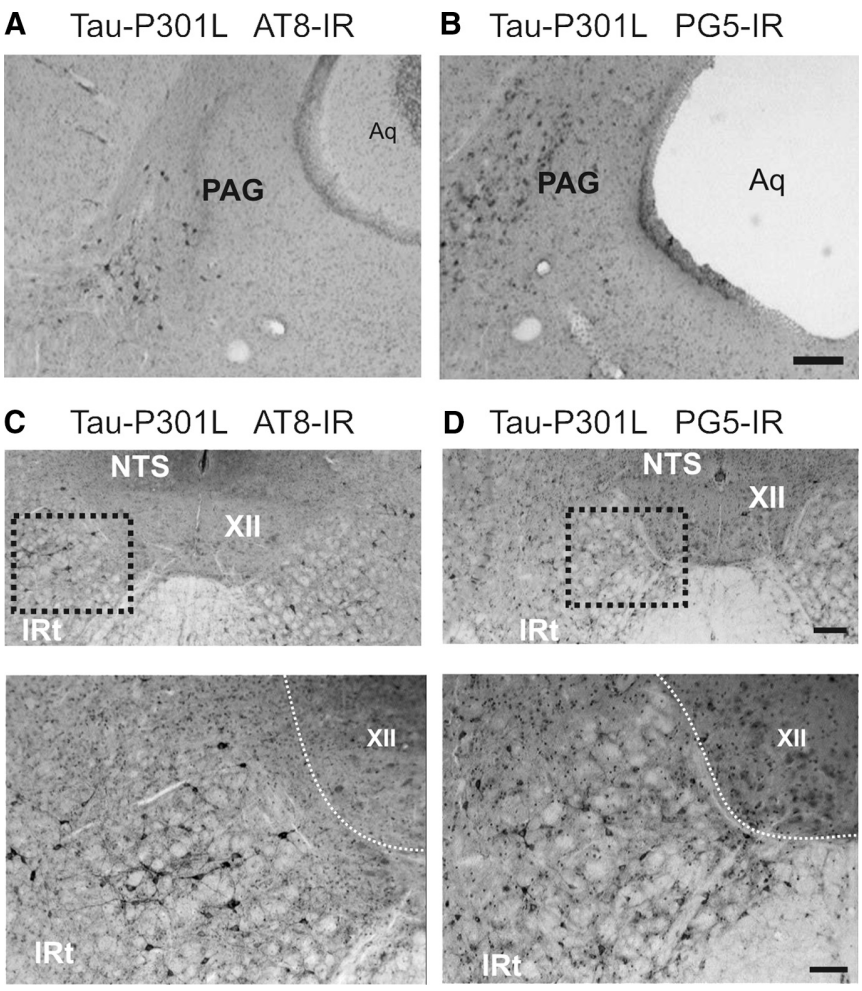

Figure 6. Tauopathy in lateral periaqueductal gray and intermediate reticular nucleus. The photomicrographs in ***A*** and ***B*** illustrate staining for phospho-epitopes AT8 and PG5 in the lateral periaqueductal gray (PAG) of Tau-P301L mouse. The photomicrographs in ***C*** and ***D*** illustrate staining in a Tau-P301L mouse for phospho-epitopes AT8 and PG5 in the intermediate reticular nucleus (IRt), which is located ventrolateral to the nucleus of the solitary tract (NTS) and lateral to hypoglossal nucleus (XII). Scale bars: low magnification, 300 μm; high magnification, 50 μm. Aq, Aqueduct.

Discussion

Postmortem analysis of AD patients reveals tauopathy, not only in limbic regions but also in midbrain and hindbrain regions (Parvizi et al., 1998; Rüb et al., 2001, 2002; Thai, 2002). The generation of transgenic mice that express mutant protein tau associated with frontotemporal dementia allows detailed investigation into the pathophysiological changes in brain functions in mouse models for tauopathy (Lewis et al., 2001; Oddo et al., 2003; Götz et al., 2004; Terwel et al., 2005, 2008). Here, we analyzed the transgenic mouse strain with neuron-specific, postnatal expression at near-physiological levels of mutant human Tau-P301L (Terwel et al., 2005, 2008; Boekhoorn et al., 2006). In old Tau-P301L mice, our study reveals a consistent pattern of expression Tau protein phospho-epitopes AT8 and PG5 in defined nuclei of midbrain pons and brainstem that are closely linked to the observed airway dysfunction and breathing deficits *in vivo* and *in situ*. In the many clinical types of primary and secondary tauopathies, vast regional differences are observed in the CNS structures that are affected. However, neither analyses of human patient nor animal models has so far yielded satisfactory explanations for the vast differential susceptibility of brain circuits for tau pathology.

Tauopathy in neural circuits associated with upper airway control

The breathing phenotype we detected in Tau-P301L mice strongly points toward a dysfunction in the laryngeal valve that dynamically controls upper airway resistance and respiratory airflow across the respiratory cycle and during various oropharyngeal behaviors. The data obtained from *in situ* preparations showed reduced postinspiratory activity recorded from the vagal nerve, which drives laryngeal adductor (constrictor) muscles under physiological conditions. The laryngeal adductors are important to break expiratory airflow, counteract elastic lung recoil after lung inflation, and regulate expiratory airflow, and are crucially involved in vocal–respiratory coupling (Dutschmann and Paton, 2002a; Dutschmann et al., 2004, 2008). The potential shift of postinspiratory laryngeal activity into inspiration and the reduced airflow accompanying increased chest movements fully support a paradoxical increase of airway resistance during inhalation in old Tau-P301L mice. The potential laryngeal dysfunction in old Tau-301L mice can be well correlated with tauopathy in specific brain circuits. The KF was reported to gate the postinspiratory motor output to laryngeal adductor (constrictor) muscles in the upper airways (Dutschmann and Herbert, 2006) and has also important functions in the mediation of inspiratory–expiratory phase switch, in the control of respiratory phase durations, and in vocal–respiratory coupling (Chamberlin and Saper, 1994; Dick et al., 1994; Lara et al., 2002; Alheid et al., 2004; Dutschmann et al., 2004; Dutschmann

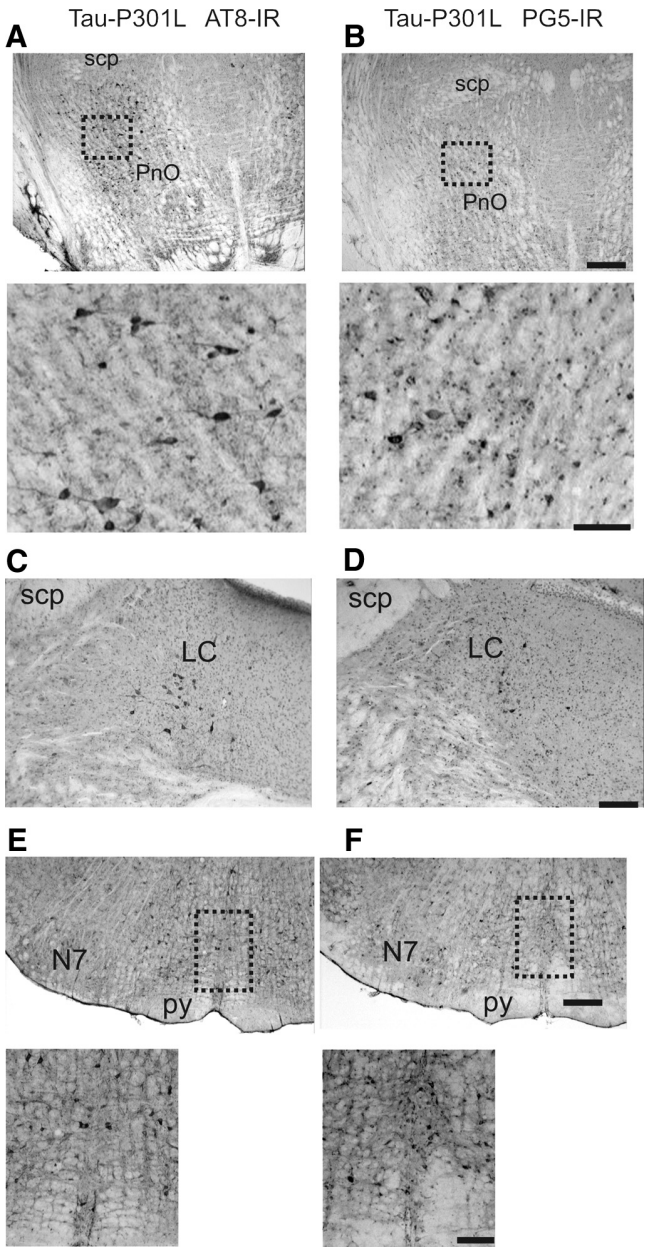

Figure 7. Tauopathy in pontine reticular nucleus, locus ceruleus, and raphe obscurus. ***A*** and ***B*** show AT8 and PG5 immunoreactivity (IR) in the dorsal aspect of the oral part of pontine reticular nucleus (PnO). Scale bars: low magnification, 300 μm; high magnification, 100 μm. The photomicrographs in ***C*** and ***D*** illustrate staining for phospho-epitopes AT8 and PG5 in the locus ceruleus (LC) of Tau-P301L mouse. ***E*** and ***F*** show the same immunoreactivity (IR) in the raphe obscurus nucleus (ROb), mediolateral to the facial nucleus (7N). Scale bars: low magnification, 300 μm; high magnification, 100 μm. scp, Superior cerebellar peduncle; py, pyramidal tract.

and Herbert, 2006; Ezure and Tanaka, 2006; Smotherman et al., 2006). Tauopathy is particularly observed in KF neurons and correlates well with the observed breathing phenotype in Tau-P301L mice, but the effects of tauopathy on synaptic function of KF neurons remain unknown. In addition, it has to be considered that the respiratory motor pattern *in situ* is generated in absence of relevant afferent inputs from the periphery. Under *in vivo* conditions, strength and duration of postinspiratory activity may be modulated by upper brain structures and by sensory feedback arising from pulmonary stretch receptors (Kubin et al., 2006). Interestingly, the terminal field of stretch receptor afferents within the ventrolateral nucleus of the solitary tract (NTS) revealed tauopathy in terminal-like structures. Thus, the observation of decreased postinspiratory activity *in situ* and airflow reduction *in vivo* is linked to tauopathy within NTS/KF axis, which has an essential role in the regulation of postinspiratory motor activity (for review, see Dutschmann et al., 2008).

Importantly, autopsy of brains from patients with AD revealed strong tauopathy in the medial parabrachial and KF nuclei (Figs. 2, 3) (Rüb et al., 2001) (note that the anatomical position of the KF overlaps with subpeduncular pigmented nucleus in this study). However, tauopathy in the NTS of AD patients is not reported yet. Our mouse data may connect the described brainstem tauopathy of AD patients to upper airway disorder, which is a common feature in various forms of dementias. For instance, progressive aphasia in frontotemporal dementia associated with downstream motor speech deficits (Hillert, 1999; Tolnay and Probst, 2002). In addition, postinspiratory activity is essential for laryngeal closure during swallowing to prevent aspiration of food into the airways (Gestreau et al., 2005). Indeed, dysphagia and aspiration pneumonia belong to the most serious complications, and eventual cause of death, in AD patients (Kalia, 2003).

Nevertheless, tauopathy in old Tau-P301L mice was widespread in midbrain, pons, and brainstem, and was also observed in respiratory motor neurons in cervical and thoracic spinal cord. Therefore, various other nuclei may also contribute to the upper airway phenotype observed in Tau-P301L mice. Of main interest here are the PAG, which strongly modulates breathing during behavioral tasks associated with emotion and particularly during vocalization (Davis et al., 1996; Jürgens, 2002; Subramanian et al., 2008), and the intermediate reticular nucleus in the medulla oblongata. The latter brain region contains a large population of hypoglossal premotor neurons involved in the control of tongue movements during oropharyngeal behaviors such as swallowing and vocalization (Gestreau et al., 2005). Thus, overlapping and closely interacting neural circuits for upper airway control are stressed by the tauopathy in old Tau-P301L mice.

In old Tau-P301L mice, *in vivo* and *in situ* studies did not show altered respiratory rhythmogenesis, and immunohistochemistry revealed that primary medullary respiratory centers such as the entire ventral respiratory column including the primary rhythm generating areas (e.g., parafacial respiratory group and pre-Bötzinger complex) were mostly devoid of tauopathy. We propose two explanations for these observations. First, dementia is not lethal per se and thus unaltered rhythmogenic circuits would make sense. Second, it was reported that Thy1 promoter used for the generation of Tau-P301L mice has limitations in targeting neurons in the ventral medulla (Winter et al., 2007), and therefore tauopathy did not develop in the ventral respiratory group for technical reasons.

Enhanced upper airway dysfunction during hypercapnia

Tauopathy was detected in brainstem areas such as the serotonergic medullary raphe nuclei, the noradrenergic locus ceruleus, and the A5 region, which principally belong to the arousal system (for discussion, see below), but have also major implications in central chemosensitivity and the state-dependent modulation of breathing (Bou-Flores et al., 2000; Nattie, 2001; Richter et al., 2003; Ballantyne et al., 2004; Hilaire et al., 2004; Richerson, 2004; Viemari et al., 2005; Zanella et al., 2008; Besnard et al., 2009). The tauopathy in these nuclei may contribute to the enhanced upper airway phenotype during exposure to hypercapnia *in situ* and *in vivo*. Our data provide evidence that activation of the respiratory network and associated arousal/chemosensitive systems during

hypercapnia contribute to evoke paradoxical activation of laryngeal adductor muscles during the inspiratory phase, leading to inspiratory airflow limitation. This phenomenon was reported to occur specifically after blockade of brainstem glycinergic neurotransmission (Dutschmann and Paton, 2002a,b) and during severe hypoxia (Dutschmann and Paton, 2005). However, the verification of potentially reduced glycinergic inhibition within the ponto-medullary brainstem of Tau-P301L mice requires future experimental analysis.

Finally, the described upper airway dysfunction with reduced respiratory airflow versus enlarged chest muscular work could trigger spells of systemic hypoxia. In turn, hypoxia is considered to contribute (Zhang et al., 2008) or even trigger AD (Peers et al., 2007). Therefore, the onset of breathing disorders most likely aggravates neurodegenerative processes in the brains of Tau-P301L mice, causing spread of tauopathy to forebrain structures, as previously reported (Terwel et al., 2005, 2008).

Summary

Aged Tau-P301L mice show defined patterns of tauopathy in vital brain circuits in midbrain, pons, brainstem, and spinal cord. The present study identified breathing deficits in older Tau-P301L mice, which strongly connect to tauopathy in defined neural circuits controlling upper airway function and to reported upper airway dysfunction in dementia patients. The observed tauopathy in other brain regions of Tau-P301L mice also correlates well with other dysfunctions of the autonomic nervous system described in dementia patients, which begs for additional experimental analysis.

References

Alheid GF, Milsom WK, McCrimmon DR (2004) Pontine influences on breathing: an overview. Respir Physiol Neurobiol 143:105–114.

Andorfer CA, Davies P (2000) PKA phosphorylations on tau: developmental studies in the mouse. Dev Neurosci 22:303–309.

Ballantyne D, Andrzejewski M, Mückenhoff K, Scheid P (2004) Rhythms, synchrony and electrical coupling in the locus coeruleus. Respir Physiol Neurobiol 143:199–214.

Besnard S, Denise P, Cappelin B, Dutschmann M, Gestreau C (2009) Stimulation of the rat medullary raphe nuclei induces differential responses in respiratory muscle activity. Respir Physiol Neurobiol 165:208–214.

Boekhoorn K, Terwel D, Biemans B, Borghgraef P, Wiegert O, Ramakers GJ, de Vos K, Krugers H, Tomiyama T, Mori H, Joels M, van Leuven F, Lucassen PJ (2006) Improved long-term potentiation and memory in young tau-P301L transgenic mice before onset of hyperphosphorylation and tauopathy. J Neurosci 26:3514–3523.

Bou-Flores C, Lajard AM, Monteau R, De Maeyer E, Seif I, Lanoir J, Hilaire G (2000) Abnormal phrenic motoneuron activity and morphology in neonatal monoamine oxidase A-deficient transgenic mice: possible role of a serotonin excess. J Neurosci 20:4646–4656.

Buée L, Bussière T, Buée-Scherrer V, Delacourte A, Hof PR (2000) Tau protein isoforms, phosphorylation and role in neurodegenerative disorders. Brain Res Brain Res Rev 33:95–130.

Chamberlin NL, Saper CB (1994) Topographic organization of respiratory responses to glutamate microstimulation of the parabrachial nucleus in the rat. J Neurosci 14:6500–6510.

Davis PJ, Zhang SP, Winkworth A, Bandler R (1996) Neural control of vocalization: respiratory and emotional influences. J Voice 10:23–38.

Denk F, Wade-Martins R (2009) Knock-out and transgenic mouse models of tauopathies. Neurobiol Aging 30:1–13.

Dick TE, Bellingham MC, Richter DW (1994) Pontine respiratory neurons in anesthetized cats. Brain Res 636:259–269.

Dutschmann M, Herbert H (2006) The Kölliker-Fuse nucleus gates the post-inspiratory phase of the respiratory cycle to control inspiratory off-switch and upper airway resistance in rat. Eur J Neurosci 24:1071–1084.

Dutschmann M, Paton JF (2002a) Inhibitory synaptic mechanisms regulating upper airway patency. Respir Physiol Neurobiol 131:57–63.

Dutschmann M, Paton JF (2002b) Glycinergic inhibition is essential for coordinating cranial and spinal respiratory motor outputs in the neonatal rat. J Physiol 543:643–653.

Dutschmann M, Paton JF (2005) Dynamic changes in glottal resistance during exposure to severe hypoxia in neonatal rats in situ. Pediatr Res 58:193–198.

Dutschmann M, Mörschel M, Kron M, Herbert H (2004) Development of adaptive behaviour of the respiratory network: implications for the pontine Kolliker-Fuse nucleus. Respir Physiol Neurobiol 143:155–165.

Dutschmann M, Mörschel M, Reuter J, Zhang W, Gestreau C, Stettner GM, Kron M (2008) Postnatal emergence of synaptic plasticity associated with dynamic adaptation of the respiratory motor pattern. Respir Physiol Neurobiol 164:72–79.

Ezure K, Tanaka I (2006) Distribution and medullary projection of respiratory neurons in the dorsolateral pons of the rat. Neuroscience 141:1011–1123.

Gestreau C, Dutschmann M, Obled S, Bianchi AL (2005) Activation of XII motoneurons and premotor neurons during various oropharyngeal behaviors. Respir Physiol Neurobiol 147:159–176.

Goedert M, Jakes R (2005) Mutations causing neurodegenerative tauopathies. Biochim Biophys Acta 1739:240–250.

Götz J, Streffer JR, David D, Schild A, Hoerndli F, Pennanen L, Kurosinski P, Chen F (2004) Transgenic animal models of Alzheimer's disease and related disorders: histopathology, behavior and therapy. Mol Psychiatry 9:664–683.

Hilaire G, Viemari JC, Coulon P, Simonneau M, Bévengut M (2004) Modulation of the respiratory rhythm generator by the pontine noradrenergic A5 and A6 groups in rodents. Respir Physiol Neurobiol 143:187–197.

Hillert D (1999) On processing lexical meanings in aphasia and Alzheimer's disease: some (re)considerations. Brain Lang 69:95–118.

Janus C (2008) Conditionally inducible tau mice—designing a better mouse model of neurodegenerative diseases. Genes Brain Behav 7 [Suppl 1]:12–27.

Jürgens U (2002) Neural pathways underlying vocal control. Neurosci Biobehav Rev 26:235–258.

Kalia M (2003) Dysphagia and aspiration pneumonia in patients with Alzheimer's disease. Metabolism 52 [Suppl 2]:36–38.

Kubin L, Alheid GF, Zuperku EJ, McCrimmon DR (2006) Central pathways of pulmonary and lower airway vagal afferents. J Appl Physiol 101:618–627.

Lara JP, Dawid-Milner MS, López MV, Montes C, Spyer KM, González-Barón S (2002) Laryngeal effects of stimulation of rostral and ventral pons in the anaesthetized rat. Brain Res 934:97–106.

Lewis J, Dickson DW, Lin WL, Chisholm L, Corral A, Jones G, Yen SH, Sahara N, Skipper L, Yager D, Eckman C, Hardy J, Hutton M, McGowan E (2001) Enhanced neurofibrillary degeneration in transgenic mice expressing mutant tau and APP. Science 293:1487–1491.

Nattie EE (2001) Central chemosensitivity, sleep, and wakefulness. Respir Physiol 129:257–268.

Oddo S, Caccamo A, Shepherd JD, Murphy MP, Golde TE, Kayed R, Metherate R, Mattson MP, Akbari Y, LaFerla FM (2003) Triple-transgenic model of Alzheimer's disease with plaques and tangles: intracellular Abeta and synaptic dysfunction. Neuron 39:409–421.

Parvizi J, Van Hoesen GW, Damasio A (1998) Severe pathological changes of parabrachial nucleus in Alzheimer's disease. Neuroreport 9:4151–4154.

Paton JFR (1996) A working heart-brainstem preparation of the mouse. J Neurosci Methods 65:63–68.

Peers C, Pearson HA, Boyle JP (2007) Hypoxia and Alzheimer's disease. Essays Biochem 43:153–164.

Richerson GB (2004) Serotonergic neurons as carbon dioxide sensors that maintain pH homeostasis. Nat Rev Neurosci 5:449–461.

Richter DW, Manzke T, Wilken B, Ponimaskin E (2003) Serotonin receptors: guardians of stable breathing. Trends Mol Med 9:542–548.

Rüb U, Del Tredici K, Schultz C, Thal DR, Braak E, Braak H (2001) The autonomic higher order processing nuclei of the lower brain stem are among the early targets of the Alzheimer's disease-related cytoskeletal pathology. Acta Neuropathol 101:555–564.

Rüb U, Del Tredici K, Schultz C, de Vos RA, Jansen Steur EN, Arai K, Braak H (2002) Progressive supranuclear palsy: neuronal and glial cytoskeletal pathology in the higher order processing autonomic nuclei of the lower brainstem. Neuropathol Appl Neurobiol 28:12–22.

Smotherman M, Kobayasi K, Ma J, Zhang S, Metzner W (2006) A mecha-

nism for vocal-respiratory coupling in the mammalian parabrachial nucleus. J Neurosci 26:4860–4869.

Stettner GM, Huppke P, Brendel C, Richter DW, Gärtner J, Dutschmann M (2007) Breathing dysfunctions associated with impaired control of post-inspiratory activity in *Mecp2*$^{-/y}$ knockout mice. J Physiol 579:863–876.

Subramanian HH, Balnave RJ, Holstege G (2008) The midbrain periaqueductal gray control of respiration. J Neurosci 28:12274–12283.

Takashima A (2008) Hyperphosphorylated tau is a cause of neuronal dysfunction in tauopathy. J Alzheimers Dis 14:371–375.

Tatebayashi Y, Miyasaka T, Chui DH, Akagi T, Mishima K, Iwasaki K, Fujiwara M, Tanemura K, Murayama M, Ishiguro K, Planel E, Sato S, Hashikawa T, Takashima A (2002) Tau filament formation and associative memory deficit in aged mice expressing mutant (R406W) human tau. Proc Natl Acad Sci U S A 99:13896–13901.

Terwel D, Dewachter I, Van Leuven F (2002) Axonal transport, tau protein, and neurodegeneration in Alzheimer's disease. Neuromolecular Med 2:151–165.

Terwel D, Lasrado R, Snauwaert J, Vandeweert E, Van Haesendonck C, Borghgraef P, Van Leuven F (2005) Changed conformation of mutant Tau-P301L mice underlies the moribund tauopathy, absent in progressive, nonlethal axonopathy of Tau-4R/2N transgenic mice. J Biol Chem 280:3963–3973.

Terwel D, Muyllaert D, Dewachter I, Borghgraef P, Croes S, Devijver H, Van Leuven F (2008) Mutant APP and GSK-3β aggravate tauopathy similarly in cortex and hippocampus of tau bigenic mice. Am J Pathol 172:786–798.

Thai DR (2002) Excitatory amino acid transporter EAAT-2 in tangle-bearing neurons in Alzheimer's disease. Brain Pathol 12:405–411.

Tolnay M, Probst A (2002) Frontotemporal lobar degeneration—tau as a pied piper? Neurogenetics 4:63–75.

Viemari JC, Roux JC, Tryba AK, Saywell V, Burnet H, Peña F, Zanella S, Bévengut M, Barthelemy-Requin M, Herzing LB, Moncla A, Mancini J, Ramirez JM, Villard L, Hilaire G (2005) Mecp2 deficiency disrupts norepinephrine and respiratory systems in mice. J Neurosci 25:11521–11530.

Weaver CL, Espinoza M, Kress Y, Davies P (2000) Conformational change as one of the earliest alterations of tau in Alzheimer's disease. Neurobiol Aging 21:719–727.

Winter SM, Hirrlinger J, Kirchhoff F, Hülsmann S (2007) Transgenic expression of fluorescent proteins in respiratory neurons. Respir Physiol Neurobiol 159:108–114.

Zanella S, Watrin F, Mebarek S, Marly F, Roussel M, Gire C, Diene G, Tauber M, Muscatelli F, Hilaire G (2008) Necdin plays a role in the serotonergic modulation of the mouse respiratory network: implication for Prader–Willi syndrome. J Neurosci 28:1745–1755.

Zhang B, Dong Y, Zhang G, Moir RD, Xia W, Yue Y, Tian M, Culley DJ, Crosby G, Tanzi RE, Xie Z (2008) The inhalation anesthetic desflurane induces caspase activation and increases amyloid beta-protein levels under hypoxic conditions. J Biol Chem 283:11866–11875.

2 - La tauopathie dans les raphés altère le métabolisme de la sérotonine et l'activité respiratoire chez les souris Tau-P301L terminales : implications potentielles pour les tauopathies et la maladie d'Alzheimer

Menuet C., Borghgraef P., Matarazzo V., Gielis L., Lajard A.M., Voituron N., Gestreau C., Dutschmann M., Van Leuven F. & Hilaire G.
Publié dans *Respiratory Physiology & Neurobiology*, en 2011.

Résumé en français :

Les tauopathies, incluant la maladie d'Alzheimer, sont les maladies neurodégénératives les plus fréquentes chez les personnes âgées. Les patients développent des troubles cognitifs et comportementaux induits par la tauopathie dans le prosencéphale, même si la plupart présentent également de la tauopathie dans le tronc cérébral, avec des troubles oro-pharyngés et sérotoninergiques (5-HT). Nous avons étudié ces aspects chez les souris Tau-P301L, qui expriment une forme mutante de protéine tau humaine et développent une tauopathie en premier dans le rhombencéphale, avec des troubles cognitifs, moteurs et des voies aériennes supérieures à partir de 7-8 mois, jusqu'à la mort prématurée avant l'âge de 12 mois. Utilisant la pléthysmographie, l'immunohistochimie et la biochimie, nous avons examiné les sytèmes respiratoires et 5-HT de souris Tau-P301L âgées et de souris contrôles. A 8 mois, les souris Tau-P301L développent une dysfonction des voies aériennes supérieures mais conservent un rythme et des régulations respiratoires normaux. Dans les semaines qui ont suivies, les souris Tau-P301L sont entrées dans le stade terminal de la maladie avec une perte de poids corporel, des fermetures des membres ("clasping") induisant progressivement une léthargie. Comparées à l'âge de 8 mois, les souris Tau-P301L terminales présentaient une dysfonction des voies aériennes supérieures aggravée, un rythme et des régulations respiratoires anormaux. En plus, elles étaient atteintes par une tauopathie sévère dans le noyau de Kölliker-Fuse, dans le raphé obscurus et dans le raphé magnus, mais pas dans les noyaux du bulbe rachidien liés à la respiration. Même si la tauopathie des raphés concerne principalement des neurones non 5-HT, le métabolisme de la 5-HT des souris Tau-P301L terminales était altéré. Nous proposons que la tauopathie progressive dans les raphés affecte le métabolisme de la 5-HT, qui affecte à son tour la modulation 5-HT du réseau respiratoire et ainsi le patron moteur respiratoire. Par conséquent, les altérations 5-HT contribuent au

phénotype moribond des souris Tau-P301L, et potentiellement à celui des patients souffrant de tauopathies, incluant la maladie d'Alzheimer.

Author's personal copy

Respiratory Physiology & Neurobiology 178 (2011) 290–303

Contents lists available at ScienceDirect

Respiratory Physiology & Neurobiology

journal homepage: www.elsevier.com/locate/resphysiol

Raphé tauopathy alters serotonin metabolism and breathing activity in terminal Tau.P301L mice: Possible implications for tauopathies and Alzheimer's disease

Clément Menuet[a], Peter Borghgraef[b], Valéry Matarazzo[a], Lies Gielis[b], Anne-Marie Lajard[a], Nicolas Voituron[a,1], Christian Gestreau[a], Mathias Dutschmann[c], Fred Van Leuven[b], Gérard Hilaire[a,*]

[a] Maturation, Plasticity, Physiology and Pathology of Respiration (MP3-Respiration), Unité Mixte de Recherche (UMR) 6231, Centre National de la Recherche Scientifique, Université de la Méditerranée, Université Paul Cézanne, Faculté Saint Jérôme (Service 362), 13397 Marseille Cedex 20, France
[b] Experimental Genetics Group, Department of Human Genetics, Katholieke Universiteit Leuven, B-3000 Leuven, Belgium
[c] Institute of Membrane and Systems Biology Garstang Building, University of Leeds, Leeds LS2 9JT, United Kingdom

ARTICLE INFO

Article history:
Accepted 30 June 2011

Keywords:
Tauopathy
Breathing
Respiratory regulations
Serotonin
Raphé
Non-serotonergic raphé neurons
Kolliker-fuse

ABSTRACT

Tauopathies, including Alzheimer's disease are the most frequent neurodegenerative disorders in elderly people. Patients develop cognitive and behaviour defects induced by the tauopathy in the forebrain, but most also display early brainstem tauopathy, with oro-pharyngeal and serotoninergic (5-HT) defects. We studied these aspects in Tau.P301L mice, that express human mutant tau protein and develop tauopathy first in hindbrain, with cognitive, motor and upper airway defects from 7 to 8 months onwards, until premature death before age 12 months. Using plethysmography, immunohistochemistry and biochemistry, we examined the respiratory and 5-HT systems of aging Tau.P301L and control mice. At 8 months, Tau.P301L mice developed upper airway dysfunction but retained normal respiratory rhythm and normal respiratory regulations. In the following weeks, Tau.P301L mice entered terminal stages with reduced body weight, progressive limb clasping and lethargy. Compared to age 8 months, terminal Tau.P301L mice showed aggravated upper airway dysfunction, abnormal respiratory rhythm and abnormal respiratory regulations. In addition, they showed severe tauopathy in Kolliker-Fuse, raphé obscurus and raphé magnus nuclei but not in medullary respiratory-related areas. Although the raphé tauopathy concerned mainly non-5-HT neurons, the 5-HT metabolism of terminal Tau.P301L mice was altered. We propose that the progressive raphé tauopathy affects the 5-HT metabolism, which affects the 5-HT modulation of the respiratory network and therefore the breathing pattern. Then, 5-HT deficits contribute to the moribund phenotype of Tau.P301L mice, and possibly in patients suffering from tauopathies, including Alzheimer's disease.

© 2011 Elsevier B.V. All rights reserved.

1. Introduction

Alzheimer's disease (AD), the most prevalent neurodegenerative disorder in elderly people, is characterized by memory loss, cognitive defects and behavioural abnormalities. AD is a secondary tauopathy, i.e. extracellular amyloid deposits in brain are combined with intraneuronal neurofibrillary tangles and dendritic neuropil threads of abnormally phosphorylated tau protein. The associated synaptic defects cause cognitive problems and altered functions in major brain networks. Patients with primary tauopathies also suffer brainstem tauopathy, sleep-disordered breathing and oro-pharyngeal problems. At early stages, patients show swallowing impairment, which eventually leads to aspiration pneumonia at later stages, a recognized cause of death in AD (Humbert et al., 2010; Suh et al., 2009; Attems et al., 2005; Priefer and Robbins, 1997). Up to 48% of AD patients also suffer obstructive sleep apnoeas and the related hypoxic spells possibly affect brain networks function (Onen and Onen, 2010). Links between breathing defects and AD are supported by mental impairment accompanying sleep obstructive

Abbreviations: AD, Alzheimer disease; ASp, airflow spirogram; CSp, chest spirogram; g7, genu of the facial nerve; KF, kolliker-fuse nucleus; LPB, lateral parabrachial nucleus; mcp, middle cerebellar peduncle; nA, nucleus ambiguus; n7, facial motor nucleus; nTS, nucleus tractus solitarius; PnO, pontine reticular nucleus; PnR, raphé pontis nucleus; pr5DM, principal trigeminal sensory nucleus dorso-median; Rf, respiratory frequency; RMg, raphé magnus; ROb, raphé obscurus; RPa, raphé pallidus; scp, superior cerebella peduncle; SubC, subcoeruelus nucleus; Ti, duration of inspiration; Te, duration of expiration; Ttot, total respiratory cycle duration; VT, tidal volume; 5-HT, serotonin; 5-HIAA, 5-hydroxy-indol acid acetic; 12r, intra-medullary rootlet of hypoglossal nerve.

* Corresponding author at: Mp3-Respiration Team, CRN2M, UMR 6231, CNRS – Université Aix-Marseille II & III, Faculté Saint Jérôme, Service 362, 13397 Marseille Cedex 20, France. Tel.: +33 491 28 81 72; fax: +33 491 28 83 97.
E-mail address: gerard.hilaire@univ-cezanne.fr (G. Hilaire).
[1] Present address: Laboratoire Réponses Cellulaires et Fonctionnelles à l'Hypoxie, EA2363, Université Paris13, Bobigny, France.

1569-9048/$ – see front matter © 2011 Elsevier B.V. All rights reserved.
doi:10.1016/j.resp.2011.06.030

Author's personal copy

apnoeas, low risk to develop AD in persons with good respiratory function at midlife (Guo et al., 2007), reduced brain atrophy in AD patients retaining cardiorespiratory fitness (Burns et al., 2008) and improved behaviours in AD patients treated with continuous positive airway pressure (Daulatzai, 2010; Cooke et al., 2006, 2009; Ancoli-Israel et al., 2008; Chong et al., 2006). Neurodegeneration in AD could even originate in the brainstem (Simic et al., 2009), and associated anomalies of the serotonin (5-HT) system causing sleep-disordered breathing contribute to AD progression (Kovacs et al., 2003; Mössner et al., 2000; Parvizi et al., 2001; Rüb et al., 2000; Storga et al., 1996; Gottfries, 1990).

As the respiratory rhythm generator (RRG) spontaneously produces easily recordable motor output, an interesting experimental model for examining onset and progression of networks dysfunction is offered by mutant mouse models of neurodevelopmental and neurodegenerative diseases (Viemari et al., 2005; Katz et al., 2009; Voituron et al., 2009, 2010a,b; Dutschmann et al., 2010). Here, we examined the RRG function in Tau.P301L mice, a mutant mouse model for tauopathy and AD (Terwel et al., 2005; Muyllaert et al., 2006). Tau.P301L mice were produced on the FVB/N background to express the longest human tau isoform bearing the P301L mutation specifically in neurons (Terwel et al., 2005). With age, Tau.P301L mice develop brain tauopathy, cognitive and motor defects, until premature death before age 10–12 months. From 8 months onwards, tauopathy affects the kolliker-fuse (KF) nucleus, which alters the KF control of the laryngeal motoneuron activity and induces upper airway dysfunction: Tau.P301L mice show a paradoxical tendency to upper airway narrowing during inspiration that they compensate by producing enlarged chest respiratory movements (Dutschmann et al., 2010).

Using plethysmography, biochemistry and immunohistochemistry in Tau.P301L and age-matched FVB/N wild-type mice, we report that despite upper airway dysfunction, Tau.P301L mice retained normal RRG function and regulations at 8 months, but showed aggravated upper airway dysfunction, altered RRG function and regulations at 9–10 months when entering the terminal stage of the disease. In addition, terminal Tau.P301L mice developed severe tauopathy in the raphé areas and abnormal 5-HT metabolism. The resulting breathing defects likely contribute essentially to the moribund phenotype of Tau.P301L mice, and by extension in tauopathies and AD patients.

2. Materials and methods

The experimental procedures were performed in accordance with European and national guidelines for care and use of laboratory animals (Council Directive 2010/63/EU). They were previously reported in details elsewhere (Terwel et al., 2005, 2008; Dutschmann et al., 2010; Voituron et al., 2009, 2010a,b; Menuet et al., 2011).

2.1. Animals

Transgenic Tau.P301L mice, produced in the FVB/N genetic background, expressed the longest human tau isoform bearing the P301L mutation (Tau.4R/2N-P301L) under control of the mouse thy1 gene promoter aiming for neuron-specific expression starting in the third postnatal week (Terwel et al., 2005, 2008). Tau.P301L mice ($n = 28$), genotyped by PCR, were compared with age- and sex-matched control FVB/N mice ($n = 23$) at three different ages (different mice were studied at different ages): 4–5 months ($n = 7$ Tau.P301L and $n = 7$ FVB/N), 8 months ($n = 7$ Tau.P301L and $n = 8$ FVB/N) and 9–11 months ($n = 14$ Tau.P301L and $n = 8$ FVB/N).

2.2. Plethysmography and RRG function at rest

As reported previously (Dutschmann et al., 2010; Voituron et al., 2009, 2010a,b; Menuet et al., 2011), we used constant flow whole-body plethysmography and double-chamber plethysmography in conscious mice. To avoid stress, the mice were habituated to the plethysmograph before the recording sessions. Spirograms were stored on disk and analyzed afterwards, selecting recording periods without artefacts and body movements. Whole body plethysmography was used to measure the respiratory frequency (Rf; expressed in respiratory cycles per minute, c min^{-1}), the duration of the inspiratory and expiratory periods (Ti and Te, respectively; expressed in ms), the distribution of total respiratory cycle duration (Ttot), and the production of transient apnoeas > two Ttot. Because of unreliability of measurements of tidal volume (VT) with plethysmography, VT was not studied.

Double-chamber plethysmography was used to simultaneously record the chest respiratory movement produced in the body chamber (Chest Spirogram, CSp) and the resulting airflow in the head chamber (airflow spirogram, ASp). This enabled the detection of upper airway defects when the ratio ASp/CSp drops to a value <1 (for details see Dutschmann et al., 2010). In addition, this enabled the identification of total obstructive apnoeas when rhythmic CSp signal persisted in the absence of phasic ASp signals as reported in other transgenic mice (Voituron et al., 2010b). The peak amplitudes of paired CSp and ASp values during quiet breathing were measured on consecutive respiratory cycles, normalized and expressed as increments of the difference between min and max amplitudes. Bravais–Pearson tests were performed to calculate the correlation coefficient between variables and the slope of the linear regression.

2.3. Plethysmography and RRG regulations

We examined the Rf changes during hypoxia, hypercapnia and peri-sigh periods (Voituron et al., 2009, 2010a; Menuet et al., 2011). Tau.P301L and FVB/N mice of matched age were subjected to short lasting (5 min) moderate hypoxic (10% O_2) or hypercapnic (4% CO_2) challenges. Rf was measured prior to respiratory challenges (control Rf) and during the last 3–5 min period of respiratory challenges, with changes expressed in increments (c min^{-1}) vs. control Rf. The effect of sigh occurrence on the Rf was studied by measuring the Rf every second during 30 s (from the 10 s period preceding the sigh to the 20 s period following the sigh). For a given mouse, at least 7 peri-sigh periods were analyzed and data averaged to obtain an individual Post-Sigh Time Histogram (PSTH) representative of Rf changes (in Hz every second) prior to and after sigh occurrence. Mice of a given genotype (Tau.P301L or FVB/N mice) were grouped and the individual PSTH were pooled to built an averaged PSTH representative of the mean Rf changes (expressed as % of control every second) prior to and after sigh for a given group of mice.

2.4. Immunohistochemistry, optic and confocal microscopy

Methods for immunohistochemistry were reported in details elsewhere (Terwel et al., 2005, 2008; Dutschmann et al., 2010). First, mice were anaesthetized (Nembutal; 120 mg/kg, i.p.), transcardiacally perfused (ice-cold saline, 2 ml/min, 2 min) and brainstems were removed, fixed (4% paraformaldehyde, 24 h), and stored (0.1% sodium azide in PBS at 4 °C) until sectioning (40 μm coronal vibratome sections). Thereafter, procedures were as follows: rinsing (PBS; 15 min with 1.5% H_2O_2 in 50% methanol/PBS), blocking of non-specific binding sites (10% fetal calf serum, 0.1% Triton X-100 in PBS), incubation with primary monoclonal antibodies AT8 (mouse anti-AT8, 1/2500) or AT100 (mouse anti-AT100, 1/1400), washing, 1 h incubation

Author's personal copy

with the secondary goat antimouse IgG antiserum coupled to horseradish peroxidase (1/500 in blocking buffer; Dako, Denmark), 5 min incubation in 50 mM Tris HCl, pH 7.6, enzymatic staining with 3,3′-diaminobenzidine (0.5 mg/ml), 0.3%H_2O_2 in 50 mM Tris HCl, pH 7.6. Sections were counterstained with hematoxylin, ethanol dehydrated, delipidated in xylol and mounted for microscopic analysis of AT8 and AT100 immunoreactivity.

AT8 and AT100 are monoclonal antibodies specifically directed against phosphorylated human protein Tau, respectively at epitopes pS198/pS202pS/pS205 and pT231/pS235 (Innogenetics, Gent, Belgium). AT8 is to be considered a marker on the border between physiology and pathology because AT8 may be observed during brain development of young adults and children (Braak and Del Tredici, 2011; Duyckaerts, 2011). Even in human pathology, AT8 is a "pre-tangle" marker, i.e. the phoshorylation precedes the hyper-phosphorylation of protein Tau that is typically observed post-mortem in the final, pathological neurofibrillary tangles. AT100 however is a recognized pathological phospho-epitope, typical for AD and primary tauopathies (Terwel et al., 2005).

We examined AT8 and AT100 expression profile in the brainstem of 4–5 months ($n = 7$) and terminal ($n = 5$) Tau.P301L mice. We specifically analyzed distinct brainstem areas, including the medullary respiratory-related areas (Feldman, 2011; Onimaru et al., 2009; Fortin and Thoby-Brisson, 2009; Wittmeier et al., 2008), the midline raphé nuclei (raphé pallidus, RPa, raphé magnus, RMg, raphé obscurus, ROb, raphé pontis, RPn) and the pontine KF nucleus (Dutschmann et al., 2010). These areas were defined from neuroanatomical reference points in mouse atlas (Paxinos and Franklin, 2001). For a given mouse, about 120 consecutive coronal sections of 40 μm were cut, from the pyramidal decussation to about 4800 μm more rostral. One section every three sections was stained with either AT8 (first section) or AT100 (second section) or retained for other studies (third section). Then, about forty AT8 and forty AT100 stained sections were analyzed per mouse (120 μm between two consecutive AT8 stained sections or AT100 stained sections). As the AT8 and AT100 staining was obviously different between young (almost no staining) and terminal (marked staining) Tau.P301L mice, we performed no statistical quantitative comparisons between the two age groups. We measured the AT8 staining in the raphé and KF nuclei of terminal Tau.P301L mice with two different protocols. For the raphé nuclei where AT8 positively stained (AT8+) neurons were easily discernible, we counted the AT8+ neurons in medial areas extending 200 μm bilaterally from the midline (400 μm) of 2–3 consecutive sections per mouse. Data from different mice were averaged to obtain the mean number of AT8+ neurons in a given raphé nucleus. As previously (Dutschmann et al., 2010), AT8+ neurons were defined as neurons with visible nucleus, well-defined soma, and high staining intensity. For the KF nucleus, extending on both left and right sides of the pons is 6–8 consecutive sections (about 720–960 μm rostro-caudal extension for a given mouse) and containing frequent and intermingled AT8+ neurons, counting of AT8+ neurons was rather difficult. We therefore used dedicated software to quantify the mean optical density of AT8 staining in the whole KF nucleus (ImageJ created by Wayne Rasband, NIH, USA). For each KF section, we defined a 500 μm × 500 μm square area centred on the KF nucleus, i.e. positioned ventral to the lateral parabrachial nucleus (LPB), lateral to the superior cerebella peduncle (scp), medial to the middle cerebellar peduncle (mcp), and dorsal to the principal trigeminal sensory nucleus dorso-median (pr5DM). Digital camera and light microscope (Olympus BX50) were used to take pictures of the KF area in different slices and mice. To minimize variations in the KF square positioning and the intensity of the AT8 staining between different sections and between different mice, the analysis was performed by the same person (CM) using standardized protocols (homogenisation for positioning, brightness and contrast adjustments; colour threshold set to remove 3/4 of the blue spectrum). For each given rostro-caudal KF section, the AT8 optical density was measured and the mean AT8 optical density of the whole KF sections for a given mouse was obtained by averaging values of individual sections. The mean value representative of the AT8 optical density of the KF of terminal Tau.P301L mice was obtained by averaging mean values from different mice. Although this protocol did not totally abolish individual variations between different sections and mice, it significantly weakened it as attested by weak standard error of the mean (about 10%).

For confocal study of AT8 and 5-HT expressions in raphé neurons, coronal cryo-sections of 40 μm were cut. Following two rinses in 0.1 M PBS, sections were positioned on glass slides and permeabilized using 0.1 M PBS containing 0.2% Triton X-100 for 30 min. Thereafter, sections were pre-incubated for 1 h in 0.1 M PBS containing 4% of goat serum and incubated overnight at 4 °C with the corresponding primary antibody: rabbit anti-serotonin (1/2000, Sigma, USA); mouse anti-AT8 (1/2000) (Terwel et al., 2005). Following primary antibody incubation, sections were washed twice in 0.1 M PBS and incubated 1 h at room temperature with the appropriate secondary antibody: goat anti-mouse Alexa 488, goat anti-rabbit Alexa 594 (1/400; Invitrogen, France). Z-stacks confocal images were captured with a Carl Zeiss LSM 700 confocal laser scanning system on an Axio Observer.Z1 inverted microscope stand (Carl Zeiss, Germany), equipped with a 488 nm and 555 nm laser lines and monitored with Zen 2009 image acquisition software (Carl Zeiss, Germany).

2.5. Biochemistry

Values of pH, pO_2 and pCO_2 (mm of Hg) were measured in venous mixed blood samples of non-anaesthetized mice as previously reported (Menuet et al., 2011). After tail blood vessels dilatation with water at 40–42 °C and small incision at the tip of the tail, 100 μL blood samples were collected in plastic capillaries with electrolyte-balanced heparin (Radiometer, 70 IU heparin per ml) and analyzed with ABL 80 Flex analyser (Radiometer, France).

To analyze the 5-HT metabolism (Menuet et al., 2011), first the mouse brainstem was quickly removed after decapitation, stored at −80 °C and thereafter, the brainstem contents of 5-HT and its main catabolite 5-hydroxy-indol acid acetic (5-HIAA) from the monoamine oxydase A (MAOA) degradation pathway were measured by high pressure liquid chromatography (HPLC) and electrochemical detection (Waters System: pump P510, electrochemical detector EC2465; Atlantis column DC18; mobile phase: citric acid, 50 mM; orthophosphoric acid, 50 mM; sodium octane sulfonic acid, 0.112 mM; EDTA, 0.06 mM; methanol, 5%; NaCl, 2 mM; pH 2.95). Contents were expressed in ng per structure. Terminal Tau.P301L mice, identified by low body weight, limb clasping, lethargy and immobility, were sacrificed for HPLC study 1–3 days after plethysmographic measurements of their breathing parameters.

2.6. Statistics

Values are expressed as mean ± standard error of the mean (SEM). Statistical comparisons between age-matched Tau.P301L and FVB/N mice were performed using Student's unpaired *t*-test. To compare coefficient of correlations between CSp and ASp amplitudes in 8 month old and terminal Tau.P301L mice, Fisher transformation was used before performing Student's *t*-test. Statistical differences were regarded as significant if $p < 0.05$.

Author's personal copy

3. Results

3.1. Normal breathing in 8 month old Tau.P301L mice

Young Tau.P301L mice (4–5 months) had normal RRG activity and upper airway function (Dutschmann et al., 2010). To examine the effects of aging on RRG function in conscious Tau.P301L and control FVB/N mice, we used non-invasive plethysmography and compared their Rf, Ti, Te, Ti/Te ratio and Ttot (whole-body plethysmography) as well as the ratio between airflow spirogram (ASp) and chest spirogram (CSp) (double-chamber plethysmography).

3.1.1. Normal baseline activity of the RRG of 8 month old Tau.P301L mice

At age 8 months, whole-body plethysmography did not reveal significant differences in RRG function of Tau.P301L ($n=7$) and FVB/N ($n=8$) mice when breathing room air (Fig. 1A1 and B1). Tau.P301L and FVB/N mice had similar Rf, Ti, Te and Ti/Te ratio (Table 1). The RRG activity of Tau.P301L and FVB/N mice was robust as attested by narrow distribution of Ttot (Fig. 1A2 and B2), and rareness of transient apnoeas (0.07 ± 0.05 and 0.11 ± 0.07 per min, respectively; $p=0.363$).

Whole-body plethysmography showed spirograms of larger amplitude in Tau.P301L than FVB/N mice, suggesting 2-fold larger VT. As demonstrated previously (Dutschmann et al., 2010), the enlarged spirograms of aged Tau.P301L mice did not reflect an actual increase of VT but reflected the enhanced chest movements to compensate for the constricted upper airways. This was further confirmed here using double-chamber plethysmography to simultaneously record CSp and ASp (Fig. 2A).Young Tau.P301L ($n=4$) and FVB/N ($n=4$) mice produced similar ASp and CSp, leading to similar ASp/CSp ratio (1.58 ± 0.46 and 1.37 ± 0.06, respectively; $p=0.375$). In contrast, 8 month old Tau.P301L mice ($n=7$) had enlarged CSp, reduced ASp, and consequently weaker ASp/CSp ratio than FVB/N ($n=8$) mice (0.85 ± 0.17 and 2.67 ± 0.40, respectively; $p=0.001$) (Fig. 2B). Furthermore, we analyzed CSp and ASp during transient apnoeas (Fig. 2C). Both CSp and ASp signals remained at baseline during apnoea in Tau.P301L and FVB/N mice. Centrally mediated breath-hold as identified in Mecp2-deficient mice (see Voituron et al., 2010a,b,c) were never observed in Tau.P301L and FVB/N mice. Recording during quiet breathing revealed synchronized changes in amplitude of ASp and CSp signals (Fig. 2E). Plotting of paired ASp and CSp variables from consecutive respiratory cycles revealed a significant linear relationship in Tau.P301L ($n=3$) and FVB/N ($n=3$) (Fig. 2D and F), with similar although marginally weaker coefficient of correlations in Tau.P301L than FVB/N mice (0.592 ± 0.184 and 0.792 ± 0.118, respectively; $p=0.076$). The slope of the linear relationship did not differ between strains (0.804 ± 0.078 and 0.902 ± 0.072, respectively; $p=0.215$).

3.1.2. Normal respiratory regulations in 8 month old Tau.P301L mice

In a next series of experiments, we examined whether the RRG of 8 month old Tau.P301L mice was normally regulated. When subjected to a short moderate hypercapnic challenge (CO_2 4%), Tau.P301L ($n=7$) and FVB/N ($n=8$) mice significantly increased their Rf (Fig. 3A1 and A2, B1 and B2). They reached similar mean Rf during the last 3–5 min period of hypercapnia (Table 1 and Fig. 3C), and similar mean Rf increments were measured in Tau.P301L and FVB/N mice (91 ± 9 and 98 ± 8 c min^{-1}, respectively; $p=0.285$). Rf was increased via shortenings of both Ti and Te (Table 1): Ti became significantly shorter in Tau.P301L than FVB/N mice but Te was similar in both groups, which induced a marginally lower Ti/Te ratio during hypercapnia in Tau.P301L than FVB/N mice.

When subjected to a short moderate hypoxic challenge (O_2 10%), Tau.P301L ($n=7$) and FVB/N ($n=8$) mice also significantly increased their Rf (Fig. 3A3 and B3) and reached similar mean Rf during the last 3–5 min period of hypoxia (Table 1 and Fig. 3C). Rf was increased by shortening Ti and Te in both groups with a trend for shorter Ti and prolonged Te in Tau.P301L compared to FVB/N mice. This induced a significantly lower Ti/Te ratio during hypoxia in Tau.P301L than FVB/N mice. Spirogram amplitudes were increased by 3–4 folds under either hypoxia or hypercapnia in both strains (Fig. 3A and B).

Spontaneous sighs are augmented inspirations that mobilize VT that is twice baseline VT. Sighs improve alveolar oxygenation, activate pulmonary stretch receptors, and reduce the Rf during the post-sigh period via chemosensitive feedback and Hering-Breuer regulations (Menuet et al., 2011; Voituron et al., 2009). Sighs were observed at a low frequency (1 sigh/2 min) in both genotypes and commonly reduced Rf in 8 month old Tau.P301L (Fig. 1A3 and A4) and FVB/N (Fig. 1B3 and B4) mice. However the changes in post-sigh Rf were not stereotyped in freely behaving mice. To allow comparison of post-sigh breathing in Tau.P301L and FVB/N mice, we measured Rf during the peri-sigh period for at least 7 sighs and illustrate representative Rf changes in a given mouse using Post-Sigh Triggered Histogram (PSTH). Pooled PSTH of Tau.P301L ($n=7$) and FVB/N ($n=8$) revealed similar changes in the post-sigh Rf in both strains: the Rf initially dropped by about 20% in the first second following the sigh, transiently increased but then remained decreased by 30–40% of the control Rf for 3–6 s after the sigh (Fig. 1A5 and B5).

To summarize, we confirmed the previously reported upper airway dysfunction of 8 month old Tau.P301L mice (Dutschmann et al., 2010) and showed that despite upper airway dysfunction, their RRG retained unimpaired baseline activity and unimpaired regulations.

3.2. Altered breathing in terminal Tau.P301L mice

Tau.P301L mice progress into the terminal stages after 8 months on average. The terminal phenotype includes dramatically reduced body weight (females <16 g), lordosis, lethargy with reduced locomotor activity and severe clasping. Thereafter, Tau.P301L mice do not survive more than a week with death before 10–12 months (Terwel et al., 2005, 2008).

3.2.1. Altered baseline activity of the RRG of terminal Tau.P301L mice

Using whole-body plethysmography, we successfully recorded the breathing of terminal Tau.P301L mice ($n=8$) and compared it to that of age-matched FVB/N mice (9–11 months; $n=6$). As shown in Table 1, terminal Tau.P301L mice showed a drastic, significant reduction of Rf when compared to age-matched FVB/N mice. The Rf reduction in terminal Tau.P301L was characterized by an increase of both Ti and Te, but the Ti/Te ratio remained similar in terminal Tau.P301L and age-matched FVB/N mice. Although terminal Tau.P301L mice did hardly move in the plethysmograph chamber, they showed unstable breathing patterns, with increased Ttot variability (Fig. 4A1, A2, B1, and B2).

Double-chamber plethysmography revealed persisting upper airway dysfunction in terminal Tau.P301L mice and a drastically reduced ASp/CSp ratio (0.51 ± 0.13) when compared to that of young Tau.P301L, young FVB/N mice and old FVB/N mice (all >1). However, the ratio reduction did not reach the significance when comparing terminal Tau.P301L mice to 8 month old Tau.P301L mice ($p=0.129$). In three terminal Tau.P301L mice, ASp and CSp values were significantly coupled (Fig. 2G and H) but the mean coefficient of correlation (0.41 ± 0.09; $p=0.030$) and slope (0.61 ± 0.07; $p=0.017$) were significantly weaker than in 8 month old Tau.P301L mice. These data revealed a further reduction in efficiency of chest movements to induce adequate ventilation in the terminal Tau.P301L mice. No obstructive apnoeas were observed in terminal

Author's personal copy

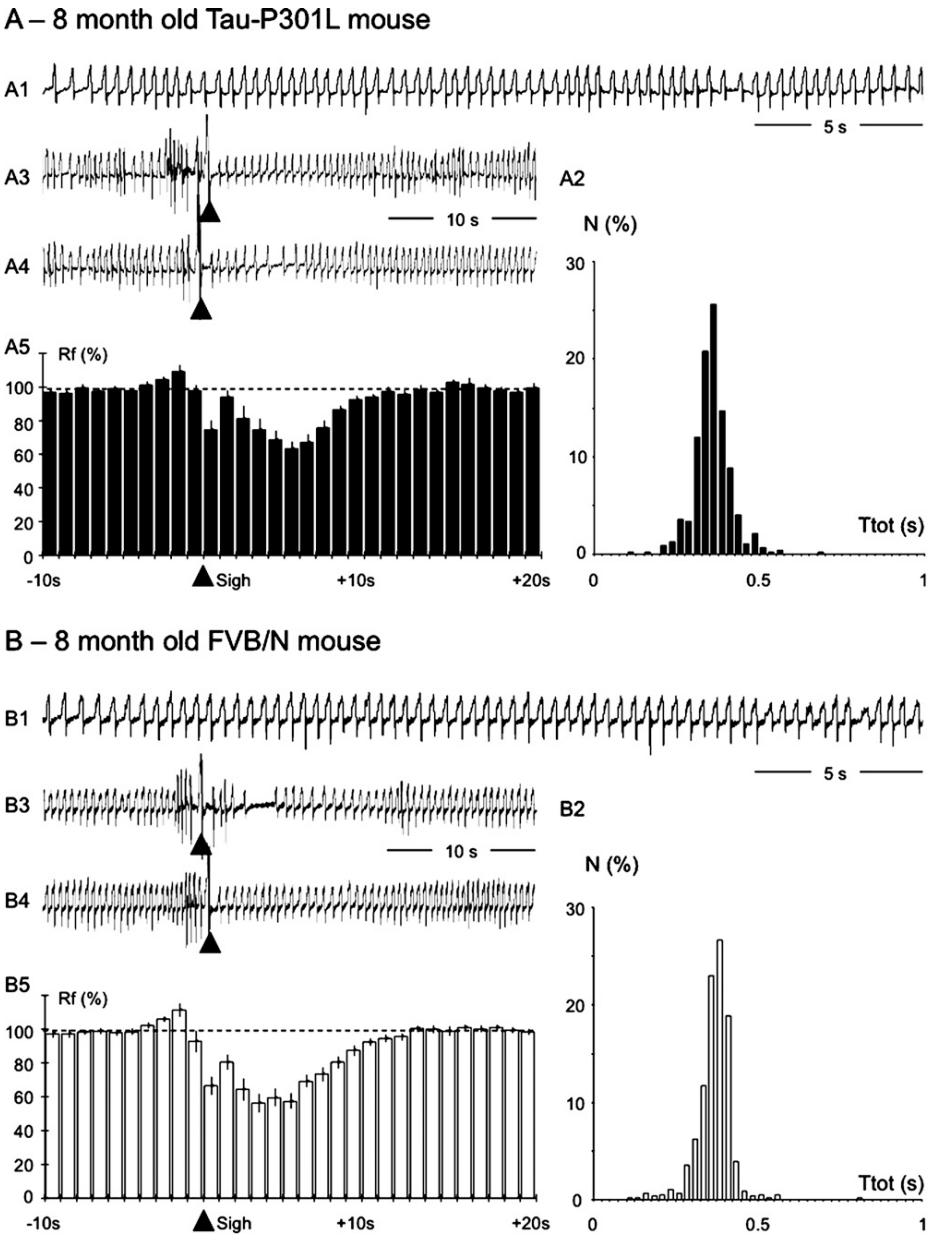

Fig. 1. Conscious, unrestrained Tau.P301L and FVB/N mice had similar breathing pattern at 8 months of age. (A and B) Spirograms recorded with whole-body plethysmography in two given conscious, unrestrained mice at 8 months, a Tau.P301L (A1, A3, A4) and a FVB/N mice (B1, B3, B4). Note the bradypnoea occurring after the sigh production (triangles) in Tau.P301L (A3 and A4) and FVB/N (B3 and B4) mice. (A2 and B2) Histograms show the distribution of the duration of total respiratory cycle (Ttot) for the two illustrated Tau.P301L and FVB/N mice (black and white columns, respectively); *N* is the % of count in a given time class (25 ms bins) for 4–5 min recording. Note the narrow distribution of Ttot in both Tau.P301L and FVB/N mice. (A5 and B5) Averaged PSTH show the mean (and SEM) changes in respiratory frequency (Rf, expressed in % of control Rf measured prior to the sigh, 100%) every second from 10 s prior to the sigh to 20 s after the sigh in Tau.P301L ($n = 7$) and FVB/N ($n = 8$) mice. Note the similar time-course of Rf changes in both types of mice, with the weak pre-sigh tachypnoea and the marked post-sigh bradypnoea.

Tau.P301L mice and transient apnoeas as described above occurred at the same rate as in 8 month old Tau.P301L mice. Sleep/wake stages were not analyzed, so no data are available about eventual sleep-disordered breathing in terminal Tau.P301L mice, an aspect that deserves further exploration.

3.2.2. Altered respiratory regulations in terminal Tau.P301L mice

To avoid premature death of terminal Tau.P301L mice by the experiment, they were not subjected to hypoxic challenges. However, five Tau.P301L mice were subjected to a hypercapnic challenge to which they responded by moderate increases of Rf (Table 1). During the last 3–5 min of hypercapnia, the Rf increment was 2-fold weaker in terminal than 8 month old Tau.P301L mice (Fig. 4D). The Rf was increased via shortenings of both Ti and Te, with a trend of the Ti/Te ratio under hypercapnia to be lower in terminal than 8 month old Tau.P301L mice ($p = 0.060$). Effects on Rf of sigh occurrence were analyzed in four terminal Tau.P301L mice. When sighs occurred (triangles in Fig. 4), they were followed by either bradypnoea (Fig. 4A2) or no Rf change (Fig. 4A1) or transient tachypnoea (Fig. 4B2). Post-sigh bradypnoea failed to reproducibly occur even during periods with rather stable Ttot and neither individual PSTH nor averaged PSTH revealed significant Rf changes during the post-sigh period in terminal Tau.P301L mice (Fig. 4C).

Author's personal copy

Table 1
Breathing parameters of conscious, unrestrained Tau.P301L and FVB/N mice.

Strains	Age (months)	Breathing mixture	Rf (c min^{-1})	Ti (ms)	Te (ms)	Ti/Te ratio
Tau.P301L			161 ± 4	125 ± 11	249 ± 10	0.51 ± 0.06
vs.	8	Air	p = 0.114	p = 0.176	p = 0.122	p = 0. 421
FVB/N			150 ± 7	136 ± 4	274 ± 17	0.50 ± 0.02
Tau.P301L			251 ± 6	89 ± 2	151 ± 5	0.60 ± 0.03
vs.	8	CO_2 4%	p = 0.273	p = 0.017	p = 0.325	p = 0.071
FVB/N			245 ± 9	102 ± 5	146 ± 9	0.72 ± 0.08
Tau.P301L			211 ± 7	95 ± 4	193 ± 8	0.49 ± 0.02
vs.	8	O_2 10%	p = 0.231	p = 0.070	p = 0.062	p = 0.001
FVB/N			221 ± 12	108 ± 7	172 ± 10	0.63 ± 0.02
TerminalTau.P301L			99 ± 7	242 ± 40	645 ± 19	0.44 ± 0.09
vs.	9–11	Air	p < 0.001	p < 0.001	p < 0.001	p = 0.212
FVB/N			138 ± 4	148 ± 13	285 ± 21	0.52 ± 0.03
TerminalTau.P301L			129 ± 15	191 ± 10	377 ± 9	0.51 ± 0.03
vs.	9–11	CO_2 4%	p < 0.001	p < 0.001	p < 0.001	p = 0.142
FVB/N			235 ± 19	102 ± 15	153 ± 16	0.67 ± 0.15

Values are mean ± SEM. Student's unpaired t-test between breathing parameters of age-matched Tau.P301L and FVB/N mice (whole body plethysmography) breathing air, hypercapnic (CO_2 4%) or hypoxic mixtures (O_2 10%).

The reduced Rf, the variable Ttot and the lack of post-sigh bradypnoea of terminal Tau.P301L mice did not reflect the normal characteristics of physiological aging. Three age-matched Tau.P301L mice that did not yet enter the terminal stage (body-weight near normal, no limb clasping, no lethargy) retained a normal breathing pattern (Fig. 4E1), with normal Rf (131 ± 7 c min^{-1}), rather robust drive although an increased variability of Ttot was observed (Fig. 4E3) and normal post-sigh bradypnoea (Fig. 4E2). Rf responses to hypercapnia were not tested in these old, non terminal Tau.P301L mice.

As aggravated upper airway dysfunction, impaired baseline activity of the RRG and impaired respiratory regulations might affect blood oxygenation, we measured pH, pCO_2 and pO_2 levels in mixed blood samples taken from the tail vein of a terminal Tau.P301L mouse. Although these are anecdotic values, pH, pCO_2 and pO_2 of the terminal Tau.P301L mouse deviated from those of young healthy Tau.P301L mice at 4 months (n = 4), suggesting acidosis (7.12 vs. 7.16 ± 0.02), hypercapnia (85 mm of Hg vs. 69 ± 8 mm of Hg) and hypoxemia (46 mm of Hg vs. 52 ± 5 mm of Hg) during the terminal phase of Tau.P301L mice.

3.3. Tauopathy in brainstem of terminal Tau.P301L mice

Aging Tau.P301L mice develop brain and brainstem tauopathy (Terwel et al., 2005; Dutschmann et al., 2010). In coronal brainstem sections of young (4–5 months) and terminal Tau.P301L mice, we analyzed the expression of the phospho-epitope of human protein Tau using two different monoclonal antibodies, AT8 and AT100. AT8 is a marker on the border between physiology and pathology (Braak and Del Tredici, 2011; Duyckaerts, 2011) whereas AT100 is a recognized pathological marker (Terwel et al., 2005). In brainstem sections, AT8 and AT100 staining was absent in FVB/N mice, weak and almost absent in young Tau.P301L mice but obvious in terminal Tau.P301L mice where AT8 positive (AT8+) and AT100 positive (AT100+) neurons were scattered in the whole brainstem, from the caudal retro ambiguus nucleus to the rostral peri aqueductal gray. Herein, we specifically examined the medullary respiratory-related areas (Fig. 5A), the pontine KF area (Fig. 5B and C) and the midline raphé area (Figs. 6 and 7).

3.3.1. Lack of tauopathy in medullary respiratory-related areas of terminal Tau.P301L mice

In the medulla of Tau.P301L mice, we analyzed three distinct respiratory-related areas (Feldman, 2011; Onimaru et al., 2009; Fortin and Thoby-Brisson, 2009; Wittmeier et al., 2008): first, the Pre-Bötzinger Complex (Pre-BötzC) area extending in the ventro-lateral medulla below the nucleus ambiguous (nA) and involved in respiratory rhythmogenesis, second the retro-trapezoid nucleus/para-facial group (RTN/pFRG) laying close to the ventral surface below the facial nucleus (n7) and involved in central chemosensitivity, and third the nucleus tractus solitarius (nTS) know to integrate the peripheral regulatory inputs entering the dorsal medulla. In young Tau.P301L mice, almost no AT8+ neurons were found in the areas of the Pre-BötzC (Fig. 5A1), RTN/pFRG (Fig. 5A2) and nTS (Fig. 5A3). In terminal Tau.P301L mice, AT8+ neurons were more frequent and well stained but they were not more frequent in the PreBötzC (Fig. 5A4), RTN/pFRG (Fig. 5A5) and nTS (Fig. 5A6) areas than in surrounding tissues. Similar results were obtained with the pathological marker AT100 that revealed scattered AT100+ neurons in the brainstem but not specifically in the PreBötzC, nTS and RTN/pFRG areas of terminal Tau.P301L mice. Then, the altered breathing pattern and altered respiratory regulations of terminal Tau.P301L mice could hardly be explained by a severe tauopathy in the medullary respiratory-related areas.

3.3.2. KF tauopathy in terminal Tau.P301L mice (Fig. 6)

The pontine KF contributes to the regulation of upper airway patency (Dutschmann and Herbert, 2006). It has been previously reported that tauopathy develops with age in the KF of Tau.P301L mice, which alters upper airway function (Dutschmann et al., 2010). AT8 staining of the KF of Tau.P301L mice was weak, almost absent at 4–5 months (Fig. 5B1) but marked at terminal stages (Fig. 5B2). In the KF area of terminal Tau.P301L mice, the AT8 staining well delimitated an easily identifiable group of AT8+ neurons extending between the lateral parabrachial nucleus (LPB), the superior cerebella peduncle (scp), the middle cerebellar peduncle (mcp), and the principal trigeminal sensory nucleus dorso-median (pr5DM) (Fig. 5B2). In TauP.301L mice, we measured the mean optical density of the AT8 signal in this KF area on 6–8 consecutive sections per mouse, averaged individual data from a given mouse and finally averaged data from different mice. We found no significant AT8 optical signal in the KF at 4-5 months (1 ± 0) but large AT8 optical signals at terminal stages (23 ± 2). In addition, we found frequent AT100+ neurons in the KF of terminal mice (Fig. 5C). Then, the tauopathy that developed with age in the KF of 8 month old Tau.P301L mice (Dutschmann et al., 2010) persisted at terminal stages of the disease, the AT100 pathologic marker confirming a severe KF tauopathy that highly likely contributed to upper airway dysfunction.

Author's personal copy

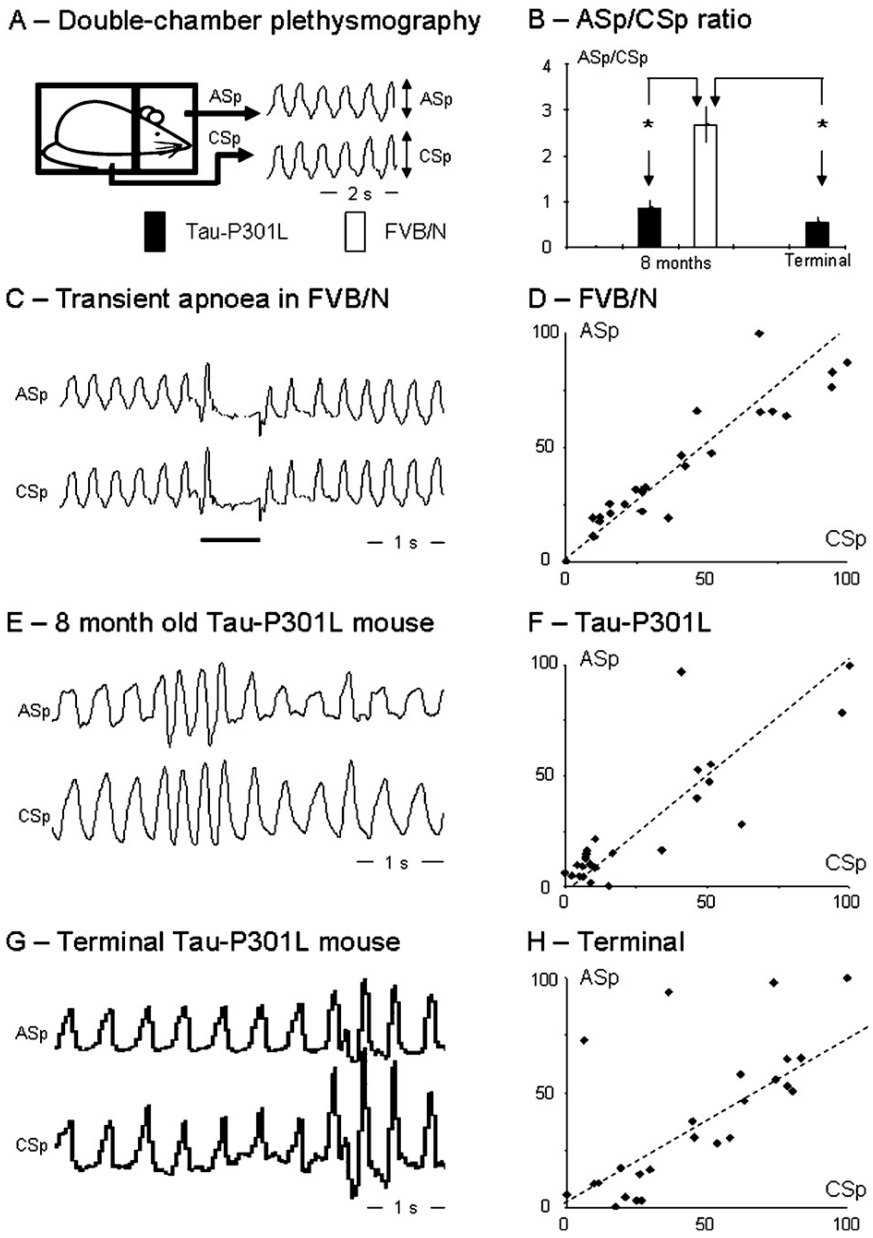

Fig. 2. Upper airway defects in conscious 8 month old and terminal Tau.P301L mice. (A) Schematic presentation of the double-chamber plethysmographic set-up allowing the simultaneous recordings of chest spirogram (CSp; in the body chamber) and airflow spirogram (ASp; in the head chamber) in conscious mice. (B) Histograms show the ASp/CSp ratio measured in 8 month old Tau.P301L and FVB/N mice (black and white columns, respectively) and terminal Tau.P301L mice. * indicates significant differences between ASp/CSp ratios of Tau.P301L and FVB/N mice. (C, E and G) ASp and CSp spirograms recorded with double-chamber plethysmography in 8 month old FVB/N (C), 8 month old Tau.P301L (E) and terminal Tau.P301L (D) mice. In C, note the transient apnoea (horizontal black bar); they were rare in Tau.P301L and FVB/N mice but when they occurred, both CSp and ASp were simultaneously zeroed. (D, F and H) *XY* plotting of normalized CSp and ASp changes in amplitude (min = 0; max = 100) measured from consecutive respiratory cycles of 8 month old FVB/N (D), Tau.P301L (F) and terminal (H) mice. Note the significant linear relationship between CSp and ASp (Bravais–Pearson coefficients of correlation: 0.865, 0.734 and 0.469; for D, F and H, respectively).

3.3.3. Raphé tauopathy in terminal Tau.P301L mice

It is well established that the 5-HT system contributes to respiratory function and dysfunction in various neurological diseases (Hilaire et al., 2010). Therefore we investigated potential alterations in the raphé system of young ($n = 7$) and terminal ($n = 5$) Tau.P301L mice. In midline raphé areas, we observed only few, weakly stained AT8+ neurons in young Tau.P301L mice (Fig. 6A) but frequent, heavily stained AT8+ neurons in terminal Tau.P301L mice (Fig. 6B). Counting AT8+ raphé neurons in terminal mice revealed that they were few in the caudal raphé pallidus, RPa (3 ± 1 neurons/section), frequent in the raphé obscurus, ROb (12 ± 3 neurons/section; Fig. 6B1 and B2) and raphé magnus, RMg (33 ± 5 neurons/section; Fig. 6B3, B4, and B5) and almost absent in the rostral raphé pontis and dorsalis. The aspects of the immune reaction in terminal Tau.P301L mice were consistent with the presence protein tau as hyper-phosphorylated fibrillar aggregates, typical for tauopathy. Second, we examined the expression profile of AT100 in raphé areas. AT100+ raphé neurons were absent in young Tau.P301L mice (data not shown) but obvious and frequent in terminal stages in the ROb (Fig. 6C1 and C2), and RMg (Fig. 6C3–C5). They were rare in the RPa, nearly absent in the raphé pontis (Fig. 5C1) and dorsalis nuclei (data not shown). Third,

Author's personal copy

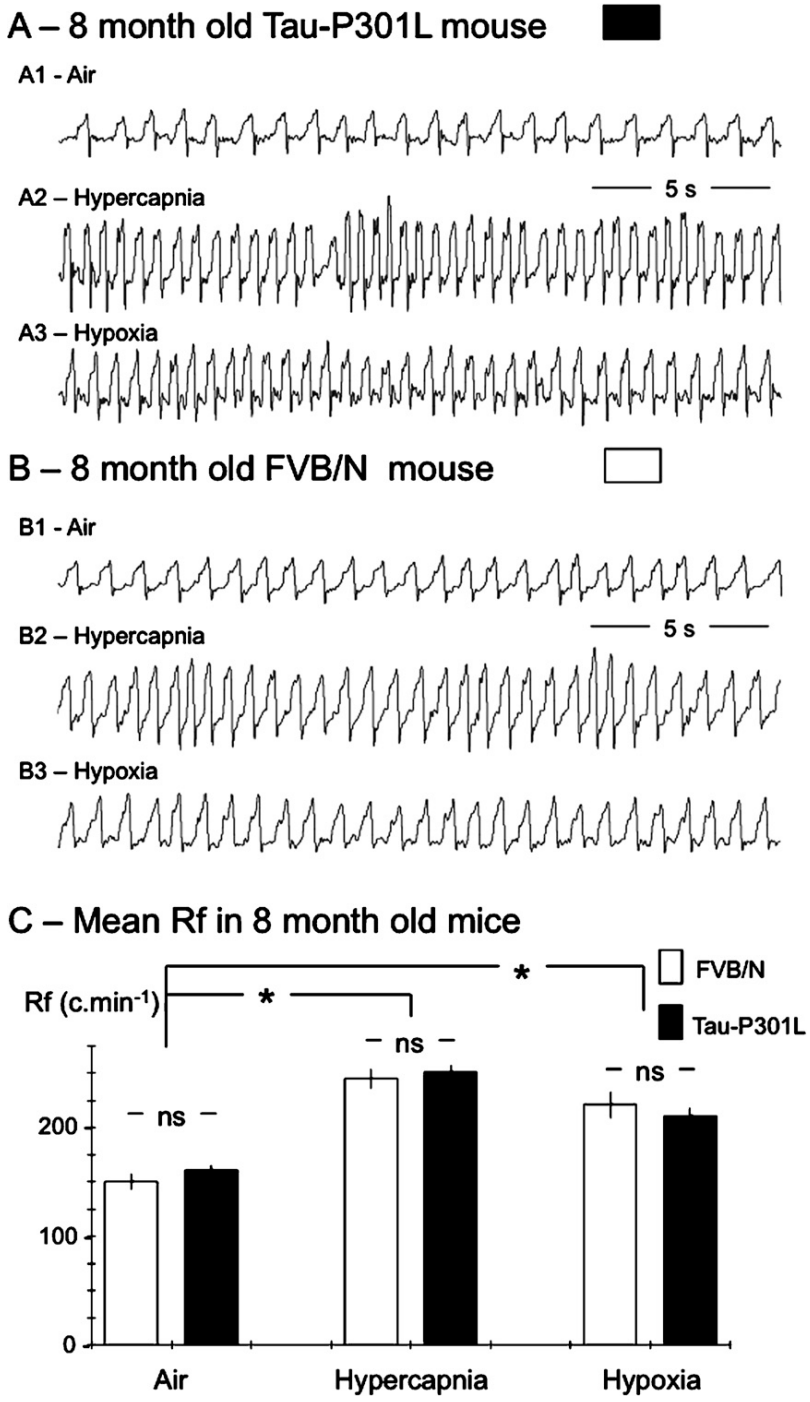

Fig. 3. Conscious, unrestrained Tau.P301L and FVB/N mice similarly responded to hypoxia and hypercapnia at 8 months of age. (A and B) Spirograms from 8 month old Tau.P301L (A) and FVB/N (B) mice under air (A1 and B1), hypercapnia (A2 and B2) and hypoxia (A3 and B3). (C) Histograms show the mean Rf (and SEM) in 8 month old Tau.P301L ($n = 7$) and FVB/N ($n = 8$) mice (black and white columns, respectively) when mice breathed either air, hypercapnic or hypoxic mixtures as indicated. Values (expressed in c min^{-1}) were measured during the 3–5 min period of the respiratory challenges. Note the similar Rf responses in both groups of mice (ns and *, non-significant and significant changes at $P < 0.05$).

given that the raphé nuclei contained not only 5-HT neurons but also non-5-HT neurons (Monti, 2010a,b; Holmes et al., 1994), we used immunofluorescence coupled with confocal microscopy to examine whether the AT8+ raphé neurons were actually 5-HT neurons. In two terminal Tau.P301L mice, almost no 5-HT neurons were AT8+ in the RPa (Fig. 7A) and only a few (5–10%) co-expressed AT8 and 5-HT in the ROb (Fig. 7B) and RMg (Fig. 7C).

3.4. Abnormal 5-HT metabolism in terminal Tau.P301L mice

Finally, we examined whether tauopathy in the raphé nuclei of terminal mice affected the 5-HT metabolism. We used HPLC and electrochemical detection to measure the content of 5-HT and its catabolite 5-HIAA. At 4 months, no differences were observed in the medulla of Tau.P301L ($n = 4$) and FVB/N

Author's personal copy

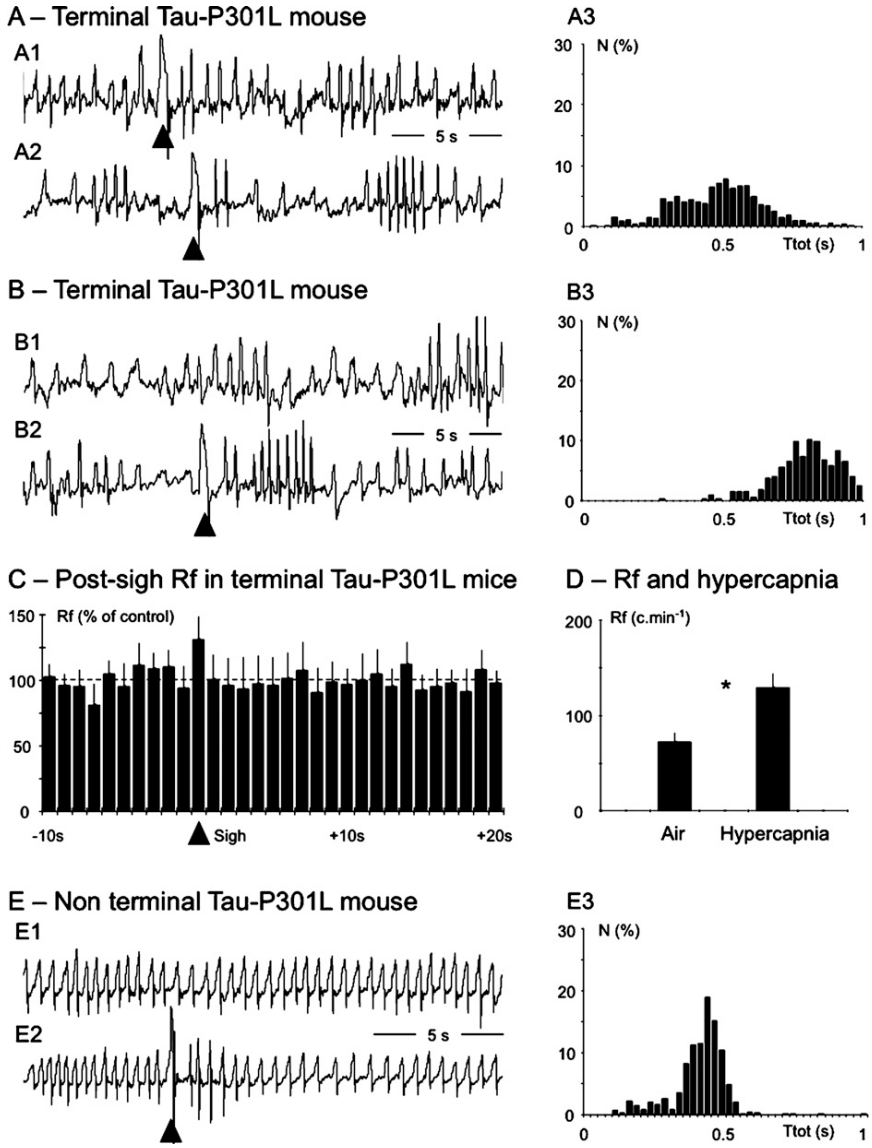

Fig. 4. Conscious, unrestrained terminal Tau.P301L mice had abnormal respiratory rhythm and regulations. (A and B) Spirograms were from two different terminal Tau.P301L mice (triangles in A1, A2 and B2 indicated sighs). Histograms in A3 and B3 show a wide distribution of Ttot for the two terminal mice; *N* is the % of count in a given time class (25 ms bins) for 4–5 min recording. Aside the wide Ttot distribution, note the reduced Rf and the lack of post-sigh bradypnoea in terminal Tau.P301L mice. (C) Averaged PSTH build from 4 terminal Tau.P301L mice shows the lack of post-sigh bradypnoea. (D) Columns in histogram show the mean (and SEM) Rf of terminal Tau.P301L mice when breathing air or hypercpanic mixture. Note the low Rf under air and the significant (*) but weak increment of Rf under hypercapnic mixture. (E) As in A and B, but for an old, non-terminal Tau.P301L mouse; spirograms and histograms show normal Rf with stable rhythm (E1), post-sigh bradypnoea (E2, sigh at triangle) and intermediate Ttot distribution (E3).

($n=4$) mice, with similar contents of 5-HT (3.35 ± 0.15 and 3.09 ± 0.19 ng/medulla, respectively; $p=0.172$) and 5-HIAA (1.90 ± 0.10 and 1.81 ± 0.31 ng/medulla, respectively; $p=0.391$), leading to similar 5-HT/5-HIAA ratio (1.76 ± 0.08 and 1.83 ± 0.25, respectively; $p=0.463$). However significant differences were observed in the medulla of terminal Tau.P301L ($n=6$) and age-matched FVB/N ($n=8$) mice (Fig. 7D1). We observed similar 5-HT contents in both groups (3.25 ± 0.23 and 3.26 ± 0.20 ng/medulla, respectively; $p=0.488$) but a significantly higher 5-HIAA content in Tau.P301L mice than in FVB/N mice (1.99 ± 0.07 and 1.39 ± 0.09 ng per medulla, respectively; $p=0.001$). Consequently the 5-HT/5-HIAA ratio was significantly lower in Tau.P301L than FVB/N mice (1.63 ± 0.09 and 2.36 ± 0.12; $p=0.001$). In the pons (Fig. 7D2), we also found similar 5-HT contents in both groups (3.22 ± 0.63 and 3.40 ± 0.26 ng per pons; $p=0.499$), marginally larger 5HIAA contents in terminal mice (2.94 ± 0.46 and 2.29 ± 0.17 ng per pons; $p=0.07$), and significantly lower 5-HT/5-HIAA ratio in terminal Tau.P301L than FVB/N mice (1.06 ± 0.06 and 1.49 ± 0.07 ng per pons, respectively; $p=0.007$).

Then, terminal Tau.P301L mice showed severe raphé tauopathy that mainly concerned non-5-HT neurons, but altered their 5-HT metabolism and subsequently RRG function and RRG regulations (Hilaire et al., 2010).

4. Discussion

In Tau.P301L mice, we confirm upper airway dysfunction at 8 months (Dutschmann et al., 2010), show normal RRG function and regulations at this age and report, at terminal stages, aggravated upper airway dysfunction, altered RRG function and regulations,

Author's personal copy

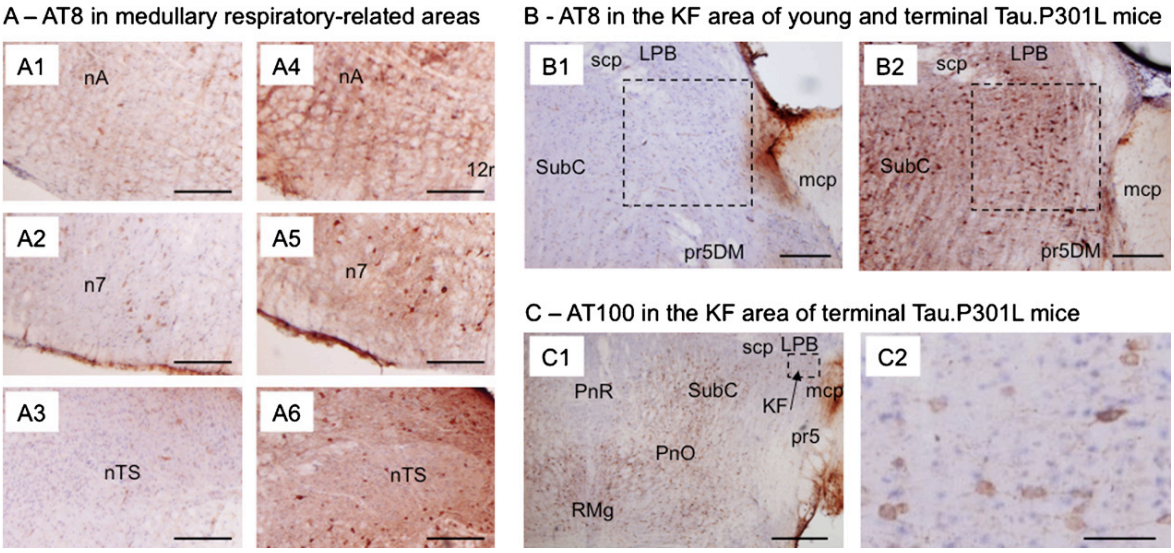

Fig. 5. AT8 expression in medullary respiratory-related areas and KF of young and terminal Tau.P301L mice. Brainstem coronal sections (40 μm) are shown with dorsal and ventral sides upward and downward, respectively, in all histological figures except Fig. 6C5. Abbreviations in Figs. 5 and 6 (from Paxinos and Franklin, 2001): g7, genu of the facial nerve; KF, kolliker-fuse nucleus; LPB, lateral parabrachial nucleus; mcp, middle cerebellar peduncle; nA, nucleus ambiguus; n7, facial motor nucleus; nTS, nucleus tractus solitarius; PnO, pontine reticular nucleus; PnR, raphé pontis nucleus; pr5DM, principal trigeminal sensory nucleus dorso-median; RMg, raphé magnus; ROb, raphé obscurus; scp, superior cerebella peduncle; SubC, subcoeruelus nucleus; 12r, intra-medullary rootlet of hypoglossal nerve. (A) AT8 immunoreactivity in the medulla of 5 month old Tau.P301L mice shows only a very few, weakly stained AT8+ neurons in the ventral Pre-BotzC area below the nA (A1), the ventral RTN/pFRG area below the n7 (A2), and the dorsal nTS area (A3). In terminal Tau.P301L mice; dark-brown stained AT8+ medullary neurons were frequent but not in the Pre-BotzC (A4), RTN/pFRG (A5), and nTS (A6) areas. Indeed, medullary respiratory-related area did not develop thauopathy in terminal Tau.P301L mice. B–AT8 immunoreactivity in the KF area shows almost no AT8+ neurons in 5 month old Tau.P301L mice (B1) but highly frequent, dark-brown stained AT8+ neurons in terminal Tau.P301L mice (A2). The dotted boxes in B1 and B2 show the 500 μm × 500 μm square area analyzed for measuring the AT8 optical density in the KF area, positioned ventral to the LPB, lateral to the scp, medial to the mcp, and dorsal to the pr5DM. (C) AT100 immunoreactivity in sections from terminal Tau.P301L mice reveals AT100+ neurons in pontine areas, especially the KF area (C2 is an enlargement of the dotted box in C1). Indeed, KF developed thauopathy in terminal Tau.P301L mice. AT100+ neurons were also found in the SubC, the PnO and the RMg but not the PnR. Scale bars: 200 μm in A1–A6 and B1 and B2; 500 μm in C1; 40 μm in C2.

altered 5-HT metabolism, and tauopathy in KF and raphé areas but not medullary respiratory-related areas. Breathing is strictly controlled by complex brainstem neural networks including at least three functional entities: (1) the RRG producing the rhythmic drive, (2) the central pattern generator (CPG) controlling the motor drive towards chest and upper airway muscles, and (3) the regulatory loops adapting the RRG and CPG drives to metabolic demands and behaviour. Given that the 5-HT system modulates the RRG, CPG and regulatory loops (Hilaire et al., 2010), we propose a causal link between raphé tauopathy, altered 5-HT metabolism, altered breathing and subsequently altered brain oxygenation in terminal Tau.P301L mice, and possibly in tauopathy and AD patients.

4.1. Raphé tauopathy, breathing and 5-HT defects in terminal Tau.P301L mice

AT8 is a pre-tangle marker of tauopathy, while AT100 is a typical pathological marker (Terwel et al., 2005, 2008; Braak and Del Tredici, 2011; Duyckaerts, 2011). AT8 immunoreaction in the brainstem of Tau.P301L mice is very weak at 4–5 months, but marked at 8 months, revealing diffuse brainstem tauopathy that specifically delineates specified structures such as the KF and the raphé nuclei (Dutschmann et al., 2010). At terminal stage, AT8 and AT100 are expressed in the same brainstem structures but do not specifically label the medullary respiratory-related areas. Consequently, the breathing defects of terminal Tau.P301L mice are unlikely to originate from direct tauopathy-associated alterations of intrinsic rhythmogenic mechanisms of the RRG, consistently with their normal Ti/Te ratio.

The raphé tauopathy concerned mainly non-5-HT neurons and some rare 5-HT neurons. Compelling evidence demonstrates that the raphé contains besides 5-HT neurons, numerous non-5-HT neurons that express distinct neurotransmitters, including dopamine, GABA and glutamate, modulating the activity of 5-HT raphé neurons (Monti, 2010a,b; Rice et al., 2009; Holmes et al., 1994). Both 5-HT and non-5-HT raphé neurons send axonal projections to the respiratory network and control breathing (Zanella et al., 2008; Rice et al., 2009). Tauopathy in non-5-HT raphé neurons therefore can indirectly affect the 5-HT system and breathing. In addition, tauopathy in GABAergic raphé neurons can directly affect gain modulation of respiratory neurons (Zuperku and McCrimmon, 2002). In Tau.P301L mice, biochemical and histological data correlate well with plethysmographic data, showing normal raphé, 5-HT metabolism and breathing at 4 months but altered raphé, 5-HT metabolism and breathing at terminal stages. Identifying the neurotransmitter phenotype of the numerous AT8+ but non-5-HT raphé neurons requires further experiments.

4.2. 5-HT defects and RRG activity in terminal Tau.P301L mice

The RRG is composed of two coupled, interacting networks, the pre-BötzC and the RTN/pFRG, and is modulated by endogenous 5-HT (Hilaire et al., 2010; Doi and Ramirez, 2010; Viemari and Tryba, 2009; Bou-Flores et al., 2000). Pharmacological reduction of the 5-HT facilitation of the RRG slows down its activity in neonates and almost stops it in fetuses (Di Pasquale et al., 1994). The RRG of mutant mice with genetically induced alterations of the 5-HT system produces an instable rhythmic drive (Bou-Flores et al., 2000; Zanella et al., 2008; Viemari et al., 2005). Finally, subjecting mice to 5-HT agents affects the RRG activity (Abdala et al., 2010; Real et al., 2009; Stettner et al., 2008; Burnet et al., 2001).

The transgenic Tau.P301L mice were produced on the FVB/N genetic background (Terwel et al., 2005, 2008). The genetic back-

Author's personal copy

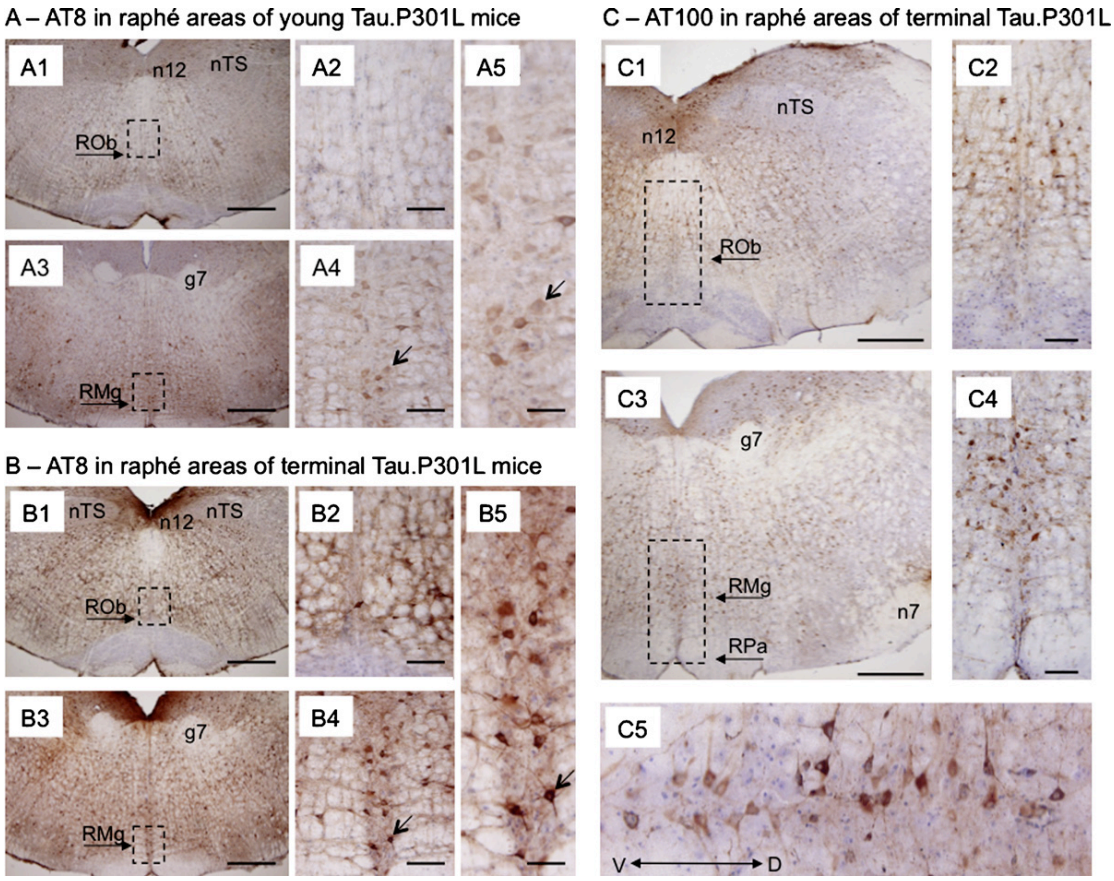

Fig. 6. AT8 and AT100 expression in midline raphé areas of young and terminal Tau.P301L mice. Medullary coronal sections in young (A) and terminal (B and C) Tau.P301L mice stained with AT8 (A and B) and AT100 (C). (A) AT8 immunoreactivity in sections passing through the rostral end of the n12 (A1) and the g7 (A3) of 5 month old Tau.P301L mice shows few, weakly stained AT8+ neurons in the ROb (A1) and RMg (A3) areas. A2 and A4 are enlargements of dotted boxes in A1 and A3, respectively. In A4 and A5 (double magnification of A4), note the arrow pointing to the same faintly stained neuron. (B) As above but for terminal Tau.P301L mice; note the frequent, dark-brown AT8+ neurons in the ROb (B1) and RMg (B3) areas. B2 and B4 are enlargements of dotted boxes in B1 and B3, respectively. In B4 and B5 (double magnification of B4), the arrow is pointing to the same dark-brown stained AT8+ neuron. In B5, note the numerous AT8 stained somata and arborisations. (C) AT100 immunoreactivity in sections passing through the rostral end of the n12 (C1) and the g7 (C3) of a terminal Tau.P301L mouse shows AT100+ neurons in the ROb (C1), RMg and RPa (C3) areas; note the lack of AT100+ neurons in the dorsal nTS area (C1) and the ventral medullary surface below n7 (C3). C2 and C4 are enlargements of dotted boxes in C1 and C3, respectively. (C5) AT100+ neurons in the ROb area of another terminal Tau.P301L mouse (ventral and dorsal sides at left- and right-hand, respectively). Scale bars, 500 μm for A1, A3, B1, B3, C1 and C3; 100 μm for A2, A4, B2, B4, C2 and C4; 50 μm for A5, B5 and C5 (double-head arrow).

ground can significantly affect the breathing phenotype and it is important to emphasize that the RRG of FVB/N mice produces a very robust drive (Menuet et al., 2011). Here, we report that the RRG of 8 month old Tau.P301L mice generates a fast and stable rhythm, similar to that of age-matched FVB/N mice. In contrast, a slow and instable rhythm becomes evident in terminal Tau.P301L mice, correlating with progressively increased phosphorylation of protein tau (Terwel et al., 2005, 2008). Given that AT8/AT100 immunoreactions remain weak in pre-BötzC and RTN/pFRG areas, the slow and instable rhythm of terminal mice is proposed not to originate from direct, tauopathy-induced RRG dysfunction but more likely from tauopathy-induced alteration of the 5-HT modulation of the RRG.

4.3. 5-HT defects and altered RRG regulations in terminal Tau.P301L mice

Regulatory loops adapt the RRG activity to CO_2/pH, O_2 and lung inflation levels. CO_2/pH changes are centrally detected by RTN/pFRG neurons (Onimaru et al., 2009; Guyenet et al., 2009). Lung inflation and hypoxemia are peripherally detected by pulmonary stretch receptors and carotid body chemoceptors, respectively, which synaptically target nTS relay neurons. The nTS integrates these regulatory inputs and adapts the activity of the RRG and the whole ventral respiratory column (Hayashi et al., 1996). The nTS contributes to the post-sigh bradypnoea: the sigh overactivates the pulmonary stretch receptors and improves alveolar oxygenation, which in turn induces bradypnoea via Hering-Breuer and chemosensory reflexes (Voituron et al., 2010a,b,c; Menuet et al., 2011).

All these respiratory regulations are modulated by 5-HT which affects the RRG responses to lung inflations (Burnet et al., 2001) and to CO_2/pH changes (Depuy et al., 2011; Corcoran et al., 2009; Bouyer et al., 2004; Voituron et al., 2010a,b,c; Penatti et al., 2011; Zanella et al., 2008). Given that tauopathy remains weak in the nTS and RTN/pFRG areas of terminal mice, direct tauopathy-induced dysfunctions of nTS and RTN/pFRG networks cannot explain the altered responses to hypercapnia and sighing whereas an altered 5-HT metabolism may contribute to these defects.

4.4. 5-HT defects and altered CPG function in terminal Tau.P301L mice

The respiratory CPG is a complex network extending within the whole brainstem that adjusts and co-ordinates the activity of chest

Author's personal copy

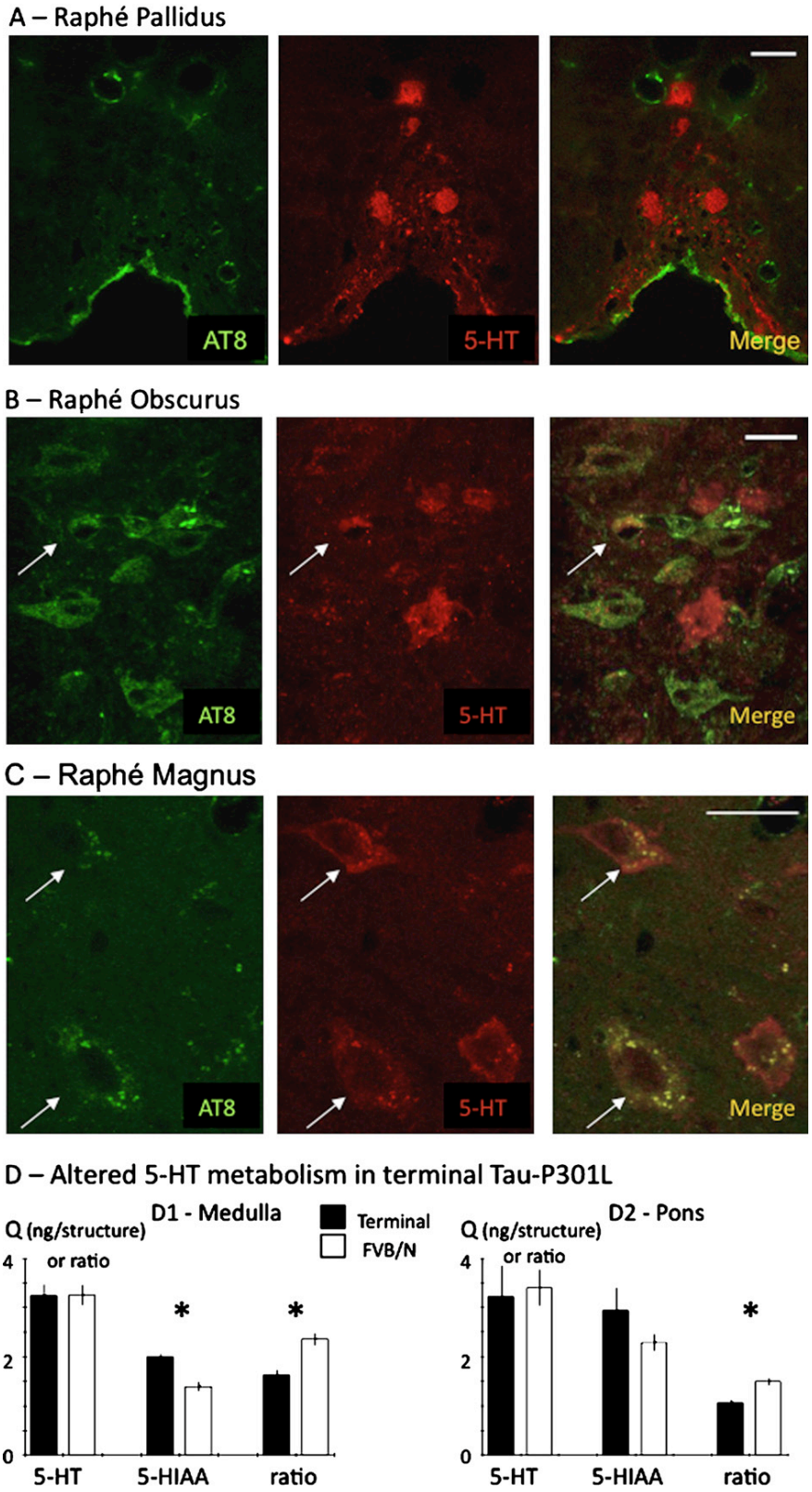

Fig. 7. Raphé AT8 expression and 5-HT system of terminal Tau.P301L mice. (A–C) Confocal analysis of RPa (A) and RMg (B and C) nuclei of terminal Tau.P301L mice reveal that most of the numerous AT8+ raphé neurons are non-5-HT neurons. White arrows indicate a few raphé neurons that contain 5-HT (red), are AT8+ (green) and appear yellow when colours are merged. Scale bars: 20 μm. (D) Histograms show mean (and SEM) contents of 5-HT and 5-HIAA and the ratio 5-HT/5-HIAA (measured by HPLC and electrochemical detection and expressed in ng per structure) in medulla (D1) and pons (D2) of terminal Tau.P301L ($n = 7$) and age-matched FVB/N ($n = 8$) mice (black and white columns, respectively). Note that the 5-HT contents are similar in both groups whereas the 5-HIAA contents are higher in terminal Tau.P301L than FVB/N mice, leading to significantly (*) different 5-HT/5-HIAA ratio. (For interpretation of the references to color in this figure caption, the reader is referred to the web version of the article.)

Author's personal copy

and upper airway motoneurons. Within the CPG, the KF is essentially involved in the control of laryngeal adductor activity as the major determinant of upper airway patency and airflow resistance (Dutschmann and Herbert, 2006). The laryngeal adductor activity controlled by the KF is also crucially linking breathing and swallowing (Bianchi and Gestreau, 2009; Rybak et al., 2007; Gestreau et al., 2005; Bonis et al., 2011). The severe KF tauopathy correlates well with upper airway dysfunction in 8 month old (Dutschmann et al., 2010) and terminal Tau.P301L mice (present results). As aging Tau.P301L mice must produce ever larger respiratory chest movements to ventilate, the increased respiratory work-load and the high metabolic demands of such abnormal breathing may contribute to their severe and rapid wasting and body-weight loss (Dutschmann et al., 2010). In terminal Tau.P301L mice, the upper airway dysfunction is aggravated, with weaker ASp/CSp ratio and weaker correlation between CSp and ASp. The further reduced efficiency of chest respiratory movements to induce adequate ventilation may be associated with altered 5-HT metabolism. Indeed, the KF and raphé nuclei are interconnected and 5-HT differentially affects the chest and upper airway motor systems (Besnard et al., in press). It is noteworthy that old Tau.P301L mice despite upper airway dysfunction do not produce total obstructive apnoeas as those reported in Mecp2-deficient mice, which produce persisting chest movements against totally closed upper airways (Voituron et al., 2010a,b,c). This may reflect differences in the 5-HT system of FVB/N and C57BL/6 genetic backgrounds used for producing these two mutants (Menuet et al., 2011).

4.5. 5-HT anomalies in terminal Tau.P301L mice and AD patients

Terminal Tau.P301L mice suffer upper airway and breathing dysfunctions that originate, at least in part, from altered 5-HT metabolism. Tauopathy and AD patients, besides their cognitive problems, suffer severe functional problems including, but not limited to swallowing impairment, sleep-disordered breathing and typical 5-HT dependent defects. In AD patients, post-mortem studies show increased AT8 expression and cytoskeletal pathology in raphé areas (Rüb et al., 2000), abnormal 5HT and 5HIAA brain content (Storga et al., 1996; Gottfries, 1990), altered expression of 5-HT synthesizing enzymes (Sawada et al., 1987) and altered 5HT/5HIAA ratio (Arai et al., 1984). Abnormal density of 5-HT receptor positive cells (Yeung et al., 2010), decreased number of neurons synthesizing 5HT (Kovacs et al., 2003) and loss of 5HT transporter (Mössner et al., 2000) have been also reported. Genetically, AD psychotic symptoms may be associated with polymorphisms in the 5-HT2A receptor (Ramanathan and Glatt, 2009; Rocchi et al., 2003). Finally, among the plethora of candidate drugs for AD, several 5-HT receptor antagonists and agonists have been suggested (Geldenhuys and Van der Schyf, 2009; Tabira, 2010; Martorana et al., 2010), which is consistent with the 5-HT role in mood, cognition, sleep (Monti, 2010a), sleep apnoeas (Real et al., 2009), upper airway patency (Besnard et al., in press) and swallowing (Sessle and Henry, 1989; Hashim and Bieger, 1987).

We conclude that oro-pharyngeal and breathing dysfunctions correlate well with raphé tauopathy and altered 5-HT system. Tauopathy in the raphé nuclei of AD patients is well documented and therefore the present results in Tau.P301L mice may translate to further understanding of human pathology in neurodegeneration.

Acknowledgments

The authors thank the support of the Centre National de la Recherche Scientifique, the Université Paul Cézanne and the Université de la Méditerranée (Unité Mixte de Recherche 6231), Eugeen Vanmechelen (Innogenetics, Gent) for generous gifts of antibodies. PB, LG, FVL acknowledge support by Fonds Wetenschappelijk Onderzoek-Vlaanderen (FWO-Vlaanderen), Instituut voor Wetenschap en Techniek (IWT), KULeuven-Research Fund (BOF), KULeuven-Research & Development and EEC Framework programs FP6 & FP7. MD was supported by NHLBI (Cluster Grant R33HL087377).

References

Abdala, A.P., Dutschmann, M., Bissonnette, J.M., Paton, J.F., 2010. Correction of respiratory disorders in a mouse model of Rett syndrome. Proc. Natl. Acad. Sci. U.S.A. 107, 18208–18213.

Ancoli-Israel, S., Palmer, B.W., Cooke, J.R., Corey-Bloom, J., Fiorentino, L., Natarajan, L., Liu, L., Ayalon, L., He, F., Loredo, J.S., 2008. Cognitive effects of treating obstructive sleep apnea in Alzheimer's disease: a randomized controlled study. J. Am. Geriatr. Soc. 56 (11), 2076–2081.

Arai, H., Kosaka, K., Iizuka, R., 1984. Changes of biogenic amines and their metabolites in postmortem brains from patients with Alzheimer-type dementia. J. Neurochem. 43 (2), 388–393.

Attems, J., König, C., Huber, M., Lintner, F., Jellinger, K.A., 2005. Cause of death in demented and non-demented elderly inpatients; an autopsy study of 308 cases. J. Alzheimers Dis. 8 (1), 57–62.

Besnard, S., Khemiri, H., Masse, F., Denise, P., Verdaguer, M., Gestreau, C. Differential respiratory control of the upper airway and diaphragm muscles induced by 5-HT1A receptor ligands. Sleep Breath, in press.

Bianchi, A.L., Gestreau, C., 2009. The brainstem respiratory network: an overview of a half century of research. Respir. Physiol. Neurobiol. 168 (1–2), 4–12.

Bonis, J.M., Neumueller, S.E., Marshall, B.D., Krause, K.L., Qian, B., Pan, L.G., Hodges, M.R., Forster, H.V., 2011. The effects of lesions in the dorsolateral pons on the coordination of swallowing and breathing in awake goats. Respir. Physiol. Neurobiol. 175 (2), 272–282.

Bou-Flores, C., Lajard, A.-M., Monteau, R., De Maeyer, E., Seif, I., Lanoir, J., Hilaire, G., 2000. Abnormal phrenic motoneuron activity and morphology in neonatal monoamine oxidase A-deficient transgenic mice: possible role of a serotonin excess. J. Neurosci. 20, 4646–4656.

Bouyer, P., Bradley, S.R., Zhao, J., Wang, W., Richerson, G.B., Boron, W.F., 2004. Effect of extracellular acid–base disturbances on the intracellular pH of neurones cultured from rat medullary raphé or hippocampus. J. Physiol. 559 (1), 85–101.

Burnet, H., Bevengut, M., Chakri, F., Bou-Flores, C., Coulon, P., Gaytan, S., Pasaro, R., Hilaire, G., 2001. Altered respiratory activity and respiratory regulations in adult monoamine oxidase A-deficient mice. J. Neurosci. 21 (14), 5212–5221.

Burns, J.M., Cronk, B.B., Anderson, H.S., Donnelly, J.E., Thomas, G.P., Harsha, A., Brooks, W.M., Swerdlow, R.H., 2008. Cardiorespiratory fitness and brain atrophy in early Alzheimer disease. Neurology 71 (3), 210–216.

Braak, H., Del Tredici, K., 2011. The pathological process underlying Alzheimer's disease in individuals under thirty. Acta Neuropathol. 121 (2), 171–181.

Chong, M.S., Ayalon, L., Marler, M., Loredo, J.S., Corey-Bloom, J., Palmer, B.W., Liu, L., Ancoli-Israel, S., 2006. Continuous positive airway pressure reduces subjective daytime sleepiness in patients with mild to moderate Alzheimer's disease with sleep disordered breathing. J. Am. Geriatr. Soc. 54 (5), 777–781.

Cooke, J.R., Ayalon, L., Palmer, B.W., Loredo, J.S., Corey-Bloom, J., Natarajan, L., Liu, L., Ancoli-Israel, S., 2009. Sustained use of CPAP slows deterioration of cognition, sleep, and mood in patients with Alzheimer's disease and obstructive sleep apnea: a preliminary study. J. Clin. Sleep. Med. 5 (4), 305–309.

Cooke, J.R., Liu, L., Natarajan, L., He, F., Marler, M., Loredo, J.S., Corey-Bloom, J., Palmer, B.W., Greenfield, D., Ancoli-Israel, S., 2006. The effect of sleep-disordered breathing on stages of sleep in patients with Alzheimer's disease. Behav. Sleep Med. 4 (4), 219–227.

Corcoran, A.E., Hodges, M.R., Wu, Y., Wang, W., Wylie, C.J., Deneris, E.S., Richerson, G.B., 2009. Medullary serotonin neurons and central CO_2 chemoreception. Respir. Physiol. Neurobiol. 168 (1–2), 49–58.

Daulatzai, M.A., 2010. Early stages of pathogenesis in memory impairment during normal senescence and Alzheimer's disease. J. Alzheimers Dis. 20 (2), 355–367.

Depuy, S.D., Kanbar, R., Coates, M.B., Stornetta, R.L., Guyenet, P.G., 2011. Control of breathing by raphé obscurus serotonergic neurons in mice. J. Neurosci. 31 (6), 1981–1990.

Di Pasquale, E., Monteau, R., Hilaire, G., 1994. Endogenous serotonin modulates the fetal respiratory rhythm: an in vitro study in the rat. Brain Res. Dev. Brain Res. 80 (1–2), 222–232.

Doi, A., Ramirez, J.M., 2010. State-dependent interactions between excitatory neuromodulators in the neuronal control of breathing. J. Neurosci. 30 (24), 8251–8262.

Dutschmann, M., Herbert, H., 2006. The Kölliker-Fuse nucleus gates the postinspiratory phase of the respiratory cycle to control inspiratory off-switch and upper airway resistance in rat. Eur. J. Neurosci. 24 (4), 1071–1084.

Dutschmann, M., Menuet, C., Stettner, G.M., Gestreau, C., Borghgraef, P., Devijver, H., Gielis, L., Hilaire, G., Van Leuven, F., 2010. Upper airway dysfunction of Tau.P301L mice correlates with tauopathy in midbrain and ponto-medullary brainstem nuclei. J. Neurosci. 30 (5), 1810–1821.

Duyckaerts, C., 2011. Tau pathology in children and young adults: can you still be unconditionally baptist? Acta Neuropathol. 121 (2), 145–147.

Feldman, J.L., 2011. Looking forward to breathing. Prog. Brain Res. 188, 213–218.

Author's personal copy

Fortin, G., Thoby-Brisson, M., 2009. Embryonic emergence of the respiratory rhythm generator. Respir. Physiol. Neurobiol. 168 (1–2), 86–91.
Geldenhuys, W.J., Van der Schyf, C.J., 2009. The serotonin 5-HT6 receptor: a viable drug target for treating cognitive deficits in Alzheimer's disease. Expert Rev. Neurother. 9 (7), 1073–1085.
Gestreau, C., Dutschmann, M., Obled, S., Bianchi, A.L., 2005. Activation of XII motoneurons and premotor neurons during various oropharyngeal behaviors. Respir. Physiol. Neurobiol. 147 (2–3), 159–176.
Gottfries, C.G., 1990. Disturbance of the 5-hydroxytryptamine metabolism in brains from patients with Alzheimer's dementia. J. Neural Transm. Suppl. 30, 33–43.
Guo, X., Waern, M., Sjögren, K., Lissner, L., Bengtsson, C., Björkelund, C., Ostling, S., Gustafson, D., Skoog, I., 2007. Midlife respiratory function and Incidence of Alzheimer's disease: a 29-year longitudinal study in women. Neurobiol. Aging 28 (3), 343–350.
Guyenet, P.G., Bayliss, D.A., Stornetta, R.L., Fortuna, M.G., Abbott, S.B., DePuy, S.D., 2009. Retrotrapezoid nucleus, respiratory chemosensitivity and breathing automaticity. Respir. Physiol. Neurobiol. 168 (1–2), 59–68.
Hashim, M.A., Bieger, D., 1987. Excitatory action of 5-HT on deglutitive substrates in the rat solitary complex. Brain Res. Bull. 18 (3), 355–363.
Hayashi, F., Coles, S.K., McCrimmon, D.R., 1996. Respiratory neurons mediating the Breuer-Hering reflex prolongation of expiration in rat. J. Neurosci. 16 (20), 6526–6536.
Hilaire, G., Voituron, N., Menuet, C., Ichiyama, R.M., Subramanian, H.H., Dutschmann, M., 2010. The role of serotonin in respiratory function and dysfunction. Respir. Physiol. Neurobiol. 174 (1–2), 76–88.
Holmes, C.J., Mainville, L.S., Jones, B.E., 1994. Distribution of cholinergic, GABAergic and serotonergic neurons in the medial medullary reticular formation and their projections studied by cytotoxic lesions in the cat. Neuroscience 62 (4), 1155–1178.
Humbert, I.A., McLaren, D.G., Kosmatka, K., Fitzgerald, M., Johnson, S., Porcaro, E., Kays, S., Umoh, E.O., Robbins, J., 2010. Early deficits in cortical control of swallowing in Alzheimer's disease. J. Alzheimers Dis. 19 (4), 1185–1197.
Katz, D.M., Dutschmann, M., Ramirez, J.M., Hilaire, G., 2009. Breathing disorders in Rett syndrome: progressive neurochemical dysfunction in the respiratory network after birth. Respir. Physiol. Neurobiol. 168 (1–2), 101–108.
Kovacs, G.G., Klöppel, S., Fischer, I., Dorner, S., Lindeck-Pozza, E., Birner, P., Bötefür, I.C., Pilz, P., Volk, B., Budka, H., 2003. Nucleus-specific alteration of raphé neurons in human neurodegenerative disorders. Neuroreport 14 (1), 73–76.
Martorana, A., Esposito, Z., Koch, G., 2010. Beyond the cholinergic hypothesis: do current drugs work in Alzheimer's disease? CNS Neurosci. Ther. 16 (4), 235–245.
Menuet, C., Kourdougli, N., Hilaire, G., Voituron, N., 2011. Differences in serotoninergic metabolism possibly contribute to differences in breathing phenotype of FVB/N and C57BL/6J mice. J. Appl. Physiol. 110 (6), 1572–1581.
Monti, J.M., 2010a. The role of dorsal raphé nucleus serotonergic and non-serotonergic neurons, and of their receptors, in regulating waking and rapid eye movement (REM) sleep. Sleep Med. Rev. 14 (5), 319–327.
Monti, J.M., 2010b. The structure of the dorsal raphé nucleus and its relevance to the regulation of sleep and wakefulness. Sleep Med. Rev. 14 (5), 307–317.
Mössner, R., Schmitt, A., Syagailo, Y., Gerlach, M., Riederer, P., Lesch, K.P., 2000. The serotonin transporter in Alzheimer's and Parkinson's disease. J. Neural Transm. Suppl. 60, 345–350.
Muyllaert, D., Terwel, D., Borghgraef, P., Devijver, H., Dewachter, I., Van Leuven, F., 2006. Transgenic mouse models for Alzheimer's disease: the role of GSK-3B in combined amyloid and Tau.pathology. Rev. Neurol. (Paris) 162 (10), 903–907.
Onen, F., Onen, H., 2010. Obstructive sleep apnea and cognitive impairment in the elderly. Psychol. Neuropsychiatr. Vieil. 8 (3), 163–169.
Onimaru, H., Ikeda, K., Kawakami, K., 2009. Phox2b, RTN/pFRG neurons and respiratory rhythmogenesis. Respir. Physiol. Neurobiol. 168 (1–2), 13–18.
Parvizi, J., Van Hoesen, G.W., Damasio, A., 2001. The selective vulnerability of brainstem nuclei to Alzheimer's disease. Ann. Neurol. 49 (1), 53–66.
Paxinos, G., Franklin, K.B., 2001. The Mouse Brain in Stereotaxic Coordinates, 2nd edition. Academic Press, San Diego, CA.
Penatti, E.M., Barina, A.E., Raju, S., Li, A., Kinney, H.C., Commons, K.G., Nattie, E.E., 2011. Maternal dietary tryptophan deficiency alters cardiorespiratory control in rat pups. J. Appl. Physiol. 110, 318–328.
Priefer, B.A., Robbins, J., 1997. Eating changes in mild-stage Alzheimer's disease: a pilot study. Dysphagia 12 (4), 212–221.
Ramanathan, S., Glatt, S.J., 2009. Serotonergic system genes in psychosis of Alzheimer dementia: meta-analysis. Am. J. Geriatr. Psychiatry 17 (10), 839–846.
Real, C., Seif, I., Adrien, J., Escourrou, P., 2009. Ondansetron and fluoxetine reduce sleep apnea in mice lacking monoamine oxidase A. Respir. Physiol. Neurobiol. 168, 230–238.
Rice, C.D., Lois, J.H., Kerman, I.A., Yates, B.J., 2009. Localization of serotoninergic neurons that participate in regulating diaphragm activity in the cat. Brain Res. 1279, 71–81.
Rocchi, A., Micheli, D., Ceravolo, R., Manca, M.L., Tognoni, G., Siciliano, G., Murri, L., 2003. Serotoninergic polymorphisms (5-HTTLPR and 5-HT2A): association studies with psychosis in Alzheimer disease. Genet. Test. 7 (4), 309–314.
Rüb, U., Del Tredici, K., Schultz, C., Thal, D.R., Braak, E., Braak, H., 2000. The evolution of Alzheimer's disease-related cytoskeletal pathology in the human raphé nuclei. Neuropathol. Appl. Neurobiol. 26 (6), 553–567.
Rybak, I.A., Abdala, A.P., Markin, S.N., Paton, J.F., Smith, J.C., 2007. Spatial organization and state-dependent mechanisms for respiratory rhythm and pattern generation. Prog. Brain Res. 165, 201–220.
Sawada, M., Hirata, Y., Arai, H., Iizuka, R., Nagatsu, T., 1987. Tyrosine hydroxylase, tryptophan hydroxylase, biopterin, and neopterin in the brains of normal controls and patients with senile dementia of Alzheimer type. J. Neurochem. 48 (3), 760–764.
Sessle, B.J., Henry, J.L., 1989. Neural mechanisms of swallowing: neurophysiological and neurochemical studies on brain stem neurons in the solitary tract region. Dysphagia 4 (2), 61–75.
Simic, G., Stanic, G., Mladinov, M., Jovanov-Milosevic, N., Kostovic, I., Hof, P.R., 2009. Does Alzheimer's disease begin in the brainstem? Neuropathol. Appl. Neurobiol. 35 (6), 532–554.
Stettner, G.M., Zanella, S., Hilaire, G., Dutschmann, M., 2008. 8-OH-DPAT suppresses spontaneous central apneas in the C57BL/6J mouse strain. Respir. Physiol. Neurobiol. 161, 10–15.
Storga, D., Vrecko, K., Birkmayer, J.G., Reibnegger, G., 1996. Monoaminergic neurotransmitters, their precursors and metabolites in brains of Alzheimer patients. Neurosci. Lett. 203 (1), 29–32.
Suh, M.K., Kim, H., Na, D.L., 2009. Dysphagia in patients with dementia: Alzheimer versus vascular. Alzheimer Dis. Assoc. Disord. 23 (2), 178–184.
Tabira, T., 2010. Development of new drugs for Alzheimer's disease. Brain Nerve 62 (7), 787–796.
Terwel, D., Lasrado, R., Snauwaert, J., Vandeweert, E., Van Haesendonck, C., Borghgraef, P., Van Leuven, F., 2005. Changed conformation of mutant Tau.P301L mice underlies the moribund tauopathy, absent in progressive, nonlethal axonopathy of Tau.4R/2N transgenic mice. J. Biol. Chem. 280, 3963–3973.
Terwel, D., Muyllaert, D., Dewachter, I., Borghgraef, P., Croes, S., Devijver, H., Van Leuven, F., 2008. Mutant APP and GSK-3beta aggravate tauopathy similarly in cortex and hippocampus of tau bigenic mice. Am. J. Pathol. 172, 786–798.
Viemari, J.C., Roux, J.C., Tryba, A.K., Saywell, V., Burnet, H., Peña, F., Zanella, S., Bévengut, M., Barthelemy-Requin, M., Herzing, L.B., Moncla, A., Mancini, J., Ramirez, J.M., Villard, L., Hilaire, G., 2005. Mecp2 deficiency disrupts norepinephrine and respiratory systems in mice. J. Neurosci. 25 (50), 11521–11530.
Viemari, J.C., Tryba, A.K., 2009. Bioaminergic neuromodulation of respiratory rhythm in vitro. Respir. Physiol. Neurobiol. 168 (1–2), 69–75.
Voituron, N., Menuet, C., Dutschmann, M., Hilaire, G., 2010a. Physiological definition of upper airway obstructions in mouse model for Rett syndrome. Respir. Physiol. Neurobiol. 173 (2), 146–156.
Voituron, N., Shvarev, Y., Menuet, C., Bevengut, M., Fasano, C., Vigneault, E., El Mestikawy, S., Hilaire, G., 2010b. Fluoxetine treatment abolishes the in vitro respiratory response to acidosis in neonatal mice. PLoS One 5 (10), e13644.
Voituron, N., Zanella, S., Menuet, C., Dutschmann, M., Hilaire, G., 2009. Early breathing defects after moderate hypoxia or hypercapnia in a mouse model of Rett syndrome. Respir. Physiol. Neurobiol. 168 (1–2), 109–118.
Voituron, N., Zanella, S., Menuet, C., Lajard, A.M., Dutschmann, M., Hilaire, G., 2010c. Early abnormalities of post-sigh breathing in a mouse model of Rett syndrome. Respir. Physiol. Neurobiol. 170 (2), 173–182.
Wittmeier, S., Song, G., Duffin, J., Poon, C.S., 2008. Pacemakers handshake synchronization mechanism of mammalian respiratory rhythmogenesis. Proc. Natl. Acad. Sci. U.S.A. 105, 18000–18005.
Yeung, L.Y., Kung, H.F., Yew, D.T., 2010. Localization of 5-HT1A and 5-HT2A positive cells in the brainstems of control age-matched and Alzheimer individuals. Age (Dordr) 32 (4), 483–495.
Zanella, S., Watrin, F., Mebarek, S., Marly, F., Roussel, M., Gire, C., Diene, G., Tauber, M., Muscatelli, F., Hilaire, G., 2008. Necdin plays a role in the serotonergic modulation of the mouse respiratory network: implication for Prader-Willi syndrome. J. Neurosci. 28 (7), 1745–1755.
Zuperku, E.J., McCrimmon, D.R., 2002. Gain modulation of respiratory neurons. Respir. Physiol. Neurobiol. 131 (1–2), 121–133.

3 - Altérations liées à l'âge de la vocalisation ultrasonore des souris Tau-P301L : implication potentielle pour les troubles progressifs du langage

Menuet C.*, Cazals Y.*, Gestreau C., Borghgraef P., Gielis L., Dutschmann M., Van Leuven F. & Hilaire G.
*Ces auteurs ont contribué de manière égale au travail.
Accepté dans *Plos One*.

Résumé en français :

Les tauopathies, incluant la maladie d'Alzheimer, sont les maladies neurodégénératives les plus fréquentes chez les personnes âgées, et causent des déficits cognitifs, comportementaux et moteurs variés, mais également des troubles progressifs du langage. Pour la communication et les interactions sociales, les souris produisent des vocalisations ultrasonores (USV) *via* leur flux aérien expiratoire à travers le larynx. Nous avons examiné les USV des souris Tau-P301L, un modèle murin de tauopathie qui exprime une isoforme humaine de protéine tau mutée et développe des déficits cognitifs, moteurs et des voies aériennes supérieures. A l'âge de 4-5 mois, les souris Tau-P301L présentaient des USV et un flux expiratoire normaux, et pas de tauopathie dans le tronc cérébral. A l'âge de 8-10 mois, les souris Tau-P301L présentaient une altération des USV, un flux expiratoire réduit et une tauopathie sévère dans la substance grise périaqueducale, dans le noyau de Kölliker-Fuse et dans le noyau rétroambigu. La tauopathie dans ces noyaux qui contrôlent les voies aériennes supérieures et la vocalisation corrèle avec l'altération des USV chez les souris Tau-P301L âgées. Cette altération liée à l'âge de la vocalisation des souris Tau-P301L pourrait rappeler les troubles progressifs du langage des personnes âgées souffrant de tauopathie, et pourrait nous aider dans la compréhension de l'impact des maladies neurodégénératives sur cette faculté propre à l'Homme qu'est le langage.

*Manuscript
Click here to download Manuscript: Final Version USV 30.06.2011.doc

Title:

Age-related impairment of ultrasonic vocalization in Tau.P301L mice: possible implication for progressive language disorders

Authors:

Clément MENUET[1,*], Yves CAZALS[2,*], Christian GESTREAU[1], Peter BORGHGRAEF[3], Lies GIELIS[3], Mathias DUTSCHMANN[4], Fred VAN LEUVEN[3] and Gérard HILAIRE[1,§]

Affiliations:

[1], Maturation, Plasticity, Physiology and Pathology of Respiration (MP3-Respiration), Unité Mixte de Recherche (UMR) 6231, Centre National de la Recherche Scientifique, Université de la Méditerranée, Université Paul Cézanne, Faculté Saint Jérôme (Service 362) 13397 Marseille Cedex 20, France.

[2], Neurovegetative physiology laboratory, Unité Mixte de Recherche (UMR) 6231, Centre National de la Recherche Scientifique, Université de la Méditerranée, Université Paul Cézanne, Faculté Saint Jérôme (Service 362) 13397 Marseille Cedex 20, France.

[3], Experimental Genetics Group, LEGTEGG, Department of Human Genetics, Katholieke Universiteit Leuven, B-3000 Leuven, Belgium

[4], Institute of Membrane and Systems Biology Garstang Building, University of Leeds, Leeds LS2 9JT, United Kingdom

*, both authors equally contributed to the work

Running title: Vocalization disorders in Tau.P301L mice

Keywords: Tauopathy; vocalization; upper airway; Alzheimer disease; neurodegenerative diseases; progressive language disorders; speech; periaqueductal gray; Kolliker-Fuse; retroambiguus; aging; mice

§, *Corresponding author:* Gérard Hilaire, Mp3-respiration team, CRN2M, UMR 6231, CNRS - Université Aix-Marseille II & III, Faculté Saint Jérôme, Service 362, 13397 Marseille Cedex 20, France. Email address: gerard.hilaire@univ-cezanne.fr

Tel: (+33) 491 28 81 72 - Fax (+33) 491 28 83 97 -

Abstract

Background: Tauopathies, including Alzheimer Disease are the most frequent neurodegenerative diseases in elderly people and cause various cognitive, behavioural and motor defects, but also progressive language disorders. For communication and social interactions, mice produce ultrasonic vocalization (USV) via expiratory airflow through the larynx. We examined USV of Tau.P301L mice, a mouse model for tauopathy expressing human mutant tau protein and developing cognitive, motor and upper airway defects.

Methodology/Principal Findings: At age 4-5 months, Tau.P301L mice had normal USV, normal expiratory airflow and no brainstem tauopathy. At age 8-10 months, Tau.P301L mice presented impaired USV, reduced expiratory airflow and severe tauopathy in the periaqueductal gray, Kolliker-Fuse and retroambiguus nuclei. Tauopathy in these nuclei that control upper airway function and vocalization correlates well with the USV impairment of old Tau.P301L mice.

Conclusions: The age-related vocalization impairment of Tau.P301L mice could be reminiscent of progressive language disorders of elderly suffering tauopathy, and might help us to understand the impact of neurodegenerative diseases on the most human faculty of speech and language.

Introduction

Tauopathies, including Alzheimer's disease (AD), are the most prevalent neurodegenerative disorders in elderly people and are characterized by defective learning and memory, besides other cognitive and behavioural symptoms. Tauopathies are accompanied by problems with swallowing, breathing and language. Swallowing disorders, with aspiration of foreign objects often result in pneumonia, a major cause of death in AD [1-3]. Sleep-disordered breathing, with obstructive apnoeas and subsequent hypoxic events possibly contributes to altered brain oxygenation and function in AD [4-8]. Problems with speech and language also develop during AD and in many other neurodegenerative diseases [9-13]. Although clinical and neuroanatomical correlates of progressive language disorders are not well understood, they are often associated with tauopathy-induced alterations of synaptic processes in forebrain networks [10,11,13-16].

Herein we examined vocalization in transgenic Tau.P301L mice, a validated mouse model of tauopathy, produced in the FVB/N genetic background and with specific expression of the human mutant Tau.P301L protein in neurons [17]. From 7-8 months onwards, Tau.P301L mice develop brain tauopathy, cognitive and motor disorders, but also upper airway dysfunction and thereafter breathing defects leading to premature death at 10-12 months [17-20]. For communication and social interactions, mice use ultrasonic vocalization (USV) produced by expiratory airflow through the larynx [21-23]. Different USV patterns, possibly representing different lexicons, behaviours or innate variations in vocal repertoires have been reported in genetically distinct mouse strains [21-26]. We report here for the first time a drastic age-related impairment of USV in transgenic Tau.P301L mice that correlates well with their upper airway dysfunction, reduced expiratory airflow and tauopathy in midbrain and brainstem areas controlling vocalization. Tau.P301L mice present as a promising mouse model for progressive language disorders in patients suffering tauopathies.

Ethics Statement:

The experiments were performed on adult mice housed with food and water *ad libitum,* and in accordance with French national legislation (JO 87-848) and European Communities Council Directive (22 September 2010, 2010/63/EU, 74). Permit numbers A13-505, 13-47 and 13-227 were delivered to C. Menuet, Y. Cazals and C. Gestreau, respectively, by the Direction Départementale de la Protection des Populations, Préfecture des Bouches du Rhône, France. The procedures for genetic analysis, plethysmography and histology were already reported in detail [17-20].

Animals

Transgenic Tau.P301L mice were produced in the FVB/N genetic background [17,18]. They expressed the longest human tau isoform bearing the P301L mutation (Tau.4R/2N-P301L) under control of the mouse thy1 gene promoter aiming for neuron-specific expression starting in the third postnatal week. Homozygous Tau.P301L mice, genotyped by PCR and qPCR, were compared with age- and sex-matched wild-type FVB/N mice as controls. Mice were studied at two different ages: at 4-5 months because that is pathologically pre-symptomatic and at age 8-10 months, which is in the pathological phase with progressive motor defects, clasping, brain tauopathy, loss of body-weight and breathing defects [17,19].

USV recordings

USV recordings were performed in a custom-build, double-walled concrete acoustic chamber. Conscious, unrestrained mice were placed in clean rectangular polyethylene cages (29x18x12.5 cm) covered by a metal wire lid. A free field microphone (type 4191, Bruel & Kjaer, Denmark) was placed 2 cm above the metal lid, in the centre of the cage. The microphone signal was sampled through audio chip (SoundMax Integrated HD) and dedicated software (Adobe Audition 1.5) at a rate of 192 kHz allowing the recording of the frequency range 10 to 90 kHz, corresponding to the USV range of adult mice [22,27].

The experimental paradigm consisted in placing three mice of the same age and genotype into the recording cage. Each group of three mice consisted of one male and two females that had no interactions prior to the recording session, and was considered as n=1 (Table 1). Recordings lasted 6 minutes and data were stored and analysed off line in a blind manner. The detection of USV was performed visually using a custom program (MATLAB based) with a spectrographic display and plotting USV as frequencies (kHz) vs. time (Fig. 1A1). Using a graphic pointer on the spectrograms, each USV emission was tagged at its beginning and its end, and also at each slope change to mark its different frequency glide segments (Fig. 1A2). Based on these coordinates (Time/Frequency), different USV parameters were calculated: 1) the duration of USV ($Dur_{(USV)}$, expressed in ms), 2) the number of USV produced per second of recording ($Nb_{(USV)}$), 3) the mean frequency at all tags within the USV ($Freq_{(USV)}$, expressed in kHz), 4) the $Freq_{(USV)}$ range within the USV (RangeFreq, expressed in kHz), i.e. the difference between max $Freq_{(USV)}$ and min $Freq_{(USV)}$ between tags, and 5) the complexity, i.e., the number of segments composing the USV (ranging from 1 to 5 for low and high complexity, respectively). The total time of USV emission ($totT_{(USV)}$, expressed in s per minute of recording) was obtained by summation of individual $Dur_{(USV)}$ and the distribution of $totT_{(USV)}$ vs. $Freq_{(USV)}$ was analyzed. Visual observations of behavioural responses of Tau.P301L mice to noise and odours did not reveal any obvious alterations in hearing and smelling compared to wild-type FVB/N mice.

Double-chamber plethysmography

We used constant flow, double-chamber plethysmography to examine breathing parameters and upper airway function of young (4-5 months) and old (8-10 months) conscious mice [19,20]. We simultaneously recorded the chest respiratory movements in the body chamber (Chest Spirogram, CSp) and the resulting airflow in the head chamber (Airflow Spirogram, ASp) (Fig. 3A). Small air volumes were injected within the head chamber and body chamber for checking proper sealing of chambers and for calibration purposes. To minimize stress, the mice were habituated to the plethysmograph chamber before the recording sessions. Spirograms were recorded, stored and analyzed afterwards, using only periods with stable breathing frequency. We calculated the ASp/CSp ratio; a reduced ASp vs. an increased CSp resulting in ratio < 1 was considered as

indicative of upper airway dysfunction impairing the chest respiratory movement to produce adequate airflow [19,20]. After averaging of about 100 respiratory cycles, we measured the mean expiratory airflow (expressed in µl per g per second, µL/g/s). We also measured the mean respiratory frequency (expressed in cycles per min) and the duration of inspiratory and expiratory periods (expressed in ms).

Immunohistochemistry

After anaesthesia (Nembutal; 120 mg/kg, i.p.) and transcardiac perfusion (ice-cold saline 5 ml/min, 8 min; paraformaldehyde 2 ml/min, 10 min), brain and brainstems were removed, post fixed overnight (4% paraformaldehyde), and stored (0.1% sodium azide in PBS at 4°C) until sectioning (40 µm coronal vibratome sections). Briefly, the following procedures were performed [17-20]: rinsing (PBS; 15 min with 1.5% H2O2 in 50% methanol/PBS), blockade of non-specific binding sites (10% fetal calf serum, 0.1% Triton X-100 in PBS), incubation with primary monoclonal antibodies AT8 (mouse anti-AT8, 1/2500) or AT100 (mouse anti-AT100, 1/1400), 1h incubation with the secondary goat antimouse IgG antiserum coupled to PAP (1:500 in blocking buffer; Dako), 5 min incubation in 50mM Tris HCl, pH 7.6, enzymatic staining with 3,3' -diaminobenzidine (0.5 mg/ml), 0.3%H2O2 in 50 mM Tris HCl, pH 7.6. Sections were counterstained with hematoxylin, ethanol dehydrated, delipidated in xylol and mounted for microscopic analysis of AT8 and AT100 immunoreactivity.

AT8 and AT100 are monoclonal antibodies specifically directed against phosphorylated human protein tau at epitopes pS198/pS202pS/pS205 and pT231/pS235, respectively (Innogenetics, Gent, Belgium). AT8 is observed in brain of young adults and children and is a marker on the border between physiology and pathology whereas AT100 is a recognized pathological phospho-epitope, typical for AD and primary tauopathies [17,28,29]. AT8 and AT100 expression profiles in brainstem sections were examined using neuroanatomical reference points from mouse atlas [30]. For a given mouse, about 140-150 consecutive coronal sections were cut, from about 0.5 mm caudal to the pyramidal decussation to about 5 mm more rostral. Sections were stained in groups of three with AT8 (first section), AT100 (second section) or saved (third section). In sections from old Tau.P301L mice, we counted the AT100 positively stained (AT100+) neurons, defined as neurons

with visible nucleus, well-marked soma, and high staining intensity. Counting neurons twice was not possible because AT100 stained sections are at least 80 μm apart.

Statistics

Statistical analysis of USV and breathing parameters in young and old FVB/N and Tau.P301L mice was performed using ANOVA with post-hoc Newman-Keuls test in the case of normally distributed data, or Kruskal-Wallis with post-hoc Dunn test in the case of non-normally distributed data (Igor Pro software; WaveMetrics, Oregon, USA). Values are given as mean ± standard error of the mean (S.E.M.). Statistical differences were regarded as significant if $p < 0.05$.

Results

Ultrasonic Vocalisation (USV) disorders in old Tau.P301L mice

We analyzed USV parameters (Fig. 1A1, A2) of conscious, unrestrained and age-matched Tau.P301L and FVB/N mice. USV parameters were similar for both genotypes in young mice (4-5 months) but differed substantially in old mice (8-10 months) (Table 1).

In young mice, no differences were observed in either the duration of individual USV ($Dur_{(USV)}$; Fig. 1B), or the number of USV produced per min ($Nb_{(USV)}$; Fig.1C), or the total amount of time spent in producing USV ($totT_{(USV)}$; Fig. 1D). Tau.P301L and FVB/N mice used the same frequency of about 65 kHz, although slightly lower in Tau.P301L than in FVB/N mice ($Freq_{(USV)}$; Fig. 2A). Within the USV, the range of $Freq_{(USV)}$ (RangeFreq = max $Freq_{(USV)}$ - min $Freq_{(USV)}$) was similar in Tau.P301L and FVB/N mice (Fig. 2B) as well as the distribution of $totT_{(USV)}$ within the different classes of $Freq_{(USV)}$ (Fig. 2C). To produce USV young Tau.P301L and FVB/N mice preferentially used high 50-70 kHz $Freq_{(USV)}$, and occasionally the low 30-40 kHz $Freq_{(USV)}$. We also analyzed the USV complexity by counting the number of segments within USV (tags in Fig. 1A2). In both strains (Fig. 2E), most USV had low complexity (1 or 2 segments) with only some of higher complexity (>2 segments).

In the old mice, significant differences were observed, with shorter, more rare and much simpler USV in transgenic Tau.P301L mice than in wild-type FVB/N mice (Table 1). In Tau.P301L

mice, the duration of USV decreased with age and $Dur_{(USV)}$ became significantly 2-fold shorter in old relative to young Tau.P301L mice (Fig. 1B). In FVB/N mice, $Dur_{(USV)}$ did not significantly decrease with age, in contrast to the significant 2-fold reduction in old Tau.P301L mice . The number of USV $Nb_{(USV)}$ decreased with age in both strains (Fig. 1C), but the $Nb_{(USV)}$ reduction was dramatic in Tau.P301L mice (20-fold reduction) versus modest in wild-type FVB/N mice (2-fold reduction). Not surprisingly, the substantial reductions of both $Dur_{(USV)}$ and $Nb_{(USV)}$ in old Tau.P301L mice dramatically reduced $totT_{(USV)}$ (Fig. 1D): i.e. 30-fold weaker in old than in young Tau.P301L mice and 15-fold weaker in old Tau.P301L than in old FVB/N mice. In addition, the USV pattern became simpler and more monotonous in old Tau.P301L than in old FVB/N mice, while the preferential 65 kHz $Freq_{(USV)}$ remained nearly unchanged (Fig. 2A). In old Tau.P301L mice, the RangeFreq was significantly reduced compared to young Tau.P301L mice and to old FVB/N mice (Fig. 1B). Plotting $totT_{(USV)}$ vs. $Freq_{(USV)}$ revealed that old Tau.P301L mice never used the low 30-40 kHz $Freq_{(USV)}$ they occasionally used at younger age, whereas old FVB/N mice still used both high and low $Freq_{(USV)}$ (Fig. 2D). In addition, the USV complexity became significantly reduced in old Tau.P301L mice (Fig. 2F), with a doubling of the number of the simplest USV (only one segment) versus only half the number of the more complex USV (2 and 3 segments). In contrast, the USV complexity did not change in aged FVB/N mice.

In summary, although young Tau.P301L and FVB/N mice produced similar USV, old Tau.P301L mice developed a drastic impairment of USV meanwhile wild-type FVB/N mice only showed a modest reduction in the number of USV with aging.

Upper Airway dysfunction reduces expiratory airflow in old Tau.P301L mice

USV are produced by expiratory airflow through the larynx [31-34]. From 7-8 months onwards, Tau.P301L mice develop upper airway dysfunction and abnormal expiratory laryngeal activity [19], which may significantly affect their USV.

We therefore measured the expiratory airflow of conscious, young and old transgenic Tau.P301L mice and wild-type FVB/N mice (Table 2). We used double-chamber plethysmography (Fig. 3A) to record the chest spirogram (CSp) produced by the chest respiratory movements in the body chamber and the resulting airflow spirogram (ASp) in the head chamber. We calculated the

ASp/CSp ratio, an index of upper airway function [19]. Young Tau.P301L and FVB/N mice had similar ASp/CSp ratio >1, indicative of correct upper airway function (Fig. 3B, 3D). Measuring the expiratory airflow revealed similar values in young Tau.P301L and FVB/N mice (Fig. 3E). In old mice however, significant differences were observed with reduced ASp and increased CSp in old Tau.P301L mice (Fig. 3C) but not in old FVB/N mice. Moreover, the ASp/CSp ratio was significantly reduced in old Tau.P301L mice (Fig. 3D) but not in old FVB/N mice. The ASp/CSp ratio <1 in old Tau.P301L mice corroborated their upper airway dysfunction [19,20]. The expiratory airflow was significantly reduced in old Tau.P301L mice but not in old FVB/N mice (Fig. 3E): it became 2-fold weaker in old Tau.P301L mice relative to young Tau.P301L mice, and to young and old FVB/N mice. Despite their upper airway dysfunction, old Tau.P301L mice retained normal respiratory frequency, duration of inspiratory period and duration of expiratory period when compared to the other three groups of mice (Table 2).

Tauopathy develops in brainstem areas of old Tau.P301L mice

From 7-8 months onwards, Tau.P301L mice progressively develop brainstem tauopathy [17,19,20], which may affect central networks controlling upper airways and vocalization.

We therefore examined by immunohistochemistry sections of midbrain and brainstem of young and old mice using two distinct antibodies against phosphorylated tau epitopes, AT8 and AT100. AT100, a recognized marker of tauopathy, was not expressed in any of the young or old FVB/N mice (n=3), and very weakly or practically absent in young Tau.P301L mice (n=3), while markedly expressed in old Tau.P301L mice (n=3), as reported previously [17]. The AT100 signal was particularly expressed in midbrain and brainstem sections of old Tau.P301L mice with most dramatic tauopathy in the midbrain periaqueductal gray (PAG), containing the highest density of AT100 positive (AT100+) neurons in the brainstem (Fig. 4). We counted around 100 well-stained AT100+ neurons per PAG section in the three studied old Tau.P301L mice. Numerous AT100+ neurons were observed at all rostro-caudal levels of the PAG and in all the PAG sub-regions, i.e. the ventro-lateral part (Fig. 4A2), the dorso-median part (Fig. 4B2) and the dorso-lateral part (Fig. 4B3). Secondly, we observed a high density of AT100+ neurons in the nucleus retroambiguus (NRA) in the caudal medulla (Fig. 5A) and in the Kolliker-Fuse (KF) nucleus in the dorso-lateral

pons (Fig. 5B). AT100+ neurons delimitated well the KF area, extending between the middle and superior cerebellar peduncles, below the lateral parabrachial nucleus and above the principal sensory trigeminal nucleus (scp, LPB and sp5, respectively, in Fig. 5B). We counted around 25-50 well-stained AT100+ neurons per sections all along the whole rostro-caudal extension of the KF (about 700-1000 µm). In the caudal medulla, frequent AT100+ neurons were also found in the NRA area, previously defined in mouse brainstem [35]. We consistently counted around 10 well-stained, packed AT100+ neurons per studied section from about 500 µm caudal to 500 µm rostral to the pyramidal decussation. Asides the PAG, KF and NRA areas, AT100+ neurons were observed scattered in the whole brainstem, but were especially dense in the raphé obscurus, raphé magnus, locus coeruleus (data not shown), oral pontine reticular nucleus and subcoeruleus (PnO and SubC, respectively, in Fig. 5C).

Conversely, some other areas appeared markedly spared by tauopathy. We found almost no AT100+ neurons in the nucleus ambiguus and the nucleus tractus solitarius (nA and nTS, respectively in Fig. 5B), the raphé dorsalis (RD in Fig. 5C) and most of the cranial motor nuclei (data not shown). The hypoglossal motor nucleus was also generally spared by tauopathy but some AT100+ neurons were observed in the caudal part of the hypoglossal nucleus of one of the three studied Tau.P301L mice (n12, in Fig. 5A). In addition, as previously reported in Tau.P301L mice at the terminal stages [20], the respiratory-related areas implicated in respiratory rhythmogenesis (in the ventral medulla below the nA) and in central chemosensitivity (in the very ventral medulla below the facial motor nucleus) did not contain significant amount of AT100+ neurons.

The epitope defined by AT8 is a marker on the border between physiology and pathology, and we confirmed its previously reported expression profile in the brainstem of old Tau.P301L mice [19,20]. Dense AT8 expression was evident in the PAG, KF and NRA areas, and more scattered in the whole reticular formation, with increased density in the raphé obscurus and magnus, locus coeruleus (data not shown). Only rare AT8+ neurons were in the nA, the nTS, the n12 (some in one mouse), the other motor cranial nuclei and the respiratory-related areas of the ventral medulla (data not shown).

To summarize, both AT100 and AT8 revealed severe tauopathy in old Tau.P301L mice, especially affecting the midbrain PAG, pontine KF and medullary NRA areas, known to control upper airway and vocalization.

Discussion

Compelling evidence exists that mice produce USV for communications and social interactions [21-23] and that mouse models of Angelman Syndrome [24], autism [25] or AD [26] produce specific USV. However, these aspects have been studied mainly in young dams and pups, not in aging mice. In the aging Tau.P301L mouse model of tauopathy [17,18], we report for the first time a dramatic age-related impairment of USV which may be reminiscent of progressive language disorders of elderly people suffering tauopathy and neurodegenerative diseases.

USV impairment of Tau.P301L mice is linked to upper airway dysfunction

Respiration and vocalization are two tightly linked motor acts that implicate the same groups of chest, abdominal and upper airway muscles. USV emission originates from expiratory airflow through the larynx as demonstrated by larynx excision, tracheotomy and motor nerve transection [31-34]. The motor neurons controlling the laryngeal muscles belong to the nA, with intermingled dilatator and constrictor motor neurons. They are multi-functional neurons driven by several central pattern generators, including those for respiration, vocalization and swallowing [36]. During USV, the inspiratory dilatator nA neurons become silent meanwhile the expiratory constrictor nA neurons are activated, mostly prior to USV [37,38].

From 7-8 months onwards, Tau.P301L mice develop upper airway dysfunction [19]: an inspiratory shift of the period of activity of expiratory laryngeal motor neurons induces a paradoxical tendency to laryngeal closure during inspiration, which subsequently reduces air entry within the lungs. Consistent with these previous results, we report here that the expiratory airflow is halved in old Tau.P301L mice. Thus the abnormal laryngeal motor activity and the expiratory airflow reduction highly likely contribute to reduce ability of old Tau.P301L mice to produce frequent, long-lasting

and complex USV. Conversely, old wild-type FVB/N mice retain normal expiratory laryngeal discharge [19], normal expiratory airflow and rather spared USV, with only a modest reduction of USV number. As discussed below with AT100 expression, the impairments of laryngeal discharge, expiratory airflow and USV production in old Tau.P301L mice do not originate from a direct alteration of laryngeal motor neurons but result from alteration of their central drivers.

USV impairment of Tau.P301L mice originates from PAG, KF and NRA tauopathy

We previously reported that Tau.P301L mice develop brainstem tauopathy from 7-8 months onwards, with frequent AT8+ neurons in the KF revealing an altered control of upper airway function [17,19]. Here, we used the late tau pathological marker AT100 to confirm the KF alteration in old Tau.P301L mice and reported numerous AT100+ neurons in the pontine KF but also the midbrain PAG and medullary NRA nuclei. These three structures are crucial in control of upper airway function and vocalization. The PAG is the main descending relay of the emotional motor system which converts higher emotional and cognitive commands into motor activity for complex behaviours, including respiration, vocalization and copulation [39-42]. The PAG projects to both the KF [43] and the NRA [40,42,44]. It also targets many other structures such as the locus coeruleus [45,46], the rostro ventromedial medulla [47] and the raphé magnus [48,49]. The PAG does not directly control the chest, abdominal and upper airway motor neurons but uses the NRA as a relay [50] and the NRA in turn projects to the PAG [51]. The NRA contains multifunctional pre-motoneurons that target the laryngeal nA motor neurons and the thoraco-abdominal motor neurons [35,44,50,52,53] and controls their activity during respiration [54], vocalization [42,50,55], coughing, sneezing [56,57] and copulation [42,58]. The KF modulates the activity of laryngeal and tongue motor neurons [59-61], controlling the upper airway function [19], the expression of learned upper airway behaviours [62] and the vocal patterning [63].

In conclusion, we propose that tauopathy-induced alterations of the crucial PAG, KF and NRA networks play a major role in the USV impairment of old Tau.P301L mice, while not excluding the implication of additional networks. Old Tau.P301L mice develop tauopathy in cortical and thalamic areas [17], which may impact on their social interactions, emotional status and subsequently USV, possibly via the PAG, KF and NRA relays. Old Tau.P301L mice also develop tauopathy in the

locus coeruleus and some raphe nuclei, which may affect the monoaminergic modulations. USV are affected by the serotoninergic system [64] and the serotonin metabolism of Tau.P301L mice becomes abnormal at terminal stages of the disease [20]. On the other hand, AT100+ neurons are rare, almost absent in the nA, which excludes a direct alteration of nA motor neurons and reinforces the concept of indirect effects via alterations of PAG, KF and NRA networks. Similarly, AT100+ neurons are rare in the nTS where the peripheral respiratory inputs are integrated and in the ventral medulla where the respiratory rhythm is, at least in part, generated. Consistently, old Tau.P301L retain normal respiratory frequency, duration of inspiration and duration of expiration (present results) and develop marked breathing defects only at terminal stages of the disease [20].

Translational aspects of mouse USV impairment to progressive language disorders

In mice, the different strain-specific USV patterns are viewed as different lexicons or innate variations in vocal repertoires [21-26]. USV are proposed as models for speech and socio-cognitive disorders [65] and for drugs and genes effects on social motivation, affect regulation and communication [21]. It is outside the scope of this study to define or speculate on the USV impairment in old Tau.P301L mice in terms of social interactions, lexicon or semantic defects. However, the possible link between the USV impairment in Tau.P301L mouse and the progressive language disorders in patients is worth noticing.

Aging from 4-5 to 8-10 months has only minor effects on USV of wild-type FVB/N mice, only reducing the USV number, in contrast to the major effects on USV of old Tau.P301L mice, dramatically reducing their duration, number, and complexity. In healthy humans, aging affects respiration and vocalization, reducing the ability to generate the required air pressure for speech production [66,67]. Old persons initiate speech at a higher lung volume and produce fewer syllables per breath than young adults [68,69]. These age-related reductions of speech performance are negligible compared to pathological language disorders. Progressive language disorders concern a group of clinically, genetically and pathologically heterogeneous neurodegenerative disorders, with different variants based on motor speech, linguistic and cognitive features [9,15,70,71]. However, neither language disorder phenotyping nor brain imaging alone appears a reliable predictor of pathology [72]. A few case reports suggest possible links between language disorder, swallowing

impairment, respiratory difficulties and brainstem alterations [73-77]. In addition, PAG abnormalities have been reported in some cases of mutism [78], in AD [79] and possibly in frontotemporal dementia [80] and Parkinson disease [81]. But these reports are rare and atypical when compared to the plethora of reports about forebrain imaging and language disorders. From our data, the USV impairment of old Tau.P301L mice correlates well with tauopathy-induced alteration of PAG, KF and NRA networks. It has been suggested in recent reviews that mouse USV may be used as models for communication, motivation and socio-cognitive disorders [21,65]. Similarly, we propose Tau.P301L mice as mouse model for neurodegenerative language disorders.

Author Contributions

Conceived and designed the experiments: CM, YC. Performed the experiments: CM, YC, PB, LG. Analyzed the data: CM. Wrote the paper: GH, CG, MD, FVL, CM.

FIGURE LEGEND

Fig. 1: altered USV production in old Tau.P301L mice

A1- Rough USV spectrographic display with frequency and time scales in kHz and ms, respectively.

A2 – As above but showing the tags (Tg, white dots) placed at slope changes in frequency on the rough USV and the analyzed USV parameters: duration of USV ($Dur_{(USV)}$), frequency at tags ($Freq_{(USV)}$), max and min $Freq_{(USV)}$ (RangeFreq), complexity (number of segments delimited by tags), and number of USV produced per minute of recording ($Nb_{(USV)}$). The total time of USV per minute ($totT_{(USV)}$) was obtained by summation of individual $Dur_{(USV)}$.

B – Columns in histograms show $Dur_{(USV)}$ (expressed in ms) in Tau.P301L (black columns) and FVB/N (white columns) mice at age 4-5 months and 8-10 months (young and old mice, respectively). Note the significant reduction of $Dur_{(USV)}$ in old Tau.P301L mice.

C – As in B but for $Nb_{(USV)}$ (expressed in events per s). Note the drastic reduction of $Nb_{(USV)}$ in old Tau.P301L mice.

D – As in B but $totT_{(USV)}$ (expressed in s per min of recording). Note the significant and drastic reduction of $totT_{(USV)}$ in old Tau.P301L mice.

* indicates a significant inter-strain difference at a given class of age and $ a significant age-related difference for a given strain; ns, non significant inter-strain difference.

Fig. 2: altered USV pattern in old Tau.P301L mice

A – Columns in histograms show $Freq_{(USV)}$ (expressed in kHz) used to produce USV in Tau.P301L (black columns) and FVB/N (white columns) mice at age 4-5 and 8-10 months. Note $Freq_{(USV)}$ was similar in old Tau.P301L and FVB/N mice.

B – As in A, but for RangeFreq (= max $Freq_{(USV)}$ – min $Freq_{(USV)}$, see Fig. 1A2). Note RangeFreq of old Tau.P301L mice was significantly reduced when compared to that of old FVB/N and young Tau.P301L mice.

C - Columns in histograms show the distribution of $totT_{(USV)}$ (in %) vs. frequency (Freq), expressed in class of 10 kHz from 30 to 80 kHz in young Tau.P301L (black columns) and FVB/N (white

columns) mice. Note 1) that most USV used high 50-70 kHz frequency but some used low 30-40 kHz frequency, and 2) that $totT_{(USV)}$ was similar distributed in Tau.P301L (black columns) and FVB/N (white columns) mice at age 4-5 months.

D – As in C, but for 8-10 months old mice. Note that old Tau.P301L mice never used the low 30-40 kHz frequency whereas old FVB/N mice still used both low and high frequency, and that $totT_{(USV)}$ was differently distributed between old mice.

E - Columns in histograms show the occurrence (%) of USV of different complexity level as defined by the number of segments (see tags in Fig. 1A2) within the USV. Complexity ranged from low (1) to high (5). Note the similar distribution of complexity in Tau.P301L (black columns) and FVB/N (white columns) young mice.

F – As in E but for old mice. Note the increased occurrence of USV of low complexity and the reduced occurrence of USV of higher complexity (>1) in old Tau.P301L mice compared to old FVB/N and young Tau.P301L mice. Complexity of old FVB/N mice did not change when compared to that of young FVB/N mice.

* indicates a significant inter-strain difference at a given class of age and $ a significant age-related difference for a given strain; ns, non significant inter-strain difference.

Fig. 3: Reduced expiratory airflow in old Tau.P301L mice

A - Schematic presentation of the double-chamber plethysmographic set-up allowing the simultaneous recordings of chest spirogram (CSp; in the body chamber) and airflow spirogram (ASp; in the head chamber) in conscious mice.

B, C – Averaging of about 100 successive respiratory cycles during quiet period of breathing in young (B) and old (C) mice allowed the measurements of mean ASp and CSp, the calculation of the ASp/CSp ratio and the measurement of expiratory airflow during lung emptying period (gray areas).

D - Columns in histograms show the ASp/CSp ratio in Tau.P301L (black columns) and FVB/N (white columns) young and old mice. Note 1) the ratio was similar in young Tau.P301L and FVB/N mice, and 2) the ratio was significantly reduced and increased in old Tau.P301L and FVB/N mice, respectively.

E – As in D but for the expiratory airflow. Note the expiratory airflow was similar in young Tau.P301L and FVB/N mice, significantly halved in old Tau.P301L mice and unchanged in old FVB/N mice.

* indicates a significant inter-strain difference at a given class of age and $ a significant age-related difference for a given strain; ns, non significant inter-strain difference.

Fig. 4: Tauopathy in the PAG of old Tau.P301L mice

Immunohistochemistry with AT100 as tauopathy marker on midbrain coronal sections of old Tau.P301L mice reveals dramatic tauopathy in the whole PAG, affecting both its caudal (A) and rostral (B) parts. A2, B2 and B3 are enlargements of the dotted line boxes drawn in A1 and B1, and show high density of AT100+ neurons in the caudal, ventro-lateral PAG (A2), the rostral, dorso-median PAG (B2) and the rostral dorso-lateral PAG (B3) of the same old Tau.P301L mouse. B4 shows frequent AT100+ neurons in the rostral, dorso-lateral PAG of another old Tau.P301L mice. Calibration bars: 500 µm for A1, B1; 100 µm for A2, B2-B4.

Fig. 5: Tauopathy in the NRA and KF areas of old Tau.P301L mice

Immunohistochemistry with AT100 as tauopathy marker on brainstem coronal sections of a given Tau.P301L mouse (as in Fig. 4). Right hand pictures are enlargements of the dotted line boxes drawn in left hand pictures. Sections show that AT100+ neurons are frequent in the NRA (A) and the KF (B) but lacking in the nucleus tractus solitarius and nucleus ambiguus (C). Calibration bars: 500 and 100 µm for left and right hand pictures, respectively.

Abbreviations: KF, Kolliker-Fuse nucleus; LPB, lateral parabrachial nucleus; nA, nucleus ambiguus; nTS, nucleus tractus solitarius; n12: hypoglossal motor nucleus; PnO, oral pontine reticular nucleus; Pr5, principal trigeminal sensory nucleus; Py, pyramidal tract; Pyx, pyramidal decussation; scp, superior cerebella peduncle; RD, raphé dorsalis; subC, subcoeruelus nucleus; 12r, intra-medullary rootlet of hypoglossal nerve.

REFERENCE LIST

1. Humbert IA, McLaren DG, Kosmatka K, Fitzgerald M, Johnson S, et al. (2010) Early **deficits in cortical control of swallowing in Alzheimer's disease. J. Alzheimers Dis** 19: 1185-1197. doi:10.3233/JAD-2010-1316

2. Suh MK, Kim H, Na DL (2009) Dysphagia in patients with dementia: Alzheimer versus vascular. Alzheimer Dis Assoc Disord 23: 178-184. doi:10.1097/WAD.0b013e318192a539

3. Attems J, König C, Huber M, Lintner F, Jellinger KA (2005) Cause of death in demented and non-demented elderly inpatients; an autopsy study of 308 cases. J. Alzheimers Dis 8: 57-62.

4. Onen F, Onen H (2010) [Obstructive sleep apnea and cognitive impairment in the elderly]. Psychol Neuropsychiatr Vieil 8: 163-169. doi:10.1684/pnv.2010.0219

5. Cooke JR, Liu L, Natarajan L, He F, Marler M, et al. (2006) The effect of sleep-**disordered breathing on stages of sleep in patients with Alzheimer's disease. Behav Sleep** Med 4: 219-27. doi:10.1207/s15402010bsm0404_2

6. Cooke JR, Ayalon L, Palmer BW, Loredo JS, Corey-Bloom J, et al. (2009) Sustained use **of CPAP slows deterioration of cognition, sleep, and mood in patients with Alzheimer's** disease and obstructive sleep apnea: a preliminary study. J Clin Sleep Med 5: 305-309.

7. Ancoli-Israel S, Palmer BW, Cooke JR, Corey-Bloom J, Fiorentino L, et al. (2008) **Cognitive effects of treating obstructive sleep apnea in Alzheimer's disease: a** randomized controlled study. J Am Geriatr Soc 56: 2076-2081. doi:10.1111/j.1532-5415.2008.01934.x

8. Chong MS, Ayalon L, Marler M, Loredo JS, Corey-Bloom J, et al. (2006) Continuous positive airway pressure reduces subjective daytime sleepiness in patients with mild to **moderate Alzheimer's disease with sleep disordered breathing.** J Am Geriatr Soc 54: 777-81. doi:10.1111/j.1532-5415.2006.00694.x

9. Rohrer JD, Schott JM (2011) Primary Progressive Aphasia - Defining Genetic and Pathological Subtypes. Curr Alzheimer Res. Available: http://www.ncbi.nlm.nih.gov/pubmed/21222598. Accessed 24 Jun 2011.

10. Rohrer JD, Rossor MN, Warren JD (2010) Syndromes of nonfluent primary progressive aphasia: a clinical and neurolinguistic analysis. Neurology 75: 603-610. doi:10.1212/WNL.0b013e3181ed9c6b

11. Rohrer JD, Rossor MN, Warren JD (2010) Apraxia in progressive nonfluent aphasia. J. Neurol 257: 569-574. doi:10.1007/s00415-009-5371-4

12. Grossman M (2010) Primary progressive aphasia: clinicopathological correlations. Nat Rev Neurol 6: 88-97. doi:10.1038/nrneurol.2009.216

13. Taler V, Phillips **NA (2008) Language performance in Alzheimer's disease and mild** cognitive impairment: a comparative review. J Clin Exp Neuropsychol 30: 501-556. doi:10.1080/13803390701550128

14. Mesulam M, Wicklund A, Johnson N, Rogalski E, Léger GC, et al. (2008) Alzheimer and frontotemporal pathology in subsets of primary progressive aphasia. Ann. Neurol 63: 709-719. doi:10.1002/ana.21388

15. Ogar JM, Dronkers NF, Brambati SM, Miller BL, Gorno-Tempini ML (2007) Progressive nonfluent aphasia and its characteristic motor speech deficits. Alzheimer Dis Assoc Disord 21: S23-30. doi:10.1097/WAD.0b013e31815d19fe

16. Gerstner E, Lazar RM, Keller C, Honig LS, Lazar GS, et al. (2007) A case of progressive apraxia of speech in pathologically verified Alzheimer disease. Cogn Behav Neurol 20: 15-20. doi:10.1097/WNN.0b013e31802b6c45

17. Terwel D, Lasrado R, Snauwaert J, Vandeweert E, Van Haesendonck C, et al. (2005) Changed conformation of mutant Tau-P301L underlies the moribund tauopathy, absent in progressive, nonlethal axonopathy of Tau-4R/2N transgenic mice. J. Biol. Chem 280: 3963-3973. doi:10.1074/jbc.M409876200

18. Terwel D, Muyllaert D, Dewachter I, Borghgraef P, Croes S, et al. (2008) Amyloid activates GSK-3beta to aggravate neuronal tauopathy in bigenic mice. Am J Pathol 172: 786-98. doi:10.2353/ajpath.2008.070904

19. Dutschmann M, Menuet C, Stettner GM, Gestreau C, Borghgraef P, et al. (2010) Upper airway dysfunction of Tau-P301L mice correlates with tauopathy in midbrain and ponto-medullary brainstem nuclei. J. Neurosci 30: 1810-1821. doi:10.1523/JNEUROSCI.5261-09.2010

20. Menuet C, Borghgraef P, Matarazzo V, Gielis L, Lajard A-M, et al. (2011) Raphé tauopathy alters serotonin metabolism and breathing activity in terminal Tau.P301L mice: possible implications for tauopat**hies and Alzheimer's Disease. Respir Physiol** Neurobiol in press.

21. Lahvis GP, Alleva E, Scattoni ML (2011) Translating mouse vocalizations: prosody and frequency modulation. Genes Brain Behav 10: 4-16. doi:10.1111/j.1601-183X.2010.00603.x

22. Grimsley JMS, Monaghan JJM, Wenstrup JJ (2011) Development of social vocalizations in mice. PLoS ONE 6: e17460. doi:10.1371/journal.pone.0017460

23. Portfors CV (2007) Types and functions of ultrasonic vocalizations in laboratory rats and mice. J. Am. Assoc. Lab. Anim. Sci 46: 28-34.

24. Jiang Y-H, Pan Y, Zhu L, Landa L, Yoo J, et al. (2010) Altered ultrasonic vocalization and impaired learning and memory in Angelman syndrome mouse model with a large maternal deletion from Ube3a to Gabrb3. PLoS ONE 5: e12278. doi:10.1371/journal.pone.0012278

25. Scattoni ML, Gandhy SU, Ricceri L, Crawley JN (2008) Unusual repertoire of vocalizations in the BTBR T+tf/J mouse model of autism. PLoS ONE 3: e3067. doi:10.1371/journal.pone.0003067

26. Scattoni ML, Gasparini L, Alleva E, Goedert M, Calamandrei G, et al. (2010) Early behavioural markers of disease in P301S tau transgenic mice. Behav. Brain Res 208: 250-257. doi:10.1016/j.bbr.2009.12.002

27. Holy TE, Guo Z (2005) Ultrasonic songs of male mice. PLoS Biol 3: e386. doi:10.1371/journal.pbio.0030386

28. **Braak H, Del Tredici K (2011) The pathological process underlying Alzheimer's disease** in individuals under thirty. Acta Neuropathol 121: 171-181. doi:10.1007/s00401-010-0789-4

29. Duyckaerts C (2011) Tau pathology in children and young adults: can you still be unconditionally baptist? Acta Neuropathol 121: 145-147. doi:10.1007/s00401-010-0794-7

30. Paxinos G, Franklin KB (2001) The mouse brain in stereotaxic coordinates. 2nd ed. p.

31. Johnson AM, Ciucci MR, Russell JA, Hammer MJ, Connor NP (2010) Ultrasonic output from the excised rat larynx. J. Acoust. Soc. Am 128: EL75-79. doi:10.1121/1.3462234

32. Suthers RA, Narins PM, Lin W-Y, Schnitzler H-U, Denzinger A, et al. (2006) Voices of the dead: complex nonlinear vocal signals from the larynx of an ultrasonic frog. J. Exp. Biol 209: 4984-4993. doi:10.1242/jeb.02594

33. Hofer MA, Shair HN (1993) Ultrasonic vocalization, laryngeal braking, and thermogenesis in rat pups: a reappraisal. Behav. Neurosci 107: 354-362.

34. Nunez AA, Pomerantz SM, Bean NJ, Youngstrom TG (1985) Effects of laryngeal denervation on ultrasound production and male sexual behavior in rodents. Physiol. Behav 34: 901-905.

35. Vanderhorst VGJM (2005) Nucleus retroambiguus-spinal pathway in the mouse: Localization, gender differences, and effects of estrogen treatment. J. Comp. Neurol 488: 180-200. doi:10.1002/cne.20574

36. Bianchi AL, Gestreau C (2009) The brainstem respiratory network: an overview of a half century of research. Respir Physiol Neurobiol 168: 4-12. doi:10.1016/j.resp.2009.04.019

37. Yajima Y, Hayashi Y (1983) Ambiguous motoneurons discharging synchronously with ultrasonic vocalization in rats. Exp Brain Res 50: 359-366.

38. Jourdan D, Ardid D, Chapuy E, Le Bars D, Eschalier A (1997) Audible and ultrasonic vocalization elicited by a nociceptive stimulus in rat: relationship with respiration. J Pharmacol Toxicol Methods 38: 109-116.

39. Holstege G (1989) Anatomical study of the final common pathway for vocalization in the cat. J. Comp. Neurol 284: 242-252. doi:10.1002/cne.902840208

40. Holstege G, Kerstens L, Moes MC, Vanderhorst VG (1997) Evidence for a periaqueductal gray-nucleus retroambiguus-spinal cord pathway in the rat. Neuroscience 80: 587-598.

41. Subramanian HH, Balnave RJ, Holstege G (2008) The midbrain periaqueductal gray control of respiration. J. Neurosci 28: 12274-12283. doi:10.1523/JNEUROSCI.4168-08.2008

42. Vanderhorst VG, Terasawa E, Ralston HJ 3rd, Holstege G (2000) Monosynaptic projections from the lateral periaqueductal gray to the nucleus retroambiguus in the rhesus monkey: implications for vocalization and reproductive behavior. J. Comp. Neurol 424: 251-268.

43. Gerrits PO, Holstege G (1996) Pontine and medullary projections to the nucleus retroambiguus: a wheat germ agglutinin-horseradish peroxidase and autoradiographic tracing study in the cat. J. Comp. Neurol 373: 173-185. doi:10.1002/(SICI)1096-9861(19960916)373:2<173::AID-CNE2>3.0.CO;2-0

44. Oka T, Tsumori T, Yokota S, Yasui Y (2008) Neuroanatomical and neurochemical organization of projections from the central amygdaloid nucleus to the nucleus retroambiguus via the periaqueductal gray in the rat. Neurosci. Res 62: 286-298. doi:10.1016/j.neures.2008.10.004

45. Bajic D, Proudfit HK, Van Bockstaele EJ (2000) Periaqueductal gray neurons monosynaptically innervate extranuclear noradrenergic dendrites in the rat pericoerulear region. J. Comp. Neurol 427: 649-662.

46. Bajic D, Proudfit HK (1999) Projections of neurons in the periaqueductal gray to pontine and medullary catecholamine cell groups involved in the modulation of nociception. J. Comp. Neurol 405: 359-379.

47. Morgan MM, Whittier KL, Hegarty DM, Aicher SA (2008) Periaqueductal gray neurons project to spinally projecting GABAergic neurons in the rostral ventromedial medulla. Pain 140: 376-386. doi:10.1016/j.pain.2008.09.009

48. Braz JM, Enquist LW, Basbaum AI (2009) Inputs to serotonergic neurons revealed by conditional viral transneuronal tracing. J. Comp. Neurol 514: 145-160. doi:10.1002/cne.22003

49. Li YQ, Shinonaga Y, Takada M, Mizuno N (1993) Demonstration of axon terminals of projection fibers from the periaqueductal gray onto neurons in the nucleus raphe magnus which send their axons to the trigeminal sensory nuclei. Brain Res 608: 138-140.

50. Boers J, Klop EM, Hulshoff AC, de Weerd H, Holstege G (2002) Direct projections from the nucleus retroambiguus to cricothyroid motoneurons in the cat. Neurosci. Lett 319: 5-8.

51. Klop E-M, Mouton LJ, Holstege G (2002) Nucleus retroambiguus projections to the periaqueductal gray in the cat. J. Comp. Neurol 445: 47-58.

52. Boers J, Kirkwood PA, de Weerd H, Holstege G (2006) Ultrastructural evidence for direct excitatory retroambiguus projections to cutaneous trunci and abdominal external oblique muscle motoneurons in the cat. Brain Res. Bull 68: 249-256. doi:10.1016/j.brainresbull.2005.08.011

53. VanderHorst VG, Terasawa E, Ralston HJ 3rd (2001) Monosynaptic projections from the nucleus retroambiguus region to laryngeal motoneurons in the rhesus monkey. Neuroscience 107: 117-125.

54. Subramanian HH, Holstege G (2009) The nucleus retroambiguus control of respiration. J. Neurosci 29: 3824-3832. doi:10.1523/JNEUROSCI.0607-09.2009

55. Zhang SP, Bandler R, Davis PJ (1995) Brain stem integration of vocalization: role of the nucleus retroambigualis. J. Neurophysiol 74: 2500-2512.

56. Baekey DM, Morris KF, Gestreau C, Li Z, Lindsey BG, et al. (2001) Medullary respiratory neurones and control of laryngeal motoneurones during fictive eupnoea and cough in the cat. J. Physiol. (Lond.) 534: 565-581.

57. Shiba K, Nakazawa K, Ono K, Umezaki T (2007) Multifunctional laryngeal premotor neurons: their activities during breathing, coughing, sneezing, and swallowing. J. Neurosci 27: 5156-5162. doi:10.1523/JNEUROSCI.0001-07.2007

58. Vanderhorst VG, Holstege G (1995) Caudal medullary pathways to lumbosacral motoneuronal cell groups in the cat: evidence for direct projections possibly representing the final common pathway for lordosis. J. Comp. Neurol 359: 457-475. doi:10.1002/cne.903590308

59. Gestreau C, Dutschmann M, Obled S, Bianchi AL (2005) Activation of XII motoneurons and premotor neurons during various oropharyngeal behaviors. Respir Physiol Neurobiol 147: 159-176. doi:10.1016/j.resp.2005.03.015

60. Dutschmann M, Herbert H (2006) The Kölliker-Fuse nucleus gates the postinspiratory phase of the respiratory cycle to control inspiratory off-switch and upper airway resistance in rat. Eur. J. Neurosci 24: 1071-1084. doi:10.1111/j.1460-9568.2006.04981.x

61. Bonis JM, Neumueller SE, Marshall BD, Krause KL, Qian B, et al. (2011) The effects of lesions in the dorsolateral pons on the coordination of swallowing and breathing in awake goats. Respir Physiol Neurobiol 175: 272-282. doi:10.1016/j.resp.2010.12.002

62. Dutschmann M, Mörschel M, Rybak IA, Dick TE (2009) Learning to breathe: control of the inspiratory-expiratory phase transition shifts from sensory- to central-dominated during postnatal development in rats. J. Physiol. (Lond.) 587: 4931-4948. doi:10.1113/jphysiol.2009.174599

63. Sugiyama Y, Shiba K, Nakazawa K, Suzuki T, Hisa Y (2010) Brainstem vocalization area in guinea pigs. Neurosci. Res 66: 359-365. doi:10.1016/j.neures.2009.12.006

64. Nastiti K, Benton D, Brain PF, Haug M (1991) The effects of 5-HT receptor ligands on ultrasonic calling in mouse pups. Neurosci Biobehav Rev 15: 483-487.

65. Fischer J, Hammerschmidt K (2011) Ultrasonic vocalizations in mouse models for speech and socio-cognitive disorders: insights into the evolution of vocal communication. Genes Brain Behav 10: 17-27. doi:10.1111/j.1601-183X.2010.00610.x

66. Huber JE (2008) Effects of utterance length and vocal loudness on speech breathing in older adults. Respir Physiol Neurobiol 164: 323-330. doi:10.1016/j.resp.2008.08.007

67. Huber JE, Spruill J 3rd (2008) Age-related changes to speech breathing with increased vocal loudness. J. Speech Lang. Hear. Res 51: 651-668. doi:10.1044/1092-4388(2008/047)

68. Hoit JD, Hixon TJ (1987) Age and speech breathing. J Speech Hear Res 30: 351-366.

69. Sperry EE, Klich RJ (1992) Speech breathing in senescent and younger women during oral reading. J Speech Hear Res 35: 1246-1255.

70. Wilson SM, Henry ML, Besbris M, Ogar JM, Dronkers NF, et al. (2010) Connected speech production in three variants of primary progressive aphasia. Brain 133: 2069-2088. doi:10.1093/brain/awq129

71. Gunawardena D, Ash S, McMillan C, Avants B, Gee J, et al. (2010) Why are patients with progressive nonfluent aphasia nonfluent? Neurology 75: 588-594. doi:10.1212/WNL.0b013e3181ed9c7d

72. Hu WT, McMillan C, Libon D, Leight S, Forman M, et al. (2010) Multimodal predictors for Alzheimer disease in nonfluent primary progressive aphasia. Neurology 75: 595-602. doi:10.1212/WNL.0b013e3181ed9c52

73. Tsuchiya K, Ozawa E, Fukushima J, Yasui H, Kondo H, et al. (2000) Rapidly progressive aphasia and motor neuron disease: a clinical, radiological, and pathological study of an autopsy case with circumscribed lobar atrophy. Acta Neuropathol 99: 81-87.

74. Lee E, Uchihara T, Machida A, Watabiki S (2007) [Slowly progressive anarthria and disturbed voluntary respiration--a case report]. Brain Nerve 59: 629-632.

75. Fuh JL, Liao KK, Wang SJ, Lin KN (1994) Swallowing difficulty in primary progressive aphasia: a case report. Cortex 30: 701-705.

76. Munoz DG, Ros R, Fatas M, Bermejo F, de Yebenes JG (2007) Progressive nonfluent aphasia associated with a new mutation V363I in tau gene. Am J Alzheimers Dis Other Demen 22: 294-299. doi:10.1177/1533317507302320

77. Chapman SB, Rosenberg RN, Weiner MF, Shobe A (1997) Autosomal dominant progressive syndrome of motor-speech loss without dementia. Neurology 49: 1298-1306.

78. Esposito A, Demeurisse G, Alberti B, Fabbro F (1999) Complete mutism after midbrain periaqueductal gray lesion. Neuroreport 10: 681-685.

79. Parvizi J, Van Hoesen GW, Damasio A (2000) Selective pathological changes of the **periaqueductal gray matter in Alzheimer's disease. Ann. Neurol 48: 344**-353.

80. Boccardi M, Sabattoli F, Laakso MP, Testa C, Rossi R, et al. (2005) Frontotemporal dementia as a neural system disease. Neurobiol. Aging 26: 37-44. doi:10.1016/j.neurobiolaging.2004.02.019

81. Braak H, Rüb U, Sandmann-Keil D, Gai WP, de Vos RA, et al. **(2000) Parkinson's** disease: affection of brain stem nuclei controlling premotor and motor neurons of the somatomotor system. Acta Neuropathol 99: 489-495.

Table 1
Click here to download Table: Table 1.doc

Table 1: Main USV parameters of young and old Tau.P301L and FVB/N mice

Mouse strain	Age	n	$Dur_{(USV)}$	$Nb_{(USV)}$	$totT_{(USV)}$	$Freq_{(USV)}$	RangeFreq
Tau.P301L	Young	18	51 ± 2	2.2 ± 0.4	6.7 ± 1.1	63 ± 2	11.2 ± 0.4
P(inter-strain diff.)			*0.186*	*0.375*	*0.174*	*0.044*	*0.277*
FVB/N	Young	21	66 ± 14	2.6 ± 0.4	9.1 ± 1.2	67 ± 1	10.2 ± 0.4
Tau.P301L	Old	18	25 ± 2	0.1 ± 0.0	0.2 ± 0.1	66 ± 1	5.9 ± 0.9
P(inter-strain diff.)			*0.047*	*0.041*	*0.047*	*0.499*	*0.002*
FVB/N	Old	24	48 ± 5	1.1 ± 0.3	3.5 ± 1.5	64 ± 1	9.0 ± 0.7
P(inter-age diff.)Tau.P301L			*0.037*	*<0.001*	*0.002*	*0.181*	*<0.001*
P(inter-age diff.)FVB/N			*0.088*	*0.002*	*0.002*	*0.157*	*0.182*

Mean ± SEM values expressed in ms for $Dur_{(USV)}$, number USV per s for $Nb_{(USV)}$, s per min of recording for $totT_{(USV)}$, kHz for $Freq_{(USV)}$ and RangeFreq; *p* values for inter-strain (Tau.P301L vs. FVB/N) and inter-age (young vs. old) comparisons are considered significant when $p<0.05$.

Table 2
Click here to download Table: Table 2.doc

Table 2: Main breathing parameters of young and old Tau.P301L and FVB/N mice

Mouse strain	Age	n	ASp/CSp	Exp Airflow	Rf	Ti	Te
Tau.P301L	Young	8	1.39 ± 0.24	1.72 ± 0.11	207 ± 9	155 ± 14	149 ± 11
P(inter-strain diff.)			*0.356*	*0.274*	*0.259*	*0.266*	*0.168*
FVB/N	Young	6	1.53 ± 0.11	1.85 ± 0.16	201 ± 12	169 ± 26	172 ± 36
Tau.P301L	Old	15	0.63 ± 0.4	0.97 ± 0.09	193 ± 10	176 ± 13	142 ± 7
P(inter-strain diff.)			*<0.001*	*<0.001*	*0.207*	*0.405*	*0.233*
FVB/N	Old	20	2.71 ± 0.22	2.10 ± 0.16	208 ± 13	177 ± 16	134 ± 16
P(inter-age diff.)Tau.P301L			*<0.001*	*<0.001*	*0.221*	*0.194*	*0.266*
P(inter-age diff.)FVB/N			*0.004*	*0.202*	*0.482*	*0.477*	*0.085*

Mean ± SEM values expressed in mL/g/s for expiratory airflow (Exp Airflow), cycle per min for respiratory frequency (Rf), and ms for duration of inspiratory (Ti) and expiratory (Te) periods; *p* values for inter-strain (Tau.P301L vs. FVB/N) and inter-age (young vs. old) comparisons are considered significant when $p<0.05$.

Figure 1

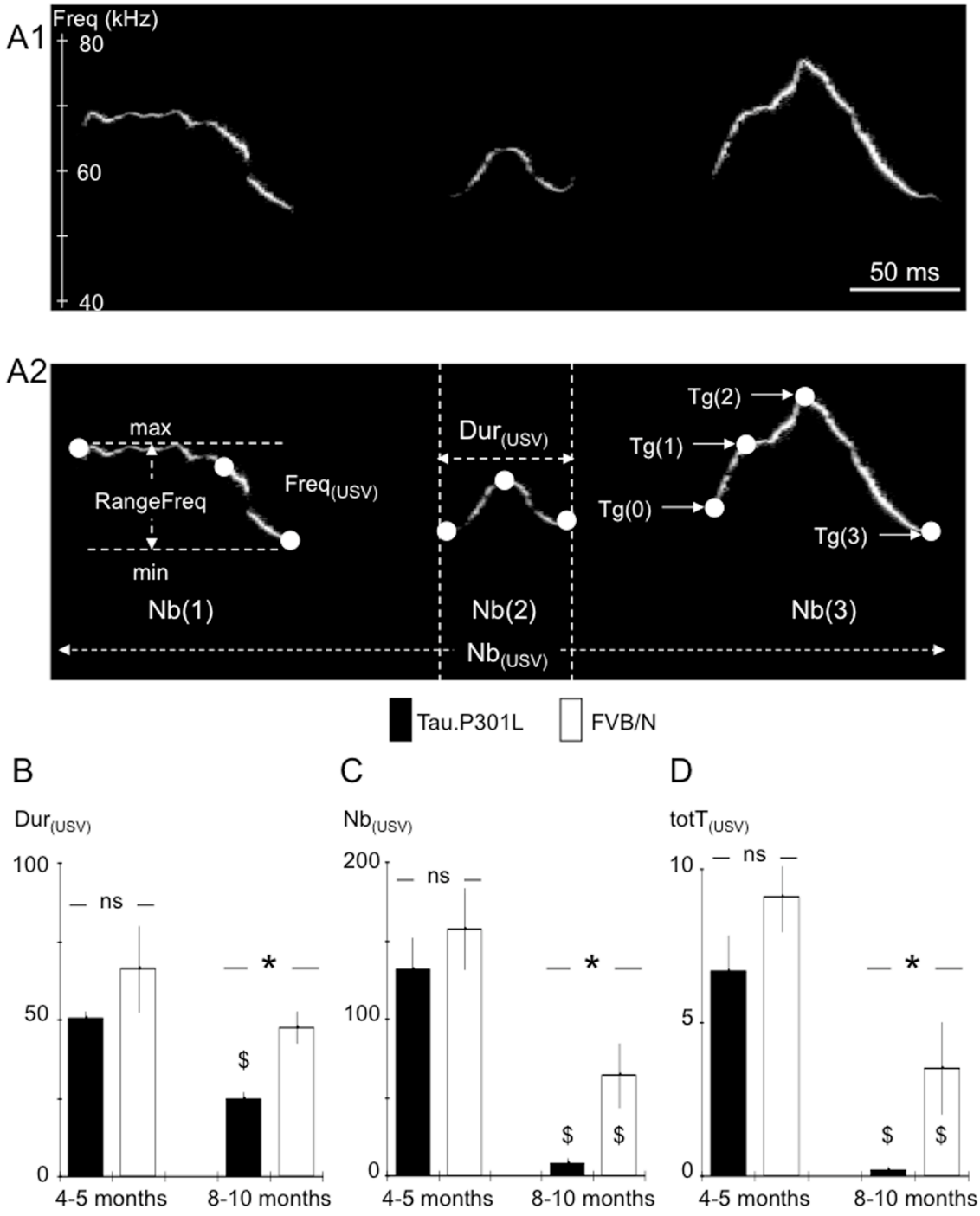
A1
Freq (kHz)
80
60
40
50 ms
A2
max
RangeFreq
min
Freq(USV)
Dur(USV)
Tg(2)
Tg(1)
Tg(0)
Tg(3)
Nb(1)
Nb(2)
Nb(3)
Nb(USV)
Tau.P301L
FVB/N
B
Dur(USV)
100
50
0
ns
*
$
4-5 months
8-10 months
C
Nb(USV)
200
100
0
ns
*
$
$
4-5 months
8-10 months
D
totT(USV)
10
5
0
ns
*
$
$
4-5 months
8-10 months

Figure 2

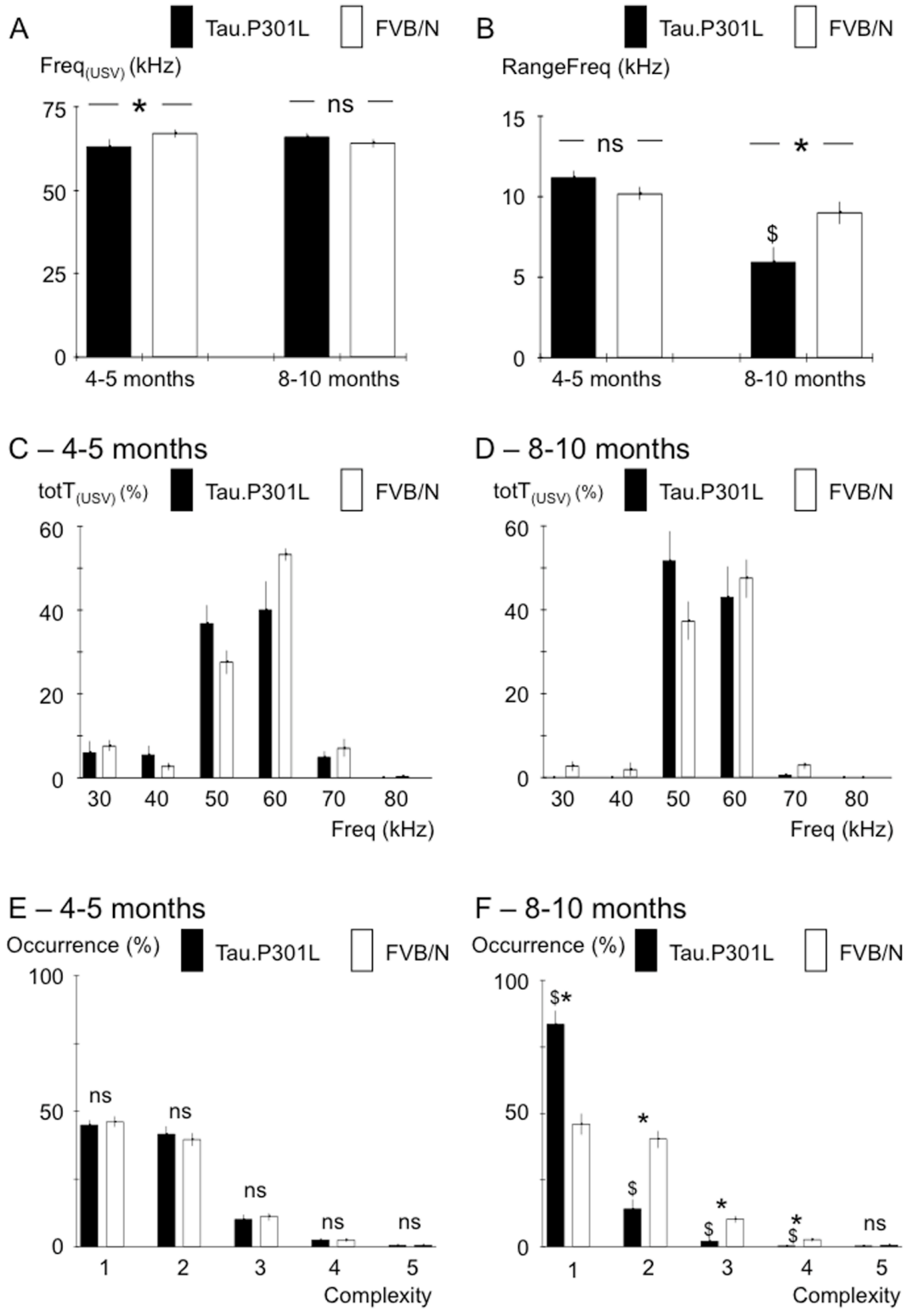
A
Tau.P301L
FVB/N
Freq(USV) (kHz)
75
50
25
0
*
ns
4-5 months
8-10 months
B
Tau.P301L
FVB/N
RangeFreq (kHz)
15
10
5
0
ns
*
$
4-5 months
8-10 months
C – 4-5 months
totT(USV) (%)
Tau.P301L
FVB/N
60
40
20
0
30
40
50
60
70
80
Freq (kHz)
D – 8-10 months
totT(USV) (%)
Tau.P301L
FVB/N
60
40
20
0
30
40
50
60
70
80
Freq (kHz)
E – 4-5 months
Occurrence (%)
Tau.P301L
FVB/N
100
50
0
ns
ns
ns
ns
ns
1
2
3
4
5
Complexity
F – 8-10 months
Occurrence (%)
Tau.P301L
FVB/N
100
50
0
$*
*
$
*
$
*
$
ns
1
2
3
4
5
Complexity

Figure 3

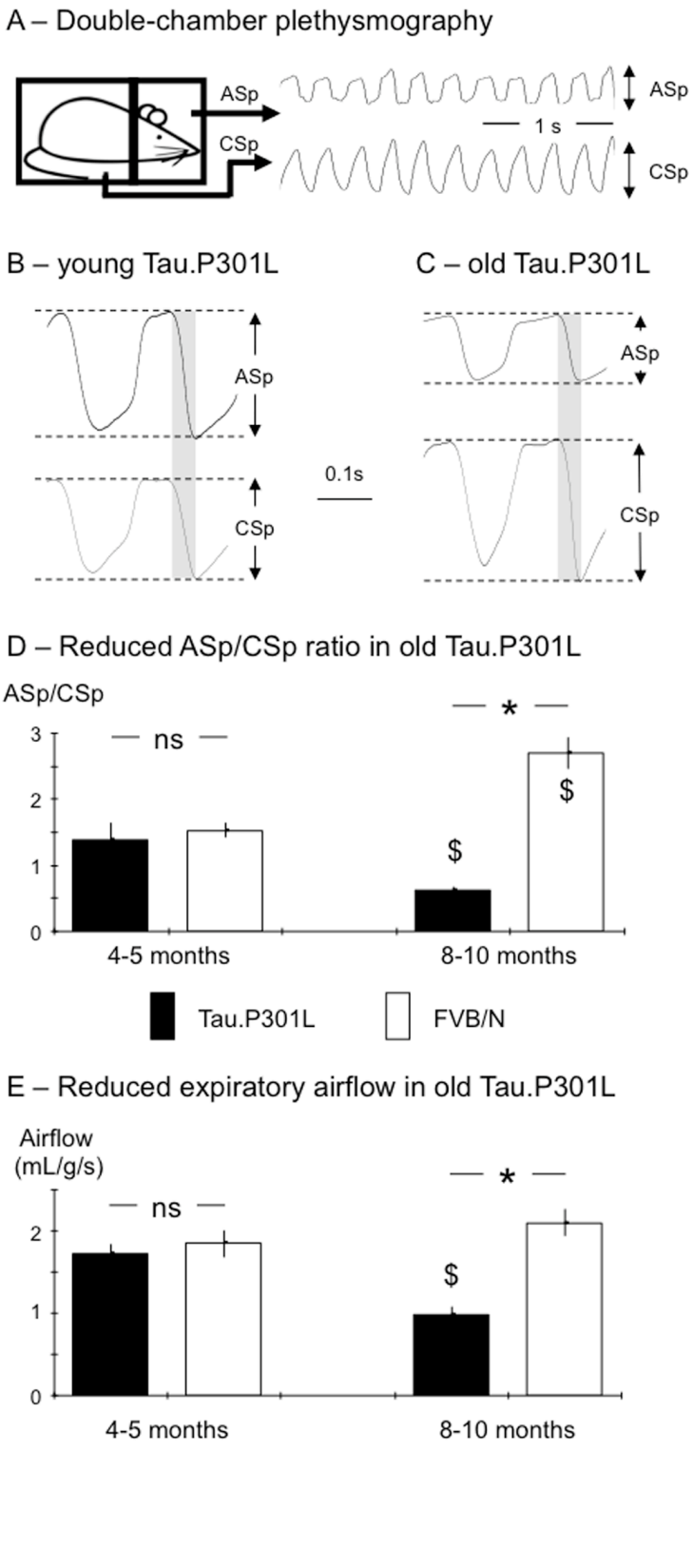
A – Double-chamber plethysmography
ASp
CSp
1 s
ASp
CSp
B – young Tau.P301L
C – old Tau.P301L
ASp
CSp
0.1s
ASp
CSp
D – Reduced ASp/CSp ratio in old Tau.P301L
ASp/CSp
3
2
1
0
ns
*
$
$
4-5 months
8-10 months
Tau.P301L
FVB/N
E – Reduced expiratory airflow in old Tau.P301L
Airflow
(mL/g/s)
2
1
0
ns
*
$
4-5 months
8-10 months

Figure 4

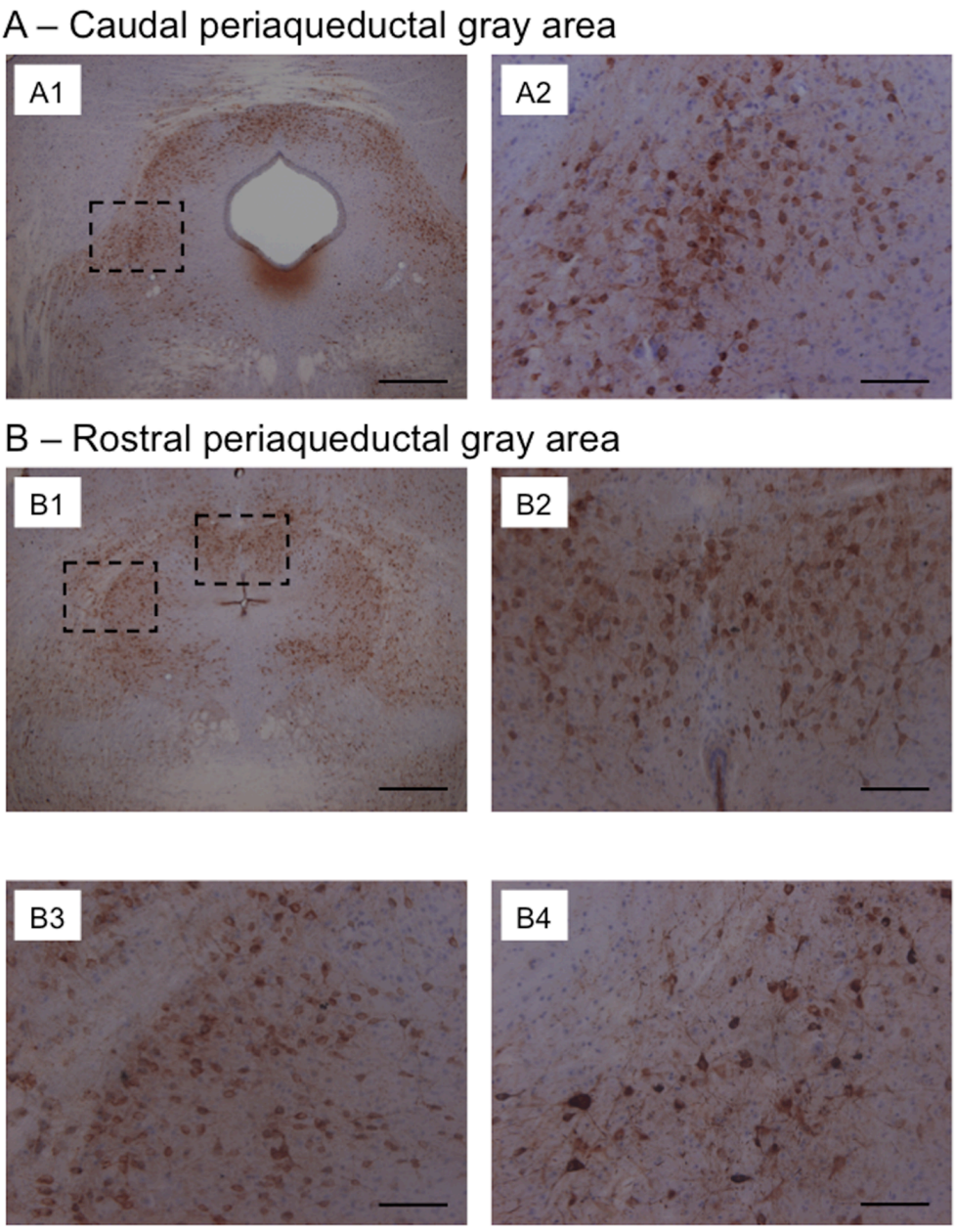
A – Caudal periaqueductal gray area
A1
A2
B – Rostral periaqueductal gray area
B1
B2
B3
B4

Figure 5

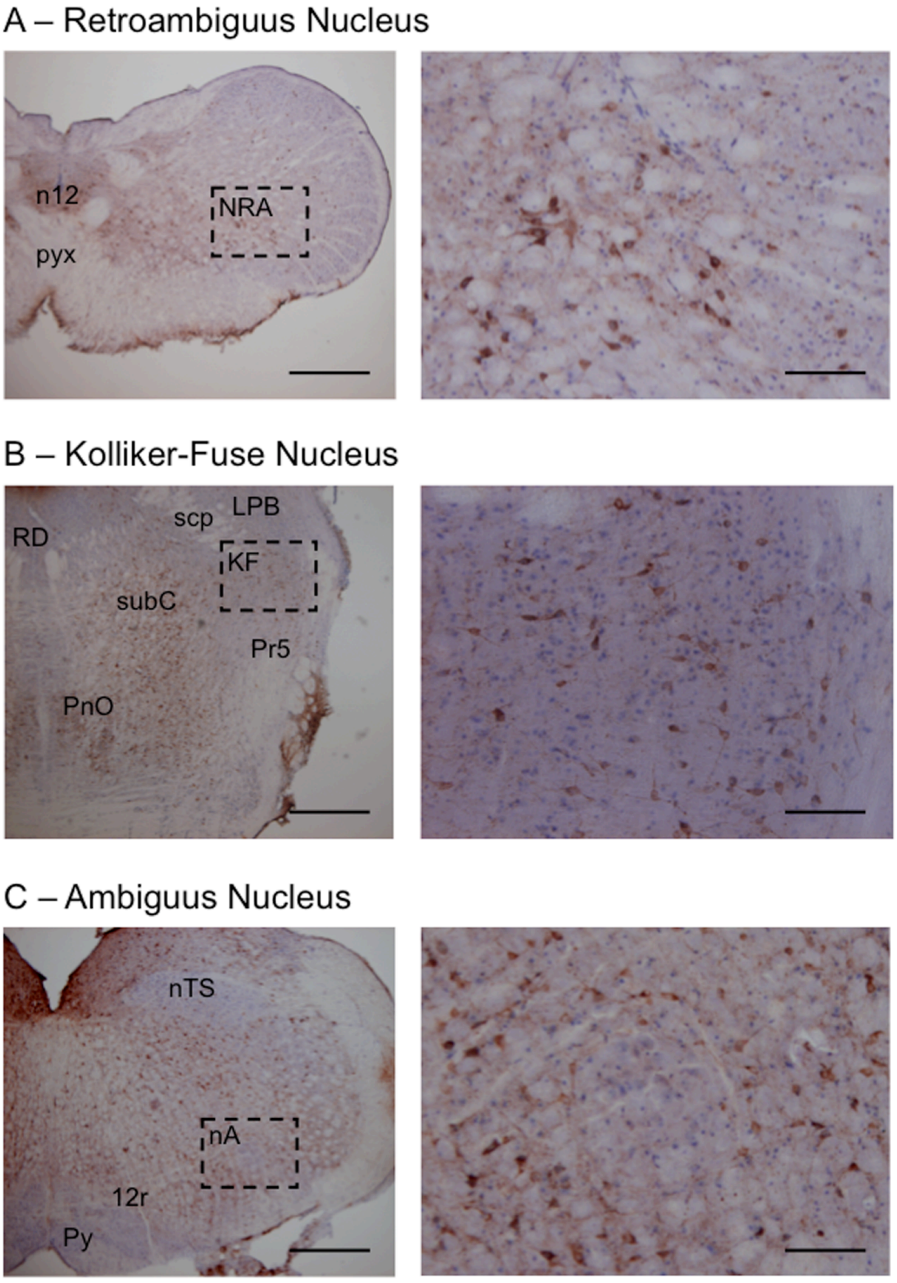
A – Retroambiguus Nucleus
n12
NRA
pyx
B – Kolliker-Fuse Nucleus
RD
scp
LPB
KF
subC
Pr5
PnO
C – Ambiguus Nucleus
nTS
nA
12r
Py

4 - L'anesthésie à l'isoflurane précipite la tauopathie et les dysfonctions des voies aériennes supérieures chez les souris Tau-P301L pré-symptomatiques

Menuet C., Borghgraef P., Voituron N., Gestreau C., Gielis L., Devijver H., Dutschmann M., Van Leuven F. & Hilaire G.

Soumis à *The Journal of Neuroscience*.

Résumé en français :

Le déclin cognitif postopératoire résultant de l'anesthésie volatile est de plus en plus considéré comme un problème de santé majeur. Il est suspecté que l'isoflurane, un anesthésique couramment utilisé, précipiterait la neurodégénérescence dans la maladie d'Alzheimer par des mécanismes inconnus. Nous avons précédemment montré que les souris Tau-P301L âgées souffrent d'altérations des voies aériennes supérieures, qui sont liées à la tauopathie dans le noyau de Kölliker-Fuse qui les contrôle. Nous montrons ici que l'anesthésie à l'isoflurane chez des souris Tau-P301L jeunes et pré-symptomatiques a déclenché des altérations précoces des voies aériennes supérieures et de la tauopathie dans plusieurs noyaux du tronc cérébral, incluant le noyau ambigu qui contient les motoneurones des voies aériennes supérieures et dans le noyau de Kölliker-Fuse. L'administration de la drogue mémantine, un antagoniste des récepteurs NMDA, a empêché l'apparition des dysfonctions post-anesthésiques des voies aériennes supérieures et de la tauopathie du noyau ambigu et du noyau de Kölliker-Fuse. Egalement, nous avons identifié des protocoles d'anesthésie chez les souris Tau-P301L jeunes qui réduisent les effets négatifs de l'anesthésie à l'isoflurane. Ainsi, nos données expérimentales chez un modèle murin validé de tauopathie renforcent le lien entre anesthésie à l'isoflurane, tauopathie et troubles fonctionnels précoces, soulignent l'implication des récepteurs NMDA dans les mécanismes qui induisent les effets négatifs de l'isoflurane, et potentiellement identifient des protocoles plus prudents pour l'anesthésie des patients atteints de tauopathie.

Title Page

Classification*:* Biological Sciences - Neurobiology

Title: Isoflurane anesthesia precipitates tauopathy and upper airways dysfunction in pre-symptomatic Tau.P301L mice

Authors: Clément Menuet[1], Peter Borghgraef[2], Nicolas Voituron[1], Christian Gestreau[1], Lies Gielis[2], Herman Devijver[2], Mathias Dutschmann[3], Fred Van Leuven[2] and Gérard Hilaire[1]

Author affiliations:

[1] MP3-respiration team, Unité Mixte de Recherche 6231, Centre de Recherche en Neurobiologie et Neurophysiologie de Marseille, Faculté Saint Jérôme, service 362, 13 Marseille, France.

[2] Experimental Genetics Group, LEGTEGG, Department Human Genetics, KULeuven - Campus Gasthuisberg ON1-06.602, B-3000 Leuven, Belgium

[3], Institute of Membrane and Systems Biology, Garstang Building, University of Leeds, Leeds LS2 9JT, UK

Running Title: Post-anesthesia upper airways sequels

Keywords: Tauopathy, anesthesia, upper airways, respiration, brainstem

Corresponding Author:

Gérard Hilaire, MP3-respiration team, Unité Mixte de Recherche 6231, Centre de Recherche en Neurobiologie et Neurophysiologie de Marseille, Faculté Saint Jérôme, service 362, 13 Marseille, France. Phone (33) 491 28 81 72 - Fax (33) 491 28 83 97 – Email: gerard.hilaire@univ-cezanne.fr

Abstract

The postoperative cognitive decline resulting from volatile anesthesia is gaining acceptance as a major health problem. The common anesthetic isoflurane is suspected to precipitate neurodegeneration in Alzheimer disease by unknown mechanisms. We previously validated that old Tau.P301L mice suffer upper airways defects related to tauopathy within the Kolliker-Fuse nucleus that controls upper airways function. We now report that isoflurane anesthesia in young, pre-symptomatic Tau.P301L mice triggered precocious upper airways defects and tauopathy in several brainstem nuclei, including the nucleus ambiguous that contains upper airways motor neurons and the Kolliker-Fuse. The prescription drug memantine, identified as a NMDA receptor antagonist, prevented the post-anesthesia upper airways dysfunction and alleviated tauopathy in the nucleus ambiguus and Kolliker-Fuse. We further identified protocols of anesthesia in young Tau.P301L mice that mitigated adverse effects of isoflurane anesthesia. Thus, our experimental findings in a validated mouse model for tauopathy strengthen the link between isoflurane anesthesia, earlier tauopathy and earlier onset of functional defects, highlight the implication of NMDA-receptors in the mechanisms mediating the adverse effects of isoflurane, and potentially identify safer protocols for anesthesia in patients with tauopathy.

\body

Introduction

Postoperative cognitive decline is a common phenomenon after anesthesia with volatile anaesthetics such as isoflurane (ISO). The problem is gaining additional importance as a secondary health concern in tauopathy patients, including Alzheimer's Disease (AD) with a possible link between anesthesia and disease onset and progression (1-3). AD is characterized by the formation of extraneuronal plaques of aggregated β-amyloid protein and intraneuronal tangles of fibrillar aggregates of the microtubule-associated Tau protein that are thought to alter the functioning of neural networks, resulting in cognitive, motor and mental dysfunctions. Tau phosphorylation is reduced by memantine, a partial NMDA-receptor antagonist, approved for treatment of AD (4-6).
In transgenic Tau.P301L mice, a mouse model of tauopathy, we previously reported development of cognitive defects (age 4-6 months, mo), motor and upper airways (UA) dysfunction (age 7-9 mo) and breathing defects leading to premature death (age 9-12 mo) (7-9). From 8 mo onwards, Tau.P301L mice develop a paradoxical tendency to UA closure during inspiration that they compensate by producing enlarged respiratory movements of the chest (8). In the same time-frame, they develop tauopathy within the pontine Kolliker-Fuse nucleus (KF) (8), a multifunctional network, contributing to the off-switch of inspiration (10-13), the control of UA (10) and the coupling of respiration with swallowing (14-17), vocalization (10), thermoregulation (18) and cardiovascular regulations (19-21). Thus, the KF tauopathy of old Tau.P301L mice correlates well with their UA dysfunction that may be reminiscent of the well-known oro-pharyngeal problems in tauopathy and AD patients (22-26).
ISO anesthesia of Tau.P301L mice, especially coupled with hypothermia, precipitates tau hyper-phosphorylation via poorly understood mechanisms (27). Here, we examined the effects of ISO anesthesia in young, pre-symptomatic Tau.P301L mice on UA dysfunction and brainstem tauopathy. First, we defined that subjecting young Tau.P301L mice to ISO anesthesia provoked precocious onset of UA dysfunction, correlating with precocious onset of tauopathy in the KF but also the nucleus ambiguus (nA) that contains UA motor neurons. Secondly, we obtained evidence that the adverse effects of ISO on UA function, nA and KF tauopathy were alleviated by distinct protocols of anesthesia, including memantine pre-treatment, which highlights implication of NMDA-R in these pathological mechanisms. Thus, our results strengthen the link between ISO anesthesia, tauopathy and disease onset, at least in Tau.P301L mice, and identify possible safer protocols for anesthesia in patients suffering tauopathy.

Manuscript Text

Results

Tau.P301L mice had normal breathing and UA function at age 4 mo

Because we aimed to define the eventual negative effects of ISO anesthesia in young, pre-symptomatic Tau.P301L mice, we first established that they breathed normally, like WT mice, at age 4 mo and that they developed UA defect only later in life, at age 8 mo (8).

In conscious Tau.P301L and WT mice, we used whole-body plethysmography to examine respiratory frequency (Rf), biochemical analysis of tail blood samples to measure pH, pCO_2 and pO_2 and double-chamber plethysmography to record chest spirograms (CSp) and airflow spirograms (ASp) and calculate the ASp/CSp ratio, a sensitive index of UA function. At age 4 mo, young Tau.P301L and WT mice had similar Rf, pH, pCO_2 and pO_2 values (Table S1) and ASp/CSp >1 (Fig. 1a-c). At age 8 mo, Rf was still similar in both genotypes but ASp/CSp was significantly reduced in old Tau.P301L compared to old WT mice (Fig. 1 c).

We conclude that the brainstem respiratory network produces normal Rf and motor drives to chest and UA muscles in young Tau.P301L mice, and normal Rf but altered motor drives at age 8 mo, consistent with UA defect (8).

Isoflurane anesthesia of young Tau.P301L mice precipitated UA defect

Having demonstrated that young Tau.P301L mice had normal UA function, we went on to analyse the effects of ISO anesthesia at age 4 mo.

Young Tau.P301L and WT mice were anaesthetized for 4 h by exposure to ISO (1.3% in 30% O_2). ISO anesthesia progressively lowered body temperature, hear rate and Rf, resulting in similar hypothermia, bradycardia and bradypnoea in Tau.P301L and WT mice (Fig. 1d-f), which however did not significantly alter pH, pCO2 and pO2 values at the end of ISO session (Table S1).

In both genotypes, bradypnoea developed with an abnormal pattern of discharge of chest inspiratory muscles (chest EMG). Initially during anesthesia, chest EMG showed a classical ramp-pattern with a progressive increase in amplitude during inspiration until maximum, and a rapid decline at the inspiratory off-switch (Fig. 1g, upper traces). After 4 h of ISO, the chest EMG normally increased at the beginning of inspiration to reach the maximum, but remained at the plateau level for about 100 ms (Fig. 1g, lower trace), leading to a significant lengthening of the duration of the chest EMG.

All mice recovered well from the 4 h ISO session. When analyzed again 7 d later, they showed normal Rf, pH, pO_2 and pCO_2 (SI Table 1). Unexpectedly, double-chamber plethysmography revealed UA defect in the young Tau.P301L mice, which was never observed in WT mice (Fig. 1h). Post-ISO session, Tau.P301L mice produced enlarged chest respiratory movements (large CSp) but weak airflow (weak ASp), which resulted in ASp/CSp <1. The ASp/CSp of ISO-exposed Tau.P301L mice was significantly reduced (0.50 ± 0.06) compared to either ISO-exposed WT mice

(1.40 ± 0.21; p=0.011) or age-matched Tau.P301L mice never subjected to ISO (1.45 ± 0.37; p=0.014). The ASp/CSp of ISO-exposed Tau.P301L mice at 4 mo was similar to that of symptomatic Tau.P301L mice at 8 mo (p=0.242). Thus, subjecting young Tau.P301L mice to ISO anesthesia precipitated the UA defect they normally developed 4 mo later.

We went on to define whether the UA defect of young Tau.P301L mice post- ISO was either permanent or only transient. Tau.P301L mice were subjected to the identical ISO session, but were analyzed at 15 d post-ISO. Their ASp/CSp was still significantly reduced (0.59 ± 0.09; p=0.013) compared to that of control mice (Fig. 1k).

We concluded that young Tau.P301L mice exhibited a severe UA defect after 4 h ISO and that this functional deficit lasted for a prolonged period following termination of anesthesia.

Isoflurane anesthesia protocols and onset of UA defect

We therefore went on to examine the eventual contributions of hypothermia, bradypnoea and bradycardia in the precocious onset of UA defect. We defined first whether counteracting the hypothermia accompanying ISO anesthesia counteracted the onset of UA defect. We used the same 4 h ISO protocol as before, but the body temperature of the mice was controlled by external heating. After 4 h ISO anesthesia with controlled body-temperature, Tau.P301L mice had normal temperature, less severe bradycardia and bradypnoea (Fig. 2a-c, Warm) and normal pattern of chest EMG (Fig. 2d1). All Tau.P301L mice recovered well from the ISO session with controlled body-temperature and their ASp/CSp recorded 7 d post-ISO was not significantly reduced compared to control (Fig. 2e, ISO+Warm).

We conclude that maintaining normothermia during ISO anesthesia of Tau.P301L mice prevented the abnormal breathing pattern during anesthesia and the UA sequel subsequent to the ISO.

We went on to examine whether the abnormal functioning of the respiratory network during ISO contributed to the UA defect. To prevent the abnormal functioning of the respiratory network under ISO, we subjected Tau.P301L mice to ISO by forced artificial ventilation, with mice breathing the same O_2 enriched air mixture as before. The ventilator rhythm was set at the Rf of warmed/ISO-exposed mice (100 cycle per min, c/min) and the volume adjusted to 0.4 ml to silent the respiratory network and abolish chest EMG (Fig. 2d2). After 4 h ISO, the Tau.P301L mice were hypothermic and bradycardic (Fig. 2a-c, Vent). All mice recovered from ISO and showed no UA defect at 7d post-ISO, with ASp/CSp not different from control (Fig. 2e, ISO+Vent).

To exclude any extraneous effects exerted by intubation and mechanical ventilation, we subjected Tau.P301L mice to the same ISO session with forced ventilation and no body-temperature control but mice were ventilated with either hypoxic (10% O_2, 90% N_2) or hyperoxic/hypercapnic (7% CO_2, 30% O_2, 63% N_2) gas mixtures. Forced ventilation with these gas mixtures maintained activity

of the respiratory network and chest EMG during ISO session. After 4 h ISO, the hypoxic- or hyperoxic/hypercapnic-ventilated mice again displayed hypothermia, bradycardia and bradypnoea with prolonged chest EMG. At 7d post-ISO, their ASp/CSp was significantly depressed (0.61 ± 0.11 and 0.60 ± 0.04) relative to control.

We conclude that silencing the respiratory network by forced ventilation prevented the UA defect in young Tau.P301L mice imposed by the ISO anesthesia. These data imply that besides hypothermia and hypoxia, other factors contribute to the precocious onset of UA defect by ISO.

The NMDA-R antagonist memantine prevented ISO-induced UA defect

The claims that the NMDA-R antagonist memantine reduced tauopathy in cell-cultures (5, 6) and transgenic mice (4) incited us to examine whether memantine affected the ISO-induced UA defect of Tau.P301L mice. Young Tau.P301L mice were administered the compound memantine (20 mg.kg-1) 1 h prior to ISO session without forced-ventilation and body-temperature correction. Memantine pre-treatment did not affect the acute hypothermia, bradycardia, bradypnoea (Fig. 2a-c, Mem) and lengthening of chest EMG (Fig. 2d3) during the 4 h ISO, as observed in young Tau.P301L mice analyzed in the foregoing sections. All the memantine-treated mice recovered well from ISO. At 7d post-ISO, their ASp/CSp was high (1.79 ± 0.17) (Fig. 2e, ISO+Mem), not significantly different from that of non-anaesthetised Tau.P301L mice.

Consequently, we conclude that although memantine pre-treatment did not prevent the acute hypothermia, bradypnoea and bradycardia inflicted by 4 h ISO, it did prevent the post-hoc UA defect, revealing the implication of NMDA-R in mediating ISO-induced UA defect.

Isoflurane anesthesia of young Tau.P301L mice precipitated tauopathy in brainstem areas

Because older Tau.P301L mice at age 8 mo developed both UA defect and tauopathy in the KF nucleus controlling UA function (8), we tested the hypothesis that ISO anesthesia of Tau.P301L mice at 4 mo precipitated not only UA defect but also tauopathy in the KF.

First in 4 mo old Tau.P301L mice that were not subjected to ISO (n=3), we performed a detailed immunohistochemical analysis of the expression of human mutant protein Tau.P301L phosphorylated at epitope AT8, the classical method to "stage" tauopathy in human brain (28). Consistently with our previous report (8), we found a diffuse, weak AT8 staining without clear tauopathy in the brainstem and midbrain of young Tau.P301L mice.

Conversely, in ISO-exposed young Tau.P301L mice (no warming, no forced ventilation) sacrificed 7d post-hoc (n=3), marked AT8 signal and tauopathy were evident in several brainstem areas, frequently with a typical pattern of stained somata and processes similar to the tauopathy previously reported in symptomatic Tau.P301L mice at age 8 mo (8). The Tau.P301L mice post-ISO already

showed frequent AT8 positively stained (AT8+) neurons at age 4 mo. Well stained AT8+ neurons were scattered in the reticular formation (arrows in Fig. 3a) but their density was high in the KF (Fig. 3c, c1), raphe obscurus (Rob; Fig. 3b, b2), A6 (Fig. 3c,c2), periaqueductal gray (PAG) (Fig. 3d, d2) and nucleus retroambiguus (NRA) (Fig. 4c). As previously reported in old and terminal Tau.P301L mice (8, 9), the nucleus tractus solitarius (nTS) and the respiratory-related areas of the ventral medulla of post-ISO Tau.P301L mice did not show frequent AT8+ neurons, which was consistent with their normal Rf, pH, pCO2 and pO2. However, highly frequent, well stained AT8+ neurons were found in hypoglossal (n12; Fig. 3a, a1, a2), facial, trigeminal (Mo5; Fig. 3c, 3d1) and ambiguous (nA; Fig. 3b, b1) nuclei, an AT8 expression profile not observed previously in old Tau.P301L mice (8, 9). Because the UA muscles are innervated by nA motor neurons and because nA motor neurons are controlled by NRA, KF and PAG interneurons, the tauopathy in the nA, NRA, KF and PAG network of post-ISO Tau.P301L mice correlated well with the precocious onset of UA defects.

In the three groups of Tau.P301L mice that retained normal UA function at 7d post-ISO, a similar AT8 expression was observed in most brainstem and midbrain areas but not in the nA and KF. Frequent, well-stained AT8+ neurons were similarly found in the NRA, n12, Mo5, Rob, A6 and PAG nuclei of temperature-controlled Tau.P301L mice (n=3), air-ventilated Tau.P301L mice (n=3; Fig. S1 and Legend S1) and memantine pre-treated Tau.P301L mice (n=3; Fig. S2 and Legend S2). However only a weak AT8 staining was observed in the nA and KF of these mice, especially in the memantine group. To ascertain the reduction of tauopathy in the nA and KF, we counted the number of AT8+ neurons per section in the nA that contained large, tightly packed and easily discernable motor neurons (Fig. 4a) and measured the optical density of the AT8 signal in the KF that contained small, intermingled interneurons in a rather extended area (Fig. 4b). We confirmed a significant reduction of both number of AT8+ neurons in the nA and AT8 optical density in the KF in mice that retained normal UA function post-ISO when compared to mice with UA defect post-ISO. No significant reduction of AT8+ neurons was observed in other areas with tauopathy, including the n12, Mo5, Rob, A6, PAG and NRA nuclei (Fig. S1, Legend S1, and Fig. S2, Legend S2). Because the NRA pre-motor neurons project to and control the KF and nA motor neurons (29), we further counted AT8+ neurons in the NRA of mice with and without UA defect post-ISO and found no significant intergroup differences (Fig. 4c).

We conclude first that our combined data from plethysmography and AT8 immunohistochemistry considerably strengthen the hypothesis of a deleterious effect of ISO anesthesia on the onset of the disease in the Tau.P301L mouse model of tauopathy, second that UA defect in Tau.P301L mice is closely linked to nA and KF tauopathy, and third that NMDA-R contribute to the deleterious effects of ISO.

Discussion

In the Tau.P301L mouse model of tauopathy with brainstem tauopathy and UA defect from 8 mo onwards (8, 9), we show that ISO anesthesia during the pre-symptomatic period prematurely induces brainstem tauopathy and UA defect at age 4 mo. Our mouse results fully support a link between ISO anesthesia and onset of AD (3), argue for implication of NMDA-R in the ISO adverse effects and identify safer protocols for anesthesia of patients at AD risks.

Pathological consequences of ISO-induced upper airways dysfunction

AD, the most prevalent neurodegenerative disorder in elderly people, is characterized by memory, cognition and behavioral defects. AD is also accompanied with breathing, swallowing and language disorders, which suggests UA defects. At 4 mo, Tau.P301L mice have normal UA function and no brainstem tauopathy but show UA defect and brainstem tauopathy post-ISO, especially in the KF, NRA and monoaminergic areas, resembling those previously reported in older Tau.P301L mice (8, 9). Post-ISO, young Tau.P301L mice retain normal Rf, which is consistent with the lack of tauopathy in the ventro-lateral medulla areas that contribute to respiratory rhythm generation and in the nTS areas that integrate peripheral regulatory inputs, as reported in older Tau.P301L mice (8). Conversely to older Tau.P301L mice, young Tau.P301L mice post-ISO show tauopathy in all cranial motor nuclei, including the nA. The nA motor neurons innervate UA muscles, are driven by inputs from the brainstem respiratory network, the medullary NRA pre-motor neurons, the pontine KF interneurons, and further upstream, the PAG that controls the KF and NRA (29). As a whole, the nA, NRA, KF and PAG constitute a multifunctional network that contributes to respiration (10), swallowing (14, 15), vocalization (29). Thus, the precocious onset of tauopathy within this network correlates well with UA defect of Tau.P301L mice and possibly with oro-pharyngeal symptoms of AD. Tau.P301L mice post-ISO must enhance their chest respiratory movements to compensate airflow reduction caused by paradoxical UA narrowing during inspiration (8, 9). This breathing strategy efficiently secures pH, pCO2 and pO2 but requires an increased respiratory work-load, which may contribute to their weight loss with aging (7), a predictor of mortality in AD (34). Post-ISO, UA defect possibly alters swallowing and therefore food intake, which may also contribute to weight loss and facilitate aspiration, a recognized cause of death in AD (22-24). In addition, tauopathy in n12, facial, Mo5 motor neurons highly likely alters mastication, swallowing and food intake (15). Upper airways defect may facilitate sleep obstructive apnoeas, which alters brain oxygenation during sleep, a process possibly contributing to AD evolution (35, 36). Finally, UA defect may affect vocalization, which may be reminiscent of progressive language disorders of AD patients (37). Our mouse results fully support the consensus reached about deleterious effects of

ISO anesthesia in AD onset and evolution (3). Indeed, ISO by precipitating tauopathy in the network controlling UA may induce distinct deleterious effects in pre-symptomatic Tau.P301L mice, and possibly AD patients.

NMDA mechanisms and ISO-induced tauopathy

AD is characterized by extraneuronal plaques and tauopathy. In young Tau.P301L mice, we confirm that ISO precipitates tau phosphorylation (27) and identify tauopathy in the network controlling UA. The mechanisms through which ISO induces tauopathy are poorly understood. First, hypothermia coupled with ISO has been reported to induce tauopathy (27). Indeed, we show that preventing hypothermia during anesthesia of Tau.P301L mice prevents UA defect. However, hyperventilating hypothermic Tau.P301L mice during anesthesia also prevents UA defect, revealing that hypothermia is not the single, main factor. Hypoxia during anesthesia has been proposed to be crucial too: ISO exposure of cell-cultures enhanced hypoxia-induced caspase-3 activation and β-Amyloid protein (Aβ) accumulation, while caspase activation and hypoxia-induced neurotoxicity may contribute to AD (1). We show that imposing hypoxia during anesthesia of forced-ventilated Tau.P301L mice induces UA defect. However, preventing hypoxia during anesthesia of forced-ventilated Tau.P301L mice with a hyperoxic / hypercapnic mixture does not prevent UA defect. In addition, spontaneously breathing Tau.P301L mice exposed to 4 h ISO did not develop hypoxia, as attested by normal pO2 levels in blood samples, but did develop UA defect. Then, neither hypothermia nor hypoxia coupled with ISO is the single, main factor. On the other hand, we show that pre-treatment with the NMDA-R antagonist memantine efficiently alleviates tauopathy and prevents UA defect in Tau.P301L mice, which fully supports NMDA-R implication.

The nA motor neurons and their KF drivers both express NMDA-R, with an especial high density in the KF where most neurons express NMDA-R (31, 38). The KF controls the off-switch of inspiration via NMDA-R and their blockade prolongs inspiration (11, 12, 36). Anesthesia depresses or leaves unchanged the activity of most respiratory neurons, but specifically activates the KF neurons (39). Anesthesia (40), hypothermia (18), cardio-respiratory changes (19-21, 39) induce c-fos expression in KF neurons, with c-fos and NMDA-R co-expression (19, 34, 40). Thus, during the 4 h ISO session, anesthesia, hypothermia, bradypnoea and bradycardia cumulatively over-activated the KF neurons. On the short term (4 h ISO), the massive activation of KF neurons induced excessive calcium influx, free radical formation (42, 43), and subsequent KF alteration, which delayed inspiratory off-switch and prolonged chest EMG in WT and Tau.P301L mice. On the long term (7d post-ISO), this induced no sequels in WT mice but KF tauopathy and UA defect in Tau.P301L mice, that were both prevented by blockade of NMDA-R with memantine pre-treatment. Memantine is a partial NMDA-R antagonist that preferentially blocks excessive NMDA-

R activity (44). Memantine did not abolish the acute hypothermia, bradycardia, bradypnoea induced by the 4 h ISO but possibly reduced the over-activation of KF neurons by the cumulative actions of anesthesia, hypothermia and cardio-vascular changes, therefore alleviating both KF tauopathy and UA defect. That memantine specifically alleviates tauopathy in the nA and KF but not in n12, Mo5, Rob and A6 is possibly related to different expression profiles of NMDA-R sub-types, density levels and cellular sites of expression, which deserves further investigations. Suppressing only one of the factors over-activating KF neurons during ISO (with warming or forced ventilation) significantly reduces, but does not abolish, the KF tauopathy. Nevertheless, the reduction of the KF tauopathy is sufficient to prevent UA defect, which suggests that tauopathy must pass beyond a threshold level in the KF to induce functional pathology of UA. In the nA, where neurons also express NMDA-R (38), the tauopathy profile is fairly different from that observed in the KF, with a kind of "all or none" response of the nA: tauopathy affects almost all nA motor neurons after the simplest ISO protocol (no warming, forced-ventilation, and memantine) but almost none of the nA motor neurons after ISO with forced-ventilation or ISO with memantine pre-treatment. This may be explained by weak, non-detectable reduction of tauopathy by forced-ventilation or memantine pre-treatment in the network upstream the nA. Minor reduction of tauopathy in the PAG, NRA, raphe, and A6, coupled to the marked reduction of KF tauopathy, may significantly protect the nA.
In conclusion, using the respiratory network of young, conscious Tau.P301L mice as model for examining the onset and progression of neural defects during neurodegenerative disease, we show normal UA function prior to, but not after ISO. Indeed, ISO anesthesia of young Tau.P301L mice precociously induced tauopathy in the network controlling UA, a pathological process implicating NMDA-R and inducing UA dysfunction and its cohort of deleterious effects. The efficiency of memantine pre-treatment and distinct protocols of anesthesia to alleviate tauopathy and UA dysfunction in Tau.P301L mice offers new, promising issues for safer anesthesia of AD patients.

Material and Methods

All methods are detailed in SI Methods. Briefly, AT8 immunohistochemistry and plethysmography were used in conscious FVB/N and transgenic Tau.P301L mice as previously reported (8, 9, 7). Tau.P301L mice, produced in the FVB/N genetic background, express the longest human tau isoform bearing the P301L mutation in neurons (7). Consistently with previous reports on onset of tauopathy by ISO anesthesia of Tau-P301L mice (27), 4 mo old mice were subjected to 4 h exposure to ISO at 1 MAC (Minimum Alveolar Concentration, 1.3% ISO) with hyperoxic gas mixture (30% O_2 in air). Mice were either kept freely breathing during ISO session (with or without control of body temperature) or intubated and ventilated with hyperoxic (30% O_2 in air) or hypoxic (10% O_2, 90% N_2) or hyperoxic / hypercapnic gas mixture (7% CO2, 30 % O2, 63% N2). After

mouse lethal anesthesia (Nembutal), the brain was removed, fixed and sectioned (40 μm coronal vibratome sections). Sections were stained with AT8, a monoclonal antibody specifically directed against phosphorylated human protein tau at epitopes pS198/pS202pS/pS205, a marker on the border between physiology and pathology (9). Brainstem structures were defined from neuroanatomical points in mouse atlas (45). Values are given as mean ± standard error of the mean (S.E.M.) and considered statistically different at $P < 0.05$.

Acknowledgments

The authors thank the support of the Unité Mixte de Recherche 6231, the Fonds Wetenschappelijk Onderzoek-Vlaanderen (FWO-Vlaanderen), Instituut voor Wetenschap en Techniek (IWT), KULeuven-Research Fund (BOF), KULeuven-Research&Development and EEC Framework programs FP6 & FP7 and NHLBI.

Footnotes

(no footnotes)

References

1. Pan C et al. (2011) The Potential Dual Effects of Anesthetic Isoflurane on Hypoxia-Induced Caspase-3 Activation and Increases in {beta}-Site Amyloid Precursor Protein-Cleaving Enzyme Levels. *Anesth. Analg* 113:145-152.

2. Bilotta F et al. (2010) Postoperative cognitive dysfunction: toward the Alzheimer's disease pathomechanism hypothesis. *J. Alzheimers Dis* 22 Suppl 3:81-89.

3. Baranov D et al. (2009) Consensus statement: First International Workshop on Anesthetics and Alzheimer's disease. *Anesth. Analg* 108:1627-1630.

4. Martinez-Coria H et al. (2010) Memantine improves cognition and reduces Alzheimer's-like neuropathology in transgenic mice. *Am. J. Pathol* 176:870-880.

5. Song MS, Rauw G, Baker GB, Kar S (2008) Memantine protects rat cortical cultured neurons against beta-amyloid-induced toxicity by attenuating tau phosphorylation. *Eur. J. Neurosci* 28:1989-2002.

6. Li L, Sengupta A, Haque N, Grundke-Iqbal I, Iqbal K (2004) Memantine inhibits and reverses the Alzheimer type abnormal hyperphosphorylation of tau and associated neurodegeneration. *FEBS Lett* 566:261-269.

7. Terwel D et al. (2005) Changed conformation of mutant Tau-P301L underlies the moribund tauopathy, absent in progressive, nonlethal axonopathy of Tau-4R/2N transgenic mice. *J. Biol. Chem* 280:3963-3973.

8. Dutschmann M et al. (2010) Upper airway dysfunction of Tau-P301L mice correlates with tauopathy in midbrain and ponto-medullary brainstem nuclei. *J. Neurosci* 30:1810-1821.

9. Menuet C et al. (2011) Raphé tauopathy alters serotonin metabolism and breathing activity in terminal Tau.P301L mice: possible implications for tauopathies and Alzheimer's disease. *Respir Physiol Neurobiol* In Press, Accepted Manuscript. Available at: http://www.sciencedirect.com/science/article/pii/S1569904811002436 [Accessed July 15, 2011].

10. Dutschmann M, Herbert H (2006) The Kölliker-Fuse nucleus gates the postinspiratory phase of the respiratory cycle to control inspiratory off-switch and upper airway resistance in rat. *Eur. J. Neurosci* 24:1071-1084.

11. Ling L, Karius DR, Speck DF (1994) Role of N-methyl-D-aspartate receptors in the pontine pneumotaxic mechanism in the cat. *J. Appl. Physiol* 76:1138-1143.

12. Fung ML, Wang W, St John WM (1994) Involvement of pontile NMDA receptors in inspiratory termination in rat. *Respir Physiol* 96:177-188.

13. Villard MF, Caille D, Hugelin A (1984) Dissociation between respiratory phase switching and phasic phrenic response on low-intensity stimulation of pneumotaxic complex and nearby structures. *J. Physiol. (Paris)* 79:11-16.

14. Bonis JM et al. (2011) The effects of lesions in the dorsolateral pons on the coordination of swallowing and breathing in awake goats. *Respir Physiol Neurobiol* 175:272-282.

15. Gestreau C, Dutschmann M, Obled S, Bianchi AL (2005) Activation of XII motoneurons and premotor neurons during various oropharyngeal behaviors. *Respir Physiol Neurobiol* 147:159-176.

16. Kuna ST, Remmers JE (1999) Premotor input to hypoglossal motoneurons from Kölliker-Fuse neurons in decerebrate cats. *Respir Physiol* 117:85-95.

17. Nunez-Abades PA, Portillo F, Pásaro R (1990) Characterisation of afferent projections to the nucleus ambiguus of the rat by means of fluorescent double labelling. *J. Anat* 172:1-15.

18. Bhatnagar S, Dallman M (1998) Neuroanatomical basis for facilitation of hypothalamic-pituitary-adrenal responses to a novel stressor after chronic stress. *Neuroscience* 84:1025-1039.

19. Dutschmann M, Herbert H (1998) NMDA and GABAA receptors in the rat Kolliker-Fuse area control cardiorespiratory responses evoked by trigeminal ethmoidal nerve stimulation. *J. Physiol. (Lond.)* 510 (Pt 3):793-804.

20. Guo Z-L, Li P, Longhurst JC (2002) Central pathways in the pons and midbrain involved in cardiac sympathoexcitatory reflexes in cats. *Neuroscience* 113:435-447.

21. Horiuchi J, Potts PD, Polson JW, Dampney RA (1999) Distribution of neurons projecting to the rostral ventrolateral medullary pressor region that are activated by sustained hypotension. *Neuroscience* 89:1319-1329.

22. Humbert IA et al. (2010) Early deficits in cortical control of swallowing in Alzheimer's disease. *J. Alzheimers Dis* 19:1185-1197.

23. Suh MK, Kim H, Na DL (2009) Dysphagia in patients with dementia: Alzheimer versus vascular. *Alzheimer Dis Assoc Disord* 23:178-184.

24. Wada H et al. (2001) Risk factors of aspiration pneumonia in Alzheimer's disease patients. *Gerontology* 47:271-276.

25. Priefer BA, Robbins J (1997) Eating changes in mild-stage Alzheimer's disease: a pilot study. *Dysphagia* 12:212-221.

26. Horner J, Alberts MJ, Dawson DV, Cook GM (1994) Swallowing in Alzheimer's disease. *Alzheimer Dis Assoc Disord* 8:177-189.

27. Planel E et al. (2009) Acceleration and persistence of neurofibrillary pathology in a mouse model of tauopathy following anesthesia. *FASEB J* 23:2595-2604.

28. Braak H, Braak E (1994) Morphological criteria for the recognition of Alzheimer's disease and the distribution pattern of cortical changes related to this disorder. *Neurobiol. Aging* 15:355-356; discussion 379-380.

29. Subramanian HH, Balnave RJ, Holstege G (2008) The midbrain periaqueductal gray control of respiration. *J. Neurosci* 28:12274-12283.

30. Hansen M-LH, Waldorff FB, Waldemar G (2011) Prognostic Factors for Weight Loss Over 1-year Period in Patients Recently Diagnosed With Mild Alzheimer Disease. *Alzheimer Dis Assoc Disord*. Available at: http://www.ncbi.nlm.nih.gov/pubmed/21285857 [Accessed July 15, 2011].

31. Cooke JR et al. (2009) Sustained use of CPAP slows deterioration of cognition, sleep, and mood in patients with Alzheimer's disease and obstructive sleep apnea: a preliminary study. *J Clin Sleep Med* 5:305-309.

32. Daulatzai MA (2010) Early stages of pathogenesis in memory impairment during normal senescence and Alzheimer's disease. *J. Alzheimers Dis* 20:355-367.

33. Rohrer JD, Schott JM (2011) Primary Progressive Aphasia - Defining Genetic and Pathological Subtypes. *Curr Alzheimer Res*. Available at: http://www.ncbi.nlm.nih.gov/pubmed/21222598 [Accessed June 24, 2011].

34. Guthmann A, Herbert H (1999) Expression of N-methyl-D-aspartate receptor subunits in the rat parabrachial and Kölliker-Fuse nuclei and in selected pontomedullary brainstem nuclei. *J. Comp. Neurol* 415:501-517.

35. Yamazaki H, Ohi Y, Haji A (2009) Mu-opioid and N-methyl-D-aspartate receptors are localized at laryngeal motoneurons of guinea pigs. *Biol. Pharm. Bull* 32:293-296.

36. Harris MB, Milsom WK (2003) Apneusis follows disruption of NMDA-type glutamate receptors in vagotomized ground squirrels. *Respir Physiol Neurobiol* 134:191-207.

37. Caille D, Vibert JF, Bertrand F, Gromysz H, Hugelin A (1979) Pentobarbitone effects on respiration related units; selective depression of bulbopontine reticular neurones. *Respir Physiol* 36:201-216.

38. Roda F, Pio J, Bianchi A-L, Gestreau C (2004) Effects of anesthetics on hypoglossal nerve discharge and c-Fos expression in brainstem hypoglossal premotor neurons. *J. Comp. Neurol* 468:571-586.

39. Teppema LJ et al. (1997) Expression of c-fos in the rat brainstem after exposure to hypoxia and to normoxic and hyperoxic hypercapnia. *J. Comp. Neurol* 388:169-190.

40. Dutschmann M, Guthmann A, Herbert H (1998) NMDA receptor subunit NR1-immunoreactivity in the rat pons and brainstem and colocalization with Fos induced by nasal stimulation. *Brain Res* 809:221-230.

41. Chen H-SV, Lipton SA (2006) The chemical biology of clinically tolerated NMDA receptor antagonists. *J. Neurochem* 97:1611-1626.

42. Lipton SA (2006) Paradigm shift in neuroprotection by NMDA receptor blockade: memantine and beyond. *Nat Rev Drug Discov* 5:160-170.

43. Lipton SA (2007) Pathologically-activated therapeutics for neuroprotection: mechanism of NMDA receptor block by memantine and S-nitrosylation. *Curr Drug Targets* 8:621-632.

44. Paxinos G, Franklin KB (2001) *The mouse brain in stereotaxic coordinates.* 2nd Ed.

Figure Legends

Figure 1: Isoflurane anesthesia precipitates UA dysfunction in young Tau.P301L mice

a-b: Representation of the double plethysmography setup (a) to record chest and airways spirograms (ASp and CSp, respectively) in conscious mice. c: histogram shows mean and SEM of ASp/CSp in WT and Tau.P301L mice (white and black columns, respectively) at age 4 mo (n=7 WT and n=6 Tau.P301L mice) and 8 mo (n= 8 WT and n=8 Tau.P301L mice). ASp/CSp was similar (ns) in both strains at 4 mo but significantly different (*, $p<0.05$) at 8 mo. d-f: Curves show similar development of hypothermia (d, temp in °C), bradypnoea (e, respiratory frequency, Rf, in c/min) and bradycardia (f, Heart Rate, HR, in c/min) vs. time (in hour, h) during isoflurane anesthesia of 4 mo old WT (n=7) and Tau.P301L (n=6) mice. g: Chest EMG recording at the beginning (1h) and end (4h) of isoflurane session show EMG lengthening at 4 h. h: mean and SEM of ASp/CSp in WT and Tau.P301L mice prior to isoflurane anesthesia (con, no ISO; n= 7 WT and n= 6 Tau.P301L mice), 7 d (7d post-ISO; n= 7 WT and n= 6 Tau.P301L mice) and 15 d after isoflurane anesthesia (15d post-ISO; n= 3 Tau.P301L mice). Isoflurane significantly reduced the ASp/CSp in Tau.P301L but not WT mice (ns and * for non-significant and significant changes, respectively, vs. control at $p<0.05$).

Figure 2: Effect of temperature, forced-ventilation and memantine pre-treatment on the isoflurane-induced alteration of UA function in young Tau.P301L mice

a-c: as in Fig.1 d-f, curves show development of hypothermia (a), bradypnoea (b) and bradycardia (c) vs. duration of isoflurane anesthesia in 4 mo old Tau.P301L mice that were either warmed to prevent hypothermia (+Warm; n=6), hyperventilated to silent the respiratory network (+Vent; n=6) or pre-treated with memantine (Mem; n=8). d: Chest EMG at the end of the isoflurane session in warmed (d1, ISO+Warm), hyperventilated (d2, ISO+Vent) and memantine pre-treated (d3,

ISO+Mem) Tau.P301L mice; note the normal EMG in dl, its lack in d2 (hyperventilated, non-breathing mice) and its lengthening in d3 (vertical traces in d1 and d2 were electrocardiogram). e: mean and SEM of ASp/CSp in 4 mo old Tau.P301L mice prior to (con, no ISO; n=6) and 7 d after isoflurane anesthesia in mice simply exposed to isoflurane (ISO; n=6) or warmed (ISO+Warm; n=6) or hyperventilated (ISO+Vent; n=6) or pre-treated with memantine (ISO+Mem; n=8). All treatments prevented the isoflurane-induced reduction of ASp/CSp (ns and * for non-significant and significant changes, respectively, vs. control at $p<0.05$).

Figure 3: AT8 expression in brainstem of Tau.P301L mice 7 d post-isoflurane.
Successive 40 µm coronal sections stained with AT8 in a given Tau.P301L mice sacrificed 7 d after isoflurane anesthesia; right-hand pictures are enlargements of the doted black box drawn in the corresponding left-hand pictures; arrows indicate some AT8+ neurons. (Fig. 3 is to be compared with Fig. S1 and Fig. S2). a: caudal medulla; AT8+ neurons were present in the reticular formation (arrows) and external cuneatus (Cun) and hypoglossal motor nucleus (n12; enlargement in a1) but almost absent in the nucleus tractus solitarius (nTS); a2: n12 at a more caudal level. b: rostral medulla, note the high density of AT8+ neurons in the nucleus ambiguus (nA) (enlargement in b1), the raphe obscurus (Rob; enlargement in b2), prepositus (pp) and catecholaminergic C2 group (c2). c: pontine level; the KF (enlargement in c1), A6 (A6; enlargement in c2) and trigeminal motor nucleus (Mo5; enlargement in d1) contained high density of AT8+ neurons; note the KF location between the superior cerebellar peduncle (scp) and the principal sensory trigeminal nucleus (Pr5). d: midbrain; the periaqueductal gray (PAG) contained weakly stained AT8+ neurons in the ventrolateral part (enlargement in d2). Calibration bars: 400 and 200 µm for left- and right-hand pictures, respectively; 100 µm for the KF enlargement in c1.

Figure 4: Effects of forced-ventilation and memantine pre-treatment on AT8 expression in the brainstem of Tau.P301L mice 7 d post-isoflurane
a: AT8+ neurons in the nA of Tau.P301L mice 7 d post- isoflurane without other treatments (ISO) or with forced-ventilation (ISO+Vent) or with memantine pre-treatment (ISO+Mem). Histogram show mean and SEM of number of AT8+ neurons in the nA of ISO (n=3), ISO+Vent (n=3) and ISO+Mem (n=3) mice. Ventilation or memantine pre-treatment almost zeroed the number of AT8+ neurons in the nA (*, $p<0.05$). b: AT8+ neurons and AT8 optical density in the KF. Ventilation or memantine pre-treatment significantly reduced (*, $p<0.05$), but not zeroed, the AT8 optical density in the KF. c: as in a but for the NRA. Ventilation or memantine pre-treatment did not significantly reduce (ns, $p>0.05$) the number of AT8+ neurons. Calibration bars: 100 µm.

Table Legends

Figure 1

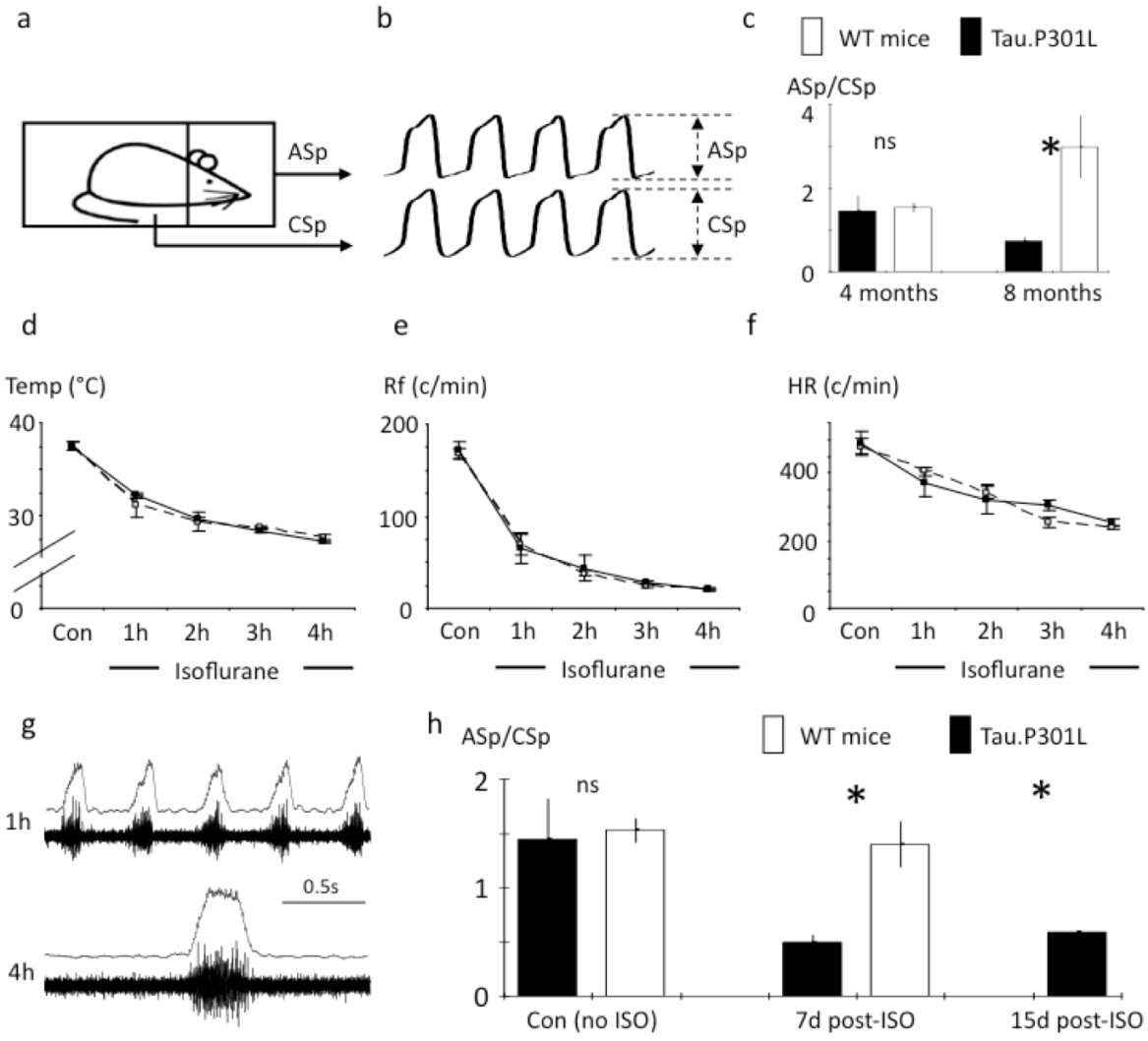
a
b
c
ASp
CSp
ASp
CSp
WT mice
Tau.P301L
ASp/CSp
ns
*
4 months
8 months
d
e
f
Temp (°C)
Rf (c/min)
HR (c/min)
Con
1h
2h
3h
4h
Isoflurane
g
h
1h
4h
0.5s
ASp/CSp
ns
*
*
Con (no ISO)
7d post-ISO
15d post-ISO

Figure 2

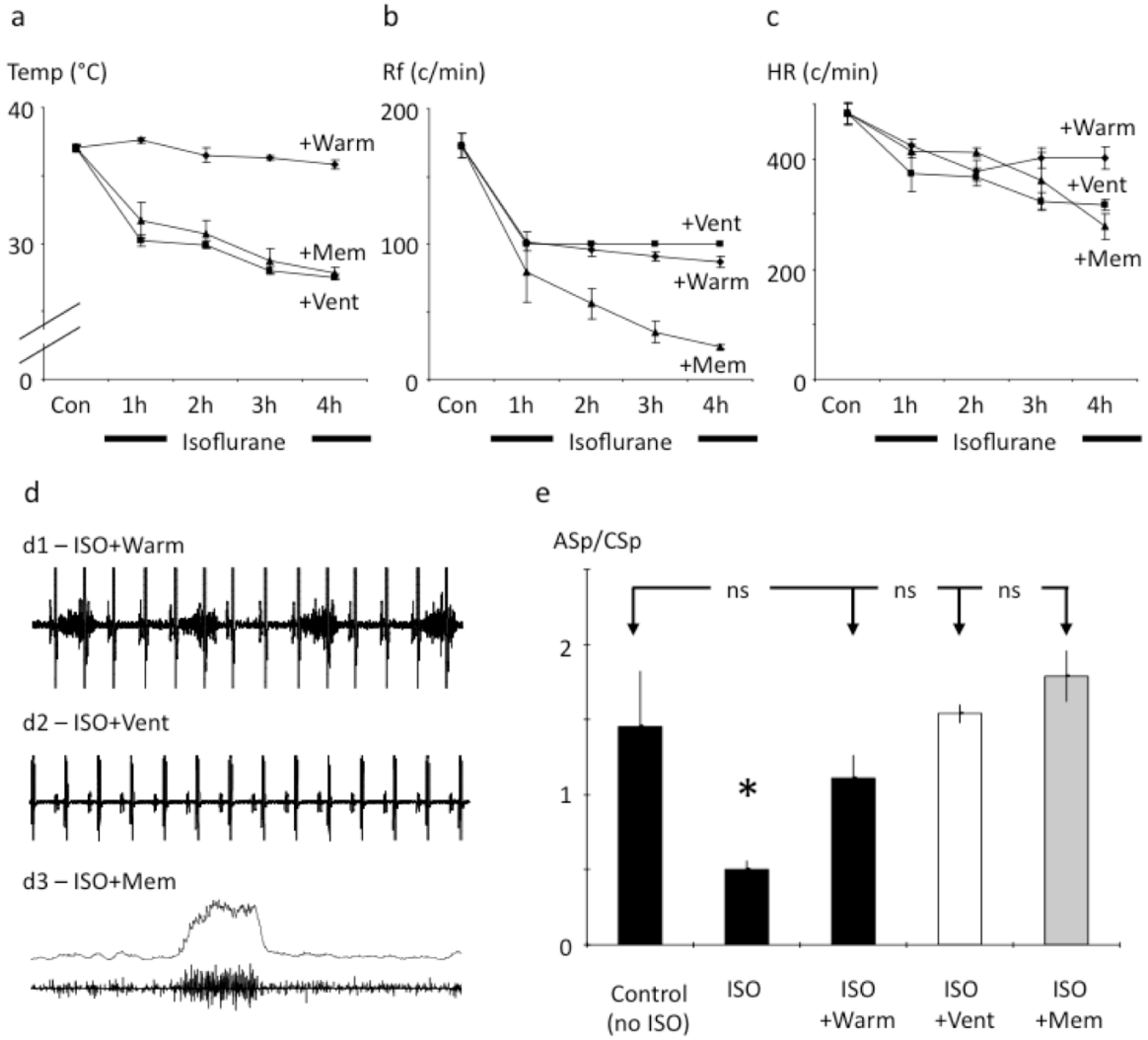
a
Temp (°C)
40
30
0
+Warm
+Mem
+Vent
Con
1h
2h
3h
4h
Isoflurane
b
Rf (c/min)
200
100
0
+Vent
+Warm
+Mem
Con
1h
2h
3h
4h
Isoflurane
c
HR (c/min)
400
200
0
+Warm
+Vent
+Mem
Con
1h
2h
3h
4h
Isoflurane
d
d1 – ISO+Warm
d2 – ISO+Vent
d3 – ISO+Mem
e
ASp/CSp
ns
ns
ns
2
1
0
*
Control
(no ISO)
ISO
ISO
+Warm
ISO
+Vent
ISO
+Mem

Figure 3

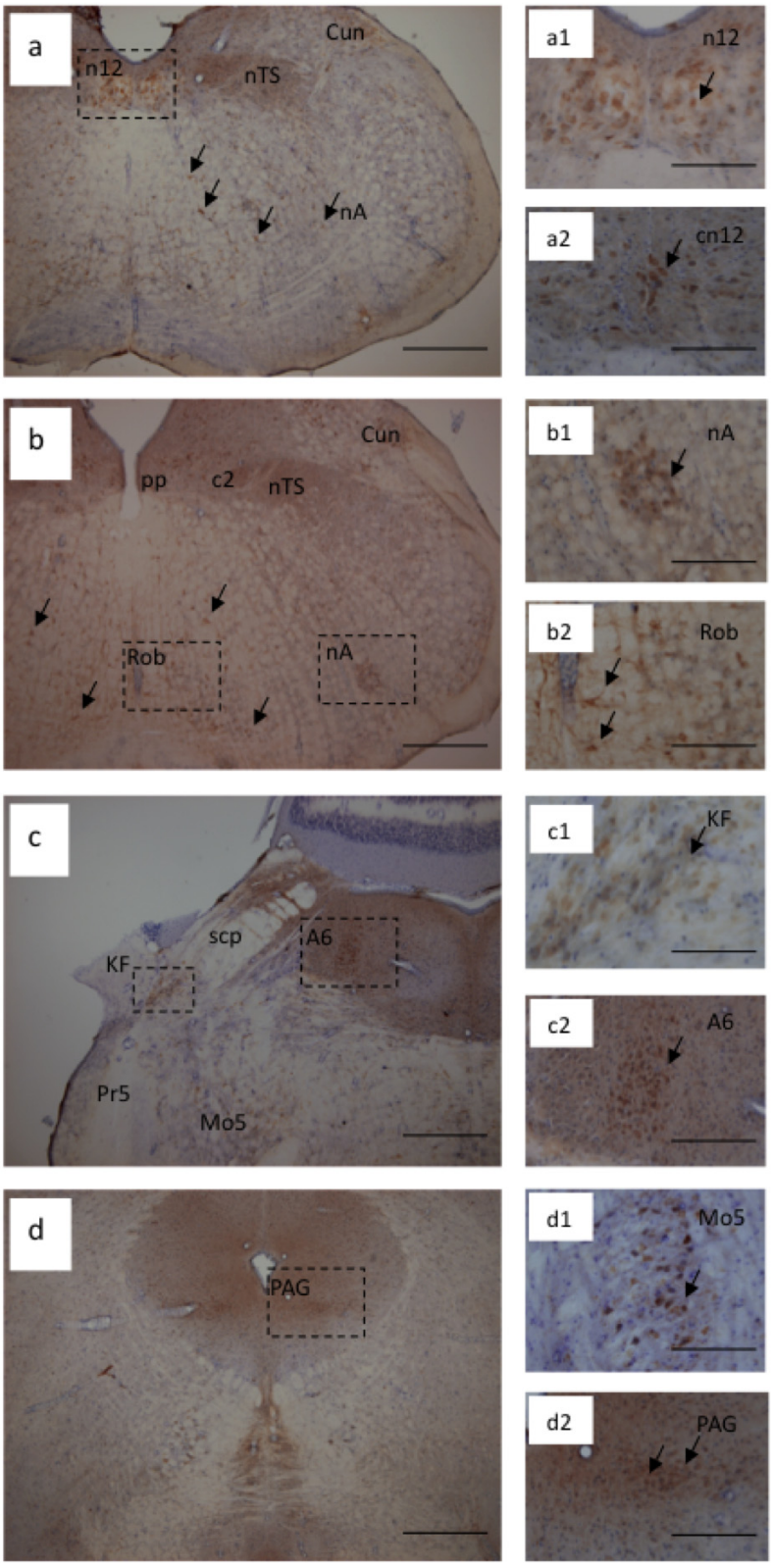
a
n12
nTS
Cun
nA
a1
n12
a2
cn12
b
pp
c2
nTS
Cun
Rob
nA
b1
nA
b2
Rob
c
scp
KF
A6
Pr5
Mo5
c1
KF
c2
A6
d
PAG
d1
Mo5
d2
PAG

Figure 4

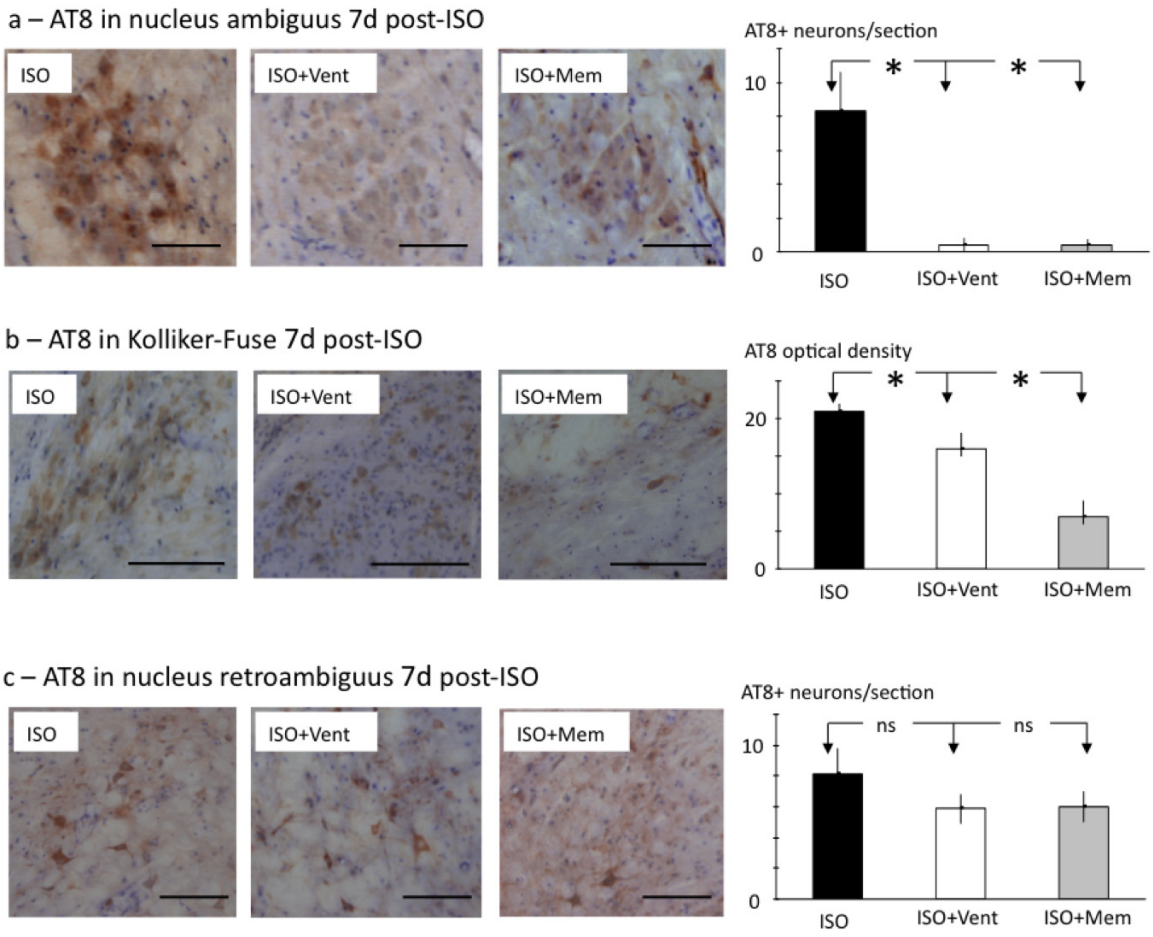
a – AT8 in nucleus ambiguus 7d post-ISO
ISO
ISO+Vent
ISO+Mem
AT8+ neurons/section
10
0
*
*
ISO
ISO+Vent
ISO+Mem
b – AT8 in Kolliker-Fuse 7d post-ISO
ISO
ISO+Vent
ISO+Mem
AT8 optical density
20
0
*
*
ISO
ISO+Vent
ISO+Mem
c – AT8 in nucleus retroambiguus 7d post-ISO
ISO
ISO+Vent
ISO+Mem
AT8+ neurons/section
10
0
ns
ns
ISO
ISO+Vent
ISO+Mem

Supplementary information (SI):

Material and Methods

We already reported in details methods for genetics, immunohistochemistry and breathing analysis (7, 8, 9). Isoflurane anesthesia protocols, consistent with those previously reported to precociously onset tauopathy in Tau-P301L mice (27), were adapted for special purposes.

Animals:

Experiments were performed in wild type (WT) FVB/N and transgenic Tau.P301L mice at age 4 and 8 mo. Tau.P301L mice were produced in the FVB/N genetic background to express the longest human tau isoform bearing the P301L mutation (Tau.4R/2N-P301L) under control of the mouse thy1 gene promoter aiming for neuron-specific expression starting in the third postnatal week (7). Tau.P301L mice, genotyped by PCR, were compared with age- and sex-matched control FVB/N mice.

Isoflurane anesthesia protocols:

Consistently with previous reports on precocious onset of tauopathy by isoflurane anesthesia of Tau-P301L mice (27), young mice at age 4 mo were subjected to 4 h exposure to isoflurane (1-chloro-2,2,2-trifluoroethyl difluoromethyl ether; AErrane; Baxter S.A., Belgium) at 1 MAC (Minimum Alveolar Concentration, 1.3% isoflurane) with hyperoxic gas mixture (30% O_2 in air instead of 21% O_2). At onset of anesthesia and every following h, we recorded rectal temperature (type T Thermocouple model 5005, Bioblock Scientific, France), respiratory frequency (home made constraint gauges), electromyogram (EMG) of chest respiratory muscles and electrocardiogram (epidermal electrodes inserted within the rib cage). Mice were either kept freely breathing during isoflurane exposure (with or without control of body temperature via external heater) or were intubated and ventilated. Forced ventilation was adjusted at 100 cycle per min (c/min) with 0.4 ml per cycle (SAR-830 ventilator, Bioseb, U.S.A.) and mice breathed either the same hyperoxic gas mixture as above (30% O_2 in air) or hypoxic gas mixture (10% O_2, 90% N_2) or hyperoxic / hypercapnic gas mixture (7% CO2, 30 % O2, 63% N2).

Plethysmographic analysis of breathing parameters:

As previously reported (8, 9), whole-body plethysmography was used to measure respiratory frequency (Rf, expressed in c/min) in conscious, unrestrained mice and double-chamber plethysmography to record the chest respiratory movements in the body chamber (Chest Spirogram, CSp) and the resulting airflow in the head chamber (Airflow Spirogram, ASp) (Fig. 1a). A reduced ASp vs. an increased CSp resulting in ASp/CSp ratio < 1 was indicative of upper airways dysfunction impairing the chest respiratory movement to produce adequate airflow. To minimize stress, the mice were habituated to the plethysmograph chamber before the recording sessions.

Biochemical analysis of blood parameters:

Values of pH, pO2 and pCO2 levels (mm of Hg) were measured in venous mixed blood samples of WT and Tau-P301L mice at age 4 mo (9). After tail blood vessels dilatation with hot water (40 – 42 °C°C) and small incision at the tip of the tail, 100 µL blood samples were collected in plastic capillaries with electrolyte-balanced heparin (Radiometer, 70 IU heparin per mL) and analysed with ABL 80 Flex analyser (Radiometer). Measurements were performed in different mice either prior to (control) or after 4 h isoflurane anesthesia or at 7 d post-isoflurane.

AT8 immunohistochemistry:

After mouse anesthesia (Nembutal; 120 mg/kg, i.p.) and transcardiac perfusion (ice-cold saline, 2 ml/min, 2 min), brainstems were removed, fixed (4% paraformaldehyde), and stored (0.1% sodium azide in PBS at 4°C) until sectioning (40 µm coronal vibratome sections). Briefly, the following procedures were performed (7, 8, 9): rinsing (PBS; 15 min with 1.5% H2O2 in 50% methanol/PBS), blockade of non-specific binding sites (10% fetal calf serum, 0.1% Triton X-100 in PBS), incubation with primary monoclonal antibodies AT8 (mouse anti-AT8, 1/2500) and AT100 (mouse anti-AT100, 1/1400), 1h incubation with the secondary goat antimouse IgG antiserum coupled to PAP (1:500 in blocking buffer; Dako), 5 min incubation in 50mM Tris HCl, pH 7.6, enzymatic staining with 3,3’ -diaminobenzidine (0.5 mg/ml), 0.3%H2O2 in 50 mM Tris HCl, pH 7.6.

Sections were counterstained with hematoxylin, ethanol dehydrated, delipidated in xylol and mounted for microscopic analysis of AT8 immunoreactivity. AT8 is a monoclonal antibody specifically directed against phosphorylated human protein tau at epitopes pS198/pS202pS/pS205 (Innogenetics, Gent, Belgium), possibly on the border between

physiology and pathology (7, 8, 9). AT8 immunoreactivity is the classical method to "stage" tauopathy in human brain (28).

Histological analysis:

For a given mouse, about 140-150 consecutive coronal sections were cut (from about 0.5 mm caudal to the pyramidal decussation to about 5 mm more rostral) and one section every three was stained with AT8. As previously in terminal Tau.P301L mice (9), we either counted AT8 positively stained (AT8+) neurons or measured the AT8 optical density to quantify AT8 staining in different structures defined from neuroanatomical points in mouse atlas (44). Mean values were obtained by averaging data from at least three different mice subjected to a given protocol of isoflurane anesthesia (either isoflurane alone, or isoflurane + warming, or isoflurane + ventilation, or isoflurane + memantine pre-treatment). In the nucleus ambiguus (nA) that contained large, easily discernible, AT8+ neurons on 3-4 sections (about 360-480 µm rostro-caudal extension), we counted the number of AT8+ neurons per section in a given mouse and averaged data from different mice to obtain the mean number of AT8+ neurons per nA. The same procedure was used for the nucleus retroambiguus (NRA). For the Kölliker-Fuse (KF) nucleus that extended on 6-8 consecutive sections (about 720-960 µm rostro-caudal extension) and contained small, intermingled AT8+ neurons, counting was rather difficult. Therefore, we used dedicated software to quantify the mean optical density of AT8 staining in the whole KF area of a given mouse (ImageJ created by Wayne Rasband, NIH, USA). For each KF section, pictures were taken of a 500x500 µm square area centered on the KF (ventral to the lateral parabrachial nucleus, lateral to the superior cerebella peduncle, medial to the middle cerebellar peduncle, and dorsal to the principal trigeminal sensory nucleus). To minimize variations in the square positioning and the intensity of the AT8 staining between different sections and different mice, the analysis was performed by the same person (CM) using standardized protocols (homogenisation for positioning, brightness and contrast adjustments; colour threshold set to remove ¾ of the blue spectrum). In a given mouse, the AT8 optical density was measured for each section containing the KF and individual values were averaged to obtain the mean AT8 optical density of the KF of this mouse. Data from different mice were averaged to obtain the mean value of the AT8 optical density in the KF.

Statistics:

Values are given as mean ± standard error of the mean (S.E.M.). First, normal distribution of values was assessed prior to statistical tests. Intra-group statistics were performed using paired Student *t* test, inter-group statistics were performed using Student *t* test (2 groups) or one-way analysis of variance (ANOVA) with post-hoc Newman-Keuls (>2 groups) (Igor Pro software; WaveMetrics, Oregon, USA). Statistical differences were regarded as significant if $P < 0.05$.

Table 1: Mean and SEM of blood parameters and respiratory frequency (Rf) of young Tau.P301L (Tau) and WT mice prior to, during (4th hour) and 7 days after isoflurane exposure (ns and * indicate non significant and significant differences, respectively).

Conditions	Strain	pH	pCO2 (mm Hg)	pO2 (mm Hg)	Rf (c/min)
Prior to ISO exposure	WT (n=8)	7.18 ± 0.02	60.37 ± 4.46	44.88 ± 6.22	175 ± 4
	Tau vs. WT	*ns*	*ns*	*ns*	*ns*
	Tau (n=8)	7.20 ± 0.02	60.63 ± 5.30	51.50 ± 3.54	173 ± 6
4th h of ISO exposure	WT (n=4)	7.28 ± 0.03	44.50 ± 3.48	43.75 ± 4.59	20 ± 1
	Tau vs. WT	*ns*	*ns*	*ns*	*ns*
	Tau (n=4)	7.24 ± 0.02	43.75 ± 4.25	42.50 ± 1.49	21 ± 1
	WT (prior vs. 4h)	*ns*	*ns*	*ns*	*
	Tau (prior vs. 4h)	*ns*	*ns*	*ns*	*
7 d after ISO exposure	WT (n=4)	7.20 ± 0.04	62.67 ± 2.19	46.33 ± 3.71	177 ± 8
	Tau vs. WT	*ns*	*ns*	*ns*	*ns*
	Tau (n=4)	7.22 ± 0.01	55.00 ± 2.48	58.25 ± 7.06	183 ± 9
	WT (7 d vs. 4 h)	*ns*	*ns*	*ns*	*
	Tau (7d vs. 4 h)	*ns*	*ns*	*ns*	*
	WT (7d vs. prior)	*ns*	*ns*	*ns*	*ns*
	Tau (7d vs. prior)	*ns*	*ns*	*ns*	*ns*

Figure S1

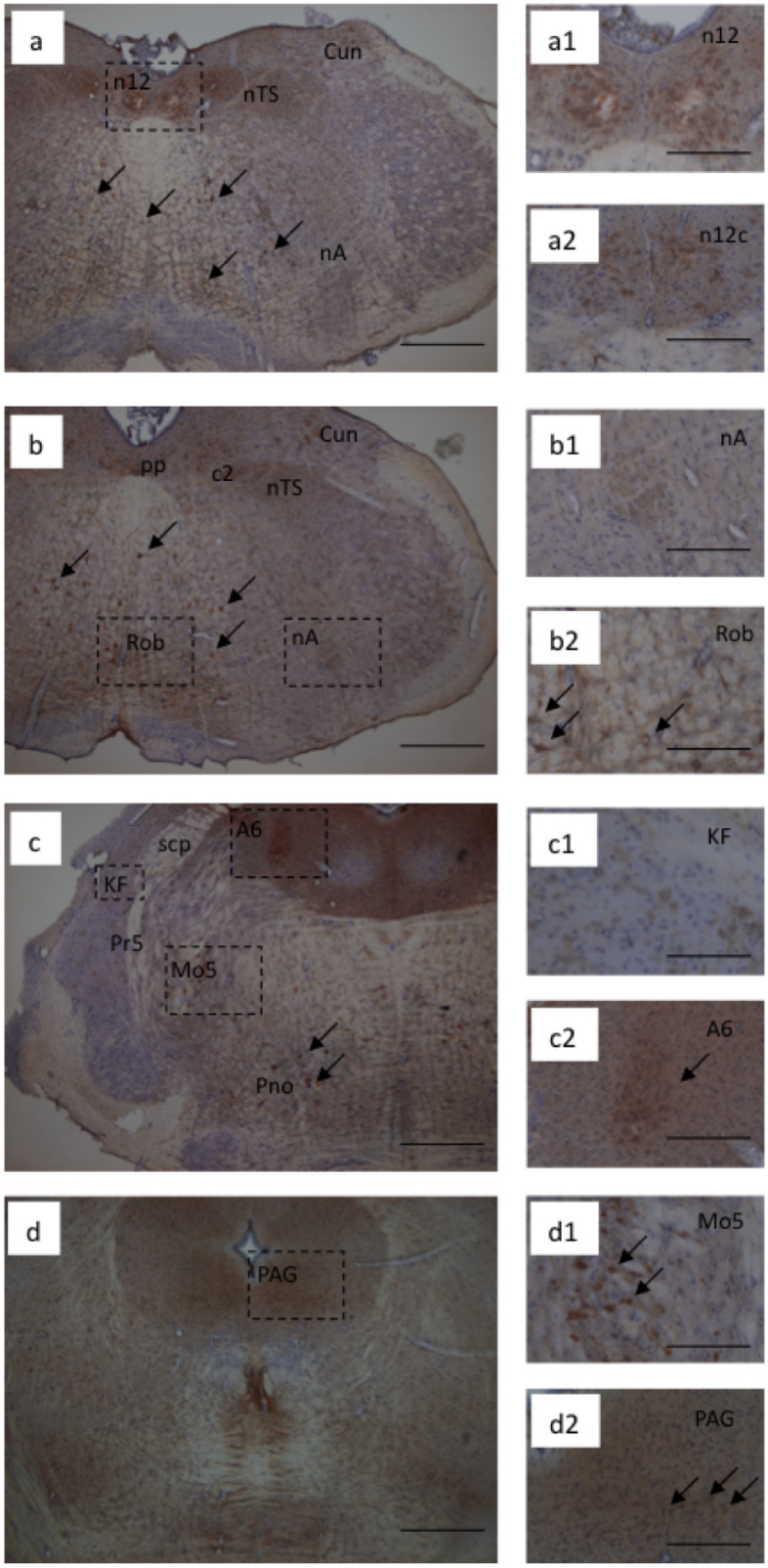
a
Cun
n12
nTS
nA
a1
n12
a2
n12c
b
Cun
pp
c2
nTS
Rob
nA
b1
nA
b2
Rob
c
scp
A6
KF
Pr5
Mo5
Pno
c1
KF
c2
A6
d
PAG
d1
Mo5
d2
PAG

Figure S1: Effect of forced-ventilation during isoflurane anesthesia on AT8 expression in brainstem of Tau.P301L mice 7 d post-isoflurane.

To be compared with Fig. 3 (isoflurane anesthesia without ventilation). Successive coronal brainstem sections (thickness 40 µm) stained with AT8 in a given Tau.P301L mice (age 4 mo), sacrificed 7 d after isoflurane anesthesia with forced ventilation; right-hand pictures are enlargements of the doted black box drawn in the corresponding left-hand pictures. Arrows show some AT8+ neurons.

a: caudal medulla; AT8+ neurons were observed in the reticular formation, especially in the external cuneatus (Cun) and hypoglossal motor nucleus (n12; enlargement in a1) but were almost absent in the nucleus tractus solitarius (nTS); b2 shows AT8+ neurons in the n12 of the same mouse but at a more caudal level.

b: rostral medulla, note the faint labeling of the nA (enlargement in b1) and the frequent, well stained AT8+ neurons in the raphe obscurus (Rob; enlargement in b2), reticular formation (arrows), prepositus (pp) and catecholaminergic C2 group (c2).

c: pontine level; note the weak AT8 labeling of the KF (enlargement in c1) but the frequent, well stained AT8+ neurons in the locus coeruleus (A6; enlargement in c2), the oral pontine reticular nucleus (Pno; arrows show some AT8+ neurons) and trigeminal motor nucleus (Mo5; enlargement in d1).

d: midbrain; the periaqueductal gray (PAG) contained some weakly stained AT8+ neurons in its ventrolateral part (enlargement in d2).

Calibration bars: 400 and 200 µm for left- and right-hand pictures, respectively; 100 µm for the KF enlargement in c1.

Figure S2

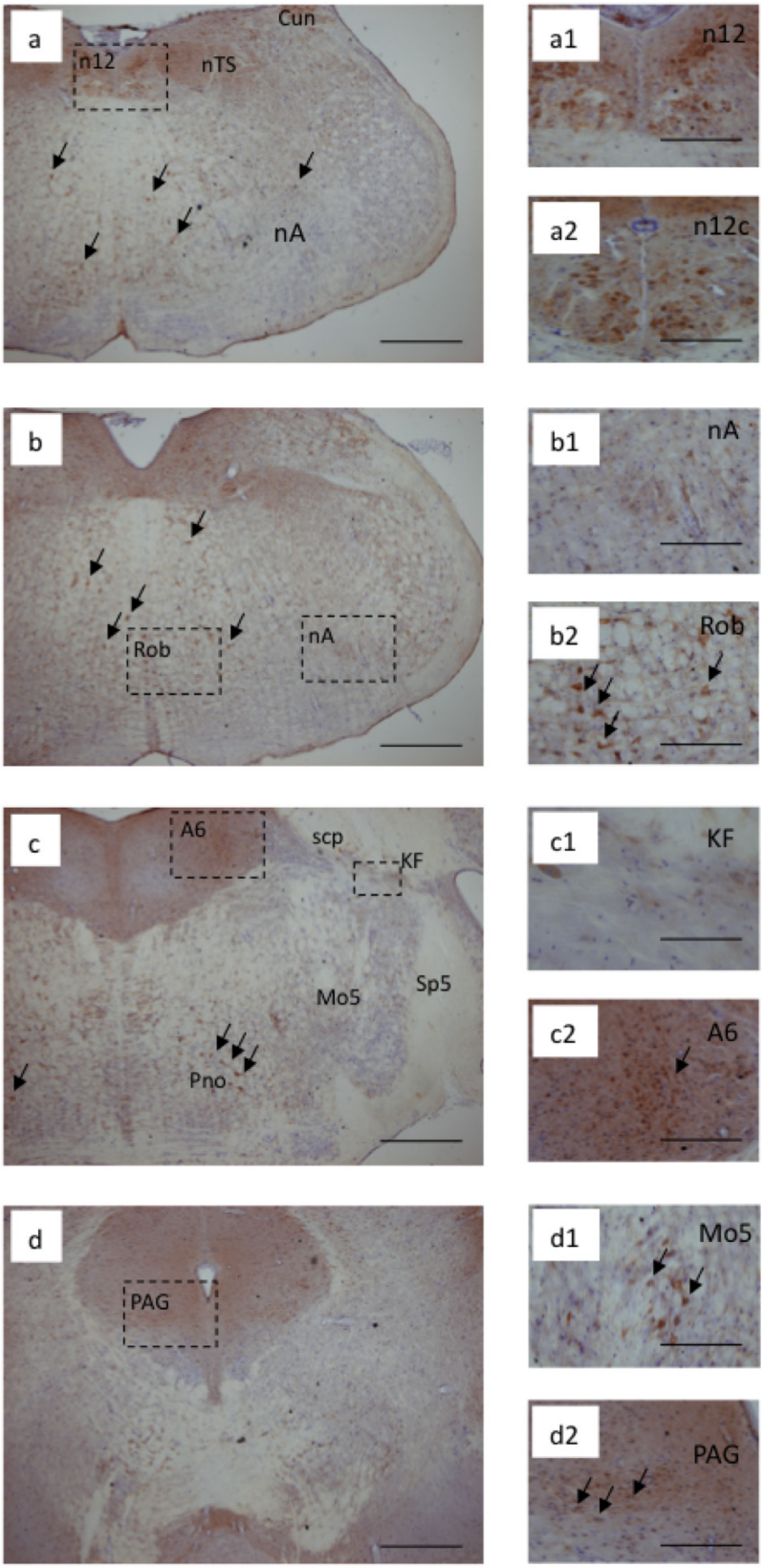
a
Cun
n12
nTS
nA
a1
n12
a2
n12c
b
Rob
nA
b1
nA
b2
Rob
c
A6
scp
KF
Mo5
Sp5
Pno
c1
KF
c2
A6
d
PAG
d1
Mo5
d2
PAG

Figure S2: Effect of memantine treatment prior to isoflurane anesthesia on AT8 expression in brainstem of Tau.P301L mice 7 d post-isoflurane.

To be compared with Fig. 3 (isoflurane anesthesia without memantine pre-treatment). Successive coronal brainstem sections (thickness 40 µm) stained with AT8 in a given Tau.P301L mice (age 4 mo), sacrificed 7 d after isoflurane anesthesia preceded by memantine pre-treatment. right-hand pictures are enlargements of the doted black box drawn in the corresponding left-hand pictures. Arrows show some AT8+ neurons.

a: caudal medulla; AT8+ neurons were observed in the reticular formation, especially in the external cuneatus (Cun) and hypoglossal motor nucleus (n12; enlargement in a1) but were almost absent in the nucleus tractus solitarius (nTS); b2 shows AT8+ neurons in the n12 of the same mouse but at a more caudal level.

b: rostral medulla, note the faint labeling of the nA (enlargement in b1) and the frequent, well stained AT8+ neurons in the raphe obscurus (Rob; enlargement in b2), reticular formation (arrows), prepositus (pp) and catecholaminergic C2 group (c2).

c: pontine level; note the weak AT8 labeling of the KF (enlargement in c1) but the frequent, well stained AT8+ neurons in the locus coeruleus (A6; enlargement in c2), the oral pontine reticular nucleus (Pno; arrows show some AT8+ neurons) and trigeminal motor nucleus (Mo5; enlargement in d1).

d: midbrain; the periaqueductal gray (PAG) contained some weakly stained AT8+ neurons in its ventrolateral part (enlargement in d2).

Calibration bars: 400 and 200 µm for left- and right-hand pictures, respectively; 100 µm for the KF enlargement in c1.

Discussion

I - Synthèse des résultats présentés dans cette thèse

Tout au long de la vie d'un organisme, le système respiratoire doit équilibrer l'apport en O_2 avec sa consommation. Chez les mammifères, les voies aériennes supérieures (VAS) leur confèrent un avantage évolutif, leur permettant de dissocier respiration et mastication, et de vocaliser. Mais cet avantage a un coût, celui d'une grande complexité dans le contrôle nerveux de la commande respiratoire et des actes moteurs associés, notamment pour la coordination entre les VAS et la pompe respiratoire thoracique. Deux périodes sont particulièrement perméables à une altération de cette coordination : la maturation et la sénescence. L'enjeu principal de la respiration étant le maintien de l'homéostasie gazeuse sanguine, toute incapacité, totale ou partielle, de régulation de la respiration en réponse à des variations de pressions partielles sanguines en O_2, CO_2 et/ou pH entraîne souvent une situation pathologique, dont la gravité diffère en fonction de l'âge. Dans cette thèse, nous nous sommes intéressés à l'altération du système respiratoire et en particulier des VAS dans deux modèles murins de pathologies humaines, une neurodéveloppementale (souris *Mecp2*$^{-/y}$) et une neurodégénérative (souris Tau.P301L). Nous avons également étudié différents mécanismes induisant des défauts respiratoires chez la souris, sauvage ou transgénique, et en particulier en réponse à l'hypercapnie.

Les souris *Mecp2*$^{-/y}$ sont un modèle murin reconnu du Syndrome de Rett (SR), une maladie rare causée par la mutation du gène codant pour la protéine 2 liée au méthyl-CpG (protéine MeCP2), un répresseur transcriptionnel. Les souris *Mecp2*$^{-/y}$, comme les patientes atteintes par le Syndrome de Rett, respirent normalement à la naissance mais développent pendant la période postnatale des troubles respiratoires graves, souvent associés à leur mortalité précoce. Chez les souris *Mecp2*$^{-/y}$, ces troubles respiratoires apparaissent vers le 30^{e} jour post-natal (P30), sous la forme d'un rythme respiratoire erratique interrompu d'apnées longues et fréquentes. Dans cette thèse, nous montrons que les anomalies de la rythmogenèse respiratoire des souris *Mecp2*$^{-/y}$ sont précédées par des anomalies des régulations respiratoires. En effet, pendant la période pré-symptomatique (avant P30), l'exposition des souris *Mecp2*$^{-/y}$ à une hypoxie ou à une hypercapnie modérée provoque l'apparition prématurée d'altérations du rythme, semblables à celles observées plus tard en période symptomatique (après P30). De plus, pendant la période pré-symptomatique (avant P30), les souris *Mecp2*$^{-/y}$ présentent une

respiration anormale après un soupir spontané, ce qui confirme des anomalies précoces des régulations respiratoires par l'état d'inflation pulmonaire et le niveau d'oxygénation sanguine. Avec l'âge, les anomalies des régulations respiratoires des souris *Mecp2*$^{-/y}$ s'aggravent : à P30, la réponse ventilatoire à l'hypoxie (RVH) est exacerbée, la respiration après un soupir est erratique et la fréquence des apnées est considérablement accrue. La moitié des apnées sont désormais de type obstructif, révélant un défaut de coordination des VAS chez les souris *Mecp2*$^{-/y}$ en période pathologique, avec des muscles respiratoires thoraciques qui luttent contre la fermeture des VAS. Ces résultats suggèrent que l'altération de la rythmogenèse respiratoire chez les souris *Mecp2*$^{-/y}$ est postérieure à l'altération de la coordination de l'activité des VAS pendant les différentes phases du cycle respiratoire. Cette altération de la commande des VAS qui n'est discernable que pendant la période tardive de maturation du réseau respiratoire, est potentiellement induite sinon aggravée par des hypoxies et hypercapnies modérées.

Chez les souris, il existe de nombreux fonds génétiques traditionnellement utilisés dans la recherche scientifique. Les souris C57Bl/6J et FVB/N sont deux fonds génétiques très répandus pour la transgénèse, or le génotype de fond peut avoir un effet en soi sur le phénotype de ces souris, et notamment sur le phénotype respiratoire. Dans cette thèse, nous montrons que dès la naissance, la respiration des souris C57Bl/6J est irrégulière, parsemée d'apnées d'origine centrale, contrairement aux souris FVB/N chez qui la respiration est robuste. Nous montrons que cette différence persiste avec l'âge et ce au moins jusqu'à l'âge de 1 an. Les souris C57Bl/6J ont une RVH et une réponse ventilatoire à l'hypercapnie (RVHC) plus faibles et une diminution de la ventilation liée à l'âge plus forte que les souris FVB/N. Egalement, les gaz du sang et le métabolisme de la sérotonine (5-HT) sont différents entre les souris C57Bl/6J et FVB/N. Or les neurones 5-HT jouent un rôle prépondérant dans la chémosensibilité centrale et donc dans la RVHC. Nous montrons sur le réseau respiratoire isolé *in vitro* du nouveau-né que des manipulations pharmacologiques du système 5-HT (et en particulier *via* la fluoxétine, un inhibiteur de la recapture de la sérotonine engendrant une augmentation des taux endogènes de 5-HT) altèrent la réponse respiratoire à l'acidose (mimant *in vitro* l'hypercapnie), ce qui pourrait être le signe d'une altération du dialogue synaptique entre les neurones 5-HT et les neurones chémosensibles du noyau rétrotrapézoïde. Ce travail s'inscrit également dans le cadre d'une revue de la littérature traitant de l'implication de la 5-HT dans la physiologie et les pathologies respiratoires. De plus, nous nous sommes intéressés à un autre mécanisme déprimant la RVHC chez la souris adulte,

impliquant l'érythropoïétine (EPO). L'EPO, une cytokine connue pour son effet stimulateur de l'érythropoïèse, possède de nombreuses autres actions notamment centrales, et contribue à l'acclimatation respiratoire à l'hypoxie chronique. Nous montrons dans cette thèse que l'EPO diminue la RVHC par une action directe à la fois au niveau périphérique (corps carotidiens) et central (réseau respiratoire du tronc cérébral), mais aussi par une action indirecte *via* la polyglobulie. Cette désensibilisation de la RVHC pourrait jouer un rôle majeur dans la survenue du mal chronique des montagnes.

Les tauopathies, dont fait partie la maladie d'Alzheimer (MA), sont des pathologies neurodégénératives caractérisées par la formation d'agrégats neurofibrillaires de protéines tau hyperphosphorylées. La protéine tau est une protéine associée aux microtubules, dont le niveau de phosphorylation détermine si elle est sous la forme liée aux microtubules (peu phosphorylée) ou libre dans le cytosole (hyperphosphorylée). Les recherches scientifiques et médicales se sont quasiment toutes focalisées sur les structures supérieures du cerveau atteintes par la tauopathie, et ont négligé l'atteinte du tronc cérébral et ses répercutions. Dans cette thèse, nous avons utilisé un modèle murin de tauopathie, les souris Tau-P301L, qui expriment une isoforme humaine mutée de la protéine tau dans les neurones. Chez ces souris Tau-P301L qui meurent précocement vers l'âge de 10 mois, nous avons montré pour la première fois une altération précoce de la commande post-inspiratoire des VAS : dès l'âge de 8 mois, la commande post-inspiratoire des VAS induit paradoxalement une fermeture partielle des VAS pendant l'inspiration. Les souris Tau-P301L doivent donc fournir un effort respiratoire accru pour inspirer un faible volume d'air. Cette altération de la commande post-inspiratoire des VAS est liée à une atteinte par la tauopathie de certains noyaux respiratoires, et en particulier du noyau de Kölliker-Fuse (KF). Egalement, l'hypercapnie aggrave les déficits respiratoires des souris Tau-P301L. Nous avons ensuite montré que l'altération de la commande des VAS affecte avec l'âge une autre activité : la vocalisation. En effet, la vocalisation ultrasonore des souris Tau-P301L âgées de 8 mois est très altérée comparée à celle des souris Tau-P301L jeunes (4 mois) ou des souris contrôles âgées de 8 mois. Cette altération qui se caractérise par une forte diminution qualitative et quantitative des vocalisations, est certainement liée à la tauopathie du KF (intervenant dans la coordination entre respiration et vocalisation), mais aussi et surtout à la tauopathie affectant la substance grise périaqueducale (PAG) et le noyau rétro-ambigu (NRA). L'altération de la vocalisation des souris Tau-P301L âgées peut rappeler dans une certaine mesure l'altération du langage des patients âgés souffrant de la MA. En stade terminal de la pathologie, nous avons montré

que les troubles respiratoires des souris Tau-P301L s'aggravent, induisant même des anomalies du rythme et des régulations respiratoires. A cet âge avancé, les régions 5-HT étant atteintes anatomiquement par la tauopathie, le métabolisme de la 5-HT est altéré, ce qui peut contribuer à l'aggravation des troubles respiratoires. L'altération 5-HT et l'aggravation des troubles respiratoires des souris Tau-P301L âgées peut rappeler dans une certaine mesure les désordres respiratoires au cours du sommeil des patients âgés souffrant de la MA. Enfin, nous montrons qu'une anesthésie de type clinique (mais sans chirurgie associée) des souris Tau-P301L jeunes (4 mois, donc en période pré-symptomatique) induit prématurément une hyperphosphorylation de tau dans le KF, le NRA et la PAG, ainsi qu'une altération marquée de la commande post-inspiratoire des VAS, ces altérations persistant après l'anesthésie. L'anesthésie des souris Tau-P301L jeunes induisant précocement les symptômes des souris âgées, nos résultats sont en parfait accord avec le bilan dressé par un consensus scientifique sur les dangers potentiels liés à l'anesthésie des patients à risque de MA. Dans un contexte appliqué, nous montrons chez la souris Tau-P301L que la ventilation artificielle pendant l'anesthésie ou un prétraitement à la mémantine, un antagoniste des récepteurs NMDA, empêche l'apparition des symptômes prématurés. Il se pourrait ainsi qu'un mécanisme d'excitotoxicité impliquant les récepteurs NMDA des centres respiratoires puisse conduire au déclenchement de la tauopathie et aux altérations respiratoires consécutives.

Dans cette discussion, nous allons montrer les interactions qui existent entre les différentes études réalisées au cours de cette thèse, afin d'en dégager les fils conducteurs, et en particulier la maturation / vieillissement du contrôle central respiratoire et de la RVHC. De plus, nous allons développer certaines avancées permises par ces études en les situant dans leur contexte scientifique, abordant certains points précis non discutés dans les articles présents dans cette thèse. Nous terminerons en évoquant des travaux encore en cours de réalisation, et les perspectives qu'ils offrent.

II - Influence du génotype sur le contrôle central respiratoire et en particulier sur la commande des VAS

Dans cette thèse, nous nous sommes particulièrement intéressés à l'atteinte du système respiratoire lors de deux pathologies, le Syndrome de Rett qui est une neuropathologie neurodéveloppementale, et la tauopathie au sens large, une maladie neurodégénérative. Nous avons étudié ces pathologies chez des modèles murins transgéniques, les souris *Mecp2*$^{-/y}$ pour le Syndrome de Rett et les souris Tau-P301L pour la tauopathie. Or les souris de laboratoire ont été sélectionnées génétiquement, certaines comme les C57Bl6 depuis plus d'un siècle (The Jackson Laboratory, n.d.). Des accouplements consanguins successifs ont permis la stabilisation de certains génotypes, afin de réduire la variabilité phénotypique au sein d'une même lignée. Grâce à cela, il est possible de connaître par exemple l'effet d'une drogue ou d'une mutation génétique en n'ayant recours qu'à de petits échantillons d'animaux, ce qui entre dans la logique éthique de réduction du nombre d'animaux utilisés lors des expérimentations scientifiques. Cependant, le lissage génétique par la consanguinité réduit le spectre phénotypique des souris étudiées, réduisant par conséquent les interactions potentielles de l'objet des recherches avec l'organisme murin. Pour essayer de pallier ce problème et d'offrir une diversité génétique permettant l'étude comparée de différents phénotypes, plusieurs souches consanguines de souris ont été créées. Parmi les plus utilisées se trouvent les souris C57Bl/6J et les souris FVB/N, notamment car elles sont particulièrement permissives à la transgénèse (Taketo et al., 1991; Montagutelli, 2000; Giménez and Montoliu, 2001).

Les souris *Mecp2*$^{-/y}$ que nous avons étudiées sont de fond C57Bl/6J, et les souris Tau-P301L sont de fond FVB/N. Or nous avons montré que ces deux fonds génétiques influencent de manière significative le contrôle central respiratoire, les souris C57Bl/6J présentant une respiration beaucoup plus irrégulière et beaucoup plus d'apnées que les souris FVB/N. Ces résultats sont en accord avec des travaux antérieurs de notre équipe de recherche, qui ont montré que les apnées spontanées des souris C57Bl/6J sont dues à un prolongement anormalement long de la phase post-inspiratoire générant la fermeture des VAS (Stettner et al., 2008b). Egalement, chez des souris déficientes pour la protéine Teashirt 3, une altération

des motoneurones laryngés cause la mort postnatale de ces souris, et ce de manière plus précoce et dramatique quand la mutation est exprimée sur le fond C57Bl/6J que sur le fond CD1 (des souris blanches issus du fond Swiss, comme les FVB/N) (Caubit et al., 2008, 2010). Il se pourrait donc que le fond C57Bl/6J soit particulièrement propice aux altérations des VAS, ce qui peut être un facteur aggravant pour les troubles des VAS observés chez les souris *Mecp2*$^{-/y}$. En effet, nous avons montré que la respiration erratique des souris *Mecp2*$^{-/y}$ est composée *in vivo* d'une proportion importante (≈ 40%) d'apnées obstructives d'origine centrale, induisant une fermeture prolongée des VAS contre laquelle lutte la pompe respiratoire thoracique. Ces résultats complètent ceux de Stettner et collaborateurs, qui avaient montré précédemment *in situ* que les pauses respiratoires des souris *Mecp2*$^{-/y}$ sont dues à un prolongement de la phase post-inspiratoire (Stettner et al., 2007). Ainsi, il est troublant de remarquer que les caractéristiques des apnées des souris *Mecp2*$^{-/y}$ ressemblent à celles des souris C57Bl/6J. Toutefois, il faut garder à l'esprit que les apnées des souris *Mecp2*$^{-/y}$ sont nettement plus fréquentes, en particulier après P40, que celles des souris C57Bl/6J (Viemari et al., 2005; Stettner et al., 2007).

A l'inverse, la stabilité respiratoire des souris FVB/N peut représenter un facteur atténuant la sévérité des altérations respiratoires liées à une mutation. Les souris FVB/N présentent un ratio flux aérien / mouvements thoraciques respiratoires (ASp/CSp, pour Airflow Spirogram/Chest Spirogram) mesuré en pléthysmographie double chambre largement supérieur à 1, signe d'une bonne efficacité ventilatoire entre la pompe ventilatoire thoracique et les VAS. Ce ratio passe même à 3 chez les souris FVB/N âgées de 8 mois, ce qui traduirait une amélioration de l'efficacité ventilatoire avec l'âge, amélioration absente chez les souris C57Bl/6J. Cela n'empêche pas la survenue des altérations respiratoires chez les souris Tau-P301L à 8 mois, avec un déclenchement de la phase post-inspiratoire pendant l'inspiration, engendrant ainsi un effort ventilatoire accru pour un flux aérien diminué (ratio ASp/CSp largement < à 1). On peut postuler que l'altération respiratoire des souris Tau-P301L est sévère, car s'exprimant sur un fond génétique peu enclin à exprimer ce type de déficit et que l'altération respiratoire aurait été extrêmement plus marquée si la mutation avait été réalisée sur un autre fond génétique, comme le fond C57Bl/6J. Toutefois, ce postulat n'est pas vérifiable car il n'existe pas de souris Tau-P301L créée sur fond pur C57Bl/6J, toutes les autres transgénèses de ce type ayant été réalisées sur des fonds mixtes C57Bl/6J / DBA / SW etc. (Lewis et al., 2000; Götz et al., 2001; Alzforum, 2010). Egalement, le principe même de la transgénèse est variable, en fonction du promoteur utilisé, de son site d'insertion dans

l'ADN etc., ce qui peut influencer grandement le phénotype respiratoire. De manière contre-intuitive, lorsque la même mutation du gène *Mecp2* (une délétion exonique étendue) est effectuée sur un fond pur 129 ou sur un fond mixte 129 / C57Bl/6J, les premières ont une espérance de vie moitié moindre par rapport aux deuxièmes (Pelka et al., 2006). D'autres auteurs ont réalisé cette délétion exonique dans le gène *Mecp2* sur un fond mixte 129 / C57Bl/6J / BALB/c, résultant en une survenue des atteintes respiratoires et de la mortalité dans les mêmes délais que ceux que l'on a retrouvés sur fond pur C57Bl/6J (Chen et al., 2001). Il est par conséquent difficile d'anticiper l'interaction entre un fond génétique et une mutation, mais au regard de la variabilité inter-génotypes qui existe au niveau de la commande respiratoire, il est important de ne pas négliger le fond génétique utilisé et de prendre en compte l'influence qu'il peut engendrer sur les résultats obtenus.

Un soupir est une inspiration très ample, qui est considérée comme servant à lutter contre l'atélectasie pulmonaire, maintenir la compliance pulmonaire, et améliorer transitoirement l'oxygénation alvéolaire (Poets et al., 1997; Patroniti et al., 2002; Qureshi et al., 2009). Le soupir est normalement suivi d'une bradypnée en deux phases, la première imputée au réflexe de Hering-Breuer, la seconde à l'hyperoxygénation sanguine induite par le soupir. Stettner et collaborateurs ont montré que lors de stimulations vagales successives *in situ* visant à reproduire artificiellement un réflexe de Hering-Breuer, les souris C56Bl/6J présentent un échappement respiratoire après plusieurs stimulations (Stettner et al., 2007). Cet échappement respiratoire est en fait une désensibilisation du réseau respiratoire à la stimulation vagale, avec un arrêt de l'apnée et un retour des décharges respiratoires alors que la stimulation vagale continue. Non seulement les souris *Mecp2*$^{-/y}$ ne présentent pas d'échappement respiratoire, mais elles produisent même une apnée de plusieurs secondes après l'arrêt de la stimulation vagale. Ces résultats sont concordants avec nos données qui montrent que les souris *Mecp2*$^{-/y}$ présentent *in vivo* une altération de la respiration post-soupir, avec une apnée de longue durée due à une fermeture des VAS. Cette atteinte spécifique post-soupir ne se retrouve pas sur les souris contrôles fond C57Bl/6J, et constitue donc certainement une altération propre à la mutation du gène *Mecp2*. Nous avons vérifié la régulation respiratoire post-soupir sur les souris FVB/N et les souris Tau-P301L, aucune différence inter-spécifique n'a été décelée. Il est possible que le niveau de maturation du système respiratoire ait une importance cruciale dans cette différence, comme nous le verrons dans le chapitre suivant.

III - Le vieillissement du contrôle respiratoire et en particulier des VAS, de la maturation à la sénescence

La maturation et la sénescence du contrôle nerveux respiratoire sont deux périodes particulièrement permissives aux pathologies, en particulier celles affectant les VAS. Au cours de la maturation, la transition de phase dans le cycle respiratoire entre inspiration et post-inspiration passe d'une activité réflexe sous-tendue par les afférences pulmonaires, à une activité codée centralement modulée par les afférences pulmonaires. Cette maturation implique tout particulièrement les VAS, car elles sont l'effecteur principal de la post-inspiration. Egalement, Dutschmann et collaborateurs ont montré chez la souris, que P15 est un âge critique autour duquel se fait la maturation de la phase post-inspiratoire (Dutschmann et al., 2009). Chez les souris *Mecp2*$^{-/y}$, les altérations respiratoires sont traditionnellement décrites comme apparaissant après P30, s'aggravant progressivement jusqu'à la mort de l'animal vers P60-80 (Viemari et al., 2005; Katz et al., 2009). Dans cette thèse nous montrons que des stimuli périphériques respiratoires comme une hypoxie ou une hypercapnie modérée, et les afférences sensorielles post-soupir, démasquent dès P15 des altérations du contrôle central respiratoire chez les souris *Mecp2*$^{-/y}$. Cette concordance temporelle avec la maturation de la post-inspiration est intéressante, et peut contribuer à expliquer l'impression de régression maturationnelle qui ressort des analyses respiratoires des souris *Mecp2*$^{-/y}$. Il semble notamment que la post-inspiration ne devient jamais une phase codée centralement et demeure une activité réflexe dépendante des afférences pulmonaires, comme suggéré par la non-apparition d'un échappement respiratoire lors de stimulations électriques vagales et les apnées suivant ces stimulations vagales (Stettner et al., 2007). Cette régression maturationnelle pourrait expliquer la déstabilisation du réseau respiratoire qui s'ensuit, avec l'apparition et l'augmentation croissante d'apnées centrales obstructives et non-obstructives, et d'irrégularités du rythme respiratoire. En effet, la phase post-inspiratoire est la plus modulable de toutes les phases du cycle respiratoire, permettant l'intégration d'activités complexes comme la vocalisation et la déglutition. Le Syndrome de Rett est une maladie épigénétique, car liée à l'absence d'un répresseur transcriptionnel (la protéine 2 liée au méthyl-CpG) (Amir et al., 1999; Shahbazian et al., 2002). Si le développement et la maturation de la phase post-inspiratoire sont compromis, cela peut entraîner une altération de

la plasticité du contrôle respiratoire central, notamment face à des stimuli variés d'origines périphériques et d'afférences sensorielles, favorisant un cercle vicieux potentiel de perturbations supplémentaires épigénétiques. Ces hypothèses sont par exemple confortées par le décours du Syndrome de Rett chez les patientes, qui présentent un développement normal jusqu'à environ 1 an, certaines ayant acquis la marche et commençant à parler, pour ensuite régresser et perdre les acquis potentiels comme le langage (Chahrour and Zoghbi, 2007). Des données présentes dans cette thèse tendent à confirmer l'importance de la coordination entre les noyaux KF, PAG et NRA pour la genèse de la vocalisation et son insertion dans la phase post-inspiratoire du cycle respiratoire. Ainsi il est troublant de remarquer que parmi les premiers déficits fonctionnels présents chez les patientes Rett se trouvent l'arrêt de l'acquisition du langage et sa perte, ce qui pourrait probablement se passer dans la période de transition entre phase post-inspiratoire générée par les afférences pulmonaires et phase post-inspiratoire codée centralement. Toutefois, Guy et collaborateurs ont montré que la restauration de l'expression du gène *Mecp2* chez la souris modèle de Syndrome de Rett environ 4 semaines après la naissance réverse les altérations phénotypiques de ces souris et tend à rétablir une espérance de vie normale (Guy et al., 2007). Egalement, McGraw et collaborateurs ont montré que la délétion du gène *Mecp2* chez la souris adulte induit rapidement des altérations phénotypiques similaires à celles que développent les souris *Mecp2*$^{-/y}$ dont l'invalidation génétique n'est pas retardée (McGraw et al., 2011). Ces données tendent à montrer la dissociation entre effets pathologiques de la mutation du gène *Mecp2* et période maturationnelle, même si les altérations respiratoires n'ont été quasiment pas abordées, ce qui ne permet pas de conclure sur ce point précis. Il serait donc tentant de considérer le Syndrome de Rett comme une maladie neurodégénérative, et non pas développementale, avec d'abord l'arrêt de la maturation tardive du contrôle central respiratoire, puis sa neurodégénérescence.

Traditionnellement, les maladies neurodégénératives sont dues à une perte de fonction puis à la mort neuronale. Le principal facteur de risque de ces maladies lorsqu'elles sont d'origine non génétique est l'âge, comme par exemple pour les maladies d'Alzheimer ou de Parkinson. L'apparition de ces maladies est considérée comme un vieillissement pathologique, à l'inverse d'un vieillissement dit sain ou "réussi" lorsqu'aucune pathologie invalidante sur le long terme ne se développe. Il existe de nombreuses hypothèses sur le vieillissement, où comment il conduit à la sénescence cellulaire et la perte progressive de certaines fonctions. On peut regrouper un bon nombre de ces hypothèses sous le postulat

d'une accumulation de déchets intra et extracellulaires, *via* de multiples mécanismes comme la peroxydation lipidique, le "cross-link" et l'agrégation spontanée de protéines etc. Une des hypothèses historiques de la tauopathie est fondée sur les théories d'accumulations de déchets et en particulier de protéines tau hyperphosphorylées s'agrégeant et formant des espèces toxiques. Tous les individus accumulent au cours de leur vie des agrégats de protéines tau, la différence entre un sujet âgé sain et un malade étant un surplus d'agrégats de protéines tau chez le sujet malade. Dans ce contexte, nous avons montré sur un modèle murin de tauopathie, les souris Tau-P301L, que le contrôle central respiratoire est altéré par la tauopathie. Toutefois, cette atteinte est très spécifique, tant en terme de régionalisation anatomique des agrégats de protéines tau que d'altération fonctionnelle de la commande respiratoire. Il en ressort une question importante : pourquoi l'atteinte neuronale par la tauopathie n'est-elle pas ubiquitaire ? En d'autres termes, comment cela se fait-il que certains noyaux soient protégés ? Chez les souris Tau-P301L, la rythmogenèse respiratoire n'est pas affectée, elle n'est que légèrement déstabilisée en toute fin de vie comme le montre une augmentation de l'irrégularité de la fréquence respiratoire. Cette propriété de rythmogenèse intrinsèque, au cœur du réseau respiratoire, semble d'ailleurs particulièrement robuste dans l'ensemble des maladies neurodégénératives et en particulier celles qui affectent la respiration. Chez les patients Alzheimer, la maladie neurodégénérative la plus répandue, l'atteinte du tronc cérébral affecte principalement les groupes bioaminergiques, et quelques noyaux respiratoires pontiques comme le noyau pigmenté subpédonculaire qui chevauche le KF chez l'Homme (Rüb et al., 2000, 2001; Simic et al., 2009; Braak and Del Tredici, 2011a, 2011b). De plus, comme pour toutes les tauopathies, la principale cause de mortalité chez les personnes atteintes de MA est la dysphagie avec pneumonie d'aspiration (Kalia, 2003). Il semble évident que les personnes atteintes de MA souffrent d'altération des VAS, et nos données expérimentales supportent ce point en l'étendant à la fonction respiratoire. Dans la MA, ce serait la coordination des VAS et son implication pour la mécanique ventilatoire plutôt qu'un défaut de rythmogenèse respiratoire qui conduirait à des déficits respiratoires. Dans d'autres pathologies neurodégénératives, comme l'atrophie systémique multiple ou le syndrome Shy-Drager, l'origine de la mortalité par défaillance respiratoire est avérée et établie (Chester et al., 1988; Benarroch, 2007). Ces deux maladies sont des neuropathologies complexes, constituées notamment de parkinsonisme mais aussi d'autres atteintes neurodégénératives. Dans ces deux pathologies, la défaillance respiratoire pourrait être liée à des altérations des afférences respiratoires, et s'exprimerait finalement comme une atteinte des VAS. En particulier, dans l'atrophie systémique multiple, les muscles adducteurs des

cordes vocales présentent des activités toniques de longue durée, générant des apnées obstructives d'origine centrale (Benarroch, 2007). Les patients atteints d'atrophie systémique multiple présentent également un défaut de réponse ventilatoire à l'hypoxie, avec des périodes de respiration de type Cheyne-Stokes etc. Le syndrome de Perry est une autre pathologie neurodégénérative, celle-ci très rare (environ 50 patients dans le monde) et vraisemblablement d'origine génétique, caractérisée par des troubles parkinsoniens, des altérations psychiatriques, une perte de poids et une hypoventilation centrale (Wider and Wszolek, 2008; Tsuboi et al., 2008). Les personnes atteintes par cette pathologie décèdent de défaillance respiratoire quelques années après la déclaration de la maladie, et présentent dans la région ventrolatérale du bulbe une diminution des neurones possédant le récepteur à la neurokinine 1 (NK1) (fortement exprimé dans le complexe de PréBötzinger, PréBötC) et des neurones exprimant la tyrosine hydroxylase (TH, un marqueur des neurones catécholaminergiques), mais aussi une perte de neurones 5-HT dans les raphés bulbaires et une perte de neurones dans la substance noire (Tsuboi et al., 2008). Dans cette maladie rare, l'altération respiratoire présente d'abord dyspnées et tachypnées, puis des apnées importantes et une insuffisance respiratoire. Il est possible qu'une altération de la rythmogenèse respiratoire soit présente dans cette maladie particulière, même si cette hypothèse n'a pas encore été analysée.

Il est ainsi intéressant de remarquer que d'une manière générale, la coordination des VAS dans l'acte moteur respiratoire et les activités associées comme la vocalisation, est particulièrement altérée dans les maladies neurodégénératives, et à l'inverse la genèse du rythme respiratoire semble peu touchée. Or toutes les pathologies neurodégénératives citées ci-dessus présentent une prédominance des altérations respiratoires nocturnes sur les diurnes, ce qui est corrélé à l'atteinte systématique des systèmes régulateurs bioaminergiques. Il est d'ailleurs très probable que les défaillances respiratoires dans ces maladies proviennent de dysfonctionnements des régulations respiratoires.

IV - L'influence des régulations respiratoires

1 - Sérotonine et tauopathie

Les bioamines sont très impliquées dans la régulation des rythmes veille/sommeil, et leur atteinte lors des maladies neurodégénératives peut être corrélée avec l'altération de la respiration pendant la nuit. Dans cette thèse, nous avons montré chez les souris Tau-P301L une atteinte par la tauopathie des raphés, ce qui est en adéquation avec les données obtenues chez les patients Alzheimer (Simic et al., 2009). De plus, nous avons montré une altération du métabolisme de la 5-HT chez les souris Tau-P301L, en mesurant par chromatographie liquide à haute pression (HPLC) une quantité d'acide 5-hydroxyindole acétique (5-HIAA ; le métabolite final de la voie de dégradation de la sérotonine) plus élevée chez les souris Tau-P301L que chez les souris contrôles. D'ailleurs, un autre modèle de souris transgénique exprimant une isoforme humaine mutante de protéine tau (THY-Tau22) présente un déficit de 5-HT et de 5-HIAA dans l'hippocampe, donc une altération plus marquée du métabolisme de la 5-HT que celle trouvée dans le tronc cérébral des souris Tau-P301L (Van der Jeugd et al., 2011). Ces résultats sont cohérents, notamment parce que les raphés pontiques, qui contiennent les neurones 5-HT qui projettent dans les structures supérieures du cerveau, sont ceux qui anatomiquement sont les plus atteints par la tauopathie. A l'inverse, les raphés bulbaires, bien moins touchés par la tauopathie, contiennent les neurones 5-HT qui projettent dans le tronc cérébral, et sont impliqués dans la régulation respiratoire. De plus, il semblerait que la biosynthèse de la 5-HT se déroule dans les corps cellulaires, la 5-HT étant ensuite transportée le long des axones dans des vésicules, d'où elle peut être libérée "en passant", ou être finalement mise en attente au niveau des terminaisons pour une potentielle exocytose synaptique (Goldman and Schwartz, 1974; Goldman et al., 1976; Leger et al., 2001; Moss et al., 2005). Vu que tous les corps cellulaires des neurones 5-HT sont dans le tronc cérébral, et considérant l'hypothèse historique d'altération du transport axonal par la tauopathie, il est probable que la biosynthèse de la 5-HT soit correcte chez les souris THY-Tau22, mais que moins de 5-HT ne parvienne dans l'hippocampe à cause d'un transport axonal perturbé. A l'inverse, comme la mesure HPLC de la quantité de sérotonine dans le tronc cérébral ne permet pas de différencier la 5-HT présente dans les corps cellulaires de la 5-HT présente dans les terminaisons synaptiques, il se peut que chez les souris Tau-P301L, les neurones 5-

HT projetant dans le tronc cérébral contiennent moins de 5-HT à destination des terminaisons synaptiques. Dans ce cas, un excès de 5-HIAA, le produit de dégradation terminal de la 5-HT, peut s'expliquer, car l'enzyme de dégradation de la 5-HT, la monoamine oxydase A (MAOA), est une enzyme mitochondriale et les mitochondries sont également transportées le long des axones, transport une fois de plus altéré par la tauopathie (Zhu et al., 2006; Ballatore et al., 2007). Ainsi, une stagnation de la 5-HT et des mitochondries dans le corps cellulaire des neurones sérotoninergiques peut conduire à une accélération du catabolisme de la 5-HT. Ces hypothèses mériteraient d'être testées expérimentalement, au regard de l'importance d'une atteinte du système 5-HT qui est « virtuellement impliqué dans tout », et qui peut donc « tout » altérer (Jacobs and Fornal, 2000).

D'une manière générale, les troubles 5-HT sont très fréquents dans les pathologies qui induisent des altérations respiratoires, comme le SR, le syndrome de Prader-Willi, ou encore les pathologies neurodégénératives citées ci-dessus (Zanella et al., 2008; Katz et al., 2009; Abdala et al., 2010). Dans la MA, les neurones 5-HT semblent même être parmi les premiers neurones atteints par la tauopathie, et pourraient servir de vecteur de transmission trans-synaptique de la pathologie dans tout le système nerveux central (Simic et al., 2009; Braak and Del Tredici, 2011b). La MA est une maladie typique du vieillissement, dont la cause la plus probable est l'accumulation tout au long de la vie d'agrégats de protéines tau et de plaques ß-amyloïdes. Un des enjeux importants est de comprendre pourquoi et comment certaines de ces espèces deviennent toxiques. Egalement, la MA est généralement diagnostiquée tardivement, car ses symptômes initiaux sont similaires à ceux du vieillissement physiologique. Dans ce contexte, il n'est pas étonnant que des troubles 5-HT soient présents à la fois dans la MA et dans le processus de vieillissement en soi. Nous avons montré que les altérations 5-HT chez les souris Tau-P301L peuvent participer à l'aggravation de leur phénotype respiratoire en période terminale. Cette aggravation passe par une déstabilisation du rythme respiratoire, mais aussi par une intensification de la dysfonction des VAS. Behan et collaborateurs ont montré chez le rat âgé que la facilitation à long terme (LTF) du nerf hypoglosse induite par des hypoxies intermittentes est altérée, voire annulée, et ce, de façon concomitante à une réduction du nombre de terminaisons 5-HT et une altération de la morphologie des boutons synaptiques projetant sur l'hypoglosse (Behan and Brownfield, 1999; Zabka et al., 2001a, 2001b, 2003, 2005; Behan et al., 2003; Behan and Wenninger, 2008). De plus, ces auteurs ont montré que ce sont surtout les rats mâles âgés chez qui la LTF de l'hypoglosse est annulée avec l'âge, résultats qui pourraient expliquer la proportion très

majoritaire chez les hommes par rapport aux femmes d'augmentation d'apnées du sommeil avec l'âge (Young et al., 1993; Hla et al., 1994; Bixler et al., 1998, 2001; Ware et al., 2000). Comme la LTF est dépendante de la 5-HT et que les souris Tau-P301L présentent des altérations 5-HT, il serait intéressant de vérifier si la LTF de l'hypoglosse est altérée chez les souris Tau-P301L, et si le sexe est également un facteur déterminant. Cela pourrait trouver une résonance particulière avec des données montrant que la MA pourrait être provoquée / facilitée par des hypoxies, ce qui pourrait alors participer à l'altération du fonctionnement des VAS et contribuer à expliquer les troubles moteurs du langage, de déglutition etc. retrouvés chez le patient Alzheimer (Hillert, 1999; Tolnay and Probst, 2002; Kalia, 2003; Peers et al., 2007; Zhang et al., 2008).

2 - Implications du tonus excitateur hypercapnique

Dans cette thèse, nous nous sommes particulièrement intéressés à l'influence du tonus excitateur hypercapnique sur le contrôle central respiratoire. L'hypercapnie et/ou la baisse de pH sanguin qui y est associée active(nt) de manière plus importante les centres respiratoires que l'hypoxie. L'hypercapnie peut ainsi servir de stress révélant des déficits sous-liminaires ou latents, ce qui est le cas pour les souris Mecp2$^{+/-}$ et les souris Tau-P301L. L'hypercapnie cause une aggravation *in situ* et *in vivo* du phénotype respiratoire pathologique des souris Tau-P301L de 8 mois. On remarquera que chez les souris Tau-P301L à 8 mois, la RVHC n'est pas altérée en terme d'efficacité de la chémosensibilité, de réponse en fréquence, seule la dysfonction des VAS est aggravée. Il serait toutefois intéressant de vérifier si un stress hypoxique produit le même effet, sachant que les souris Tau-P301L de 8 mois ont une RVH également correcte. Par contre, chez les souris Tau-P301L en stade terminal, la RVHC est diminuée par rapport aux souris contrôles. Les raphés contiennent des neurones chémosensibles, et sont avec le noyau rétrotrapézoïde (RTN) un des sites principaux responsables de la RVHC (Severson et al., 2003; Richerson, 2004; Guyenet et al., 2010; Hodges and Richerson, 2010). Or ce sont les raphés bulbaires qui projettent dans le tronc cérébral, qui sont responsables de l'excitation des centres respiratoires, les raphés pontiques intervenant plutôt dans les voies menant à l'excitation d'éveil. Chez les souris Tau-P301L, les raphés pontiques sont dans l'ensemble plus atteints par la tauopathie que les raphés bulbaires, ce qui est montré principalement par des marquages AT100, un marqueur pathologique reconnu. Il est donc possible que les raphés bulbaires des souris Tau-P301L de 8 mois ne

soient pas encore suffisamment atteints par la tauopathie pour engendrer des déficits de RVHC. Par contre, en stade terminal lorsque la tauopathie arrive à son paroxysme, l'atteinte des raphés bulbaires serait suffisante pour provoquer une altération de la RVHC. En effet, le RTN et les noyaux respiratoires de la surface ventrale du bulbe rachidien ne sont pas touchés par la tauopathie, même au stade terminal de la maladie. Enfin, l'atteinte des structures catécholaminergiques, et en particulier celle du locus cœruleus, est très marquée chez les souris Tau-P301L, or ces structures sont également chémosensibles, ce qui peut avoir un rôle dans l'altération de la RVHC des souris terminales.

Dans cette thèse, nous avons également étudié plusieurs mécanismes contribuant à ou altérant la RVHC. En particulier, nous avons montré que l'érythropoïétine (EPO) désensibilise la RVHC par une action directe périphérique (certainement sur les corps carotidiens, CC) et centrale, certainement sur les groupes respiratoires du tronc cérébral. Egalement, l'EPO désensibilise la RVH de manière indirecte, *via* la polyglobulie qu'elle induit. Dans cette étude deux modèles murins transgéniques ont été utilisés, tous deux créés sur le fond C57Bl/6J. Cependant, les souris contrôles de ces modèles étaient de souches légèrement différentes, l'une sur fond pur C57Bl/6J, l'autre sur fond C57Bl/6J mais issu des portées d'une des souches mutantes. Cette très légère différence a tout de même conduit à une RVHC plus ample chez les C57Bl/6J issues des portées de souris mutantes que chez les C57Bl/6J de fond pur. Dans un autre article de cette thèse, nous montrons que les souris C57Bl/6J ont une RVH et une RVHC moins amples que les souris FVB/N. Il semblerait donc que le fond pur C57Bl/6J soit particulièrement peu sensible aux variations de concentrations en O_2 et CO_2, et qu'une petite dérive génétique puisse augmenter cette sensibilité. Ces données confirment l'impression générale que les souris du fond C57Bl/6J sont peu robustes au niveau de leurs paramètres physiologiques. En outre, Stettner et collaborateurs ont montré que les souris C57Bl/6J présentent naturellement des apnées d'origine centrale, ce qui pourrait conduire à des hypoxies intermittentes (Stettner et al., 2008b, 2008a). Or nous avons montré que les souris C57Bl/6J ont un hématocrite et une pression partielle artério-veineuse en CO_2 plus élevés, et un pH plus faible que les souris FVB/N. Au regard de ces paramètres, il est très probable que les souris C57Bl/6J aient un taux élevé d'EPO, ce qui expliquerait l'hématocrite élevé, la RVHC plus faible que chez les souris FVB/N et les souris C57Bl/6J de souche non pure (par rapport à nos travaux sur la désensibilisation de la RVHC par l'EPO). Ceci expliquerait aussi le pH plus faible et la pression partielle artério-veineuse en CO_2 plus élevée car le tonus excitateur qu'ils exercent sur la respiration est diminué par l'EPO. Dans

cette même ligne de pensée, nos résultats sur l'EPO et la RVHC peuvent participer à la compréhension du mal chronique des montagnes (MCM), une pathologie qui touche les personnes habitant en haute altitude et qui développent pour une raison inconnue une baisse de la ventilation d'altitude, qui entraîne une hypoxémie, une surproduction d'EPO, une polyglobulie majeure, puis en conséquence une hypertension artérielle pulmonaire et une hypertrophie du ventricule droit qui mènent à la mort du sujet (Monge and Whittembury, 1976; León-Velarde et al., 2010). Egalement, les sujets atteints de MCM ont une pression partielle de CO_2 dans l'air expiré plus élevée et un pH sanguin plus faible que les sujets sains vivant à la même altitude ; la diminution de ventilation d'altitude des sujets atteints de MCM pourrait être corrélée avec une réduction de leur chémosensibilité centrale au CO_2 (Hurtado, 1960; Fatemian et al., 2003; León-Velarde and Richalet, 2006; León-Velarde et al., 2010). On remarquera les similitudes entre les sujets atteints de MCM et les souris C57Bl/6J : dans les deux cas, une concentration élevée d'EPO peut entraîner un cercle vicieux de désensibilisation de la RVHC et donc de diminution du tonus excitateur du CO_2 sur la respiration, résultant en une baisse générale des paramètres respiratoires qui peut selon les circonstances (par exemple la haute altitude) devenir pathologique.

La théorie de la neuro-archéologie propose que des désordres neurologiques comme l'épilepsie infantile, le retard mental, et même dans certaines conditions les maladies de Huntington et d'Alzheimer, pourraient être en partie causés par des troubles précoces du développement (Ben-Ari, 2008). Cette théorie a été démontrée comme vraie dans d'autres systèmes biologiques, le plus connu étant certainement le système endocrinien. En particulier, l'exposition d'une mère enceinte à des perturbateurs endocriniens comme les phthalates ou le bisphénol A (présents dans la majorité des produits industriels : plastiques, vêtements, jouets etc.), peut causer chez l'enfant de nombreux troubles comme une diminution de la fertilité et une atrophie des organes génitaux, mais aussi plus tard des risques élevés d'obésité et de cancers (Soto and Sonnenschein, 2010; Walker and Gore, 2011; Goodman et al., 2011; Weiss, 2011). D'ailleurs, l'explosion du nombre de cancers du sein au cours des dernières années est de plus en plus imputée à l'exposition notamment intra-utérine aux perturbateurs endocriniens. Dans cette thèse, nous nous sommes penchés sur ce paradigme du développement de la pathologie en période pré-symptomatique, chez les souris *Mecp2*$^{-/y}$ et Tau-P301L. Chez les souris *Mecp2*$^{-/y}$, nous avons montré qu'une hypoxie ou une hypercapnie modérée déclenche de façon anticipée (dès P15) des troubles respiratoires similaires à ceux présents en période symptomatique (après P30), et que ces troubles sont transitoires, la

respiration revenant ensuite à la normale. De même, les souris *Mecp2*$^{-/y}$ présentent dès P15 des altérations de la respiration post-soupir. Ces altérations précoces pourraient représenter les prémices de la pathologie Rett sur le système respiratoire, et pourraient permettre un diagnostic plus précoce. Egalement, ces altérations montrent toute l'importance des régulations respiratoires, même pour la rythmogenèse, des variations modestes de pressions partielles sanguines en O_2 ou CO_2 perturbant *a posteriori* la stabilité du rythme respiratoire et entraînant même des apnées. L'hypothèse réseau de la rythmogenèse respiratoire considère le réseau respiratoire comme étant en permanence sous une forte pression inhibitrice notamment GABAergique. Ceci pourrait expliquer le succès de l'augmentation pharmacologique du GABA chez les souris *Mecp2*$^{-/y}$ restaurant leur stabilité respiratoire, en adéquation avec les démonstrations récentes de l'importance de l'altération du système GABAergique pour le développement des troubles liés à la mutation du gène *Mecp2* (Medrihan et al., 2008; Katz et al., 2009; Abdala et al., 2010; Chao et al., 2010; Voituron and Hilaire, 2011). Chez les souris Tau-P301L, nous avons montré qu'une anesthésie à l'isoflurane en période pré-symptomatique, c'est-à-dire à l'âge de 4 mois, déclenche prématurément l'hyperphosphorylation de tau dans certaines régions du tronc cérébral et des troubles respiratoires similaires à ceux des souris Tau-P301L de 8 mois. De plus, ces troubles respiratoires perdurent jusqu'à deux semaines post-anesthésie. Ces données démontrent que l'anesthésie peut précipiter le déclenchement d'une pathologie encore non déclarée mais latente, et ce certainement *via* des mécanismes d'excitotoxicité à travers les récepteurs au NMDA, comme suggéré par l'effet protecteur d'un traitement avec la mémantine, un antagoniste des récepteurs au NMDA, avant l'anesthésie. De plus, nous montrons que le tonus excitateur hypoxique ou hypercapnique sur le réseau respiratoire pendant l'anesthésie participe au déclenchement des altérations respiratoires post-anesthésie. Ces données montrent une fois de plus le rôle crucial des régulations respiratoires dans l'apparition d'altérations respiratoires. Dans cette étude, nous avons utilisé l'anticorps AT8 pour marquer l'hyperphosphorylation de tau ; les troubles respiratoires étaient corrélés à la présence et à l'intensité du marquage AT8. Cependant, cet anticorps est généralement décrit comme étant à la frontière entre la physiologie et la pathologie. Notre étude montre que dans certains cas, la présence d'AT8 peut être reliée à la pathologie, ce qui pourrait coïncider avec l'hypothèse de plus en plus prégnante de la toxicité des espèces intermédiaires des protéines tau hyperphosphorylées comme les oligomères, par rapport au rôle certainement non néfaste des agrégats neurofibrillaires de tau.

V - Conclusion et perspectives

Dans cette thèse nous avons développé plusieurs axes de recherche, avec deux fils conducteurs principaux : 1) l'étude du vieillissement du contrôle nerveux de la respiration, de sa maturation à sa sénescence, et en particulier au cours de deux neuropathologies caractérisant chacune de ces périodes ; 2) l'étude de l'impact du CO_2 sur la commande centrale respiratoire, des facteurs modulant la réponse ventilatoire à l'hypercapnie à l'influence du CO_2 dans les pathologies de la maturation et de la sénescence étudiées.

L'objet principal et l'originalité de cette thèse reposent essentiellement sur l'étude de l'altération respiratoire des souris Tau-P301L, modèle reconnu de tauopathie, et donc de la maladie d'Alzheimer (MA).

La MA, maladie neurodégénérative actuellement la plus répandue, est devenue ces dernières années un enjeu sociétal majeur. L'effort de recherche sur la MA au niveau international est monumental, la communauté de scientifiques s'y consacrant intensément et les subventions tant publiques que privées étant très importantes. Cependant, aucune thérapie n'a encore été découverte ; les rares outils thérapeutiques existant actuellement amoindrissent les symptômes de la MA, ralentissent le développement de la MA, mais sans pour autant l'arrêter ni bloquer son aggravation. La plus grande partie des recherches et essais cliniques thérapeutiques se sont concentrés sur les plaques ß-amyloïdes, en raison de l'hypothèse principale sur l'étiologie MA, la "cascade amyloïde", qui place la pathologie liée au peptide amyloïde (Aß) comme initiale. Les échecs successifs des essais cliniques sur des traitements liés à Aß, faisant pourtant suite à des résultats quasi-miraculeux sur les modèles murins, ont notamment contribué ces dernières années à un regain d'attention sur la tauopathie.

Toutes les expérimentations effectuées au cours de cette thèse ne sont pas présentées dans ce manuscrit, comme l'étude réalisée en collaboration avec le Docteur Françoise Muscatelli et son équipe (INMED, Marseille) sur les souris *Necdin*$^{+/-p}$, un modèle murin du syndrome de Prader-Willi, et l'étude réalisée en collaboration avec le Professeur Giuseppe Testa et son équipe (IFOM-IEO, Milan) sur l'importance épigénétique de *JMJD3* pour le développement du réseau respiratoire. Mais, grâce à notre collaboration avec le Professeur Fred Van Leuven (LEGTEGG, Leuven), nous avons également pu étudier de manière approfondie le rôle de la phosphorylation de tau pour la pathologie respiratoire des souris Tau-P301L, avec des pistes thérapeutiques.

Tout d'abord, en utilisant des souris transgéniques Tau-P301L qui surexpriment l'enzyme GSK3ß (Glycogène Synthase kinase 3ß), la principale kinase phosphorylant la protéine tau, nous avons noté de manière surprenante que l'excès de GSK3ß annule les altérations respiratoires des souris Tau-P301L à 8 mois et double leur durée de vie. A l'inverse, les souris Tau-P301L qui n'expriment plus GSK3ß ont une durée de vie réduite de moitié, et des altérations respiratoires encore plus sévères que les souris Tau-P301L à 8 mois. Ces résultats sont inattendus, car on aurait supposé que l'excès de GSK3ß aurait aggravé la tauopathie dans le tronc cérébral et donc les altérations respiratoires, et inversement avec la délétion de GSK3ß. Ceci est d'autant plus surprenant que la surexpression de GSK3ß chez les souris Tau-P301L aggrave la tauopathie dans le télencéphale, ainsi que les atteintes cognitives et comportementales. La compréhension du ou des mécanismes responsable(s) de cette dichotomie dans l'action de GSK3ß sur tau entre le tronc cérébral et le télencéphale représente un enjeu majeur, permettant d'offrir des perspectives thérapeutiques.

Enfin, la protéine tau peut être modifiée post-translationnellement de diverses manières, et notamment par l'O-GlcNAcylation. L'O-GlcNAcylation de la protéine tau est d'ailleurs supposée antagoniser sa phosphorylation. Nous avons pu tester l'effet d'un inhibiteur de l'O-GlcNAcase (l'enzyme clivant O-GlcNAc et protéine tau) chez les souris Tau-P301L à 6 mois et à 8 mois. Dans les deux cas, la respiration des souris était très significativement améliorée, et la survie des animaux considérablement prolongée. Cette étude est encore en cours, notamment pour la partie biochimique, mais elle permet déjà d'envisager l'inhibition de l'O-GlcNAcase comme une piste potentielle thérapeutique pour les tauopathies et la MA.

Bibliographie

Abbott SBG, Stornetta RL, Fortuna MG, Depuy SD, West GH, Harris TE, Guyenet PG (2009) Photostimulation of retrotrapezoid nucleus phox2b-expressing neurons in vivo produces long-lasting activation of breathing in rats. J. Neurosci 29:5806-5819 Available at: [Accessed May 8, 2009].

Abdala APL, Dutschmann M, Bissonnette JM, Paton JFR (2010) Correction of respiratory disorders in a mouse model of Rett syndrome. Proc. Natl. Acad. Sci. U.S.A 107:18208-18213 Available at: [Accessed June 24, 2011].

Abu-Shaweesh JM (2004) Maturation of respiratory reflex responses in the fetus and neonate. Semin Neonatol 9:169-180 Available at: [Accessed May 23, 2011].

Acker H (2005) The oxygen sensing signal cascade under the influence of reactive oxygen species. Philos. Trans. R. Soc. Lond., B, Biol. Sci 360:2201-2210 Available at: [Accessed June 30, 2011].

Adametz J, O'Leary JL (1959) Experimental mutism resulting from periaqueductal lesions in cats. Neurology 9:636-642 Available at: [Accessed June 2, 2011].

Adrian ED (1933) Afferent impulses in the vagus and their effect on respiration. J. Physiol. (Lond.) 79:332-358 Available at: [Accessed July 14, 2011].

Aghajanian GK, Sprouse JS, Sheldon P, Rasmussen K (1990) Electrophysiology of the central serotonin system: receptor subtypes and transducer mechanisms. Ann. N. Y. Acad. Sci 600:93-103; discussion 103 Available at: [Accessed June 1, 2011].

Ahmed M, Giesbrecht GG, Serrette C, Georgopoulos D, Anthonisen NR (1991) Ventilatory response to hypoxia in elderly humans. Respir Physiol 83:343-351 Available at: [Accessed June 13, 2011].

Albert MS, Dekosky ST, Dickson D, Dubois B, Feldman HH, Fox NC, Gamst A, Holtzman DM, Jagust WJ, Petersen RC, Snyder PJ, Carrillo MC, Thies B, Phelps CH (2011) The diagnosis of mild cognitive impairment due to Alzheimer's disease: Recommendations from the National Institute on Aging-Alzheimer's Association workgroups on diagnostic guidelines for Alzheimer's disease. Alzheimers Dement 7:270-279 Available at: [Accessed June 17, 2011].

Alberts B, Alexander Johnson, Julian Lewis, Martin Raff, Keith Roberts, Peter Walter (2002) Molecular Biology of the Cell, 4th edition New York: Garland Science.

Aletrino MA, Vogels OJ, Van Domburg PH, Ten Donkelaar HJ (1992) Cell loss in the nucleus raphes dorsalis in Alzheimer's disease. Neurobiol. Aging 13:461-468 Available at: [Accessed June 23, 2011].

Alheid GF, Gray PA, Jiang MC, Feldman JL, McCrimmon DR (2002) Parvalbumin in respiratory neurons of the ventrolateral medulla of the adult rat. J. Neurocytol 31:693-717 Available at: [Accessed May 11, 2011].

Alheid GF, McCrimmon DR (2008) The chemical neuroanatomy of breathing. Respir Physiol Neurobiol 164:3-11 Available at: [Accessed April 26, 2011].

Alheid GF, Milsom WK, McCrimmon DR (2004) Pontine influences on breathing: an overview. Respir Physiol Neurobiol 143:105-114 Available at: [Accessed May 8, 2011].

Alvarez JE, Bodani J, Fajardo CA, Kwiatkowski K, Cates DB, Rigatto H (1993) Sighs and their relationship to apnea in the newborn infant. Biol. Neonate 63:139-146 Available at: [Accessed July 14, 2011].

Alzforum (2010) Tau Research Models. Available at: http://www.alzforum.org/res/com/tra/tau/default.asp.

Alzheimer A, Stelzmann RA, Schnitzlein HN, Murtagh FR (1995) An English translation of Alzheimer's 1907 paper, "Uber eine eigenartige Erkankung der Hirnrinde." Clin Anat 8:429-431 Available at: [Accessed June 17, 2011].

Amiel J, Dubreuil V, Ramanantsoa N, Fortin G, Gallego J, Brunet J-F, Goridis C (2009) PHOX2B in respiratory control: lessons from congenital central hypoventilation syndrome and its mouse models. Respir Physiol Neurobiol 168:125-132 Available at: [Accessed July 13, 2011].

Amin AH, CRAWFORD TB, GADDUM JH (1954) The distribution of substance P and 5-hydroxytryptamine in the central nervous system of the dog. J. Physiol. (Lond.) 126:596-618 Available at: [Accessed May 31, 2011].

Amir RE, Van den Veyver IB, Wan M, Tran CQ, Francke U, Zoghbi HY (1999) Rett syndrome is caused by mutations in X-linked MECP2, encoding methyl-CpG-binding protein 2. Nat. Genet 23:185-188 Available at: [Accessed June 24, 2011].

Ancoli-Israel S, Palmer BW, Cooke JR, Corey-Bloom J, Fiorentino L, Natarajan L, Liu L, Ayalon L, He F, Loredo JS (2008) Cognitive effects of treating obstructive sleep apnea in Alzheimer's disease: a randomized controlled study. J Am Geriatr Soc 56:2076-2081 Available at: [Accessed June 23, 2011].

Arango V, Ruggiero DA, Callaway JL, Anwar M, Mann JJ, Reis DJ (1988) Catecholaminergic neurons in the ventrolateral medulla and nucleus of the solitary tract in the human. J. Comp. Neurol 273:224-240 Available at: [Accessed June 29, 2011].

Arita H, Ichikawa K, Kuwana S, Kogo N (1989) Possible locations of pH-dependent central chemoreceptors: intramedullary regions with acidic shift of extracellular fluid pH during hypercapnia. Brain Res 485:285-293 Available at: [Accessed July 12, 2011].

Arita H, Kogo N, Koshiya N (1987) Morphological and physiological properties of caudal medullary expiratory neurons of the cat. Brain Res 401:258-266 Available at: [Accessed May 11, 2011].

Armstrong DD (1997) Review of Rett syndrome. J. Neuropathol. Exp. Neurol 56:843-849 Available at: [Accessed June 24, 2011].

Arnold CS, Johnson GV, Cole RN, Dong DL, Lee M, Hart GW (1996) The microtubule-associated protein tau is extensively modified with O-linked N-acetylglucosamine. J. Biol. Chem 271:28741-28744 Available at: [Accessed June 16, 2011].

Aronov S, Aranda G, Behar L, Ginzburg I (2001) Axonal tau mRNA localization coincides with tau protein in living neuronal cells and depends on axonal targeting signal. J. Neurosci 21:6577-6587 Available at: [Accessed June 15, 2011].

Arriagada PV, Growdon JH, Hedley-Whyte ET, Hyman BT (1992)(a) Neurofibrillary tangles but not senile plaques parallel duration and severity of Alzheimer's disease. Neurology 42:631-639 Available at: [Accessed July 23, 2010].

Arriagada PV, Marzloff K, Hyman BT (1992)(b) Distribution of Alzheimer-type pathologic changes in nondemented elderly individuals matches the pattern in Alzheimer's disease. Neurology 42:1681-1688 Available at: [Accessed June 20, 2011].

Aston-Jones G, Ennis M, Pieribone VA, Nickell WT, Shipley MT (1986) The brain nucleus locus coeruleus: restricted afferent control of a broad efferent network. Science 234:734-737 Available at: [Accessed May 10, 2011].

Babcock MA, Badr MS (1998) Long-term facilitation of ventilation in humans during NREM sleep. Sleep 21:709-716 Available at: [Accessed June 13, 2011].

Bach KB, Mitchell GS (1996) Hypoxia-induced long-term facilitation of respiratory activity is serotonin dependent. Respir Physiol 104:251-260 Available at: [Accessed July 12, 2011].

Baekey DM, Morris KF, Gestreau C, Li Z, Lindsey BG, Shannon R (2001) Medullary respiratory neurones and control of laryngeal motoneurones during fictive eupnoea and cough in the cat. J. Physiol. (Lond.) 534:565-581 Available at: [Accessed June 5, 2011].

Bailey EF, Fregosi RF (2006) Modulation of upper airway muscle activities by bronchopulmonary afferents. J. Appl. Physiol 101:609-617 Available at: [Accessed July 14, 2011].

Bajić J, Zuperku EJ, Tonković-Capin M, Hopp FA (1994) Interaction between chemoreceptor and stretch receptor inputs at medullary respiratory neurons. Am. J. Physiol 266:R1951-1961 Available at: [Accessed July

14, 2011].

Baker TL, Fuller DD, Zabka AG, Mitchell GS (2001) Respiratory plasticity: differential actions of continuous and episodic hypoxia and hypercapnia. Respir Physiol 129:25-35 Available at: [Accessed July 12, 2011].

Baker-Herman TL, Fuller DD, Bavis RW, Zabka AG, Golder FJ, Doperalski NJ, Johnson RA, Watters JJ, Mitchell GS (2004) BDNF is necessary and sufficient for spinal respiratory plasticity following intermittent hypoxia. Nat. Neurosci 7:48-55 Available at: [Accessed July 12, 2011].

Baker-Herman TL, Mitchell GS (2002) Phrenic long-term facilitation requires spinal serotonin receptor activation and protein synthesis. J. Neurosci 22:6239-6246 Available at: [Accessed June 9, 2011].

Ballantyne D, Scheid P (2001) Central chemosensitivity of respiration: a brief overview. Respir Physiol 129:5-12 Available at: [Accessed July 13, 2011].

Ballanyi K, Panaitescu B, Ruangkittisakul A (2010) Control of breathing by "nerve glue." Sci Signal 3:pe41 Available at: [Accessed June 10, 2011].

Ballard C, Gauthier S, Corbett A, Brayne C, Aarsland D, Jones E (2011) Alzheimer's disease. Lancet 377:1019-1031 Available at: [Accessed June 15, 2011].

Ballatore C, Lee VM-Y, Trojanowski JQ (2007) Tau-mediated neurodegeneration in Alzheimer's disease and related disorders. Nat. Rev. Neurosci 8:663-672 Available at: [Accessed June 18, 2011].

Bandler R, Carrive P (1988) Integrated defence reaction elicited by excitatory amino acid microinjection in the midbrain periaqueductal grey region of the unrestrained cat. Brain Res 439:95-106 Available at: [Accessed June 4, 2011].

Bautista TG, Burke PGR, Sun Q-J, Berkowitz RG, Pilowsky PM (2010) The generation of post-inspiratory activity in laryngeal motoneurons: a review. Adv. Exp. Med. Biol 669:143-149 Available at: [Accessed May 4, 2011].

Beckman KB, Ames BN (1998) The free radical theory of aging matures. Physiol. Rev 78:547-581 Available at: [Accessed June 7, 2011].

Behan M, Brownfield MS (1999) Age-related changes in serotonin in the hypoglossal nucleus of rat: implications for sleep-disordered breathing. Neurosci. Lett 267:133-136 Available at: [Accessed June 9, 2011].

Behan M, Zabka AG, Mitchell GS (2002) Age and gender effects on serotonin-dependent plasticity in respiratory motor control. Respir Physiol Neurobiol 131:65-77 Available at: [Accessed June 13, 2011].

Behan M, Wenninger JM (2008) Sex steroidal hormones and respiratory control. Respir Physiol Neurobiol 164:213-221 Available at: [Accessed June 12, 2011].

Behan M, Zabka AG, Thomas CF, Mitchell GS (2003) Sex steroid hormones and the neural control of breathing. Respir Physiol Neurobiol 136:249-263 Available at: [Accessed June 9, 2011].

Behbehani MM (1995) Functional characteristics of the midbrain periaqueductal gray. Prog. Neurobiol 46:575-605 Available at: [Accessed June 3, 2011].

Bellingham MC (1998) Driving respiration: the respiratory central pattern generator. Clin. Exp. Pharmacol. Physiol 25:847-856 Available at: [Accessed May 5, 2011].

Ben-Ari Y (2008) Neuro-archaeology: pre-symptomatic architecture and signature of neurological disorders. Trends Neurosci 31:626-636 Available at: [Accessed July 9, 2011].

Benarroch EE (2007) Brainstem respiratory control: substrates of respiratory failure of multiple system atrophy. Mov. Disord 22:155-161 Available at: [Accessed July 7, 2011].

von Bergen M, Barghorn S, Li L, Marx A, Biernat J, Mandelkow EM, Mandelkow E (2001) Mutations of tau

protein in frontotemporal dementia promote aggregation of paired helical filaments by enhancing local beta-structure. J. Biol. Chem 276:48165-48174 Available at: [Accessed June 20, 2011].

Berger AJ (1977) Dorsal respiratory group neurons in the medulla of cat: spinal projections, responses to lung inflation and superior laryngeal nerve stimulation. Brain Res 135:231-254 Available at: [Accessed May 11, 2011].

Berger Z, Roder H, Hanna A, Carlson A, Rangachari V, Yue M, Wszolek Z, Ashe K, Knight J, Dickson D, Andorfer C, Rosenberry TL, Lewis J, Hutton M, Janus C (2007) Accumulation of pathological tau species and memory loss in a conditional model of tauopathy. J. Neurosci 27:3650-3662 Available at: [Accessed June 22, 2011].

Berridge CW (2008) Noradrenergic modulation of arousal. Brain Res Rev 58:1-17 Available at: [Accessed May 10, 2011].

Bertram L, Tanzi RE (2005) The genetic epidemiology of neurodegenerative disease. J. Clin. Invest 115:1449-1457 Available at: [Accessed June 18, 2011].

Besnard S, Denise P, Cappelin B, Dutschmann M, Gestreau C (2009) Stimulation of the rat medullary raphe nuclei induces differential responses in respiratory muscle activity. Respir Physiol Neurobiol 165:208-214 Available at: [Accessed May 31, 2011].

Besnard S, Massé F, Verdaguer M, Cappelin B, Meurice JC, Gestreau C (2007) Time- and dose-related effects of three 5-HT receptor ligands on the genioglossus activity in anesthetized and conscious rats. Sleep Breath 11:275-284 Available at: [Accessed June 1, 2011].

Besnard S, Khemiri H, Masse F, Denise P, Verdaguer M, Gestreau C (2011) Differential respiratory control of the upper airway and diaphragm muscles induced by 5-HT1A receptor ligands. Sleep Breath Available at: http://www.ncbi.nlm.nih.gov/pubmed/21221824 [Accessed June 1, 2011].

Biancardi V, Bícego KC, Almeida MC, Gargaglioni LH (2008) Locus coeruleus noradrenergic neurons and CO2 drive to breathing. Pflugers Arch 455:1119-1128 Available at: [Accessed July 13, 2011].

Bianchi AL (1969) [Antidromic activation of bulbar respiratory neurons]. J. Physiol. (Paris) 61 Suppl 1:91 Available at: [Accessed May 5, 2011].

Bianchi AL (1971) [Localization and study of respiratory medullary neurons. Antidromic starting by spinal cord or vagal stimulation]. J. Physiol. (Paris) 63:5-40 Available at: [Accessed May 5, 2011].

Bianchi AL (1974) [Modalities of discharge and anatomo-functional properties of medullary respiratory neurons]. J. Physiol. (Paris) 68:555-587 Available at: [Accessed May 5, 2011].

Bianchi AL, Barillot JC (1982) Respiratory neurons in the region of the retrofacial nucleus: pontile, medullary, spinal and vagal projections. Neurosci. Lett 31:277-282 Available at: [Accessed May 11, 2011].

Bianchi AL, Denavit-Saubié M, Champagnat J (1995) Central control of breathing in mammals: neuronal circuitry, membrane properties, and neurotransmitters. Physiol. Rev 75:1-45 Available at: [Accessed May 4, 2011].

Bianchi AL, Gestreau C (2009)(a) The brainstem respiratory network: an overview of a half century of research. Respir Physiol Neurobiol 168:4-12 Available at: [Accessed May 4, 2011].

Bianchi AL, Gestreau C (2009)(b) The brainstem respiratory network: an overview of a half century of research. Respir Physiol Neurobiol 168:4-12 Available at: [Accessed October 2, 2009].

Bierer LM, Hof PR, Purohit DP, Carlin L, Schmeidler J, Davis KL, Perl DP (1995) Neocortical neurofibrillary tangles correlate with dementia severity in Alzheimer's disease. Arch. Neurol 52:81-88 Available at: [Accessed June 18, 2011].

Biscoe TJ, Purves MJ, Sampson SR (1970) The frequency of nerve impulses in single carotid body

chemoreceptor afferent fibres recorded in vivo with intact circulation. J. Physiol. (Lond.) 208:121-131 Available at: [Accessed June 29, 2011].

Bixler EO, Vgontzas AN, Lin HM, Ten Have T, Rein J, Vela-Bueno A, Kales A (2001) Prevalence of sleep-disordered breathing in women: effects of gender. Am. J. Respir. Crit. Care Med 163:608-613 Available at: [Accessed June 13, 2011].

Bixler EO, Vgontzas AN, Ten Have T, Tyson K, Kales A (1998) Effects of age on sleep apnea in men: I. Prevalence and severity. Am. J. Respir. Crit. Care Med 157:144-148 Available at: [Accessed June 13, 2011].

Blackburn EH (2000) Telomere states and cell fates. Nature 408:53-56 Available at: [Accessed June 8, 2011].

Blain GM, Smith CA, Henderson KS, Dempsey JA (2009) Contribution of the carotid body chemoreceptors to eupneic ventilation in the intact, unanesthetized dog. J. Appl. Physiol 106:1564-1573 Available at: [Accessed June 29, 2011].

Blanco CE, Dawes GS, Hanson MA, McCooke HB (1984) The response to hypoxia of arterial chemoreceptors in fetal sheep and new-born lambs. J. Physiol. (Lond.) 351:25-37 Available at: [Accessed May 23, 2011].

Blennow K, de Leon MJ, Zetterberg H (2006) Alzheimer's disease. Lancet 368:387-403 Available at: [Accessed June 18, 2011].

Bliwise DL (2002) Sleep apnea, APOE4 and Alzheimer's disease 20 years and counting? J Psychosom Res 53:539-546 Available at: [Accessed June 23, 2011].

Bodineau L, Cayetanot F, Frugière A (2000)(a) Possible role of retrotrapezoid nucleus and parapyramidal area in the respiratory response to anoxia: an in vitro study in neonatal rat. Neurosci. Lett 295:67-69 Available at: [Accessed July 11, 2011].

Bodineau L, Frugière A, Marlot D, Wallois F (2000)(b) Connections between retrotrapezoid nucleus and nucleus tractus solitarii in cat. Neurosci. Lett 280:111-114 Available at: [Accessed May 11, 2011].

Bodineau L, Frugière A, Marlot D, Wallois F (2000)(c) Effect of hypoxia on the activity of respiratory and non-respiratory modulated retrotrapezoid neurons of the cat. Auton Neurosci 86:70-77 Available at: [Accessed May 11, 2011].

Boers J, Klop EM, Hulshoff AC, de Weerd H, Holstege G (2002) Direct projections from the nucleus retroambiguus to cricothyroid motoneurons in the cat. Neurosci. Lett 319:5-8 Available at: [Accessed June 4, 2011].

Bondareff W, Mountjoy CQ, Roth M (1982) Loss of neurons of origin of the adrenergic projection to cerebral cortex (nucleus locus ceruleus) in senile dementia. Neurology 32:164-168 Available at: [Accessed June 23, 2011].

Bonora M, Gautier H (1989) Effects of hypoxia on thermal polypnea in intact and carotid body-denervated conscious cats. J. Appl. Physiol 67:578-583 Available at: [Accessed July 2, 2011].

Botez MI, Carp N (1968) Nouvelles données sur le problème du mécanisme de déclenchement de a parole. Rev Roum Neurol 5:153-158

Boutin AT, Weidemann A, Fu Z, Mesropian L, Gradin K, Jamora C, Wiesener M, Eckardt K-U, Koch CJ, Ellies LG, Haddad G, Haase VH, Simon MC, Poellinger L, Powell FL, Johnson RS (2008) Epidermal sensing of oxygen is essential for systemic hypoxic response. Cell 133:223-234 Available at: [Accessed June 15, 2009].

Braak H, Braak E (1991) Neuropathological stageing of Alzheimer-related changes. Acta Neuropathol 82:239-259 Available at: [Accessed June 18, 2011].

Braak H, Braak E (1995) Staging of Alzheimer's disease-related neurofibrillary changes. Neurobiol. Aging 16:271-278; discussion 278-284 Available at: [Accessed June 18, 2011].

Braak H, Braak E (1997) Frequency of stages of Alzheimer-related lesions in different age categories. Neurobiol. Aging 18:351-357 Available at: [Accessed June 22, 2011].

Braak H, Del Tredici K (2011)(a) The pathological process underlying Alzheimer's disease in individuals under thirty. Acta Neuropathol 121:171-181 Available at: [Accessed June 23, 2011].

Braak H, Del Tredici K (2011)(b) Alzheimer's pathogenesis: is there neuron-to-neuron propagation? Acta Neuropathol 121:589-595 Available at: [Accessed June 23, 2011].

Bradley SR, Pieribone VA, Wang W, Severson CA, Jacobs RA, Richerson GB (2002) Chemosensitive serotonergic neurons are closely associated with large medullary arteries. Nat. Neurosci 5:401-402 Available at: [Accessed June 28, 2011].

Bramble DM, Carrier DR (1983) Running and breathing in mammals. Science 219:251-256 Available at: [Accessed June 5, 2011].

Brandes IF, Zuperku EJ, Stucke AG, Jakovcevic D, Hopp FA, Stuth EAE (2006) Serotonergic modulation of inspiratory hypoglossal motoneurons in decerebrate dogs. J. Neurophysiol 95:3449-3459 Available at: [Accessed June 12, 2011].

Brandt R, Léger J, Lee G (1995) Interaction of tau with the neural plasma membrane mediated by tau's amino-terminal projection domain. J. Cell Biol 131:1327-1340 Available at: [Accessed June 16, 2011].

Brandão ML, Zanoveli JM, Ruiz-Martinez RC, Oliveira LC, Landeira-Fernandez J (2008) Different patterns of freezing behavior organized in the periaqueductal gray of rats: association with different types of anxiety. Behav. Brain Res 188:1-13 Available at: [Accessed June 3, 2011].

Breuer J (1868) Die Selbststeurung der Athmung durch den Nervus vagus. Akad Wiss Wien 58:909-937

Brion JP, Flament-Durand J, Dustin P (1986) Alzheimer's disease and tau proteins. Lancet 2:1098 Available at: [Accessed June 20, 2011].

Brion S, Plas J, Jeanneau A (1991) [Pick's disease. Anatomo-clinical point of view]. Rev. Neurol. (Paris) 147:693-704 Available at: [Accessed June 22, 2011].

Brischetto MJ, Millman RP, Peterson DD, Silage DA, Pack AI (1984) Effect of aging on ventilatory response to exercise and CO2. J Appl Physiol 56:1143-1150 Available at: [Accessed June 13, 2011].

Browne HAK, Adams L, Simonds AK, Morrell MJ (2003) Ageing does not influence the sleep-related decrease in the hypercapnic ventilatory response. Eur. Respir. J 21:523-529 Available at: [Accessed June 13, 2011].

Brugniaux JV, Pialoux V, Foster GE, Duggan CTC, Eliasziw M, Hanly PJ, Poulin MJ (2011) Effects of intermittent hypoxia on erythropoietin, soluble erythropoietin receptor and ventilation in humans. Eur. Respir. J 37:880-887 Available at: [Accessed July 8, 2011].

Bryce SD, Morrison V, Craig NJ, Forsyth NR, Fitzsimmons SA, Ireland H, Cuthbert AP, Newbold RF, Parkinson EK (2002) A mortality gene(s) for the human adenocarcinoma line HeLa maps to a 130-kb region of human chromosome 4q22-q23. Neoplasia 4:544-550 Available at: [Accessed June 8, 2011].

Buckler KJ (2007) TASK-like potassium channels and oxygen sensing in the carotid body. Respir Physiol Neurobiol 157:55-64 Available at: [Accessed June 29, 2011].

Bunn HF, Poyton RO (1996) Oxygen sensing and molecular adaptation to hypoxia. Physiol. Rev 76:839-885 Available at: [Accessed July 3, 2011].

Burlhis TM, Aghajanian GK (1987) Pacemaker potentials of serotonergic dorsal raphe neurons: contribution of a low-threshold Ca2+ conductance. Synapse 1:582-588 Available at: [Accessed June 1, 2011].

Burns JM, Cronk BB, Anderson HS, Donnelly JE, Thomas GP, Harsha A, Brooks WM, Swerdlow RH (2008) Cardiorespiratory fitness and brain atrophy in early Alzheimer disease. Neurology 71:210-216 Available at:

[Accessed June 23, 2011].

Buée L, Bussière T, Buée-Scherrer V, Delacourte A, Hof PR (2000) Tau protein isoforms, phosphorylation and role in neurodegenerative disorders. Brain Res. Brain Res. Rev 33:95-130 Available at: [Accessed June 21, 2011].

Byrum CE, Guyenet PG (1987) Afferent and efferent connections of the A5 noradrenergic cell group in the rat. J. Comp. Neurol 261:529-542 Available at: [Accessed May 10, 2011].

de Calignon A, Fox LM, Pitstick R, Carlson GA, Bacskai BJ, Spires-Jones TL, Hyman BT (2010) Caspase activation precedes and leads to tangles. Nature Available at: http://www.ncbi.nlm.nih.gov/pubmed/20357768.

de Calignon A, Spires-Jones TL, Pitstick R, Carlson GA, Hyman BT (2009) Tangle-bearing neurons survive despite disruption of membrane integrity in a mouse model of tauopathy. J. Neuropathol. Exp. Neurol 68:757-761 Available at: [Accessed June 22, 2011].

Cantillon D, Bradford A (2000) Effects of age and gender on rat upper airway muscle contractile properties. J. Gerontol. A Biol. Sci. Med. Sci 55:B396-400 Available at: [Accessed June 11, 2011].

Carrive P (1993) The periaqueductal gray and defensive behavior: functional representation and neuronal organization. Behav. Brain Res 58:27-47 Available at: [Accessed June 3, 2011].

Carroll JL (2003) Developmental plasticity in respiratory control. J. Appl. Physiol 94:375-389 Available at: [Accessed May 6, 2011].

Carroll MS, Patwari PP, Weese-Mayer DE (2010) Carbon dioxide chemoreception and hypoventilation syndromes with autonomic dysregulation. J. Appl. Physiol 108:979-988 Available at: [Accessed July 13, 2011].

Carruth MK, Fowler AA, Fairman RP, Mayer DJ, Leichnetz GR (1992) Respiratory failure without pulmonary edema following injection of a glutamate agonist into the ventral medullary raphe of the rat. Brain Res. Bull 28:365-378 Available at: [Accessed July 13, 2011].

Cass H, Reilly S, Owen L, Wisbeach A, Weekes L, Slonims V, Wigram T, Charman T (2003) Findings from a multidisciplinary clinical case series of females with Rett syndrome. Dev Med Child Neurol 45:325-337 Available at: [Accessed June 24, 2011].

de Castro D, Lipski J, Kanjhan R (1994) Electrophysiological study of dorsal respiratory neurons in the medulla oblongata of the rat. Brain Res 639:49-56 Available at: [Accessed May 12, 2011].

Caubit X, Lye CM, Martin E, Coré N, Long DA, Vola C, Jenkins D, Garratt AN, Skaer H, Woolf AS, Fasano L (2008) Teashirt 3 is necessary for ureteral smooth muscle differentiation downstream of SHH and BMP4. Development 135:3301-3310 Available at: [Accessed July 5, 2011].

Caubit X, Thoby-Brisson M, Voituron N, Filippi P, Bévengut M, Faralli H, Zanella S, Fortin G, Hilaire G, Fasano L (2010) Teashirt 3 regulates development of neurons involved in both respiratory rhythm and airflow control. J. Neurosci 30:9465-9476 Available at: [Accessed July 5, 2011].

Cerami A (1985) Hypothesis. Glucose as a mediator of aging. J Am Geriatr Soc 33:626-634 Available at: [Accessed June 8, 2011].

Chahrour M, Zoghbi HY (2007) The story of Rett syndrome: from clinic to neurobiology. Neuron 56:422-437 Available at: [Accessed June 24, 2011].

Chamberlin NL, Saper CB (1994) Topographic organization of respiratory responses to glutamate microstimulation of the parabrachial nucleus in the rat. J. Neurosci 14:6500-6510 Available at: [Accessed May 24, 2011].

Champagnat J, Denavit-Saubié M, Henry JL, Leviel V (1979) Catecholaminergic depressant effects on bulbar respiratory mechanisms. Brain Res 160:57-68 Available at: [Accessed May 29, 2011].

Champagnat J, Morin-Surun M-P, Bouvier J, Thoby-Brisson M, Fortin G (2011) Prenatal development of central rhythm generation. Respir Physiol Neurobiol Available at: http://www.ncbi.nlm.nih.gov/pubmed/21527363 [Accessed May 23, 2011].

Chao H-T, Chen H, Samaco RC, Xue M, Chahrour M, Yoo J, Neul JL, Gong S, Lu H-C, Heintz N, Ekker M, Rubenstein JLR, Noebels JL, Rosenmund C, Zoghbi HY (2010) Dysfunction in GABA signalling mediates autism-like stereotypies and Rett syndrome phenotypes. Nature 468:263-269 Available at: [Accessed June 24, 2011].

Chapman KR, Cherniack NS (1987) Aging effects on the interaction of hypercapnia and hypoxia as ventilatory stimuli. J Gerontol 42:202-209 Available at: [Accessed June 13, 2011].

Chen RZ, Akbarian S, Tudor M, Jaenisch R (2001) Deficiency of methyl-CpG binding protein-2 in CNS neurons results in a Rett-like phenotype in mice. Nat. Genet 27:327-331 Available at: [Accessed July 5, 2011].

Cherniack NS, von Euler C, Głogowska M, Homma I (1981) Characteristics and rate of occurrence of spontaneous and provoked augmented breaths. Acta Physiol. Scand 111:349-360 Available at: [Accessed July 14, 2011].

Chester CS, Gottfried SB, Cameron DI, Strohl KP (1988) Pathophysiological findings in a patient with Shy-Drager and alveolar hypoventilation syndromes. Chest 94:212-214 Available at: [Accessed July 7, 2011].

Chung S, Yoon I-Y, Lee CH, Kim J-W (2009) Effects of age on the clinical features of men with obstructive sleep apnea syndrome. Respiration 78:23-29 Available at: [Accessed June 9, 2011].

Clavaguera F, Bolmont T, Crowther RA, Abramowski D, Frank S, Probst A, Fraser G, Stalder AK, Beibel M, Staufenbiel M, Jucker M, Goedert M, Tolnay M (2009) Transmission and spreading of tauopathy in transgenic mouse brain. Nat. Cell Biol Available at: http://www.ncbi.nlm.nih.gov/pubmed/19503072 [Accessed June 15, 2009].

Coates EL, Li A, Nattie EE (1993) Widespread sites of brain stem ventilatory chemoreceptors. J. Appl. Physiol 75:5-14 Available at: [Accessed July 13, 2011].

Cohen MI (1979) Neurogenesis of respiratory rhythm in the mammal. Physiol. Rev 59:1105-1173 Available at: [Accessed May 5, 2011].

Cohen TJ, Guo JL, Hurtado DE, Kwong LK, Mills IP, Trojanowski JQ, Lee VMY (2011) The acetylation of tau inhibits its function and promotes pathological tau aggregation. Nat Commun 2:252 Available at: [Accessed June 16, 2011].

Conde SV, Obeso A, Rigual R, Monteiro EC, Gonzalez C (2006) Function of the rat carotid body chemoreceptors in ageing. J. Neurochem 99:711-723 Available at: [Accessed June 13, 2011].

Connelly CA, Ellenberger HH, Feldman JL (1989) Are there serotonergic projections from raphe and retrotrapezoid nuclei to the ventral respiratory group in the rat? Neurosci. Lett 105:34-40 Available at: [Accessed May 10, 2011].

Connelly CA, Ellenberger HH, Feldman JL (1990) Respiratory activity in retrotrapezoid nucleus in cat. Am. J. Physiol 258:L33-44 Available at: [Accessed May 10, 2011].

Cooke JR, Ayalon L, Palmer BW, Loredo JS, Corey-Bloom J, Natarajan L, Liu L, Ancoli-Israel S (2009) Sustained use of CPAP slows deterioration of cognition, sleep, and mood in patients with Alzheimer's disease and obstructive sleep apnea: a preliminary study. J Clin Sleep Med 5:305-309 Available at: [Accessed June 23, 2011].

Cosmi EV, Anceschi MM, Cosmi E, Piazze JJ, La Torre R (2003) Ultrasonographic patterns of fetal breathing movements in normal pregnancy. Int J Gynaecol Obstet 80:285-290 Available at: [Accessed May 17, 2011].

Crapo RO, Morris AH, Clayton PD, Nixon CR (1982) Lung volumes in healthy nonsmoking adults. Bull Eur Physiopathol Respir 18:419-425 Available at: [Accessed June 11, 2011].

Cripps D, Thomas SN, Jeng Y, Yang F, Davies P, Yang AJ (2006) Alzheimer disease-specific conformation of hyperphosphorylated paired helical filament-Tau is polyubiquitinated through Lys-48, Lys-11, and Lys-6 ubiquitin conjugation. J. Biol. Chem 281:10825-10838 Available at: [Accessed June 16, 2011].

Dahlstrom A, Fuxe K (1964) EVIDENCE FOR EXISTENCE OF MONOAMINE-CONTAINING NEURONS IN CENTRAL NERVOUS SYSTEM .I. DEMONSTRATION OF MONOAMINES IN CELL BODIES OF BRAIN STEM NEURONS. ACTA PHYSIOLOGICA SCANDINAVICA 62:5-& Available at: [Accessed May 31, 2011].

Dale-Nagle EA, Satriotomo I, Mitchell GS (2011) Spinal Vascular Endothelial Growth Factor Induces Phrenic Motor Facilitation via Extracellular Signal-Regulated Kinase and Akt Signaling. J. Neurosci 31:7682-7690 Available at: [Accessed July 12, 2011].

Davies JG, Kirkwood PA, Sears TA (1985) The distribution of monosynaptic connexions from inspiratory bulbospinal neurones to inspiratory motoneurones in the cat. J. Physiol. (Lond.) 368:63-87 Available at: [Accessed May 5, 2011].

Davis SE, Solhied G, Castillo M, Dwinell M, Brozoski D, Forster HV (2006) Postnatal developmental changes in CO2 sensitivity in rats. J. Appl. Physiol 101:1097-1103 Available at: [Accessed July 13, 2011].

Dawid-Milner MS, Lara JP, Gonzaléz-Barón S, Spyer KM (2001) Respiratory effects of stimulation of cell bodies of the A5 region in the anaesthetised rat. Pflugers Arch 441:434-443 Available at: [Accessed May 30, 2011].

Dawson HN, Ferreira A, Eyster MV, Ghoshal N, Binder LI, Vitek MP (2001) Inhibition of neuronal maturation in primary hippocampal neurons from tau deficient mice. J. Cell. Sci 114:1179-1187 Available at: [Accessed June 16, 2011].

Delclaux B, Orcel B, Housset B, Whitelaw WA, Derenne JP (1994) Arterial blood gases in elderly persons with chronic obstructive pulmonary disease (COPD). Eur. Respir. J 7:856-861 Available at: [Accessed June 11, 2011].

Depuy SD, Kanbar R, Coates MB, Stornetta RL, Guyenet PG (2011) Control of breathing by raphe obscurus serotonergic neurons in mice. J. Neurosci 31:1981-1990 Available at: [Accessed May 30, 2011].

Derenne JP, Debru A, Grassino AE, Whitelaw WA (1995) History of diaphragm physiology: the achievements of Galen. Eur. Respir. J 8:154-160 Available at: [Accessed May 6, 2011].

Destexhe A, Marder E (2004) Plasticity in single neuron and circuit computations. Nature 431:789-795 Available at: [Accessed June 2, 2011].

Dick TE, Baekey DM, Paton JFR, Lindsey BG, Morris KF (2009) Cardio-respiratory coupling depends on the pons. Respir Physiol Neurobiol 168:76-85 Available at: [Accessed June 5, 2011].

Digicaylioglu M, Lipton SA (2001) Erythropoietin-mediated neuroprotection involves cross-talk between Jak2 and NF-kappaB signalling cascades. Nature 412:641-647 Available at: [Accessed July 3, 2011].

Dixit R, Ross JL, Goldman YE, Holzbaur ELF (2008) Differential regulation of dynein and kinesin motor proteins by tau. Science 319:1086-1089 Available at: [Accessed June 16, 2011].

Dobbins EG, Feldman JL (1994)(a) Brainstem network controlling descending drive to phrenic motoneurons in rat. J. Comp. Neurol 347:64-86 Available at: [Accessed May 5, 2011].

Dobbins EG, Feldman JL (1994)(b) Brainstem network controlling descending drive to phrenic motoneurons in rat. J. Comp. Neurol 347:64-86 Available at: [Accessed May 11, 2011].

Dollemore D (2006) Aging under the microscope - A biological quest.

Donald Jr. Bartlett (1986) Upper airway motor system In Handbook for Physiology The American Physiological Society, p. 223-245.

Van Dorpe J, Spittaels K, Van den Haute CV, Dewachter I, Moechars D, Geerts H, Van Leuven F (2003) Neuropathobiology in transgenic mice. The case of Alzheimer's disease. Methods Mol. Biol 209:333-361 Available at: [Accessed June 21, 2011].

Dorval V, Fraser PE (2006) Small ubiquitin-like modifier (SUMO) modification of natively unfolded proteins tau and alpha-synuclein. J. Biol. Chem 281:9919-9924 Available at: [Accessed June 16, 2011].

Douglas WW, Toh CC (1953) The respiratory stimulant action of 5-hydroxytryptamine (serotonin) in the dog. J. Physiol. (Lond.) 120:311-318 Available at: [Accessed May 31, 2011].

Dreshaj IA, Haxhiu MA, Martin RJ (1998) Role of the medullary raphe nuclei in the respiratory response to CO2. Respir Physiol 111:15-23 Available at: [Accessed July 13, 2011].

Dubois B et al. (2010) Revising the definition of Alzheimer's disease: a new lexicon. Lancet Neurol 9:1118-1127 Available at: [Accessed June 17, 2011].

Dubreuil V, Barhanin J, Goridis C, Brunet J-F (2009)(a) Breathing with phox2b. Philos. Trans. R. Soc. Lond., B, Biol. Sci 364:2477-2483 Available at: [Accessed July 13, 2011].

Dubreuil V, Ramanantsoa N, Trochet D, Vaubourg V, Amiel J, Gallego J, Brunet J-F, Goridis C (2008) A human mutation in Phox2b causes lack of CO2 chemosensitivity, fatal central apnea, and specific loss of parafacial neurons. Proc. Natl. Acad. Sci. U.S.A 105:1067-1072 Available at: [Accessed May 11, 2011].

Dubreuil V, Thoby-Brisson M, Rallu M, Persson K, Pattyn A, Birchmeier C, Brunet J-F, Fortin G, Goridis C (2009)(b) Defective respiratory rhythmogenesis and loss of central chemosensitivity in Phox2b mutants targeting retrotrapezoid nucleus neurons. J. Neurosci 29:14836-14846 Available at: [Accessed July 13, 2011].

Duffin J (2003) A commentary on eupnoea and gasping. Respir Physiol Neurobiol 139:105-111 Available at: [Accessed June 9, 2011].

Dujardin E, Jürgens U (2005) Afferents of vocalization-controlling periaqueductal regions in the squirrel monkey. Brain Res 1034:114-131 Available at: [Accessed June 2, 2011].

Dujardin E, Jürgens U (2006) Call type-specific differences in vocalization-related afferents to the periaqueductal gray of squirrel monkeys (Saimiri sciureus). Behav. Brain Res 168:23-36 Available at: [Accessed June 2, 2011].

Duncan JR, Paterson DS, Hoffman JM, Mokler DJ, Borenstein NS, Belliveau RA, Krous HF, Haas EA, Stanley C, Nattie EE, Trachtenberg FL, Kinney HC (2010) Brainstem serotonergic deficiency in sudden infant death syndrome. JAMA 303:430-437 Available at: [Accessed June 1, 2011].

Dunn HG (2001) Neurons and neuronal systems involved in the pathophysiologies of Rett syndrome. Brain Dev 23 Suppl 1:S99-S100 Available at: [Accessed June 24, 2011].

Dunn HG, MacLeod PM (2001) Rett syndrome: review of biological abnormalities. Can J Neurol Sci 28:16-29 Available at: [Accessed June 24, 2011].

Dutschmann M, Guthmann A, Herbert H (1998) NMDA receptor subunit NR1-immunoreactivity in the rat pons and brainstem and colocalization with Fos induced by nasal stimulation. Brain Res 809:221-230 Available at: [Accessed May 9, 2011].

Dutschmann M, Herbert H (1996) The Kölliker-Fuse nucleus mediates the trigeminally induced apnoea in the rat. Neuroreport 7:1432-1436 Available at: [Accessed May 24, 2011].

Dutschmann M, Herbert H (1998) NMDA and GABAA receptors in the rat Kolliker-Fuse area control cardiorespiratory responses evoked by trigeminal ethmoidal nerve stimulation. J. Physiol. (Lond.) 510 (Pt 3):793-804 Available at: [Accessed May 9, 2011].

Dutschmann M, Wilson RJ, Paton JF (2000) Respiratory activity in neonatal rats. Auton Neurosci 84:19-29 Available at: [Accessed January 20, 2009].

Dutschmann M, Herbert H (2006) The Kölliker-Fuse nucleus gates the postinspiratory phase of the respiratory cycle to control inspiratory off-switch and upper airway resistance in rat. Eur. J. Neurosci 24:1071-1084 Available at: [Accessed May 8, 2011].

Dutschmann M, Mörschel M, Kron M, Herbert H (2004) Development of adaptive behaviour of the respiratory network: implications for the pontine Kolliker-Fuse nucleus. Respir Physiol Neurobiol 143:155-165 Available at: [Accessed May 8, 2011].

Dutschmann M, Mörschel M, Rybak IA, Dick TE (2009) Learning to breathe: control of the inspiratory-expiratory phase transition shifts from sensory- to central-dominated during postnatal development in rats. J. Physiol. (Lond.) 587:4931-4948 Available at: [Accessed May 22, 2011].

Duyckaerts C, Delatour B, Potier M-C (2009) Classification and basic pathology of Alzheimer disease. Acta Neuropathol 118:5-36 Available at: [Accessed June 18, 2011].

Eastman NJ (1954) Mount Everest in utero. Am. J. Obstet. Gynecol 67:701-711 Available at: [Accessed May 23, 2011].

Ebneth A, Godemann R, Stamer K, Illenberger S, Trinczek B, Mandelkow E (1998) Overexpression of tau protein inhibits kinesin-dependent trafficking of vesicles, mitochondria, and endoplasmic reticulum: implications for Alzheimer's disease. J. Cell Biol 143:777-794 Available at: [Accessed June 16, 2011].

Eikermann M, Jordan AS, Chamberlin NL, Gautam S, Wellman A, Lo Y-L, White DP, Malhotra A (2007) The influence of aging on pharyngeal collapsibility during sleep. Chest 131:1702-1709 Available at: [Accessed June 11, 2011].

Elam M, Yao T, Thorén P, Svensson TH (1981) Hypercapnia and hypoxia: chemoreceptor-mediated control of locus coeruleus neurons and splanchnic, sympathetic nerves. Brain Res 222:373-381 Available at: [Accessed July 13, 2011].

Eldridge FL, Kiley JP, Millhorn DE (1984) Respiratory effects of carbon dioxide-induced changes of medullary extracellular fluid pH in cats. J. Physiol. (Lond.) 355:177-189 Available at: [Accessed July 12, 2011].

Elian M, Rudolf ND (1991) EEG and respiration in Rett syndrome. Acta Neurol. Scand 83:123-128 Available at: [Accessed June 24, 2011].

Ellenberger HH, Feldman JL (1990) Brainstem connections of the rostral ventral respiratory group of the rat. Brain Res 513:35-42 Available at: [Accessed May 10, 2011].

Ellenberger HH, Feldman JL, Goshgarian HG (1990) Ventral respiratory group projections to phrenic motoneurons: electron microscopic evidence for monosynaptic connections. J. Comp. Neurol 302:707-714 Available at: [Accessed May 5, 2011].

Enright PL, Kronmal RA, Manolio TA, Schenker MB, Hyatt RE (1994) Respiratory muscle strength in the elderly. Correlates and reference values. Cardiovascular Health Study Research Group. Am. J. Respir. Crit. Care Med 149:430-438 Available at: [Accessed June 10, 2011].

Errchidi S, Hilaire G, Monteau R (1990) Permanent release of noradrenaline modulates respiratory frequency in the newborn rat: an in vitro study. J. Physiol. (Lond.) 429:497-510 Available at: [Accessed May 29, 2011].

Errchidi S, Monteau R, Hilaire G (1991) Noradrenergic modulation of the medullary respiratory rhythm generator in the newborn rat: an in vitro study. J. Physiol. (Lond.) 443:477-498 Available at: [Accessed May 29, 2011].

Esposito A, Demeurisse G, Alberti B, Fabbro F (1999) Complete mutism after midbrain periaqueductal gray lesion. Neuroreport 10:681-685 Available at: [Accessed June 2, 2011].

Evans AM, Mustard KJW, Wyatt CN, Peers C, Dipp M, Kumar P, Kinnear NP, Hardie DG (2005) Does AMP-activated protein kinase couple inhibition of mitochondrial oxidative phosphorylation by hypoxia to calcium signaling in O2-sensing cells? J. Biol. Chem 280:41504-41511 Available at: [Accessed June 30, 2011].

Ezure K (1990) Synaptic connections between medullary respiratory neurons and considerations on the genesis of respiratory rhythm. Prog. Neurobiol 35:429-450 Available at: [Accessed May 11, 2011].

Ezure K, Tanaka I (1996) Pump neurons of the nucleus of the solitary tract project widely to the medulla. Neurosci. Lett 215:123-126 Available at: [Accessed July 14, 2011].

Ezure K, Tanaka I (2004) GABA, in some cases together with glycine, is used as the inhibitory transmitter by pump cells in the Hering-Breuer reflex pathway of the rat. Neuroscience 127:409-417 Available at: [Accessed May 12, 2011].

Ezure K, Tanaka I (2006) Distribution and medullary projection of respiratory neurons in the dorsolateral pons of the rat. Neuroscience 141:1011-1023 Available at: [Accessed May 9, 2011].

Ezure K, Tanaka I, Miyazaki M (1998) Pontine projections of pulmonary slowly adapting receptor relay neurons in the cat. Neuroreport 9:411-414 Available at: [Accessed July 14, 2011].

Ezure K (2004) Reflections on respiratory rhythm generation. Prog. Brain Res 143:67-74 Available at: [Accessed June 7, 2011].

Ezure K, Tanaka I, Kondo M (2003)(a) Glycine is used as a transmitter by decrementing expiratory neurons of the ventrolateral medulla in the rat. J. Neurosci 23:8941-8948 Available at: [Accessed May 11, 2011].

Ezure K, Tanaka I, Saito Y (2003)(b) Brainstem and spinal projections of augmenting expiratory neurons in the rat. Neurosci. Res 45:41-51 Available at: [Accessed May 11, 2011].

Ezure K, Tanaka I, Saito Y, Otake K (2002) Axonal projections of pulmonary slowly adapting receptor relay neurons in the rat. J. Comp. Neurol 446:81-94 Available at: [Accessed July 14, 2011].

Fabris G, Anselmo-Franci JA, Branco LG (1999) Role of nitric oxide in hypoxia-induced hyperventilation and hypothermia: participation of the locus coeruleus. Braz. J. Med. Biol. Res 32:1389-1398 Available at: [Accessed July 11, 2011].

Fabris G, Steiner AA, Anselmo-Franci JA, Branco LG (2000) Role of nitric oxide in rat locus coeruleus in hypoxia-induced hyperventilation and hypothermia. Neuroreport 11:2991-2995 Available at: [Accessed July 11, 2011].

Fallert M, Böhmer G, Dinse HR, Sommer TJ, Bittner A (1979) Microelectrophoretic application of putative neurotransmitters onto various types of bulbar respiratory neurons. Arch Ital Biol 117:1-12 Available at: [Accessed May 31, 2011].

Farias GA, Muñoz JP, Garrido J, Maccioni RB (2002) Tubulin, actin, and tau protein interactions and the study of their macromolecular assemblies. J. Cell. Biochem 85:315-324 Available at: [Accessed June 16, 2011].

Farmer CG (1999) Evolution of the vertebrate cardio-pulmonary system. Annu. Rev. Physiol 61:573-592 Available at: [Accessed May 2, 2011].

Fatemian M, Gamboa A, Léon-Velarde F, Rivera-Ch M, Palacios J-A, Robbins PA (2003) Selected contribution: Ventilatory response to CO2 in high-altitude natives and patients with chronic mountain sickness. J. Appl. Physiol 94:1279-1287; discussion 1253-1254 Available at: [Accessed April 19, 2010].

Fedorko L, Hoskin RW, Duffin J (1989) Projections from inspiratory neurons of the nucleus retroambigualis to phrenic motoneurons in the cat. Exp. Neurol 105:306-310 Available at: [Accessed May 5, 2011].

Fedorko L, Merrill EG, Lipski J (1983) Two descending medullary inspiratory pathways to phrenic motoneurones. Neurosci. Lett 43:285-291 Available at: [Accessed May 5, 2011].

Feldman JL, Mitchell GS, Nattie EE (2003) Breathing: rhythmicity, plasticity, chemosensitivity. Annu. Rev. Neurosci 26:239-266 Available at: [Accessed July 12, 2011].

Feldman JL, Del Negro CA (2006)(a) Looking for inspiration: new perspectives on respiratory rhythm. Nat.

Rev. Neurosci 7:232-242 Available at: [Accessed May 10, 2011].

Feldman JL, Del Negro CA (2006)(b) Looking for inspiration: new perspectives on respiratory rhythm. Nat. Rev. Neurosci 7:232-242 Available at: [Accessed May 4, 2011].

Feldman JL (1986) Neurophysiology of breathing in mammals. In Handbook of physiology-the nervous system American Physiology Society, p. 463-524.

Fenik P, Veasey SC (2003) Pharmacological characterization of serotonergic receptor activity in the hypoglossal nucleus. Am. J. Respir. Crit. Care Med 167:563-569 Available at: [Accessed June 12, 2011].

Feuillette S, Miguel L, Frébourg T, Campion D, Lecourtois M (2010) Drosophila models of human tauopathies indicate that Tau protein toxicity in vivo is mediated by soluble cytosolic phosphorylated forms of the protein. J. Neurochem 113:895-903 Available at: [Accessed June 22, 2011].

Finch CE, Tanzi RE (1997) Genetics of aging. Science 278:407-411 Available at: [Accessed June 8, 2011].

Finkel T, Holbrook NJ (2000) Oxidants, oxidative stress and the biology of ageing. Nature 408:239-247 Available at: [Accessed June 8, 2011].

Finley JC, Katz DM (1992) The central organization of carotid body afferent projections to the brainstem of the rat. Brain Res 572:108-116 Available at: [Accessed June 29, 2011].

Finley JC, Polak J, Katz DM (1992) Transmitter diversity in carotid body afferent neurons: dopaminergic and peptidergic phenotypes. Neuroscience 51:973-987 Available at: [Accessed May 11, 2011].

Flourens P (1842) Recherches expérimentales sur les propriétés et les fonctions du système nerveux dans les animaux vertébrés. Baillière Ed. Paris.

Flourens P (1851) Note sur le point vital de la moelle allongée.

Fordyce WE (1987) Hypoxic ventilatory control in the awake cat five years after carotid body resection. Respir Physiol 69:209-225 Available at: [Accessed July 2, 2011].

Fortuna MG, Stornetta RL, West GH, Guyenet PG (2009) Activation of the retrotrapezoid nucleus by posterior hypothalamic stimulation. J. Physiol. (Lond.) 587:5121-5138 Available at: [Accessed July 13, 2011].

Froelich S, Basun H, Forsell C, Lilius L, Axelman K, Andreadis A, Lannfelt L (1997) Mapping of a disease locus for familial rapidly progressive frontotemporal dementia to chromosome 17q12-21. Am. J. Med. Genet 74:380-385 Available at: [Accessed June 22, 2011].

Frost B, Jacks RL, Diamond MI (2009) Propagation of tau misfolding from the outside to the inside of a cell. J. Biol. Chem 284:12845-12852 Available at: [Accessed June 22, 2011].

Fulga TA, Elson-Schwab I, Khurana V, Steinhilb ML, Spires TL, Hyman BT, Feany MB (2007) Abnormal bundling and accumulation of F-actin mediates tau-induced neuronal degeneration in vivo. Nat. Cell Biol 9:139-148 Available at: [Accessed June 16, 2011].

Fung ML, St John WM (1995) The functional expression of a pontine pneumotaxic centre in neonatal rats. J. Physiol. (Lond.) 489 (Pt 2):579-591 Available at: [Accessed May 24, 2011].

Gallez C (2005) Rapport sur la maladie d'Alzheimer et les maladies apparentées.

Gang S, Sato Y, Kohama I, Aoki M (1995) Afferent projections to the Bötzinger complex from the upper cervical cord and other respiratory related structures in the brainstem in cats: retrograde WGA-HRP tracing. J. Auton. Nerv. Syst 56:1-7 Available at: [Accessed May 10, 2011].

Gassmann M, Heinicke K, Soliz J, Ogunshola OO (2003) Non-erythroid functions of erythropoietin. Adv. Exp. Med. Biol 543:323-330 Available at: [Accessed July 3, 2011].

Gassmann M, Soliz J (2009) Erythropoietin modulates the neural control of hypoxic ventilation. Cell. Mol. Life Sci 66:3575-3582 Available at: [Accessed July 3, 2011].

Gatti PJ, Shirahata M, Johnson TA, Massari VJ (1995) Synaptic interactions of substance P immunoreactive nerve terminals in the baro- and chemoreceptor reflexes of the cat. Brain Res 693:133-147 Available at: [Accessed May 11, 2011].

Gautier H, Bonora M (1979) Effects of carotid body denervation on respiratory pattern of awake cats. J Appl Physiol 46:1127-1131 Available at: [Accessed July 12, 2011].

Gaytán SP, Pásaro R (1998) Connections of the rostral ventral respiratory neuronal cell group: an anterograde and retrograde tracing study in the rat. Brain Res. Bull 47:625-642 Available at: [Accessed May 5, 2011].

Gaytán SP, Pásaro R, Coulon P, Bevengut M, Hilaire G (2002)(a) Identification of central nervous system neurons innervating the respiratory muscles of the mouse: a transneuronal tracing study. Brain Res. Bull 57:335-339 Available at: [Accessed May 5, 2011].

Gaytán SP, Pásaro R, Coulon P, Bevengut M, Hilaire G (2002)(b) Identification of central nervous system neurons innervating the respiratory muscles of the mouse: a transneuronal tracing study. Brain Res. Bull 57:335-339 Available at: [Accessed May 11, 2011].

German DC, Manaye KF, White CL 3rd, Woodward DJ, McIntire DD, Smith WK, Kalaria RN, Mann DM (1992) Disease-specific patterns of locus coeruleus cell loss. Ann. Neurol 32:667-676 Available at: [Accessed June 23, 2011].

Geschwind DH (2003) Tau phosphorylation, tangles, and neurodegeneration: the chicken or the egg? Neuron 40:457-460 Available at: [Accessed June 20, 2011].

Gestreau C, Bianchi AL, Grélot L (1997) Differential brainstem Fos-like immunoreactivity after laryngeal-induced coughing and its reduction by codeine. J. Neurosci 17:9340-9352 Available at: [Accessed June 2, 2011].

Gestreau C, Grélot L, Bianchi AL (2000) Activity of respiratory laryngeal motoneurons during fictive coughing and swallowing. Exp Brain Res 130:27-34 Available at: [Accessed May 4, 2011].

Gestreau C, Milano S, Bianchi AL, Grélot L (1996) Activity of dorsal respiratory group inspiratory neurons during laryngeal-induced fictive coughing and swallowing in decerebrate cats. Exp Brain Res 108:247-256 Available at: [Accessed May 4, 2011].

Gestreau C, Dutschmann M, Obled S, Bianchi AL (2005) Activation of XII motoneurons and premotor neurons during various oropharyngeal behaviors. Respir Physiol Neurobiol 147:159-176 Available at: [Accessed May 4, 2011].

Gestreau C, Heitzmann D, Thomas J, Dubreuil V, Bandulik S, Reichold M, Bendahhou S, Pierson P, Sterner C, Peyronnet-Roux J, Benfriha C, Tegtmeier I, Ehnes H, Georgieff M, Lesage F, Brunet J-F, Goridis C, Warth R, Barhanin J (2010) Task2 potassium channels set central respiratory CO2 and O2 sensitivity. Proc. Natl. Acad. Sci. U.S.A 107:2325-2330 Available at: [Accessed July 11, 2011].

Giannakopoulos P, Herrmann FR, Bussière T, Bouras C, Kövari E, Perl DP, Morrison JH, Gold G, Hof PR (2003) Tangle and neuron numbers, but not amyloid load, predict cognitive status in Alzheimer's disease. Neurology 60:1495-1500 Available at: [Accessed June 18, 2011].

Giménez E, Montoliu L (2001) A simple polymerase chain reaction assay for genotyping the retinal degeneration mutation (Pdeb(rd1)) in FVB/N-derived transgenic mice. Lab. Anim 35:153-156 Available at: [Accessed July 5, 2011].

Ginzel KH, Kottegoda SR (1954) The action of 5-hydroxytryptamine and tryptamine on aortic and carotid sinus receptors in the cat. J. Physiol. (Lond.) 123:277-288 Available at: [Accessed May 31, 2011].

Di Giulio C, Cacchio M, Bianchi G, Rapino C, Di Ilio C (2003) Selected contribution: Carotid body as a model for aging studies: is there a link between oxygen and aging? J. Appl. Physiol 95:1755-1758 Available at:

[Accessed June 13, 2011].

Goedert M, Spillantini MG, Jakes R, Rutherford D, Crowther RA (1989)(a) Multiple isoforms of human microtubule-associated protein tau: sequences and localization in neurofibrillary tangles of Alzheimer's disease. Neuron 3:519-526 Available at: [Accessed June 15, 2011].

Goedert M, Spillantini MG, Potier MC, Ulrich J, Crowther RA (1989)(b) Cloning and sequencing of the cDNA encoding an isoform of microtubule-associated protein tau containing four tandem repeats: differential expression of tau protein mRNAs in human brain. EMBO J 8:393-399 Available at: [Accessed June 15, 2011].

Goedert M, Jakes R (2005) Mutations causing neurodegenerative tauopathies. Biochim. Biophys. Acta 1739:240-250 Available at: [Accessed June 20, 2011].

Goldman JE, Kim KS, Schwartz JH (1976) Axonal transport of [3H]serotonin in an identified neuron of Aplysia californica. J. Cell Biol 70:304-318 Available at: [Accessed July 7, 2011].

Goldman JE, Schwartz JH (1974) Cellular specificity of serotonin storage and axonal transport in identified neurones of Aplysia californica. J. Physiol. (Lond.) 242:61-76 Available at: [Accessed July 7, 2011].

Gonzalez C, Agapito MT, Rocher A, Gonzalez-Martin MC, Vega-Agapito V, Gomez-Niño A, Rigual R, Castañeda J, Obeso A (2007) Chemoreception in the context of the general biology of ROS. Respir Physiol Neurobiol 157:30-44 Available at: [Accessed June 30, 2011].

Gonzalez C, Almaraz L, Obeso A, Rigual R (1994) Carotid body chemoreceptors: from natural stimuli to sensory discharges. Physiol. Rev 74:829-898 Available at: [Accessed June 29, 2011].

Gonzalez C, Sanz-Alyayate G, Agapito MT, Obeso A (2004) Effects of reducing agents on glutathione metabolism and the function of carotid body chemoreceptor cells. Biol. Chem 385:265-274 Available at: [Accessed June 30, 2011].

Goodman A, Schorge J, Greene MF (2011) The long-term effects of in utero exposures--the DES story. N. Engl. J. Med 364:2083-2084 Available at: [Accessed July 9, 2011].

Gourine AV, Kasymov V, Marina N, Tang F, Figueiredo MF, Lane S, Teschemacher AG, Spyer KM, Deisseroth K, Kasparov S (2010) Astrocytes control breathing through pH-dependent release of ATP. Science 329:571-575 Available at: [Accessed July 1, 2011].

Gourine AV, Llaudet E, Dale N, Spyer KM (2005)(a) Release of ATP in the ventral medulla during hypoxia in rats: role in hypoxic ventilatory response. J. Neurosci 25:1211-1218 Available at: [Accessed July 11, 2011].

Gourine AV, Llaudet E, Dale N, Spyer KM (2005)(b) ATP is a mediator of chemosensory transduction in the central nervous system. Nature 436:108-111 Available at: [Accessed July 1, 2011].

Graeff FG (2004) Serotonin, the periaqueductal gray and panic. Neurosci Biobehav Rev 28:239-259 Available at: [Accessed June 3, 2011].

Gray PA, Janczewski WA, Mellen N, McCrimmon DR, Feldman JL (2001) Normal breathing requires preBötzinger complex neurokinin-1 receptor-expressing neurons. Nat. Neurosci 4:927-930 Available at: [Accessed May 19, 2011].

Gray PA, Rekling JC, Bocchiaro CM, Feldman JL (1999) Modulation of respiratory frequency by peptidergic input to rhythmogenic neurons in the preBötzinger complex. Science 286:1566-1568 Available at: [Accessed May 11, 2011].

Grelot L, Iscoe S, Bianchi AL (1988) Effects of amino acids on the excitability of respiratory bulbospinal neurons in solitary and para-ambigual regions of medulla in cat. Brain Res 443:27-36 Available at: [Accessed May 11, 2011].

Grimsley JMS, Monaghan JJM, Wenstrup JJ (2011) Development of social vocalizations in mice. PLoS ONE 6:e17460 Available at: [Accessed May 15, 2011].

Grinberg LT, Rüb U, Ferretti REL, Nitrini R, Farfel JM, Polichiso L, Gierga K, Jacob-Filho W, Heinsen H (2009) The dorsal raphe nucleus shows phospho-tau neurofibrillary changes before the transentorhinal region in Alzheimer's disease. A precocious onset? Neuropathol. Appl. Neurobiol 35:406-416 Available at: [Accessed June 23, 2011].

Grossman P, Taylor EW (2007) Toward understanding respiratory sinus arrhythmia: relations to cardiac vagal tone, evolution and biobehavioral functions. Biol Psychol 74:263-285 Available at: [Accessed June 5, 2011].

Groups TLaM (1994) Clinical and neuropathological criteria for frontotemporal dementia. The Lund and Manchester Groups. J. Neurol. Neurosurg. Psychiatr 57:416-418 Available at: [Accessed June 22, 2011].

Grudzien A, Shaw P, Weintraub S, Bigio E, Mash DC, Mesulam MM (2007) Locus coeruleus neurofibrillary degeneration in aging, mild cognitive impairment and early Alzheimer's disease. Neurobiol. Aging 28:327-335 Available at: [Accessed June 23, 2011].

Grundke-Iqbal I, Iqbal K, Tung YC, Quinlan M, Wisniewski HM, Binder LI (1986) Abnormal phosphorylation of the microtubule-associated protein tau (tau) in Alzheimer cytoskeletal pathology. Proc Natl Acad Sci U S A 83:4913-7 Available at: [Accessed February 18, 2009].

Grélot L, Barillot JC, Bianchi AL (1989) Central distributions of the efferent and afferent components of the pharyngeal branches of the vagus and glossopharyngeal nerves: an HRP study in the cat. Exp Brain Res 78:327-335 Available at: [Accessed May 5, 2011].

Grélot L, Bianchi AL, Iscoe S, Remmers JE (1988) Expiratory neurones of the rostral medulla: anatomical and functional correlates. Neurosci. Lett 89:140-145 Available at: [Accessed May 5, 2011].

Grélot L, Milano S, Portillo F, Miller AD, Bianchi AL (1992) Membrane potential changes of phrenic motoneurons during fictive vomiting, coughing, and swallowing in the decerebrate cat. J. Neurophysiol 68:2110-2119 Available at: [Accessed June 2, 2011].

Gu Y, Oyama F, Ihara Y (1996) Tau is widely expressed in rat tissues. J. Neurochem 67:1235-1244 Available at: [Accessed June 15, 2011].

Guarente L, Kenyon C (2000) Genetic pathways that regulate ageing in model organisms. Nature 408:255-262 Available at: [Accessed June 8, 2011].

Gulyás B, Brockschnieder D, Nag S, Pavlova E, Kása P, Beliczai Z, Légrádi A, Gulya K, Thiele A, Dyrks T, Halldin C (2010) The norepinephrine transporter (NET) radioligand (S,S)-[18F]FMeNER-D2 shows significant decreases in NET density in the human brain in Alzheimer's disease: a post-mortem autoradiographic study. Neurochem. Int 56:789-798 Available at: [Accessed June 23, 2011].

Guo X, Waern M, Sjögren K, Lissner L, Bengtsson C, Björkelund C, Ostling S, Gustafson D, Skoog I (2007) Midlife respiratory function and Incidence of Alzheimer's disease: a 29-year longitudinal study in women. Neurobiol. Aging 28:343-350 Available at: [Accessed June 23, 2011].

Gura T (1999) Gene defect linked to Rett syndrome. Science 286:27 Available at: [Accessed June 24, 2011].

Guthmann A, Herbert H (1999) Expression of N-methyl-D-aspartate receptor subunits in the rat parabrachial and Kölliker-Fuse nuclei and in selected pontomedullary brainstem nuclei. J. Comp. Neurol 415:501-517 Available at: [Accessed May 9, 2011].

Gutrecht JA (1992) Autonomic cardiovascular reflexes in progressive supranuclear palsy. J. Auton. Nerv. Syst 39:29-35 Available at: [Accessed June 23, 2011].

Guy J, Gan J, Selfridge J, Cobb S, Bird A (2007) Reversal of neurological defects in a mouse model of Rett syndrome. Science 315:1143-1147 Available at: [Accessed July 6, 2011].

Guyenet PG (1984) Baroreceptor-mediated inhibition of A5 noradrenergic neurons. Brain Res 303:31-40 Available at: [Accessed May 10, 2011].

Guyenet PG, Koshiya N, Huangfu D, Verberne AJ, Riley TA (1993) Central respiratory control of A5 and A6 pontine noradrenergic neurons. Am. J. Physiol 264:R1035-1044 Available at: [Accessed May 30, 2011].

Guyenet PG, Wang H (2001) Pre-Bötzinger neurons with preinspiratory discharges "in vivo" express NK1 receptors in the rat. J. Neurophysiol 86:438-446 Available at: [Accessed May 11, 2011].

Guyenet PG, Mulkey DK, Stornetta RL, Bayliss DA (2005)(a) Regulation of ventral surface chemoreceptors by the central respiratory pattern generator. J. Neurosci 25:8938-8947 Available at: [Accessed May 11, 2011].

Guyenet PG, Sevigny CP, Weston MC, Stornetta RL (2002) Neurokinin-1 receptor-expressing cells of the ventral respiratory group are functionally heterogeneous and predominantly glutamatergic. J. Neurosci 22:3806-3816 Available at: [Accessed May 11, 2011].

Guyenet PG, Stornetta RL, Bayliss DA (2010) Central respiratory chemoreception. J. Comp. Neurol 518:3883-3906 Available at: [Accessed February 28, 2011].

Guyenet PG, Stornetta RL, Bayliss DA, Mulkey DK (2005)(b) Retrotrapezoid nucleus: a litmus test for the identification of central chemoreceptors. Exp. Physiol 90:247-253; discussion 253-257 Available at: [Accessed May 11, 2011].

Guénard H, Marthan R (1996) Pulmonary gas exchange in elderly subjects. Eur. Respir. J 9:2573-2577 Available at: [Accessed June 11, 2011].

Gómez-Ramos A, Díaz-Hernández M, Rubio A, Miras-Portugal MT, Avila J (2008) Extracellular tau promotes intracellular calcium increase through M1 and M3 muscarinic receptors in neuronal cells. Mol. Cell. Neurosci 37:673-681 Available at: [Accessed June 22, 2011].

Gómez-Ramos A, Díaz-Hernández M, Cuadros R, Hernández F, Avila J (2006) Extracellular tau is toxic to neuronal cells. FEBS Lett 580:4842-4850 Available at: [Accessed June 22, 2011].

Götz J, Chen F, Barmettler R, Nitsch RM (2001)(a) Tau filament formation in transgenic mice expressing P301L tau. J. Biol. Chem 276:529-534 Available at: [Accessed July 5, 2011].

Götz J, Chen F, van Dorpe J, Nitsch RM (2001)(b) Formation of neurofibrillary tangles in P301l tau transgenic mice induced by Abeta 42 fibrils. Science 293:1491-1495 Available at: [Accessed June 19, 2009].

Götz J, Probst A, Spillantini MG, Schäfer T, Jakes R, Bürki K, Goedert M (1995) Somatodendritic localization and hyperphosphorylation of tau protein in transgenic mice expressing the longest human brain tau isoform. EMBO J 14:1304-1313 Available at: [Accessed June 20, 2011].

Götz J, Streffer JR, David D, Schild A, Hoerndli F, Pennanen L, Kurosinski P, Chen F (2004) Transgenic animal models of Alzheimer's disease and related disorders: histopathology, behavior and therapy. Mol. Psychiatry 9:664-683 Available at: [Accessed June 15, 2011].

Götz J, Ittner LM, Kins S (2006) Do axonal defects in tau and amyloid precursor protein transgenic animals model axonopathy in Alzheimer's disease? J. Neurochem 98:993-1006 Available at: [Accessed June 16, 2011].

Haass C, Selkoe DJ (2007) Soluble protein oligomers in neurodegeneration: lessons from the Alzheimer's amyloid beta-peptide. Nat. Rev. Mol. Cell Biol 8:101-112 Available at: [Accessed June 18, 2011].

Hagberg B, Aicardi J, Dias K, Ramos O (1983) A progressive syndrome of autism, dementia, ataxia, and loss of purposeful hand use in girls: Rett's syndrome: report of 35 cases. Ann. Neurol 14:471-479 Available at: [Accessed June 24, 2011].

Haglund M, Sjöbeck M, Englund E (2006) Locus ceruleus degeneration is ubiquitous in Alzheimer's disease: possible implications for diagnosis and treatment. Neuropathology 26:528-532 Available at: [Accessed June 23, 2011].

Haji A, Takeda R, Okazaki M (2000) Neuropharmacology of control of respiratory rhythm and pattern in mature mammals. Pharmacol. Ther 86:277-304 Available at: [Accessed June 7, 2011].

Halliday GM, McCann HL, Pamphlett R, Brooks WS, Creasey H, McCusker E, Cotton RG, Broe GA, Harper CG (1992) Brain stem serotonin-synthesizing neurons in Alzheimer's disease: a clinicopathological correlation. Acta Neuropathol 84:638-650 Available at: [Accessed June 23, 2011].

Harada A, Oguchi K, Okabe S, Kuno J, Terada S, Ohshima T, Sato-Yoshitake R, Takei Y, Noda T, Hirokawa N (1994) Altered microtubule organization in small-calibre axons of mice lacking tau protein. Nature 369:488-491 Available at: [Accessed June 20, 2011].

Hardy J, Selkoe DJ (2002) The amyloid hypothesis of Alzheimer's disease: progress and problems on the road to therapeutics. Science 297:353-356 Available at: [Accessed June 18, 2011].

Harley CB, Futcher AB, Greider CW (1990) Telomeres shorten during ageing of human fibroblasts. Nature 345:458-460 Available at: [Accessed June 8, 2011].

Haxhiu MA, Tolentino-Silva F, Pete G, Kc P, Mack SO (2001) Monoaminergic neurons, chemosensation and arousal. Respir Physiol 129:191-209 Available at: [Accessed July 13, 2011].

Haxhiu MA, Yung K, Erokwu B, Cherniack NS (1996) CO2-induced c-fos expression in the CNS catecholaminergic neurons. Respir Physiol 105:35-45 Available at: [Accessed July 13, 2011].

Hayflick L, Moorhead PS (1961) The serial cultivation of human diploid cell strains. Exp. Cell Res 25:585-621 Available at: [Accessed June 8, 2011].

Hayward LF, Castellanos M, Davenport PW (2004) Parabrachial neurons mediate dorsal periaqueductal gray evoked respiratory responses in the rat. J. Appl. Physiol 96:1146-1154 Available at: [Accessed June 5, 2011].

Hayward LF, Swartz CL, Davenport PW (2003) Respiratory response to activation or disinhibition of the dorsal periaqueductal gray in rats. J. Appl. Physiol 94:913-922 Available at: [Accessed June 5, 2011].

He HJ, Wang XS, Pan R, Wang DL, Liu MN, He RQ (2009) The proline-rich domain of tau plays a role in interactions with actin. BMC Cell Biol 10:81 Available at: [Accessed June 16, 2011].

Heath D (1991) The human carotid body in health and disease. J. Pathol 164:1-8 Available at: [Accessed June 13, 2011].

Helmer C, Pasquier F, Dartigues J-F (2006) [Epidemiology of Alzheimer disease and related disorders]. Med Sci (Paris) 22:288-296 Available at: [Accessed June 17, 2011].

Hendricksen M, Thomas AJ, Ferrier IN, Ince P, O'Brien JT (2004) Neuropathological study of the dorsal raphe nuclei in late-life depression and Alzheimer's disease with and without depression. Am J Psychiatry 161:1096-1102 Available at: [Accessed June 23, 2011].

Hering E (1868) Die Selbststeurung der Athmung durch den Nervus vagus. Akad Wiss Wien 57:672-677

Hermann DM, Luppi PH, Peyron C, Hinckel P, Jouvet M (1996) Forebrain projections of the rostral nucleus raphe magnus shown by iontophoretic application of choleratoxin b in rats. Neurosci. Lett 216:151-154 Available at: [Accessed May 31, 2011].

Hermann DM, Luppi PH, Peyron C, Hinckel P, Jouvet M (1997) Afferent projections to the rat nuclei raphe magnus, raphe pallidus and reticularis gigantocellularis pars alpha demonstrated by iontophoretic application of choleratoxin (subunit b). J. Chem. Neuroanat 13:1-21 Available at: [Accessed May 31, 2011].

Heymans C, Bouckaert JJ (1930) Sinus caroticus and respiratory reflexes: I. Cerebral blood flow and respiration. Adrenaline apnoea. J. Physiol. (Lond.) 69:254-266 Available at: [Accessed June 29, 2011].

Hilaire GG, Nicholls JG, Sears TA (1983) Central and proprioceptive influences on the activity of levator costae motoneurones in the cat. J. Physiol. (Lond.) 342:527-548 Available at: [Accessed July 14, 2011].

Hilaire G, Duron B (1999) Maturation of the mammalian respiratory system. Physiol. Rev 79:325-360 Available at: [Accessed May 23, 2011].

Hilaire G, Monteau R (1976) [Connections between inspiratory medullary neurons and phrenic or intercostal motoneurones (author's transl)]. J. Physiol. (Paris) 72:987-1000 Available at: [Accessed July 14, 2011].

Hilaire G, Monteau R, Bianchi AL (1984) A cross-correlation study of interactions among respiratory neurons of dorsal, ventral and retrofacial groups in cat medulla. Brain Res 302:19-31 Available at: [Accessed May 5, 2011].

Hilaire G, Monteau R, Errchidi S (1989) Possible modulation of the medullary respiratory rhythm generator by the noradrenergic A5 area: an in vitro study in the newborn rat. Brain Res 485:325-332 Available at: [Accessed May 29, 2011].

Hilaire G, Morin D, Lajard AM, Monteau R (1993) Changes in serotonin metabolism may elicit obstructive apnoea in the newborn rat. J. Physiol. (Lond.) 466:367-381 Available at: [Accessed May 31, 2011].

Hilaire G (2006) Endogenous noradrenaline affects the maturation and function of the respiratory network: possible implication for SIDS. Auton Neurosci 126-127:320-331 Available at: [Accessed May 30, 2011].

Hilaire G, Pásaro R (2003) Genesis and control of the respiratory rhythm in adult mammals. News Physiol. Sci 18:23-28 Available at: [Accessed May 5, 2011].

Hilaire G, Viemari J-C, Coulon P, Simonneau M, Bévengut M (2004) Modulation of the respiratory rhythm generator by the pontine noradrenergic A5 and A6 groups in rodents. Respir Physiol Neurobiol 143:187-197 Available at: [Accessed May 8, 2011].

Hillert D (1999) On processing lexical meanings in aphasia and Alzheimer's disease: some (re)considerations. Brain Lang 69:95-118 Available at: [Accessed June 23, 2011].

Hillman RS, Finch CA (1971) Erythropoiesis. N. Engl. J. Med 285:99-101 Available at: [Accessed July 3, 2011].

Hirokawa N, Funakoshi T, Sato-Harada R, Kanai Y (1996) Selective stabilization of tau in axons and microtubule-associated protein 2C in cell bodies and dendrites contributes to polarized localization of cytoskeletal proteins in mature neurons. J. Cell Biol 132:667-679 Available at: [Accessed June 15, 2011].

Hirtz D, Thurman DJ, Gwinn-Hardy K, Mohamed M, Chaudhuri AR, Zalutsky R (2007) How common are the "common" neurologic disorders? Neurology 68:326-337 Available at: [Accessed June 17, 2011].

Hla KM, Young TB, Bidwell T, Palta M, Skatrud JB, Dempsey J (1994) Sleep apnea and hypertension. A population-based study. Ann. Intern. Med 120:382-388 Available at: [Accessed June 9, 2011].

Hodges MR, Opansky C, Qian B, Davis S, Bonis JM, Krause K, Pan LG, Forster HV (2005) Carotid body denervation alters ventilatory responses to ibotenic acid injections or focal acidosis in the medullary raphe. J. Appl. Physiol 98:1234-1242 Available at: [Accessed July 13, 2011].

Hodges MR, Opansky C, Qian B, Davis S, Bonis J, Bastasic J, Leekley T, Pan LG, Forster HV (2004) Transient attenuation of CO2 sensitivity after neurotoxic lesions in the medullary raphe area of awake goats. J. Appl. Physiol 97:2236-2247 Available at: [Accessed July 13, 2011].

Hodges MR, Richerson GB (2008)(a) Contributions of 5-HT neurons to respiratory control: neuromodulatory and trophic effects. Respir Physiol Neurobiol 164:222-232 Available at: [Accessed June 12, 2011].

Hodges MR, Richerson GB (2008)(b) Interaction between defects in ventilatory and thermoregulatory control in mice lacking 5-HT neurons. Respir Physiol Neurobiol 164:350-357 Available at: [Accessed July 11, 2011].

Hodges MR, Richerson GB (2010) Medullary serotonin neurons and their roles in central respiratory chemoreception. Respir Physiol Neurobiol 173:256-263 Available at: [Accessed June 28, 2011].

Hodges MR, Tattersall GJ, Harris MB, McEvoy SD, Richerson DN, Deneris ES, Johnson RL, Chen Z-F, Richerson GB (2008) Defects in breathing and thermoregulation in mice with near-complete absence of central serotonin neurons. J. Neurosci 28:2495-2505 Available at: [Accessed July 11, 2011].

Hof PR, Bouras C, Perl DP, Morrison JH (1994) Quantitative neuropathologic analysis of Pick's disease cases: cortical distribution of Pick bodies and coexistence with Alzheimer's disease. Acta Neuropathol 87:115-124 Available at: [Accessed June 22, 2011].

Hoffman MS, Mitchell GS (2011) Spinal 5-HT7 receptor activation induces long-lasting phrenic motor facilitation. J. Physiol. (Lond.) 589:1397-1407 Available at: [Accessed July 12, 2011].

Hoffmann F, Musolf K, Penn DJ (2009) Freezing urine reduces its efficacy for eliciting ultrasonic vocalizations from male mice. Physiol. Behav 96:602-605 Available at: [Accessed June 5, 2011].

Holmes CJ, Mainville LS, Jones BE (1994) Distribution of cholinergic, GABAergic and serotonergic neurons in the medial medullary reticular formation and their projections studied by cytotoxic lesions in the cat. Neuroscience 62:1155-1178 Available at: [Accessed May 31, 2011].

Holstege G (1989) Anatomical study of the final common pathway for vocalization in the cat. J. Comp. Neurol 284:242-252 Available at: [Accessed June 2, 2011].

Holstege G, Kerstens L, Moes MC, Vanderhorst VG (1997) Evidence for a periaqueductal gray-nucleus retroambiguus-spinal cord pathway in the rat. Neuroscience 80:587-598 Available at: [Accessed June 4, 2011].

Holstege G, Kuypers HG (1982) The anatomy of brain stem pathways to the spinal cord in cat. A labeled amino acid tracing study. Prog. Brain Res 57:145-175 Available at: [Accessed June 5, 2011].

Holstege G (2010) The emotional motor system and micturition control. Neurourol. Urodyn 29:42-48 Available at: [Accessed June 3, 2011].

Holtman JR Jr (1988) Immunohistochemical localization of serotonin- and substance P-containing fibers around respiratory muscle motoneurons in the nucleus ambiguus of the cat. Neuroscience 26:169-178 Available at: [Accessed May 31, 2011].

Holtman JR Jr, Dick TE, Berger AJ (1986) Involvement of serotonin in the excitation of phrenic motoneurons evoked by stimulation of the raphe obscurus. J. Neurosci 6:1185-1193 Available at: [Accessed May 31, 2011].

Holtman JR Jr, Dick TE, Berger AJ (1987) Serotonin-mediated excitation of recurrent laryngeal and phrenic motoneurons evoked by stimulation of the raphe obscurus. Brain Res 417:12-20 Available at: [Accessed May 31, 2011].

Holtman JR Jr, Marion LJ, Speck DF (1990) Origin of serotonin-containing projections to the ventral respiratory group in the rat. Neuroscience 37:541-552 Available at: [Accessed May 10, 2011].

Holy TE, Guo Z (2005) Ultrasonic songs of male mice. PLoS Biol 3:e386 Available at: [Accessed May 15, 2011].

Holzer P (2009) Acid-sensitive ion channels and receptors. Handb Exp Pharmacol:283-332 Available at: [Accessed July 12, 2011].

Hong X-P, Peng C-X, Wei W, Tian Q, Liu Y-H, Yao X-Q, Zhang Y, Cao F-Y, Wang Q, Wang J-Z (2010) Essential role of tau phosphorylation in adult hippocampal neurogenesis. Hippocampus 20:1339-1349 Available at: [Accessed June 16, 2011].

Hooper SL, Moulins M (1990) Cellular and synaptic mechanisms responsible for a long-lasting restructuring of the lobster pyloric network. J. Neurophysiol 64:1574-1589 Available at: [Accessed June 2, 2011].

Hoover BR, Reed MN, Su J, Penrod RD, Kotilinek LA, Grant MK, Pitstick R, Carlson GA, Lanier LM, Yuan L-L, Ashe KH, Liao D (2010) Tau mislocalization to dendritic spines mediates synaptic dysfunction independently of neurodegeneration. Neuron 68:1067-1081 Available at: [Accessed June 22, 2011].

Horn EM, Dillon GH, Fan YP, Waldrop TG (1999) Developmental aspects and mechanisms of rat caudal hypothalamic neuronal responses to hypoxia. J. Neurophysiol 81:1949-1959 Available at: [Accessed July 11, 2011].

Horn EM, Waldrop TG (1994) Modulation of the respiratory responses to hypoxia and hypercapnia by synaptic input onto caudal hypothalamic neurons. Brain Res 664:25-33 Available at: [Accessed July 13, 2011].

Hornung J-P (2003) The human raphe nuclei and the serotonergic system. J. Chem. Neuroanat 26:331-343 Available at: [Accessed May 31, 2011].

Housley GD, Martin-Body RL, Dawson NJ, Sinclair JD (1987) Brain stem projections of the glossopharyngeal nerve and its carotid sinus branch in the rat. Neuroscience 22:237-250 Available at: [Accessed June 29, 2011].

Huang LE, Gu J, Schau M, Bunn HF (1998) Regulation of hypoxia-inducible factor 1alpha is mediated by an O2-dependent degradation domain via the ubiquitin-proteasome pathway. Proc. Natl. Acad. Sci. U.S.A 95:7987-7992 Available at: [Accessed July 3, 2011].

Huang Q, St John WM (1988) Respiratory neural activities after caudal-to-rostral ablation of medullary regions. J. Appl. Physiol 64:1405-1411 Available at: [Accessed May 24, 2011].

Huang ZG, Subramanian SH, Balnave RJ, Turman AB, Moi Chow C (2000) Roles of periaqueductal gray and nucleus tractus solitarius in cardiorespiratory function in the rat brainstem. Respir Physiol 120:185-195 Available at: [Accessed June 5, 2011].

Humbert IA, Robbins J (2008) Dysphagia in the elderly. Phys Med Rehabil Clin N Am 19:853-866, ix-x Available at: [Accessed June 13, 2011].

Hurtado A (1960) Some clinical aspects of life at high altitudes. Ann. Intern. Med 53:247-258 Available at: [Accessed February 25, 2011].

Hutton M et al. (1998) Association of missense and 5'-splice-site mutations in tau with the inherited dementia FTDP-17. Nature 393:702-705 Available at: [Accessed June 22, 2011].

Hwang SC, Jhon DY, Bae YS, Kim JH, Rhee SG (1996) Activation of phospholipase C-gamma by the concerted action of tau proteins and arachidonic acid. J. Biol. Chem 271:18342-18349 Available at: [Accessed June 16, 2011].

Ichikawa H, Terayama R, Yamaai T, Yan Z, Sugimoto T (2007) Brain-derived neurotrophic factor-immunoreactive neurons in the rat vagal and glossopharyngeal sensory ganglia; co-expression with other neurochemical substances. Brain Res 1155:93-99 Available at: [Accessed May 11, 2011].

Ichiyama A, Nakamura S, Nishizuka Y, Hayaishi O (1968) Tryptophan-5-hydroxylase in mammalian brain. Adv Pharmacol 6:5-17 Available at: [Accessed May 31, 2011].

Ide S, Itoh M, Goto Y-ichi (2005) Defect in normal developmental increase of the brain biogenic amine concentrations in the mecp2-null mouse. Neurosci. Lett 386:14-17 Available at: [Accessed June 24, 2011].

Ihara Y (2001) PHF and PHF-like fibrils--cause or consequence? Neurobiol. Aging 22:123-126 Available at: [Accessed June 18, 2011].

Iizuka M (1999) Intercostal expiratory activity in an in vitro brainstem-spinal cord-rib preparation from the neonatal rat. J. Physiol. (Lond.) 520 Pt 1:293-302 Available at: [Accessed June 6, 2011].

Ikegami S, Harada A, Hirokawa N (2000) Muscle weakness, hyperactivity, and impairment in fear conditioning in tau-deficient mice. Neurosci. Lett 279:129-132 Available at: [Accessed June 20, 2011].

Isaacs JS, Murdock M, Lane J, Percy AK (2003) Eating difficulties in girls with Rett syndrome compared with other developmental disabilities. J Am Diet Assoc 103:224-230 Available at: [Accessed June 24, 2011].

Iscoe S (1998) Control of abdominal muscles. Prog. Neurobiol 56:433-506 Available at: [Accessed May 4, 2011].

Isoda K, Morimoto M, Matsui F, Hasegawa T, Tozawa T, Morioka S, Chiyonobu T, Nishimura A, Yoshimoto K, Hosoi H (2010) Postnatal changes in serotonergic innervation to the hippocampus of methyl-CpG-binding

protein 2-null mice. Neuroscience 165:1254-1260 Available at: [Accessed June 24, 2011].

Ittner LM, Götz J (2011) Amyloid-β and tau--a toxic pas de deux in Alzheimer's disease. Nat. Rev. Neurosci 12:65-72 Available at: [Accessed June 14, 2011].

Ittner LM, Ke YD, Delerue F, Bi M, Gladbach A, van Eersel J, Wölfing H, Chieng BC, Christie MJ, Napier IA, Eckert A, Staufenbiel M, Hardeman E, Götz J (2010) Dendritic function of tau mediates amyloid-beta toxicity in Alzheimer's disease mouse models. Cell 142:387-397 Available at: [Accessed June 15, 2011].

Iturriaga R, Alcayaga J (2004) Neurotransmission in the carotid body: transmitters and modulators between glomus cells and petrosal ganglion nerve terminals. Brain Res. Brain Res. Rev 47:46-53 Available at: [Accessed June 29, 2011].

Iwatsubo T, Kuzuhara S, Kanemitsu A, Shimada H, Toyokura Y (1990) Corticofugal projections to the motor nuclei of the brainstem and spinal cord in humans. Neurology 40:309-312 Available at: [Accessed June 3, 2011].

Jaakkola P, Mole DR, Tian YM, Wilson MI, Gielbert J, Gaskell SJ, Kriegsheim Av, Hebestreit HF, Mukherji M, Schofield CJ, Maxwell PH, Pugh CW, Ratcliffe PJ (2001) Targeting of HIF-alpha to the von Hippel-Lindau ubiquitylation complex by O2-regulated prolyl hydroxylation. Science 292:468-472 Available at: [Accessed July 3, 2011].

Jack L. Feldman (1986) Neurophysiology of breathing in mammals In Handbook of physiology; section I: The nervous system. Volume IV: Intrinsic regulatory systems of the brain Am. Physiol. Soc., Washington, DC, p. 463-524.

Jacobs BL, Azmitia EC (1992) Structure and function of the brain serotonin system. Physiol. Rev 72:165-229 Available at: [Accessed May 31, 2011].

Jacobs BL, Fornal CA (1991) Activity of brain serotonergic neurons in the behaving animal. Pharmacol. Rev 43:563-578 Available at: [Accessed July 13, 2011].

Jacobs BL, Fornal CA (2000) Serotonin and Behavior: A General Hypothesis In Psychopharmacology - 4th Generation of Progress American College of Neuropsychopharmacology.

Jakus J, Poliacek I, Halasova E, Murin P, Knocikova J, Tomori Z, Bolser DC (2008) Brainstem circuitry of tracheal-bronchial cough: c-fos study in anesthetized cats. Respir Physiol Neurobiol 160:289-300 Available at: [Accessed June 2, 2011].

Janczewski WA, Feldman JL (2006) Distinct rhythm generators for inspiration and expiration in the juvenile rat. J. Physiol. (Lond.) 570:407-420 Available at: [Accessed June 9, 2011].

Janssens JP, Pache JC, Nicod LP (1999) Physiological changes in respiratory function associated with ageing. Eur. Respir. J 13:197-205 Available at: [Accessed June 6, 2011].

Javaheri S, Teppema LJ, Evers JA (1988) Effects of aminophylline on hypoxemia-induced ventilatory depression in the cat. J. Appl. Physiol 64:1837-1843 Available at: [Accessed July 2, 2011].

Jaworski T, Dewachter I, Seymour CM, Borghgraef P, Devijver H, Kügler S, Van Leuven F (2010) Alzheimer's disease: old problem, new views from transgenic and viral models. Biochim. Biophys. Acta 1802:808-818 Available at: [Accessed June 15, 2011].

Jeganathan S, Hascher A, Chinnathambi S, Biernat J, Mandelkow E-M, Mandelkow E (2008) Proline-directed pseudo-phosphorylation at AT8 and PHF1 epitopes induces a compaction of the paperclip folding of Tau and generates a pathological (MC-1) conformation. J. Biol. Chem 283:32066-32076 Available at: [Accessed June 21, 2011].

Jelkmann W (2007) Erythropoietin after a century of research: younger than ever. Eur. J. Haematol 78:183-205 Available at: [Accessed July 3, 2011].

Van der Jeugd A, Burnouf S, Belarbi K, Hamdame M, Grosjean M-E, Humez S, Blum D, Buée L, D'Hooge R

(2011) Non-cognitive behaviours in a tau transgenic model of Alzheimer's disease. In Barcelona, Spain.

Jian L, Nagarajan L, de Klerk N, Ravine D, Bower C, Anderson A, Williamson S, Christodoulou J, Leonard H (2006) Predictors of seizure onset in Rett syndrome. J. Pediatr 149:542-547 Available at: [Accessed June 24, 2011].

Jiang M, Alheid GF, Calandriello T, McCrimmon DR (2004) Parabrachial-lateral pontine neurons link nociception and breathing. Respir Physiol Neurobiol 143:215-233 Available at: [Accessed May 9, 2011].

Jodkowski JS, Coles SK, Dick TE (1997) Prolongation in expiration evoked from ventrolateral pons of adult rats. J. Appl. Physiol 82:377-381 Available at: [Accessed May 30, 2011].

Johnson PL, Hollis JH, Moratalla R, Lightman SL, Lowry CA (2005) Acute hypercarbic gas exposure reveals functionally distinct subpopulations of serotonergic neurons in rats. J. Psychopharmacol. (Oxford) 19:327-341 Available at: [Accessed July 13, 2011].

Julu PO, Kerr AM, Apartopoulos F, Al-Rawas S, Engerström IW, Engerström L, Jamal GA, Hansen S (2001) Characterisation of breathing and associated central autonomic dysfunction in the Rett disorder. Arch. Dis. Child 85:29-37 Available at: [Accessed June 24, 2011].

Jürgens U (1994) The role of the periaqueductal grey in vocal behaviour. Behav. Brain Res 62:107-117 Available at: [Accessed June 4, 2011].

Jürgens U (2009) The neural control of vocalization in mammals: a review. J Voice 23:1-10 Available at: [Accessed June 3, 2011].

Jürgens U, von Cramon D (1982) On the role of the anterior cingulate cortex in phonation: a case report. Brain Lang 15:234-248 Available at: [Accessed June 4, 2011].

Jürgens U, Pratt R (1979) Role of the periaqueductal grey in vocal expression of emotion. Brain Res 167:367-378 Available at: [Accessed June 2, 2011].

Jürgens U (2002) Neural pathways underlying vocal control. Neurosci Biobehav Rev 26:235-258 Available at: [Accessed June 4, 2011].

Jürgens U, Ehrenreich L (2007) The descending motorcortical pathway to the laryngeal motoneurons in the squirrel monkey. Brain Res 1148:90-95 Available at: [Accessed June 4, 2011].

Kadotani H, Kadotani T, Young T, Peppard PE, Finn L, Colrain IM, Murphy GM Jr, Mignot E (2001) Association between apolipoprotein E epsilon4 and sleep-disordered breathing in adults. JAMA 285:2888-2890 Available at: [Accessed June 23, 2011].

Kalia M (2003) Dysphagia and aspiration pneumonia in patients with Alzheimer's disease. Metab. Clin. Exp 52:36-38 Available at: [Accessed June 23, 2011].

Kaluz S, Kaluzová M, Stanbridge EJ (2008) Regulation of gene expression by hypoxia: integration of the HIF-transduced hypoxic signal at the hypoxia-responsive element. Clin. Chim. Acta 395:6-13 Available at: [Accessed July 3, 2011].

Kamura T, Sato S, Iwai K, Czyzyk-Krzeska M, Conaway RC, Conaway JW (2000) Activation of HIF1alpha ubiquitination by a reconstituted von Hippel-Lindau (VHL) tumor suppressor complex. Proc. Natl. Acad. Sci. U.S.A 97:10430-10435 Available at: [Accessed July 3, 2011].

Kanbar R, Stornetta RL, Cash DR, Lewis SJ, Guyenet PG (2010) Photostimulation of Phox2b medullary neurons activates cardiorespiratory function in conscious rats. Am. J. Respir. Crit. Care Med 182:1184-1194 Available at: [Accessed July 13, 2011].

Karadottir R, Hamilton NB, Bakiri Y, Attwell D (2008) Spiking and nonspiking classes of oligodendrocyte precursor glia in CNS white matter. Nat Neurosci 11:450-456 Available at: [Accessed June 2, 2011].

Kato T, Hayashi F, Tatsumi K, Kuriyama T, Fukuda Y (2000) Inhibitory mechanisms in hypoxic respiratory depression studied in an in vitro preparation. Neurosci. Res 38:281-288 Available at: [Accessed July 11, 2011].

Katz DM, Dutschmann M, Ramirez J-M, Hilaire G (2009) Breathing disorders in Rett syndrome: progressive neurochemical dysfunction in the respiratory network after birth. Respir Physiol Neurobiol 168:101-108 Available at: [Accessed June 23, 2011].

Kawahara K, Kumagai S, Nakazono Y, Miyamoto Y (1989) Coupling between respiratory and stepping rhythms during locomotion in decerebrate cats. J. Appl. Physiol 67:110-115 Available at: [Accessed June 5, 2011].

Kawai A, Okada Y, Mückenhoff K, Scheid P (1995) Theophylline and hypoxic ventilatory response in the rat isolated brainstem-spinal cord. Respir Physiol 100:25-32 Available at: [Accessed July 11, 2011].

Kawai A, Onimaru H, Homma I (2006) Mechanisms of CO2/H+ chemoreception by respiratory rhythm generator neurons in the medulla from newborn rats in vitro. J. Physiol. (Lond.) 572:525-537 Available at: [Accessed July 12, 2011].

Kawai Y, Senba E (1999) Electrophysiological and morphological characterization of cytochemically-defined neurons in the caudal nucleus of tractus solitarius of the rat. Neuroscience 89:1347-1355 Available at: [Accessed May 11, 2011].

Kayed R, Head E, Thompson JL, McIntire TM, Milton SC, Cotman CW, Glabe CG (2003) Common structure of soluble amyloid oligomers implies common mechanism of pathogenesis. Science 300:486-489 Available at: [Accessed June 18, 2011].

Kepe V, Barrio JR, Huang S-C, Ercoli L, Siddarth P, Shoghi-Jadid K, Cole GM, Satyamurthy N, Cummings JL, Small GW, Phelps ME (2006) Serotonin 1A receptors in the living brain of Alzheimer's disease patients. Proc. Natl. Acad. Sci. U.S.A 103:702-707 Available at: [Accessed June 23, 2011].

Kerr AM, Armstrong DD, Prescott RJ, Doyle D, Kearney DL (1997) Rett syndrome: analysis of deaths in the British survey. Eur Child Adolesc Psychiatry 6 Suppl 1:71-74 Available at: [Accessed June 24, 2011].

Kerr AM, Belichenko P, Woodcock T, Woodcock M (2001) Mind and brain in Rett disorder. Brain Dev 23 Suppl 1:S44-49 Available at: [Accessed June 24, 2011].

Kerr AM, Julu PO (1999) Recent insights into hyperventilation from the study of Rett syndrome. Arch. Dis. Child 80:384-387 Available at: [Accessed June 24, 2011].

Kinkead R (2009) Phylogenetic trends in respiratory rhythmogenesis: insights from ectothermic vertebrates. Respir Physiol Neurobiol 168:39-48 Available at: [Accessed May 2, 2011].

Kinney HC, Richerson GB, Dymecki SM, Darnall RA, Nattie EE (2009) The brainstem and serotonin in the sudden infant death syndrome. Annu Rev Pathol 4:517-550 Available at: [Accessed May 23, 2011].

Klein C, Kramer E-M, Cardine A-M, Schraven B, Brandt R, Trotter J (2002) Process outgrowth of oligodendrocytes is promoted by interaction of fyn kinase with the cytoskeletal protein tau. J. Neurosci 22:698-707 Available at: [Accessed June 15, 2011].

Klein WL, Krafft GA, Finch CE (2001) Targeting small Abeta oligomers: the solution to an Alzheimer's disease conundrum? Trends Neurosci 24:219-224 Available at: [Accessed June 18, 2011].

Kline DD, Ogier M, Kunze DL, Katz DM (2010) Exogenous brain-derived neurotrophic factor rescues synaptic dysfunction in Mecp2-null mice. J. Neurosci 30:5303-5310 Available at: [Accessed June 24, 2011].

Klose RJ, Bird AP (2006) Genomic DNA methylation: the mark and its mediators. Trends Biochem. Sci 31:89-97 Available at: [Accessed June 24, 2011].

Knudson RJ, Slatin RC, Lebowitz MD, Burrows B (1976) The maximal expiratory flow-volume curve. Normal standards, variability, and effects of age. Am. Rev. Respir. Dis 113:587-600 Available at: [Accessed June 11, 2011].

Ko ML, King MA, Gordon TL, Crisp T (1997) The effects of aging on spinal neurochemistry in the rat. Brain Res. Bull 42:95-98 Available at: [Accessed June 9, 2011].

Kobayashi K, Lemke RP, Greer JJ (2001) Ultrasound measurements of fetal breathing movements in the rat. J. Appl. Physiol 91:316-320 Available at: [Accessed May 17, 2011].

Kobayashi RM, Palkovits M, Kopin IJ, Jacobowitz DM (1974) Biochemical mapping of noradrenergic nerves arising from the rat locus coeruleus. Brain Res 77:269-279 Available at: [Accessed May 10, 2011].

Kotani S, Nishida E, Kumagai H, Sakai H (1985) Calmodulin inhibits interaction of actin with MAP2 and Tau, two major microtubule-associated proteins. J. Biol. Chem 260:10779-10783 Available at: [Accessed June 16, 2011].

Kovacs GG, Klöppel S, Fischer I, Dorner S, Lindeck-Pozza E, Birner P, Bötefür IC, Pilz P, Volk B, Budka H (2003) Nucleus-specific alteration of raphe neurons in human neurodegenerative disorders. Neuroreport 14:73-76 Available at: [Accessed June 23, 2011].

Krause KL, Forster HV, Kiner T, Davis SE, Bonis JM, Qian B, Pan LG (2009) Normal breathing pattern and arterial blood gases in awake and sleeping goats after near total destruction of the presumed pre-Botzinger complex and the surrounding region. J. Appl. Physiol 106:605-619 Available at: [Accessed May 19, 2011].

Kronenberg RS, Drage CW (1973) Attenuation of the ventilatory and heart rate responses to hypoxia and hypercapnia with aging in normal men. J. Clin. Invest 52:1812-1819 Available at: [Accessed June 13, 2011].

Krumpe PE, Knudson RJ, Parsons G, Reiser K (1985) The aging respiratory system. Clin. Geriatr. Med 1:143-175 Available at: [Accessed June 13, 2011].

Kubin L, Tojima H, Reignier C, Pack AI, Davies RO (1996) Interaction of serotonergic excitatory drive to hypoglossal motoneurons with carbachol-induced, REM sleep-like atonia. Sleep 19:187-195 Available at: [Accessed June 13, 2011].

Kubin L, Alheid GF, Zuperku EJ, McCrimmon DR (2006) Central pathways of pulmonary and lower airway vagal afferents. J. Appl. Physiol 101:618-627 Available at: [Accessed May 4, 2011].

Kukley M, Capetillo-Zarate E, Dietrich D (2007) Vesicular glutamate release from axons in white matter. Nat Neurosci 10:311-320 Available at: [Accessed June 2, 2011].

Kuret J, Congdon EE, Li G, Yin H, Yu X, Zhong Q (2005) Evaluating triggers and enhancers of tau fibrillization. Microsc. Res. Tech 67:141-155 Available at: [Accessed June 21, 2011].

Kurozumi M, Matsushita T, Hosokawa M, Takeda T (1994) Age-related changes in lung structure and function in the senescence-accelerated mouse (SAM): SAM-P/1 as a new murine model of senile hyperinflation of lung. Am. J. Respir. Crit. Care Med 149:776-782 Available at: [Accessed June 10, 2011].

Kuwana S-ichi, Tsunekawa N, Yanagawa Y, Okada Y, Kuribayashi J, Obata K (2006) Electrophysiological and morphological characteristics of GABAergic respiratory neurons in the mouse pre-Bötzinger complex. Eur. J. Neurosci 23:667-674 Available at: [Accessed May 11, 2011].

Kuypers HG (1958) Corticobular connexions to the pons and lower brain-stem in man: an anatomical study. Brain 81:364-388 Available at: [Accessed June 3, 2011].

LaManna JC, Kutina-Nelson KL, Hritz MA, Huang Z, Wong-Riley MT (1996) Decreased rat brain cytochrome oxidase activity after prolonged hypoxia. Brain Res 720:1-6 Available at: [Accessed July 2, 2011].

Ladas T, Chan S-A, Ogier M, Smith C, Katz DM (2009) Enhanced dense core granule function and adrenal hypersecretion in a mouse model of Rett syndrome. Eur. J. Neurosci 30:602-610 Available at: [Accessed June 24, 2011].

Lahiri S, Ehleben W, Acker H (1999) Chemoreceptor discharges and cytochrome redox changes of the rat carotid body: role of heme ligands. Proc. Natl. Acad. Sci. U.S.A 96:9427-9432 Available at: [Accessed June 30,

2011].

Lalley PM, Benacka R, Bischoff AM, Richter DW (1997) Nucleus raphe obscurus evokes 5-HT-1A receptor-mediated modulation of respiratory neurons. Brain Res 747:156-159 Available at: [Accessed May 31, 2011].

Lalley PM, Bischoff AM, Richter DW (1994) 5-HT-1A receptor-mediated modulation of medullary expiratory neurones in the cat. J. Physiol. (Lond.) 476:117-130 Available at: [Accessed May 31, 2011].

Lalley PM, Bischoff AM, Schwarzacher SW, Richter DW (1995) 5-HT2 receptor-controlled modulation of medullary respiratory neurones in the cat. J. Physiol. (Lond.) 487 (Pt 3):653-661 Available at: [Accessed May 31, 2011].

Landgraf R, Kessler MS, Bunck M, Murgatroyd C, Spengler D, Zimbelmann M, Nussbaumer M, Czibere L, Turck CW, Singewald N, Rujescu D, Frank E (2007) Candidate genes of anxiety-related behavior in HAB/LAB rats and mice: focus on vasopressin and glyoxalase-I. Neurosci Biobehav Rev 31:89-102 Available at: [Accessed June 5, 2011].

Landhuis E (2011) San Francisco: Tau-Time to Shine as Therapeutic Target ? Available at: http://www.alzforum.org/new/detail.asp?id=2792.

Larnicol N, Wallois F, Berquin P, Gros F, Rose D (1994) c-fos-like immunoreactivity in the cat's neuraxis following moderate hypoxia or hypercapnia. J. Physiol. Paris 88:81-88 Available at: [Accessed July 13, 2011].

LeGallois JJC (1812) Expériences sur le Principe de la Vie, notamment sur celui des mouvements du coeur, et sur le siège de ce principe. A Paris: Chez D'Hautel.

Ledesma MD, Bonay P, Colaço C, Avila J (1994) Analysis of microtubule-associated protein tau glycation in paired helical filaments. J. Biol. Chem 269:21614-21619 Available at: [Accessed June 16, 2011].

Lee G, Newman ST, Gard DL, Band H, Panchamoorthy G (1998) Tau interacts with src-family non-receptor tyrosine kinases. J. Cell. Sci 111 (Pt 21):3167-3177 Available at: [Accessed June 16, 2011].

Lee L-Y, Shuei Lin Y, Gu Q, Chung E, Ho C-Y (2003) Functional morphology and physiological properties of bronchopulmonary C-fiber afferents. Anat Rec A Discov Mol Cell Evol Biol 270:17-24 Available at: [Accessed July 14, 2011].

Lee Y-M, Kim B-J, Chun Y-S, So I, Choi H, Kim M-S, Park J-W (2006) NOX4 as an oxygen sensor to regulate TASK-1 activity. Cell. Signal 18:499-507 Available at: [Accessed June 30, 2011].

Leger L, Charnay Y, Hof PR, Bouras C, Cespuglio R (2001) Anatomical distribution of serotonin-containing neurons and axons in the central nervous system of the cat. J. Comp. Neurol 433:157-182 Available at: [Accessed May 31, 2011].

Leist M et al. (2004) Derivatives of erythropoietin that are tissue protective but not erythropoietic. Science 305:239-242 Available at: [Accessed July 3, 2011].

Leiter JC, St -John WM (2004) Phrenic, vagal and hypoglossal activities in rat: pre-inspiratory, inspiratory, expiratory components. Respir Physiol Neurobiol 142:115-126 Available at: [Accessed May 19, 2011].

Leusen IR (1954) Chemosensitivity of the respiratory center; influence of CO2 in the cerebral ventricles on respiration. Am. J. Physiol 176:39-44 Available at: [Accessed July 12, 2011].

Van Leuven F (2000) Single and multiple transgenic mice as models for Alzheimer's disease. Prog. Neurobiol 61:305-312 Available at: [Accessed June 21, 2011].

Levitzky MG (1984) Effects of aging on the respiratory system. Physiologist 27:102-107 Available at: [Accessed June 10, 2011].

Lewis J, Dickson DW, Lin WL, Chisholm L, Corral A, Jones G, Yen SH, Sahara N, Skipper L, Yager D,

Eckman C, Hardy J, Hutton M, McGowan E (2001) Enhanced neurofibrillary degeneration in transgenic mice expressing mutant tau and APP. Science 293:1487-1491 Available at: [Accessed June 21, 2011].

Lewis J, McGowan E, Rockwood J, Melrose H, Nacharaju P, Van Slegtenhorst M, Gwinn-Hardy K, Paul Murphy M, Baker M, Yu X, Duff K, Hardy J, Corral A, Lin WL, Yen SH, Dickson DW, Davies P, Hutton M (2000) Neurofibrillary tangles, amyotrophy and progressive motor disturbance in mice expressing mutant (P301L) tau protein. Nat. Genet 25:402-405 Available at: [Accessed November 12, 2009].

León-Velarde F, Richalet J-P (2006) Respiratory control in residents at high altitude: physiology and pathophysiology. High Alt. Med. Biol 7:125-137 Available at: [Accessed April 19, 2010].

León-Velarde F, Villafuerte FC, Richalet J-P (2010) Chronic mountain sickness and the heart. Prog Cardiovasc Dis 52:540-549 Available at: [Accessed February 25, 2011].

Li A, Nattie E (2008) Serotonin transporter knockout mice have a reduced ventilatory response to hypercapnia (predominantly males) but not hypoxia. J. Physiol. (Lond.) 586:2321-9

Li A, Emond L, Nattie E (2008) Brainstem catecholaminergic neurons modulate both respiratory and cardiovascular function. Adv. Exp. Med. Biol 605:371-376 Available at: [Accessed February 24, 2011].

Li A, Nattie E (2002) CO2 dialysis in one chemoreceptor site, the RTN: stimulus intensity and sensitivity in the awake rat. Respir Physiol Neurobiol 133:11-22 Available at: [Accessed July 13, 2011].

Li A, Nattie E (2006) Catecholamine neurones in rats modulate sleep, breathing, central chemoreception and breathing variability. J. Physiol. (Lond.) 570:385-396 Available at: [Accessed July 13, 2011].

Lindsay AD, Feldman JL (1993) Modulation of respiratory activity of neonatal rat phrenic motoneurones by serotonin. J. Physiol. (Lond.) 461:213-233 Available at: [Accessed June 1, 2011].

Ling L (2008) Serotonin and NMDA receptors in respiratory long-term facilitation. Respir Physiol Neurobiol 164:233-241 Available at: [Accessed July 12, 2011].

Lipski J, Duffin J (1986) An electrophysiological investigation of propriospinal inspiratory neurons in the upper cervical cord of the cat. Exp Brain Res 61:625-637 Available at: [Accessed May 12, 2011].

Lipski J, Martin-Body RL (1987) Morphological properties of respiratory intercostal motoneurons in cats as revealed by intracellular injection of horseradish peroxidase. J. Comp. Neurol 260:423-434 Available at: [Accessed May 5, 2011].

Litvan I, Agid Y, Jankovic J, Goetz C, Brandel JP, Lai EC, Wenning G, D'Olhaberriague L, Verny M, Chaudhuri KR, McKee A, Jellinger K, Bartko JJ, Mangone CA, Pearce RK (1996) Accuracy of clinical criteria for the diagnosis of progressive supranuclear palsy (Steele-Richardson-Olszewski syndrome). Neurology 46:922-930 Available at: [Accessed June 22, 2011].

Liu F, Iqbal K, Grundke-Iqbal I, Hart GW, Gong C-X (2004) O-GlcNAcylation regulates phosphorylation of tau: a mechanism involved in Alzheimer's disease. Proc. Natl. Acad. Sci. U.S.A 101:10804-10809 Available at: [Accessed June 21, 2011].

Livingston CA, Berger AJ (1989) Immunocytochemical localization of GABA in neurons projecting to the ventrolateral nucleus of the solitary tract. Brain Res 494:143-150 Available at: [Accessed May 11, 2011].

Loeschcke HH (1982) Central chemosensitivity and the reaction theory. J. Physiol. (Lond.) 332:1-24 Available at: [Accessed July 12, 2011].

Loewy AD, Burton H (1978) Nuclei of the solitary tract: efferent projections to the lower brain stem and spinal cord of the cat. J. Comp. Neurol 181:421-449 Available at: [Accessed May 24, 2011].

Loewy AD, McKellar S, Saper CB (1979) Direct projections from the A5 catecholamine cell group to the intermediolateral cell column. Brain Res 174:309-314 Available at: [Accessed May 10, 2011].

Long WQ, Giesbrecht GG, Anthonisen NR (1993) Ventilatory response to moderate hypoxia in awake chemodenervated cats. J. Appl. Physiol 74:805-810 Available at: [Accessed June 30, 2011].

Loomis PA, Howard TH, Castleberry RP, Binder LI (1990) Identification of nuclear tau isoforms in human neuroblastoma cells. Proc. Natl. Acad. Sci. U.S.A 87:8422-8426 Available at: [Accessed June 16, 2011].

Lopez-Barneo J, Pardal R, Ortega-Sáenz P (2001) Cellular mechanism of oxygen sensing. Annu. Rev. Physiol 63:259-287 Available at: [Accessed June 30, 2011].

Lorier AR, Lipski J, Housley GD, Greer JJ, Funk GD (2008) ATP sensitivity of preBötzinger complex neurones in neonatal rat in vitro: mechanism underlying a P2 receptor-mediated increase in inspiratory frequency. J. Physiol. (Lond.) 586:1429-1446 Available at: [Accessed July 11, 2011].

Lorier AR, Huxtable AG, Robinson DM, Lipski J, Housley GD, Funk GD (2007) P2Y1 receptor modulation of the pre-Bötzinger complex inspiratory rhythm generating network in vitro. J. Neurosci 27:993-1005 Available at: [Accessed July 11, 2011].

Lovick TA (1993) The periaqueductal gray-rostral medulla connection in the defence reaction: efferent pathways and descending control mechanisms. Behav. Brain Res 58:19-25 Available at: [Accessed June 3, 2011].

Lu CL, Jürgens U (1993) Effects of chemical stimulation in the periaqueductal gray on vocalization in the squirrel monkey. Brain Res. Bull 32:143-151 Available at: [Accessed June 4, 2011].

Van Luijtelaar MG, Tonnaer JA, Steinbusch HW (1992) Aging of the serotonergic system in the rat forebrain: an immunocytochemical and neurochemical study. Neurobiol. Aging 13:201-215 Available at: [Accessed June 9, 2011].

Lumbroso D, Joseph V (2009) Impaired acclimatization to chronic hypoxia in adult male and female rats following neonatal hypoxia. Am. J. Physiol. Regul. Integr. Comp. Physiol 297:R421-427 Available at: [Accessed May 22, 2011].

Lumsden T (1923)(a) Observations on the respiratory centres in the cat. J. Physiol. (Lond.) 57:153-160 Available at: [Accessed May 9, 2011].

Lumsden T (1923)(b) Observations on the respiratory centres. JOURNAL OF PHYSIOLOGY-LONDON 57:354-367 Available at: [Accessed May 18, 2011].

Lumsden T (1923)(c) The regulation of respiration. Part I. JOURNAL OF PHYSIOLOGY-LONDON 58:0081-0091 Available at: [Accessed May 18, 2011].

Van Lunteren E, Vafaie H, Salomone RJ (1995) Comparative effects of aging on pharyngeal and diaphragm muscles. Respir Physiol 99:113-125 Available at: [Accessed June 11, 2011].

Lyness SA, Zarow C, Chui HC (2003) Neuron loss in key cholinergic and aminergic nuclei in Alzheimer disease: a meta-analysis. Neurobiol. Aging 24:1-23 Available at: [Accessed June 23, 2011].

López-Barneo J, Ortega-Sáenz P, Pardal R, Pascual A, Piruat JI (2008) Carotid body oxygen sensing. Eur. Respir. J 32:1386-1398 Available at: [Accessed June 29, 2011].

MacFarlane PM, Satriotomo I, Windelborn JA, Mitchell GS (2009) NADPH oxidase activity is necessary for acute intermittent hypoxia-induced phrenic long-term facilitation. J. Physiol. (Lond.) 587:1931-1942 Available at: [Accessed July 12, 2011].

MacFarlane PM, Wilkerson JER, Lovett-Barr MR, Mitchell GS (2008) Reactive oxygen species and respiratory plasticity following intermittent hypoxia. Respir Physiol Neurobiol 164:263-271 Available at: [Accessed July 12, 2011].

Maeda S, Sahara N, Saito Y, Murayama M, Yoshiike Y, Kim H, Miyasaka T, Murayama S, Ikai A, Takashima A (2007) Granular tau oligomers as intermediates of tau filaments. Biochemistry 46:3856-3861 Available at: [Accessed June 22, 2011].

Malhotra A, Huang Y, Fogel R, Lazic S, Pillar G, Jakab M, Kikinis R, White DP (2006) Aging influences on pharyngeal anatomy and physiology: the predisposition to pharyngeal collapse. Am. J. Med 119:72.e9-14 Available at: [Accessed June 9, 2011].

Manaker S, Tischler LJ (1993) Origin of serotoninergic afferents to the hypoglossal nucleus in the rat. J. Comp. Neurol 334:466-476 Available at: [Accessed May 31, 2011].

Mandelkow EM, Mandelkow E (1998) Tau in Alzheimer's disease. Trends Cell Biol 8:425-427 Available at: [Accessed June 20, 2011].

Mandelkow EM, Schweers O, Drewes G, Biernat J, Gustke N, Trinczek B, Mandelkow E (1996) Structure, microtubule interactions, and phosphorylation of tau protein. Ann. N. Y. Acad. Sci 777:96-106 Available at: [Accessed June 15, 2011].

Mandell JW, Banker GA (1996) A spatial gradient of tau protein phosphorylation in nascent axons. J. Neurosci 16:5727-5740 Available at: [Accessed June 16, 2011].

Mann DM, Lincoln J, Yates PO, Stamp JE, Toper S (1980) Changes in the monoamine containing neurones of the human CNS in senile dementia. Br J Psychiatry 136:533-541 Available at: [Accessed June 23, 2011].

Manzke T, Dutschmann M, Schlaf G, Mörschel M, Koch UR, Ponimaskin E, Bidon O, Lalley PM, Richter DW (2009) Serotonin targets inhibitory synapses to induce modulation of network functions. Philos. Trans. R. Soc. Lond., B, Biol. Sci 364:2589-2602 Available at: [Accessed June 1, 2011].

Manzke T, Guenther U, Ponimaskin EG, Haller M, Dutschmann M, Schwarzacher S, Richter DW (2003) 5-HT4(a) receptors avert opioid-induced breathing depression without loss of analgesia. Science 301:226-229 Available at: [Accessed May 31, 2011].

Manzke T, Niebert M, Koch UR, Caley A, Vogelgesang S, Hülsmann S, Ponimaskin E, Müller U, Smart TG, Harvey RJ, Richter DW (2010) Serotonin receptor 1A-modulated phosphorylation of glycine receptor α3 controls breathing in mice. J. Clin. Invest 120:4118-4128 Available at: [Accessed June 2, 2011].

Manzke T, Preusse S, Hülsmann S, Richter DW (2008) Developmental changes of serotonin 4(a) receptor expression in the rat pre-Bötzinger complex. J. Comp. Neurol 506:775-790 Available at: [Accessed June 1, 2011].

Marcus CL, Carroll JL, McColley SA, Loughlin GM, Curtis S, Pyzik P, Naidu S (1994) Polysomnographic characteristics of patients with Rett syndrome. J. Pediatr 125:218-224 Available at: [Accessed June 24, 2011].

Marder E, Calabrese RL (1996) Principles of rhythmic motor pattern generation. Physiol. Rev 76:687-717 Available at: [Accessed June 2, 2011].

Marina N, Abdala AP, Trapp S, Li A, Nattie EE, Hewinson J, Smith JC, Paton JFR, Gourine AV (2010) Essential role of Phox2b-expressing ventrolateral brainstem neurons in the chemosensory control of inspiration and expiration. J. Neurosci 30:12466-12473 Available at: [Accessed June 28, 2011].

Martin SE, Mathur R, Marshall I, Douglas NJ (1997) The effect of age, sex, obesity and posture on upper airway size. Eur. Respir. J 10:2087-2090 Available at: [Accessed June 9, 2011].

Martin-Body RL, Robson GJ, Sinclair JD (1986) Restoration of hypoxic respiratory responses in the awake rat after carotid body denervation by sinus nerve section. J. Physiol. (Lond.) 380:61-73 Available at: [Accessed July 2, 2011].

Massari VJ, Shirahata M, Johnson TA, Gatti PJ (1996) Carotid sinus nerve terminals which are tyrosine hydroxylase immunoreactive are found in the commissural nucleus of the tractus solitarius. J. Neurocytol 25:197-208 Available at: [Accessed May 11, 2011].

Maxwell PH, Wiesener MS, Chang GW, Clifford SC, Vaux EC, Cockman ME, Wykoff CC, Pugh CW, Maher ER, Ratcliffe PJ (1999) The tumour suppressor protein VHL targets hypoxia-inducible factors for oxygen-dependent proteolysis. Nature 399:271-275 Available at: [Accessed July 3, 2011].

Mazanetz MP, Fischer PM (2007) Untangling tau hyperphosphorylation in drug design for neurodegenerative diseases. Nat Rev Drug Discov 6:464-479 Available at: [Accessed June 20, 2011].

Mazzone SB, Geraghty DP (1999) Altered respiratory response to substance P and reduced NK1 receptor binding in the nucleus of the solitary tract of aged rats. Brain Res 826:139-142 Available at: [Accessed June 9, 2011].

McCrimmon DR, Lalley PM (1982) Inhibition of respiratory neural discharges by clonidine and 5-hydroxytryptophan. J. Pharmacol. Exp. Ther 222:771-777 Available at: [Accessed May 31, 2011].

McGraw CM, Samaco RC, Zoghbi HY (2011) Adult Neural Function Requires MeCP2. Science Available at: http://www.ncbi.nlm.nih.gov/pubmed/21636743 [Accessed July 6, 2011].

McKhann GM, Knopman DS, Chertkow H, Hyman BT, Jack CR Jr, Kawas CH, Klunk WE, Koroshetz WJ, Manly JJ, Mayeux R, Mohs RC, Morris JC, Rossor MN, Scheltens P, Carrillo MC, Thies B, Weintraub S, Phelps CH (2011) The diagnosis of dementia due to Alzheimer's disease: Recommendations from the National Institute on Aging-Alzheimer's Association workgroups on diagnostic guidelines for Alzheimer's disease. Alzheimers Dement 7:263-269 Available at: [Accessed June 17, 2011].

Medrihan L, Tantalaki E, Aramuni G, Sargsyan V, Dudanova I, Missler M, Zhang W (2008) Early defects of GABAergic synapses in the brain stem of a MeCP2 mouse model of Rett syndrome. J. Neurophysiol 99:112-121 Available at: [Accessed July 9, 2011].

Melton JE, Chae LO, Neubauer JA, Edelman NH (1991) Extracellular potassium homeostasis in the cat medulla during progressive brain hypoxia. J. Appl. Physiol 70:1477-1482 Available at: [Accessed July 2, 2011].

Mendez R, De Occa MM, Rassulo J, Celli B (1996) Effects of age on ventilatory drive response to CO2. Chest 110

Merrill EG (1970)(a) The lateral respiratory neurones of the medulla: their associations with nucleus ambiguus, nucleus retroambigualis, the spinal accessory nucleus and the spinal cord. Brain Res 24:11-28 Available at: [Accessed May 5, 2011].

Merrill EG (1970)(b) The lateral respiratory neurones of the medulla: their associations with nucleus ambiguus, nucleus retroambigualis, the spinal accessory nucleus and the spinal cord. Brain Res 24:11-28 Available at: [Accessed May 11, 2011].

Merrill EG, Lipski J (1987) Inputs to intercostal motoneurons from ventrolateral medullary respiratory neurons in the cat. J. Neurophysiol 57:1837-1853 Available at: [Accessed May 5, 2011].

Meyrand P, Simmers J, Moulins M (1994) Dynamic construction of a neural network from multiple pattern generators in the lobster stomatogastric nervous system. J. Neurosci 14:630-644 Available at: [Accessed June 2, 2011].

Miller AD, Tan LK, Lakos SF (1989) Brainstem projections to cats' upper lumbar spinal cord: implications for abdominal muscle control. Brain Res 493:348-356 Available at: [Accessed May 5, 2011].

Millhorn DE, Eldridge FL, Waldrop TG (1980) Prolonged stimulation of respiration by a new central neural mechanism. Respir Physiol 41:87-103 Available at: [Accessed July 12, 2011].

Min S-W, Cho S-H, Zhou Y, Schroeder S, Haroutunian V, Seeley WW, Huang EJ, Shen Y, Masliah E, Mukherjee C, Meyers D, Cole PA, Ott M, Gan L (2010) Acetylation of tau inhibits its degradation and contributes to tauopathy. Neuron 67:953-966 Available at: [Accessed June 16, 2011].

Mitchell GS (2004) Back to the future: carbon dioxide chemoreceptors in the mammalian brain. Nat. Neurosci 7:1288-1290 Available at: [Accessed July 13, 2011].

Mitchell GS, Johnson SM (2003) Neuroplasticity in respiratory motor control. J. Appl. Physiol 94:358-374 Available at: [Accessed June 13, 2011].

Mitchell RA, Loeschcke HH, Massion WH, Severinghaus JW (1963) Respiratory responses mediated through superficial chemosensitive areas on the medulla. J Appl Physiol 18:523 -533 Available at: [Accessed July 13, 2011].

Miyasaka T, Watanabe A, Saito Y, Murayama S, Mann DMA, Yamazaki M, Ravid R, Morishima-Kawashima M, Nagashima K, Ihara Y (2005) Visualization of newly deposited tau in neurofibrillary tangles and neuropil threads. J. Neuropathol. Exp. Neurol 64:665-674 Available at: [Accessed June 16, 2011].

Mizuno M (1991) Human respiratory muscles: fibre morphology and capillary supply. Eur. Respir. J 4:587-601 Available at: [Accessed June 10, 2011].

Mizusawa A, Ogawa H, Kikuchi Y, Hida W, Kurosawa H, Okabe S, Takishima T, Shirato K (1994) In vivo release of glutamate in nucleus tractus solitarii of the rat during hypoxia. J. Physiol. (Lond.) 478 (Pt 1):55-66 Available at: [Accessed May 11, 2011].

Mocanu M-M, Nissen A, Eckermann K, Khlistunova I, Biernat J, Drexler D, Petrova O, Schönig K, Bujard H, Mandelkow E, Zhou L, Rune G, Mandelkow E-M (2008) The potential for beta-structure in the repeat domain of tau protein determines aggregation, synaptic decay, neuronal loss, and coassembly with endogenous Tau in inducible mouse models of tauopathy. J. Neurosci 28:737-748 Available at: [Accessed June 22, 2011].

Moechars D, Dewachter I, Lorent K, Reversé D, Baekelandt V, Naidu A, Tesseur I, Spittaels K, Haute CV, Checler F, Godaux E, Cordell B, Van Leuven F (1999) Early phenotypic changes in transgenic mice that overexpress different mutants of amyloid precursor protein in brain. J. Biol. Chem 274:6483-6492 Available at: [Accessed June 21, 2011].

Monge CC, Whittembury J (1976) Chronic mountain sickness. Johns Hopkins Med J 139 SUPPL:87-89 Available at: [Accessed July 8, 2011].

Montagutelli X (2000) Effect of the genetic background on the phenotype of mouse mutations. J. Am. Soc. Nephrol 11 Suppl 16:S101-105 Available at: [Accessed July 5, 2011].

Monteau R, Morin D, Hennequin S, Hilaire G (1990) Differential effects of serotonin on respiratory activity of hypoglossal and cervical motoneurons: an in vitro study on the newborn rat. Neurosci. Lett 111:127-132 Available at: [Accessed May 31, 2011].

Monteau R, Di Pasquale E, Hilaire G (1994) Further evidence that various 5-HT receptor subtypes modulate central respiratory activity: in vitro studies with SR 46349B. Eur. J. Pharmacol 259:71-74 Available at: [Accessed June 1, 2011].

Monti JM (2010)(a) The role of dorsal raphe nucleus serotonergic and non-serotonergic neurons, and of their receptors, in regulating waking and rapid eye movement (REM) sleep. Sleep Med Rev 14:319-327 Available at: [Accessed May 31, 2011].

Monti JM (2010)(b) The structure of the dorsal raphe nucleus and its relevance to the regulation of sleep and wakefulness. Sleep Med Rev 14:307-317 Available at: [Accessed May 31, 2011].

Moore RY, Bloom FE (1979) Central catecholamine neuron systems: anatomy and physiology of the norepinephrine and epinephrine systems. Annu. Rev. Neurosci 2:113-168 Available at: [Accessed May 10, 2011].

Morelli C, Badr MS, Mateika JH (2004) Ventilatory responses to carbon dioxide at low and high levels of oxygen are elevated after episodic hypoxia in men compared with women. J. Appl. Physiol 97:1673-1680 Available at: [Accessed June 13, 2011].

Morgan DG, May PC, Finch CE (1987) Dopamine and serotonin systems in human and rodent brain: effects of age and neurodegenerative disease. J Am Geriatr Soc 35:334-345 Available at: [Accessed June 12, 2011].

Morin D, Hennequin S, Monteau R, Hilaire G (1990)(a) Serotonergic influences on central respiratory activity: an in vitro study in the newborn rat. Brain Res 535:281-287 Available at: [Accessed May 31, 2011].

Morin D, Hennequin S, Monteau R, Hilaire G (1990)(b) Depressant effect of raphe stimulation on inspiratory activity of the hypoglossal nerve: in vitro study in the newborn rat. Neurosci. Lett 116:299-303 Available at: [Accessed June 1, 2011].

Morin D, Monteau R, Hilaire G (1992) Compared effects of serotonin on cervical and hypoglossal inspiratory activities: an in vitro study in the newborn rat. J. Physiol. (Lond.) 451:605-629 Available at: [Accessed May 31, 2011].

Morin D, Di Pasquale E, Hilaire G, Monteau R (1994) Possible involvement of serotonin in obstructive apnea of the newborn. Biol. Neonate 65:176-181 Available at: [Accessed June 1, 2011].

Morin D, Viala D (2002) Coordinations of locomotor and respiratory rhythms in vitro are critically dependent on hindlimb sensory inputs. J. Neurosci 22:4756-4765 Available at: [Accessed June 5, 2011].

Morris M, Maeda S, Vossel K, Mucke L (2011) The many faces of tau. Neuron 70:410-426 Available at: [Accessed May 13, 2011].

Morrison SF, Cravo SL, Wilfehrt HM (1994) Pontine lesions produce apneusis in the rat. Brain Res 652:83-86 Available at: [Accessed May 24, 2011].

Mortola JP, Fisher JT, Sant'Ambrogio G (1984) Vagal control of the breathing pattern and respiratory mechanics in the adult and newborn rabbit. Pflugers Arch 401:281-286 Available at: [Accessed May 24, 2011].

Moss BL, Fuller AD, Sahley CL, Burrell BD (2005) Serotonin modulates axo-axonal coupling between neurons critical for learning in the leech. J. Neurophysiol 94:2575-2589 Available at: [Accessed May 31, 2011].

Mueller RA, Towle AC, Breese GR (1985) The role of vagal afferents and carbon dioxide in the respiratory response to thyrotropin-releasing hormone. Regul. Pept 10:157-166 Available at: [Accessed July 13, 2011].

Mulkey DK, Mistry AM, Guyenet PG, Bayliss DA (2006) Purinergic P2 receptors modulate excitability but do not mediate pH sensitivity of RTN respiratory chemoreceptors. J. Neurosci 26:7230-7233 Available at: [Accessed July 13, 2011].

Mulkey DK, Rosin DL, West G, Takakura AC, Moreira TS, Bayliss DA, Guyenet PG (2007)(a) Serotonergic neurons activate chemosensitive retrotrapezoid nucleus neurons by a pH-independent mechanism. J. Neurosci 27:14128-14138 Available at: [Accessed May 11, 2011].

Mulkey DK, Stornetta RL, Weston MC, Simmons JR, Parker A, Bayliss DA, Guyenet PG (2004)(a) Respiratory control by ventral surface chemoreceptor neurons in rats. Nat. Neurosci 7:1360-1369 Available at: [Accessed February 28, 2011].

Mulkey DK, Stornetta RL, Weston MC, Simmons JR, Parker A, Bayliss DA, Guyenet PG (2004)(b) Respiratory control by ventral surface chemoreceptor neurons in rats. Nat. Neurosci 7:1360-1369 Available at: [Accessed May 11, 2011].

Mulkey DK, Talley EM, Stornetta RL, Siegel AR, West GH, Chen X, Sen N, Mistry AM, Guyenet PG, Bayliss DA (2007)(b) TASK channels determine pH sensitivity in select respiratory neurons but do not contribute to central respiratory chemosensitivity. J. Neurosci 27:14049-14058 Available at: [Accessed July 11, 2011].

Murase S, Takayama M, Nosaka S (1993) Chemical stimulation of the nucleus locus coeruleus: cardiovascular responses and baroreflex modification. Neurosci. Lett 153:1-4 Available at: [Accessed May 10, 2011].

Muyllaert D, Kremer A, Jaworski T, Borghgraef P, Devijver H, Croes S, Dewachter I, Van Leuven F (2008) Glycogen synthase kinase-3beta, or a link between amyloid and tau pathology? Genes Brain Behav 7 Suppl 1:57-66 Available at: [Accessed February 16, 2009].

Muyllaert D, Terwel D, Borghgraef P, Devijver H, Dewachter I, Van Leuven F (2006) Transgenic mouse models for Alzheimer's disease: the role of GSK-3B in combined amyloid and tau-pathology. Rev Neurol (Paris) 162:903-7 Available at: [Accessed February 16, 2009].

Mössner R, Schmitt A, Syagailo Y, Gerlach M, Riederer P, Lesch KP (2000) The serotonin transporter in Alzheimer's and Parkinson's disease. J. Neural Transm. Suppl:345-350 Available at: [Accessed June 23, 2011].

Nagatsu T, LEVITT M, UDENFRIEND S (1964) TYROSINE HYDROXYLASE. THE INITIAL STEP IN NOREPINEPHRINE BIOSYNTHESIS. J. Biol. Chem 239:2910-2917 Available at: [Accessed May 29, 2011].

Nakayama S, Von Baumgarten (1964) [LOCALIZATION OF DESCENDING RESPIRATORY NEURONS IN THE SPINAL CORD OF THE CAT BY MEANS OF ANTIDROMIC STIMULATION]. Pflugers Arch Gesamte Physiol Menschen Tiere 281:231-244 Available at: [Accessed May 5, 2011].

Nattie E (1999) CO2, brainstem chemoreceptors and breathing. Prog. Neurobiol 59:299-331 Available at: [Accessed July 12, 2011].

Nattie E (2000) Multiple sites for central chemoreception: their roles in response sensitivity and in sleep and wakefulness. Respir Physiol 122:223-235 Available at: [Accessed July 12, 2011].

Nattie EE, Fung ML, Li A, St John WM (1993) Responses of respiratory modulated and tonic units in the retrotrapezoid nucleus to CO2. Respir Physiol 94:35-50 Available at: [Accessed May 11, 2011].

Nattie EE, Li A (2001) CO2 dialysis in the medullary raphe of the rat increases ventilation in sleep. J. Appl. Physiol 90:1247-1257 Available at: [Accessed July 13, 2011].

Nattie EE, Forster HV (2010) Special Issue on Central Chemoreception. Foreword. Respir Physiol Neurobiol 173:193-194 Available at: [Accessed June 29, 2011].

Nattie EE, Li A (2002)(a) Substance P-saporin lesion of neurons with NK1 receptors in one chemoreceptor site in rats decreases ventilation and chemosensitivity. J. Physiol. (Lond.) 544:603-616 Available at: [Accessed May 11, 2011].

Nattie EE, Li A (2002)(b) CO2 dialysis in nucleus tractus solitarius region of rat increases ventilation in sleep and wakefulness. J. Appl. Physiol 92:2119-2130 Available at: [Accessed July 13, 2011].

Nattie EE, Li A, Richerson GB, Richerson G, Lappi DA (2004) Medullary serotonergic neurones and adjacent neurones that express neurokinin-1 receptors are both involved in chemoreception in vivo. J. Physiol. (Lond.) 556:235-253 Available at: [Accessed June 28, 2011].

Neary D, Snowden JS, Gustafson L, Passant U, Stuss D, Black S, Freedman M, Kertesz A, Robert PH, Albert M, Boone K, Miller BL, Cummings J, Benson DF (1998) Frontotemporal lobar degeneration: a consensus on clinical diagnostic criteria. Neurology 51:1546-1554 Available at: [Accessed June 22, 2011].

Del Negro CA, Koshiya N, Butera RJ Jr, Smith JC (2002) Persistent sodium current, membrane properties and bursting behavior of pre-bötzinger complex inspiratory neurons in vitro. J. Neurophysiol 88:2242-2250 Available at: [Accessed May 18, 2011].

Del Negro CA, Morgado-Valle C, Hayes JA, Mackay DD, Pace RW, Crowder EA, Feldman JL (2005) Sodium and calcium current-mediated pacemaker neurons and respiratory rhythm generation. J. Neurosci 25:446-453 Available at: [Accessed May 18, 2011].

Nielsen AM, Bisgard GE, Mitchell GS (1986) Phrenic nerve responses to hypoxia and CO2 in decerebrate dogs. Respir Physiol 65:267-283 Available at: [Accessed July 13, 2011].

Niewoehner DE, Kleinerman J, Liotta L (1975) Elastic behavior of postmortem human lungs: effects of aging and mild emphysema. J Appl Physiol 39:943-949 Available at: [Accessed June 10, 2011].

Nishimura A, Ueda S, Takeuchi Y, Matsushita H, Sawada T, Kawata M (1998) Vulnerability to aging in the rat serotonergic system. Acta Neuropathol 96:581-595 Available at: [Accessed June 12, 2011].

Noble W, Planel E, Zehr C, Olm V, Meyerson J, Suleman F, Gaynor K, Wang L, LaFrancois J, Feinstein B, Burns M, Krishnamurthy P, Wen Y, Bhat R, Lewis J, Dickson D, Duff K (2005) Inhibition of glycogen synthase kinase-3 by lithium correlates with reduced tauopathy and degeneration in vivo. Proc. Natl. Acad. Sci. U.S.A

102:6990-6995 Available at: [Accessed June 22, 2011].

Nomura Y, Segawa M, Higurashi M (1985) Rett syndrome--an early catecholamine and indolamine deficient disorder? Brain Dev 7:334-341 Available at: [Accessed June 24, 2011].

Nomura Y (2005) Early behavior characteristics and sleep disturbance in Rett syndrome. Brain Dev 27 Suppl 1:S35-S42 Available at: [Accessed June 24, 2011].

Nuding SC, Segers LS, Shannon R, O'Connor R, Morris KF, Lindsey BG (2009) Central and peripheral chemoreceptors evoke distinct responses in simultaneously recorded neurons of the raphé-pontomedullary respiratory network. Philos. Trans. R. Soc. Lond., B, Biol. Sci 364:2501-2516 Available at: [Accessed June 29, 2011].

Nurse CA, Zhang M (2001) Synaptic mechanisms during re-innervation of rat arterial chemoreceptors in co-culture. Comp. Biochem. Physiol., Part A Mol. Integr. Physiol 130:241-251 Available at: [Accessed June 29, 2011].

Nurse CA (2005) Neurotransmission and neuromodulation in the chemosensory carotid body. Auton Neurosci 120:1-9 Available at: [Accessed June 29, 2011].

Nygren LG, Olson L (1977) A new major projection from locus coeruleus: the main source of noradrenergic nerve terminals in the ventral and dorsal columns of the spinal cord. Brain Res 132:85-93 Available at: [Accessed May 10, 2011].

Núñez-Abades PA, Morillo AM, Pásaro R (1993) Brainstem connections of the rat ventral respiratory subgroups: afferent projections. J. Auton. Nerv. Syst 42:99-118 Available at: [Accessed May 5, 2011].

Núñez-Abades PA, Pásaro R, Bianchi AL (1991) Localization of respiratory bulbospinal and propriobulbar neurons in the region of the nucleus ambiguus of the rat. Brain Res 568:165-172 Available at: [Accessed May 5, 2011].

Núñez-Abades PA, Pásaro R, Bianchi AL (1992) Study of the topographical distribution of different populations of motoneurons within rat's nucleus ambiguus, by means of four different fluorochromes. Neurosci. Lett 135:103-107 Available at: [Accessed May 11, 2011].

Oddo S, Billings L, Kesslak JP, Cribbs DH, LaFerla FM (2004) Abeta immunotherapy leads to clearance of early, but not late, hyperphosphorylated tau aggregates via the proteasome. Neuron 43:321-332 Available at: [Accessed June 21, 2011].

Ogier M, Wang H, Hong E, Wang Q, Greenberg ME, Katz DM (2007) Brain-derived neurotrophic factor expression and respiratory function improve after ampakine treatment in a mouse model of Rett syndrome. J. Neurosci 27:10912-10917 Available at: [Accessed June 24, 2011].

Okabe S, Mackiewicz M, Kubin L (1997) Serotonin receptor mRNA expression in the hypoglossal motor nucleus. Respir Physiol 110:151-160 Available at: [Accessed June 12, 2011].

Okazaki M, Takeda R, Yamazaki H, Haji A (2002) Synaptic mechanisms of inspiratory off-switching evoked by pontine pneumotaxic stimulation in cats. Neurosci. Res 44:101-110 Available at: [Accessed May 8, 2011].

Oku Y, Dick TE (1992) Phase resetting of the respiratory cycle before and after unilateral pontine lesion in cat. J. Appl. Physiol 72:721-730 Available at: [Accessed May 24, 2011].

Oliven A, Carmi N, Coleman R, Odeh M, Silbermann M (2001) Age-related changes in upper airway muscles morphological and oxidative properties. Exp. Gerontol 36:1673-1686 Available at: [Accessed June 11, 2011].

Olson EB Jr, Dempsey JA, McCrimmon DR (1979) Serotonin and the control of ventilation in awake rats. J. Clin. Invest 64:689-693 Available at: [Accessed May 31, 2011].

Onai T, Miura M (1986) Projections of supraspinal structures to the phrenic motor nucleus in cats studied by a horseradish peroxidase microinjection method. J. Auton. Nerv. Syst 16:61-77 Available at: [Accessed May 11,

2011].

Onimaru H, Homma I (1987) Respiratory rhythm generator neurons in medulla of brainstem-spinal cord preparation from newborn rat. Brain Res 403:380-384 Available at: [Accessed May 10, 2011].

Onimaru H, Homma I (2003) A novel functional neuron group for respiratory rhythm generation in the ventral medulla. J. Neurosci 23:1478-1486 Available at: [Accessed May 10, 2011].

Onimaru H, Homma I (2005) Optical imaging of respiratory neuron activity from the dorsal view of the lower brainstem. Clin. Exp. Pharmacol. Physiol 32:297-301 Available at: [Accessed May 12, 2011].

Onimaru H, Ikeda K, Kawakami K (2008) CO2-sensitive preinspiratory neurons of the parafacial respiratory group express Phox2b in the neonatal rat. J. Neurosci 28:12845-12850 Available at: [Accessed May 18, 2011].

Onimaru H, Kumagawa Y, Homma I (2006) Respiration-related rhythmic activity in the rostral medulla of newborn rats. J. Neurophysiol 96:55-61 Available at: [Accessed May 10, 2011].

Oriander PR, Nader S (1996) Endocrinology. Youthful hormones. Lancet 348 Suppl 2:sII6 Available at: [Accessed June 8, 2011].

Otake K, Ezure K, Lipski J, Wong She RB (1992) Projections from the commissural subnucleus of the nucleus of the solitary tract: an anterograde tracing study in the cat. J. Comp. Neurol 324:365-378 Available at: [Accessed May 11, 2011].

Otake K, Sasaki H, Ezure K, Manabe M (1988) Axonal projections from Bötzinger expiratory neurons to contralateral ventral and dorsal respiratory groups in the cat. Exp Brain Res 72:167-177 Available at: [Accessed May 5, 2011].

Otake K, Sasaki H, Mannen H, Ezure K (1987) Morphology of expiratory neurons of the Bötzinger complex: an HRP study in the cat. J. Comp. Neurol 258:565-579 Available at: [Accessed May 5, 2011].

Oyamada Y, Ballantyne D, Mückenhoff K, Scheid P (1998) Respiration-modulated membrane potential and chemosensitivity of locus coeruleus neurones in the in vitro brainstem-spinal cord of the neonatal rat. J. Physiol. (Lond.) 513 (Pt 2):381-398 Available at: [Accessed July 13, 2011].

O'Leary JC 3rd, Li Q, Marinec P, Blair LJ, Congdon EE, Johnson AG, Jinwal UK, Koren J 3rd, Jones JR, Kraft C, Peters M, Abisambra JF, Duff KE, Weeber EJ, Gestwicki JE, Dickey CA (2010) Phenothiazine-mediated rescue of cognition in tau transgenic mice requires neuroprotection and reduced soluble tau burden. Mol Neurodegener 5:45 Available at: [Accessed June 22, 2011].

Pagliardini S, Janczewski WA, Tan W, Dickson CT, Deisseroth K, Feldman JL (2011) Active expiration induced by excitation of ventral medulla in adult anesthetized rats. J. Neurosci 31:2895-2905 Available at: [Accessed March 21, 2011].

Panayotis N, Ghata A, Villard L, Roux J-C (2011) Biogenic amines and their metabolites are differentially affected in the Mecp2-deficient mouse brain. BMC Neurosci 12:47 Available at: [Accessed June 24, 2011].

Parvizi J, Van Hoesen GW, Damasio A (1998) Severe pathological changes of parabrachial nucleus in Alzheimer's disease. Neuroreport 9:4151-4154 Available at: [Accessed June 23, 2011].

Parvizi J, Van Hoesen GW, Damasio A (2000) Selective pathological changes of the periaqueductal gray matter in Alzheimer's disease. Ann. Neurol 48:344-353 Available at: [Accessed June 23, 2011].

Parvizi J, Van Hoesen GW, Damasio A (2001) The selective vulnerability of brainstem nuclei to Alzheimer's disease. Ann. Neurol 49:53-66 Available at: [Accessed June 23, 2011].

Pascual O, Morin-Surun M-P, Barna B, Denavit-Saubié M, Pequignot J-M, Champagnat J (2002) Progesterone reverses the neuronal responses to hypoxia in rat nucleus tractus solitarius in vitro. J. Physiol. (Lond.) 544:511-520 Available at: [Accessed July 11, 2011].

Di Pasquale E, Lindsay A, Feldman J, Monteau R, Hilaire G (1997) Serotonergic inhibition of phrenic motoneuron activity: an in vitro study in neonatal rat. Neurosci. Lett 230:29-32 Available at: [Accessed June 1, 2011].

Di Pasquale E, Monteau R, Hilaire G (1992) In vitro study of central respiratory-like activity of the fetal rat. Exp Brain Res 89:459-464 Available at: [Accessed May 30, 2011].

Paterson DS, Hilaire G, Weese-Mayer DE (2009) Medullary serotonin defects and respiratory dysfunction in sudden infant death syndrome. Respir Physiol Neurobiol 168:133-143 Available at: [Accessed June 1, 2011].

Paterson DS, Trachtenberg FL, Thompson EG, Belliveau RA, Beggs AH, Darnall R, Chadwick AE, Krous HF, Kinney HC (2006) Multiple serotonergic brainstem abnormalities in sudden infant death syndrome. JAMA 296:2124-2132 Available at: [Accessed June 1, 2011].

Paton JF (1996)(a) The ventral medullary respiratory network of the mature mouse studied in a working heart-brainstem preparation. J. Physiol. (Lond.) 493 (Pt 3):819-831 Available at: [Accessed May 4, 2011].

Paton JF (1996)(b) A working heart-brainstem preparation of the mouse. J. Neurosci. Methods 65:63-68 Available at: [Accessed May 23, 2011].

Paton JF, Li YW, Kasparov S (1999) Reflex response and convergence of pharyngoesophageal and peripheral chemoreceptors in the nucleus of the solitary tract. Neuroscience 93:143-154 Available at: [Accessed May 24, 2011].

Paton JFR, Abdala APL, Koizumi H, Smith JC, St-John WM (2006) Respiratory rhythm generation during gasping depends on persistent sodium current. Nat. Neurosci 9:311-313 Available at: [Accessed May 19, 2011].

Paton JFR, St-John WM (2007) Counterpoint: Medullary pacemaker neurons are essential for gasping, but not eupnea, in mammals. J. Appl. Physiol 103:718-720; discussion 721-722 Available at: [Accessed May 19, 2011].

Patrickson JW, Smith TE, Zhou SS (1991) Motor neurons of the laryngeal nerves. Anat. Rec 230:551-556 Available at: [Accessed June 2, 2011].

Patroniti N, Foti G, Cortinovis B, Maggioni E, Bigatello LM, Cereda M, Pesenti A (2002) Sigh improves gas exchange and lung volume in patients with acute respiratory distress syndrome undergoing pressure support ventilation. Anesthesiology 96:788-794 Available at: [Accessed July 6, 2011].

Peano CA, Shonis CA, Dillon GH, Waldrop TG (1992) Hypothalamic GABAergic mechanism involved in respiratory response to hypercapnia. Brain Res. Bull 28:107-113 Available at: [Accessed July 13, 2011].

Pearce RA, Stornetta RL, Guyenet PG (1989) Retrotrapezoid nucleus in the rat. Neurosci. Lett 101:138-142 Available at: [Accessed May 10, 2011].

Peers C, Pearson HA, Boyle JP (2007) Hypoxia and Alzheimer's disease. Essays Biochem 43:153-164 Available at: [Accessed June 23, 2011].

Pelka GJ, Watson CM, Radziewic T, Hayward M, Lahooti H, Christodoulou J, Tam PPL (2006) Mecp2 deficiency is associated with learning and cognitive deficits and altered gene activity in the hippocampal region of mice. Brain 129:887-898 Available at: [Accessed July 5, 2011].

Perez M, Santa-Maria I, Gomez de Barreda E, Zhu X, Cuadros R, Cabrero JR, Sanchez-Madrid F, Dawson HN, Vitek MP, Perry G, Smith MA, Avila J (2009) Tau--an inhibitor of deacetylase HDAC6 function. J. Neurochem 109:1756-1766 Available at: [Accessed June 16, 2011].

Pete G, Mack SO, Haxhiu MA, Walbaum S, Gauda EB (2002) CO(2)-induced c-Fos expression in brainstem preprotachykinin mRNA containing neurons. Respir Physiol Neurobiol 130:265-274 Available at: [Accessed July 13, 2011].

Peterson DD, Pack AI, Silage DA, Fishman AP (1981) Effects of aging on ventilatory and occlusion pressure responses to hypoxia and hypercapnia. Am. Rev. Respir. Dis 124:387-391 Available at: [Accessed June 13,

2011].

Pilowsky PM, de Castro D, Llewellyn-Smith I, Lipski J, Voss MD (1990) Serotonin immunoreactive boutons make synapses with feline phrenic motoneurons. J. Neurosci 10:1091-1098 Available at: [Accessed May 31, 2011].

Planel E, Bretteville A, Liu L, Virag L, Du AL, Yu WH, Dickson DW, Whittington RA, Duff KE (2009) Acceleration and persistence of neurofibrillary pathology in a mouse model of tauopathy following anesthesia. FASEB J 23:2595-2604 Available at: [Accessed August 4, 2009].

Planel E, Krishnamurthy P, Miyasaka T, Liu L, Herman M, Kumar A, Bretteville A, Figueroa HY, Yu WH, Whittington RA, Davies P, Takashima A, Nixon RA, Duff KE (2008) Anesthesia-induced hyperphosphorylation detaches 3-repeat tau from microtubules without affecting their stability in vivo. J. Neurosci 28:12798-12807 Available at: [Accessed October 26, 2009].

Planel E, Richter KEG, Nolan CE, Finley JE, Liu L, Wen Y, Krishnamurthy P, Herman M, Wang L, Schachter JB, Nelson RB, Lau L-F, Duff KE (2007) Anesthesia leads to tau hyperphosphorylation through inhibition of phosphatase activity by hypothermia. J. Neurosci 27:3090-3097 Available at: [Accessed October 26, 2009].

Poets CF, Rau GA, Neuber K, Gappa M, Seidenberg J (1997) Determinants of lung volume in spontaneously breathing preterm infants. Am. J. Respir. Crit. Care Med 155:649-653 Available at: [Accessed July 6, 2011].

Pokorski M, Antosiewicz J (2010) Alterations in the hypoxic ventilatory response with advancing age in awake rats. J. Physiol. Pharmacol 61:227-232 Available at: [Accessed June 13, 2011].

Pokorski M, Marczak M (2003) Ventilatory response to hypoxia in elderly women. Ann. Hum. Biol 30:53-64 Available at: [Accessed June 13, 2011].

Pokorski M, Walski M, Dymecka A, Marczak M (2004) The aging carotid body. J. Physiol. Pharmacol 55 Suppl 3:107-113 Available at: [Accessed June 13, 2011].

Poliacek I, Jakus J, Stránsky A, Baráni H, Halasová E, Tomori Z (2004) Cough, expiration and aspiration reflexes following kainic acid lesions to the pontine respiratory group in anesthetized cats. Physiol Res 53:155-163 Available at: [Accessed June 2, 2011].

Poliacek I, Stránsky A, Szereda-Przestaszewska M, Jakus J, Baráni H, Tomori Z, Halasová E (2005) Cough and laryngeal muscle discharges in brainstem lesioned anaesthetized cats. Physiol Res 54:645-654 Available at: [Accessed June 2, 2011].

Polkey MI, Harris ML, Hughes PD, Hamnegärd CH, Lyons D, Green M, Moxham J (1997) The contractile properties of the elderly human diaphragm. Am. J. Respir. Crit. Care Med 155:1560-1564 Available at: [Accessed June 10, 2011].

Portillo F, Grélot L, Milano S, Bianchi AL (1994) Brainstem neurons with projecting axons to both phrenic and abdominal motor nuclei: a double fluorescent labeling study in the cat. Neurosci. Lett 173:50-54 Available at: [Accessed May 5, 2011].

Portillo F, Pásaro R (1987) Axonal projections to the ventrolateral nucleus of the solitary tract revealed by double labelling of retrograde fluorescent markers in the cat. Neurosci. Lett 76:280-284 Available at: [Accessed May 5, 2011].

Portillo F, Pásaro R (1988) Location of bulbospinal neurons and of laryngeal motoneurons within the nucleus ambiguus of the rat and cat by means of retrograde fluorescent labelling. J. Anat 159:11-18 Available at: [Accessed May 5, 2011].

Potts JT, Spyer KM, Paton JF (2000) Somatosympathetic reflex in a working heart-brainstem preparation of the rat. Brain Res Bull 53:59-67 Available at: [Accessed January 20, 2009].

Potts JT, Rybak IA, Paton JFR (2005) Respiratory rhythm entrainment by somatic afferent stimulation. J. Neurosci 25:1965-1978 Available at: [Accessed May 10, 2011].

Prasad M, Fearon IM, Zhang M, Laing M, Vollmer C, Nurse CA (2001) Expression of P2X2 and P2X3 receptor subunits in rat carotid body afferent neurones: role in chemosensory signalling. J. Physiol. (Lond.) 537:667-677 Available at: [Accessed June 29, 2011].

Putnam RW (2001) Intracellular pH regulation of neurons in chemosensitive and nonchemosensitive areas of brain slices. Respir Physiol 129:37-56 Available at: [Accessed July 13, 2011].

Putnam RW, Filosa JA, Ritucci NA (2004) Cellular mechanisms involved in CO(2) and acid signaling in chemosensitive neurons. Am. J. Physiol., Cell Physiol 287:C1493-1526 Available at: [Accessed July 12, 2011].

Pásaro R, Lobera B, González-Barón S, Delgado-García JM (1981) [Localization of laryngeal muscle motoneurons in rat (author's transl)]. Rev. Esp. Fisiol 37:317-322 Available at: [Accessed May 11, 2011].

Qiang L, Yu W, Andreadis A, Luo M, Baas PW (2006) Tau protects microtubules in the axon from severing by katanin. J. Neurosci 26:3120-3129 Available at: [Accessed June 16, 2011].

Querfurth HW, LaFerla FM (2010) Alzheimer's disease. N. Engl. J. Med 362:329-344 Available at: [Accessed June 17, 2011].

Qureshi M, Khalil M, Kwiatkowski K, Alvaro RE (2009) Morphology of sighs and their role in the control of breathing in preterm infants, term infants and adults. Neonatology 96:43-49 Available at: [Accessed July 6, 2011].

Rabie T, Marti HH (2008) Brain protection by erythropoietin: a manifold task. Physiology (Bethesda) 23:263-274 Available at: [Accessed July 3, 2011].

Ramaroson H, Helmer C, Barberger-Gateau P, Letenneur L, Dartigues J-F (2003) [Prevalence of dementia and Alzheimer's disease among subjects aged 75 years or over: updated results of the PAQUID cohort]. Rev. Neurol. (Paris) 159:405-411 Available at: [Accessed June 17, 2011].

Ramirez JM, Pearson KG (1988) Generation of motor patterns for walking and flight in motoneurons supplying bifunctional muscles in the locust. J. Neurobiol 19:257-282 Available at: [Accessed June 2, 2011].

Ramirez J-M, Garcia A 3rd (2007) Point: Medullary pacemaker neurons are essential for both eupnea and gasping in mammals. J. Appl. Physiol 103:717-718; discussion 722 Available at: [Accessed May 19, 2011].

Rapoport M, Dawson HN, Binder LI, Vitek MP, Ferreira A (2002) Tau is essential to beta -amyloid-induced neurotoxicity. Proc. Natl. Acad. Sci. U.S.A 99:6364-6369 Available at: [Accessed June 21, 2011].

Rapport MM, Green AA, Page IH (1948) Crystalline Serotonin. Science 108:329-330 Available at: [Accessed May 31, 2011].

Ray AD, Ogasa T, Magalang UJ, Krasney JA, Farkas GA (2008) Aging increases upper airway collapsibility in Fischer 344 rats. J. Appl. Physiol 105:1471-1476 Available at: [Accessed June 9, 2011].

Rebeiz JJ, Kolodny EH, Richardson EP Jr (1968) Corticodentatonigral degeneration with neuronal achromasia. Arch. Neurol 18:20-33 Available at: [Accessed June 22, 2011].

Reid G, Rand M (1951) Physiological actions of the partially purified serum vasoconstrictor (serotonin). Aust J Exp Biol Med Sci 29:401-415 Available at: [Accessed May 31, 2011].

Rekling JC, Champagnat J, Denavit-Saubié M (1996) Thyrotropin-releasing hormone (TRH) depolarizes a subset of inspiratory neurons in the newborn mouse brain stem in vitro. J. Neurophysiol 75:811-819 Available at: [Accessed May 11, 2011].

Rett A (1966) [On a unusual brain atrophy syndrome in hyperammonemia in childhood]. Wien Med Wochenschr 116:723-726 Available at: [Accessed June 24, 2011].

Reyes EP, Fernández R, Larraín C, Zapata P (2007) Effects of combined cholinergic-purinergic block upon cat carotid body chemoreceptors in vitro. Respir Physiol Neurobiol 156:17-22 Available at: [Accessed June 29,

2011].

Reyes JF, Reynolds MR, Horowitz PM, Fu Y, Guillozet-Bongaarts AL, Berry R, Binder LI (2008) A possible link between astrocyte activation and tau nitration in Alzheimer's disease. Neurobiol. Dis 31:198-208 Available at: [Accessed June 16, 2011].

Rhein V, Song X, Wiesner A, Ittner LM, Baysang G, Meier F, Ozmen L, Bluethmann H, Dröse S, Brandt U, Savaskan E, Czech C, Götz J, Eckert A (2009) Amyloid-beta and tau synergistically impair the oxidative phosphorylation system in triple transgenic Alzheimer's disease mice. Proc. Natl. Acad. Sci. U.S.A 106:20057-20062 Available at: [Accessed June 21, 2011].

Ricardo JA, Koh ET (1978) Anatomical evidence of direct projections from the nucleus of the solitary tract to the hypothalamus, amygdala, and other forebrain structures in the rat. Brain Res 153:1-26 Available at: [Accessed May 24, 2011].

Richerson GB (2004) Serotonergic neurons as carbon dioxide sensors that maintain pH homeostasis. Nat Rev Neurosci 5:449-61 Available at: [Accessed April 17, 2009].

Richter DW (1982) Generation and maintenance of the respiratory rhythm. J. Exp. Biol 100:93-107 Available at: [Accessed May 4, 2011].

Rinne JO, Lee MS, Thompson PD, Marsden CD (1994) Corticobasal degeneration. A clinical study of 36 cases. Brain 117 (Pt 5):1183-1196 Available at: [Accessed June 22, 2011].

Ritucci NA, Dean JB, Putnam RW (2005) Somatic vs. dendritic responses to hypercapnia in chemosensitive locus coeruleus neurons from neonatal rats. Am. J. Physiol., Cell Physiol 289:C1094-1104 Available at: [Accessed July 13, 2011].

Roberson ED, Halabisky B, Yoo JW, Yao J, Chin J, Yan F, Wu T, Hamto P, Devidze N, Yu G-Q, Palop JJ, Noebels JL, Mucke L (2011) Amyloid-β/Fyn-induced synaptic, network, and cognitive impairments depend on tau levels in multiple mouse models of Alzheimer's disease. J. Neurosci 31:700-711 Available at: [Accessed June 20, 2011].

Roberson ED, Scearce-Levie K, Palop JJ, Yan F, Cheng IH, Wu T, Gerstein H, Yu G-Q, Mucke L (2007) Reducing endogenous tau ameliorates amyloid beta-induced deficits in an Alzheimer's disease mouse model. Science 316:750-4 Available at: [Accessed April 15, 2009].

Roberta A Pagon TDB (1998) Alzheimer Disease Overview. Available at: http://www.ncbi.nlm.nih.gov/books/NBK1161/?log$=disease5_name [Accessed June 22, 2011].

Rocher A, Geijo-Barrientos E, Cáceres AI, Rigual R, González C, Almaraz L (2005) Role of voltage-dependent calcium channels in stimulus-secretion coupling in rabbit carotid body chemoreceptor cells. J. Physiol. (Lond.) 562:407-420 Available at: [Accessed June 30, 2011].

Roda F, Gestreau C, Bianchi AL (2002) Discharge patterns of hypoglossal motoneurons during fictive breathing, coughing, and swallowing. J. Neurophysiol 87:1703-1711 Available at: [Accessed May 4, 2011].

Romaniuk JR, Kasicki S, Kazennikov OV, Selionov VA (1994) Respiratory responses to stimulation of spinal or medullary locomotor structures in decerebrate cats. Acta Neurobiol Exp (Wars) 54:11-17 Available at: [Accessed June 5, 2011].

Rosenberg KJ, Ross JL, Feinstein HE, Feinstein SC, Israelachvili J (2008) Complementary dimerization of microtubule-associated tau protein: Implications for microtubule bundling and tau-mediated pathogenesis. Proc. Natl. Acad. Sci. U.S.A 105:7445-7450 Available at: [Accessed June 16, 2011].

Rosin DL, Chang DA, Guyenet PG (2006) Afferent and efferent connections of the rat retrotrapezoid nucleus. J. Comp. Neurol 499:64-89 Available at: [Accessed May 10, 2011].

Rossi F, Maione S, Berrino L (1994) Periaqueductal gray area and cardiovascular function. Pharmacol. Res 29:27-36 Available at: [Accessed June 3, 2011].

Roux E (2002) [Origin and evolution of the respiratory tract in vertebrates]. Rev Mal Respir 19:601-615 Available at: [Accessed April 28, 2011].

Roux J-C, Dura E, Villard L (2008) Tyrosine hydroxylase deficit in the chemoafferent and the sympathoadrenergic pathways of the Mecp2 deficient mouse. Neurosci. Lett 447:82-86 Available at: [Accessed June 24, 2011].

Roy S, Zhang B, Lee VM-Y, Trojanowski JQ (2005) Axonal transport defects: a common theme in neurodegenerative diseases. Acta Neuropathol 109:5-13 Available at: [Accessed June 18, 2011].

Rubens AB (1975) Aphasia with infarction in the territory of the anterior cerebral artery. Cortex 11:239-250 Available at: [Accessed June 4, 2011].

Rudman D, Feller AG, Nagraj HS, Gergans GA, Lalitha PY, Goldberg AF, Schlenker RA, Cohn L, Rudman IW, Mattson DE (1990) Effects of human growth hormone in men over 60 years old. N. Engl. J. Med 323:1-6 Available at: [Accessed June 8, 2011].

Rüb U, Del Tredici K, Schultz C, Thal DR, Braak E, Braak H (2000) The evolution of Alzheimer's disease-related cytoskeletal pathology in the human raphe nuclei. Neuropathol. Appl. Neurobiol 26:553-567 Available at: [Accessed June 23, 2011].

Rüb U, Del Tredici K, Schultz C, Thal DR, Braak E, Braak H (2001) The autonomic higher order processing nuclei of the lower brain stem are among the early targets of the Alzheimer's disease-related cytoskeletal pathology. Acta Neuropathol 101:555-564 Available at: [Accessed November 13, 2009].

Rüb U, Del Tredici K, Schultz C, de Vos RAI, Jansen Steur ENH, Arai K, Braak H (2002) Progressive supranuclear palsy: neuronal and glial cytoskeletal pathology in the higher order processing autonomic nuclei of the lower brainstem. Neuropathol. Appl. Neurobiol 28:12-22 Available at: [Accessed June 23, 2011].

Sagen J, Proudfit HK (1986) Alterations in nociception following lesions of the A5 catecholamine nucleus. Brain Res 370:93-101 Available at: [Accessed May 10, 2011].

Sahara N, Maeda S, Takashima A (2008) Tau oligomerization: a role for tau aggregation intermediates linked to neurodegeneration. Curr Alzheimer Res 5:591-598 Available at: [Accessed June 22, 2011].

Saito Y, Tanaka I, Ezure K (2002) Morphology of the decrementing expiratory neurons in the brainstem of the rat. Neurosci. Res 44:141-153 Available at: [Accessed May 11, 2011].

Sakanaka M, Wen TC, Matsuda S, Masuda S, Morishita E, Nagao M, Sasaki R (1998) In vivo evidence that erythropoietin protects neurons from ischemic damage. Proc. Natl. Acad. Sci. U.S.A 95:4635-4640 Available at: [Accessed July 3, 2011].

Salter MW, Kalia LV (2004) Src kinases: a hub for NMDA receptor regulation. Nat. Rev. Neurosci 5:317-328 Available at: [Accessed June 16, 2011].

Sanai N, Tramontin AD, Quinones-Hinojosa A, Barbaro NM, Gupta N, Kunwar S, Lawton MT, McDermott MW, Parsa AT, Manuel-Garcia Verdugo J, Berger MS, Alvarez-Buylla A (2004) Unique astrocyte ribbon in adult human brain contains neural stem cells but lacks chain migration. Nature 427:740-744 Available at: [Accessed June 2, 2011].

Sanchez PE, Fares RP, Risso J-J, Bonnet C, Bouvard S, Le-Cavorsin M, Georges B, Moulin C, Belmeguenai A, Bodennec J, Morales A, Pequignot J-M, Baulieu E-E, Levine RA, Bezin L (2009) Optimal neuroprotection by erythropoietin requires elevated expression of its receptor in neurons. Proc. Natl. Acad. Sci. U.S.A 106:9848-9853 Available at: [Accessed July 3, 2011].

Santacruz K, Lewis J, Spires T, Paulson J, Kotilinek L, Ingelsson M, Guimaraes A, DeTure M, Ramsden M, McGowan E, Forster C, Yue M, Orne J, Janus C, Mariash A, Kuskowski M, Hyman B, Hutton M, Ashe KH (2005) Tau suppression in a neurodegenerative mouse model improves memory function. Science 309:476-81 Available at: [Accessed April 15, 2009].

Sara SJ (2009) The locus coeruleus and noradrenergic modulation of cognition. Nat. Rev. Neurosci 10:211-223 Available at: [Accessed June 23, 2011].

Sasaki H, Otake K, Mannen H, Ezure K, Manabe M (1989) Morphology of augmenting inspiratory neurons of the ventral respiratory group in the cat. J. Comp. Neurol 282:157-168 Available at: [Accessed May 5, 2011].

Sasaki R (2003) Pleiotropic functions of erythropoietin. Intern. Med 42:142-149 Available at: [Accessed July 3, 2011].

Scattoni ML, Crawley J, Ricceri L (2009) Ultrasonic vocalizations: a tool for behavioural phenotyping of mouse models of neurodevelopmental disorders. Neurosci Biobehav Rev 33:508-515 Available at: [Accessed June 5, 2011].

Scattoni ML, Gandhy SU, Ricceri L, Crawley JN (2008) Unusual repertoire of vocalizations in the BTBR T+tf/J mouse model of autism. PLoS ONE 3:e3067 Available at: [Accessed June 5, 2011].

Scattoni ML, Gasparini L, Alleva E, Goedert M, Calamandrei G, Spillantini MG (2010) Early behavioural markers of disease in P301S tau transgenic mice. Behav. Brain Res 208:250-257 Available at: [Accessed June 5, 2011].

Schelegle ES (2003) Functional morphology and physiology of slowly adapting pulmonary stretch receptors. Anat Rec A Discov Mol Cell Evol Biol 270:11-16 Available at: [Accessed July 14, 2011].

Schlaefke ME, See WR, Loeschcke HH (1970) Ventilatory response to alterations of H+ ion concentration in small areas of the ventral medullary surface. Respir Physiol 10:198-212 Available at: [Accessed July 13, 2011].

Schmidt CD, Dickman ML, Gardner RM, Brough FK (1973) Spirometric standards for healthy elderly men and women. 532 subjects, ages 55 through 94 years. Am. Rev. Respir. Dis 108:933-939 Available at: [Accessed June 11, 2011].

Schreihofer AM, Stornetta RL, Guyenet PG (1999) Evidence for glycinergic respiratory neurons: Bötzinger neurons express mRNA for glycinergic transporter 2. J. Comp. Neurol 407:583-597 Available at: [Accessed May 11, 2011].

Schwab RJ, Gupta KB, Gefter WB, Metzger LJ, Hoffman EA, Pack AI (1995) Upper airway and soft tissue anatomy in normal subjects and patients with sleep-disordered breathing. Significance of the lateral pharyngeal walls. Am. J. Respir. Crit. Care Med 152:1673-1689 Available at: [Accessed June 11, 2011].

Schwarzacher SW, Pestean A, Günther S, Ballanyi K (2002) Serotonergic modulation of respiratory motoneurons and interneurons in brainstem slices of perinatal rats. Neuroscience 115:1247-1259 Available at: [Accessed June 12, 2011].

Schöner G, Kelso JA (1988) Dynamic pattern generation in behavioral and neural systems. Science 239:1513-1520 Available at: [Accessed June 2, 2011].

Seebart BR, Stoffel RT, Behan M (2007) Age-related changes in the serotonin 2A receptor in the hypoglossal nucleus of male and female rats. Respir Physiol Neurobiol 158:14-21 Available at: [Accessed June 9, 2011].

Selkoe DJ (2001) Alzheimer's disease: genes, proteins, and therapy. Physiol. Rev 81:741-766 Available at: [Accessed June 18, 2011].

Selkoe DJ (2002) Alzheimer's disease is a synaptic failure. Science 298:789-791 Available at: [Accessed June 20, 2011].

Semenza GL (2001) HIF-1, O(2), and the 3 PHDs: how animal cells signal hypoxia to the nucleus. Cell 107:1-3 Available at: [Accessed July 3, 2011].

Semenza G (2002) Signal transduction to hypoxia-inducible factor 1. Biochem. Pharmacol 64:993-998 Available at: [Accessed July 3, 2011].

Semenza GL, Shimoda LA, Prabhakar NR (2006) Regulation of gene expression by HIF-1. Novartis Found. Symp 272:2-8; discussion 8-14, 33-36 Available at: [Accessed July 3, 2011].

Semenza GL (2007) Life with Oxygen. Science 318:62 -64 Available at: [Accessed March 24, 2011].

Serebrovskaya TV, Karaban IN, Kolesnikova EE, Mishunina TM, Swanson RJ, Beloshitsky PV, Ilyin VN, Krasuk AN, Safronova OS, Kuzminskaya LA (2000) Geriatric men at altitude: hypoxic ventilatory sensitivity and blood dopamine changes. Respiration 67:253-260 Available at: [Accessed June 13, 2011].

Severson CA, Wang W, Pieribone VA, Dohle CI, Richerson GB (2003) Midbrain serotonergic neurons are central pH chemoreceptors. Nat. Neurosci 6:1139-1140 Available at: [Accessed June 28, 2011].

Shahbazian M, Young J, Yuva-Paylor L, Spencer C, Antalffy B, Noebels J, Armstrong D, Paylor R, Zoghbi H (2002) Mice with truncated MeCP2 recapitulate many Rett syndrome features and display hyperacetylation of histone H3. Neuron 35:243-254 Available at: [Accessed June 24, 2011].

Shiba K, Satoh I, Kobayashi N, Hayashi F (1999) Multifunctional laryngeal motoneurons: an intracellular study in the cat. J. Neurosci 19:2717-2727 Available at: [Accessed May 24, 2011].

Shiba K, Nakazawa K, Ono K, Umezaki T (2007) Multifunctional laryngeal premotor neurons: their activities during breathing, coughing, sneezing, and swallowing. J. Neurosci 27:5156-5162 Available at: [Accessed June 5, 2011].

Simic G, Stanic G, Mladinov M, Jovanov-Milosevic N, Kostovic I, Hof PR (2009) Does Alzheimer's disease begin in the brainstem? Neuropathol. Appl. Neurobiol 35:532-554 Available at: [Accessed June 23, 2011].

Simms AE, Paton JFR, Allen AM, Pickering AE (2010) Is augmented central respiratory-sympathetic coupling involved in the generation of hypertension? Respir Physiol Neurobiol 174:89-97 Available at: [Accessed June 5, 2011].

Simms AE, Paton JFR, Pickering AE, Allen AM (2009) Amplified respiratory-sympathetic coupling in the spontaneously hypertensive rat: does it contribute to hypertension? J. Physiol. (Lond.) 587:597-610 Available at: [Accessed June 5, 2011].

Simonyan K, Jürgens U (2003) Efferent subcortical projections of the laryngeal motorcortex in the rhesus monkey. Brain Res 974:43-59 Available at: [Accessed June 3, 2011].

Skultety FM (1962) Experimental mutism in dogs. Arch. Neurol 6:235-241 Available at: [Accessed June 4, 2011].

Smith CA, Forster HV, Blain GM, Dempsey JA (2010) An interdependent model of central/peripheral chemoreception: evidence and implications for ventilatory control. Respir Physiol Neurobiol 173:288-297 Available at: [Accessed June 29, 2011].

Smith JC, Abdala APL, Koizumi H, Rybak IA, Paton JFR (2007) Spatial and functional architecture of the mammalian brain stem respiratory network: a hierarchy of three oscillatory mechanisms. J. Neurophysiol 98:3370-3387 Available at: [Accessed May 4, 2011].

Smith JC, Ellenberger HH, Ballanyi K, Richter DW, Feldman JL (1991) Pre-Bötzinger complex: a brainstem region that may generate respiratory rhythm in mammals. Science 254:726-729 Available at: [Accessed May 11, 2011].

Smith JC, Greer JJ, Liu GS, Feldman JL (1990) Neural mechanisms generating respiratory pattern in mammalian brain stem-spinal cord in vitro. I. Spatiotemporal patterns of motor and medullary neuron activity. J. Neurophysiol 64:1149-1169 Available at: [Accessed May 19, 2011].

Smith JC, Morrison DE, Ellenberger HH, Otto MR, Feldman JL (1989) Brainstem projections to the major respiratory neuron populations in the medulla of the cat. J. Comp. Neurol 281:69-96 Available at: [Accessed May 10, 2011].

Smith JC, Abdala APL, Rybak IA, Paton JFR (2009) Structural and functional architecture of respiratory networks in the mammalian brainstem. Philos. Trans. R. Soc. Lond., B, Biol. Sci 364:2577-2587 Available at: [Accessed May 6, 2011].

Smith WD, Poulin MJ, Paterson DH, Cunningham DA (2001) Dynamic ventilatory response to acute isocapnic hypoxia in septuagenarians. Exp. Physiol 86:117-126 Available at: [Accessed June 13, 2011].

Smotherman M, Kobayasi K, Ma J, Zhang S, Metzner W (2006) A mechanism for vocal-respiratory coupling in the mammalian parabrachial nucleus. J. Neurosci 26:4860-4869 Available at: [Accessed May 8, 2011].

Soffe SR (1993) Two distinct rhythmic motor patterns are driven by common premotor and motor neurons in a simple vertebrate spinal cord. J. Neurosci 13:4456-4469 Available at: [Accessed June 2, 2011].

Soliz J, Gassmann M, Joseph V (2007)(a) Soluble erythropoietin receptor is present in the mouse brain and is required for the ventilatory acclimatization to hypoxia. J. Physiol. (Lond.) 583:329-336 Available at: [Accessed June 9, 2009].

Soliz J, Joseph V, Soulage C, Becskei C, Vogel J, Pequignot JM, Ogunshola O, Gassmann M (2005) Erythropoietin regulates hypoxic ventilation in mice by interacting with brainstem and carotid bodies. J. Physiol. (Lond.) 568:559-571 Available at: [Accessed July 3, 2011].

Soliz J, Soulage C, Hermann DM, Gassmann M (2007)(b) Acute and chronic exposure to hypoxia alters ventilatory pattern but not minute ventilation of mice overexpressing erythropoietin. Am. J. Physiol. Regul. Integr. Comp. Physiol 293:R1702-1710 Available at: [Accessed July 3, 2011].

Soliz J, Thomsen JJ, Soulage C, Lundby C, Gassmann M (2009) Sex-dependent regulation of hypoxic ventilation in mice and humans is mediated by erythropoietin. Am. J. Physiol. Regul. Integr. Comp. Physiol 296:R1837-1846 Available at: [Accessed July 3, 2011].

Solomon IC, Edelman NH, Neubauer JA (2000) Pre-Bötzinger complex functions as a central hypoxia chemosensor for respiration in vivo. J. Neurophysiol 83:2854-2868 Available at: [Accessed July 11, 2011].

Song G, Poon C-S (2004) Functional and structural models of pontine modulation of mechanoreceptor and chemoreceptor reflexes. Respir Physiol Neurobiol 143:281-292 Available at: [Accessed May 10, 2011].

Song G, Yu Y, Poon C-S (2006) Cytoarchitecture of pneumotaxic integration of respiratory and nonrespiratory information in the rat. J. Neurosci 26:300-310 Available at: [Accessed May 9, 2011].

Soto AM, Sonnenschein C (2010) Environmental causes of cancer: endocrine disruptors as carcinogens. Nat Rev Endocrinol 6:363-370 Available at: [Accessed July 9, 2011].

Soulage C, Pequignot J-M, Perrin D (2004) Breathing pattern and hypoxic sensitivity during ageing in a new model of obesity-resistant rat. Respir Physiol Neurobiol 144:45-57 Available at: [Accessed June 13, 2011].

Sperling RA et al. (2011) Toward defining the preclinical stages of Alzheimer's disease: Recommendations from the National Institute on Aging-Alzheimer's Association workgroups on diagnostic guidelines for Alzheimer's disease. Alzheimers Dement 7:280-292 Available at: [Accessed June 17, 2011].

Spillantini MG, Murrell JR, Goedert M, Farlow MR, Klug A, Ghetti B (1998) Mutation in the tau gene in familial multiple system tauopathy with presenile dementia. Proc. Natl. Acad. Sci. U.S.A 95:7737-7741 Available at: [Accessed June 22, 2011].

Spirduso WW (1995) Physical Dimensions of Aging. In Champaign, II: Human Kinetics.

Spyer KM (2009) To breathe or not to breathe? That is the question. Exp. Physiol 94:1-10 Available at: [Accessed May 6, 2011].

St John WM (1996) Medullary regions for neurogenesis of gasping: noeud vital or noeuds vitals? J. Appl. Physiol 81:1865-1877 Available at: [Accessed May 19, 2011].

St John WM, Bledsoe TA (1985) Genesis of rhythmic respiratory activity in pons independent of medulla. J. Appl. Physiol 59:684-690 Available at: [Accessed May 24, 2011].

St John WM (2009) Noeud vital for breathing in the brainstem: gasping--yes, eupnoea--doubtful. Philos. Trans. R. Soc. Lond., B, Biol. Sci 364:2625-2633 Available at: [Accessed May 10, 2011].

St John WM, Leiter JC (2009) Discharge of the hypoglossal nerve cannot distinguish eupnea from gasping, as defined by phrenic discharge, in the in situ mouse. J. Appl. Physiol 107:686-695 Available at: [Accessed May 19, 2011].

St-Jacques R, St-John WM (1999) Transient, reversible apnoea following ablation of the pre-Bötzinger complex in rats. J. Physiol. (Lond.) 520 Pt 1:303-314 Available at: [Accessed May 19, 2011].

St-John WM (1998) Neurogenesis of patterns of automatic ventilatory activity. Prog. Neurobiol 56:97-117 Available at: [Accessed May 6, 2011].

St-John WM (2008) Eupnea of in situ rats persists following blockers of in vitro pacemaker burster activities. Respir Physiol Neurobiol 160:353-356 Available at: [Accessed May 19, 2011].

St-John WM, Paton JFR (2004) Role of pontile mechanisms in the neurogenesis of eupnea. Respir Physiol Neurobiol 143:321-332 Available at: [Accessed May 9, 2011].

Steinbusch HW (1981) Distribution of serotonin-immunoreactivity in the central nervous system of the rat-cell bodies and terminals. Neuroscience 6:557-618 Available at: [Accessed May 31, 2011].

Steinbusch HW, Van Luijtelaar MG, Dijkstra H, Nijssen A, Tonnaer JA (1990) Aging and regenerative capacity of the rat serotonergic system. A morphological, neurochemical and behavioral analysis after transplantation of fetal raphe cells. Ann. N. Y. Acad. Sci 600:384-402; discussion 402-404 Available at: [Accessed June 12, 2011].

Stettner GM, Huppke P, Brendel C, Richter DW, Gärtner J, Dutschmann M (2007) Breathing dysfunctions associated with impaired control of postinspiratory activity in Mecp2-/y knockout mice. J. Physiol. (Lond.) 579:863-876 Available at: [Accessed June 24, 2011].

Stettner GM, Huppke P, Gärtner J, Richter DW, Dutschmann M (2008)(a) Disturbances of breathing in Rett syndrome: results from patients and animal models. Adv. Exp. Med. Biol 605:503-507 Available at: [Accessed June 24, 2011].

Stettner GM, Zanella S, Hilaire G, Dutschmann M (2008)(b) 8-OH-DPAT suppresses spontaneous central apneas in the C57BL/6J mouse strain. Respir Physiol Neurobiol 161:10-15 Available at: [Accessed June 25, 2011].

Stettner GM, Zanella S, Huppke P, Gärtner J, Hilaire G, Dutschmann M (2008)(c) Spontaneous central apneas occur in the C57BL/6J mouse strain. Respir Physiol Neurobiol 160:21-27 Available at: [Accessed June 25, 2011].

Stornetta RL, Moreira TS, Takakura AC, Kang BJ, Chang DA, West GH, Brunet JF, Mulkey DK, Bayliss DA, Guyenet PG (2006) Expression of Phox2b by brainstem neurons involved in chemosensory integration in the adult rat. J. Neurosci 26:10305-10314 Available at: [Accessed May 11, 2011].

Stornetta RL, Rosin DL, Wang H, Sevigny CP, Weston MC, Guyenet PG (2003) A group of glutamatergic interneurons expressing high levels of both neurokinin-1 receptors and somatostatin identifies the region of the pre-Bötzinger complex. J. Comp. Neurol 455:499-512 Available at: [Accessed May 11, 2011].

Stunden CE, Filosa JA, Garcia AJ, Dean JB, Putnam RW (2001) Development of in vivo ventilatory and single chemosensitive neuron responses to hypercapnia in rats. Respir Physiol 127:135-155 Available at: [Accessed July 13, 2011].

Subramanian HH, Balnave RJ, Holstege G (2008) The midbrain periaqueductal gray control of respiration. J. Neurosci 28:12274-12283 Available at: [Accessed May 8, 2011].

Subramanian HH, Holstege G (2009) The nucleus retroambiguus control of respiration. J. Neurosci 29:3824-3832 Available at: [Accessed June 5, 2011].

Subramanian HH, Holstege G (2010) Periaqueductal gray control of breathing. Adv. Exp. Med. Biol 669:353-358 Available at: [Accessed May 8, 2011].

Sugiyama Y, Shiba K, Nakazawa K, Suzuki T, Hisa Y (2010) Brainstem vocalization area in guinea pigs. Neurosci. Res 66:359-365 Available at: [Accessed June 4, 2011].

Sultan A, Nesslany F, Violet M, Bégard S, Loyens A, Talahari S, Mansuroglu Z, Marzin D, Sergeant N, Humez S, Colin M, Bonnefoy E, Buée L, Galas M-C (2011) Nuclear tau, a key player in neuronal DNA protection. J. Biol. Chem 286:4566-4575 Available at: [Accessed June 16, 2011].

Sun MK, Reis DJ (1994) Hypoxia selectively excites vasomotor neurons of rostral ventrolateral medulla in rats. Am. J. Physiol 266:R245-256 Available at: [Accessed July 11, 2011].

Sun QJ, Goodchild AK, Chalmers JP, Pilowsky PM (1998) The pre-Bötzinger complex and phase-spanning neurons in the adult rat. Brain Res 809:204-213 Available at: [Accessed May 11, 2011].

Suratt PM, McTier RF, Wilhoit SC (1988) Upper airway muscle activation is augmented in patients with obstructive sleep apnea compared with that in normal subjects. Am. Rev. Respir. Dis 137:889-894 Available at: [Accessed June 13, 2011].

Surridge CD, Burns RG (1994) The difference in the binding of phosphatidylinositol distinguishes MAP2 from MAP2C and Tau. Biochemistry 33:8051-8057 Available at: [Accessed June 16, 2011].

Sutton D, Larson C, Lindeman RC (1974) Neocortical and limbic lesion effects on primate phonation. Brain Res 71:61-75 Available at: [Accessed June 4, 2011].

Suzue T (1984) Respiratory rhythm generation in the in vitro brain stem-spinal cord preparation of the neonatal rat. J. Physiol. (Lond.) 354:173-183 Available at: [Accessed May 19, 2011].

Suzue T (1994) Mouse fetuses in late gestation maintained in vitro by a transplacental perfusion method and their physiological activities. Neurosci. Res 21:173-176 Available at: [Accessed May 17, 2011].

Swanson LW (1976) The locus coeruleus: a cytoarchitectonic, Golgi and immunohistochemical study in the albino rat. Brain Res 110:39-56 Available at: [Accessed May 10, 2011].

Swanson LW, Hartman BK (1975) The central adrenergic system. An immunofluorescence study of the location of cell bodies and their efferent connections in the rat utilizing dopamine-beta-hydroxylase as a marker. J. Comp. Neurol 163:467-505 Available at: [Accessed May 10, 2011].

Sydow A, Van der Jeugd A, Zheng F, Ahmed T, Balschun D, Petrova O, Drexler D, Zhou L, Rune G, Mandelkow E, D'Hooge R, Alzheimer C, Mandelkow E-M (2011) Tau-induced defects in synaptic plasticity, learning, and memory are reversible in transgenic mice after switching off the toxic Tau mutant. J. Neurosci 31:2511-2525 Available at: [Accessed June 22, 2011].

Sykes RM, Spyer KM, Izzo PN (1997) Demonstration of glutamate immunoreactivity in vagal sensory afferents in the nucleus tractus solitarius of the rat. Brain Res 762:1-11 Available at: [Accessed May 11, 2011].

Tadjalli A, Duffin J, Peever J (2010) Identification of a novel form of noradrenergic-dependent respiratory motor plasticity triggered by vagal feedback. J. Neurosci 30:16886-16895 Available at: [Accessed June 9, 2011].

Takakura ACT, Moreira TS, Colombari E, West GH, Stornetta RL, Guyenet PG (2006) Peripheral chemoreceptor inputs to retrotrapezoid nucleus (RTN) CO2-sensitive neurons in rats. J. Physiol. (Lond.) 572:503-523 Available at: [Accessed May 11, 2011].

Takashima A (2008) Hyperphosphorylated tau is a cause of neuronal dysfunction in tauopathy. J. Alzheimers Dis 14:371-375 Available at: [Accessed June 20, 2011].

Taketo M, Schroeder AC, Mobraaten LE, Gunning KB, Hanten G, Fox RR, Roderick TH, Stewart CL, Lilly F, Hansen CT (1991) FVB/N: an inbred mouse strain preferable for transgenic analyses. Proc. Natl. Acad. Sci. U.S.A 88:2065-2069 Available at: [Accessed July 5, 2011].

Talley EM, Sadr NN, Bayliss DA (1997) Postnatal development of serotonergic innervation, 5-HT1A receptor expression, and 5-HT responses in rat motoneurons. J. Neurosci 17:4473-4485 Available at: [Accessed June 12, 2011].

Tan W, Janczewski WA, Yang P, Shao XM, Callaway EM, Feldman JL (2008) Silencing preBötzinger complex somatostatin-expressing neurons induces persistent apnea in awake rat. Nat. Neurosci 11:538-540 Available at: [Accessed May 11, 2011].

Tanzi RE, Bertram L (2005) Twenty years of the Alzheimer's disease amyloid hypothesis: a genetic perspective. Cell 120:545-555 Available at: [Accessed June 18, 2011].

Tashiro K, Hasegawa M, Ihara Y, Iwatsubo T (1997) Somatodendritic localization of phosphorylated tau in neonatal and adult rat cerebral cortex. Neuroreport 8:2797-2801 Available at: [Accessed June 15, 2011].

Telgkamp P, Ramirez JM (1999) Differential responses of respiratory nuclei to anoxia in rhythmic brain stem slices of mice. J. Neurophysiol 82:2163-2170 Available at: [Accessed July 11, 2011].

Teppema LJ, Dahan A (2010) The ventilatory response to hypoxia in mammals: mechanisms, measurement, and analysis. Physiol. Rev 90:675-754 Available at: [Accessed June 7, 2011].

Terwel D, Lasrado R, Snauwaert J, Vandeweert E, Van Haesendonck C, Borghgraef P, Van Leuven F (2005) Changed conformation of mutant Tau-P301L underlies the moribund tauopathy, absent in progressive, nonlethal axonopathy of Tau-4R/2N transgenic mice. J. Biol. Chem 280:3963-3973 Available at: [Accessed August 3, 2010].

Terwel D, Muyllaert D, Dewachter I, Borghgraef P, Croes S, Devijver H, Van Leuven F (2008) Amyloid activates GSK-3beta to aggravate neuronal tauopathy in bigenic mice. Am J Pathol 172:786-98 Available at: [Accessed February 16, 2009].

The Jackson Laboratory Available at: http://jaxmice.jax.org/strain/000664.html.

Thoby-Brisson M, Ramirez JM (2000) Role of inspiratory pacemaker neurons in mediating the hypoxic response of the respiratory network in vitro. J. Neurosci 20:5858-5866 Available at: [Accessed July 11, 2011].

Thoby-Brisson M, Ramirez JM (2001) Identification of two types of inspiratory pacemaker neurons in the isolated respiratory neural network of mice. J. Neurophysiol 86:104-112 Available at: [Accessed May 18, 2011].

Thoby-Brisson M, Karlén M, Wu N, Charnay P, Champagnat J, Fortin G (2009) Genetic identification of an embryonic parafacial oscillator coupling to the preBötzinger complex. Nat. Neurosci 12:1028-1035 Available at: [Accessed May 17, 2011].

Thoby-Brisson M, Trinh J-B, Champagnat J, Fortin G (2005) Emergence of the pre-Bötzinger respiratory rhythm generator in the mouse embryo. J. Neurosci 25:4307-4318 Available at: [Accessed May 18, 2011].

Thomas AJ, Hendriksen M, Piggott M, Ferrier IN, Perry E, Ince P, O'Brien JT (2006) A study of the serotonin transporter in the prefrontal cortex in late-life depression and Alzheimer's disease with and without depression. Neuropathol. Appl. Neurobiol 32:296-303 Available at: [Accessed June 23, 2011].

Tian GF, Peever JH, Duffin J (1998) Bötzinger-complex expiratory neurons monosynaptically inhibit phrenic motoneurons in the decerebrate rat. Exp Brain Res 122:149-156 Available at: [Accessed May 11, 2011].

Tolep K, Higgins N, Muza S, Criner G, Kelsen SG (1995) Comparison of diaphragm strength between healthy adult elderly and young men. Am. J. Respir. Crit. Care Med 152:677-682 Available at: [Accessed June 10, 2011].

Tolep K, Kelsen SG (1993) Effect of aging on respiratory skeletal muscles. Clin. Chest Med 14:363-378

Available at: [Accessed June 10, 2011].

Tolnay M, Probst A (2002) Frontotemporal lobar degeneration--tau as a pied piper? Neurogenetics 4:63-75 Available at: [Accessed June 23, 2011].

Tomori Z, Benacka R, Donic V (1998) Mechanisms and clinicophysiological implications of the sniff- and gasp-like aspiration reflex. Respir Physiol 114:83-98 Available at: [Accessed June 2, 2011].

Toppin VAL, Harris MB, Kober AM, Leiter JC, St-John WM (2007) Persistence of eupnea and gasping following blockade of both serotonin type 1 and 2 receptors in the in situ juvenile rat preparation. J. Appl. Physiol 103:220-227 Available at: [Accessed May 19, 2011].

Trapp S, Aller MI, Wisden W, Gourine AV (2008) A role for TASK-1 (KCNK3) channels in the chemosensory control of breathing. J. Neurosci 28:8844-8850 Available at: [Accessed June 28, 2011].

Trippenbach T (1994) Pulmonary reflexes and control of breathing during development. Biol. Neonate 65:205-210 Available at: [Accessed May 24, 2011].

Trojanowski JQ, Schuck T, Schmidt ML, Lee VM (1989) Distribution of tau proteins in the normal human central and peripheral nervous system. J. Histochem. Cytochem 37:209-215 Available at: [Accessed June 15, 2011].

Trojanowski JQ, Smith AB, Huryn D, Lee VM-Y (2005) Microtubule-stabilising drugs for therapy of Alzheimer's disease and other neurodegenerative disorders with axonal transport impairments. Expert Opin Pharmacother 6:683-686 Available at: [Accessed June 20, 2011].

Tsuboi Y, Dickson DW, Nabeshima K, Schmeichel AM, Wszolek ZK, Yamada T, Benarroch EE (2008) Neurodegeneration involving putative respiratory neurons in Perry syndrome. Acta Neuropathol 115:263-268 Available at: [Accessed July 7, 2011].

Turner JM, Mead J, Wohl ME (1968) Elasticity of human lungs in relation to age. J Appl Physiol 25:664-671 Available at: [Accessed June 10, 2011].

Twarog BM (1954) Responses of a molluscan smooth muscle to acetylcholine and 5-hydroxytryptamine. J. Cell. Physiol 44:141-163 Available at: [Accessed May 31, 2011].

Twarog BM, Page IH (1953) Serotonin content of some mammalian tissues and urine and a method for its determination. Am. J. Physiol 175:157-161 Available at: [Accessed May 31, 2011].

Ueda S, Aikawa M, Ishizuya-Oka A, Koibuchi N, Yamaoka S, Yoshimoto K (1998) Age-related degeneration of the serotoninergic fibers in the zitter rat brain. Synapse 30:62-70 Available at: [Accessed June 12, 2011].

Ugolini G (1995) Specificity of rabies virus as a transneuronal tracer of motor networks: transfer from hypoglossal motoneurons to connected second-order and higher order central nervous system cell groups. J. Comp. Neurol 356:457-480 Available at: [Accessed May 6, 2011].

Ungerstedt U (1971) Stereotaxic mapping of the monoamine pathways in the rat brain. Acta Physiol Scand Suppl 367:1-48 Available at: [Accessed May 10, 2011].

Vacher H, Mohapatra DP, Trimmer JS (2008) Localization and targeting of voltage-dependent ion channels in mammalian central neurons. Physiol. Rev 88:1407-1447 Available at: [Accessed July 12, 2011].

VanderHorst VG, Terasawa E, Ralston HJ 3rd (2001) Monosynaptic projections from the nucleus retroambiguus region to laryngeal motoneurons in the rhesus monkey. Neuroscience 107:117-125 Available at: [Accessed June 4, 2011].

Vanderhorst VG, Holstege G (1997) Nucleus retroambiguus projections to lumbosacral motoneuronal cell groups in the male cat. J. Comp. Neurol 382:77-88 Available at: [Accessed June 5, 2011].

Vanderhorst VG, Terasawa E, Ralston HJ 3rd, Holstege G (2000)(a) Monosynaptic projections from the lateral

periaqueductal gray to the nucleus retroambiguus in the rhesus monkey: implications for vocalization and reproductive behavior. J. Comp. Neurol 424:251-268 Available at: [Accessed June 4, 2011].

Vanderhorst VG, Terasawa E, Ralston HJ 3rd, Holstege G (2000)(b) Monosynaptic projections from the nucleus retroambiguus to motoneurons supplying the abdominal wall, axial, hindlimb, and pelvic floor muscles in the female rhesus monkey. J. Comp. Neurol 424:233-250 Available at: [Accessed June 4, 2011].

Varas R, Alcayaga J, Iturriaga R (2003) ACh and ATP mediate excitatory transmission in cat carotid identified chemoreceptor units in vitro. Brain Res 988:154-163 Available at: [Accessed June 29, 2011].

Varas R, Wyatt CN, Buckler KJ (2007) Modulation of TASK-like background potassium channels in rat arterial chemoreceptor cells by intracellular ATP and other nucleotides. J. Physiol. (Lond.) 583:521-536 Available at: [Accessed April 20, 2010].

Veasey SC, Fornal CA, Metzler CW, Jacobs BL (1995) Response of serotonergic caudal raphe neurons in relation to specific motor activities in freely moving cats. J. Neurosci 15:5346-5359 Available at: [Accessed July 13, 2011].

Veasey SC, Fornal CA, Metzler CW, Jacobs BL (1997) Single-unit responses of serotonergic dorsal raphe neurons to specific motor challenges in freely moving cats. Neuroscience 79:161-169 Available at: [Accessed July 13, 2011].

Velly L, Pellegrini L, Guillet B, Bruder N, Pisano P (2010) Erythropoietin 2nd cerebral protection after acute injuries: a double-edged sword? Pharmacol. Ther 128:445-459 Available at: [Accessed July 3, 2011].

Verbeken EK, Cauberghs M, Mertens I, Clement J, Lauweryns JM, Van de Woestijne KP (1992) The senile lung. Comparison with normal and emphysematous lungs. 1. Structural aspects. Chest 101:793-799 Available at: [Accessed June 10, 2011].

Viemari JC, Bévengut M, Burnet H, Coulon P, Pequignot JM, Tiveron MC, Hilaire G (2004)(a) Phox2a gene, A6 neurons, and noradrenaline are essential for development of normal respiratory rhythm in mice. J. Neurosci 24:928-937 Available at: [Accessed May 5, 2011].

Viemari JC, Maussion G, Bévengut M, Burnet H, Pequignot JM, Népote V, Pachnis V, Simonneau M, Hilaire G (2005)(a) Ret deficiency in mice impairs the development of A5 and A6 neurons and the functional maturation of the respiratory rhythm. Eur. J. Neurosci 22:2403-2412 Available at: [Accessed May 30, 2011].

Viemari J-C, Burnet H, Bévengut M, Hilaire G (2003) Perinatal maturation of the mouse respiratory rhythm-generator: in vivo and in vitro studies. Eur. J. Neurosci 17:1233-1244 Available at: [Accessed May 17, 2011].

Viemari J-C, Bévengut M, Coulon P, Hilaire G (2004)(b) Nasal trigeminal inputs release the A5 inhibition received by the respiratory rhythm generator of the mouse neonate. J. Neurophysiol 91:746-758 Available at: [Accessed May 5, 2011].

Viemari J-C, Roux J-C, Tryba AK, Saywell V, Burnet H, Peña F, Zanella S, Bévengut M, Barthelemy-Requin M, Herzing LBK, Moncla A, Mancini J, Ramirez J-M, Villard L, Hilaire G (2005)(b) Mecp2 deficiency disrupts norepinephrine and respiratory systems in mice. J. Neurosci 25:11521-11530 Available at: [Accessed June 24, 2011].

Viemari J-C, Tryba AK (2009) Bioaminergic neuromodulation of respiratory rhythm in vitro. Respir Physiol Neurobiol 168:69-75 Available at: [Accessed May 30, 2011].

Vizek M, Pickett CK, Weil JV (1987) Biphasic ventilatory response of adult cats to sustained hypoxia has central origin. J. Appl. Physiol 63:1658-1664 Available at: [Accessed June 29, 2011].

Vogel J, Gassmann M (2011) Erythropoietic and non-erythropoietic functions of erythropoietin (Epo) in mouse models. J Physiol Available at: http://www.ncbi.nlm.nih.gov.gate1.inist.fr/pubmed/21282290 [Accessed March 21, 2011].

Voituron N, Frugière A, Champagnat J, Bodineau L (2006) Hypoxia-sensing properties of the newborn rat

ventral medullary surface in vitro. J. Physiol. (Lond.) 577:55-68 Available at: [Accessed July 2, 2011].

Voituron N, Frugière A, Gros F, Macron JM, Bodineau L (2005) Diencephalic and mesencephalic influences on ponto-medullary respiratory control in normoxic and hypoxic conditions: an in vitro study on central nervous system preparations from newborn rat. Neuroscience 132:843-854 Available at: [Accessed July 2, 2011].

Voituron N, Hilaire G (2011) The benzodiazepine Midazolam mitigates the breathing defects of Mecp2-deficient mice. Respir Physiol Neurobiol 177:56-60 Available at: [Accessed June 24, 2011].

Volgin DV, Fay R, Kubin L (2003) Postnatal development of serotonin 1B, 2 A and 2C receptors in brainstem motoneurons. Eur. J. Neurosci 17:1179-1188 Available at: [Accessed June 12, 2011].

Voss MD, De Castro D, Lipski J, Pilowsky PM, Jiang C (1990) Serotonin immunoreactive boutons form close appositions with respiratory neurons of the dorsal respiratory group in the cat. J. Comp. Neurol 295:208-218 Available at: [Accessed May 31, 2011].

Vossel KA, Zhang K, Brodbeck J, Daub AC, Sharma P, Finkbeiner S, Cui B, Mucke L (2010) Tau reduction prevents Abeta-induced defects in axonal transport. Science 330:198 Available at: [Accessed June 21, 2011].

Waldrop TG (1991) Posterior hypothalamic modulation of the respiratory response to CO2 in cats. Pflugers Arch 418:7-13 Available at: [Accessed July 13, 2011].

Walker DM, Gore AC (2011) Transgenerational neuroendocrine disruption of reproduction. Nat Rev Endocrinol 7:197-207 Available at: [Accessed July 9, 2011].

Wallin IE (1926) BACTERIA AND THE ORIGIN OF SPECIES. Science 64:173-175 Available at: [Accessed April 28, 2011].

Walsh DM, Selkoe DJ (2007) A beta oligomers - a decade of discovery. J. Neurochem 101:1172-1184 Available at: [Accessed June 18, 2011].

Walsh DM, Townsend M, Podlisny MB, Shankar GM, Fadeeva JV, El Agnaf O, Hartley DM, Selkoe DJ (2005) Certain inhibitors of synthetic amyloid beta-peptide (Abeta) fibrillogenesis block oligomerization of natural Abeta and thereby rescue long-term potentiation. J. Neurosci 25:2455-2462 Available at: [Accessed June 18, 2011].

Wang GL, Semenza GL (1993) General involvement of hypoxia-inducible factor 1 in transcriptional response to hypoxia. Proc. Natl. Acad. Sci. U.S.A 90:4304-4308 Available at: [Accessed July 3, 2011].

Wang H, Liang S, Burgdorf J, Wess J, Yeomans J (2008) Ultrasonic vocalizations induced by sex and amphetamine in M2, M4, M5 muscarinic and D2 dopamine receptor knockout mice. PLoS ONE 3:e1893 Available at: [Accessed June 5, 2011].

Wang H, Chan S-an, Ogier M, Hellard D, Wang Q, Smith C, Katz DM (2006) Dysregulation of brain-derived neurotrophic factor expression and neurosecretory function in Mecp2 null mice. J. Neurosci 26:10911-10915 Available at: [Accessed June 24, 2011].

Wang MR, Kuo JS, Chai CY (2002)(a) Cardiovascular and vocalization reactions elicited by N-methyl-D-aspartate in the pretentorial periaqueductal grey of cats. Clin. Exp. Pharmacol. Physiol 29:759-771 Available at: [Accessed June 4, 2011].

Wang W, Richerson GB (1999) Development of chemosensitivity of rat medullary raphe neurons. Neuroscience 90:1001-1011 Available at: [Accessed June 28, 2011].

Wang W, Bradley SR, Richerson GB (2002)(b) Quantification of the response of rat medullary raphe neurones to independent changes in pH(o) and P(CO2). J. Physiol. (Lond.) 540:951-970 Available at: [Accessed July 12, 2011].

Wang Y, Loomis PA, Zinkowski RP, Binder LI (1993) A novel tau transcript in cultured human neuroblastoma cells expressing nuclear tau. J. Cell Biol 121:257-267 Available at: [Accessed June 16, 2011].

Ward DS, Berkenbosch A, DeGoede J, Olievier CN (1990) Dynamics of the ventilatory response to central hypoxia in cats. J. Appl. Physiol 68:1107-1113 Available at: [Accessed July 2, 2011].

Ware JC, McBrayer RH, Scott JA (2000) Influence of sex and age on duration and frequency of sleep apnea events. Sleep 23:165-170 Available at: [Accessed June 9, 2011].

Weese-Mayer DE, Lieske SP, Boothby CM, Kenny AS, Bennett HL, Ramirez J-M (2008) Autonomic dysregulation in young girls with Rett Syndrome during nighttime in-home recordings. Pediatr. Pulmonol 43:1045-1060 Available at: [Accessed June 24, 2011].

Weese-Mayer DE, Lieske SP, Boothby CM, Kenny AS, Bennett HL, Silvestri JM, Ramirez J-M (2006) Autonomic nervous system dysregulation: breathing and heart rate perturbation during wakefulness in young girls with Rett syndrome. Pediatr. Res 60:443-449 Available at: [Accessed June 24, 2011].

Wei ML, Andreadis A (1998) Splicing of a regulated exon reveals additional complexity in the axonal microtubule-associated protein tau. J. Neurochem 70:1346-1356 Available at: [Accessed June 15, 2011].

Weidemann A, Kerdiles YM, Knaup KX, Rafie CA, Boutin AT, Stockmann C, Takeda N, Scadeng M, Shih AY, Haase VH, Simon MC, Kleinfeld D, Johnson RS (2009) The glial cell response is an essential component of hypoxia-induced erythropoiesis in mice. J. Clin. Invest 119:3373-3383 Available at: [Accessed July 3, 2011].

Weingarten MD, Lockwood AH, Hwo SY, Kirschner MW (1975) A protein factor essential for microtubule assembly. Proc. Natl. Acad. Sci. U.S.A 72:1858-1862 Available at: [Accessed June 15, 2011].

Weir EK, López-Barneo J, Buckler KJ, Archer SL (2005) Acute oxygen-sensing mechanisms. N. Engl. J. Med 353:2042-2055 Available at: [Accessed June 30, 2011].

Weiss B (2011) Endocrine disruptors as a threat to neurological function. J. Neurol. Sci 305:11-21 Available at: [Accessed July 9, 2011].

Wenninger JM, Olson EB Jr, Cotter CJ, Thomas CF, Behan M (2009) Hypoxic and hypercapnic ventilatory responses in aging male vs. aging female rats. J. Appl. Physiol 106:1522-1528 Available at: [Accessed June 13, 2011].

Westlund KN, Bowker RM, Ziegler MG, Coulter JD (1982) Descending noradrenergic projections and their spinal terminations. Prog. Brain Res 57:219-238 Available at: [Accessed May 10, 2011].

Westlund KN, Bowker RM, Ziegler MG, Coulter JD (1983) Noradrenergic projections to the spinal cord of the rat. Brain Res 263:15-31 Available at: [Accessed May 10, 2011].

Weston MC, Stornetta RL, Guyenet PG (2004) Glutamatergic neuronal projections from the marginal layer of the rostral ventral medulla to the respiratory centers in rats. J. Comp. Neurol 473:73-85 Available at: [Accessed May 10, 2011].

Widdicombe J (2003) Functional morphology and physiology of pulmonary rapidly adapting receptors (RARs). Anat Rec A Discov Mol Cell Evol Biol 270:2-10 Available at: [Accessed July 14, 2011].

Widdicombe J (2006) Reflexes from the lungs and airways: historical perspective. J. Appl. Physiol 101:628-634 Available at: [Accessed July 14, 2011].

Wider C, Wszolek ZK (2008) Rapidly progressive familial parkinsonism with central hypoventilation, depression and weight loss (Perry syndrome)--a literature review. Parkinsonism Relat. Disord 14:1-7 Available at: [Accessed July 7, 2011].

Willard HF, Hendrich BD (1999) Breaking the silence in Rett syndrome. Nat. Genet 23:127-128 Available at: [Accessed June 24, 2011].

Williams SEJ, Wootton P, Mason HS, Bould J, Iles DE, Riccardi D, Peers C, Kemp PJ (2004) Hemoxygenase-2 is an oxygen sensor for a calcium-sensitive potassium channel. Science 306:2093-2097 Available at: [Accessed June 30, 2011].

Winter SM, Fresemann J, Schnell C, Oku Y, Hirrlinger J, Hülsmann S (2009) Glycinergic interneurons are functionally integrated into the inspiratory network of mouse medullary slices. Pflugers Arch 458:459-469 Available at: [Accessed May 11, 2011].

Witman GB, Cleveland DW, Weingarten MD, Kirschner MW (1976) Tubulin requires tau for growth onto microtubule initiating sites. Proc. Natl. Acad. Sci. U.S.A 73:4070-4074 Available at: [Accessed June 15, 2011].

Wszolek ZK, Pfeiffer RF, Bhatt MH, Schelper RL, Cordes M, Snow BJ, Rodnitzky RL, Wolters EC, Arwert F, Calne DB (1992) Rapidly progressive autosomal dominant parkinsonism and dementia with pallido-ponto-nigral degeneration. Ann. Neurol 32:312-320 Available at: [Accessed June 22, 2011].

Wyatt CN, Buckler KJ (2004) The effect of mitochondrial inhibitors on membrane currents in isolated neonatal rat carotid body type I cells. J. Physiol. (Lond.) 556:175-191 Available at: [Accessed June 30, 2011].

Wyatt CN, Peers C (1995) Ca(2+)-activated K+ channels in isolated type I cells of the neonatal rat carotid body. J. Physiol. (Lond.) 483 (Pt 3):559-565 Available at: [Accessed June 30, 2011].

Wyatt CN, Evans AM (2007) AMP-activated protein kinase and chemotransduction in the carotid body. Respir Physiol Neurobiol 157:22-29 Available at: [Accessed June 30, 2011].

Xu F, Zhang Z, Frazier DT (2001) Microinjection of acetazolamide into the fastigial nucleus augments respiratory output in the rat. J. Appl. Physiol 91:2342-2350 Available at: [Accessed July 13, 2011].

Yamada H, Ezure K, Manabe M (1988) Efferent projections of inspiratory neurons of the ventral respiratory group. A dual labeling study in the rat. Brain Res 455:283-294 Available at: [Accessed May 5, 2011].

Yamamoto Y, Kummer W, Atoji Y, Suzuki Y (2002) TASK-1, TASK-2, TASK-3 and TRAAK immunoreactivities in the rat carotid body. Brain Res 950:304-307 Available at: [Accessed June 29, 2011].

Yamauchi M, Ocak H, Dostal J, Jacono FJ, Loparo KA, Strohl KP (2008) Post-sigh breathing behavior and spontaneous pauses in the C57BL/6J (B6) mouse. Respir Physiol Neurobiol 162:117-125 Available at: [Accessed July 14, 2011].

Yang Y, Schmitt HP (2001) Frontotemporal dementia: evidence for impairment of ascending serotoninergic but not noradrenergic innervation. Immunocytochemical and quantitative study using a graph method. Acta Neuropathol 101:256-270 Available at: [Accessed June 23, 2011].

Yokota S, Oka T, Tsumori T, Nakamura S, Yasui Y (2007) Glutamatergic neurons in the Kölliker-Fuse nucleus project to the rostral ventral respiratory group and phrenic nucleus: a combined retrograde tracing and in situ hybridization study in the rat. Neurosci. Res 59:341-346 Available at: [Accessed May 9, 2011].

Yoshiyama Y, Higuchi M, Zhang B, Huang S-M, Iwata N, Saido TC, Maeda J, Suhara T, Trojanowski JQ, Lee VM-Y (2007) Synapse loss and microglial activation precede tangles in a P301S tauopathy mouse model. Neuron 53:337-51 Available at: [Accessed April 15, 2009].

Young T, Palta M, Dempsey J, Skatrud J, Weber S, Badr S (1993) The occurrence of sleep-disordered breathing among middle-aged adults. N. Engl. J. Med 328:1230-1235 Available at: [Accessed June 13, 2011].

Young T, Peppard PE, Gottlieb DJ (2002) Epidemiology of obstructive sleep apnea: a population health perspective. Am. J. Respir. Crit. Care Med 165:1217-1239 Available at: [Accessed June 9, 2011].

Yu J-Z, Rasenick MM (2006) Tau associates with actin in differentiating PC12 cells. FASEB J 20:1452-1461 Available at: [Accessed June 16, 2011].

Yuan A, Kumar A, Peterhoff C, Duff K, Nixon RA (2008) Axonal transport rates in vivo are unaffected by tau deletion or overexpression in mice. J. Neurosci 28:1682-1687 Available at: [Accessed June 20, 2011].

Yuzwa SA, Macauley MS, Heinonen JE, Shan X, Dennis RJ, He Y, Whitworth GE, Stubbs KA, McEachern EJ, Davies GJ, Vocadlo DJ (2008) A potent mechanism-inspired O-GlcNAcase inhibitor that blocks phosphorylation of tau in vivo. Nat. Chem. Biol 4:483-490 Available at: [Accessed September 14, 2010].

Yuzwa SA, Vocadlo DJ (2009) O-GlcNAc modification and the tauopathies: insights from chemical biology. Curr Alzheimer Res 6:451-454 Available at: [Accessed June 21, 2011].

Zabka AG, Behan M, Mitchell GS (2001)(a) Long term facilitation of respiratory motor output decreases with age in male rats. J. Physiol. (Lond.) 531:509-514 Available at: [Accessed June 9, 2011].

Zabka AG, Behan M, Mitchell GS (2001)(b) Selected contribution: Time-dependent hypoxic respiratory responses in female rats are influenced by age and by the estrus cycle. J. Appl. Physiol 91:2831-2838 Available at: [Accessed June 9, 2011].

Zabka AG, Mitchell GS, Behan M (2005) Ageing and gonadectomy have similar effects on hypoglossal long-term facilitation in male Fischer rats. J. Physiol. (Lond.) 563:557-568 Available at: [Accessed June 9, 2011].

Zabka AG, Mitchell GS, Olson EB Jr, Behan M (2003) Selected contribution: chronic intermittent hypoxia enhances respiratory long-term facilitation in geriatric female rats. J. Appl. Physiol 95:2614-2623; discussion 2604 Available at: [Accessed June 9, 2011].

Zanella S, Roux JC, Viemari JC, Hilaire G (2006) Possible modulation of the mouse respiratory rhythm generator by A1/C1 neurones. Respir Physiol Neurobiol 153:126-138 Available at: [Accessed May 30, 2011].

Zanella S, Mebarek S, Lajard A-M, Picard N, Dutschmann M, Hilaire G (2008)(a) Oral treatment with desipramine improves breathing and life span in Rett syndrome mouse model. Respir Physiol Neurobiol 160:116-121 Available at: [Accessed June 24, 2011].

Zanella S, Watrin F, Mebarek S, Marly F, Roussel M, Gire C, Diene G, Tauber M, Muscatelli F, Hilaire G (2008)(b) Necdin plays a role in the serotonergic modulation of the mouse respiratory network: implication for Prader-Willi syndrome. J Neurosci 28:1745-55 Available at: [Accessed February 4, 2009].

Zarow C, Lyness SA, Mortimer JA, Chui HC (2003) Neuronal loss is greater in the locus coeruleus than nucleus basalis and substantia nigra in Alzheimer and Parkinson diseases. Arch. Neurol 60:337-341 Available at: [Accessed June 23, 2011].

Zhan G, Shaheen F, Mackiewicz M, Fenik P, Veasey SC (2002) Single cell laser dissection with molecular beacon polymerase chain reaction identifies 2A as the predominant serotonin receptor subtype in hypoglossal motoneurons. Neuroscience 113:145-154 Available at: [Accessed June 12, 2011].

Zhan WZ, Ellenberger HH, Feldman JL (1989) Monoaminergic and GABAergic terminations in phrenic nucleus of rat identified by immunohistochemical labeling. Neuroscience 31:105-113 Available at: [Accessed May 31, 2011].

Zhang B, Dong Y, Zhang G, Moir RD, Xia W, Yue Y, Tian M, Culley DJ, Crosby G, Tanzi RE, Xie Z (2008) The inhalation anesthetic desflurane induces caspase activation and increases amyloid beta-protein levels under hypoxic conditions. J. Biol. Chem 283:11866-11875 Available at: [Accessed June 23, 2011].

Zhang B, Maiti A, Shively S, Lakhani F, McDonald-Jones G, Bruce J, Lee EB, Xie SX, Joyce S, Li C, Toleikis PM, Lee VM-Y, Trojanowski JQ (2005)(a) Microtubule-binding drugs offset tau sequestration by stabilizing microtubules and reversing fast axonal transport deficits in a tauopathy model. Proc. Natl. Acad. Sci. U.S.A 102:227-231 Available at: [Accessed June 20, 2011].

Zhang SP, Bandler R, Davis PJ (1995) Brain stem integration of vocalization: role of the nucleus retroambigualis. J. Neurophysiol 74:2500-2512 Available at: [Accessed June 3, 2011].

Zhang W, Hayward LF, Davenport PW (2005)(b) Respiratory muscle responses elicited by dorsal periaqueductal gray stimulation in rats. Am. J. Physiol. Regul. Integr. Comp. Physiol 289:R1338-1347 Available at: [Accessed June 5, 2011].

Zhang W, Hayward LF, Davenport PW (2007) Respiratory responses elicited by rostral versus caudal dorsal periaqueductal gray stimulation in rats. Auton Neurosci 134:45-54 Available at: [Accessed June 5, 2011].

Zhao Z-Q, Scott M, Chiechio S, Wang J-S, Renner KJ, Gereau RW 4th, Johnson RL, Deneris ES, Chen Z-F

(2006) Lmx1b is required for maintenance of central serotonergic neurons and mice lacking central serotonergic system exhibit normal locomotor activity. J. Neurosci 26:12781-12788 Available at: [Accessed July 13, 2011].

Zheng Y, Barillot JC, Bianchi AL (1991)(a) Patterns of membrane potentials and distributions of the medullary respiratory neurons in the decerebrate rat. Brain Res 546:261-270 Available at: [Accessed May 5, 2011].

Zheng Y, Barillot JC, Bianchi AL (1991)(b) Patterns of membrane potentials and distributions of the medullary respiratory neurons in the decerebrate rat. Brain Res 546:261-270 Available at: [Accessed May 11, 2011].

Zheng Y, Riche D, Rekling JC, Foutz AS, Denavit-Saubié M (1998) Brainstem neurons projecting to the rostral ventral respiratory group (VRG) in the medulla oblongata of the rat revealed by co-application of NMDA and biocytin. Brain Res 782:113-125 Available at: [Accessed May 9, 2011].

Zhu X, Perry G, Moreira PI, Aliev G, Cash AD, Hirai K, Smith MA (2006) Mitochondrial abnormalities and oxidative imbalance in Alzheimer disease. J. Alzheimers Dis 9:147-153 Available at: [Accessed July 7, 2011].

Ziemann AE, Allen JE, Dahdaleh NS, Drebot II, Coryell MW, Wunsch AM, Lynch CM, Faraci FM, Howard MA 3rd, Welsh MJ, Wemmie JA (2009) The amygdala is a chemosensor that detects carbon dioxide and acidosis to elicit fear behavior. Cell 139:1012-1021 Available at: [Accessed June 2, 2011].

Zoghbi HY, Milstien S, Butler IJ, Smith EO, Kaufman S, Glaze DG, Percy AK (1989) Cerebrospinal fluid biogenic amines and biopterin in Rett syndrome. Ann. Neurol 25:56-60 Available at: [Accessed June 24, 2011].

Zoghbi HY, Percy AK, Glaze DG, Butler IJ, Riccardi VM (1985) Reduction of biogenic amine levels in the Rett syndrome. N. Engl. J. Med 313:921-924 Available at: [Accessed June 24, 2011].

Vieillissement physiologique et pathologique du contrôle nerveux de la respiration : Etude chez des souris sauvages et transgéniques

Résumé

De nouveaux enjeux émergent dans le domaine de la Santé en raison du vieillissement de la population et du développement inquiétant de la Maladie d'Alzheimer (MA). Chez le sujet sain ou pathologique, peu d'études ont porté sur le vieillissement du contrôle nerveux de la respiration, en dépit de son rôle crucial pour l'oxygénation du cerveau. Cette thèse présente des recherches translationnelles, réalisées chez la souris, pour étudier le vieillissement physiologique et pathologique du contrôle nerveux de la respiration. Chez des souris transgéniques, modèles reconnus de la MA et du syndrome de Rett, nous décrivons le développement de neuropathologies respiratoires graves, conduisant à un décès prématuré. Nous montrons pour la première fois qu'une tauopathie du tronc cérébral altère le fonctionnement des voies aériennes supérieures, la vocalisation et la respiration. De plus, nos travaux suggèrent un rôle délétère de l'anesthésie pour la MA et identifient des pistes thérapeutiques nouvelles. En conclusion, nos travaux chez la souris peuvent avoir des retombées particulièrement intéressantes notamment pour la MA.

Summary

New issues are emerging in the field of Health care due to ageing of the population and the alarming development of Alzheimer's Disease (AD). In healthy or pathological living being, very few studies are dealing with the ageing of the respiratory nervous control, in spite of the crucial role of respiration for brain oxygenation. This thesis presents translational research performed in mice to examine the physiological and pathological ageing of the respiratory nervous control. In mice from two transgenic strains, recognized models for AD and Rett syndrome, we describe the development of drastic respiratory neuropathologies leading to premature death. In the AD mouse model, we show for the first time that brainstem tauopathy triggers dysfunctions of the upper airways, impairs vocalization and alters respiration and respiratory control. In addition, our work suggests a deleterious effect of anaesthesia for AD and identifies new therapeutic strategies. This mouse research could well contribute to significant improvements in AD care.